



Interactions Between Dietary Anthocyanins and the Human Gut Microbiota

By

Emad Mohamed Shehata

Food Innovation and Health Programme
Quadram Institute Bioscience

A thesis submitted for the degree of **Doctor of Philosophy (PhD)**

to the **University of East Anglia**

Norwich, United Kingdom

June 2022

©This copy of the thesis has been supplied on condition that anyone who consults it is understood to recognise that its copyright rests with the author and that use of any information derived therefrom must be in accordance with current UK Copyright Law. In addition, any quotation or extract must include full attribution

Abstract

Background: Consumption of dietary anthocyanins has been associated with various health benefits. However, anthocyanins are known to be very poorly bioavailable, and this has led to the concept that there is an important interplay between anthocyanins and the human gut microbiota, where the gut microbiota are able to break down anthocyanins into various metabolites, and that anthocyanins and/or their metabolites may alter the composition of the gut microbiota. However, these interactions are still not clear and much remains to be understood.

Objectives: (i) Investigate the *in-vitro* metabolism of black rice and bilberry anthocyanins by the gut microbiota and (ii) explore the impact of anthocyanins on the structure and function of the gut microbiota.

Approaches: Incubate black rice and bilberry anthocyanins over 24 h with human faecal samples using an *in-vitro* batch colon fermentation model and collect samples for quantifying anthocyanins and anthocyanin metabolites using HPLC-DAD and UPLC-MS-MS. Assess the gut microbiota composition differences between anthocyanin treated and non-anthocyanin treated human colon model samples using whole-genome shotgun metagenomics.

Results: It was shown that loss of anthocyanins was partly spontaneous and partly due to the gut microbiota. Anthocyanins were subject to high inter-individual variations in both spontaneous and gut microbiota-dependent degradation, and modest intra-individual variations. The gut microbiota metabolism (enzymatic) of anthocyanins generates various ring-fission metabolites, and various microbial metabolic pathways were determined such as [Cya3Glc → PCA → catechol], [Cya3Glc → PGA → PGCA → phloroglucinol], and [Cya3Glc → dihydroferulic acid → dihydrocaffeic acid → 4-methylcatechol]. The production of the microbial anthocyanin metabolites such as catechol, dihydrocaffeic acid, dihydroferulic acid, and 4-methylcatechol were completely microbiota-dependent, providing strong evidence that the gut microbiota is important for the metabolism of anthocyanins. In contrast, in the absence of live gut microbiota and in anaerobic

conditions, anthocyanins underwent classic pH-dependent transformation to give Cya hemiketal-Glc, Cya chalcone-Glc, Cya chalcone anionic-Glc and trihydroxyethenylbenzene-Glc (all colourless). But under aerobic conditions, there was a substantial increase in the number of anthocyanin breakdown products formed and these included PCA, PGA, coumarin-Glc, di- and tri-hydroxyphenyloxoacetic acid, and trihydroxyphenylacetic acid. Although there was a small increase of Bacteroidetes over Firmicutes at 6 and 12 h and small increase of *Bacteroides vulgatus* at 6 h, no significant changes were observed in the gut microbiota profile in response to anthocyanin treatments.

Conclusions: Anthocyanins are rapidly and completely degraded in the human colon by a combination of spontaneous and microbiota-dependent processes generating a series of ring fission metabolites, but they did not significantly affect the structure and function of the microbiome. These data extend our understanding of the important role of the human gut microbiota on the bioavailability of consumed anthocyanins.

Access Condition and Agreement

Each deposit in UEA Digital Repository is protected by copyright and other intellectual property rights, and duplication or sale of all or part of any of the Data Collections is not permitted, except that material may be duplicated by you for your research use or for educational purposes in electronic or print form. You must obtain permission from the copyright holder, usually the author, for any other use. Exceptions only apply where a deposit may be explicitly provided under a stated licence, such as a Creative Commons licence or Open Government licence.

Electronic or print copies may not be offered, whether for sale or otherwise to anyone, unless explicitly stated under a Creative Commons or Open Government license. Unauthorised reproduction, editing or reformatting for resale purposes is explicitly prohibited (except where approved by the copyright holder themselves) and UEA reserves the right to take immediate 'take down' action on behalf of the copyright and/or rights holder if this Access condition of the UEA Digital Repository is breached. Any material in this database has been supplied on the understanding that it is copyright material and that no quotation from the material may be published without proper acknowledgement.

Table of Contents

Table of Contents

ABSTRACT	I
TABLE OF CONTENTS	III
LIST OF FIGURES	VIII
LIST OF TABLES	XIII
ABBREVIATIONS	XIV
SYMBOLS	XVI
LIST OF PUBLICATIONS	XVII
DEDICATION	XIX
ACKNOWLEDGEMENTS	XX
CONTRIBUTIONS	XXII
CHAPTER 1: GENERAL INTRODUCTION	1
1.1. SCOPE OF THE RESEARCH IN THIS THESIS	1
1.2. DIETARY (POLY)PHENOLS.....	1
1.3. ANTHOCYANINS.....	7
1.3.1. <i>Chemical structure of anthocyanins</i>	7
1.3.2. <i>Types and distribution of anthocyanins</i>	7
1.4. ANTHOCYANIN-RICH FOODS AND DAILY INTAKE	10
1.5. CHEMICAL STABILITY OF ANTHOCYANINS.....	13
1.5.1. <i>Effect of environmental factors on anthocyanin stability</i>	13
1.5.2. <i>Effect of chemical structure on anthocyanin stability</i>	14
1.5.3. <i>Appearance of breakdown products of chemical degradation of anthocyanins</i>	14
1.6. BIOAVAILABILITY AND METABOLISM OF ANTHOCYANINS.....	16
1.7. ANTHOCYANINS AND HUMAN HEALTH	20
1.8. THE ROLE OF GUT MICROBIOTA IN HUMAN HEALTH	21
1.8.1. <i>What is gut microbiota?</i>	21
1.8.2. <i>The relation between gut microbiota and human health</i>	23
1.9. INTERACTIONS BETWEEN ANTHOCYANINS AND HUMAN GUT MICROBIOTA.....	25
1.9.1. <i>Metabolism of anthocyanin by human gut microbiota</i>	27
1.9.2. <i>The impact of anthocyanins on the structure of the human gut microbiota</i>	29
1.10. AIMS AND OBJECTIVES OF THE RESEARCH	32
CHAPTER 2: MATERIALS AND METHODS	34
2.1. EXTRACTION AND QUANTIFICATION OF ANTHOCYANINS	34
2.1.1. <i>Preparing plant materials for anthocyanin extraction using green solvents</i>	34
2.1.2. <i>Batch extraction procedure for glycerol/water solvent composition assays</i>	34
2.1.3. <i>Batch extraction procedure using 80% glycerol solvent for liquid-to-solid ratio ($R_{L/S}$) assays</i> 35	35
2.1.4. <i>Batch extraction procedure using green solvent for the effect of temperature assays</i> 35	35
2.1.5. <i>Determination of total polyphenol yield in aqueous glycerol extracts</i>	36
2.1.6. <i>Determination of total pigment yield in aqueous glycerol extracts</i>	37
2.1.7. <i>Determination of total anthocyanins in aqueous glycerol extracts using HPLC–DAD</i> 37	37
2.1.8. <i>Determination of anthocyanin content in acidified ethanol extracts using HPLC–DAD–MS</i> 38	38

2.1.9.	Statistical Analysis	38
2.2.	IN-VITRO COLON MODEL FERMENTATION.....	40
2.2.1.	Donor recruitment for in-vitro colonic fermentation experiments	40
2.2.2.	Preparation of fresh faecal slurries.....	41
2.2.3.	Preparation of glycerol-frozen faecal stock with a final faecal concentration of 37.6 %.....	41
2.2.4.	Setting up the in-vitro batch colon model	42
2.2.5.	Incubating anthocyanins with the faecal microbiota using in-vitro colon model fermentation	42
2.2.6.	Preparation of colon model samples for chromatography and mass spectrometry analysis	45
2.2.7.	Determination of anthocyanins in colon model samples using HPLC–DAD.....	45
2.2.8.	Determination of anthocyanin metabolites in the colon model sample using UPLC–MS/MS	45
2.2.9.	Observing the appearance of anthocyanin metabolites in the colon model samples using UPLC-TOF Analysis	46
2.2.10.	Statistical Analysis	46
2.3.	SPONTANEOUS DEGRADATION OF ANTHOCYANINS	47
2.3.1.	Incubating Cya3Glc in colon media and phosphate buffer solution	47
2.3.2.	Incubating anthocyanidins (Cya and Del) aerobically in phosphate buffer solution ..	48
2.3.3.	Quantify Cya3Glc, Cya, and Del concentrations and their break down products using HPLC-DAD-MS ..	48
2.3.4.	Monitoring the formation of the break down products of Cya3Glc, Cya, and Del using UPLC-TOF method.....	48
2.3.5.	Statistical Analysis	49
2.4.	CHANGES OF THE GUT MICROBIOTA STRUCTURE AND FUNCTION	50
2.4.1.	Study design for incubating anthocyanins with faecal gut microbiota using in-vitro colon model ..	50
2.4.2.	Extraction of DNA from colon model samples	50
2.4.3.	Shotgun metagenomics sequencing for extracted DNA from colon model samples ..	52
2.4.4.	Read processing for metagenomics sequencing data	52
2.4.5.	Microbial Community Profiling for metagenomics sequencing data	52
2.4.6.	Metabolic reconstruction and pathway analysis using HUMAnN3 for metagenomics sequencing data.....	53
2.4.7.	Statistical associations with MaAsLin2 for metagenomics sequencing data	54
CHAPTER 3: PREPARING ANTHOCYANIN-RICH EXTRACTS FROM BLACK RICE AND BILBERRY USING GREEN EXTRACTION PROCESSES.....		55
3.1.	ABSTRACT.....	55
3.2.	INTRODUCTION.....	56
3.3.	OBJECTIVES.....	57
3.4.	RESULTS.....	58
3.4.1.	Identification of anthocyanin composition of black rice and bilberry powders	58
3.4.2.	Effects of the glycerol to water ratio on the amounts of anthocyanins extracted from black rice and bilberry	63
3.4.3.	Determining the most effective liquid-to-solid ratios ($R_{L/S}$) for anthocyanin extraction using 80% w/v glycerol /water medium from black rice and bilberry	67
3.4.4.	The effect of temperature on anthocyanin extraction from black rice and bilberry over time ..	71
3.5.	DISCUSSION	76
3.6.	CONCLUSIONS	78
CHAPTER 4: THE METABOLISM OF ANTHOCYANINS BY THE HUMAN GUT MICROBIOTA		80
4.1.	ABSTRACT.....	80
4.2.	INTRODUCTION.....	82
4.3.	OBJECTIVES.....	84

4.4.	RESULTS.....	84
4.4.1.	<i>Chemical characterisation of the black rice and bilberry extract powders</i>	84
4.4.2.	<i>The disappearance of Cya3Glc during incubation of a black rice anthocyanin extract in the human in-vitro colon model</i>	97
4.4.3.	<i>The contribution of the faecal microbiota to the disappearance of Cya3Glc during in-vitro colon fermentation</i>	102
4.4.4.	<i>The disappearance of Cya3Glc in a simple anaerobic cabinet stirred vessel human colon model that is not pH controlled</i>	105
4.4.5.	<i>The intra-individual variations in the disappearance of Cya3Glc incubated in the in-vitro colon model fermentations</i>	107
4.4.6.	<i>The inter-individual variations in the disappearance of black rice Cya3Glc incubated in the in-vitro colon model fermentations.</i>	110
4.4.7.	<i>Assessment of the feasibility and viability of micro-organisms when using glycerol-frozen faecal stocks for investigating the disappearance of Cya3Glc during colonic fermentation.</i>	112
4.4.8.	<i>Disappearance of a mixture of fifteen bilberry anthocyanins during the human in-vitro colonic fermentation</i>	115
4.4.9.	<i>The effect of anthocyanidin B-ring and the conjugated sugars on the disappearance of anthocyanins during colonic fermentation</i>	119
4.5.	DISCUSSION	127
4.6.	CONCLUSIONS.....	132
CHAPTER 5: THE SPONTANEOUS DEGRADATION OF ANTHOCYANINS AND ANTHOCYANIDINS		134
5.1.	ABSTRACT	134
5.2.	INTRODUCTION	135
5.3.	OBJECTIVES	137
5.4.	RESULTS.....	137
5.4.1.	<i>The identification of Cya3Glc, Cya, Del, and their breakdown products on HPLC-DAD-MS</i> 137	
5.4.2.	<i>The spontaneous degradation of Cya3Glc in colon model media: Anaerobic conditions</i> 141	
5.4.3.	<i>The spontaneous degradation of Cya3Glc in phosphate buffered solution: Anaerobic conditions</i> 143	
5.4.4.	<i>The spontaneous degradation of Cya3Glc in colon media and phosphate buffer: Aerobic conditions</i> 146	
5.4.5.	<i>Investigating the breakdown products of the spontaneous degradation of Cya3Glc during anaerobic incubation</i>	150
5.4.6.	<i>Investigating the breakdown products of the spontaneous degradation of Cya3Glc during the aerobic incubation</i>	155
5.4.7.	<i>The effects of matrix, initial concentration, and buffer capacity on the aerobic spontaneous degradation of anthocyanidins: Cya</i>	162
5.4.8.	<i>The spontaneous degradation of anthocyanidins: Cya and Del</i>	169
5.4.9.	<i>Identification of breakdown products of the spontaneous degradation of Cya and Del</i> 171	
5.5.	DISCUSSION	176
5.6.	CONCLUSIONS.....	188
CHAPTER 6: ELUCIDATING METABOLIC PATHWAYS OF COLONIC DEGRADATION OF ANTHOCYANINS		189
6.1.	ABSTRACT	189
6.2.	INTRODUCTION	190
6.3.	OBJECTIVES	192
6.4.	RESULTS.....	192
6.4.1.	<i>The identification of anthocyanin metabolites</i>	192
6.4.2.	<i>The formation of anthocyanin metabolites during incubations of black rice anthocyanin extract in the human in-vitro colon model fermentations</i>	198

6.4.4.	<i>The formation of anthocyanin metabolites during the in-vitro colonic fermentation of pure anthocyanins</i>	205
6.4.5.	<i>The step-by-step metabolic pathway of anthocyanin metabolites</i>	210
6.4.6.	<i>The intra-individual variations in the formation of the black rice anthocyanin metabolites during the human in-vitro colon model fermentations</i>	214
6.4.7.	<i>The inter-individual variations in the formation of the black rice anthocyanin metabolites during the human in-vitro colon model fermentations</i>	217
6.4.8.	<i>The formation of black rice anthocyanin metabolites when using glycerol-frozen faecal stocks to inoculate the human in-vitro colon model fermentations</i>	220
6.4.9.	<i>The formation of anthocyanin metabolites during the fermentation of a mixture of fifteen bilberry anthocyanins in an in-vitro colon model</i>	223
6.5.	DISCUSSION	225
6.6.	CONCLUSIONS	236
CHAPTER 7: THE IMPACT OF ANTHOCYANINS ON THE STRUCTURE AND FUNCTION OF THE HUMAN COLONIC MICROBIOME		238
7.1.	ABSTRACT	238
7.2.	INTRODUCTION	239
7.3.	OBJECTIVES.....	240
7.4.	RESULTS	241
7.4.1.	<i>Bacterial growth during the in-vitro colon model fermentations</i>	242
7.4.2.	<i>Microbial community profiling</i>	244
7.4.3.	<i>Microbial composition: Taxonomic profiling</i>	248
7.4.4.	<i>Functional analysis: Pathways</i>	257
7.4.5.	<i>Functional analysis: Enzyme commission categories</i>	260
7.5.	DISCUSSION	265
7.6.	CONCLUSIONS	268
CHAPTER 8: GENERAL DISCUSSION		270
8.1.	SUMMARY OF MAIN FINDINGS	270
8.2.	DISCUSSION POINTS	271
8.2.1.	<i>In-vitro studies of anthocyanin degradation under aerobic conditions cannot be used to determine degradation in anaerobic environments such as the colon</i>	271
8.2.2.	<i>In-vitro studies of anthocyanin metabolism need to use appropriate models</i>	272
8.2.3.	<i>Is PCA an important metabolite of anthocyanin degradation in humans?</i>	273
8.2.4.	<i>Which anthocyanin metabolites should be studied for their possible biological activity with relevance to human health?</i>	275
8.2.5.	<i>Biomarkers of microbiota-dependent degradation of anthocyanins</i>	276
8.2.6.	<i>Current limitations in microbial gene annotation are preventing the identification of the microbial genes responsible for observed metabolic steps (Redundancy issues).</i>	277
8.2.7.	<i>Impact of polyphenols on the structure and function of the human gut microbiota</i>	278
8.3.	STRENGTHS AND LIMITATIONS OF THE RESEARCH	279
8.4.	RECOMMENDATIONS FOR FUTURE WORK	280
REFERENCES		283
APPENDIX 1		319
APPENDIX 2		321
APPENDIX 3		322
APPENDIX 4		325
APPENDIX 5		328
APPENDIX 6		329
APPENDIX 7		348

APPENDIX 8.....	355
APPENDIX 9.....	363
APPENDIX 10.....	378

List of Figures

FIGURE 1. 1. CHEMICAL STRUCTURE OF A PHENOL (HYDROXYBENZENE).	2
FIGURE 1. 2. GENERAL CLASSIFICATION OF DIETARY (POLY)PHENOLS.	3
FIGURE 1. 3. CHEMICAL STRUCTURE OF NON-FLAVONOID (POLY)PHENOLS.	4
FIGURE 1. 4. CHEMICAL STRUCTURE OF FLAVONOID (POLY)PHENOLS.	6
FIGURE 1. 5. BASIC STRUCTURE AND NUMBERING SYSTEM OF ANTHOCYANIDINS (ANTHOCYANIN AGLYCONES).	9
FIGURE 1. 6. THE SPONTANEOUS DEGRADATION OF ANTHOCYANINS AND FORMATION OF A-RING AND B-RING BREAKDOWN PRODUCTS.	15
FIGURE 1. 7. TAXONOMICAL CLASSIFICATION OF GUT MICROBIOTA COMPOSITIONS.	22
FIGURE 1. 8. BIDIRECTIONAL RELATIONSHIP BETWEEN ANTHOCYANINS AND THE HUMAN GUT MICROBIOTA.	26
FIGURE 2. 1. RAW PLANT MATERIALS OF BLACK RICE AND BILBERRY.	34
FIGURE 2. 2. BOROSILICATE STOPPERED GLASS BOTTLES CONTAINING GLYCEROL/WATER SOLVENTS AND ANTHOCYANIN-RICH POWDERS.	35
FIGURE 2. 3. OIL BATH USED FOR THE EXTRACTION OF ANTHOCYANIN-RICH POWDERS AT VARIOUS TEMPERATURES.	36
FIGURE 2. 4. SCHEMATIC OF THE COLON MODEL VESSEL.	43
FIGURE 2. 5. SCHEMATIC OF THE HUMAN IN-VITRO COLON MODEL.	44
FIGURE 3. 1. DAD CHROMATOGRAM AT 520 NM SHOWING ANTHOCYANINS IDENTIFIED IN BLACK RICE POWDER.	61
FIGURE 3. 2. DAD CHROMATOGRAM AT 520 NM SHOWING ANTHOCYANINS IDENTIFIED IN BILBERRY POWDER.	62
FIGURE 3. 3. BAR PLOT SHOWING QUANTIFICATION ASSAYS AND RECOVERIES FROM BLACK RICE POWDER ACHIEVED BY VARIOUS GLYCEROL/WATER MEDIUMS RANGING BETWEEN 10- 90%.	65
FIGURE 3. 4. BAR PLOT SHOWING QUANTIFICATION ASSAYS AND RECOVERIES FROM BILBERRY POWDER ACHIEVED BY VARIOUS GLYCEROL/WATER MEDIUMS RANGING BETWEEN 10- 90%.	66
FIGURE 3. 5. BAR PLOT SHOWING VARIOUS QUANTIFICATION ASSAYS AND RECOVERIES ACHIEVED BY USING A MEDIUM OF 80% W/V GLYCEROL WITH DIFFERENT RATIOS OF LIQUID-TO-SOLID ($R_{L/S}$) FROM BLACK RICE POWDER.	69
FIGURE 3. 6. BAR PLOT SHOWING VARIOUS QUANTIFICATION ASSAYS AND RECOVERIES ACHIEVED BY USING A MEDIUM OF 80% W/V GLYCEROL WITH DIFFERENT RATIOS OF LIQUID-TO-SOLID ($R_{L/S}$) FROM BILBERRY POWDER.	70
FIGURE 3. 7. DIFFERENT ASSAYS SHOWING RECOVERIES FROM BLACK RICE POWDER OVER 180 MIN AT VARIOUS TEMPERATURES (50, 60, 70, AND 80°C) USING 80% W/V GLYCEROL AND $R_{L/S} = 60 \text{ mL G}^{-1}$	74
FIGURE 3. 8. DIFFERENT ASSAYS SHOWING RECOVERIES FROM BILBERRY POWDER OVER 180 MIN AT VARIOUS TEMPERATURES (50, 60, 70, AND 80°C) USING 80% W/V GLYCEROL AND $R_{L/S} = 60 \text{ mL G}^{-1}$	75
FIGURE 4. 1. MS AND DAD CHROMATOGRAMS OF ANTHOCYANINS IN BLACK RICE EXTRACT POWDER.	86
FIGURE 4. 2. SIGNALS CORRESPONDING TO $m/z [M+H]^+$ OF ANTHOCYANINS IN BLACK RICE EXTRACT.	88
FIGURE 4. 3. EXTERNAL STANDARD CURVE FOR CYANIDIN-3-O-GLUCOSIDE (CYA3GLC).	89
FIGURE 4. 4. STANDARD ADDITION FOR CYANIDIN-3-O-GLUCOSIDE (CYA3GLC).	90
FIGURE 4. 5. HPLC-DAD CHROMATOGRAM OF BLACK RICE ANTHOCYANINS AT 520 NM.	92
FIGURE 4. 6. TOF MS SPECTRUM FOR THE IDENTIFIED BILBERRY ANTHOCYANINS.	94
FIGURE 4. 7. HPLC-DAD CHROMATOGRAM OF BILBERRY ANTHOCYANINS AT 520 NM.	96
FIGURE 4. 8. SCHEMATIC OF EXPERIMENTAL DESIGN FOR INVESTIGATING THE METABOLISM OF BLACK RICE ANTHOCYANINS (CYA3GLC) BY THE HUMAN FAECAL MICROBIOTA USING IN-VITRO HUMAN COLON MODEL.	98
FIGURE 4. 9. LOSS OF CYA3GLC DURING BATCH IN VITRO COLON MODEL FERMENTATIONS OF A BLACK RICE EXTRACT (C_{THEO} OF CYA3GLC = 66.8 μM).	99
FIGURE 4. 10. LOSS OF CYA3GLC DURING BATCH IN VITRO COLON MODEL FERMENTATIONS OF A BLACK RICE EXTRACT (C_{THEO} OF CYA3GLC = 133.6 μM).	101
FIGURE 4. 11. SCHEMATIC OF EXPERIMENTAL DESIGN FOR INVESTIGATING THE DIFFERENCE BETWEEN THE SPONTANEOUS AND THE GUT MICROBIOTA-DEPENDENT DEGRADATIONS OF BLACK RICE ANTHOCYANINS (CYA3GLC) USING <i>IN-VITRO</i> HUMAN COLON MODEL.	103
FIGURE 4. 12. LOSS OF BLACK RICE ANTHOCYANINS (C_{THEO} OF CYA3GLC = 133.6 μM) OVER TIME WAS PARTLY SPONTANEOUS AND PARTLY DUE THE TO GUT MICROBIOTA.	104
FIGURE 4. 13. LOSS OF BLACK RICE ANTHOCYANIN (C_{THEO} OF CYA3GLC = 133.60 μM) USING UNCONTROLLED PH MODEL.	106

FIGURE 4. 14. INTRA-INDIVIDUAL VARIATIONS IN THE LOSS OF BLACK RICE ANTHOCYANINS (C_{THEO} OF CYA3GLC 133.6 μM) OVER 24 H.	109
FIGURE 4. 15. INTER-INDIVIDUAL VARIATIONS IN THE LOSS OF BLACK RICE ANTHOCYANINS (C_{THEO} OF CYA3GLC 133.6 μM) OVER 24 H INCUBATED WITH FRESH FAECAL MICROBIOTA.	111
FIGURE 4. 16. LOSS OF BLACK RICE ANTHOCYANINS (C_{THEO} OF CYA3GLC 133.6 μM) OVER 24 H FERMENTATIONS USING GLYCEROL-FROZEN FAECAL STOCK.	113
FIGURE 4. 17. SCHEMATIC OF EXPERIMENTAL DESIGN FOR THE METABOLISM OF BILBERRY ANTHOCYANINS BY THE HUMAN FAECAL MICROBIOTA USING IN-VITRO HUMAN COLON MODEL FERMENTATION.	117
FIGURE 4. 18. LOSS OF BILBERRY ANTHOCYANINS (C_{THEO} OF TOTAL ANTHOCYANINS = 265 μM) OVER 24 H.....	118
FIGURE 4. 19. LOSS OF INDIVIDUAL BILBERRY ANTHOCYANINS OVER THE FIRST 8 H IN THE PRESENCE OF LIVE FAECAL MICROBIOTA.....	120
FIGURE 4. 20. EFFECT OF B-RING ON THE LOSS OF BILBERRY ANTHOCYANINS WHICH ARE ATTACHED TO THE SAME SUGAR MOIETY (GALACTOSE (GAL), GLUCOSE (GLC) OR ARABINOSE (ARA)) OVER THE FIRST 8 H IN THE PRESENCE OF LIVE FAECAL MICROBIOTA.	121
FIGURE 4. 21. EFFECTS OF DIFFERENT SUGAR SUBSTITUTIONS (GALACTOSE (GAL), GLUCOSE (GLC) OR ARABINOSE (ARA)) ON THE LOSS OF INDIVIDUAL BILBERRY ANTHOCYANINS OVER THE FIRST 8 H IN THE PRESENCE OF LIVE FAECAL MICROBIOTA.	122
FIGURE 4. 22. LOSS OF INDIVIDUAL BILBERRY ANTHOCYANINS OVER THE FIRST 8 H IN THE PRESENCE OF AUTOCLAVED FAECAL MICROBIOTA.....	123
FIGURE 4. 23. LOSS OF INDIVIDUAL BILBERRY ANTHOCYANINS OVER THE FIRST 8 H IN THE PRESENCE OF AUTOCLAVED FAECAL MICROBIOTA.....	124
FIGURE 4. 24. EFFECTS OF DIFFERENT SUGAR SUBSTITUTIONS (GALACTOSE (GAL), GLUCOSE (GLC) OR ARABINOSE (ARA)) ON THE LOSS OF INDIVIDUAL BILBERRY ANTHOCYANINS OVER THE FIRST 8 H IN THE ABSENCE OF AUTOCLAVED FAECAL MICROBIOTA.....	125
FIGURE 4. 25. LOSS OF INDIVIDUAL BILBERRY ANTHOCYANINS OVER THE FIRST 8 H ONLY INCUBATED WITH STERILE COLON MEDIA.....	126
FIGURE 5. 1. DAD CHROMATOGRAM λ (280 NM) OF A MIXTURE OF 30 PHENOLIC COMPOUNDS DISSOLVED IN A 10 MM PHOSPHATE BUFFER (PH 6.8).	140
FIGURE 5. 2. THE ANAEROBIC SPONTANEOUS DEGRADATION OF CYA3GLC ($C_{\text{THEO}} = 170 \mu\text{M}$) UNDER THE PHYSIOLOGICAL CONDITION OF THE COLON (NEUTRAL PH; 37°C) IN COLON MEDIA.	142
FIGURE 5. 3. THE ANAEROBIC SPONTANEOUS DEGRADATION OF CYA3GLC ($C_{\text{THEO}} = 170 \mu\text{M}$) UNDER THE PHYSIOLOGICAL CONDITION OF THE COLON (NEUTRAL PH; 37°C) IN PHOSPHATE BUFFERED SOLUTION.	144
FIGURE 5. 4. COMPARISON OF THE ANAEROBIC SPONTANEOUS DEGRADATION OF CYA3GLC IN COLON MODEL MEDIA AND PHOSPHATE BUFFER.	145
FIGURE 5. 5. THE AEROBIC SPONTANEOUS DEGRADATION OF CYA3GLC ($C_{\text{THEO}} = 170 \mu\text{M}$) AT PHYSIOLOGICAL CONDITION (NEUTRAL PH; 37°C) IN COLON MEDIA AND PHOSPHATE BUFFER.	147
FIGURE 5. 6. COMPARISON BETWEEN AEROBIC AND ANAEROBIC SPONTANEOUS DEGRADATION OF CYA3GLC IN COLON MODEL MEDIA AND PHOSPHATE BUFFER.	148
FIGURE 5. 7. THE FORMATION OF THE BREAKDOWN MASSES (PRODUCTS) DURING THE ANAEROBIC SPONTANEOUS DEGRADATION OF CYA3GLC ($C_{\text{THEO}} = 150 \mu\text{M}$) AT PHYSIOLOGICAL CONDITION (NEUTRAL PH; 37°C) IN COLON MEDIA AND PHOSPHATE BUFFER.....	152
FIGURE 5. 8. THE MASS SPECTRA OF THE PEAKS CORRESPONDING TO CYA3GLC AND ITS ANAEROBIC SPONTANEOUS BREAKDOWN PRODUCTS IN PHOSPHATE BUFFER ON LC-MS IN NEGATIVE FULL SCAN MODE, WHERE X AXIS IS $m/z[M-H]^-$ AND Y AXIS IS THE RELATIVE ABUNDANCE (100%).	154
FIGURE 5. 9. SPONTANEOUS AEROBIC DEGRADATION OF CYA3GLC (170 μM) AT NEUTRAL PH; 37°C AND THE FORMATION OF BREAKDOWN PRODUCTS OVER 24 H INCUBATION.....	157
FIGURE 5. 10. THE MASS SPECTRA OF PEAKS CORRESPONDING TO BREAKDOWN PRODUCTS FROM THE AEROBIC SPONTANEOUS DEGRADATION OF CYA3GLC IN PHOSPHATE BUFFER ON LC-MS IN NEGATIVE FULL SCAN MODE, WHERE X AXIS IS m/z AND Y AXIS IS RELATIVE ABUNDANCE (100%).	159
FIGURE 5. 11. DAD CHROMATOGRAM λ (280 NM) OF THE AEROBIC INCUBATION OF CYA3GLC AT 0, 12 AND 24 H IN A 10 MM PHOSPHATE BUFFER (PH 7.4) AT 37°C SHOWING THE DECOMPOSITION OF CYA3GLC WITH THE FORMATION OF NEW BREAKDOWN PRODUCTS.	160
FIGURE 5. 12. PICTURE OF INCUBATED CYA (1000 $\mu\text{g mL}^{-1}$) IN TWO DIFFERENT MATRICES AFTER 24 H INCUBATION AT 37°C.	163

FIGURE 5. 13. THE MASS SPECTRA (TIC) OF PEAKS WHICH APPEARED FROM THE INJECTION OF THE RESUSPENDED PRECIPITATE WHICH FORMED AFTER DISSOLVING CYA ($1000 \mu\text{G mL}^{-1}$) IN PHOSPHATE BUFFERED SOLUTION.164

FIGURE 5. 14. PICTURES OF INCUBATED AUTHENTIC CYA (WITH DIFFERENT CONCENTRATIONS AND WITH DIFFERENT % OF DMSO) IN PHOSPHATE BUFFERED SOLUTION (100 mM) AT 24 h165

FIGURE 5. 15. THE SPONTANEOUS DEGRADATION OF CYA ($150 \mu\text{M}$, WITH 1.5% DMSO) IN DIFFERENT MEDIA WITH DIFFERENT BUFFER CAPACITIES AT 0 AND 20 h167

FIGURE 5. 16. THE SPONTANEOUS DEGRADATION OF CYA ($222 \mu\text{M}$, WITH 3% DMSO) IN TWO PHOSPHATE BUFFERED SOLUTIONS WITH DIFFERENT PH (6.8 AND 7.4) OVER 12 h AT 37°C168

FIGURE 5. 17. THE SPONTANEOUS DEGRADATION OF CYA WITH C_{INITIAL} OF $100 \mu\text{G mL}^{-1}$ ($222 \mu\text{M}$) (A) AND DEL WITH C_{INITIAL} OF $100 \mu\text{G mL}^{-1}$ ($330 \mu\text{M}$) (B) AT PHYSIOLOGICAL CONDITION (NEUTRAL PH; 37°C) IN PHOSPHATE BUFFERED SOLUTION.170

FIGURE 5. 18. DAD CHROMATOGRAM $\lambda_{(280 \text{ nm})}$ OF THE INCUBATION OF $100 \mu\text{G mL}^{-1}$ ($222 \mu\text{M}$) CYA AT 0 , 6 AND 12 h INCUBATION IN A 100 mM PHOSPHATE BUFFER (PH 6.8) AT 37°C SHOWING THE DECOMPOSITION OF CYA WITH THE FORMATION OF NEW BREAKDOWN PRODUCTS.172

FIGURE 5. 19. DAD CHROMATOGRAM $\lambda_{(280 \text{ nm})}$ OF THE AEROBIC INCUBATION OF DEL AT 0 , 6 AND 12 h INCUBATION IN A 100 mM PHOSPHATE BUFFER (PH 6.8) AT 37°C SHOWING THE DECOMPOSITION OF DEL WITH THE FORMATION OF NEW BREAKDOWN PRODUCTS.174

FIGURE 5. 20. POSTULATED MECHANISM OF THE ANAEROBIC SPONTANEOUS DEGRADATION OF CYANIDIN-3-O-GLUCOSIDE (CYA3GLC).178

FIGURE 5. 21. POSTULATED MECHANISM OF THE AEROBIC SPONTANEOUS DEGRADATION OF CYANIDIN-3-GLUCOSIDE (CYA3GLC) DURING THE INCUBATION IN 10 mM PHOSPHATE BUFFER (6.8 AND 7.4 pH) AT 37°C180

FIGURE 5. 22. POSTULATED MECHANISM OF THE AEROBIC SPONTANEOUS DEGRADATION OF $100 \mu\text{G mL}^{-1}$ CYANIDIN (CYA) INCUBATED IN 10 mM PHOSPHATE BUFFER (6.8 pH) AT 37°C184

FIGURE 5. 23. POSTULATED MECHANISM OF THE AEROBIC SPONTANEOUS DEGRADATION OF $100 \mu\text{G mL}^{-1}$ DELPHINIDIN (DEL) INCUBATED IN 10 mM PHOSPHATE BUFFER (6.8 pH) AT 37°C185

FIGURE 6. 1. THE CHEMICAL STRUCTURES OF DIHYDROXYPHENYLACETIC ACID ISOMERS.196

FIGURE 6. 2. MS/MS CHROMATOGRAMS OF THE ION CURRENTS FOR 3,4-DIHYDROXYPHENYLACETIC ACID (DHPAA).197

FIGURE 6. 3. THE FORMATION OF ANTHOCYANIN METABOLITES DURING BATCH COLON MODEL FERMENTATION OVER 24 h BY USING A LOW CONCENTRATION OF BLACK RICE ANTHOCYANIN ($66.8 \mu\text{M}$ CYA3GLC).201

FIGURE 6. 4. THE FORMATION OF ANTHOCYANIN METABOLITES DURING BATCH COLON MODEL FERMENTATION OVER 24 h BY USING A LOW CONCENTRATION OF BLACK RICE ANTHOCYANIN ($66.8 \mu\text{M}$ CYA3GLC).202

FIGURE 6. 5. THE FORMATION OF ANTHOCYANIN METABOLITES DURING BATCH COLON MODEL FERMENTATION OVER 24 h BY USING A HIGH CONCENTRATION OF BLACK RICE ANTHOCYANIN ($133.6 \mu\text{M}$ CYA3GLC).203

FIGURE 6. 6. THE FORMATION OF ANTHOCYANIN METABOLITES DURING BATCH COLON MODEL FERMENTATION OVER 24 h BY USING A HIGH CONCENTRATION OF BLACK RICE ANTHOCYANIN ($133.6 \mu\text{M}$ CYA3GLC).204

FIGURE 6. 7. THE FORMATION OF CYA3GLC METABOLITES DURING BATCH COLON MODEL FERMENTATION OVER 24 h208

FIGURE 6. 8. THE FORMATION OF PEO3GLC METABOLITES DURING BATCH COLON MODEL FERMENTATION OVER 24 h209

FIGURE 6. 9. INCUBATIONS OF PCA IN THE IN-VITRO COLON MODEL OVER 24 h211

FIGURE 6. 10. INCUBATIONS OF PGA IN THE IN-VITRO COLON MODEL OVER 24 h212

FIGURE 6. 11. INCUBATIONS OF 3,4-DHPAA IN THE IN-VITRO COLON MODEL OVER 24 h213

FIGURE 6. 12. THE FORMATION OF BLACK RICE ANTHOCYANIN METABOLITES SHOWING THE INTRA-INDIVIDUAL VARIATIONS IN THE PRESENCE OF LIVE FAECAL MICROBIOTA.216

FIGURE 6. 13. THE FORMATION OF BLACK RICE ANTHOCYANIN METABOLITES SHOWING THE INTER-INDIVIDUAL VARIATIONS IN THE PRESENCE OF LIVE FAECAL MICROBIOTA.219

FIGURE 6. 14. THE FORMATION OF BLACK RICE ANTHOCYANIN METABOLITES IN THE PRESENCE OF LIVE FAECAL MICROBIOTA USING GLYCEROL-FROZEN FAECAL STOCKS.222

FIGURE 6. 15. THE FORMATION OF ANTHOCYANIN METABOLITES DURING BATCH COLON MODEL FERMENTATION OVER 24 h BY USING A CONCENTRATION OF BILBERRY ANTHOCYANIN ($50 \mu\text{G mL}^{-1}$).224

FIGURE 6. 16. PROPOSED PATHWAY OF COLONIC BIOTRANSFORMATION OF CYANIDIN-3-O-GLUCOSIDE (CYA3GLC) BY THE HUMAN GUT MICROBIOTA, WHERE THE SOLID ARROWS REPRESENT CONFIRMED ROUTES, THE DOTTED ARROWS REPRESENT PREDICTED ROUTES, AND MW IS AN ABBREVIATION FOR THE MOLECULAR WEIGHT.227

FIGURE 6. 17. PROPOSED PATHWAY OF THE COLONIC BIOTRANSFORMATION OF PEONIDIN-3-O-GLUCOSIDE (PEO3GLC), WHERE THE SOLID ARROWS REPRESENT CONFIRMED ROUTES, THE DOTTED ARROWS REPRESENT ANTICIPATED ROUTES, AND MW IS AN ABBREVIATION FOR THE MOLECULAR WEIGHT.228

FIGURE 6. 18. PROPOSED PATHWAY OF THE FORMATION OF GALLIC ACID AND PYROGALLOL FROM TANNINS, IN THE PRESENCE OF LIVE FAECAL MICROBIOTA	235
FIGURE 7. 1. SCHEMATIC OF EXPERIMENTAL DESIGN FOR INVESTIGATING THE EFFECTS OF BLACK RICE ANTHOCYANINS ON THE COMPOSITION OF THE HUMAN FAECAL MICROBIOTA USING AN IN-VITRO HUMAN COLON MODEL.	242
FIGURE 7. 2. THE BACTERIAL GROWTH CURVE DURING BATCH COLON MODEL FERMENTATION OVER 24 H.	243
FIGURE 7. 3. HIERARCHICAL CLUSTERING OF MICROBIAL PROFILES SHOWING SAMPLES ORDERED BY TIME POINT (COLUMNS) FOR THE TOP 50 SPECIES.	245
FIGURE 7. 4. MDS PLOT WHERE THE TIME POINT IS COLOUR-CODED, TRIANGLES REPRESENT CONTROL SAMPLES, AND CIRCLES REPRESENT SAMPLES FROM VESSELS TREATED WITH ANTHOCYANINS.	247
FIGURE 7. 5. COMPOSITION OF RELATIVE ABUNDANCES FOR THE 10 MOST ABUNDANT GENERA FOR EACH SAMPLE ACROSS TIME AT 0, 6, 12, AND 24 H.	249
FIGURE 7. 6. COMPOSITION IN RELATIVE ABUNDANCES OF THE TOP 10 MOST ABUNDANCE SPECIES IN THE ANTHOCYANIN-TREATED AND NON-ANTHOCYANIN-TREATED CONTROL SAMPLES FROM THE IN-VITRO COLON MODEL COLLECTED AT 0, 6, 12 AND 24 H INCUBATIONS.	250
FIGURE 7. 7. COMPOSITION IN RELATIVE ABUNDANCES OF THE TOP 10 MOST ABUNDANT SPECIES IN THE ANTHOCYANIN-TREATED AND NON-ANTHOCYANIN-TREATED CONTROL SAMPLES FROM THE IN-VITRO COLON MODEL AT 0, 6, AND 12 H TIME POINTS.	251
FIGURE 7. 8. MICROBIAL COMPOSITION AT THE PHYLUM LEVEL FOR SAMPLES TAKEN AT THE START OF THE EXPERIMENT (T0), CONTROL SAMPLES (CTRL) AND SAMPLES TREATED WITH ANTHOCYANINS (BR) AT 6H AND 12H.	253
FIGURE 7. 9. MICROBIAL COMPOSITION AT THE SPECIES LEVEL FOR SAMPLES TAKEN AT THE START OF THE EXPERIMENT (T0).	254
FIGURE 7. 10. MICROBIAL COMPOSITION AT THE SPECIES LEVEL FOR CONTROL SAMPLES (CTRL) AND TREATED ANTHOCYANINS (BR) AT 6 H (T6).	255
FIGURE 7. 11. MICROBIAL COMPOSITION AT THE SPECIES LEVEL FOR CONTROL SAMPLES (CTRL) AND TREATED ANTHOCYANINS (BR) AT 12 H (T12).	256
FIGURE 7. 12. THE EFFECT OF ANTHOCYANIN TREATMENT AND TIME ON ORTHO-CLEAVAGE PATHWAY OF CATECHOL DEGRADATION TO B-KETOADIPATE.	258
FIGURE 7. 13. THE EFFECT OF ANTHOCYANIN TREATMENT AND TIME ON ORTHO-CLEAVAGE PATHWAY OF 4-METHYLCATECHOL DEGRADATION.	259
FIGURE 7. 14. THE RELATIVE ABUNDANCES OF SPECIES LEVEL FOR THE EC GLUCAN 1,4-B-GLUCOSIDASE THAT PRESENTED DIFFERENT RELATIVE ABUNDANCES DUE TO ANTHOCYANIN TREATMENT AND TIME.	263
FIGURE 7. 15. THE RELATIVE ABUNDANCE FOR PATHWAY 1.13.11.1: CATECHOL 1,2-DIOXYGENASE, COMPARED THE RELATIVE ABUNDANCE FOR THE TWO KLEBSIELLA SPECIES IN THE PATHWAY: KLEBSIELLA OXYTOCA AND KLEBSIELLA MICHIGANENSIS.	264
FIGURE 8. 1. TIMES CITED AND PUBLICATIONS OVER TIME OF PROTOCATECHUIC ACID (PCA) AND ITS RELATIONSHIP TO HUMAN HEALTH.	275
APPENDIX FIGURE 1. 1. PRODUCT SPECIFICATIONS OF THE BLACK RICE EXTRACT USED IN THE IN-VITRO COLON MODEL STUDY.	319
APPENDIX FIGURE 1. 2. PRODUCT SPECIFICATIONS OF THE BILBERRY EXTRACT USED IN THE IN-VITRO COLON MODEL STUDY.	320
APPENDIX FIGURE 3. 1. SIGNALS CORRESPONDING TO THE $m/z[M+H]^+$ OF ANTHOCYANINS IN BLACK RICE EXTRACT.	322
APPENDIX FIGURE 3. 2. SIGNALS CORRESPONDING TO THE $m/z[M+H]^+$ OF ANTHOCYANINS IN BILBERRY EXTRACT.	324
APPENDIX FIGURE 4. 1. STANDARD CURVES IN DIFFERENT MATRICES SHOWING THE EFFECT OF FAECAL MATERIALS ON THE DETECTION OF CYA3GLC.	325
APPENDIX FIGURE 4. 2. STANDARD CURVES IN DIFFERENT MATRICES SHOWING THE EFFECT OF FAECAL MATERIALS ON THE DETECTION OF PCA.	325
APPENDIX FIGURE 4. 3. STANDARD CURVES IN DIFFERENT MATRICES SHOWING THE EFFECT OF FAECAL MATERIALS ON THE DETECTION OF PGA.	326
APPENDIX FIGURE 4. 4. STANDARD CURVES IN DIFFERENT MATRICES SHOWING THE EFFECT OF FAECAL MATERIALS ON THE DETECTION OF 3,4-DHPAA.	326

APPENDIX FIGURE 4. 5. STANDARD CURVES IN DIFFERENT MATRICES SHOWING THE EFFECT OF FAECAL MATERIALS ON THE DETECTION OF CATECHOL.....327

APPENDIX FIGURE 5. 1. DAD CHROMATOGRAM λ (280 NM) OF THE AEROBIC INCUBATION OF CYA3GLC AFTER 7 DAYS INCUBATION IN A 10 MM PHOSPHATE BUFFER (PH 7.4) AT 37°C SHOWING THE DECOMPOSITION OF CYA3GLC WITH THE FORMATION OF NEW BREAKDOWN PRODUCTS.....328

APPENDIX TABLE 7. 1. THE FOLLOWING TABLE SHOW THE SUMMARY OF THE QUALITY CONTROL, TRIMMING AND DECONTAMINATION FOR THE RAW SEQUENCING DATA.....350

APPENDIX TABLE 7. 2. THE TABLE BELOW SHOWS THE SUMMARY STATISTICS FOR THIS SAMPLE COMPARED TO OTHER BLACK RICE (BR) SAMPLES.352

APPENDIX TABLE 7. 3. SUMMARY OF QUALITY CONTROL, ADAPTER TRIMMING AND DECONTAMINATION OF SEQUENCING DATA FOR ALL CONTROLS SAMPLES354

List of Tables

TABLE 1. 1. TOTAL ANTHOCYANINS CONTENT AND PREDOMINANT ANTHOCYANINS IN COMMON DIETARY SOURCES.	12
TABLE 1. 2. PHARMACOKINETICS OF ANTHOCYANINS FOLLOWING ORAL CONSUMPTION IN HUMAN SUBJECTS*	19
TABLE 2. 1. PREPARATION OF STANDARD CURVE FOR AUTHENTIC ANTHOCYANINS	38
TABLE 3. 1. THE CONTENT OF ANTHOCYANINS IN BLACK RICE POWDER	59
TABLE 3. 2. THE CONTENT OF ANTHOCYANINS IN BILBERRY POWDER	60
TABLE 3. 3. CALCULATED LIQUID-TO-SOLID RATIO ($R_{L/S}$) BASED ON DIFFERENT SAMPLE WEIGHTS (G) IN THE 50 ML SOLVENT.	67
TABLE 4. 1. PREPARATION OF STANDARD ADDITION FOR CYA3GLC	90
TABLE 4. 2. THE CONTENT OF ANTHOCYANINS IDENTIFIED IN BLACK RICE EXTRACT POWDER*	91
TABLE 4. 3. IDENTIFIED ANTHOCYANINS AND THEIR CONTENTS IN BILBERRY EXTRACT POWDER	95
TABLE 5. 1. HPLC-DAD-MS IDENTIFICATION OF CYA3GLC, CYA, AND DEL.	138
TABLE 5. 2. HPLC-DAD-MS IDENTIFICATION OF POTENTIAL BREAKDOWN COMPOUNDS DURING THE SPONTANEOUS DEGRADATION OF CYA3GLC, CYA, AND DEL.....	139
TABLE 5. 3. COMPARISON OF THE SPONTANEOUS DEGRADATION OF CYA3GLC IN DIFFERENT CONDITIONS#	149
TABLE 5. 4. IDENTIFICATION OF CYA3GLC AND ITS PUTATIVE SPONTANEOUS BREAKDOWN PRODUCTS DURING AEROBIC AND ANAEROBIC CONDITIONS	161
TABLE 5. 5. IDENTIFICATION OF CYA AND ITS PUTATIVE SPONTANEOUS BREAKDOWN PRODUCTS DURING AEROBIC INCUBATION IN PHOSPHATE BUFFER PH 6.8 AT 37°C.	173
TABLE 5. 6. IDENTIFICATION OF DEL AND ITS PUTATIVE SPONTANEOUS BREAKDOWN PRODUCTS DURING AEROBIC INCUBATION IN PHOSPHATE BUFFER PH 6.8 AT 37°C	175
TABLE 5. 7. COMPARISON BETWEEN THE FORMED BREAKDOWN PRODUCTS FROM THE DEGRADATION OF INCUBATED ANTHOCYANINS AND ANTHOCYANIDINS IN NEUTRAL PH AT 37°C.	186
TABLE 6. 1. UPLC-MS/MS IDENTIFICATION (MRM) OF POTENTIAL ANTHOCYANIN METABOLITES DURING THE ANAEROBIC IN VITRO HUMAN COLON MODEL FERMENTATION.	194
TABLE 7. 1. THE 20 EC CATEGORIES THAT SHOW THE MOST SIGNIFICANT CHANGES BY BR ANTHOCYANIN TREATMENT AT 6H.	261
TABLE 7. 2. THE 20 EC CATEGORIES THAT SHOW THE MOST SIGNIFICANT CHANGES FOR TREATED SAMPLES WITH BR ANTHOCYANINS AT 12H.	262
TABLE 8. 1. COMPARISON BETWEEN DIFFERENT HUMAN STUDIES ON THE PROTOCATECHUIC ACID (PCA) RECOVERIES.....	274
APPENDIX TABLE 2. 1. THE MOLAR EXTINCTION COEFFICIENT ($\epsilon_{520\text{NM}}$) OF SIX COMMON ANTHOCYANINS.....	321
APPENDIX TABLE 4. 1. THE EFFECT OF IN-VITRO COLON MODEL FERMENTATION ON THE SIGNAL RESPONSES OF DIFFERENT PHENOLIC METABOLITES.....	327
APPENDIX TABLE 7. 1. THE FOLLOWING TABLE SHOW THE SUMMARY OF THE QUALITY CONTROL, TRIMMING AND DECONTAMINATION FOR THE RAW SEQUENCING DATA.	350
APPENDIX TABLE 7. 2. THE TABLE BELOW SHOWS THE SUMMARY STATISTICS FOR THIS SAMPLE COMPARED TO OTHER BLACK RICE (BR) SAMPLES.	352
APPENDIX TABLE 7. 3. SUMMARY OF QUALITY CONTROL, ADAPTER TRIMMING AND DECONTAMINATION OF SEQUENCING DATA FOR ALL CONTROLS SAMPLES.....	354

Abbreviations

Ara	Arabinose
CE	Collusion energy
Cya	Cyanidin
Cya3Ara	Cyanidin-3- <i>O</i> -arabinoside
Cya3Glc	Cyanidin-3- <i>O</i> -glucoside
Cya3Rut	Cyanidin-3- <i>O</i> -rutinoside
Cya3,5Glc	Cyanidin-3,5- <i>O</i> -diglucoside
C_{\max}	Maximum concentration
C_{theo}	Theoretical concentration
C_{initial}	Initial quantified concentration
C_{end}	End concentration
Del	Delphinidin
Del3Ara	Delphinidin-3- <i>O</i> -arabinoside
Del3Glc	Delphinidin-3- <i>O</i> -glucoside
Del3Rut	Delphinidin-3- <i>O</i> -rutinoside
DAD	Diode array detection
DHPAA	Dihydroxyphenylacetic acid
DMSO	Dimethyl sulfoxide
DNA	Deoxyribonucleic acid
FA	Formic acid
FW	Fresh weight
GI	Gastrointestinal
Gal	Galactose
Glc	Glucose
HCl	Hydrochloric acid
HPLC	High performance liquid chromatography
ISTD	Internal standard
k_{deg}	Degradation rate
m/z	Mass-to-charge ratio
Mal	Malvidin
Mal3Ara	Malvidin-3- <i>O</i> -arabinoside
Mal3Glc	Malvidin-3- <i>O</i> -glucoside
Mal3Rut	Malvidin-3- <i>O</i> -rutinoside
MRM	Multiple reaction monitoring
NaOH	Sodium hydroxide
OH	Hydroxyl group
OCH ₃	Methoxy group
PCA	Protocatechuic acid
Pel	Pelargonidin
Pel3Ara	Pelargonidin-3- <i>O</i> -arabinoside
Pel3Glc	Pelargonidin-3- <i>O</i> -glucoside
Pel3Rut	Pelargonidin-3- <i>O</i> -rutinoside
Peo	Peonidin
Peo3Ara	Peonidin-3- <i>O</i> -arabinoside
Peo3Glc	Peonidin-3- <i>O</i> -glucoside
Peo3Rut	Peonidin-3- <i>O</i> -rutinoside
Pet	Petunidin

Pet3Ara	Petunidin-3- <i>O</i> -arabinoside
Pet3Glc	Petunidin-3- <i>O</i> -glucoside
Pet3Rut	Petunidin-3- <i>O</i> -rutinoside
PGA	Phloroglucinaldehyde
PGCA	Phloroglucinol carboxylic acid
QIB	Quadram Institute Bioscience
Rha	Rhamnose
RNA	Ribonucleic acid
RT	Retention time
Rut	Rutinose
SD	Standard deviation
SPE	Solid phase extraction
SS	Stock solution
TIC	Total ion current
$t_{1/2}$	Half-life of elimination
t_{max}	Time of maximum concentration
TOF-MS	Time-of-flight mass spectrometry
UHPLC	Ultra-high performance liquid chromatography
UHPLC-MS/MS	Ultra-high performance liquid chromatography – with tandem mass spectrometry
WS	Working solution

Symbols

%	Percent
°C	Degrees Celsius
CO ₂	Carbon dioxide
g	Gram
h	Hour
kg	Kilogram
kg/m ²	Kilogram per square meter
m/s	Pulse wave velocity (meter per second)
mg	Milligram
mg/day	Milligram per day
mg/dL	Milligrams per deciliter
mg/kg	Milligram per kilogram
mg/L	Milligram per litre
min	Minute
mL	Millilitre
mL/min	Millilitre per minute
mm	Millimetre
mM	Millimolar
mmol/L	Millimole per litre
ng	Nanogram
ng/mL	Nanogram per millilitre
nM	Nanomolar
v/v	Volume per volume
w/w	Weight per weight
µg	Microgram
µg/mL	Microgram per millilitre
µL	Microlitre
µM	Micromolar

List of Publications

Peer reviewed papers

- **Published**

Shehata E., Parker A., Suzuki T., Swann J. R., Suez J., Kroon P. A., and Day-Walsh P. (2022). Microbiomes in physiology: insights into 21st-century global medical challenges. *Experimental Physiology*, 107(4), 257-264. <https://doi.org/10.1113/EP090226> (See appendix 8).

Saha S., Day-Walsh P., **Shehata E.**, and Kroon P. A. (2021). Development and validation of a LC-MS/MS technique for the analysis of short chain fatty acids in tissues and biological fluids without derivatisation using isotope labelled internal standards. *Molecules*, 26(21), 6444. <https://doi.org/10.3390/molecules26216444> (See appendix 9).

Day-Walsh P., **Shehata E.**, Saha S., Savva G. M., Nemeckova B., Speranza J., Kellingray L., Narbad A., and Kroon P. A. (2021). The use of an in-vitro batch fermentation (human colon) model for investigating mechanisms of TMA production from choline, L-carnitine, and related precursors by the human gut microbiota. *European journal of nutrition*, 60(7), 3987-3999. <https://doi.org/10.1007/s00394-021-02572-6> (See appendix 10).

- **In preparation**

Shehata E., Percival J (joint first author), and Kroon P. A. Spontaneous anthocyanin degradation and its potential importance for human health: A review.

Shehata E., Day-Walsh P., Kellingray L., Saha S., Philo M., Narbad A., and Kroon P. A. Role for spontaneous and microbiota-driven metabolism of anthocyanins in human.

Shehata E., Percival J., and Kroon P. A. Aerobic in-vitro studies of anthocyanin degradation are not useful models for anthocyanin breakdown in the colon.

Shehata E., Percival J., Day-Walsh P., Kellingray L., Saha S., Philo M., Narbad A., and Kroon P. A. In-vivo and in-vitro studies of anthocyanin colonic metabolism.

Shehata E., Percival J., Rey P., Defernez M., Day-Walsh P., Hollands WJ., and Kroon PA. Little evidence of effects of anthocyanins on the human gut microbiota structure and function: in-vitro and in-vivo studies.

Day-Walsh P., **Shehata E.**, Saha S., and Kroon PA. Effects of pomegranate peel extract on L-carnitine metabolism to TMA.

Oral Presentations

Shehata E., Day-Walsh P., Percival J., Kellingray L., Saha S., Philo M., Narbad A., and Kroon P. A. Colonic transformation of anthocyanins is partly spontaneous and partly driven by the gut microbiota. The 3rd Food Bioactives and Health Conference (**Parma, 21st-24th June 2022**).

Shehata E., Day-Walsh P., Percival J., Kellingray L., Saha S., Philo M., Narbad A., and Kroon P. A. Interactions between anthocyanins and the gut microbiota. Quadram Institute Bioscience-Student Seminar (**Online, 31st March 2021**).

Shehata E., Day-Walsh P., Percival J., Kellingray L., Narbad A., and Kroon P. A. Understanding the role of the colon microbiota in the metabolism of dietary anthocyanins. Quadram Institute Bioscience-Coffee Break Science Meeting (**Online, 26th March 2021**).

Shehata E., Day-Walsh P., Percival J., Kellingray L., Narbad A., and Kroon P. A. The gut microbial and spontaneous transformation of anthocyanins. Quadram Institute Bioscience-Food and Health Programme Meeting (**Online, 7th October 2020**).

Shehata E., Day-Walsh P., Kellingray L., Narbad A., and Kroon P. A. The interaction between anthocyanins and human gut microbiota. Knowledge Exchange Trip at the Technical University of Munich (**Munich, 16th September 2019**).

Posters

Shehata E., Day-Walsh P., Kellingray L., Saha S., Philo M., Narbad A., and Kroon P. A. The metabolic pathways of anthocyanin degradation by the human gut microbiota. 10th International Conference on Polyphenols (ICPH) (**London, April 2022**).

Shehata E., Day-Walsh P., Kellingray L., Saha S., Philo M., Narbad A., and Kroon P. A. The colonic catabolism of black rice anthocyanins by the human gut microbiota. Physiology 2021 Annual Conference (**Online, July 2021**).

Shehata E., Day-Walsh P., Kellingray L., Saha S., Philo M., Narbad A., and Kroon P. A. Colonic transformation of anthocyanins is partly spontaneous and partly driven by the gut microbiota. Norwich Institute of Healthy Aging (NIHA) Initial Partner Symposium -Won poster prize (**Online, February 2021**).

Shehata E., Day-Walsh P., Kellingray L., Saha S., Philo M., Narbad A., and Kroon P. A. Colonic transformation of anthocyanins is partly spontaneous and partly driven by the gut microbiota. Quadram Institute Bioscience-Student Science Showcase (**Norwich, June 2019**).

Dedication

All praises and thanks to Allah (God) the almighty for giving me the force, courage, guidance, and willingness to reach this point of my life, despite all the challenges. I would like also to express my deepest gratitude to my dearest father—Mohamed Shehata (May Allah have mercy upon him) and to my dearest mother—Amina Kihail, for their endless support and love. Also, I would like to recognise and accredit all people I have met throughout my life who keep good principles, and values, and always have the willing to help others. Last, I don't want to forget to mention my home— Egypt.

With all my love and consideration,

Emad Shehata

Acknowledgements

The completion of this thesis could not have been possible without my supervisor. I was lucky to be supervised by Dr Paul Kroon from whom I have learnt a lot. You have given me constant support, guidance, and advice through all the stages of my PhD journey. Thank you for being so approachable and for the kindness you have shown. Also, you were a very thoughtful football manager of the QIB football team helping us to win the NRP championship twice. I would also like to thank Professor Arjan Narbad for his support and insights throughout my project. There are also people I would like to thank who I am so grateful for the time and the scientific support these people have given me to finish my doctorate: Dr Dimitris Makris, Dr Shikha Saha, Dr Lee Kellingray, Dr Perla Rey, and Mr Mark Philo.

Additionally, I would like also to thank Newton-Mosharafa Fund Programme and BBSRC for providing the funding for this project and giving me this great opportunity to work on this project which I have truly enjoyed working on.

To the members of Kroon's research group, I could not have reached this point without all of you. Firstly to Dr Priscilla Day-Walsh: you were more than a colleague during my journey. I never forget your endless kindness and support. I remember all moments that we worked together especially on the colon model experiments when I used to turn up late in the morning but in turn, I used to stay until late at night. I also remember all discussions and funny things we went through during those lab works which gave us the patience to complete 35 colon model experiments. All the time I expected something great to happen to you, and yes, congratulations for the new prestigious position at the University of Cambridge. I wish you all the best wishes and for good things to happen for you. To Gemma Beasy: thank you for being there during my journey. I remember those funny moments when we were laughing until tears come out. Now, while my journey is about to end, I wish you a very happy life, not only because I wish it for you but also because you deserve it. I am looking forward to calling you Dr Beasy. To Jasmine Percival: I enjoyed working with you on the part of this thesis when I felt more independent doing research. I am looking forward to seeing your success in your career. To Jenna Helleur, thank you for the time we shared travelling across the globe during the EIT entrepreneurial programme. To Olla Al-Jaibaji, thank you for being there during the last stage of my journey which was a hectic and very stressful time. I remember sometimes I wanted to speak in Arabic, and you were there to listen to random things. Olla, you were the reason to keep doing my prayers on time during this period. You left precious values which I will keep remembering. May Allah bless and protect you throughout your life.

To my colleagues and friends, Tedros Yamane, Annalisa Altera, Barbora Nemeckova, Johanna Jokioja, Jannika Oßkp, Jasmine Speranza, Julia Haarhuis, Hassan Aboufarrag, Amr El-Demerdash, Sherif Hamdallah, thank you for sharing part of your time with me during my stay in the UK, I am grateful to have met you all and to have built friendships with you. I would like also to thank all the people I met in my life who I have learned values from.

I would like to thank my family who I would never have been able to get to this point without them. Mum, you did more than you could for us. Every time I talk to you, you take me 20 years back to when I can feel those beautiful days. Dad, I know you are not here anymore, but now I am sure you are proud of me. Now I understand why you were waiting for me on the last visit I saw you, it was the last goodbye before you go. The thing that makes me accept your absence is your smile when I saw you in my dream one night. I know you are in a better place, but I miss you. May God have mercy on you, Dad. Finally, to my future wife and my children, I love you all. All you need to remember is that you are the reason behind all of this and I hope one day you would be proud of me.

Contributions

The work presented in this thesis is original research undertaken by the author. Some parts of the work described in this thesis were collaborative and hence significant contributions were made by other researchers and are summarised as follows.

Chapter 3 describes the green extraction process of black rice and bilberry anthocyanins. This work was done under the supervision of Dr Dimitris Makris and Dr Paul Kroon. All experimental work was completed by the author and the data reported in this thesis was collected, analysed, and interpreted by the author.

Chapters 4 and 6 describe the metabolism of anthocyanins and gut microbiota. All work described in these two chapters was done by the author but with the help of Dr Priscilla Day-Walsh in the experimental work with the colon model and under the supervision of Dr Paul Kroon. However, the data analysis and interpretation presented in this thesis are the work of the author.

Chapter 5 explores the spontaneous degradation of anthocyanins and anthocyanidins. The work on anthocyanidins (Cya and Del) was completed collaboratively with Jasmine Percival with a 50:50 division of experimental work. However, the data analysis and interpretation presented here are the work of the author.

Chapter 7 explores the impact of anthocyanins on the structure and function of the human gut microbiota. Experimental work was completed by the author, samples were sent to Novogene for sequencing, and bioinformatics analysis was done by Dr Perla Rey in collaboration with the author. However, the interpretation of the data presented in this thesis is the work of the author.

Chapter One

General introduction

Chapter 1: General introduction

1.1. Scope of the research in this thesis

The consumption of anthocyanins, a subclass of polyphenols, in high quantities is associated with health benefits in humans. However, anthocyanins are very poorly bioavailable and there is evidence that anthocyanin-derived metabolites are the main forms found in the circulation. Therefore, it is hypothesised that the beneficial effects of anthocyanins are due to anthocyanin metabolites interacting with human cells. Currently, it is not known what processes lead to anthocyanin breakdown and to what extent the gut microbiota is involved. Thus, the research in this thesis focuses on the degradation of anthocyanins due to both the human gut microbiota activity and also as a result of spontaneous degradation. The interaction between anthocyanins and the human gut microbiota will also be investigated. Therefore, this general introduction will include sections focused on what is currently known about the spontaneous degradation of anthocyanins, the microbiota-dependent degradation of anthocyanins, the formation of the anthocyanin metabolites, and the effects of anthocyanin exposure on the structure and function of gut microbiota.

1.2. Dietary (poly)phenols

Chemically, the word (poly)phenols refer to compounds comprising at least two phenol units (**Figure 1. 1**) in their structures. However, in the field of food bioactives research, polyphenols refer to compounds containing one or more phenol units in their structures and even include compounds that contain no phenol moieties, for example, *trans*-cinnamic acid. Polyphenols are the biggest group of natural products and are widely distributed in plant-based foods. There are two pathways for the biosynthesis of polyphenols by plants, the shikimic acid and the phenylpropanoid pathways^{1,2}. Currently, up to eight thousand phenolic compounds are chemically known, and half of these are categorized as flavonoids³. Naturally, many polyphenols exist in glycoside form (where a sugar molecule is bound to polyphenol via a glycosidic bond) and/or acylated with other molecules at different positions of the polyphenol skeletons³.

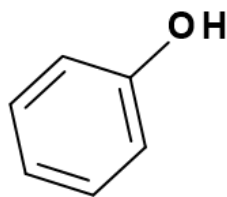


Figure 1. 1. Chemical structure of a phenol (hydroxybenzene).

There are different ways to classify polyphenols. The easiest and most common classification is based on the chemical of the aglycone moiety where polyphenols are classified into two main groups, non-flavonoids, and flavonoids. Each group is divided further into subgroups (**Figure 1. 2**). The non-flavonoid groups chemically comprise at least one phenolic unit in their structures (**Figure 1. 3**). There are commonly six subgroups of non-flavonoid polyphenols, namely hydroxybenzoic acids (e.g., gallic acid), hydroxycinnamic acids (e.g., caffeic acid), coumarins (e.g., 7-hydroxycoumarin), tannins (e.g., gallotannin), lignans (e.g., secoisolariciresinol), and stilbenes (e.g., resveratrol) (**Figure 1. 3**). These compounds linked to several health benefits such as antioxidant, anti-microbial, anti-cancer, anti-diabetic, and hepatic- and cardio-protective activities ⁴. The main source of these non-flavonoid polyphenols is fruits and vegetables such as broccoli, carrot, tomatoes, curry leaves, aubergine, kale, brussel sprouts, spinach, and red beet ⁴. Whereas grapes and wine derivatives provide the highest sources of stilbenes ⁵.

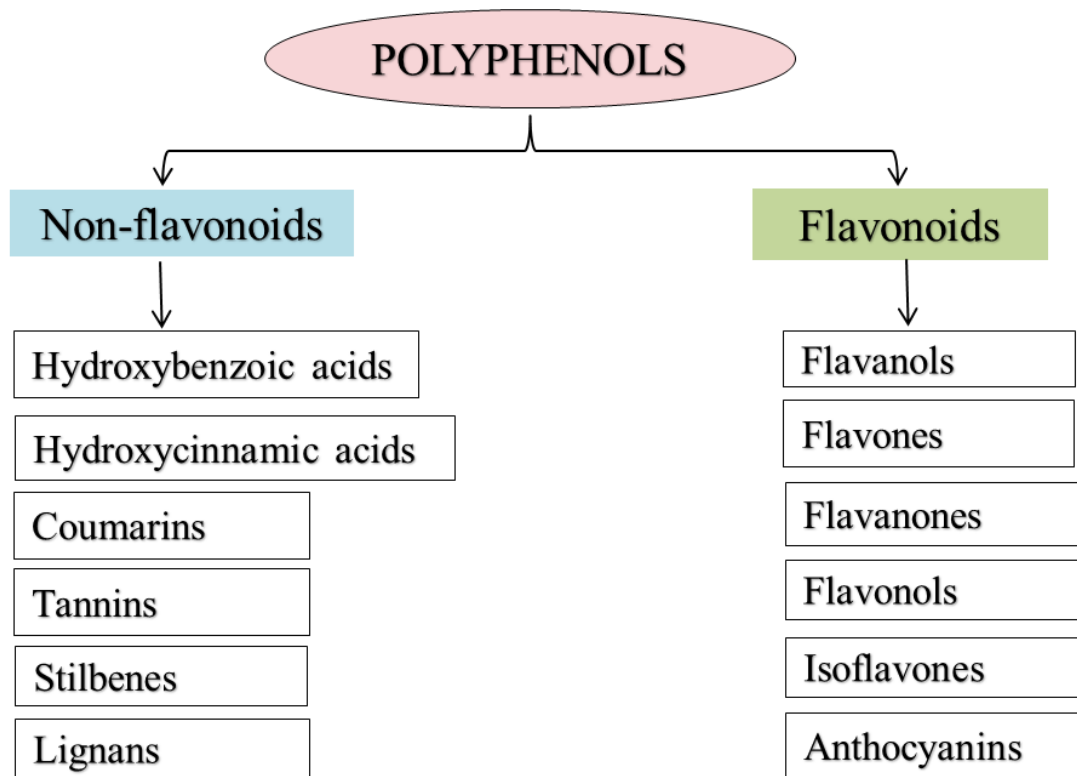
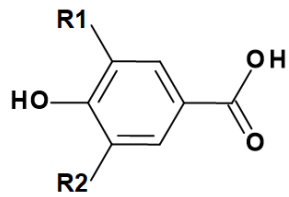
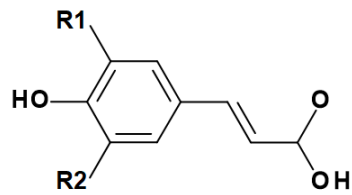


Figure 1. 2. General classification of dietary (poly)phenols.



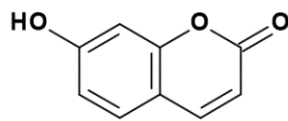
Hydroxybenzoic acid

- R1=H, R2=H (4-hydroxybenzoic acid)
- R1=OH, R2=H (Protocatechuic acid)
- R1=OH, R2=OH (Gallic acid)
- R1=H, R2=OCH₃ (Vanillic acid)



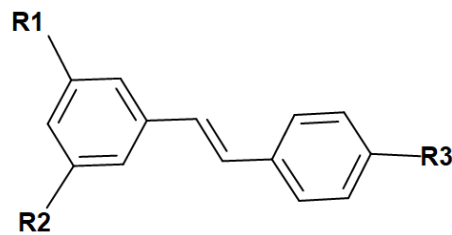
Hydroxycinnamic acid

- R1=H, R2=H (*p*-coumaric acid)
- R1=OH, R2=H (Caffeic acid)
- R1=OCH₃, R2=H (Ferulic acid)
- R1=OCH₃, R2=OCH₃ (Sinapic acid)



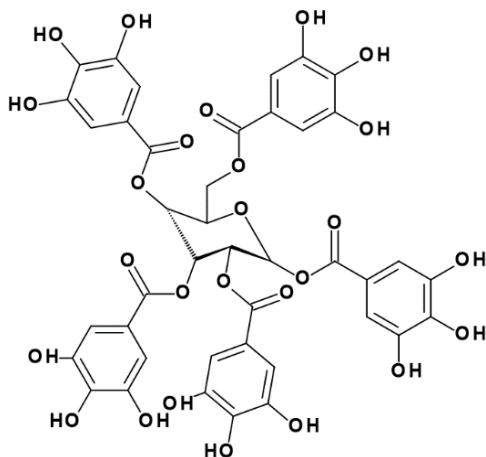
Coumarins

7-hydroxycoumarin



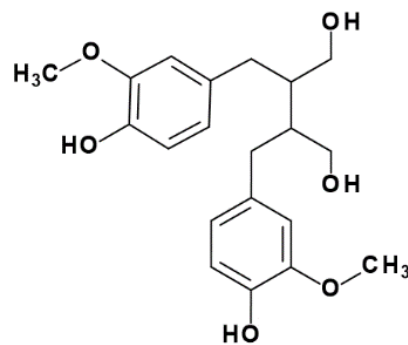
Stilbenes

- R1=OH, R2=OH, R3=H (Pinosylvin)
- R1=OH, R2=OH, R3=OH (Resveratrol)
- R1=OCH₃, R2=OCH₃, R3=OH (Pterostilbene)



Tannins

- Gallotannin



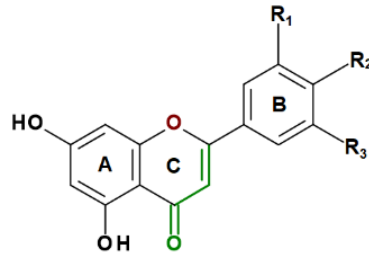
Lignans

- Secoisolariciresinol

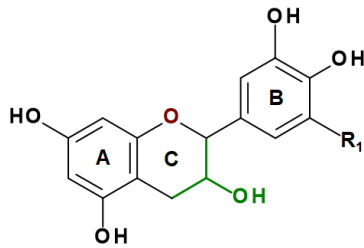
Figure 1. 3. Chemical structure of non-flavonoid (poly)phenols.

Flavonoids are another important class of polyphenols found in plants, and thus commonly consumed in human diets. Flavonoids are usually found naturally as flavonoid glycosides where the aglycone is attached to a glycone unit (sugar moiety) by a glycosidic bond ⁶. Foods with a high flavonoid content include parsley, onion, garlic, broccoli, berries (e.g., blueberries), black tea, green tea, bananas, soybean, all citrus fruits, red wine, and dark chocolate (with a cocoa content of 70% or greater) ⁶⁻⁸. Flavonoids are commonly divided into six main categories, namely flavonols (e.g., quercetin), flavones (e.g., apigenin), isoflavones (e.g., daidzein), flavanones (e.g., naringenin), flavan-3-ols (e.g., catechin), and anthocyanidins (i.e., cyanidin), where they are chemically similar in terms of their aglycone moiety with “C6–C3–C6” as a general structure in all flavonoid-type compounds (**Figure 1. 4**). The two C6 units (A-ring and B-ring) are phenolic nature; however, the C-ring (the chromane ring) is a C3 unit. Anthocyanins differ from other flavonoids as the oxygen atom in the C-ring is positively charged (+). Several reports in the literature reported that flavonoids exert various beneficial effects such as antioxidants, anti-inflammatory, hypocholesterolaemia, and cardioprotective agents ⁹.

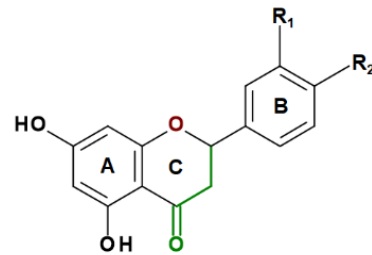
The main focus of my project was anthocyanins; thus, this class will be described in more detail.

**Flavones**

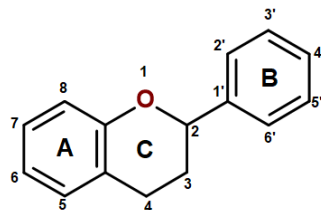
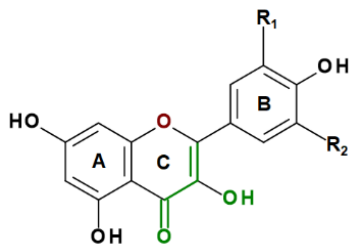
- R1=H, R2=H, R3=H (Chrysin)
- R1=H, R2=OH, R3=H (Apigenin)
- R1=H, R2=OH, R3=OH (Luteolin)

**Flavanols**

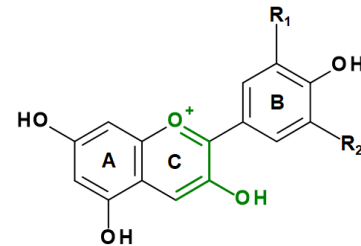
- R1=H (Catechin & Epicatechin)
- R1=OH (Epigallocatechin)

**Flavanones**

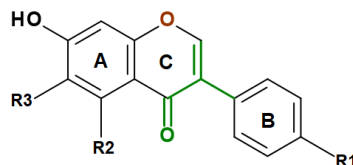
- R1=H, R2=OH (Naringenin)
- R1=OH, R2=OH (Eriodictyol)
- R1=OH, R2=OCH₃ (Hesperetin)

**Flavonoid backbone****Flavonols**

- R1=H, R2=H (Kaempferol)
- R1=OH, R2=H (Quercetin)
- R1=OH, R2=OH (Myricetin)

**Anthocyanidins**

- R1=H, R2=H (Pelargonidin)
- R1=OH, R2=H (Cyanidin)
- R1=OH, R2=OH (Delphinidin)

**Isoflavones**

- R1=OH, R2=H, R3=H (Daidzein)
- R1=OH, R2=OH, R3=H (Genistein)
- R1=OH, R2=OH, R3=OCH₃ (Glycitein)

Figure 1. 4. Chemical structure of flavonoid (poly)phenols.

1.3. Anthocyanins

Anthocyanins are an important subclass of flavonoids that give the natural colour to many fruits, flowers, seeds and other parts of plants¹⁰. The word anthocyanins originated from Greek words (anthos means flower; kianos means blue). Anthocyanins are responsible for many of the red-orange to blue-violet colours present in plant organs such as fruits, flowers, and leaves¹¹. Anthocyanins are harmless and dissolve in aqueous media, therefore they are commonly used as natural water-soluble colourants¹².

1.3.1. Chemical structure of anthocyanins

Structurally, anthocyanins are in the form of glycoside whereas anthocyanidins are known as aglycones. Anthocyanins are formed when an aglycone moiety (anthocyanidin) attaches to a sugar moiety. Anthocyanidins are derivatives of the flavylum form (2- phenylbenzopyrylium) where the C6-C3-C6 structure is the general backbone flavonoid¹³. Therefore, anthocyanidins consist of three rings (A-, B- and C-rings) (**Figure 1. 5**). The A- and C rings are fused together while the C-ring is bonded to the B-ring by a carbon-carbon bond^{14,15}. Anthocyanidins are grouped into 3-hydroxyanthocyanidins, 3-deoxyanthocyanidins, and O-methylated anthocyanidins. Whilst anthocyanins are anthocyanidin glycosides which can also carry acylated groups.

1.3.2. Types and distribution of anthocyanins

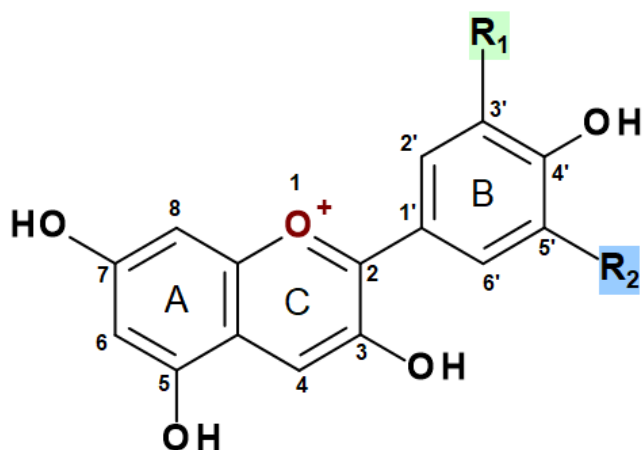
Anthocyanidins are polyhydroxy and polymethoxy derivative compounds. Many different anthocyanidins have been identified¹¹ and their differences come from the number and position of the hydroxyl (OH) and/or methoxy (OCH₃) groups, but only 6 are predominant in nature¹⁶. The A- and C- rings of anthocyanidins are identical, therefore substitution differences on B-ring give different anthocyanidin-type compounds, namely pelargonidin (Pel), cyanidin (Cya), delphinidin (Del), peonidin (Peo), petunidin (Pet), and malvidin (Mal) (**Figure 1. 5**). Like other flavonoids, anthocyanidins mainly exist in a glycosidic form (anthocyanins) where a glycosylic bond is linked to a sugar molecule on a hydroxyl group of anthocyanidin at one or more at the 3, 5, 7-positions. The sugar moieties are most usually glucose (Glc), galactose (Gal), rhamnose (Rha), or arabinose (Ara) and may be present as mono-, di-, or trisaccharide forms^{17,18}. In addition, acylated

anthocyanins are also found naturally where phenolic compounds (e.g., *p*-coumaric acid and ferulic acid) are attached to one or more of the sugar moieties of anthocyanins^{19,20}.

The aglycone moiety (anthocyanidin) is mainly responsible for the colour of anthocyanins. The chemical structures of A- and C-rings are identical in all anthocyanidins; therefore, the number of OH and/or OCH₃ groups in the B-ring is responsible for the colour shift of anthocyanidins and anthocyanins. With the increase of attached OH groups, the visible colour of the molecule shifts from orange to violet and goes toward redness if more OCH₃ groups are present^{21,22}. In addition, the presence of sugar moieties to anthocyanidins results in additional reddening of anthocyanins, whereas aliphatic or aromatic acyl moieties cause no colour change or a slight blue shift²³⁻²⁵.

Naturally, anthocyanins can form complex associations (co-pigmentation) with other compounds such as flavonoids, alkaloids, amino acids, organic acids, nucleotides, polysaccharides, metals or other anthocyanins²⁶. This phenomenon generates a change or an increase in the colour intensity by producing a hyperchromic effect and a bathochromic shift in the UV–Vis region¹².

Nevertheless, non-methylated anthocyanidins are found in 80 % of pigmented leaves, 69 % of pigmented fruits and 50 % of coloured flowers. Cya, Del, and Pel are the most distributed in nature, where 90% of the naturally occurring anthocyanins are based on only six structures (30% on Cya, 22% on Del, 18% on Pel and the rest 20% being the sum of Peo, Mal and Pet)²⁷. The glycosylated anthocyanidins with 3-monoglycosides, 3-diglycosides, and 3,5-diglycosides are most commonly sugar-bound anthocyanidins. Moreover, the 3-monoglycoside derivative occurrence is 2.5 times higher than derivatives containing the other glycosides and cyanidin-3-*O*-glucoside (Cya3Glc) is the most abundant anthocyanin type found in nature¹².



Anthocyanidin	R ₁	R ₂	Colour ^a
Pelargonidin (Pel)	H	H	Orange
Cyanidin (Cya)	OH	H	Orange-red
Peonidin (Peo)	OCH ₃	H	Blue-red
Delphinidin (Del)	OH	OH	Blue
Petunidin (Pet)	OH	OCH ₃	Blue-violet
Malvidin (Mal)	OCH ₃	OCH ₃	Violet

Figure 1. 5. Basic structure and numbering system of anthocyanidins (Anthocyanin aglycones).

The visible colour of the entire molecule shifts from orange to violet when attached hydroxyl groups increased.^a Data adapted from a report published by Ananga²⁷.

1.4. Anthocyanin-rich foods and daily intake

High consumption of anthocyanin-rich foods is associated with beneficial health effects in humans through the activation of long-term cellular adaptive physiological processes^{28,29}. Anthocyanins are mainly found in fresh berries, fruits, and some vegetables with coloured skin. Chokeberries, redberries, blueberries, elderberries, blackcurrant, blood orange, red grape and red wine are the most common and richest sources of anthocyanins among a long list of other human dietary sources²⁹. However, in processed foods (i.e., canned foods, bread, cereals, and baby foods) where anthocyanin-rich raw materials were added, anthocyanins generally are not detected³⁰. The lack of detection of anthocyanins added to processed foods may be due to their low chemical stability and possible degradation during processing, in particular the thermal process³¹.

Anthocyanin levels vary considerably in different plants as well as in the same plant according to the cultivar, level of maturation, storage conditions, and environmental and agronomic factors^{32,33}. For example, the red colour of blood orange juice significantly reduces with increasing storage temperature^{34,35}. Additionally, within different plants, the average anthocyanin content ranges between 0.25-1500 mg/100 g fresh weight (FW)^{29,30}. For example, the anthocyanin content in chokeberry, blackcurrant, blueberry, red raspberry, red grape, and strawberry were 1480, 476, 386, 92, 26, and 21 mg/ 100 g FW. More data on the total anthocyanin contents and the predominant anthocyanin-type of various anthocyanin-rich fruits and vegetables are presented in **Table 1. 1**. Furthermore, the types of anthocyanins are considerably different among food sources. For example, black raspberry contains the highest levels of cyanidin-type anthocyanins (669 mg/ 100 g FW), while black currant contains the highest levels of delphinidin-type anthocyanins (333 mg/100g FW)³⁰.

Dietary reference intakes do not currently exist for anthocyanins¹¹ and the average daily intake of anthocyanins has been shown to be considerably different among various racial/ethnic groups. Variations in daily intakes of anthocyanins depend on various factors such as the dietary habits of a population, their gender, season, and cultural practices. For example, the average daily intake of anthocyanins for men ranged from 19.8 mg (Netherlands) to 64.9 mg (Italy), whereas for women the average daily intake was 18.4

mg (Spain) to 44.1 mg (Italy). Higher consumption by Italians may result from their Mediterranean diet, which includes rich sources of anthocyanins such as berries, other red and blue-coloured fruits, and red wine and the availability of these foods ¹⁰. In addition, although they are estimated with a considerably higher average, the average daily consumption of anthocyanins has been estimated at 215 mg during the summer and 180 mg during the winter in the United States ³⁶.

Recent studies suggest a daily intake of anthocyanins to be 82, 50, and 12.5 mg/day in Finland, China, and the United States, respectively ^{11,37}. Some other reports estimated that the daily intake is somewhere between 3 to 215 mg/day, but these data may be underestimated daily intakes because they are estimated from questionnaires and dietary recalls, as anthocyanins are poorly represented in available food composition databases. Nevertheless, doses ranging from 400 to 500 mg of anthocyanins can easily be obtained from one serving (80 g) of berries and some juices such as blackberries (353 – 433 mg/serving), blueberries (579 – 705 mg/ serving), black currants (533 mg/serving) and blood orange juice (500 mg/serving) ³⁸.

Table 1. 1. Total anthocyanins content and predominant anthocyanins in common dietary sources.

Food	Total anthocyanins content (mg/100 g) ^a	Predominant anthocyanins	Reference
Purple corn	600-8200	Cyanidin-3- <i>O</i> -glucoside	39,40
Cranberry	140	Peonidin-3- <i>O</i> -galactoside	30,41
Elderberry	200-1816	Cyanidin-3- <i>O</i> -sambubioside Cyanidin-3- <i>O</i> -glucoside	30,42
Chokeberry	410-1480	Cyanidin-3- <i>O</i> -galactoside Cyanidin-3- <i>O</i> -arabinoside	22,43,44
Red grape	30-750	Malvidin-3- <i>O</i> -glucoside	45,46
Black grapes	39.23	Malvidin-3- <i>O</i> -glucoside	29,47
Apple	0.6	Cyanidin-3- <i>O</i> -galactoside	30,48
Bilberry	300-698	A mixture of anthocyanidins (cyanidin-, delphinidin-, peonidin-, petunidin- and malvidin) 3- <i>O</i> -monosaccharide (galactose, glucose, and arabinose)	49,50
Raspberry	20-687	Cyanidin-3- <i>O</i> -sophoroside	51-53
Blueberry	25-495	A mixture of anthocyanidins (cyanidin-, delphinidin-, peonidin-, petunidin- and malvidin) 3- <i>O</i> -monosaccharide (galactose, glucose, and arabinose)	54-56
Blackberry	82.5-325.9	Cyanidin-3- <i>O</i> -glucoside	51,57
Plum	5-173	Cyanidin-3- <i>O</i> -rutinoside	58,59
Strawberry	13-38	Pelargonidin-3- <i>O</i> -glucoside	51,60,61
Eggplant	750	Delphinidin-3- <i>O</i> -rutinoside, delphinidin-3-(<i>p</i> -coumaroylrutinoside)-5-glucoside	22,62,63
Cabbage	322	Cyanidin-3- <i>O</i> -diglucoside-5- <i>O</i> -glucoside	36,64
Black rice	23-327	Cyanidin-3- <i>O</i> -glucoside	65-67
Red wine	16.4-35 ^b	Malvidin-3- <i>O</i> -glucoside	68,69
Pomegranate (Juice)	44 ^b	Cyanidin-3- <i>O</i> -glucoside, Cyanidin-3,5- <i>O</i> -diglucoside	70-73
Pistachio nut	7.5	Cyanidin-3- <i>O</i> -galactoside	30,74

^a Fresh weight (FW)^b The content of anthocyanins presented as mg/100 mL

1.5. Chemical stability of anthocyanins

Anthocyanins are chemically unstable compounds, and their stability is affected by a range of factors including temperature, pH, light, metal ions, enzymes, and oxygen³⁸, which may cause loss of colour as a result of chemical or spontaneous degradation.

1.5.1. Effect of environmental factors on anthocyanin stability

The degradation of anthocyanins occurs during preharvest and postharvest stages³³ due to different environmental factors affecting anthocyanin stability and leading to the loss of colour. In the preharvest stage, anthocyanin stability is affected by vacuolar pH, growth temperature, enzyme activity, formation of metal complexes, and the level of maturation^{75,76}. However, although the main postharvest factors are the storage duration and the storage conditions, enzymatic and non-enzymatic factors play a part. For example, the red colour of blood orange juice was shown to be significantly reduced with increasing storage temperatures^{34,35}. Whereas the high storage temperature of strawberries increases the anthocyanin content⁷⁷. Regarding enzymatic factors, three main enzymes have been linked with anthocyanin degradation: namely polyphenol oxidases, β -glucosidases, and peroxidases⁷⁸. Generally enzyme activities are affected by a variety of factors such as temperature, pH, enzyme concentration, substrate concentration, and matrix⁷⁹.

The majority of anthocyanins are stable at low pH, and spontaneous degradation occurs at higher pH. Therefore, the pH of the medium is an important factor influencing anthocyanin stability. At an acidic pH, anthocyanins appear in a form of flavylium cation (a highly stable form compared to other forms) which is water soluble and red-pigmented. As pH increases to neutral, colourless carbinol pseudobase and chalcone structures are formed; and then as pH becomes alkali, anionic quinonoidal structures are formed⁸⁰⁻⁸³. Another factor affecting anthocyanin stability is temperature. As temperature increases, anthocyanin stability decreases⁸⁴. Although anthocyanins are sensitive to temperature, anthocyanidins are less stable than anthocyanins. Additionally, anthocyanins are light sensitive where fluorescent light stimulates the most degradation⁸⁵. In addition, anthocyanin stability is reduced when exposed to high levels of oxygen⁸⁴. Furthermore, at high concentrations, anthocyanins can interact with each other increasing their stability,

and it has been suggested that this may increase anthocyanin stability more than structural differences in the B-ring. Water content also adversely affects anthocyanin stability. These variables illustrate the delicate nature of anthocyanins ⁸⁶.

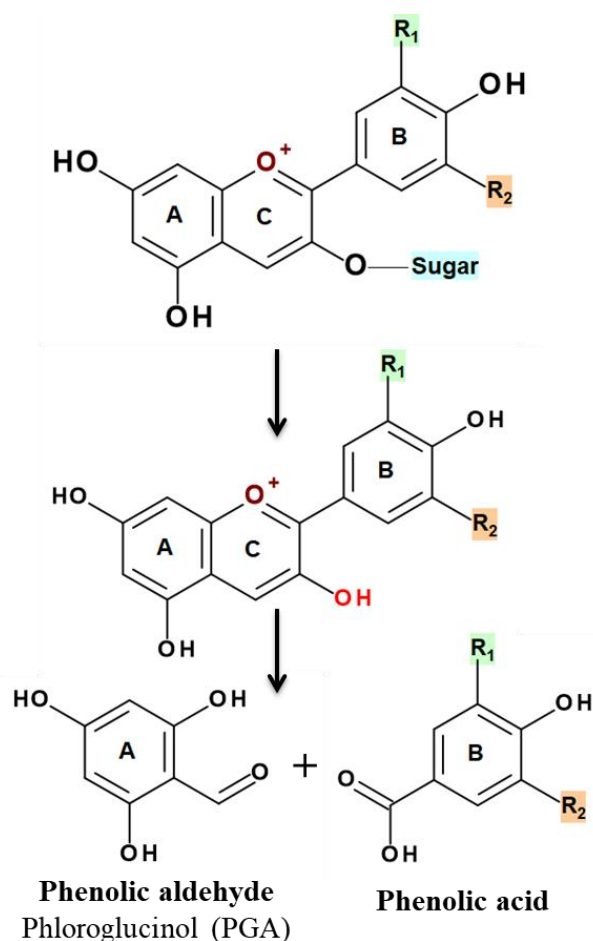
1.5.2. Effect of chemical structure on anthocyanin stability

The sugar moiety considerably increases anthocyanin stability, therefore the majority of reports in the literature have been focused on the spontaneous degradation of anthocyanidins than on their respective anthocyanins ^{38,87}. This was highlighted by Hanske and others who reported that Cya3Glc is more chemically stable than Cya ⁸⁸. In addition, disaccharide anthocyanins are more stable than monosaccharide anthocyanins ⁸⁹. Furthermore, the stability of the anthocyanin aglycone (anthocyanidin) is heavily influenced by the structure of the B-ring, with the presence of OH groups reducing stability, whilst the presence of OCH₃ groups increasing the molecule stability. Therefore, Cy3glc (which has two OH groups on the B-ring), was reported with higher chemical stability than Del-type anthocyanins (three OH groups on B-ring) and Pet-type anthocyanins (two OH groups and one OCH₃ group on B-ring) ⁹⁰.

1.5.3 Appearance of breakdown products of chemical degradation of anthocyanins

Anthocyanins undergo chemical degradation due to various environmental factors. However, pH is the most common environmental factor which causes the spontaneous degradation of anthocyanins. Although anthocyanins show stability in acidic medium (pH 1-3), they undergo structural rearrangement with increasing pH towards neutral pH. This rearrangement results in anthocyanins forming colourless chalcones and other intermediates ⁹¹. Nonetheless, small molecular weight compounds were reported as a result of chemical degradation of anthocyanins as well as anthocyanidins ^{38,87,92}. The formation of those small molecular weight compounds is the respective phenolic acids and phenolic aldehydes formed from the A- and B-ring structure. Since the chemical structure of the A-ring is identical to all anthocyanidins, phloroglucinol aldehyde (PGA) has been reported as a chemical breakdown product of all anthocyanins and/or anthocyanidins (**Figure 1. 6**). However, different phenolic acids were detected corresponding to the chemical structural variations of the B-ring within different

anthocyanidins. Therefore, 4-hydroxybenzoic acid, protocatechuic acid (PCA), gallic acid, vanillic acid, 3-O-methylgallic acid, and syringic acid were reported as breakdown products of Pel, Cy, Del, Peo, Pet, and Mal, respectively. However, there is conflicting evidence in the literature regarding the recovery of these breakdown products due to the spontaneous degradation of anthocyanins^{38,87,88,90,91,93,94}.



Anthocyanidin	Corresponding B-ring breakdown phenolics		References
	Phenolic acid	R ₁ R ₂	
Pelargonidin	4-Hydroxybenzoic acid	H H	87
Cyanidin	Protocatechuic acid	OH H	38,87–89,91,95
Delphinidin	Gallic acid	OH OH	87,93,94
Peonidin	Vanillic acid	OCH ₃ H	89,91
Petunidin	3-O-methylgallic acid	OH OCH ₃	96
Malvidin	Syringic acid	OCH ₃ OCH ₃	89,91,96

Figure 1. 6. The spontaneous degradation of anthocyanins and formation of A-ring and B-ring breakdown products.

1.6. Bioavailability and metabolism of anthocyanins

The term bioavailability refers to the extent a bioactive substance or drug enters the systemic circulation and becomes completely available to reach any specific destination and reaches the site of action ^{97,98}. However, compared to other flavonoids, the bioavailability of anthocyanins is very poor. For example, relative urinary excretion of the iso-flavone daidzin indicates that it is highly bioavailable (43% of dose) compared to that of anthocyanins (0.3% of dose) ⁹. Moreover, only a small fraction of ingested anthocyanins is absorbed by humans and a majority of studies have recorded a recovery of < 2 % ^{37,97,99,100}. The maximal plasma concentration is attained within 0.5–2 h after the consumption of anthocyanins. In addition, the absorbed anthocyanins are cleared from the circulation rapidly. In animal studies, following the consumption of berries or grapes, the systemic bioavailability of anthocyanins is estimated to be 0.26–1.8 %. In human studies, maximum plasma levels of total anthocyanins are in the range of 1–100 nM ⁹⁷. As such the biological health effects of anthocyanins are strongly associated with their absorption and metabolism *in-vivo* within the gut and also through phase II metabolism.

Anthocyanins are rapidly absorbed and detected in the circulation after consumption of their parent forms as a result of absorption through the gastrointestinal tract, in particular from the small intestine ^{101,102}. Prior and others reported that anthocyanins required 0.5 to 2 h to reach their maximum concentration (C_{max}) in plasma which is relatively faster than other flavonoids ¹⁴. Although there is little information about the absorption of anthocyanins in the oral cavity ³⁷, the quick appearance of anthocyanins in the circulation after ingestion (approximately 30 min) suggested that anthocyanins may be able to cross the upper gastric intestinal tract and reach the circulation ^{41,103}. These findings were supported in *in-vivo* and situ models (using mainly rat models) which reported that about 20% of the total absorbed anthocyanins were absorbed from the stomach in their intact forms ^{104–106}. This may be due to the acidic gastric juices increasing the stability of glycoside forms ^{57,104}. In fact, the mechanism of anthocyanin gastric absorption remains unknown and there is controversial information on whether the stomach is only an absorption organ or a metabolizing organ ¹⁰³. However, the vast majority of animal and human studies suggest that the intestine is the major site of anthocyanin absorption ¹⁰⁷.

After passing through the stomach, anthocyanins arrive in the small and large intestines where more basic conditions are present. Talavera and others reported that the intact methylated and conjugated forms of anthocyanins imply lots of absorption in the small and large intestines⁵⁷. They also reported that anthocyanin absorption is associated with enhanced activity of several hydrolysis-releasing enzymes such as lactase-phlorizin hydrolase (LPH) in the brush border of the small intestine. In addition, it was reported that aglycones undergo phase II transformation in the enterocytes, producing sulfated, glucuronidated, and/or methylated forms through the respective action of sulfotransferases, uridine-5'-diphosphate glucuronosyltransferases and catechol-O-methyltransferases¹⁰⁷. On the other hand, unabsorbed anthocyanins reached the colon where substantial structural modification occur including ring fusion and phase II metabolism which led to the production of many smaller molecules such as phenolic acids and their conjugates¹⁰⁸.

Generally, the absorption of anthocyanins is dependent on their molecular structure. In human and rat studies, the glycosylated forms are poorly absorbed compared to the aglycone forms¹⁰⁹. This may be due to the higher molecular weight of the glycosylated forms which makes their absorption less efficient. Nevertheless, anthocyanins carrying the same sugar moiety were reported to be absorbed in the following order: pelargonidin > cyanidin > delphinidin > malvidin. This may be a result of the greater number of hydroxyl groups in delphinidin or the greater hydrophobic nature of malvidin. Similarly, anthocyanins with the same aglycone type were reported to be in the order: galactoside > glucoside > arabinoside.

Comparing the amount of the intact anthocyanins absorbed and excreted in urine to the total ingested doses, anthocyanins appear to have low bioavailability with a recovery of < 1% of consumed doses of anthocyanins in the majority of studies¹¹⁰. Manach and others reviewed 97 human interventions that investigated the kinetics and extent of polyphenol absorption¹¹¹. They found that the concentration of anthocyanins measured in plasma ranged from 10-50 nmol/L and the mean time to reach C_{max} was 1.5 h for plasma after anthocyanin consumption. Additionally, the concentration of anthocyanins excreted in urine was 0.1 % of the intake and the mean time was 2.5 h. Others reported that the concentrations of anthocyanins were in the range of 1 – 100 nM in plasma and urine

following the consumption of berries and grapes¹⁴. Furthermore, another study reported low concentrations of Cya3Glc (36.47 ng) in plasma, urine, and faeces after the consumption of 500 mg of ¹³C-labelled Cya3Glc¹⁰⁰. In **Table 1. 2**, a summary of the measured bioavailability of intact anthocyanins in humans is presented.

Explaining the high bioactivity of anthocyanins despite their low recovery (bioavailability) was the most pressing issue. Therefore, few reports suggested that the bioavailability of anthocyanins has been underestimated¹¹². They claimed that the main methods used in the analysis were based on measuring anthocyanins in their coloured acidified forms (flavylium ions) and therefore, other colourless forms had not been quantified¹¹². However, this suggestion does not explain entirely the low recovery. Others suggested that the reason for the reported low bioavailability of anthocyanins is that anthocyanins are subject to extensive metabolism and biotransformation¹⁰³ where the gut microbiota most likely plays an essential role in this biotransformation¹⁰.

Anthocyanin metabolism has been reported to start in the oral cavity as a result of interaction with salivary proteins and digestive enzymes¹⁰³. In saliva samples which were collected from healthy volunteers (who participated in a human intervention study with several derivatives of black raspberry), anthocyanins were detected including their hydrolysed forms (anthocyanidins), glucuronidated conjugates and low quantities of PCA. The formation of all these derivatives was reported to be a result of β -glycosidase activity derived from oral epithelial cells or as a result of oral microbiota⁵². In fact, the degradation of anthocyanins into smaller molecules (such as phenolic acids) is the most likely event, and there are several reports supporting this notion. For example, Prior and Wu reported that 60–90 % of the anthocyanins disappeared from the gastrointestinal tract within 4 h after a meal; and just very low concentrations of intact compounds were observed, suggesting that anthocyanins were transformed into other forms¹⁴. In addition, 30 to 44% of blood orange anthocyanins were found as PCA in plasma supporting the notion that anthocyanins undergo extensive metabolism¹¹³. This notion was confirmed after using isotopically labelled anthocyanins in two reports by Czank and De Ferrars who reported a substantial number and amount of breakdown products derived from ¹³C-labelled anthocyanins and about 43% of the [¹³C] dose was recovered^{99,100}.

Table 1. 2. Pharmacokinetics of anthocyanins following oral consumption in human subjects*

Source	Period (h)	Dose (mg)	Urinary recovery (%)	C _{max} (nmol/L)	t _{max} (h)	t _{1/2} (h)	Reference
Aronia berry	24	500	0.004	12	1.6	-	114
Cranberry juice	4	94.47	0.79	4.64	1.3	-	115
Strawberry	24	200	1	274	1.1	2.1	116
Chokeberry	24	721	0.15	96.1	2.8	1.5	117
Hibiscus extract	7	147	0.018	7.6	1.5	2.6	118
Red grape juice	7	283	0.23	222.7	0.5	1.8	119
Red wine	7	280	0.18	95.5	1.5	2.0	119
Blackcurrant	7	145	0.04	-	-	1.7	120
Elderberry	7	147	0.37	-	-	1.7	120
Chokeberry	24	1300	0.048	592	-	-	121
Strawberries	24	77	1.9	-	-	-	122
Blackcurrant	4	716	0.05	35.6	0.7	-	123
Blueberry	4	1200	0.003	29.2	4.0	-	124
Blackcurrant	7	1000	0.039	-	-	-	125
Elderberry	24	720	0.08	97.4	-	-	126
Blueberry	6	690	0.004	-	-	-	126
Elderberry	-	500	0.05	-	-	-	127
Blackcurrant	5	153	0.03	-	-	-	128

C_{max}, maximum concentration derived from serum or plasma data; t_{max}, time to reach maximum concentration derived from serum or plasma data; t_{1/2}, half-life of elimination. The table is adapted from Kay (2006) in addition to some recent studies.

*Values represent total anthocyanins and include anthocyanin metabolites when identified

1.7. Anthocyanins and human health

Anthocyanins have been shown to protect against a myriad of human diseases. The free-radical scavenging and antioxidant capacities of anthocyanins are the most commonly reported biological activities through which these bioactive compounds may be used as therapeutic intervention targets in humans¹⁶. However, research suggests that other mechanisms of action are also responsible for delivering the beneficial health effects of these bioactive compounds^{129–131}. For example, anthocyanins may confer their effects by providing protection from DNA cleavage, or through altering estrogenic activity, enzyme inhibition, boosting the production of cytokines, anti-inflammatory activity, lipid peroxidation, decreasing capillary permeability and fragility, and membrane strengthening^{132–134}. In both *in-vitro* and *in-vivo* research trials, anthocyanins have demonstrated considerable ability to inhibit tumour formation¹³⁵. With regard to cardiovascular disease protection, anthocyanins are strongly linked to oxidative stress protection¹³⁶. Other reports suggest that anthocyanins can aid in the prevention of obesity and diabetes through the modification of insulin and glucose metabolism¹²⁹. Anthocyanins have also been reported to enhance memory, and prevent age-related decline in neural function¹³².

Despite the growing evidence for the beneficial health properties of dietary anthocyanins especially as cardioprotective agents, the mechanisms of action involved remain poorly defined due to a limited understanding of their bioavailability, metabolism, and elimination^{37,99,100}. This may be partly because many studies have ignored the role of the human gut microbiota in anthocyanin bioavailability and metabolism. Anthocyanins absorbed in the gastrointestinal tract, are mainly found in methylated, sulfated forms or as intact glycosides at extremely low levels in plasma and urine 10 – 2000 nM⁹⁹. Therefore, intact anthocyanins most probably remain in the gastrointestinal tract and therefore, either spontaneously degrade and/or continue to enter the colon where the majority of gut microbiota are located and subject the anthocyanins to extensive metabolism to generate a wide range of potentially bioactive metabolites that are absorbed into circulation^{89,97,99,137}.

1.8. The role of gut microbiota in human health

1.8.1. What is gut microbiota?

The term “microbiota” is a recent but now commonly used term for an "ecological community of commensal, symbiotic and pathogenic microorganisms" ¹³⁸ which exist in various parts/organs of multicellular organisms such as insects, animals, plants and humans. In addition, microbiota refers to all microorganisms such as bacteria, archaea, protists, fungi, and viruses. The human-associated microbiota is estimated to include at least 40,000 bacterial strains in 1800 genera which collectively harbour at least 46 million non-human genes^{139,140}.

The collective microorganism communities found in the human gastrointestinal tract are termed “the human gut microbiota” which constitutes a large proportion of the human microbiota^{138,141}. The human gut microbiota represents a biomass of up to 2 kg in adult humans ¹³⁹ and contributes to a wide range of physiological functions in the host including immune development, maturity and modulation, host energy metabolism, cell signalling, pathogenic bacteria colonization resistance, gut mucosal integrity, and regeneration ¹⁴². The human gut microbiome is taxonomically ordered into phylum, class, order, family, genus, and species (**Figure 1. 7**). The majority of microbes in the gut (the gut microbiota) come under the phyla Firmicutes, Bacteroidetes, Proteobacteria, Fusobacteria, Verrucomicrobia, Cyanobacteria and Actinobacteria with Firmicutes and Bacteroidetes accounting for over 90% in most cases ¹⁴³.

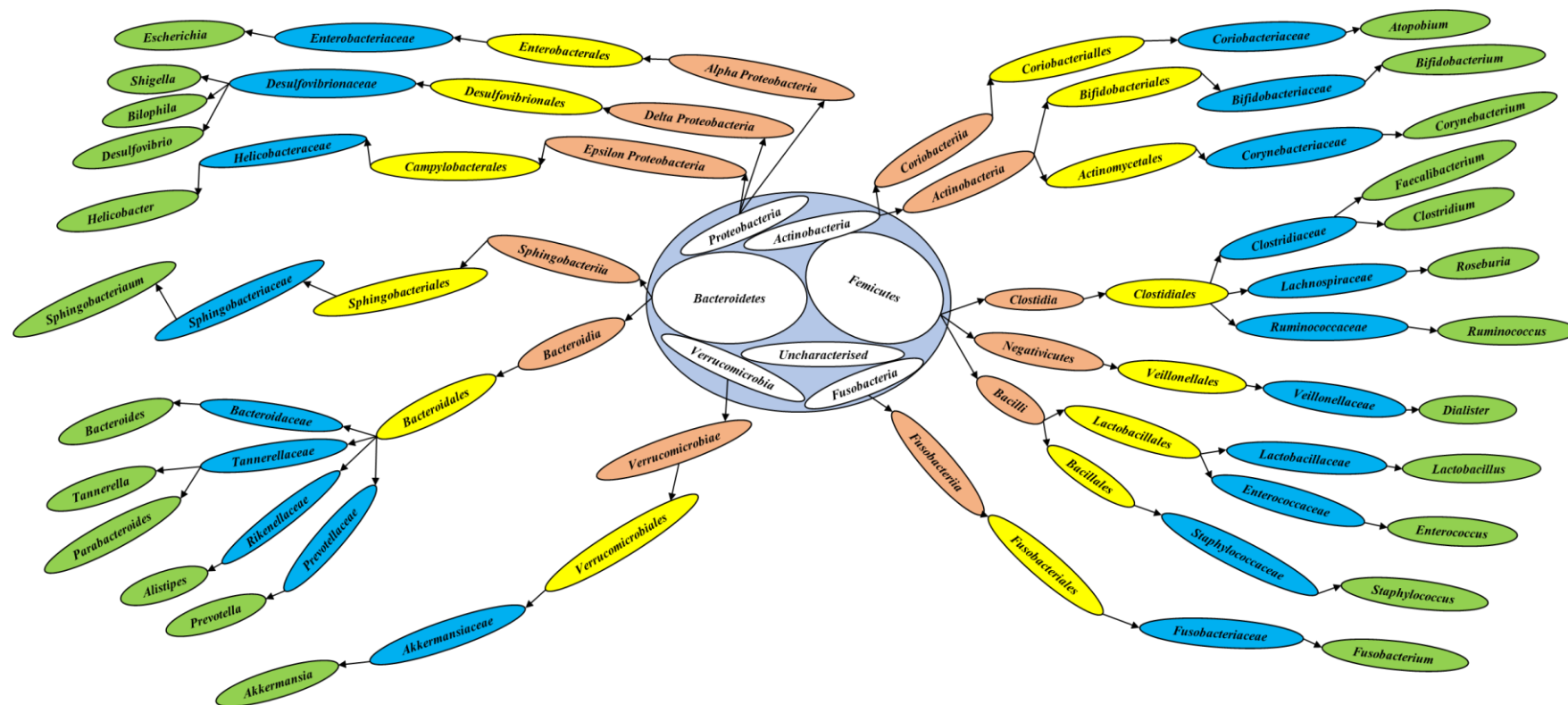


Figure 1. 7. Taxonomical classification of gut microbiota compositions.

The highest order from the pie chart radiates into the lower genus order. Light blue colour=phylum, brown colour=Class, yellow highlight=Order, blue highlight=Family, green highlight=genus. Due to the diversity of microbial species, species are not included in this figure but will be referred to wherever necessary in the text.

1.8.2. The relation between gut microbiota and human health

The gastrointestinal tract is the primary site of interaction between the host immune system and both symbiotic and pathogenic microorganisms delivered with diets ¹⁴⁴. Furthermore, the relation between gut microbiota and human health has increasingly been recognised. It is now well established that a normal gut microbiota considerably contributes to the overall health of the host ¹⁴⁵. Although each individual's gut microbiota is shaped in early life as its structure depends on some infant events/factors (i.e., birth gestational date, type of delivery, methods of milk feeding, and weaning period) and external factors such as antibiotic use. The gut microbiota in infants is dynamic but starts resembling the adult gut microbiota structure by the age of 3 years ¹⁴³. Then, the structural variations in temporal and spatial gut microbiota occur all along the individual's life span.

These individuals and their healthy native gut microbiota remain relatively stable in adulthood but differ between individuals due to factors such as geographical location, exercise frequency, lifestyle, and cultural and dietary habits. Therefore, it is difficult to define an optimal gut microbiota composition since there are both intra- and inter-individual variations. However, large microbial diversity is considered more beneficial to the host ¹⁴⁶⁻¹⁴⁸. Many studies have shown the human gut microbiota is not only critical for nutrient and energy absorption, digestion, vitamin synthesis, and metabolism but also essential for maintaining physiological homeostasis and thus can determine an individual's general health ^{149,150}. Therefore, the gut microbiota has been associated with immunologic ¹⁴⁴, and hormonal and metabolic homeostasis ^{151,152}. For example, microbial imbalance (dysbiosis) in the gut has been linked to several complex diseases such as anxiety, depression ¹⁵³ and metabolic diseases such as obesity, cardiovascular diseases, non-alcoholic fatty liver disease and diabetes ^{141,151,154}. Experimental data have demonstrated this by showing that high-fat diets, high red meat and low-fibre diets, are linked to increased relative abundances of undesirable microorganisms and thus increased production of undesired compounds/metabolites including the cardio-toxicant trimethylamine (TMAO) ¹⁵⁵⁻¹⁵⁷. Consequently, the modulation of the gut microbial population is a promising approach for potential health treatments or decreasing the risk of many chronic/metabolic diseases ¹⁴⁹. These observations emphasise that the gut microbiome is a vital element in maintaining human well-being. Not only has the gut

microbiome been shown to be critical for the metabolism of essential dietary precursors and nutrients, but there is also now further evidence that the gut microbiota may be involved in the metabolism of food bioactive compounds such as polyphenols including anthocyanins^{158–160}.

Initially, the Firmicutes/Bacteroidetes ratio was proposed to determine disease phenotype, with a high Firmicutes/Bacteroidetes ratio being indicative of diseases such as type II diabetes, obesity etc¹⁶¹. However, further studies, have suggested that while this ratio, may indeed be important in classifying some disease phenotypes, alterations in other phyla may influence this ratio and that dysbiotic changes in other phyla are not necessarily reflected by Firmicutes/Bacteroidetes ratio¹⁶². Further efforts have been made to characterise the gut microbiota composition of each individual based on clusters of bacterial communities termed enterotypes, which include; Enterotype I, predominantly consisting of the genus *Bacteroides* with a functional capacity to metabolise food components such as animal fat, carbohydrates and proteins found in the Western diet, enterotype II which is predominantly *Prevotella* with a functional capacity to metabolise simple sugars and carbohydrates mainly found in plant-rich diets consumed by non-westernised agricultural communities and western communities on the Mediterranean diet (Agrian), and Enterotype III which is predominantly *Ruminococcus* but in infants, other genera including *Enterobacteriaceae*, and *Bifidobacterium*, as well as *Proteobacteria*, also exist. It is noteworthy that the concept of enterotypes has also become a subject of debate due to other studies demonstrating that there is no clear demarcation between groups, but gradients may exist. Additionally, it has been demonstrated that other genera than the original genera contributing to the enterotype group may predominate the enterotype clusters (as in the case of *Methanobrevibacter* in Enterotype III¹⁶³). Nevertheless, this calls for a better classification of disease phenotypes-associated microbiota structures that will allow the modification of the gut microbiota towards a beneficial microbiome through therapeutic targets such as probiotics, prebiotics, and faecal microbiota transplantation.

Such approaches are compromised by the fact that the precise composition of the gut microbiota is subject to the variations between individuals where a wide range of factors

can influence the microbial composition, including, but not limited to age, gender, antibiotic use, cultural habits, diet, disease and lifestyle ¹⁴³.

1.9. Interactions between anthocyanins and human gut microbiota

Some anthocyanin metabolites have been identified post the consumption of anthocyanins, in particular phenolic acids and simple phenols which have been reported to have potential health benefits ^{100,110}. These phenolics (metabolites) have been suggested to be produced by the human gut microbiota ⁹⁹. Anthocyanins have also been suggested to change the composition and profile of the human gut microbiota ^{164–166}. The changes in gut microbiota structure are closely related to several physiological effects, and the modulation of the gut microbiota has been considered a possible mechanism by which phenolic compounds may exert their effect. Evidence for microbial-dependent anthocyanin metabolism is much less extensive than that of many other flavonoids, with the metabolic consequence(s) of anthocyanins still a matter of much debate ¹⁶⁷. This is owing to the fact that the gut microbiota has only started to be considered as a metabolic organ, hence contributing to the metabolism of polyphenols and, consequently, to their bioavailability and their biological effects ¹⁶⁸. Therefore, it has been hypothesised that gut microbiota generally interacts with dietary polyphenols (including anthocyanins) in two ways (**Figure 1. 8**): (i) the human gut microbiota metabolise polyphenols into potential bioactive molecules and/or (ii) the polyphenols and/or their metabolites act as prebiotic agents to change the structure and function of the gut microbiota ¹⁶⁸.

There is evidence of high concentrations of anthocyanins being found in the distal intestine, cecum, and colon because the majority are not absorbed in the upper gastrointestinal tract. For example, 85% of blueberry anthocyanins were reported to reach the colon ¹⁶⁹. Therefore, the colon is being considered an active site for metabolism rather than a simple excretion route and has recently been receiving much attention as a subject of further research ¹⁷⁰. Therefore, colonic metabolism is important for the absorption and the biological activities of dietary polyphenols, not only due to the direct bioactivity of the polyphenol breakdown products but also because of their prebiotic activity in reshaping the structure and function of the gut microbiota ^{168,171,172}. However, the role of the gut microbiota in anthocyanin metabolism, the influence of anthocyanins on gut

microbial populations, and how this may affect overall health is not well understood and has only been investigated by a few studies as will be discussed in the next section^{137,160,168}, and this relationship is shown in **Figure 1. 8**.

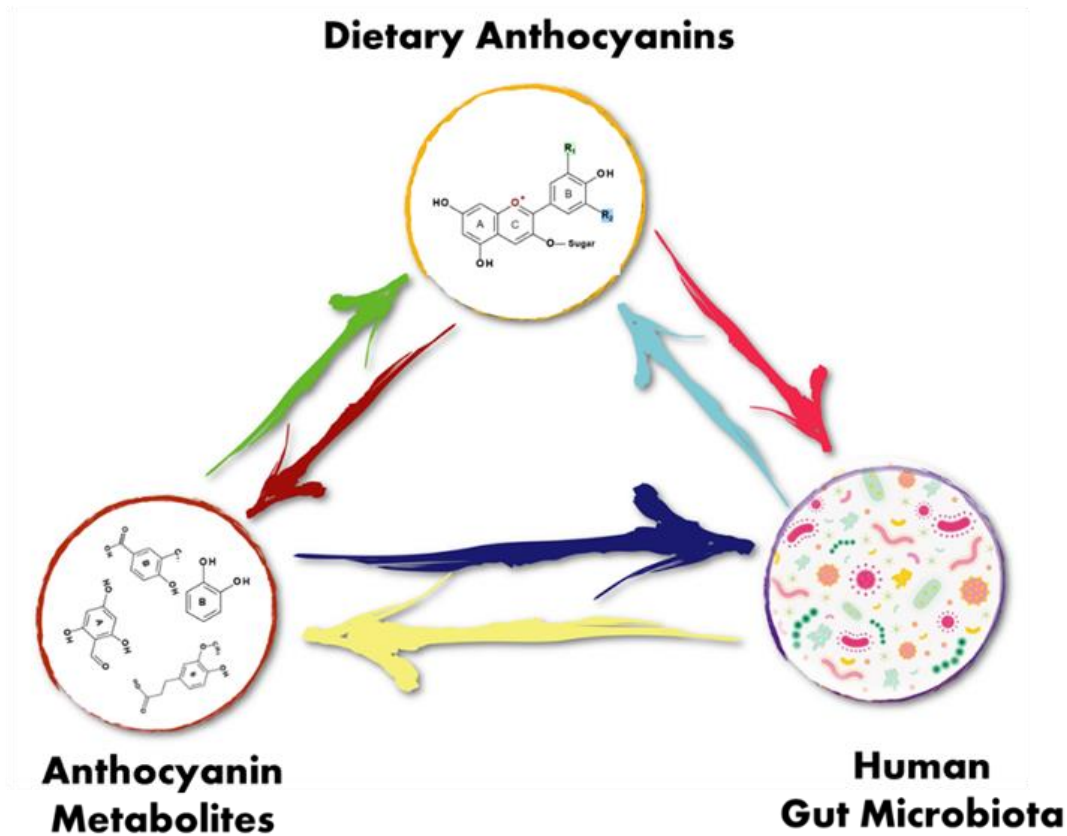


Figure 1. 8. Bidirectional relationship between anthocyanins and the human gut microbiota.

1.9.1. Metabolism of anthocyanin by human gut microbiota

A human intervention study showed that anthocyanin degradation products and derived metabolites are the bioavailable forms in circulation after anthocyanin consumption⁹⁹. Therefore, the human gut microbiota was considered an active organ for the metabolism of anthocyanins.

The majority of dietary anthocyanins are not absorbed in the upper gastrointestinal tract, therefore consumed anthocyanins can reach the human colon where the colonic gut microbiota can bio-transform anthocyanins into their metabolites⁹⁹. These anthocyanin metabolites are then absorbed and entered the circulatory system¹⁶⁸. To investigate the role of the gut microbiota metabolism, faecal samples were used as a source of gut microbiota, specifically the colonic microbiota. Therefore, early *in-vitro* studies on the metabolism of anthocyanins by the gut microbiota were conducted by incubating anthocyanins with faecal samples collected from animals such as pigs or rats. For example, two reports used the content of the larger intestine of slaughtered pigs and showed a decline in the incubated anthocyanins in the presence of pig faecal samples within a few hours (2 and 6 h, respectively)^{89,96}. Keppler and others investigated both mono- and di-saccharide anthocyanin compounds (i.e., Cya3Glc and cyanidin-3,5-*O*-diglucosides (Cya3,5Glc))⁸⁹. They observed that the addition of sugar moieties increased the stability of anthocyanins. A few other *in-vitro* studies have used human faecal samples to investigate the anthocyanin metabolism by the human faecal microbiota. For example, a study incubated 100 μ M of Cya3Glc with filtered (to eliminate the bigger organic matter) human faecal samples¹⁷³. They reported that Cya3Glc fully disappeared at 2 h incubation in the presence of active human gut microbiota and PCA was identified as a B-ring metabolite of Cya3Glc, but a smaller decline was observed in the presence of inactive gut microbiota. Another report also investigated the metabolism of anthocyanins by the human faecal gut microbiota and 90% of the initial concentration (C_{initial}) of incubated Cya3Glc disappeared after 2 h incubation⁹¹. In another study, 100 μ M of incubated Cya3Glc completely disappeared within 2 h and subsequently, the B-ring-PGA and A-ring-PCA appeared as degraded products⁸⁸. Although the incubations of the aforementioned studies were carried out using simple buffer solutions, few studies used

nutrient media such as Basal nutrient medium and Gifu anaerobic media to carry out the incubations^{174,175}.

All investigations were set up with the initial pH at neutral (between 5.5-7.5). However, there were small variations in pH, for example, different used different pH such as 5.5, 6.8, 7.2 and 7.3^{91,173,175,176}. To my knowledge, only one *in-vitro* study has used a model where the pH was controlled to remain in the range between 6.8 and 7.0¹⁷⁷. Although Hidalgo and others investigated the microbial metabolism of anthocyanins, the spontaneous degradation of anthocyanins was not investigated. In their report, however, they showed that in the presence of faecal microbiota, syringic acid and gallic acid were detected as B-ring products of Mal3Glc and Del3Glc, respectively. Furthermore, syringic acid and tyrosol were reported as the main microbial metabolites generated from a strawberry extract¹⁷⁴.

Several epidemiological, clinical, and *in-vitro* studies have demonstrated the health benefits of consuming polyphenol-rich diets against cardiovascular disease, hormone-dependent cancers and other metabolic diseases¹⁷⁸. However, there is large variability in outcome measures, very limited reproducibility between studies, and in some cases, a disparity between the results of clinical trials¹⁷⁹. Recently more evidence support that there are inter- and intra-individual variations in the metabolism of dietary bioactive compounds¹⁸⁰. As the majority of polyphenols are metabolised in the human gut, this may result in variable bioactive microbial metabolites in the small and large intestine consequently they may have a different impact on the host's health before or after absorption into the circulatory system. This variability might be due to individual differences in gut microbiota structure at phyla, genera as well as species levels¹⁸¹, resulting in variability in metabolic profiles in the circulation and consequently excreted metabolites (metabotypes). These metabolic differences are hypothesised to impact the effects of the metabolites or parent phenolic compounds on health¹⁸². To my knowledge, nothing has been reported on inter- and intra-individual variations of anthocyanin metabolism by the human colonic microbiota although some studies have been conducted using other polyphenolic compounds. For example, a study suggested the putative existence of three metabotypes in the production of flavan-3-ol colonic metabolites¹⁸³. Three metabotypes were defined and characterized based on the appearance of

flavan-3-ol microbial metabolites during the consumption of green tea and green coffee bean extracts over 8 weeks. The characterisation was based on the excretion of different amounts of trihydroxyphenyl- γ -valerolactones, dihydroxyphenyl- γ -valerolactones, and hydroxyphenylpropionic acids.

Variability in gut microbial composition between individuals can lead to the selective production of specific metabolites. This has been demonstrated with equol, where metabolism by the colonic gut microbiota potentially determines the benefits associated with the consumption of the isoflavone daidzein¹⁸⁴. Moreover, the metabotype differences in the production and excretion of colonic microbial metabolites are not restricted to a single compound but might include a set of metabolites originating from the same parent compound. For example in the case of urolithins, ellagitannin-derived microbial metabolites, can be classified into three urolithin metabotypes according to the qualitative and quantitative proportions of different urolithins excreted after consumption of ellagic acid or ellagitannins¹⁸⁵; with Metabotype A only producing urolithin-A (Uro-A), Metabotype B producing urolithin-B, isourolithin-A, and Uro-A and Metabotype O which produces none of the afore mentioned metabolites¹⁸⁶. Crucially, the benefits associated with rich sources of ellagitannins (i.e., pomegranate and walnuts) may be related to each specific metabotypes^{187,188}.

1.9.2. The impact of anthocyanins on the structure of the human gut microbiota

Phenolic compounds, including anthocyanins, are associated with a favourable change in the microbiota composition with the beneficial effects being reflected in changes in inflammatory markers, involving the down-regulation of the transcription factor NF- κ B signalling pathway^{168,169}. For example, black raspberry showed intestinal anti-inflammatory effects and changes in microbiota community¹⁸⁹. Moreover, a review paper reported that consuming anthocyanins can increase the growth of beneficial gut bacteria and/or inhibit the growth of some bacterial species that are known to have negative implications for human health¹⁹⁰.

Other reports have observed that anthocyanin metabolites appeared as a result of anthocyanin metabolism by the human gut microbiota. For example, PCA, caffeic acid, PGA, and ferulic acid have been reported as anthocyanin metabolites produced by human gut microbiota activity¹⁷⁵. Therefore, anthocyanins and their metabolites are considered as important molecules that may modulate the gut microbiota structure and function as observed with the modulation of beneficial gut microbiota, particularly an increase in *Bifidobacterium* strains¹⁶⁹. Additionally, anthocyanin degradation pathways involved have been shown to vary depending on the strains that are incubated with the anthocyanins¹⁹¹. Anthocyanins have been shown to increase the relative abundances of specific microbial communities including *Bifidobacterium* spp¹⁶⁴. For example, an *in-vitro* study with bacterial strains reported that black rice anthocyanins increased the growth of *Bifidobacterium* and *Lactobacillus* species¹⁹². Furthermore, incubation of Mal3Glc with faecal microbiota enhanced total bacterial growth, including *Bifidobacterium* species and *Lactobacillus* species, whereas gallic acid, the microbial anthocyanin metabolite, reduced *Clostridium histolyticum* but had no effect on beneficial bacteria¹⁷⁷. In agreement with this, another study reported that the growth of *C. histolyticum* in human faeces was decreased when incubated with red wine extract¹⁹³.

In regards to animal and human studies, there are relatively few studies that have investigated the effects of anthocyanin consumption on the gut microbiota structure. However, most of these studies have used plant anthocyanin extracts, not purified single compounds. For example, one mouse study reported that a black raspberry anthocyanin supplement increased the abundance of *Eubacterium rectale*, *Faecalibacterum prausnitzii*, and *Lactobacillus* whereas *Desulfovibrio* species and *Enterococcus* species were shown to be inhibited¹⁹⁴. Another mouse study reported that dietary supplementation with genetically modified apples (with high anthocyanin content) increased the relative abundance of *Bifidobacterium* species¹⁹⁵. Likewise, a human study reported that there was a significant increase in *Bifidobacterium* species after 6-week consumption of a blueberry drink¹⁶⁴. However, it should be noted that some studies have reported no effect of anthocyanin consumption on gut microbiota composition. For example, no effect of purple sweet potato anthocyanins was shown on the composition of

the microbiome ¹⁶⁶. In addition, no increase was observed in *Bifidobacterium* or *Lactobacillus* species as reported by others ¹⁹⁶.

From the data in the literature, in both *in-vitro* and animal studies, anthocyanins are hypothesised to be associated with flourishes in *Bifidobacterium* and *Lactobacillus* species. Many of these species were shown to have β -glucosidase activity and thus can catabolise polyphenolic compounds and enrich the bacterial medium with glucose. Moreover, these bacterial species are reported with an antimicrobial effect against pathogenic organisms by producing short-chain fatty acids as well as via competing for substrates and adhesion sites needed for microbial growth ¹⁹⁷.

although the evidence of changing gut microbiota structure by anthocyanin consumption is still little, the evidence of anthocyanin catabolism by gut microbiota was shown to be critical in the appearance of anthocyanin metabolites. For example, in literature as well as in chapter 6, various metabolites (i.e., PCA, PGA, catechol, PGCA, dihydroferulic acid, and dihydrocaffeic acid) were shown in the presence of live faecal microbiota from black rice anthocyanins. However, as far as literature searches have shown, no current reports have focused on the impact of anthocyanin metabolites on the structure and function of gut microbiota, opening a major area for future research.

1.10. Aims and objectives of the research

The principle aims of the thesis were to investigate the role of the human gut microbiota in the metabolism of anthocyanins and to investigate the impact of anthocyanins on the structure and function of the human gut microbiota. The following objectives were addressed.

- I. To produce an in-house solvent extraction method for purifying anthocyanins from suitable food sources to generate the quantities required for subsequent anthocyanin metabolism experiments (**Chapter 3**)
- II. Investigate the loss of anthocyanins over time in the presence of human faecal microbiota and the within and between donor variations (**Chapter 4**).
- III. Determine the relative contribution of spontaneous degradation and microbiota-dependent degradation of anthocyanins and anthocyanidins in the colon (**Chapter 4**).
- IV. Identify the products of spontaneous degradation of anthocyanins and the influence of environmental variables (**Chapter 5**).
- V. Identify the products of microbiota-dependent degradation of anthocyanins and the metabolic pathways (**Chapter 6**).
- VI. Investigate the impact of anthocyanins on the structure and function of the human gut microbiota using metagenomics and bioinformatic analyses (**Chapter 7**).

Chapter Two

Materials and methods

Chapter 2: Materials and methods

2.1. Extraction and quantification of anthocyanins

All water used was 18 M Ω /cm Milli-Q water, and solvents were of high-performance liquid chromatography (HPLC) grade. All authentic anthocyanins standards were purchased from Extrasynthese (Genay, France). Other chemicals and reagents were purchased from Sigma unless otherwise stated within the text.

2.1.1. Preparing plant materials for anthocyanin extraction using green solvents

Black rice grains were purchased from the Belazu Ingredient Company (UK) and were ground using a coffee blender (**Figure 2. 1A**) and then stored in the dry and dark at ambient temperature. The freeze-dried bilberry powder (**Figure 2. 1B**) was purchased from Biokia[®] (Finland) and stored in the dry and dark at ambient temperature.

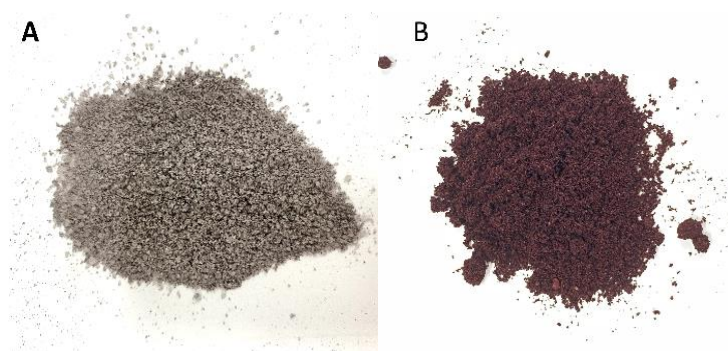


Figure 2. 1. Raw plant materials of black rice and bilberry.
Figure A is black rice powder whereas figure B is bilberry powder

2.1.2. Batch extraction procedure for glycerol/water solvent composition assays

1 g of plant powder was mixed with 50 mL of varying concentrations of aqueous glycerol (10 – 90% w/v) in a stoppered glass bottle (**Figure 2. 2**). All glycerol solutions were mixtures with water and from here on will just be referred to in terms of the percent glycerol. The ground powder was subjected to extraction under stirring at 600 rpm with

a Teflon-coated magnetic stirrer, for 180 min, at room temperature (23 ± 1 °C). At 180 min, 1 mL samples were collected and centrifuged at $10,000\times g$ for 10 min. The clear supernatant was used for further analysis.



Figure 2. 2. Borosilicate stoppered glass bottles containing glycerol/water solvents and anthocyanin-rich powders.

2.1.3. Batch extraction procedure using 80% glycerol solvent for liquid-to-solid ratio ($R_{L/S}$) assays

A range of plant powder masses (0.5, 0.625, 0.833, 1.25, and 2.5 g) was weighed out and separately mixed with 50 mL of 80% glycerol in a screw top glass bottle (**Figure 2. 2**). The plant powders were subjected to extraction under stirring at 600 rpm, with a Teflon-coated magnetic stirrer, for 180 min, at room temperature (23 ± 1 °C). Samples were collected at 180 min, then centrifuged at $10,000\times g$ for 10 min. The clear supernatants were used for further analysis.

2.1.4. Batch extraction procedure using green solvent for the effect of temperature assays

0.833 g of each of the plant powders was mixed with 50 mL ($R_{L/S} = 60$) of 80% w/v glycerol in stoppered glass bottles. The plant powder was subjected to extraction under stirring at 600 rpm, with a Teflon-coated magnetic stirrer, for 180 min, at different temperatures (50, 60, 70, and 80°C) using an oil bath (**Figure 2. 3**). Samples were taken for analysis at 5, 10, 15, 20, 30, 60, 120 and 180 min. Samples were centrifuged at $10,000\times g$ for 10 min and the clear supernatant was used for further analysis.



Figure 2. 3. Oil bath used for the extraction of anthocyanin-rich powders at various temperatures.

2.1.5. Determination of total polyphenol yield in aqueous glycerol extracts

In a 1.5-mL Eppendorf tube, 20 μL of the sample was diluted with 780 μL of Milli-Q water, and 50 μL of the reagent (Folin-Ciocalteu) was added and vortexed. After exactly 1 min, 150 μL of a freshly-prepared aqueous sodium carbonate 20% w/v was added. Then the mixture was vortexed and allowed to stand at room temperature in the dark, for 60 min. The absorbance was read at 750 nm (λ_{750}) and the total polyphenol concentration was calculated from a calibration curve, using gallic acid as a standard. The content of total polyphenols was determined as mg gallic acid equivalents (GAE) per 100 g of dry weight (dw). The measurements were carried out using a 96-well microplate where 300 μl of aliquots were spiked and the absorbance was carried out on a UV-vis plate reader (Molecular Devices, LLC VersaMax, California, United States). The blank sample was prepared from Milli-Q water.

For a standard curve, a fresh 1 mg/mL gallic acid standard was prepared in methanol. A series of gallic acid concentrations (0, 10, 50, 100, and 200 $\mu\text{g/mL}$) were prepared in Milli-Q water. The standards were analysed in the same way as the samples described above.

2.1.6. Determination of total pigment yield in aqueous glycerol extracts

An aliquot of 100 μ L of the sample was mixed with 900 μ L of 0.25 M HCl solution (prepared in ethanol) and the mixture was left to equilibrate for 10 min. The absorbance at λ ($_{520\text{ nm}}$) was obtained with 0.25 M HCl in ethanol as blank and the total pigment yield was determined as cyanidin-3-glucoside equivalents (C3GE). In a 96-well micro plate, 300 μ L of aliquots were spiked and the absorbance was carried out on a UV-visible plate reader (Molecular Devices, LLC VersaMax, California, United States).

In external standard curve preparation, a stock solution of 2 mg/mL cyanidin-3-glucoside was prepared in acidified methanol (1% aqueous HCl). Serial dilutions (0, 5, 10, 50, 100, 200 μ g/mL) were prepared in acidified ethanol (0.1% HCl) and serial dilutions treated in the same way as samples.

2.1.7. Determination of total anthocyanins in aqueous glycerol extracts using HPLC–DAD

To measure the concentration of anthocyanins, the glycerol extracts were centrifuged at 10,000 \times g for 10 min. 500 μ L of the supernatants were diluted 3-fold with 4% aqueous formic acid. The final water percent was 75%. Samples were vortexed well before injection onto HPLC.

HPLC Agilent 1100 series coupled with a diode array detector (DAD) was used. The method was performed using a reverse phase column and with gradient elution. 20 μ L of the sample was injected onto a Kinetex XB-C18 column (100 \times 4.6 mm; particle size 2.6 μ m) at 40°C using 5% aqueous formic acid (eluent A) and 5% formic acid in acetonitrile (eluent B). The gradient was 5% B with injection for 2 minutes, increased to 7% at 10 min, 10% at 15 min, 13% at 16 min, 20% at 18 min, and then re-equilibrated to initial conditions over 6 min. anthocyanins were identified against authentic standards using *RT* and their *m/z* (M-H). Anthocyanins peaks were quantified using DAD at λ ($_{520\text{ nm}}$).

For standard curves, five authentic anthocyanins (Del3Glc, Cya3Glc, Peo3Glc, Pet3Glc, and Mal3Glc) were purchased from Extrasynthese (Genay, France). Stock solutions of 1000 μ g/mL for each authentic anthocyanin compound were prepared in 0.75 mL of

glycerol/water solvent (10%, 40% and 80% glycerol/water ratios were used). 0.75 ml of 4% aqueous formic acid was added to the mixture to give a final anthocyanin concentration of 500 µg/mL. The mixture was vortexed well for 1 min and afterwards, the standard curve was plotted against various concentrations of working solutions ranging from 0 to 250 µg/mL (Table 2. 1).

Table 2. 1. Preparation of standard curve for authentic anthocyanins

W.S. ^a	Prepared Anthocyanin (µg/mL)	Volume added from higher concentration (µL)	Glycerol/water (µL)	4%FA water (µL)
1	250	500 (from S.S.)	0	500
2	125	500 (from W.S. 1)	125	375
3	62.5	500 (from W.S. 2)	125	375
4	31.25	500 (from W.S. 3)	125	375
5	15.625	500 (from W.S. 4)	125	375
6	7.8125	500 (from W.S. 5)	125	375
7	0.00	0	250	750

^aWorking Solution

2.1.8. Determination of anthocyanin content in acidified ethanol extracts using HPLC–DAD-MS

The black rice and bilberry extract powders were prepared by dissolving in acidified water (4% FA). HPLC Agilent 1100 series coupled with diode array detector (DAD) and an Agilent single Quade mass spectrometer was used. The method was performed on a reverse phase column using gradient elution. 20 µL of sample was injected into Kinetex XB-C18 column (100 × 4.6 mm; particle size 2.6 µm) at 40°C using 5% aqueous formic acid (eluent A) and 5% formic acid in acetonitrile (eluent B). The gradient was 5% B with injection for 2 minutes, increased to 7% at 10 min, 10% at 15 min, 13% at 16 min, 20% at 18 min, and then re-equilibrated to initial conditions over 6 min. Anthocyanin detection was achieved on DAD at λ_{520} nm.

2.1.9. Statistical Analysis

Unless otherwise stated, statistical analysis was performed in GraphPad Prism (version 9.3 for Windows, GraphPad Software, La Jolla California USA, www.graphpad.com).

For dependent samples, one-way analysis of variance (ANOVA) with Dunnett's Multiple Comparison Test was used to compare the means of the control and experimental samples and $p < 0.05$ was considered statistically significant. Values of $p < 0.05$ were considered significant (*, $p < 0.05$; **, $p < 0.01$; ***, $p < 0.001$; ****, $p < 0.0001$).

2.2. *in-vitro* colon model fermentation

All water used was 18 M Ω /cm Milli-Q water, and solvents were of high-performance liquid chromatography (HPLC) grade. The anthocyanin-rich extract powders prepared from black rice and bilberry were purchased from the Beijing Gingko Group (BGG), China. Cyanidin-3-*O*-glucoside (Kuromanin chloride), delphinidin-3-*O*-glucoside (Myrtillin chloride), Peonidin-3-*O*-glucoside (Peonidin-3-glucoside chloride), Malvidin-3-*O*-glucoside (Oenin chloride), Petunidin-3-*O*-glucoside (Petunidin-3-*O*-glucoside chloride) and pelargonidin-3-*O*-glucoside (Callistephin chloride) were purchased from Extrasynthese (Genay, France).

Other chemicals and reagents were purchased from Sigma unless otherwise stated within the text.

2.2.1. Donor recruitment for *in-vitro* colonic fermentation experiments

Stool samples used in the *in-vitro* colon model experiments were collected from participants recruited onto the Quadram Institute Bioscience (QIB) Colon Model study. Demographic information was collected, and recruited participants, from both gender who aged between 25 and 54 years older, who live or work within 10 miles of the Norwich Research Park. The participants who were declared to be in good health and had not ingested antibiotics for at least 4 weeks before giving faecal sample were eligible to participate onto the study. In addition, participants were required to have a normal bowel habit which meant regular defecation between three times a day and three times a week, with an average faecal type of 3–5 on the Bristol Stool Chart. Moreover, participants who declared no diagnosed chronic gastrointestinal health problems, such as irritable bowel syndrome, inflammatory bowel disease, or coeliac disease were eligible to enrol onto the study. Participants were also asked additional questions immediately prior to donating a stool sample to confirm that they had not experienced a gastrointestinal complaint, such as vomiting or diarrhoea, within the last 72 h, were not tested positive COVID-19 using lateral flow test, were not currently pregnant or breast-feeding, had not recently had an operation requiring general anaesthetic, were not taking multivitamin supplements. The study was approved by the Quadram Institute Bioscience (formally Institute of Food Research) Human Research Governance committee (IFR01/2015), and London -

Westminster Research Ethics Committee (15/LO/2169). The informed consent of all participating subjects was obtained, and the trial is registered at <http://www.clinicaltrials.gov> (NCT02653001).

All faecal samples that were used in the studies reported in this thesis have a specific code such as “**donor 01-S1**”, where each donor is designated by a unique donor number (**01**) and the sample number (**S1**) indicates the distinct stool sample provided by a donor on a specific day.

2.2.2. Preparation of fresh faecal slurries

Fresh faecal samples were delivered by donors to the Quadram Clinical Research Facility and were collected immediately on the day of the experiment. In the safety cabinet, a faecal slurry was prepared in a stomacher filter bag by diluting faecal sample 10 fold (1/10, w/v) with autoclaved 0.01 M phosphate-buffered saline (PBS) (which was placed overnight in the anaerobic cabinet prior to the day of experiment) and then homogenized in a stomacher (Seward Stomacher 400 Circulator) for 45 sec (230 rpm). The filter was separated from the stomacher bag and then discarded. The remaining solution was used for inoculation of the *in-vitro* colon model. Later, for the preparation of 1 % faecal colon media, 10 mL faecal slurry (10 % faecal sample) was added to 90 mL of colon model media.

2.2.3. Preparation of glycerol-frozen faecal stock with a final faecal concentration of 37.6 %

Autoclaved 50 mM potassium phosphate buffer and glycerol solutions were kept in the anaerobic cabinet overnight before use. In the safety cabinet, 50 g of a fresh faecal sample was weighed into a stomacher filter bag, and then 50 mL of autoclaved phosphate buffer was added. The mixture was homogenised in the stomacher for 30-45 sec at 230 rpm. The filter was separated from the bag and then discarded. In the remaining mixture, 33 mL of autoclaved glycerol was added to achieve a final glycerol concentration of 25% (v/v) and a faecal concentration of 37.6 % in a total of 133 unit of slurry (w/v). Aliquots were prepared in 15 mL Falcon tubes and stored at -80°C until use. For reuse, the frozen

glycerol-faecal stock tubes were thawed by placing them in the anaerobic cabinet (37°C) for 1 h.

2.2.4. Setting up the *in-vitro* batch colon model

300 mL colon vessels (**Figure 2. 4**) were set up, sealed, and then autoclaved before the experiment. After autoclaving, the vessels were filled with 89 mL autoclaved colon model media which was prepared previously as described by Day-Walsh and others¹⁵⁷. Briefly, before autoclaving and in 1 L Milli-q water, the colon model media was prepared by adding 2 g each of peptone water, yeast extract and NaHCO₃, 0.1 g NaCl, 0.04 g each of K₂HPO₄ and KH₂PO₄, 0.01 g each of MgSO₄·7H₂O and CaCl₂·6H₂O, 2 mL Tween, 10 µL vitamin K, 0.5 g each of cysteine and bile salts, and 0.02 g hemin (after dissolving in few drops of 0.5 M NaOH). D-glucose was added after autoclaving by dissolving 10 g in a 30 mL autoclaved colon model and then reintroduced again into the colon media through a 0.45 µm syringe filter (Sartorius). After adding the autoclaved colon media into vessels, the media was gassed overnight with O₂-free N₂ to set up an anaerobic condition. Then pH probes were introduced into vessels and the pH was adjusted to between 6.6 to 7.0 using acid (0.5 M HCl) and alkali (0.5 M NaOH). Before the addition of the faecal slurries, the temperature of the colon vessels was set at 37°C using a water bath (**Figure 2. 5**).

2.2.5. Incubating anthocyanins with the faecal microbiota using *in-vitro* colon model fermentation

All incubations were carried out by inoculating 1% w/v faecal sample in a total experiment volume of 100 mL. Therefore, for vessels containing live faecal microbiota, 10 mL of fresh faecal slurry (or 2.6 mL from glycerol-frozen faecal stock) was inoculated into a 90 mL medium (89 mL colon media + 1 mL treatment). The 1 g of faecal sample used in each fermentation vessel is expected to contain an average of 0.92×10^{11} microorganisms¹⁹⁸. For vessels containing autoclaved faecal microbiota, 10 mL of fresh faecal slurry was autoclaved before adding to the vessels. For the treatments, anthocyanin-rich extract powder of black rice or bilberry was dissolved in 1 mL milli-Q water and immediately filtered through a 0.45 µm syringe filter, then added to the growth media (1% faecal sample). For control vessels, no anthocyanin extract powder was

introduced. Samples (0.5 mL) were collected at 0, 1, 2, 4, 6, 8, 10, 12, 20 and 24 h, mixed with 0.5 mL of 4% v/v aqueous formic acid. Samples were stored at -80°C until analysis.

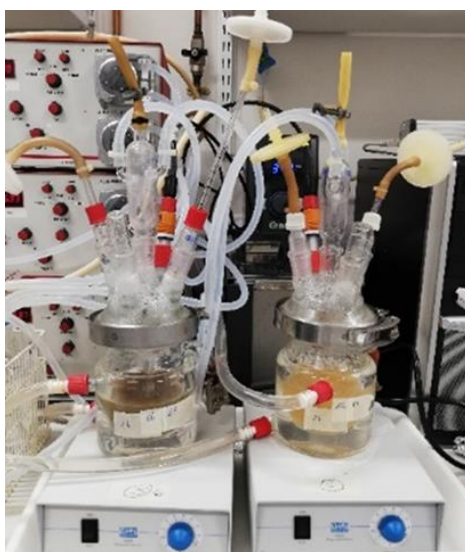
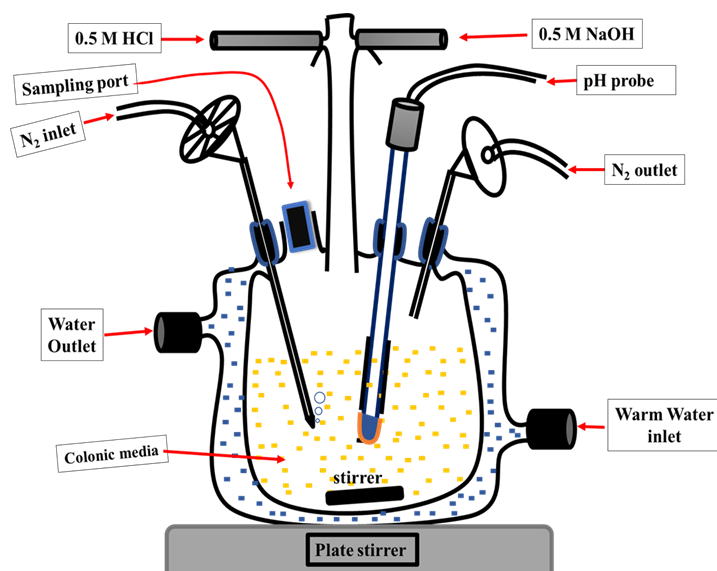


Figure 2. 4. Schematic of the colon model vessel.

The vessel was set up with a total reaction volume of 100 mL and a gas container volume of 200mL. The top figure shows the vessel with all connected ports for supplying warm water, nitrogen, acid and alkali solutions, and injection and sampling ports. The bottom picture shows the real vessel in the laboratory.

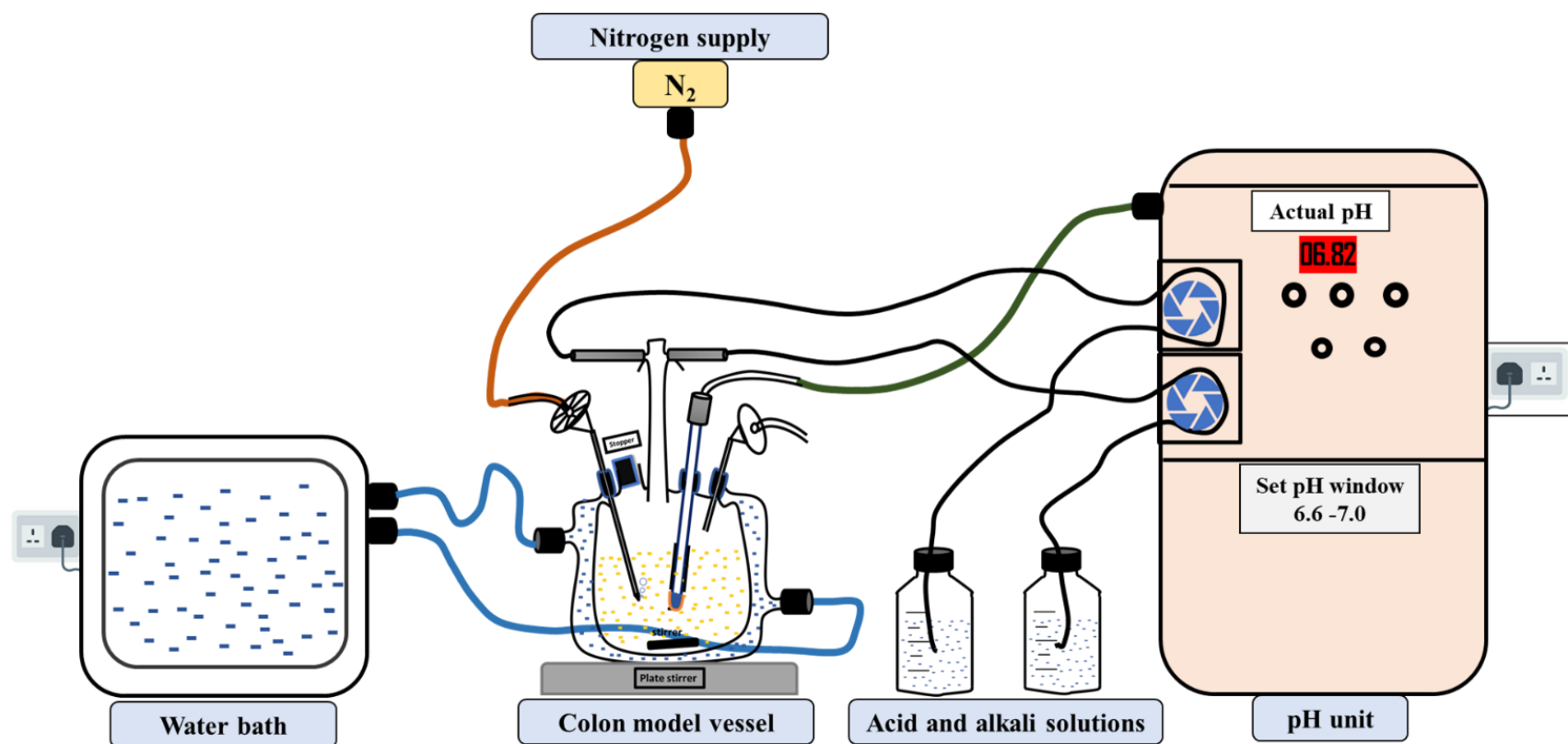


Figure 2. 5. Schematic of the human in-vitro colon model.

The model was set up with the colon model vessel, the pH unit, acid & alkali solutions, nitrogen supply, and water bath.

2.2.6. Preparation of colon model samples for chromatography and mass spectrometry analysis

Colon model samples were thawed at room temperature for 1 h, vortexed, and then centrifuged at 17,000×g for 10 min. 250 µL of supernatant was transferred into HPLC vials (300 µL inserted amber glass).

2.2.7. Determination of anthocyanins in colon model samples using HPLC–DAD

To measure the rate of loss of the incubated anthocyanins from black rice and bilberry, HPLC Agilent 1100 series coupled with a diode array detector (DAD) was used. The method was performed on a reverse phase column using gradient elution. 20 µL of sample was injected into Kinetex XB-C18 column (100 × 4.6 mm; particle size 2.6 µm) at 40°C using 5% aqueous formic acid (eluent A) and 5% formic acid in acetonitrile (eluent B). The gradient was 5% B with injection for 2 minutes, increased to 7% at 10 min, 10% at 15 min, 13% at 16 min, 20% at 18 min, and then re-equilibrated to initial conditions over 6 min. Anthocyanin detection was achieved on DAD at λ_{520} nm.

2.2.8. Determination of anthocyanin metabolites in the colon model sample using UPLC–MS/MS

Multiple reaction monitoring (MRM) technique was used for the quantification of anthocyanin metabolites on UPLC-MS/MS. The 1 µL sample (concentration of 20 µg/ml) was injected into a Water HSS T3 (C18) (100 x 2.1 x 1.7 µ) connected to an Agilent 1290 UPLC equipped with a binary pump, degasser, cooled auto-sampler, DAD detector and column oven (Agilent Technologies, Waldbronn, Germany) and an Agilent 6490 mass spectrometer (Agilent Technologies, Waldbronn, Germany) and eluted at a flow rate of 0.40 ml/min. The column temperature was maintained at 35°C. Elution was achieved using a gradient of increasing solvent B (containing 10 mM ammonium acetate in acetonitrile adjusted to pH=5.00 using acetic acid) from solvent A (10 mM ammonium acetate in water adjusted to pH= 5.00 using acetic acid). The gradient was 1% B at injection for 1 minute, increased to 5% at 3 min, 60% at 8 min, 99% at 8.5 min and then re-equilibrated to initial conditions over 3.5 min.

2.2.9. Observing the appearance of anthocyanin metabolites in the colon model samples using UPLC-TOF Analysis

This is another detection technique and was used for observing the formation of anthocyanin metabolites. Samples were analysed using a Waters Synapt G2si time of flight (TOF) mass spectrometer coupled to a Waters Acquity UPLC. Chromatography was performed using a Waters HSS T3 100 x 2.1 mm, 1.7 μm separating column at 37°C and a binary gradient of solvent A (10 mM Ammonium acetate in Water) and B (10 mM Ammonium acetate in Acetonitrile, pH= 5) at a flow rate of 400 $\mu\text{L}/\text{min}$. The gradient was 1% B with injection for 1 minute, increased to 5% at 3 min, 60% at 8 min, 99% at 8.5 min and then re-equilibrated to initial conditions over 3.5 min. Sample injections were 2 μL . The TOF was operated in negative electrospray and full scan mode, 100-1200 amu with a 0.3 sec scan time.

2.2.10. Statistical Analysis

Unless otherwise stated, statistical analysis was performed in GraphPad Prism (version 9.3 for Windows, GraphPad Software, La Jolla California USA, www.graphpad.com). One-way ANOVA with Tukey's Multiple Comparison test was used to compare the concentration means of spontaneous and microbiota-dependent at specific timepoint and $p < 0.05$ was considered statistically significant. Values of $p > 0.05$ were considered significant (*, $p < 0.05$; **, $p < 0.01$; ***, $p < 0.001$; ****, $p < 0.0001$).

2.3. Spontaneous degradation of anthocyanins

All water used was 18 M Ω /cm Milli-Q water, and solvents were of high-performance liquid chromatography (HPLC) grade. Cyanidin-3-*O*-glucoside (Kuromanin chloride), cyanidin (Cyanidin chloride), and delphinidin (Delphinidin chloride) were purchased from Extrasynthese (Genay, France). Other chemicals and reagents were purchased from Sigma unless otherwise stated.

2.3.1. Incubating Cya3Glc in colon media and phosphate buffer solution

On the day of the experiment, a fresh stock solution (SS) of Cya3Glc (2 mg/mL) was prepared by dissolving 2 mg of the authentic compound in 1 mL DMSO.

The anaerobic incubation of Cya3Glc

A colon media (0.5 mM K phosphate, pH 7.0) was prepared and autoclaved then placed in the anaerobic cabinet overnight. Inside the anaerobic cabinet and in a 10 mL vial, a 168.5 μ L of SS was added to 4831.5 μ L media to give a final volume of 5 mL with Cya3Glc concentration of 150 μ M, then immediately the first sample at 0 h was collected into a 1 mL HPLC vial, capped, taken to HPLC analysis. Other samples were collected for injections at the times to determine the Cya3Glc concentration. External standard curves of serial concentrations of Cya3Glc were prepared in acidified colon model media (4% v/v formic acid).

The aerobic incubation of Cya3Glc

A phosphate buffer (10 mM K phosphate, pH 7.4) and colon media (0.5 mM K phosphate, pH 7.0) were prepared and autoclaved. On the day of the experiment, a fresh stock solution (SS) of Cya3Glc (2 mg/mL) was prepared by dissolving 2 mg of the authentic compound in 1 mL dimethyl sulfoxide (DMSO). In 1 mL HPLC vials and separate days, two experimental vials (n=2) were prepared for each medium by adding 168.5 μ L of SS to 4831.5 μ L medium) to give a final volume of 5 mL and a Cya3Glc concentration of 150 μ M, then immediately the experimental vials were put in LC-DAD autosampler for injections at the times to determine the Cya3Glc concentration. The external standard curve of serial concentrations of Cya3Glc was prepared in acidified phosphate buffer or colon media (4% v/v formic acid).

2.3.2. Incubating anthocyanidins (Cya and Del) aerobically in phosphate buffer solution

On the day of the experiment, a fresh stock solution (SS) of Cya3Glc (2 mg/mL) was prepared by dissolving 2 mg of the authentic compound in 1 mL DMSO.

A phosphate buffer (10 mM K phosphate, pH 6.8) was prepared and autoclaved. On the day of the experiment, a fresh stock solution of Cya (1 mg/mL) was prepared by dissolving 1 mg of the authentic compound in 1 mL DMSO. In a 1mL HPLC vial, 100 μ L of SS was added to 900 μ L phosphate buffered solution to give a final Cya concentration of 222 μ M, then immediately the experimental vial was incubated in LC-DAD autosampler at 37°C and then injections were carried out at the times to determine the Cya concentration. The external standard curve of serial concentrations of Cya was prepared in acidified phosphate buffer (4% v/v formic acid). Each experiment was carried out once.

2.3.3. Quantify Cya3Glc, Cya, and Del concentrations and their break down products using HPLC-DAD-MS

The chromatographic separation was carried out on a reverse-phase HPLC column. 20 μ l of the sample was injected into Kinetex XB-C18 column (100 \times 4.6 mm; particle size 2.6 μ m) at 40°C using 1% aqueous formic acid (eluent A) and 1% formic acid in acetonitrile (eluent B) at a flow rate of 1 mL/min. The gradient started with 2% B at 0 min, increased to 10% B at 15 min, 15% at 20 min, 30% at 25 min, 50% at 27 min and then re-equilibrated to initial conditions over 2 min. The autosampler temperature was 37°C. The MS was set up on full scan mode and negative ionisation polarity.

2.3.4. Monitoring the formation of the break down products of Cya3Glc, Cya, and Del using UPLC-TOF method

This is another detection technique that was used for observing the formation of anthocyanin metabolites. Samples were analysed using a Waters Synapt G2si time of flight (TOF) mass spectrometer coupled to a Waters Acquity UPLC. Chromatography was performed using a Waters HSS T3 100 x 2.1 mm, 1.7 μ m separating column at 37°C and a binary gradient of solvent A (10 mM ammonium acetate in water) and B (10 mM

ammonium acetate in acetonitrile, pH= 5) at a flow rate of 400 $\mu\text{L}/\text{min}$. The gradient was 1% B with injection for 1 minute, increased to 5% at 3 min, 60% at 8 min, 99% at 8.5 min and then re-equilibrated to initial conditions over 3.5 min. Sample injections were 2 μL . The TOF was operated in negative electrospray and full scan mode, 100-1200 amu with a 0.3 sec scan time

2.3.5. Statistical Analysis

Unless otherwise stated, statistical analysis was performed in GraphPad Prism (version 9.3 for Windows, GraphPad Software, La Jolla California USA, www.graphpad.com). Differences between controls (purified Cya3Glc standard spiked directly into acidified medium at $t=0$) and experimental conditions (aerobic and anaerobic spontaneous degradation of Cya3Glc in colon media or phosphate buffer) were carried out using one-way analysis of variance (ANOVA) with Tukey's Multiple Comparison Test and $p < 0.05$ was considered statistically significant. Comparison between aerobic and anaerobic spontaneous degradation of Cya3Glc was analysed by unpaired t-test with two-tailed p -value and $p < 0.05$ was considered statistically significant. Values of $p > 0.05$ were considered significant (*, $p < 0.05$; **, $p < 0.01$; ***, $p < 0.001$; ****, $p < 0.0001$).

2.4. Changes of the gut microbiota structure and function

The black rice extract powder was purchased from the Beijing Gingko Group (BGG), China. FastDNA 2mL Spin Kit for Soil was purchased from MP Biomedicals (Germany). All water used was 18 MΩ/cm Milli-Q water, and solvents were of high-performance liquid chromatography (HPLC) grade.

Other chemicals and reagents were purchased from Sigma unless otherwise stated.

2.4.1. Study design for incubating anthocyanins with faecal gut microbiota using *in-vitro* colon model

Batch fermentation *in-vitro* human colon model experiment was carried out as previously described in this chapter where section (2.2.3) for preparing 10% fresh faecal slurry, section (2.2.5) for setting up the batch colon model, and section (2.2.6) for incubating the anthocyanin-rich extract in the batch colon model.

Briefly, 14 colon model vessels were prepared and filled with 89 mL autoclaved colon media the night before the experiment: 7 vessels for the treatment with black rice anthocyanins, 7 vessels as controls with no addition of black rice anthocyanins, and 2 vessels used as contamination controls where only autoclaved colon media was added. On the day of treatment, a fresh human faecal sample was diluted 1/10 w/v with phosphate buffer and homogenised to generate the faecal slurries that were used as inocula. Then 10 mL of faecal slurry was added to each vessel of treatment and control (except for contamination control vessels). In the treatment vessels, 1 mL of filtered black rice anthocyanins solution (18 mg/mL of black rice powder) was added. The final concentration of anthocyanins in a total volume of 100 mL was 133.3 μM. Samples (5 mL) were collected at 0, 6, 12, and 24 h and immediately stored at -80°C until extracting the DNA.

2.4.2. Extraction of DNA from colon model samples

Sample preparation

The frozen samples were thawed on ice, then vortexed (5 sec) and 2.5 mL of 1% w/v faecal sample were aliquoted in sterile 5 mL Eppendorf vials and centrifuged for 10 mins

at full speed (14,000 x g). The supernatant was discarded carefully (decantation), and the sediment was kept. The pellet was resuspended again using molecular grade water (400 μ L for 0 h samples, 500 μ L for 6 h samples and 600 μ L for 12 and 24 h samples). Afterwards, 400 μ L was transferred into Lysing Matrix E Tubes, then frozen at -80°C until DNA extraction.

DNA extraction

The DNA extraction was carried out as previously described by Kellingray and others¹⁹⁹ using FastDNA™ SPIN Kit for Soil. Briefly, samples were thawed on ice and 980 μ L sodium phosphate buffer and 120 μ l MT buffer were added to the sample and then vortexed. Samples were placed in a refrigerator (+4°C) for ~ 1 h. Then, samples were lysed in a Fastprep machine for 60 s three times (speed: 6.5 m/s). Afterwards, Lysing Matrix E Tubes were centrifuged for 15 min at 14000 x g. The supernatant (650 μ L x2) was transferred into a clean 2 ml Eppendorf tube, and then added 250 μ l PPS reagent and mixed by shaking the tube by hand 10 times (invert). Samples were centrifuged for 10 min at 14000 x g to precipitate the pellet. The supernatant (750 μ L x2) was then transferred into a sterile 5 ml Eppendorf tube, and 1 ml of Binding Matrix Suspension was added to the supernatant. The tubes were inverted by hand for two minutes and were then left to stand in a rack for 3 min (to allow settling of silica matrix). Approximately 1 mL of supernatant was removed and discarded, then the binding matrix was resuspended into the remaining supernatant. Approximately 700 (x2) μ L of the mixture was transferred into a SPIN Filter tube and centrifuged for 2 min at 14,000 x g. The flow-through was decanted and 500 μ l SEWS-M was added into the SPIN Filter tube and then centrifuged for 1 min at 14,000 x g. The flow-through was decanted again to perform SEWS-M wash altogether three times. the flow-through was decanted and centrifuged for 5 min at full speed (14,000 x g) to 'dry' the matrix of residual SEWS-M wash solution. Then the SPIN Filter was removed and placed into a fresh Catch Tube, then it was left in the SPIN Filter for 10 min to dry at room temperature. Afterwards, 65 μ l DES (DNase/Pyrogen Free Water) was added and the matrix was gently stirred on the filter membrane using a pipette tip for efficient elution of the DNA. Air dry samples for a few min was carried out, then centrifuged for 2 min at full speed (14,000 x g) to elute DNA (or at 6,400 x g with open lids). The collected samples were stored at -20°C until preparation for sequencing.

2.4.3. Shotgun metagenomics sequencing for extracted DNA from colon model samples

Samples concentrations were normalised to 5 ng/ μ L using molecular grade water and 15 μ L samples were pipetted into a 96-well plate. DNA samples were then quantified using Qubit broad range reagents according to manufacturer guidelines (Thermo-fisher, Cambridge, UK). Afterwards, NanoSeq (a DNA library preparation and sequencing protocol based on Duplex Sequencing) was run for all samples to create a library which was then pooled together into one tube. Metagenomics shotgun sequencing was performed by Novogene European Headquarters (Cambridge, UK), using Illumina NovaSeq, to generate 150bp paired-end libraries to a sequencing depth of \sim 30 million reads. Dr Perla Rey (Bioinformatician at QIB) checked, cleaned, and analysed the sequence data using in-house bioinformatic tools and performed taxonomic and functional profiling of the metagenomics dataset.

2.4.4. Read processing for metagenomics sequencing data

The host DNA contamination is expected in metagenomics datasets, and thus the first step in processing metagenomics sequencing data is to remove host sequences. A tool commonly used for the pre-processing of metagenomics dataset is KneadData v0.10.0 (<https://github.com/biobakery/kneaddata>), which uses bowtie and bowtie indexes for the removal of host reads. In addition, KneadData is also used to remove adapter sequences, and perform quality control using Trimmomatic²⁰⁰. Trimmomatic: A flexible trimmer for Illumina Sequence Data. Bioinformatics, btu170] and remove other contaminant sequences. The human (hg37) reference database (which includes the human genome and transcriptome) is based on the Decoy Genome (<http://www.cureffi.org/2013/02/01/the-decoy-genome/>). Other contaminant sequences were taken from Breitwieser and others²⁰¹. Finally, bacterial rRNA reads from SILVA were also removed. KneadData was used with the option `--run-trim-repetitive` for shotgun sequences to trim overrepresented sequences. Only high-quality trimmed, and non-contaminant paired reads (in which both reads passed filtering) are used for downstream analyses. This work was performed by Dr Perla Rey, QIB.

2.4.5. Microbial Community Profiling for metagenomics sequencing data

High-quality and trimmed reads are used to estimate the microbial composition profiles using MetaPhlAn v3.0.2^{202,203}. MetaPhlAn identifies the microbes and their abundance from metagenomics reads by mapping them to the ChocoPhlAn database of unique clade-specific marker genes. Clades are a group of organisms and clade-specific markers are coding sequences that are strongly conserved within the clade's genomes and are sufficiently different to any sequence outside the clade. The marker genes in the ChocoPhlAn database were identified from over 17,000 reference genomes from bacteria, archaea, viruses and eukaryotes²⁰³. An initial exploratory analysis is performed using a Multidimensional Scaling, MDS plot. An MDS plot is an ordination plot where points represent objects, in this case, samples, in which closer points are more alike than those further apart. The points on the plot are arranged so that the distances among each pair of points represent the dissimilarity between those two samples. This work was performed by Dr Perla Rey, QIB.

2.4.6. Metabolic reconstruction and pathway analysis using HUMAnN3 for metagenomics sequencing data

The HMP (Human Microbiome Project) Unified Metabolic Analysis Network, HUMAnN, is a method for profiling the abundance of microbial metabolic pathways and other molecular functions from metagenomic sequencing data. It infers community function directly from short DNA reads²⁰⁴. It uses KEGG Orthology to estimate abundance of each orthologous gene family in the community. Orthologous families are groups of genes that perform roughly the same biological roles. Pathways are sets of two or more genes with a similar function.

For the analysis of the metagenomics dataset, the latest version of HUMAnN, HUMAnN3 (v3.0.0.alpha.3) is used. The analysis starts with a search in different levels: first, a taxonomic search maps short reads to clade-specific marker genes to identify community species (using MetaPhlAn v3.0.2 and -the nucleotide database- ChocoPhlAn database v296_201901), second, mapping reads to community pangenomes of identified species (using bowtie v2.4.4), and finally, alignment of unclassified reads to a protein database (using DIAMOND v2.0.11). Mapping results are then used to estimate the per-species and community total gene family abundances which considers alignment quality, gene

length and coverage. Then, genes are mapped to metabolic reactions, and pathway quantification and coverage are estimated. A pathway is a set of two or more genes.

The analysis with HUMAnN3 was done using nucleotide mapping and translated search to provide organism-specific gene and pathway abundance profiles from our high-quality shotgun metagenomic reads. Gene families are annotated using UniRef90 definitions²⁰⁵, which is a protein database, it is the UniProt Reference Clusters that provide clustered sets of sequences. UniRef90 is built such as each cluster is composed of sequences that have at least 90% sequence identity and 80% overlap with the longest sequence of the cluster. Pathways are annotated using MetaCyc definitions^{206–208}. MetaCyc is a curated database of metabolic pathways from all domains of life. It contains 2,937 pathways from over 3,000 different organisms. Humann3 was used with the default options (minimum percentage of reads matching a species: 0.01, identity threshold for nucleotide alignments: 0.0), using uniref90 to annotate gene families. To be able to compare gene families and pathway abundances between samples with different sequencing depths, we used normalised values using “copies per million”, CPM, or sum-normalisation to relative abundance. Furthermore, using the gene family abundances, HUMAnN3 is used to reconstruct the abundance of enzyme commission (EC) categories in the microbiome using the function `humann_regroup_table`. This work was performed by Dr Perla Rey, QIB.

2.4.7. Statistical associations with MaAsLin2 for metagenomics sequencing data

MaAsLin2 is used to find associations between community total abundances with the effect of the treatment over time²⁰⁹. Specifically, MaAsLin2 is used by selecting Linear Model (LM) method to test the association between Pathway relative abundances and the effect of anthocyanins in the microbiome. The same was done using EC category relative abundances. Relative abundances are normalised using TSS normalisation and AST transformation. The following formula is used for the Linear Model, where the relative abundance of the Pathway or EC category (expression) is determined by the interaction between treatment (control, anthocyanin) and TimePoint (0h, 6h, 12h). This work was performed by Dr Perla Rey, QIB.

Chapter Three

Preparing anthocyanin-rich extracts from black rice and bilberry using green extraction processes

Chapter 3: Preparing anthocyanin-rich extracts from black rice and bilberry using green extraction processes

3.1. Abstract

Background: Anthocyanins are present in plant tissues in very small concentrations. The conventional extraction techniques for anthocyanins usually involve the use of high amounts of organic solvents which are expensive and toxic, hence highly purified anthocyanins are very expensive to purchase. However, in the last few years, eco-friendly extraction approaches have been developed with a promising recovery of bioactive compounds from plant materials. Thus, there is considerable literature on eco-friendly “green” approaches for recovering plant bioactive compounds.

Aim and approach: The overall aim of research presented in this chapter was to prepare anthocyanin-rich extracts using green solvents, and then use these anthocyanin-rich extracts for subsequent investigations into microbial metabolism of anthocyanins by the human gut microbiota. The focus of the research reported in this chapter was to carry out a step-by-step optimisation of an eco-friendly extraction methodology to recover anthocyanins from black rice grains and bilberry fruits. The specific steps were to (i) choose the optimum solvent mixture composed of glycerol and water with the highest anthocyanin recovery; (ii) investigate the optimum liquid-to-solid ratio ($R_{L/S}$) for high extraction efficacy of anthocyanins; then (iii) examine the effect of temperature on the recovery of anthocyanins from the extraction mixtures.

Results: The chemical composition of anthocyanins was determined in black rice and bilberry after their extraction using a conventional solvent. Cya3Glc was the predominant anthocyanin in black rice with 84.3% w/w of the total anthocyanins ($179 \text{ mg } 100 \text{ g}^{-1} \text{ dw}$). Whereas a mixture of fourteen anthocyanins which were predominantly delphinidin, cyanidin, petunidin, peonidin and malvidin derivatives were detected in bilberry fruits with a total concentration of $1775 \text{ mg } 100 \text{ g}^{-1} \text{ dw}$. The alternative solvent of 80% w/v glycerol/water showed better extraction efficiency for anthocyanins from black rice

(211 mg 100 g⁻¹ dw) and bilberry (2635 mg 100 g⁻¹ dw) compared to the conventional solvent. In addition, the liquid-to-solid ratio ($R_{L/S}$) = 60 mL g⁻¹ was shown to be the optimum ratio for higher recovery of anthocyanins, providing corresponding anthocyanin concentration of 190 mg 100 g⁻¹ dw black rice powder and 2600 mg 100 g⁻¹ dw bilberry powder. Extraction temperature showed a significant effect on anthocyanin recoveries, and the extraction process at 80°C gave the highest anthocyanin recoveries for a shorter extraction time of 20 min for black rice (211 mg 100 g⁻¹ dw) and 15 min for bilberry (3119 mg 100 g⁻¹ dw).

Conclusion: Compared to the conventional solvent, the extraction efficiency of black rice and bilberry anthocyanins was higher when using 80% glycerol/water solvent. However, the recovered concentrations were relatively low and in larger volumes mainly consisting of glycerol. As such it was concluded that this would not be ideal for subsequent experiments investigating the gut microbial metabolism of anthocyanins.

3.2. Introduction

The extraction approaches for plant-derived phytochemicals are varied and they depend on different parameters such as time, the number of aqueous and organic solvent phases, impact on the environment, and type of extraction medium²¹⁰. The extraction solvent used for polyphenols is mainly a mixture of both aqueous and organic solvents. Polyphenols including anthocyanins, are present in plant tissues in very small concentrations. Therefore, extraction processes of polyphenols using conventional techniques usually involve the use of high amounts of organic solvents²¹¹. In these processes, petroleum-based solvents are used usually consisting of volatile organic components such as halogenated hydrocarbons (e.g., chloroform), aromatic hydrocarbons (e.g., hexane and toluene), alcohols (e.g., methanol), ethers (e.g., diethyl ether), and ketones (e.g., acetone). Many of these organic solvents are either toxic, highly flammable or detrimental to the environment²¹². In the last few years, eco-friendly “green extraction” approaches have been expanded endeavouring to increase the recovery of phytochemical yields, meanwhile being eco-friendly to the environment²¹³. The “green extraction” is usually defined as extraction processes which involve one or more of these factors: less time, less energy, and/or less harm to health and the environment. Thus, there

is considerable literature on extraction, separation, and purification of phytochemicals using eco-friendly approaches. Other alternative solvents have also been investigated including ionic liquid, superheated water, surface active agents, supercritical fluids, bio-derived solvents, deep eutectic and natural deep eutectic solvents²¹⁰. For extraction of anthocyanins, the conventional medium used is acidified aqueous ethanol or methanol^{65,214}. Due to their notoriously poor stability, the purification and separation of anthocyanins are usually carried out using columns rather than solvent evaporation²¹⁵. This technique is laborious and is associated with high consumption of organic solvents.

In the literature, few reports have been published on the extraction of anthocyanins using eco-friendly solvents. However, the most commonly used solvents were supercritical fluids and deep eutectic solvents (usually a combination of a constituent termed as hydrogen bond donor and another one termed as hydrogen bond acceptor)²¹⁰. For example, a report showed a choline chloride-based deep eutectic solvent, containing oxalic acid with 25% water, was more effective for extracting the black-purple rice anthocyanins compared to an aqueous menthol solvent²¹². In addition, another report also obtained promising anthocyanin yield from blueberry by using natural deep eutectic solvents compared to conventional solvent (acidified aqueous methanol)²¹⁶. Another solvent alternative reported in the literature was glycerol/water medium. A mixture of 90% w/v glycerol/water was the optimum medium for phenolic recoveries from two different species of *Artemisia*²¹⁷. Similarly, glycerol/water (90% w/v) showed to be the optimal solvent for extracting phenolic and pigment compounds from onion solid waste²¹⁸. These findings showed that the mixture between glycerol and water has a high potential for extracting anthocyanins from their plant materials. In this context, a glycerol/water medium, as a cost-effective and green alternative solvent, was used to extract and prepare an anthocyanin-rich extract from two commercial materials of black rice and bilberries.

3.3. Objectives

The overall aim was to develop an extraction approach for preparing anthocyanin-rich extracts which will subsequently be used for the investigation of anthocyanin metabolism by the human gut microbiota. The approach was to use green solvents to recover

anthocyanins from black rice and bilberry raw materials. The specific objectives were to: (i) identify the anthocyanins and determine the anthocyanin composition of black rice and bilberry, (ii) investigate how different mixtures of glycerol and water affect the amount of anthocyanins extracted; (iv) determine the relationship between the liquid-to-solid ratio ($R_{L/S}$) and the amounts of anthocyanins extracted; and (iv) determine the effect of temperature on the amounts of anthocyanins extracted and (v) determine the amounts extracted using a combination of the most effective conditions.

3.4. Results

3.4.1. Identification of anthocyanin composition of black rice and bilberry powders

The anthocyanin composition of black rice and bilberry has been reported previously^{55,219–222}. However, it was necessary to determine the anthocyanin content and composition of the black rice and bilberry samples which were used to prepare anthocyanin-rich extracts. Raw plant materials of both black rice grains and bilberry fruits were purchased and then ground (**Figure 2. 1**) using a domestic coffee grinder. The extraction of anthocyanins was carried out using acidified aqueous ethanol (60% v/v) separately for each plant material. The determination of anthocyanin composition was accomplished using HPLC-DAD-MS (**Chapter 2, section 2.1.8**).

The concentration of total anthocyanins in black rice powder was 178.9 mg (100 g dw powder)⁻¹. At λ (520 nm), seven peaks were detected (**Figure 3. 1**) in black rice extract at different retention times (RT) with different masses as shown in **Table 3. 1**. Cya3Glc ($m/z[M+H]^+$ 449.1; RT 13.7) was shown to be a predominant anthocyanin (84.4 % w/w of the total anthocyanins) in black rice powder followed by Peo3Glc ($m/z[M+H]^+$ 463.1; RT 18.4) with 11 % w/w of the total anthocyanins. These anthocyanins were identified using reference standards, retention times at 520 nm, and MS data. In addition, five other peaks were detected at λ (520 nm) which are putatively identified as follows: Unknown 1 ($m/z[M+H]^+$ 737; RT 3.9), Cya35diGlc ($m/z[M+H]^+$ 611.1; RT 12.0), Cya3Glc-*p*-coumarate ($m/z[M+H]^+$ 595.1; RT 16.4), unknown 2 ($m/z[M+H]^+$ 465.1; RT 18.7), and Peo3Glc-*p*-coumarate ($m/z[M+H]^+$ 609.3; RT 19.2).

Table 3. 1. The content of anthocyanins in black rice powder

Peak	RT (min)	Parent ion m/z [M+H] ⁺	Fragment ions [M+H] ⁺	Identified anthocyanin	Content (mg 100 g ⁻¹ d.w.)
1	3.9	737.1	287.1	Unknown 1 (Cya type)	1.0 ^a
2	12.0	611.1	449.1, 287.1	Cya35diGlc	1.7 ^a
3	13.7	449.1	287.1	Cya3Glc	150.9 ^a
4	16.4	595.1	287.1	Cya3Glc- <i>p</i> -coumarate	1.9 ^a
5	18.4	463.1	301.1	Peo3Glc	19.7 ^b
6	18.7	465.1	303.1	Unknown 2	Traces
7	19.2	609.1	465.1, 433.1	Peo3Glc- <i>p</i> -coumarate	3.7 ^b
				Total	178.9

^a =expressed as Cya3Glc^b =expressed as Peo3Glc

In bilberry powder, fourteen different anthocyanin compounds were detected at λ (520nm) (Figure 3. 2) and quantified with a total anthocyanin content of 1774.6 mg (100 g dw powder)⁻¹. All individual bilberry anthocyanins are presented with their parent ion [M+H]⁺, fragment ions, and contents. Although, various anthocyanins were identified, only monosaccharide-anthocyanins were identified and no disaccharide or acylated anthocyanins were detected.

Five peaks were identified using reference standards and retention times, UV-Vis and MS data as follows: Del3Glc (m/z [M+H]⁺ 465.1; RT 10.2), Cya3Glc (m/z [M+H]⁺ 449.1; RT 13.8), Pet3Glc (m/z [M+H]⁺ 479.1; RT 16.8), Peo3Glc (m/z [M+H]⁺ 463.1; RT 18.4), and Mal3Glc (m/z [M+H]⁺ 493.1; RT 18.9). The remaining nine anthocyanins were putatively identified using their mass data and from literature²²³ as follows: Del3Glc (m/z [M+H]⁺ 465.1; RT 8.3), Cya3Gal (m/z [M+H]⁺ 449.1; RT 11.3), Del3Ara (m/z [M+H]⁺ 435.1; RT 12.1), Cya3Ara (m/z [M+H]⁺ 419.1; RT 15.0), Peo3Gal (m/z [M+H]⁺ 463.1; RT 17.5), Pet3Ara (m/z [M+H]⁺ 449.1; RT 17.9), Mal3Gal (m/z [M+H]⁺ 493.1; RT 18.6), Peo3Ara (m/z [M+H]⁺ 433.1; RT 18.7), and Mal3Ara (m/z [M+H]⁺ 463.1; RT 19.2).

Table 3. 2. The content of anthocyanins in bilberry powder

Peak	RT (min)	Parent ion [M+H] ⁺	Fragment ions [M+H] ⁺	Identified anthocyanin	Content (mg 100 g ⁻¹ d.w.)
1	8.3	465.1	303	Del3Gal	172.4 ^a
2	10.2	465.1	303	Del3Glc	272.0 ^a
3	11.3	449.1	287	Cya3Gal	107.3 ^b
4	12.1	435.1	303	Del3Ara	161.3 ^a
5	13.8	449.1	287	Cya3Glc	221.4 ^b
6	15.0	419.1	287	Cya3Ara	182.4 ^b
7	16.8	479.1	317	Pet3Glc	177.3 ^c
8	17.5	463.1	301	Peo3Gal	22.1 ^d
9	17.9	449.1	317	Pet3Ara	54.5 ^c
10	18.4	463.1	301	Peo3Glc	99.6 ^d
11	18.6	493.1	331	Mal3Gal	74.3 ^e
12	18.7	433.1	301	Peo3Ara	17.6 ^d
13	18.9	493.1	331	Mal3Glc	161.5 ^e
14	19.2	463.1	331	Mal3Ara	51.0 ^e
Total					1774.6

^a=expressed as Del3Glc, ^b=expressed as Cya3Glc, ^c=expressed as Pet3Glc, ^d=expressed as Peo3Glc, and ^e=expressed as Mal3Glc

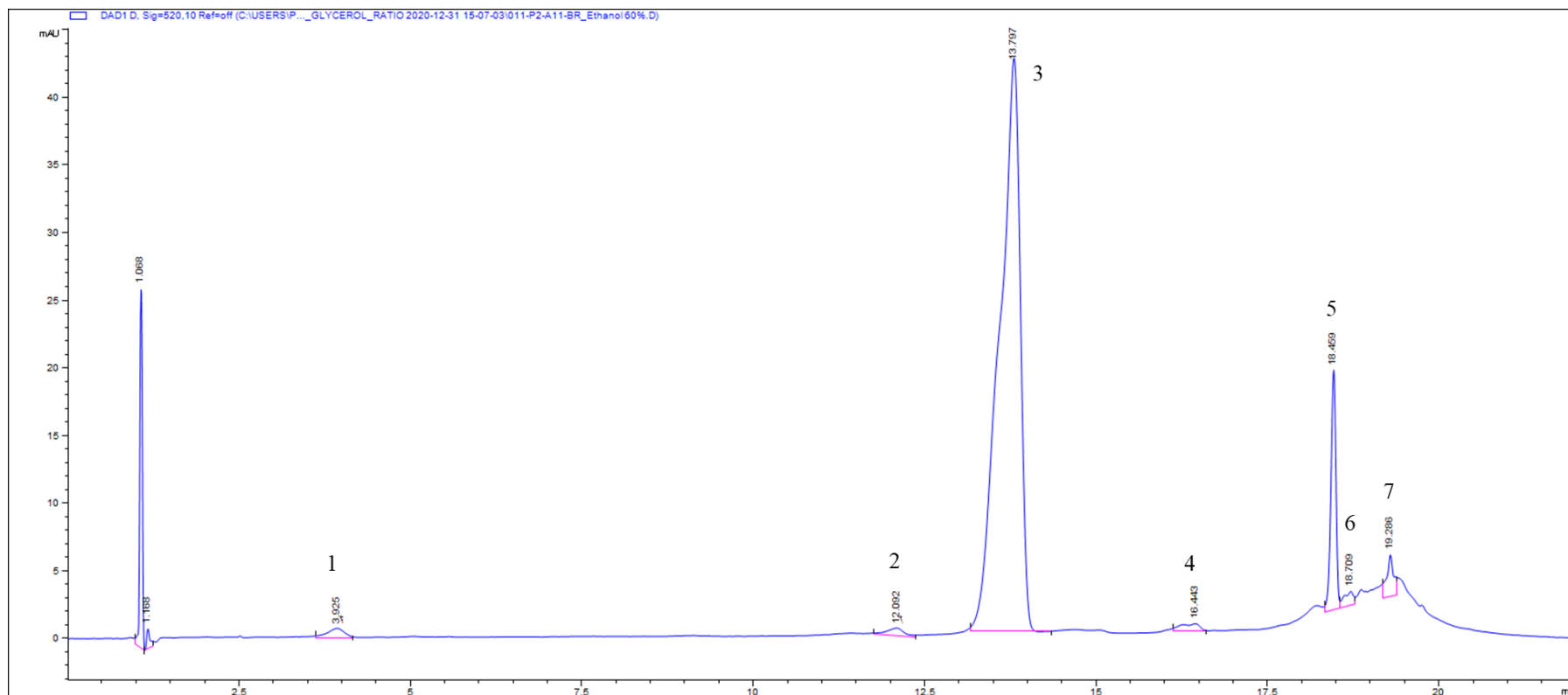


Figure 3. 1. DAD chromatogram at 520 nm showing anthocyanins identified in black rice powder.

One gram of black rice powder was subjected to the extraction process under stirring at 600 rpm with 50 mL acidified aqueous ethanol (60% v/v) for 180 min at room temperature. 20 μ L of the extracted solution was injected onto Kinetex XB-C18 column (Reversed phase; 100 \times 4.6 mm; particle size 2.6 μ m) at 40 $^{\circ}$ C using a gradient separation by 5% aqueous formic acid (eluent A) and 5% formic acid in acetonitrile (eluent B).

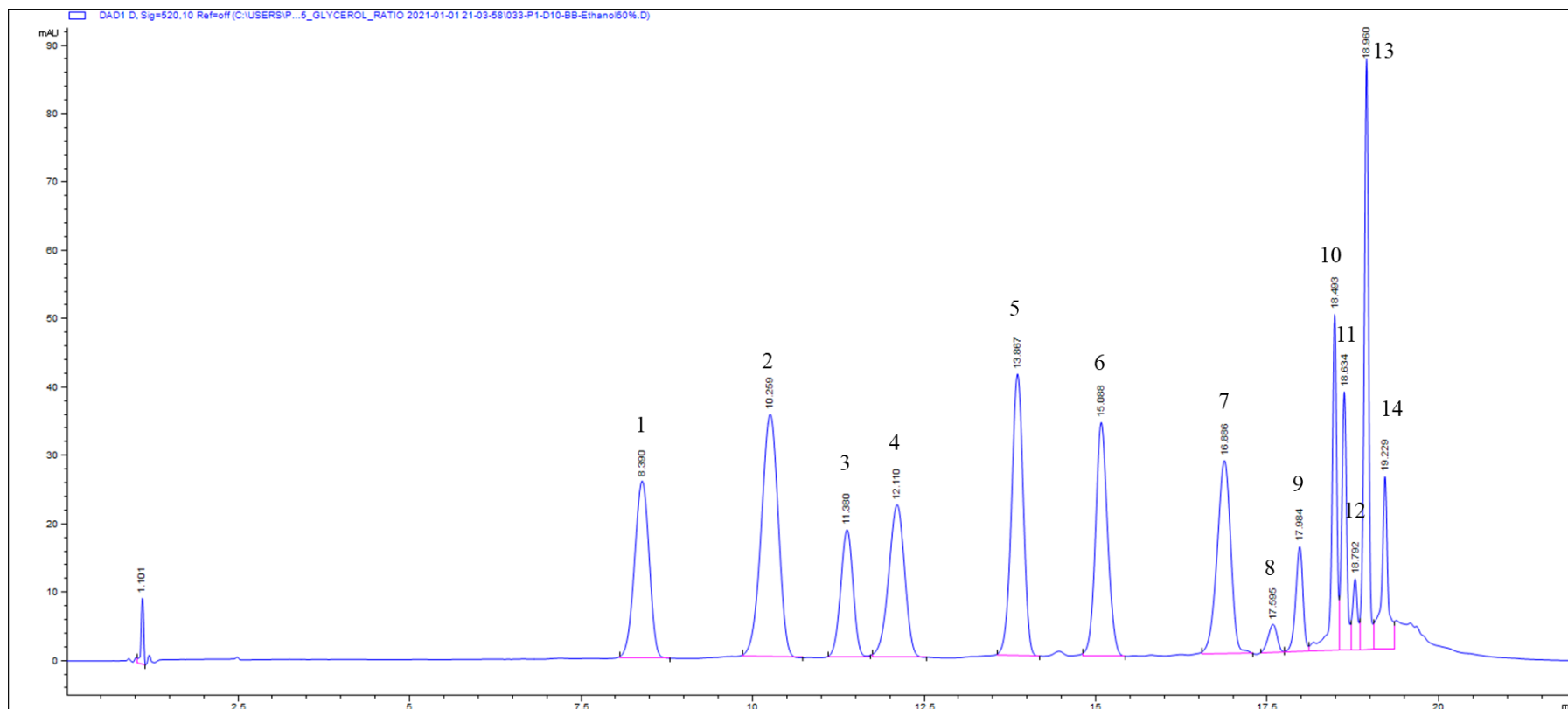


Figure 3. 2. DAD chromatogram at 520 nm showing anthocyanins identified in bilberry powder.

One gram of bilberry powder was subjected to an extraction process under stirring at 600 rpm with 50 mL acidified aqueous ethanol (60% v/v) for 180 min at room temperature. 20 μ L of the extracted solution was injected onto Kinetex XB-C18 column (Reversed phase; 100 \times 4.6 mm; particle size 2.6 μ m) at 40 $^{\circ}$ C using 5% aqueous formic acid (eluent A) and 5% formic acid in acetonitrile (eluent B).

3.4.2. Effects of the glycerol to water ratio on the amounts of anthocyanins extracted from black rice and bilberry

For a “green” extraction process, an alternative, eco-friendly and a cost-effective solvent mixture of glycerol/water was tested. To assess how different ratios affected the total quantity of anthocyanins extracted, nine different ratios ranging from 10 to 90% w/v glycerol/water were prepared. A 1 g of black rice or bilberry powders were subjected to an extraction process using 50 mL of solvent for 180 min (**Chapter 2, section 2.1.2**). A control solvent of acidified aqueous ethanol (60 % v/v) was also used for comparison. At the end of extraction, samples were collected, and spectrophotometric methods were used to quantify total polyphenols and pigments (**Chapter 2, section 2.1.5-6**), whereas HPLC-DAD was used to quantify total anthocyanins (**Chapter 2, section 2.1.7**). Polyphenols were quantified as gallic acid equivalents (GAE), while pigments were quantified as Cya3Glc equivalents (C3GE).

For black rice powder, 80% w/v glycerol/water solvent was the most effective mixture to extract anthocyanins (**Figure 3. 3**). No significant difference in total pigments between conventional solvent and various mixtures of glycerol/water solvents (60, 70, and 80%, w/v) was observed. However, the 80% w/v glycerol solvent showed better anthocyanin and polyphenol recoveries compared to the conventional solvent. For example, the recovered anthocyanin concentrations were 211 mg 100 g⁻¹ dw powder when using 80% w/v glycerol/water solvent, while it was 178 mg 100 g⁻¹ dw powder when using the conventional solvent. Furthermore, there was a significant difference ($p < 0.0001$) in recovered polyphenols between the 80% w/v glycerol/water extraction and the conventional solvent extraction (900 ± 25 and 520 ± 20 mg 100 g⁻¹ dw powder, respectively). However, no significant differences in extracted pigments between conventional solvent (360 ± 5 mg 100 g⁻¹ dw powder) and 80% w/v glycerol solvent (335 ± 10 mg 100 g⁻¹ dw powder) were observed. Regarding solvents of glycerol/water ranged from 10 to 50 % w/v, the extracted polyphenols, pigments, and anthocyanins were considerably lower than using the conventional solvent of aqueous ethanol (60%, v/v).

Similarly, for bilberry powder, the 80% w/v glycerol/water solvent gave the highest recovery of bilberry anthocyanins (**Figure 3. 4**). Significant differences were observed between conventional solvent and solvents of 80 and 90 % w/v glycerol/water on the

recovery of polyphenols ($P<0.0001$) and pigments ($P<0.0001$). For example, the conventional solvent gave a polyphenol concentration of $2850 \pm 60 \text{ mg } 100 \text{ g}^{-1} \text{ dw}$, whereas 80 and 90 % w/v glycerol solvents showed better polyphenol recoveries of 3550 ± 150 and $3420 \pm 50 \text{ mg } 100 \text{ g}^{-1} \text{ dw}$, respectively. However, the 80% glycerol solvent showed slightly better extraction of total polyphenols than the 90% w/v glycerol solvent. Although there was no significant difference in the extracted polyphenols between 80 and 90% w/v glycerol/water medium, the quantified recovered anthocyanins by 80 and 90% w/v glycerol/water solvents were significantly higher ($P<0.0001$) at 2635 and 2716 mg $100 \text{ g}^{-1} \text{ dw}$, respectively, compared to control solvent (1775 mg $100 \text{ g}^{-1} \text{ dw}$ powder). In addition, the total extracted pigment was similar between 80 and 90% w/v glycerol solvent with 2067.4 mg C3GE 100 g^{-1} and 2046.7 mg C3GE $100 \text{ g}^{-1} \text{ dw}$ powder, respectively. Furthermore, solvents of glycerol/water (ranging from 10 to 50 % w/v) showed lower extraction effectiveness in polyphenols, pigments and anthocyanins than using the conventional solvent of aqueous ethanol (60%, v/v).

Therefore, 80% w/v glycerol/water solvent was selected as a suitable solvent mixture for extraction of anthocyanins from both black rice and bilberry powders.

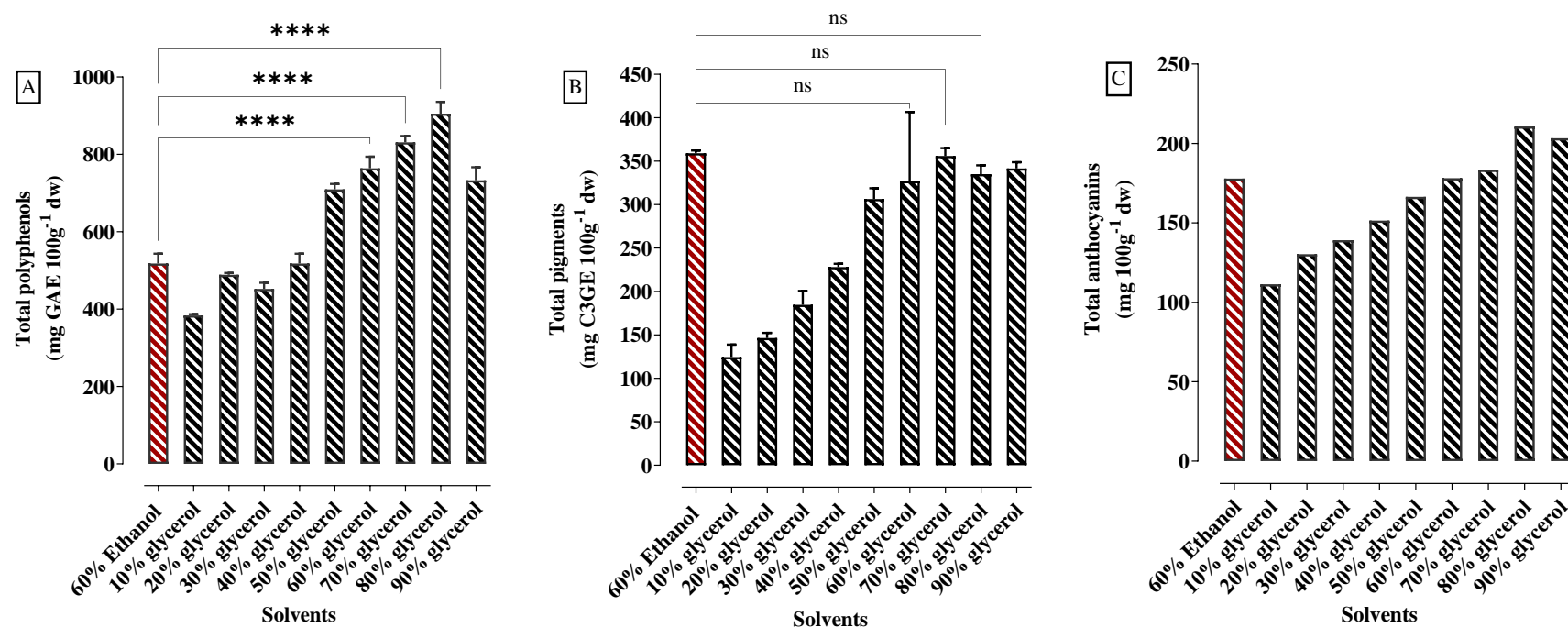


Figure 3.3. Bar plot showing quantification assays and recoveries from black rice powder achieved by various glycerol/water mediums ranging between 10-90%.

A 1 g plant powder was added to 50 mL solvent. All extractions were performed at room temperature (23 ± 1 °C) and 600 rpm for 180 min. Samples were taken at 180 min to quantify total polyphenols (A) and pigments (B) by using spectrophotometer methods whereas HPLC-DAD was used to quantify total anthocyanins (C) (Chapter 2, section 2.1). A medium of acidified aqueous ethanol was used as a control. The data shown are 3 replicates for polyphenols and pigments analysis, but one injection onto HPLC for anthocyanins analysis. Values represent means \pm SD for polyphenols and pigments and **** significance from control ($p < 0.0001$) which represent quantified extracts from using ethanol medium, using one-way analysis of variance (ANOVA) with Dunnett's Multiple Comparison Test, ns indicates non-significance.

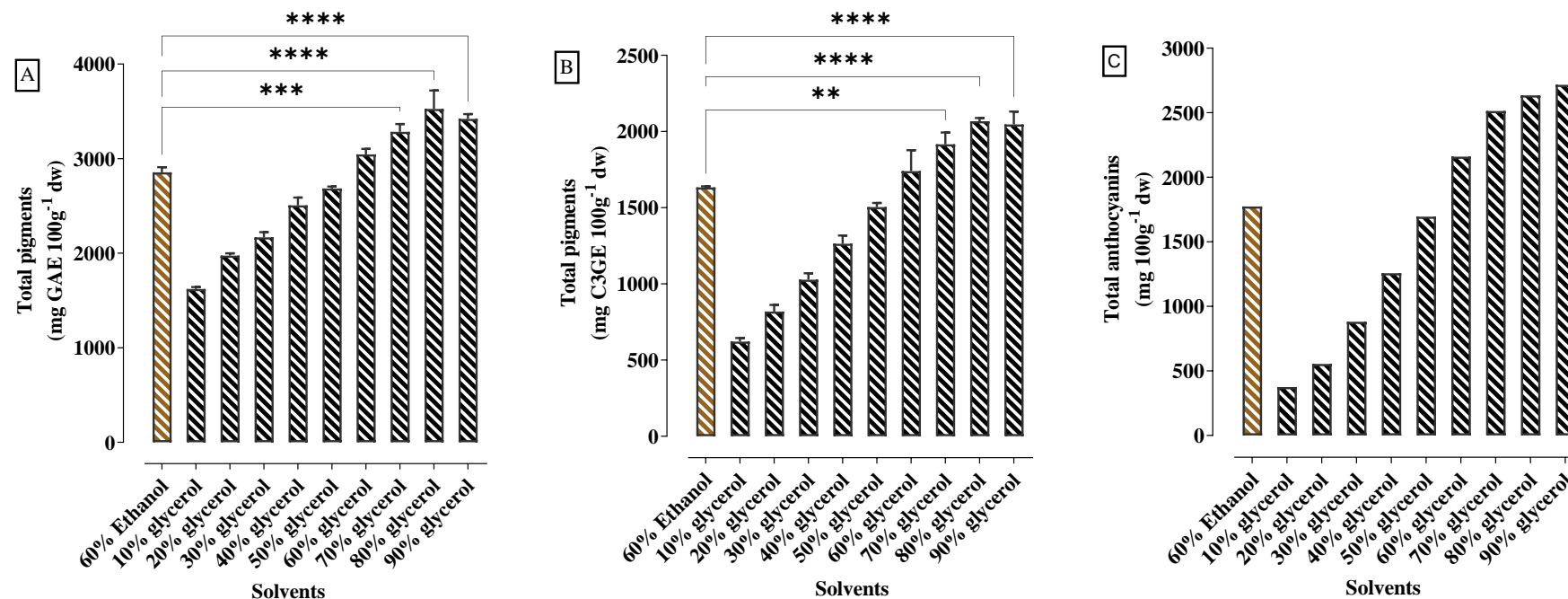


Figure 3. 4. Bar plot showing quantification assays and recoveries from bilberry powder achieved by various glycerol/water mediums ranging between 10-90%.

A 1 g plant powder was added to 50 mL solvent. All extractions were performed at room temperature (23 ± 1 °C) and 600 rpm for 180 min. Samples were taken at 180 min to quantify total polyphenols (A) and pigments (B) by using spectrophotometer methods whereas HPLC-DAD was used to quantify total anthocyanins (C) (Chapter 2.1). A solvent of acidified aqueous ethanol was used as a control. The data shown are 3 replicates for polyphenols and pigments analysis, but one injection onto HPLC-DAD for anthocyanins analysis. Values represent means \pm SD for polyphenols and pigments and **** significance from control ($p < 0.0001$), ** significance from control ($p < 0.01$), which represent quantified extracts from using ethanol medium, using one-way analysis of variance (ANOVA) with Dunnett's Multiple Comparison Test.

3.4.3. Determining the most effective liquid-to-solid ratios ($R_{L/S}$) for anthocyanin extraction using 80% w/v glycerol /water medium from black rice and bilberry

The next variable of the extraction process that was tested was the liquid-to-solid ratio ($R_{L/S}$) of plant material to solvent. This was assessed using various amounts of ground powders (Table 3. 3), which were subjected to extraction using 50 mL of 80% w/v glycerol/water for 180 min (Chapter 2, section 2.1.3). To evaluate the extraction efficiency of anthocyanins, three different assays were carried out. Samples were collected at the end of extraction and then used for the quantification of total polyphenols and total pigments using spectrophotometric methods (Chapter 2, section 2.1.5-6), and quantification of total anthocyanins using HPLC-DAD (Chapter 2, section 2.1.7).

Table 3. 3. Calculated liquid-to-solid ratio ($R_{L/S}$) based on different sample weights (g) in the 50 mL solvent.

No.	Solvent volume (mL)	Sample weight (g)	Liquid-to-solid ratio ($R_{L/S}$)
1	50	0.5	100
2	50	0.625	80
3	50	0.833	60
4	50	1.25	40
5	50	2.5	20

To determine the most effective $R_{L/S}$ for best anthocyanin extraction, a range of various $R_{L/S}$ 20 to 100 mL g⁻¹ were examined. For black rice powder, no significant differences in the concentrations of extracted polyphenols between the extraction with $R_{L/S}$ of 100 and 80 were observed (Figure 3. 5), although significant differences ($p=0.013$) were observed between $R_{L/S}$ of 100 and 60 (1150 ± 50 and 1050 ± 60 mg 100 g⁻¹, respectively), which was highly significant with $R_{L/S}$ of 40 ($P<0.0001$) with 790 ± 30 mg 100 g⁻¹. Regarding the extracted pigment content, there was no significant difference between $R_{L/S}= 100$ and 60 but a highly significant difference was observed between $R_{L/S}= 100$ and 40 ($P<0.001$). For example, the extracted pigments with $R_{L/S}$ of 100 and 60 were 430 ± 11 and 400 ± 15 mg 100 g⁻¹, respectively but the recovered pigment at 40 was 370 ± 15 mg 100 g⁻¹. Furthermore, the extracted anthocyanins showed very small differences between quantified anthocyanins within various $R_{L/S}$ in corresponding solid amounts in the same solvent volume (50 mL). For example, $R_{L/S}$ of 100 showed an extracted anthocyanin

content of $196 \text{ mg } 100 \text{ g}^{-1}$, whereas $R_{L/S}= 20$ showed a recovered concentration of $190 \text{ mg } 100 \text{ g}^{-1}$ of black rice anthocyanins. Therefore $R_{L/S}= 60$ was found to be best, giving a total polyphenol concentration of $980 \pm 60 \text{ mg } 100 \text{ g}^{-1} \text{ dw}$, total pigments of $400 \pm 15 \text{ mg } 100 \text{ g}^{-1}$, and a total of anthocyanins of $190 \text{ mg } 100 \text{ g}^{-1} \text{ dw powder}$.

For bilberry powder, the $R_{L/S}$ was also examined within a range varying from 20 to 100 mL g^{-1} . No significant differences in the yields of polyphenols between $R_{L/S}= 100$ ($4300 \pm 400 \text{ mg } 100 \text{ g}^{-1}$) and $R_{L/S}= 80$ and 60 (**Figure 3. 6**) were observed. However, significant differences ($p=0.001$) were observed between $R_{L/S}= 100$ and 40 ($3200 \pm 50 \text{ mg } 100 \text{ g}^{-1}$). In regard to recovered pigments, although no significant differences between $R_{L/S}=100$ ($2160 \pm 50 \text{ mg } 100 \text{ g}^{-1}$) and 80 , 60 , and 40 were observed; a significant difference ($P<0.0001$) was observed with $R_{L/S}=20$ ($1850 \pm 25 \text{ mg } 100 \text{ g}^{-1}$). In addition, the total anthocyanins showed small differences in recovery in association with increasing amounts of plant material in the same volume of medium (50 mL). For example, $R_{L/S}= 100$ extracted a total of anthocyanins at $2627 \text{ mg } 100 \text{ g}^{-1}$, whereas $R_{L/S}= 20$ recovered $2419 \text{ mg } 100 \text{ g}^{-1}$. Therefore $R_{L/S}= 60$ was found to be the most effective ratio to extract polyphenols from bilberry with a total polyphenol concentration of $3850 \pm 130 \text{ mg } 100 \text{ g}^{-1} \text{ dw powder}$, total pigment concentration of $2100 \pm 40 \text{ mg } 100 \text{ g}^{-1} \text{ dw powder}$, and a total anthocyanins concentration of $2600 \text{ mg } 100 \text{ g}^{-1} \text{ dw powder}$.

For anthocyanin extraction from both black rice and bilberry powders, $R_{L/S}= 60$ was an ideal ratio for maximum recovery of anthocyanins.

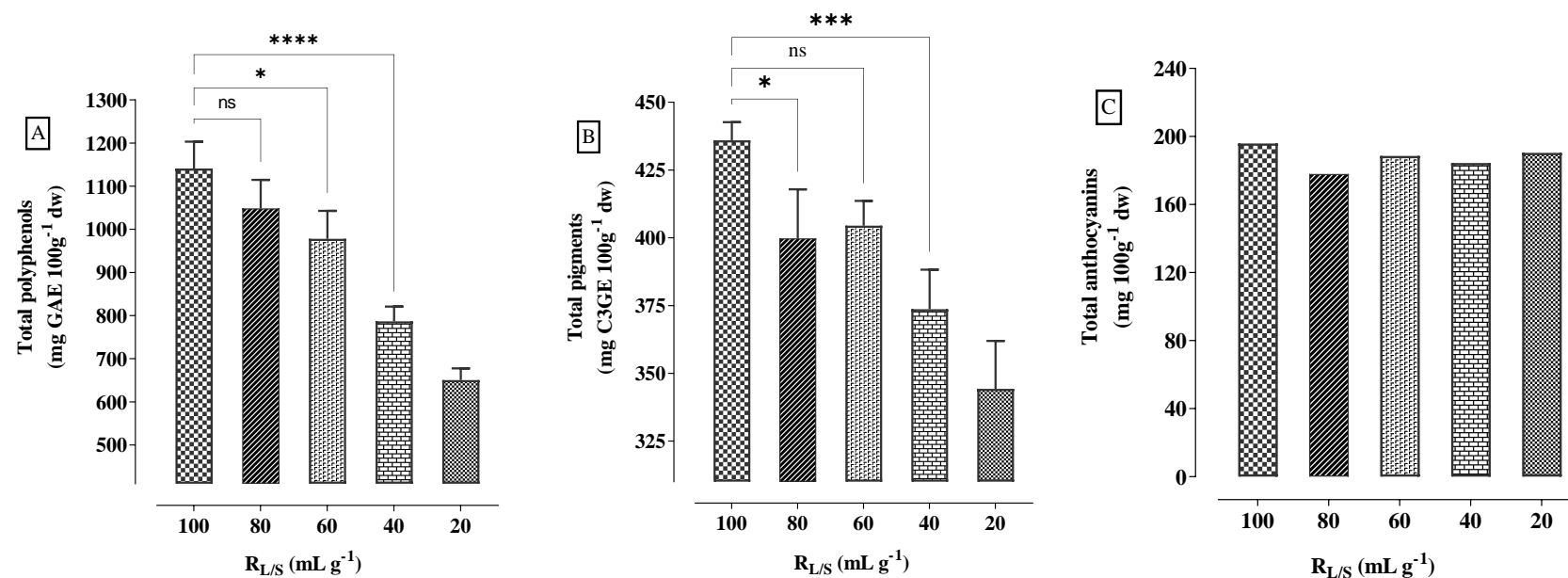


Figure 3.5. Bar plot showing various quantification assays and recoveries achieved by using a medium of 80% w/v glycerol with different ratios of liquid-to-solid (R_{L/S}) from black rice powder.

A 0.5, 0.625, 0.833, 1.25, and 2.5 g plant powder was separately added to 50 mL solvent. All extractions were performed at room temperature (23±1 °C) and 600 rpm for 180 min. Samples were taken at 180 min to quantify total polyphenols (A) and pigments (B) by using spectrophotometer methods (chapter 2, section 2.1.5-6) whereas HPLC-DAD was used to quantify total anthocyanins (C) (chapter 2, section 2.1.7). The data shown are 3 replicates for polyphenols and pigments analysis, but one injection onto HPLC for anthocyanins analysis. Values represent means ± SD for polyphenols and pigments. The significance difference from control with $p < 0.0001$ represented by ****, $p < 0.001$ represented by *** and $p < 0.05$ represented by *, (where control was extracts quantified using ethanol medium) using one-way analysis of variance (ANOVA) with Dunnett's Multiple Comparison Test.

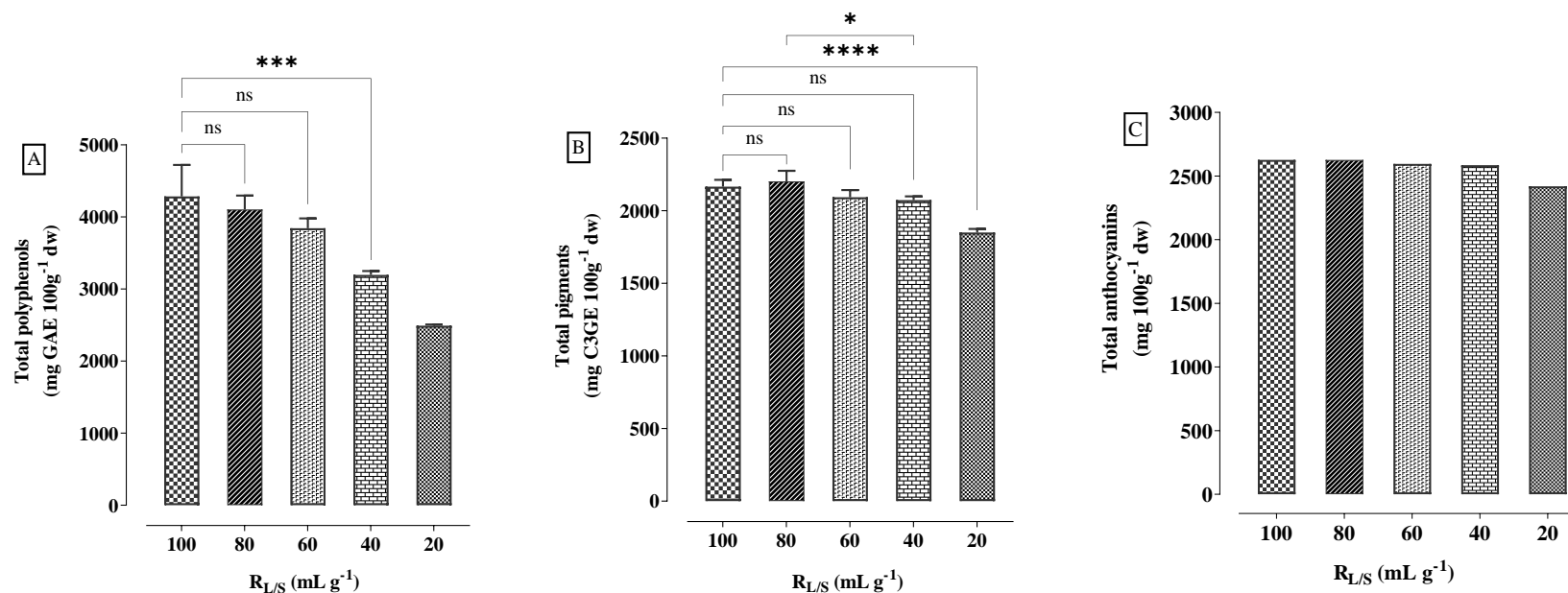


Figure 3. 6. Bar plot showing various quantification assays and recoveries achieved by using a medium of 80% w/v glycerol with different ratios of liquid-to-solid ($R_{L/S}$) from bilberry powder.

A 0.5, 0.625, 0.833, 1.25, and 2.5 g plant powder was separately added to 50 mL solvent. All extractions were performed at room temperature (23 ± 1 °C) and 600 rpm for 180 min. Samples were taken at 180 min to quantify total polyphenols (A) and pigments (B) by using spectrophotometer methods (chapter 2, section 2.1.5-6) whereas HPLC-DAD was used to quantify total anthocyanins (C) (chapter 2, section 2.1.7). The data shown are 3 replicates for polyphenols and pigments analysis, but one injection onto HPLC for anthocyanins analysis. Values represent means \pm SD for polyphenols and pigments. The significance difference from control with $p < 0.0001$ represented by ****, $p < 0.001$ represented by *** and $p < 0.05$ represented by * (where control was extracts quantified from using ethanol medium,) using one-way analysis of variance (ANOVA) with Dunnett's Multiple Comparison Test.

3.4.4. The effect of temperature on anthocyanin extraction from black rice and bilberry over time

Having selected 80% w/v glycerol/water as a suitable solvent and an $R_{L/S}$ of 60 as the most effective for anthocyanin extraction for both plant powders, the next step was to investigate the effect of temperature on anthocyanin extraction. To do this, four different temperatures (50, 60, 70, and 80°C) were tested on anthocyanin recovery from black rice and bilberry powders, using 80% w/v glycerol/water and $R_{L/S}$ of 60 ml g⁻¹. Samples were collected at time points over 180 min (**Chapter 2, section 2.1.4**). The total concentrations of polyphenols and total pigments were quantified using spectrophotometric methods (**Chapter 2, section 2.1.5-6**) and total anthocyanins were quantified using HPLC-DAD (**Chapter 2, section 2.1.7**).

For black rice powder, different temperatures showed different extraction effectiveness for polyphenols, pigments, and anthocyanins (**Figure 3. 7**). At 50 and 60°C, the recoveries of polyphenols, pigment and anthocyanins increased over the first 60 min of the extraction, then plateaued, with a small decline between 120 and 180 min. Whereas the extraction occurring at 70 and 80°C showed a rise in the polyphenols, pigments, and anthocyanins over the first 30 min, and then declined after 30 min. The decline after 30 min was insignificant regarding polyphenols but was significant with pigments and anthocyanins. For example, at the end of extraction (at 180 min), the variation in the total polyphenols at 50, 60, 70, and 80°C were not significantly different and were as follows: 1015 ± 20, 1000 ± 15, 990 ± 46, and 1033 ± 7 mg GAE 100 g⁻¹, respectively. However, the variation of the pigments, as well as anthocyanins at 180 min, were significantly different between the extraction at lower temperatures (50 and 60°C) and higher temperatures (70 and 80°C). For example, the pigments from the extraction process at 50 and 60°C were 434 ± 6 and 431 ± 11 mg 100 g⁻¹, respectively, while, during the extraction at 70 and 80°C, the quantified pigments were remarkably lower with 374 ± 20 and 359 ± 22 mg 100 g⁻¹, respectively. Likewise, the quantified anthocyanins at 180 min were higher during lower-temperature extractions at 50 and 60°C with 200 and 196 mg 100 g⁻¹, respectively: and lower during higher-temperature extractions at 70 and 80°C with 166 and 132 mg 100 g⁻¹, respectively.

However, within the four extractions at different temperatures, the highest recovered content occurred during the black rice extraction at 80°C with polyphenol concentration of $1100 \pm 40 \text{ mg } 100 \text{ g}^{-1}$ at 30 min, pigment concentration of $460 \pm 11 \text{ mg } 100 \text{ g}^{-1}$ at 20 min, and anthocyanin concentration of $211 \text{ mg } 100 \text{ mg}^{-1}$ also at 20 min. Therefore, the ideal extraction condition for higher anthocyanin recovery from black rice was achieved by using a solvent of 80% w/v glycerol/water with $R_{L/S}$ of 60 at 80°C for 20 min to obtain approximately Cya3Glc concentration of $188.7 \text{ mg } \text{g}^{-1}$ dw powder and a total anthocyanin of $211 \text{ mg } 100 \text{ g}^{-1}$ dw of black rice powder.

For bilberry powder, extractions at different temperatures showed different extraction behaviours of pigments and anthocyanins but similar behaviour with polyphenol extraction (**Figure 3. 8**). For example, extractions at 50, 60, 70, and 80°C showed that the polyphenols were increasing over time until the end of extraction time (180 min), while pigments and anthocyanins increased over the first 30 min of the extraction period, then showed a plateau with extraction temperatures at 50 and 60°C or showed a decline with high extraction temperatures at 70 and 80°C. For example, for each extraction condition, the highest recovered contents of polyphenols were achieved at 180 min (at the end of extraction time). However, compared with all different conditions, the higher temperature (80°C) showed higher polyphenol recoveries. For example, quantified polyphenols of $4090 \pm 114 \text{ mg } 100 \text{ g}^{-1}$ dw recovered after 180 min extraction at 50°C, whereas during extractions at 60, 70, and 80°C were 4210 ± 120 , 4330 ± 80 and $4520 \pm 130 \text{ mg } 100 \text{ g}^{-1}$, respectively.

Regarding pigment recoveries, there were different extraction behaviours at different temperatures. For example, during the extraction process at 80°C, the content of pigments was elevated over time until 30 min, with a total recovery of $2110 \pm 50 \text{ mg } 100 \text{ g}^{-1}$ dw, then started to decline to reach content of $1600 \pm 17 \text{ mg } 100 \text{ g}^{-1}$ dw. However, during the extraction process at 70°C, the content of pigments was lower with $2070 \pm 125 \text{ mg } 100 \text{ g}^{-1}$ dw at 30 min, and higher content of $1890 \pm 75 \text{ mg } 100 \text{ g}^{-1}$ dw at 180 min. Furthermore, the extraction at lower temperatures (50 and 60°C) showed similar behaviour where the content of pigments was increased until 60 min then plateaued to end up with a quantified content of 2100 ± 22 and $2060 \pm 40 \text{ mg } 100 \text{ g}^{-1}$ dw, respectively.

In regard to anthocyanin recoveries, extraction at different temperatures showed two stages. The first stage was an increase in anthocyanin content over time. The second process showed a plateau in the case of 50 and 60°C or a decline in the case of extractions at 70 and 80°C. For example, the anthocyanins increased during the first 30 min (except 80°C was until 15 min) after which, the quantified anthocyanins plateaued over time with extractions at 50 and 60°C and declined over time which was faster in the case of extraction at 80°C compared to extraction at 70°C. For example, at 180 min, the total anthocyanins were 3125, 3024, and 2778 mg 100 g⁻¹ at 50, 60, and 70°C, respectively, while it was considerably lower (2118 mg 100 g⁻¹) with the highest extraction temperature at 80°C.

Within the four different extraction temperatures, the highest content occurred during extraction at 80°C where the highest total polyphenols content was at 180 min with 4517 ± 135 mg 100 g⁻¹, total pigment at 30 min with 2109 ± 54 mg 100 g⁻¹, and total anthocyanins at 15 min with 3119 mg 100 g⁻¹. However, only the total anthocyanins during 50°C extraction at 60 min was slightly higher (3163 mg 100 g⁻¹) than the anthocyanins during 80°C extraction at 15 min. Therefore, the ideal extraction condition with the highest anthocyanin recovery from bilberry powder was achieved using a solvent of 80% w/v glycerol/water with R_{L/S} of 60 at 80°C for 15 min to obtain a total anthocyanins content of 3119 mg g⁻¹ dw of bilberry powder.

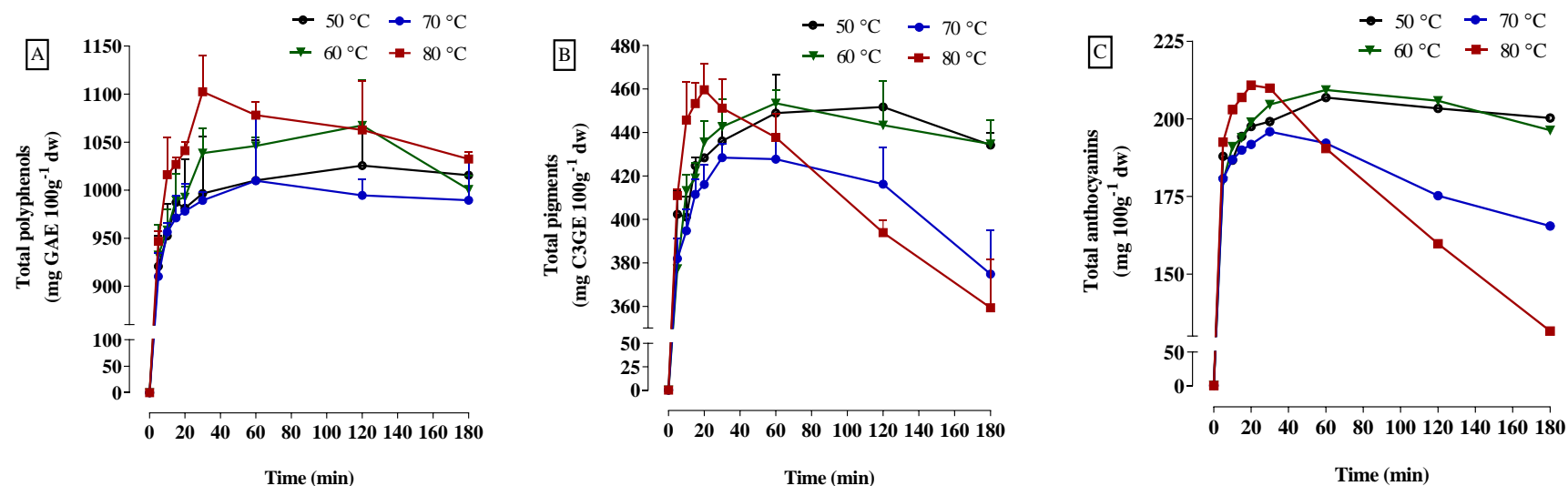


Figure 3. 7. Different assays showing recoveries from black rice powder over 180 min at various temperatures (50, 60, 70, and 80°C) using 80% w/v glycerol and $R_{L/S} = 60 \text{ mL g}^{-1}$.

All extractions were performed at 600 rpm for 180 min. Samples were taken at 5, 10, 15, 20, 30, 60, 120, and 180 min and immediately centrifuged at $10,000\times g$ for 10 min. Samples were taken at 180 min to quantify total polyphenols (A) and pigments (B) by using spectrophotometer methods (chapter 2, section 2.1.5-6) whereas HPLC-DAD was used to quantify total anthocyanins (C) (chapter 2, section 2.1.7). The data shown are 3 replicates for polyphenols and pigments analysis, and values represent means \pm SD, but one injection onto HPLC for anthocyanins analysis.

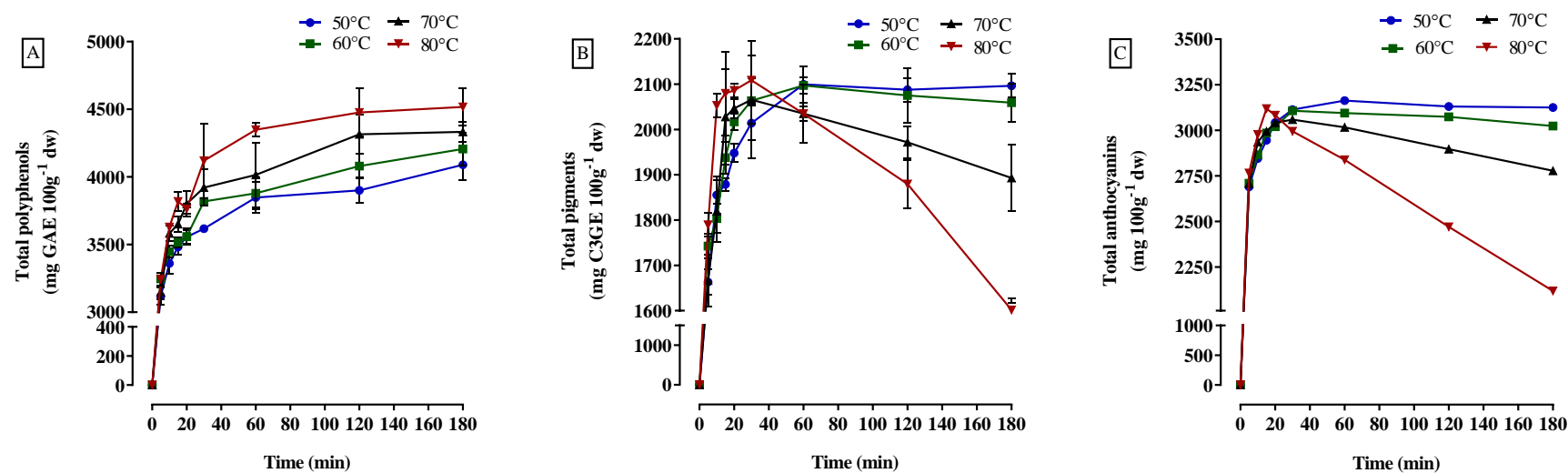


Figure 3. 8. Different assays showing recoveries from bilberry powder over 180 min at various temperatures (50, 60, 70, and 80°C) using 80% w/v glycerol and $R_{L/S} = 60 \text{ mL g}^{-1}$.

All extractions were performed at 600 rpm for 180 min. Samples were taken at 5, 10, 15, 20, 30, 60, 120, and 180 min and immediately centrifuged at 10,000×g for 10 min. Samples were taken at 180 min to quantify total polyphenols (A) and pigments (B) by using spectrophotometer methods (chapter 2, section 2.1.5-6) whereas HPLC-DAD was used to quantify total anthocyanins (C) (chapter 2, section 2.1.7). The data shown are 3 replicates for polyphenols and pigments analysis, and values represent means \pm SD, but one injection onto HPLC for anthocyanins analysis.

3.5. Discussion

The overall aim of this chapter was to prepare cost-effective, green anthocyanin-rich extracts from black rice and bilberry powders to be used for the investigations of anthocyanins metabolism by the human gut microbiota.

The main findings in this chapter were that (i) Cya3Glc was the main anthocyanin in black rice powder, whereas the bilberry anthocyanins consisted of 14 different anthocyanins (ii) the extraction of anthocyanins from black rice and bilberry was higher using the alternative solvent of 80% w/v glycerol/water compared to the conventional solvent of aqueous ethanol, (iii) the solid ratio over the solvent volume showed that $R_{L/S} = 60 \text{ mL g}^{-1}$ was the best for anthocyanin recoveries from black rice and bilberry powder, and (iv) increasing temperature also increased recovery but this varied with the time of incubation, where longer incubation times with higher temperatures, reduced the stability of anthocyanins and therefore the effectiveness of their recovery.

The data presented here demonstrate for the first time that aqueous combinations of glycerol up to 80% (w/v) can significantly increase the total extracted yields of anthocyanins with 211 and 2635 mg 100 g⁻¹ dw from black rice and bilberry, respectively. However, a higher percentage of glycerol of 93% and 90% (w/v) were reported to be suitable glycerol/water mixtures for the extraction of polyphenolic contents from olive leaves and *Artemisia* species, respectively^{217,224}. This was significantly different from the total anthocyanin yields obtained from using aqueous mixtures with ethanol, a widely used medium to extract phenolic compounds from their plant sources^{214,225}. For example, from the data presented in this chapter, the aqueous ethanol (60% v/v) recovered only total anthocyanins of 179 and 1775 mg 100 g⁻¹ dw from black rice and bilberry powders, respectively. The effectiveness of aqueous glycerol solvent was previously investigated which showed better recovery of polyphenols from other plant materials²²⁴. A report by Rupasinghe and others reported that solvent polarity is a critical factor that affected the recovery of molecules from plant matrices and thus different fractions can be obtained through modification of the polarity of the extraction solvent²²⁶. This might be afforded by reducing the dielectric constant of water ($\epsilon = 80.1$) with the addition of glycerol which has a lower dielectric constant ($\epsilon = 42.5$) which could favourably increase the extraction

effectiveness of polyphenols and anthocyanins. However, other parameters might affect the extraction efficiency of the solvents such as the solubility of phenols in different solvents and the intermolecular forces (mainly hydrogen bonds) between them and the solvent²¹⁷.

In addition, increasing the solid material over the solvent volume showed that the efficiency ratio for the recovery of anthocyanins was $R_{L/S}=60 \text{ mL g}^{-1}$ for both black rice and bilberry, providing corresponding total anthocyanins of 190 and 2600 mg 100 g⁻¹dw. This effect was ascribed to the improvement of mass transfer between the solid and the liquid. For example, mass transfer is greater when a higher liquid-to-solid ratio is applied. If the amount of solvent is not sufficient to allow adequate diffusion of the dispersed solids, thus resistance to mass transfer from the solid particles to the liquid phase is predictable. Therefore, a well-defined $R_{L/S}$ is important to achieve an adequate mix between solid and liquid as well as a high diffusion rate of solute during extraction²²⁷. In contrast with the data presented in this chapter, for example, $R_{L/S}$ of 100 mL g⁻¹ was the most effective ratio for maximum yield of polyphenols from *Artemisia* species using 90% glycerol/water solvent²¹⁷.

Furthermore, increasing extraction temperature increased anthocyanins recoveries from black rice and bilberry. However, high temperature for a long time was shown to adversely affect the stability of anthocyanins. Data presented in this chapter shows that extraction of anthocyanins is significantly different at different temperatures. In addition, the extraction duration is an important factor, which is also demonstrated by Seikova and others²²⁸. In fact, extraction temperature and duration are correlated, and they are defined as the most essential factors in phytochemical extraction process²²⁹. Although it has been undeniably shown that in most cases, increasing temperature up to 70–80°C produced higher polyphenol yields, longer extraction time not only makes a process energy-ineffective but also offers no benefit for higher extracted yields. This is because in most cases the extracted yields obey the second-order model^{230,231}. For example, at 80°C, the recovery of anthocyanins increased only until 20 and 15 min for black rice and bilberry, respectively. After reaching the highest (at 15 and 20 min) extraction yields, whether the total extracted anthocyanins decline or stay at the same concentrations depends on the plant and the temperature used. It is well known that anthocyanins degrade spontaneously

in media at neutral pH into a simple phenolic compound like PCA and PGA^{38,87}. This might be supported by the rise in quantified total polyphenols from the same samples over time in both black rice and bilberry (**Figure 3. 7** and **Figure 3. 8**). Therefore, higher recovery of anthocyanins could be achieved by using high temperature for short time or at lower temperature for longer time.

Although, in both black rice and bilberry powder, the extracted yields of anthocyanins were higher using glycerol/water solvent than acidified ethanol/water solvent, the anthocyanin-rich glycerol extracts were unsuitable to be used for the incubation in the batch colon model due to two issues: (i) the glycerol/water is hard to remove and the absolute amounts that would need to be added to colon models renders it not useable (e.g., the concentration of Cya3Glc in black rice glycerol extract was 30.4 µg/mL, thus 20 mL glycerol extract will be needed to prepare 60 µg/mL Cya3Glc in a total volume of 100 mL), (ii) adding glycerol means another carbon source for the microbes in the colon model, and (iii) the extraction does not likely just extract anthocyanins but also various phenolics which would need to be removed through one or more additional clean-ups that would be time-consuming and expensive (large scale preparative chromatography). Therefore, highly purified commercially-available anthocyanin extracts will be used for future experiments instead.

3.6. Conclusions

The research presented in this chapter focused on using an eco-friendly extraction process to prepare cost-effective anthocyanin-rich extracts from raw materials of black rice and bilberry using aqueous glycerol solvent, and to be used later for further investigations. A glycerol concentration up to 80% (w/v) with $R_{L/S}$ of 60 provided very satisfactory contents of extracted total anthocyanins from black rice and bilberry. The most effective extraction temperature was 80°C for 20 min for black rice and 15 min for bilberry. In both black rice and bilberry, longer extraction time adversely affected anthocyanins stability and thus anthocyanins degraded into low molecular weight compounds. The main black rice anthocyanins were Cya3Glc (84%) and Peo3Glc (11%) of the total black rice anthocyanins, while in bilberry a range of fourteen different monosaccharides of delphinidin, cyanidin, petunidin, peonidin and malvidin derivatives of anthocyanins were

detected. Although the extracted anthocyanins using aqueous glycerol solvent was better than aqueous ethanol solvent, the extracted anthocyanin concentration, from both plant powders, was relatively low due to the higher volume needed to be used in the incubation vessels to study the gut microbial metabolism of anthocyanins. Therefore, the highly purified commercially-available anthocyanin extracts will be used in the investigation with the human gut microbiota which will be presented in the following chapters (Chapters 4, 6, and 7).

Chapter Four

**The metabolism of
anthocyanins by the
human gut microbiota**

Chapter 4: The metabolism of anthocyanins by the human gut microbiota

4.1. Abstract

Background: Numerous reports on anthocyanins show that they are very poorly bioavailable, and this has led to the concept that the beneficial effects of consuming anthocyanin-rich foods and diets are caused by breakdown products and metabolites rather than the anthocyanins themselves. The seminal report from a study of human metabolism of penta-[¹³C] labelled cyanidin-3-glucoside (Cya3Glc) has provided more clarity as to the nature of human metabolites of this anthocyanin and confirmed that breakdown products and their metabolites are found in blood and urine at orders of magnitude higher concentrations than the intact anthocyanin⁹⁹. However, it is not clear if these breakdown products are produced through spontaneous degradation or microbiota-dependent transformation, or a combination of both. Few studies reported the degradation of anthocyanins in the presence of the human faecal microbiota, and these have used simple non-pH-controlled colon models and, apart from one, have not tried to distinguish between spontaneous and microbiota-dependent degradation.

Objective: The work presented in this chapter aimed to investigate (i) the relative contribution of the microbiota and spontaneous processes in the degradation of anthocyanins, (ii) the within-person and (iii) between person variation of these processes, and (iv) whether there are differences in anthocyanin degradation between colon models with and without pH control.

Methods: An *in-vitro* pH-controlled human colon model was used to incubate two different anthocyanin-rich extracts from black rice and bilberry, with human gut microbiota. Black rice and bilberry extracts were incubated in media with faecal inoculum over 24 h and HPLC-DAD was used to quantify the concentration of anthocyanins over the incubation time. The colon model was inoculated with both fresh human faecal samples and autoclaved human faecal samples to represent microbial-dependant

metabolism and spontaneous degradation respectively. Similar incubations were performed using a non-pH-controlled colon model also under an anaerobic environment. The feasibility of using glycerol-frozen faecal stocks to inoculate the colon model was also investigated. Intra- and inter-individual variations were determined by conducting experiments with faecal samples collected from the same donor on different days and faecal samples collected from different donors, respectively.

Results: Loss of anthocyanins occurred both in the presence and absence of live faecal inoculum. However, the rate of loss of anthocyanins was considerably faster in the presence of live faecal inoculum compared to autoclaved faeces. The rate of loss of anthocyanins varied between donors but also for faecal samples collected from the same donor but on different days. In the non-pH-controlled colon model, the rate of loss of anthocyanins was much slower and only occurred over the first 6 h of incubation and did not proceed to completion, probably due to reductions in pH caused by organic acid production (and consequent reduction in pH) by the microbiota. The breakdown of Cya3Glc was shown to occur at similar rates in glycerol-frozen faecal stocks compared to the corresponding fresh faecal sample. The rates of loss of anthocyanins varied and the differences were shown to depend on the B-ring substitution pattern and the type of sugar moiety, both for spontaneous and microbiota-dependent degradation.

Conclusion: The degradation of anthocyanins was faster in the presence of live faecal microbiota compared to autoclaved faecal microbiota. This result supports the hypothesis that the human gut microbiota is involved in anthocyanin metabolism and their microbial metabolites should be considered when evaluating the effects of anthocyanins on host health. Therefore, further studies on the spontaneous and microbial degradation of anthocyanins were carried out and presented in the following chapters (chapter 5 and chapter 6, respectively).

4.2. Introduction

There have been challenges to demonstrate physiological-relevant mechanisms of action underlying the health benefits of anthocyanins. An important reason for this relates to the very poor availability of anthocyanins which are poorly absorbed from the intestinal tract and are hardly detected in serum and/or urine ²³².

The human gastrointestinal tract is the main location of the human gut microbiota which comprises 10^{12} - 10^{14} resident microorganisms, including bacteria, viruses, fungi, and protozoa, that are commensal within the human gut ²³³. In recent years, more evidence has shown the link between the status of gut microbiota and either gastrointestinal functions and/or non-gastrointestinal diseases ¹⁵³. Meanwhile, many scientific articles have been published recently showing the importance of the mutual relationship of the human gut microbiota with our diets, and how this relationship strongly influences human health ²³⁴. Our diets contain numerous bioactive compounds, and, therefore, any dietary changes can cause rapid microbial diversity and structural as well as metabolite shifts. These alterations play a significant role in the modulation of the risk of several chronic diseases such as type 2 diabetes, obesity, inflammatory bowel disease, and cardiovascular diseases ²³⁵.

Therefore, several investigations have been conducted to understand this interaction between dietary bioactive compounds, including anthocyanins, and the human gut microbiota, especially the intestinal microbiota metabolites which are different from those that can be generated by human enzymes ¹⁵⁸. In the last 10 years, many reports have been published that investigated the relationship between anthocyanins and the human gut microbiota. The main reason was that the bioavailability studies showed that anthocyanins are hardly detected in urine or serum (less than 2% of anthocyanin intake) ⁹⁹. However, the knowledge regarding the interaction between anthocyanins and the human gut microbiota is still limited. Firstly, most of these investigations have focused on mutual interactions between polyphenol-rich diets and the gut microbiome ²³⁶. For example, Cheng and others proposed that the human gut is the main bioreactor where tea polyphenols and gut microbiota have reciprocal interactions where the polyphenols modulate gut bacteria composition and gut microbiota metabolise polyphenols to form

metabolites²³⁷. Several reports have been recently published investigating in more detail the sub-categories of polyphenols such as the flavonoid classes flavonols, isoflavones, flavones, flavanones, and flavan-3-ols.

Anthocyanins also have been investigated like other flavonoids but still need more detailed investigations using the human microbiota and including proper controls. For example, several *in-vitro* and *in-vivo* studies were conducted using animal models to investigate the relationship between anthocyanins and gut microbiota which may not be representative of metabolic processes occurring in humans⁸⁸. In addition, previous human *in-vitro* studies (where human faecal samples were used), have used anaerobic models without pH control^{91,173}. In contrast, Hidalgo and others investigated the degradation of individual anthocyanins by the human gut microflora using pH-controlled colon models¹⁷⁷. However, they did not report the role of the microbiota versus spontaneous chemical degradation such as incubating anthocyanins with heat-inactivated human faeces. Other reports used individual bacterial isolates represented in the human gut microflora to investigate the anthocyanin degradation by individual human microbes which is a simplification of the complex multi-organism structures present in the human gut⁸⁸. To my knowledge, the investigation of the intra- and inter-individual variations have not been reported yet using an established pH-controlled model with appropriate controls. Understanding the contribution of complex microbial-dependent degradation and that of spontaneous degradation, and how they determine inter-individual and intra-individual variations in metabolites produced is critical for clarifying mechanisms involved in the beneficial effects of anthocyanins and their metabolites. There is evidence suggesting that metabotypes can determine the beneficial effects of polyphenols²³⁸. To date, the interactions of anthocyanins with the human gut microbiota are still not fully understood.

The overall aim of this chapter, therefore, is to investigate the metabolism of anthocyanins by the human gut microbiota using a pH-controlled batch colon fermentation, including appropriate controls by incubating anthocyanins with inactivated faecal samples and investigating inter and intra-individual variations using faecal samples from different donors or the same donor respectively.

4.3. Objectives

The overall aim of the research presented in this chapter and chapter 6 was to investigate the metabolism of dietary anthocyanins by the human gut microbiota in more detail. The focus of the research reported in this chapter was to understand the role of the microbiota, and between-person differences, in the disappearance of anthocyanins. Subsequently, chapter 6 reports the various metabolic transformations that occur and is therefore focused on the production of (ring-fission) metabolites and their further metabolism. The *in-vitro* human colon fermentation was used as an experimental model and the metabolism of two sources of dietary anthocyanins (black rice and bilberry) was investigated. Therefore, the studies described in this chapter were focused on (i) monitoring the disappearance of anthocyanins during *in-vitro* colon fermentation in the presence of live and heat-inactivated human faecal microbiota; (ii) exploring the loss of anthocyanins in the presence as well as the absence of the human gut microbiota, and (iii) investigating the intra- and inter-individual differences on the loss of anthocyanins during *in-vitro* colon fermentation.

4.4. Results

4.4.1. Chemical characterisation of the black rice and bilberry extract powders

In chapter 3, the use of green solvents (glycerol-water mixtures) to extract anthocyanins from raw black rice grain and bilberry fruits was reported. However, despite this extraction process being efficient for extraction of anthocyanins from black rice and bilberry, the final extracts did not contain anthocyanins at a high enough concentration which would result in requiring large quantities of glycerol to be added to the colon model. At this time, commercially available anthocyanin-rich extract powders prepared from both black rice and bilberry were purchased from the Beijing Gingko Group (BGG), China (**Appendix 1**). According to a representative of BGG, the black rice and bilberry were extracted using aqueous alcohol and then the anthocyanins were purified by passing the extracts through a chromatography column before the purified solutions were dried to give anthocyanin-rich powders (Dr Paul Kroon, QIB, personal correspondence). The content and composition of anthocyanins in both extracts were determined.

HPLC- TOF- MS was used to identify the various anthocyanins in the extracts (**Chapter 2, section 2.2.9**). Then, HPLC-DAD was initially used to quantify the anthocyanins using 520 nm (**Chapter 2, section 2.2.7**). In addition, the standard addition method was carried out to confirm the quantity of anthocyanins in black rice extract powder. Moreover, the extinction coefficients for several commercially available HPLC-grade purified anthocyanins were determined using a spectrophotometer at 520 nm (**Appendix 2**) for checking the concentrations of stored standard stocks over time.

The HPLC-TOF-MS data showed that the black rice extract powder contained 6 different putative anthocyanins based on (i) the peak of absorbance at 500 nm (**Figure 4. 1**), (ii) the presence of a signal corresponding to the m/z $[M+H]^+$ of the parent anthocyanins (**Table 4. 2** and **Figure 4. 2**), (iii) the presence of a $m/z[M+H]^+$ 287.058 (corresponding to cyanidin aglycone) or a $m/z[M+H]^+$ 301.073 (corresponding to peonidin aglycone) (**Figure 4. 2**), and (iv) the majority of these identifications being consistent with the anthocyanins that were reported previously²³⁹.

The quantitative analysis was first carried out using the $A_{520\text{ nm}}$ data from the HPLC-DAD run (**Chapter 2, section 2.2.7**), with quantification done by comparing the peak area obtained for the black rice extract with peak areas obtained for a range of known concentrations of Cya3Glc reference standards (i.e., an external standard curve; **Figure 4. 3**). Using this quantitative method gave a Cya3Glc content of 284.8 ± 4.8 mg/g dry weight of black rice powder. The same method gave the content of unknown 1 (Cya-type), Cya3,5diGlc, Cya3Glc-p-coumarate, Peo3Glc, and unknown 2 (Cya-type) for 1.8 ± 0.7 , 2.4 ± 0.3 , 4.6 ± 0.2 , 19.9 ± 1.1 , and 6.8 ± 1.2 mg/g dry weight of black rice powder, respectively. The total anthocyanin was calculated as the sum of the individual anthocyanin contents at 320.2 ± 8.3 mg/g dry weight of black rice powder.

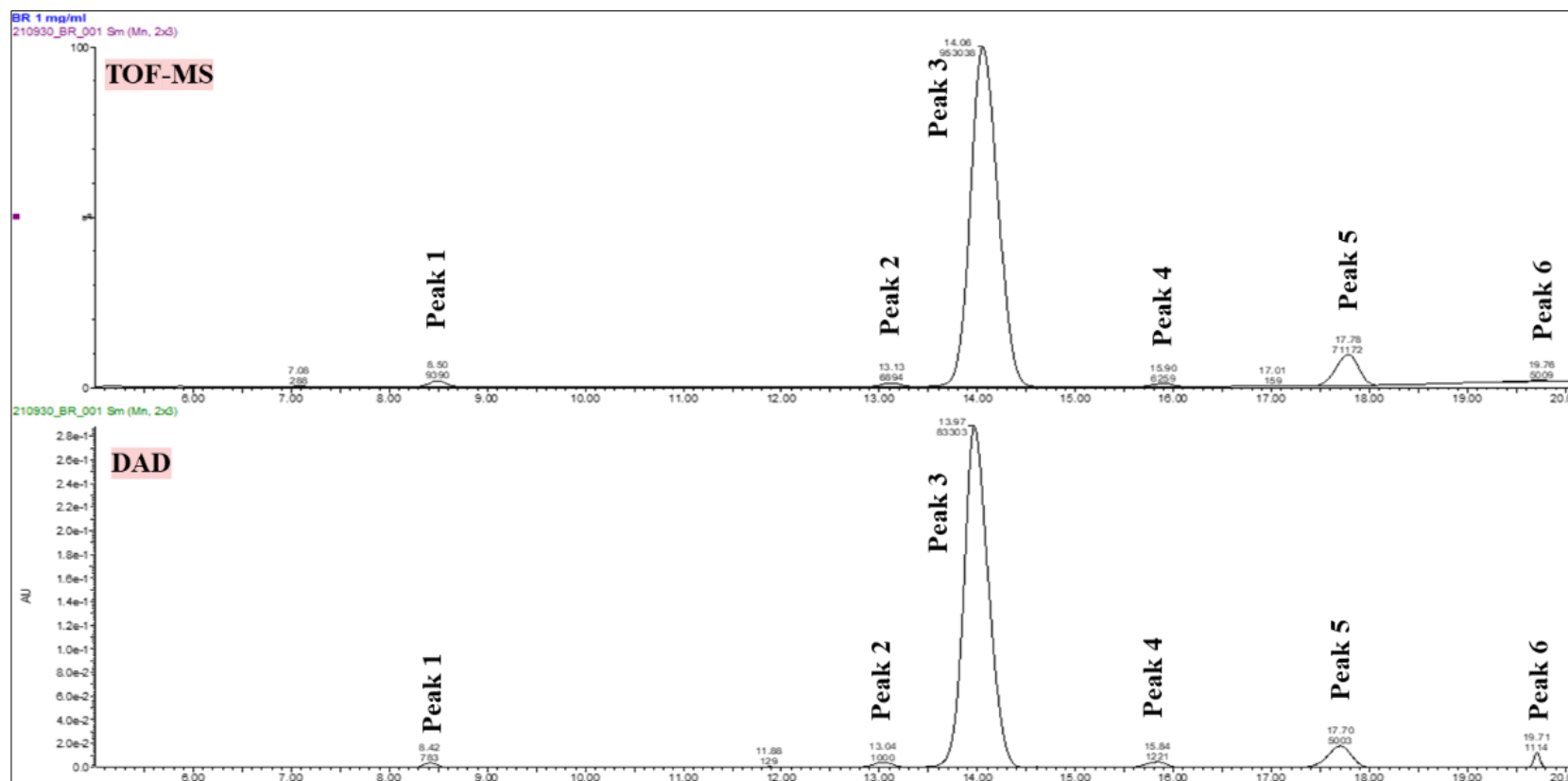


Figure 4. 1. MS and DAD chromatograms of anthocyanins in black rice extract powder.

A fresh stock solution of black rice extract powder (1 mg/mL) was prepared in acidified water (2% formic acid). A 10 μ L of prepared stock solution was injected through HPLC-ESI-TOF. Both low and high-energy collisions were scanned alongside with DAD detector at 500 nm. Gradient elution was performed using 1% v/v formic acid in water as solvent A, and 1% v/v formic acid in acetonitrile as solvent.

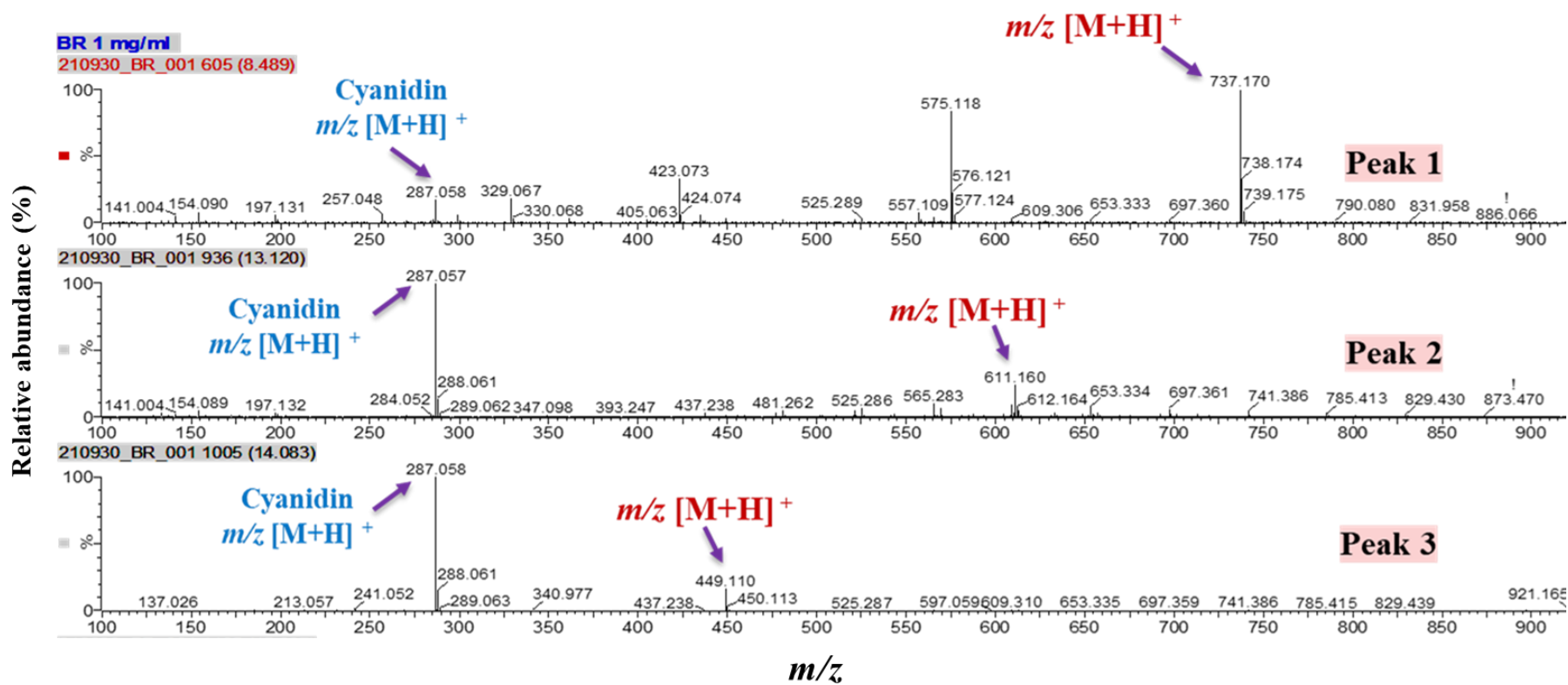


Figure to be continued.....

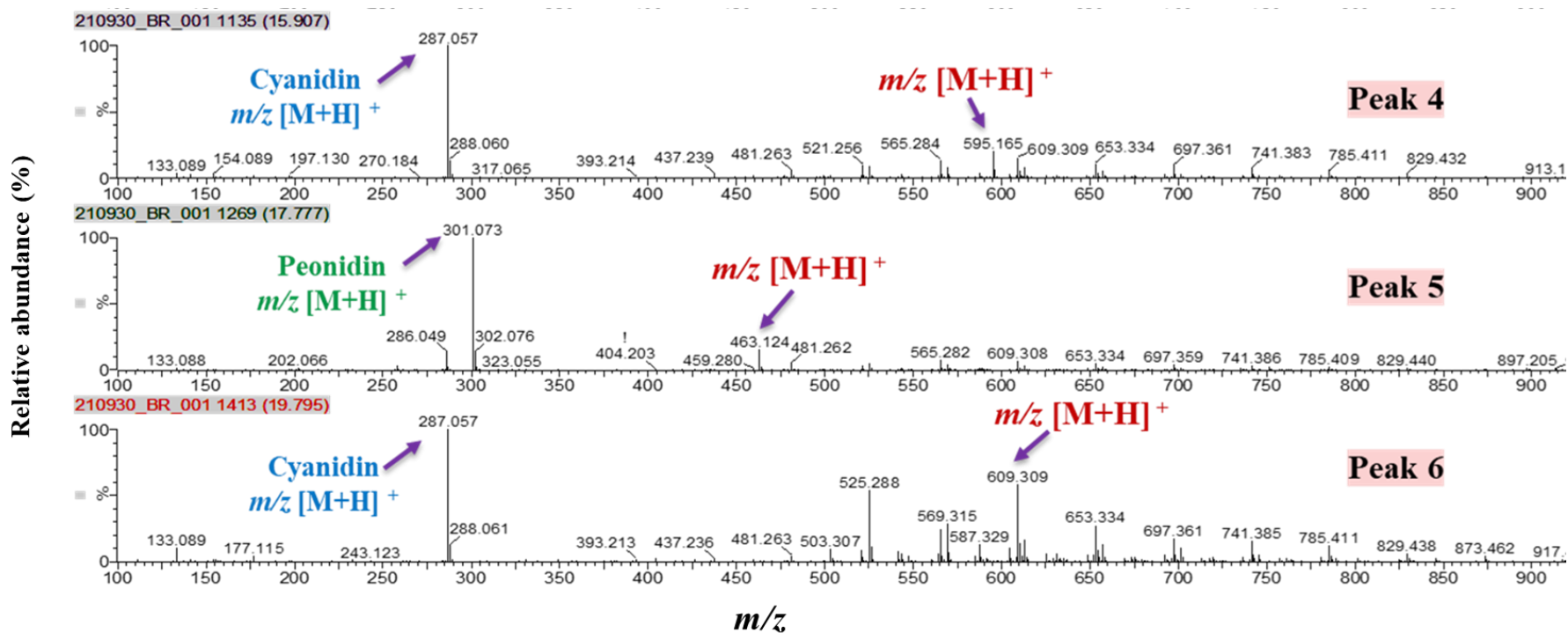


Figure 4. 2. Signals corresponding to $m/z [M+H]^+$ of anthocyanins in black rice extract.

A fresh stock solution of black rice extract powder (1 mg/mL) was prepared in acidified water (2% formic acid). A 10 μ L of prepared stock solution was injected through HPLC-ESI-TOF in positive mode. Both low and high-energy collisions were scanned alongside with DAD detector at 500 nm. Gradient elution was performed using 1% v/v formic acid in water as solvent A, and 1% v/v formic acid in acetonitrile as solvent B.

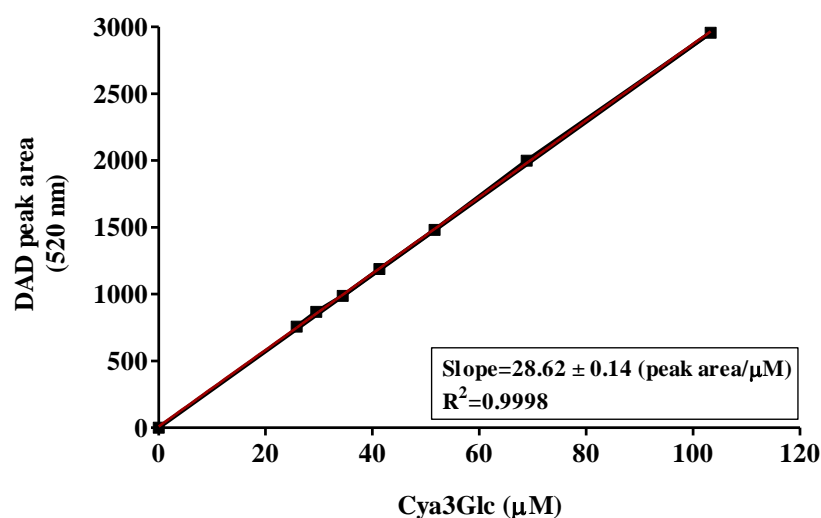


Figure 4. 3. External standard curve for cyanidin-3-O-glucoside (Cya3Glc).

A fresh stock solution from the authentic compound of Cya3Glc (1 mg/mL) was prepared in acidified water (2% formic acid). In the same matrix, serial dilutions were prepared and then injected through a reversed-phase column. Peak detection was achieved using a DAD detector at 520 nm.

In addition, the standard addition method was used to quantify the Cya3Glc in the black rice extract. The black rice extract prepared in acidified water was mixed with either acidified water (no addition) or increasing volumes of Cya3Glc (in acidified water; from the same stock as used to prepare the external standard curve) and appropriate volumes of acidified water so that all samples had a final volume of 1 mL (**Table 4. 1**). The Cya3Glc content of the black rice extract powder was estimated by plotting the DAD (520 nm) peak area against the added concentration of pure Cya3Glc (**Figure 4. 4**), which was 333.6 ± 15.3 mg/g dry weight powder (33.4 % w/w), whereas 15 different anthocyanin compounds in bilberry extract powder were quantified using (**Figure 4. 7**) the same approach described above.

Table 4. 1. Preparation of standard addition for Cya3Glc

Vials	Black rice (μL)	Pure Cya3Glc (μL)	Added Cya3Glc (μM)	Acidified water (μL)	Peak area (520 nm)
0	0.00	0.00	0.0000	1000	0.000
1	250	0.00	0.0000	750	79.32
2	250	50.0	1.7215	700	122.8
3	250	150	5.1645	600	216
4	250	250	8.6075	500	314.2
5	250	500	17.215	250	543.9

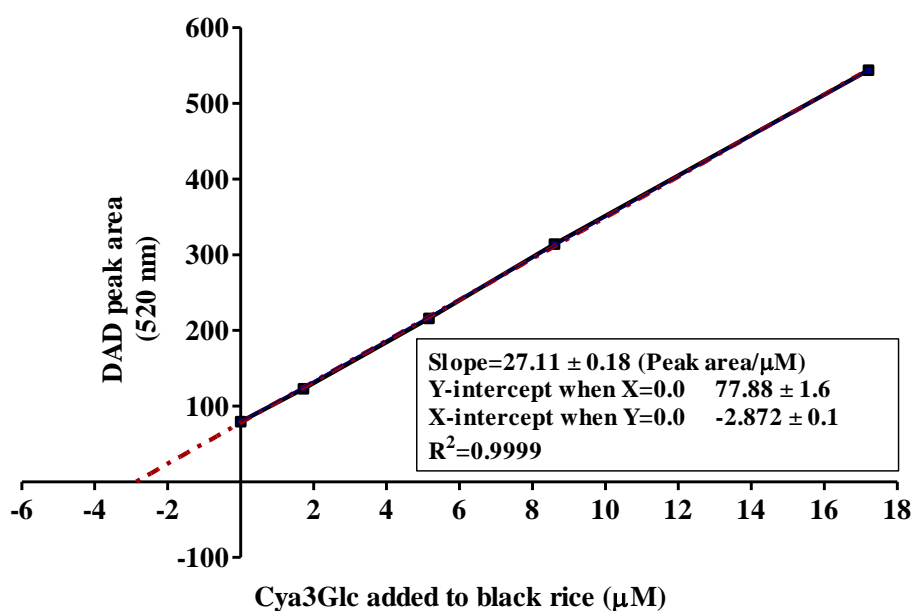


Figure 4. 4. Standard addition for cyanidin-3-O-glucoside (Cya3Glc).

A fresh stock solution of black rice extract powder (16.6667 μg/mL) was prepared in acidified water (2% formic acid). A pure authentic standard of Cya3Glc was also freshly prepared in 2% v/v aqueous formic acid with 34.430 μM (15.462 μg/mL) concentration. 250 μL of black rice stock solution was added separately in 5 different 1.5 mL-Eppendorf tubes. A serial volume from pure Cya3Glc stock was added in only 4 of the Eppendorf tubes. A blank sample was prepared using only acidified aqueous 4% v/v formic acid. All tubes were topped up to 1mL using the same acidified water. All samples were vortex and then injected through HPLC-DAD and all measurements were taken at 520 nm.

Table 4. 2. The content of anthocyanins identified in black rice extract powder*

Peak	RT TOF-MS (min)	RT DAD _{520nm} (min)	Parent ion <i>m/z</i> [M+H] ⁺	Other ions <i>m/z</i> [M+H] ⁺	Identified anthocyanin	Content [#] (mg g ⁻¹ d.w.)	% of total anthocyanins
1	8.42	3.55	737.170	575.118, 423.073, 287.058	Unknown 1 (Cya-type)	4.68 ± 0.08 ^a	1.22
2	13.13	10.42	611.160	449.108, 287.058	Cya3,5diGlc	5.98 ± 0.07 ^a	1.56
3	14.06	11.72	449.110	287.058	Cya3Glc	333.44 ± 5.4	87.21
4	15.90	15.08	595.166	287.057	Cya3Glc- <i>p</i> -coumarate	6.26 ± 0.18 ^a	1.64
5	17.81	17.92	463.124	301.073	Peo3Glc	23.48 ± 1.88	6.14
6	19.80	18.71	609.309	525.288, 287.057	Unknown 2 (Cya-type)	8.49 ± 1.34 ^a	2.22
Total						382.33 ± 8.95	100

*Identification of anthocyanins in black rice extract powder was achieved by freshly preparing three different concentrations of black rice extract powder (1, 0.05, and 0.0333 mg/mL) in 2% v/v formic acid in water and 10 μL was injected through HPLC-ESI-TOF in positive mode. Both low and high-energy collisions were scanned alongside UV-VIS detection at 500 nm. Gradient elution was performed using 1% v/v formic acid in water as solvent A, and 1% v/v formic acid in acetonitrile as solvent B. However, the quantification method was performed by using an additional standard curve for Cya3Glc but an external standard curve for other compounds. All peaks were detected at 520 nm on HPLC-DAD using a gradient elution of 5% v/v formic acid in water as solvent A, and 5% v/v formic acid in acetonitrile as solvent B. The content was calculated using the average of three different concentrations of black rice extract powder.

[#]Values are expressed as mean ± SD.

^a=expressed as Cya3Glc equivalent

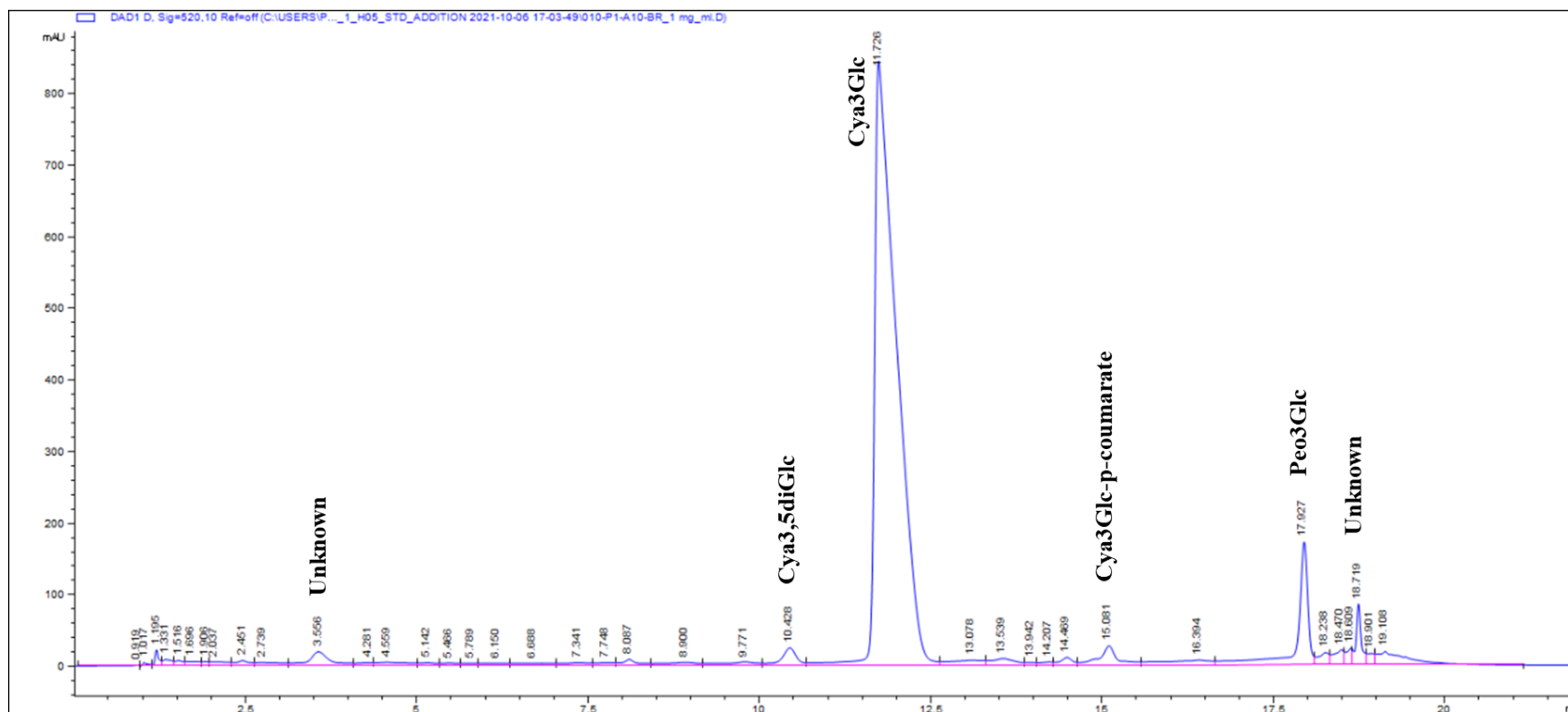


Figure 4. 5. HPLC-DAD chromatogram of black rice anthocyanins at 520 nm.

Quantification was performed by using an external standard curve for two authentic anthocyanins (Cya3Glc and Peo3Glc). A 20 μ L sample was injected onto the reversed-phase column using a gradient elution of 5% v/v formic acid in water as solvent A, and 5% v/v formic acid in acetonitrile as solvent B.

The HPLC-TOF-MS data showed that the bilberry extract powder contained 15 different putative anthocyanins based on (i) the presence of a signal corresponding to m/z $[M+H]^+$ of the parent anthocyanins (**Table 4. 3** and **appendix 3**), (ii) the presence of the fragment ions of anthocyanidins such as m/z $[M+H]^+$ 287.058 (corresponding to cyanidin aglycone), 301.073 (corresponding to peonidin aglycone), 331.083 (corresponding to malvidin aglycone), 303.052 (corresponding to delphinidin aglycone), 317.067 (corresponding to petunidin aglycone), 301.072 (corresponding to peonidin aglycone) (**Figure 4. 6**), and (iii) the literature where the majority of these identifications being consistent with the bilberry anthocyanins that were reported previously ²³⁹.

The quantitative analysis of the content of anthocyanins in bilberry extract powder was carried out using the $A_{520\text{ nm}}$ data from the HPLC-DAD run (**Chapter 2, section 2.2.7**), with quantification done by comparing the peak area obtained for the black rice extract with peak areas obtained for a range of known concentrations of reference standards (**Appendix 3**). Using this quantitative method gave individual anthocyanin contents (Table 4.6). The total anthocyanin was calculated as the sum of the individual anthocyanin contents at 262.9 ± 5.46 mg/g dry weight of bilberry powder.

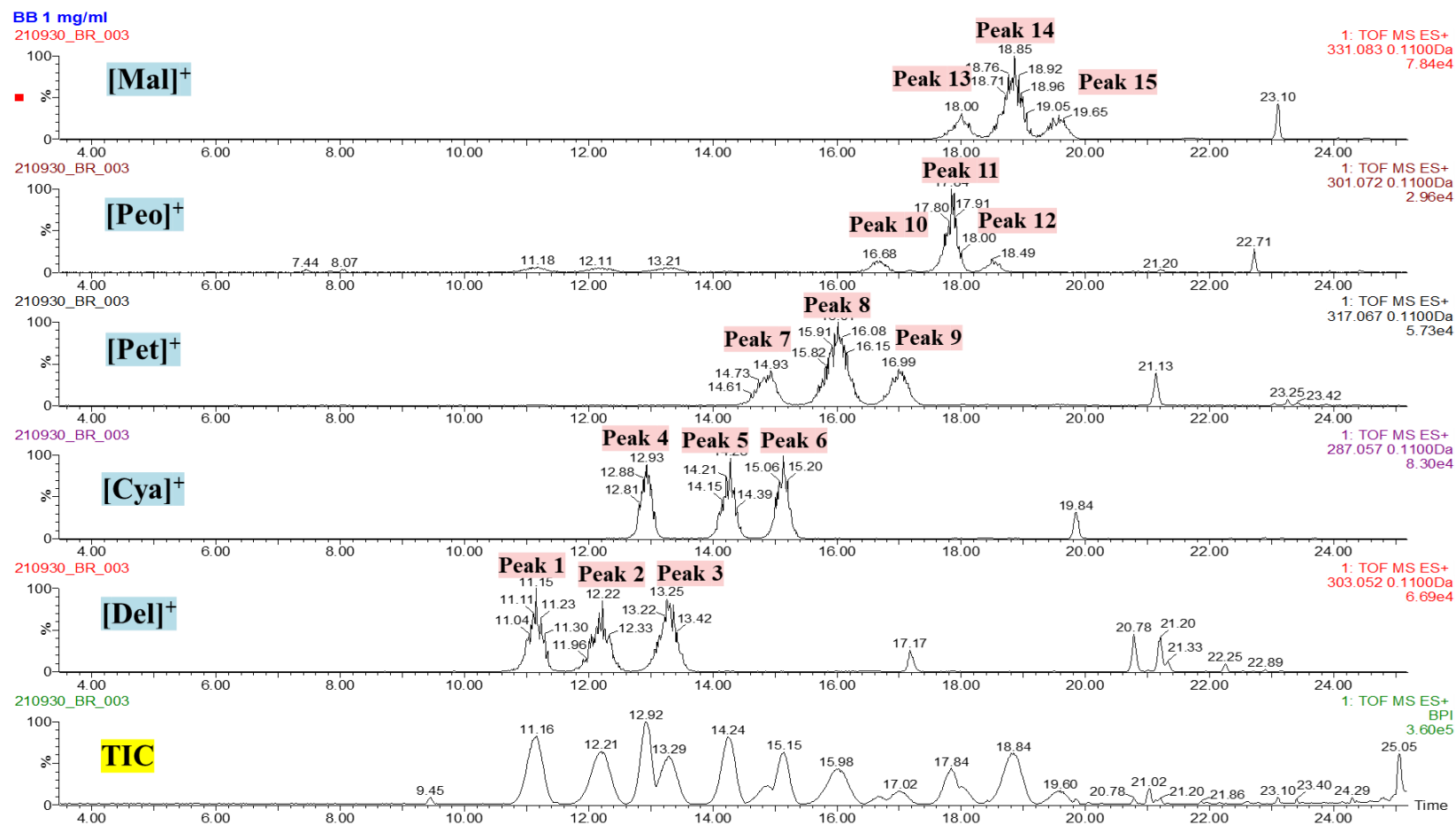


Figure 4. 6. TOF MS spectrum for the identified bilberry anthocyanins.

Table 4. 3. Identified anthocyanins and their contents in bilberry extract powder

Peak	RT TOF-MS (min)	RT DAD _{520nm} (min)	Parent ion <i>m/z</i> [M+H] ⁺	Other ions <i>m/z</i> [M+H] ⁺	Identified anthocyanin	Content [#] (mg g ⁻¹ d.w.)	% of total anthocyanins
1	11.16	7.22	465.104	303.052	Del3Gal	36.87 ± 0.66 ^a	14.0
2	12.22	8.91	465.104	303.052	Del3Glc	34.89 ± 0.67 ^a	13.3
3	12.93	9.97	449.108	287.057	Cya3Gal	26.49 ± 0.53 ^b	10.1
4	13.25	10.65	435.093	303.052	Del3Ara	32.19 ± 0.68 ^a	12.2
5	14.28	12.35	449.109	287.057	Cya3Glc	25.55 ± 0.66 ^b	9.7
6	14.93	13.03	479.119	317.067	Pet3Gal	Traces	0
7	15.13	13.65	419.099	287.057	Cya3Ara	29.71 ± 0.61 ^b	11.3
8	16.01	15.63	479.118	317.067	Pet3Glc	21.58 ± 0.40 ^c	8.2
9	16.68	16.38	463.124	301.072	Peo3Gal	2.75 ± 0.12 ^d	1.0
10	16.99	16.99	449.109	317.067	Pet3Ara	6.80 ± 0.15 ^c	2.6
11	17.84	18.08	463.124	301.073	Peo3Glc	10.39 ± 0.18 ^d	4.0
12	18.00	18.32	493.135	331.083	Mal3Gal	8.24 ± 0.18 ^e	3.1
13	18.49	18.49	433.113	301.073	Peo3Ara	1.67 ± 0.11 ^d	0.6
14	18.85	18.76	493.135	331.083	Mal3Glc	20.53 ± 0.37 ^e	7.8
15	19.65	19.06	463.124	331.082	Mal3Ara	5.20 ± 0.12 ^e	2.0
Total						262.9 ± 5.46	100

[#]The quantification method was performed by using an external standard curve at 520 nm on HPLC-DAD. The content was calculated using the average of five different concentrations of bilberry extract powder. Values are expressed as mean ± SD.

^a=expressed as Del3Glc, ^b=expressed as Cya3Glc, ^c=expressed as Pet3Glc, ^d=expressed as Peo3Glc, and ^e=expressed as Mal3Glc.

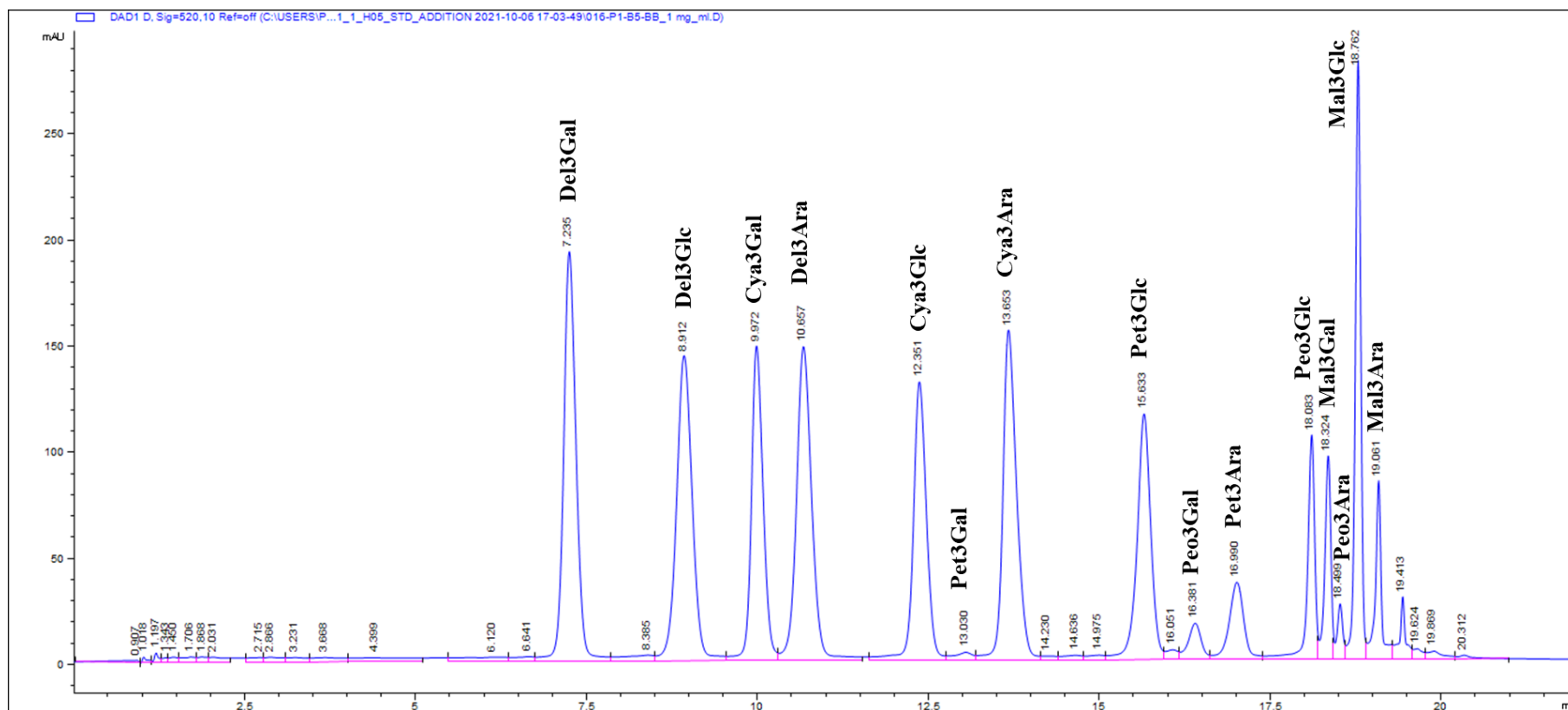


Figure 4. 7. HPLC-DAD chromatogram of bilberry anthocyanins at 520 nm.

The quantification method was performed by using an external standard curve for five authentic anthocyanins (Del3Glc, Cya3Glc, Peo3Glc, Pet3Glc, and Mal3Glc). A 20 μ L was injected into the reversed-phase column using a gradient elution of 5% v/v formic acid in water as solvent A, and 5% v/v formic acid in acetonitrile as solvent B.

4.4.2. The disappearance of Cya3Glc during incubation of a black rice anthocyanin extract in the human *in-vitro* colon model.

In order to gain an understanding of the rate at which the anthocyanins disappear during the microbial colonic fermentations, how long it takes for all the anthocyanins to disappear, and what would be a suitable starting concentration, preliminary investigations were carried out. First, black rice extract was incubated with human fresh faecal samples in the batch *in-vitro* colon model (**Figure 4. 8**) as described in detail in Chapter 2 (**Section 2.2**). Two different concentrations of black rice extract powder were tested (**Figure 4. 9** and **Figure 4. 10**). Control vessels were inoculated with a human fresh faecal sample but without black rice extract.

No Cya3Glc was detected in any of the samples from the control vessels and was detected in samples from vessels treated with black rice extract. However, the initial quantified concentration (C_{initial}) of Cya3Glc at 0 h was significantly lower than the initial theoretical concentration (C_{theo} , 66.80 μM) with a 42.2 % and 44.9 % reduction when using the faecal slurries from donor 01-S1 and donor 04-S1, respectively. Cya3Glc concentration declined rapidly over time with complete disappearance of Cya3Glc by 8 h in donor 01-S1 and by 4 h in donor 04- S1 (**Figure 4. 9**). The initial rate of loss of anthocyanin was estimated by comparing the concentration of Cya3Glc at 0 h with that at the 2 h time point. The initial decline rate was 7.75 $\mu\text{M}/\text{h}$ for donor 01-S1 and 13.08 $\mu\text{M}/\text{h}$ for donor 04-S1.

A higher starting concentration of black rice extract was also tested (133.60 μM Cya3Glc) (**Figure 4. 10**). Only one faecal sample was used from donor 01-S2. The quantified Cya3Glc at 0 h was 73.3 μM with a reduction of 45.1 % than the initial C_{theo} (133.36 μM). However, the initial decline rate of the Cya3Glc concentration over the first 2 h was 13.95 $\mu\text{M}/\text{h}$, which was almost twice as fast as for the same donor 01-S1 sample result obtained at half the Cya3Glc concentration (**Figure 4. 9**). At the higher concentration of Cya3Glc, the time required for the complete disappearance of Cya3Glc was somewhere between 8 and 24 h and therefore not observed in this experiment. Although in **Figure 4. 9** there is only a small reduction in the rate of loss of Cya3Glc over the time of its disappearance (i.e., largely straight-line loss of Cya3Glc over time), at the higher concentration, the rate of loss of Cya3Glc noticeably slowed over the time course (**Figure 4. 10**).

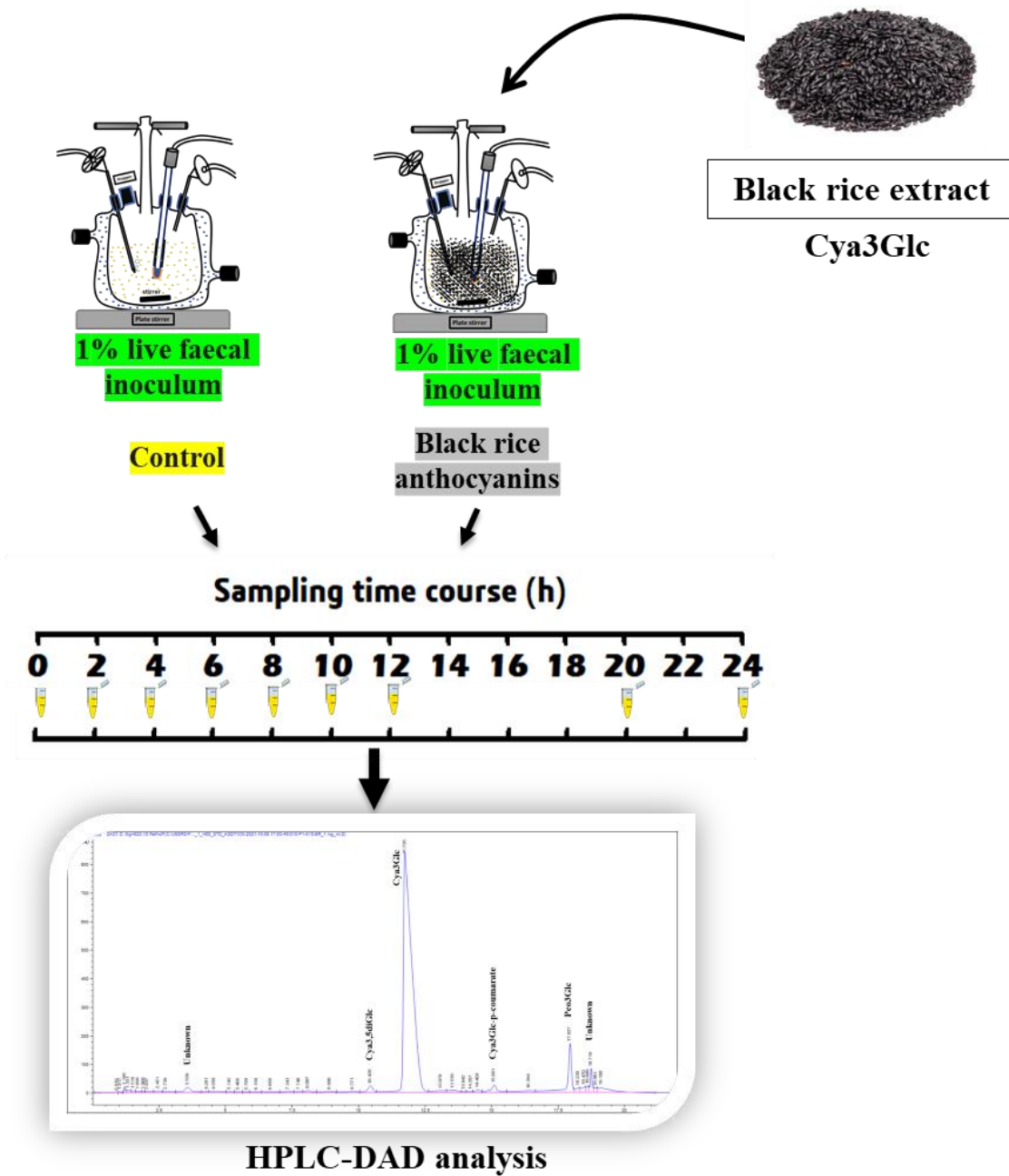


Figure 4. 8. Schematic of experimental design for investigating the metabolism of black rice anthocyanins (Cya3Glc) by the human faecal microbiota using in-vitro human colon model. Black rice extract powder was incubated with live faecal slurry. Control vessel was prepared by inoculating sterile colon media with live-faecal inoculum and no black rice extract was added. Incubation was carried out at pH 6.6-7.0 and 37°C, over 24 h. Samples (0.5 mL) were removed at the times shown in the figure, mixed with 0.5 mL of 4 % v/v aqueous formic acid, and after sample preparation (chapter 2, section 2.2.6), analysed using HPLC-DAD to determine Cya3Glc concentration.

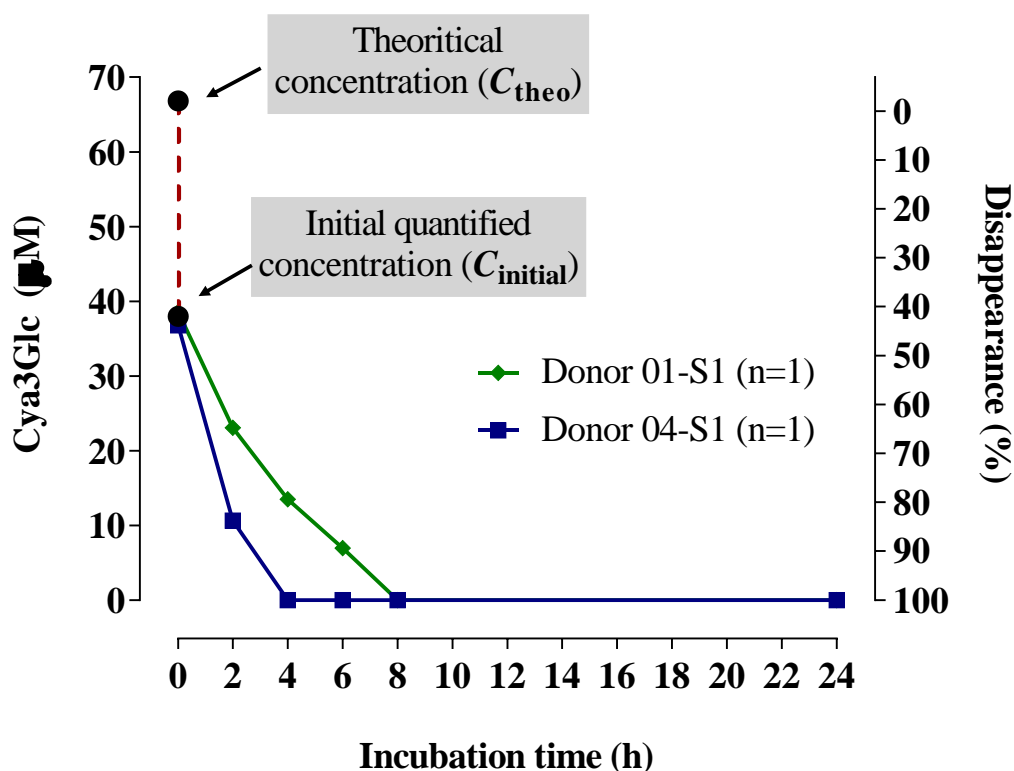


Figure 4. 9. Loss of Cya3Glc during batch in vitro colon model fermentations of a black rice extract (C_{theo} of Cya3Glc = 66.8 μM).

Black rice extract (9 mg, containing 33.36 % w/w Cya3Glc) was dissolved in 1 mL water, filtered and immediately added to a colon model vessel pre-filled with sterile media (89 mL) and human faecal slurry (10 mL of a 10 % slurry from a fresh stool) to give a final volume of 100 mL and a Cya3Glc concentration of 66.80 μM (30 $\mu\text{g}/\text{mL}$). The media was also pre-equilibrated with nitrogen overnight prior to sample inoculation to maintain anaerobicity. Control vessels were prepared by incubating fresh faecal inoculum in the same colon model media but without black rice extract. Incubation was carried out at pH 6.6-7.0 and 37°C, over 24 h with continuous nitrogen flow. Samples (0.5 mL) were collected at the times shown in the figure, mixed with 0.5 mL of 4 % v/v aqueous formic acid, and after sample preparation (chapter 2, section 2.2.6) analysed using HPLC-DAD to determine the Cya3Glc concentration. The experiment was repeated once on a separate occasion using a stool sample from a different donor. No Cya3Glc was detected in control vessels lacking black rice extract (data not shown). Each donor is designated by a unique donor number (here donor 01 and donor 04) and the sample number indicates the distinct stool sample provided by a donor on a specific day; ‘sample 1’ here indicates that for both donors this was the first stool samples they donated that was used in the studies reported in this thesis. No Cya3Glc was detected in control vessels lacking black rice extract (data not shown).

Since there may be significant individual variations in the rate of loss of Cya3Glc, more sampling points at 10, 12 and 20 h were added as it was likely for Cya3Glc to fully disappear before the 24 h sample point.

The time between introducing the black rice extract to the vessels and the first time point sample (0 h) is ranged from 1 to 3 mins. It is possible that part of Cya3Glc broke down immediately once black rice extract was been added as anthocyanin is extremely unstable in neutral pH^{38,87}. In addition, before introducing the black rice and inoculating the colon media with faecal slurry, some of the acid (HCl 0.5 M) and/or base (NaOH 0.5 M) solutions were added initially and automatically into vessels to normalise the colon media pH to 6.6-7.0 if the pH is out of this range. This addition of acid and/or base may cause dilution to the initial concentration of the Cya3Glc. Therefore, it was decided that the final volumes inside the vessels to be measured at the end of each experiment which would then be used to work out the total volume in the vessel and correct for this in the final Cya3Glc concentration at each time point. All upcoming figures will present the quantified concentration of Cya3Glc from the first time point sampling as 0 h samples. Therefore, any concentrations or rates that correlate with the initial concentration, will be presented in this thesis based on the initial quantified concentration (C_{initial}) collected from sample at 0 h, not based on the theoretical concentration (C_{theo}).

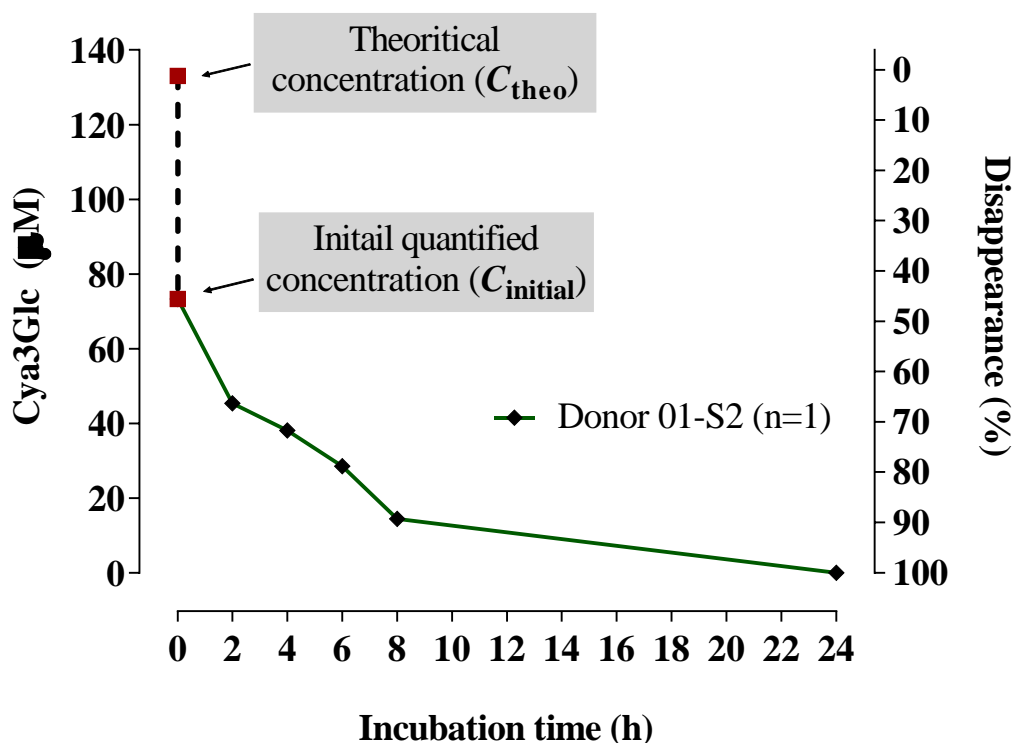


Figure 4. 10. Loss of Cya3Glc during batch in vitro colon model fermentations of a black rice extract (C_{theo} of Cya3Glc = 133.6 μ M).

Black rice extract (18 mg, containing 33.36 % w/w Cya3Glc) was dissolved in 1 mL water, filtered and immediately added to a colon model vessel pre-filled with sterile media (89 mL) and human faecal slurry (10 mL of a 10 % slurry from a fresh stool) to give a final volume of 100 mL and a Cya3Glc concentration of 133.60 μ M (60 μ g/mL). Control vessels were prepared by incubating fresh faecal inoculum in the same colon model media but without black rice extract. Incubation was carried out at pH 6.6-7.0 and 37°C, over 24 h with continuous nitrogen flow. Samples (0.5 mL) were collected at the times shown in the figure, mixed with 0.5 mL of 4 % v/v aqueous formic acid, and after sample preparation (chapter 2, section 2.2.6), analysed using HPLC-DAD to determine the Cya3Glc concentration. No Cya3Glc was detected in control vessels lacking black rice extract (data not shown).

4.4.3. The contribution of the faecal microbiota to the disappearance of Cya3Glc during *in-vitro* colon fermentation

Having observed that Cya3Glc disappears during a 24 h incubation in a human *in-vitro* colon model, the next question that was addressed was whether this was entirely, partly or not at all caused by the activity of the faecal microbiota. In order to explore this, incubations of black rice anthocyanin extract with a human faecal inoculum were conducted with both fresh and autoclaved faecal slurry (**Figure 4. 11**), where the autoclaving process served to kill all the viable microorganisms in the faecal slurry and therefore representing spontaneous degradation. A control vessel containing non-autoclaved faecal slurry, but no black rice extract was also included in the experimental design.

No Cya3Glc was detected in any samples taken from the control vessels that had not been supplemented with black rice extract. In the vessels supplemented with black rice extract, Cya3Glc was detected in the 0 h timepoint samples at 109 ± 17.1 and 110.2 ± 6.1 μM concentration in vessels containing fresh faecal slurry and autoclaved faecal slurry, respectively (**Figure 4. 12**). Compared to the initial C_{theo} of Cya3Glc (133.36 μM), the C_{initial} of Cya3Glc were significantly lower, with 18.4 % and 17.5 % reduction in fresh faecal slurry and autoclaved faecal slurry, respectively.

In the vessels containing live faecal microbiota, Cya3Glc declined over the time course with an initial rate of 16.8 ± 7.8 $\mu\text{M}/\text{h}$ over the first 2 h. In contrast, in vessels containing autoclaved faecal slurry, Cya3Glc declined at a significantly slower rate (12.7 ± 5.2 $\mu\text{M}/\text{h}$ over the first 2 h) compared to similar vessels containing live faecal microbiota. In addition, at 24 h time point sample, Cya3Glc was detectable at 30.8 ± 27.3 μM in samples taken from vessels containing autoclaved faecal slurry, whereas Cya3Glc was not detectable in any samples taken after 8 h from vessels containing live faecal microbiota.

These data demonstrate that the disappearance of Cya3Glc (the black rice anthocyanin) incubated anaerobically at pH 6.6-7.0, 37°C and in the presence of live faecal microbiota is partly microbiota-dependent and partly not due to the activity of the faecal microbiota. It is widely known that anthocyanins are not stable at near neutral pH³⁸ and the non-

microbiota-dependent components of Cya3Glc disappearance likely reflect chemical instability and will be referred to “spontaneous degradation”.

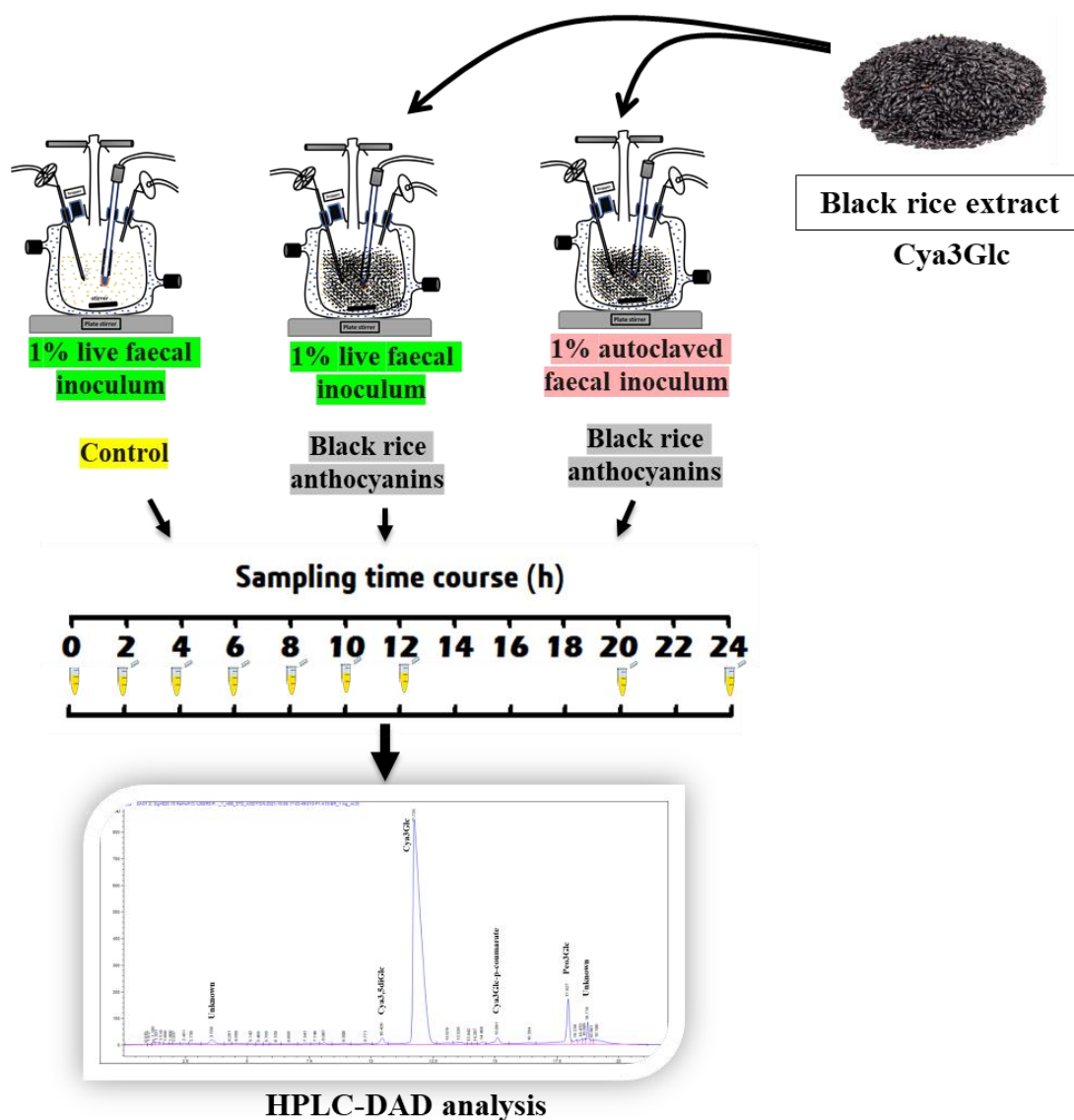


Figure 4. 11. Schematic of experimental design for investigating the difference between the spontaneous and the gut microbiota-dependent degradations of black rice anthocyanins (Cya3Glc) using *in-vitro* human colon model.

Black rice extract powder was incubated with live faecal slurry and separately with autoclaved faecal slurry. Control vessel was prepared by inoculating sterile colon media with live-faecal inoculum and no black rice extract was added. Incubation was carried out at pH 6.6-7.0 and 37°C, over 24 h with continuous nitrogen flow. Samples (0.5 mL) were removed at the times shown in the figure, mixed with 0.5 mL of 4 % v/v aqueous formic acid, and after sample preparation (chapter 2, section 2.2.6), analysed using HPLC-DAD to determine Cya3Glc concentration.

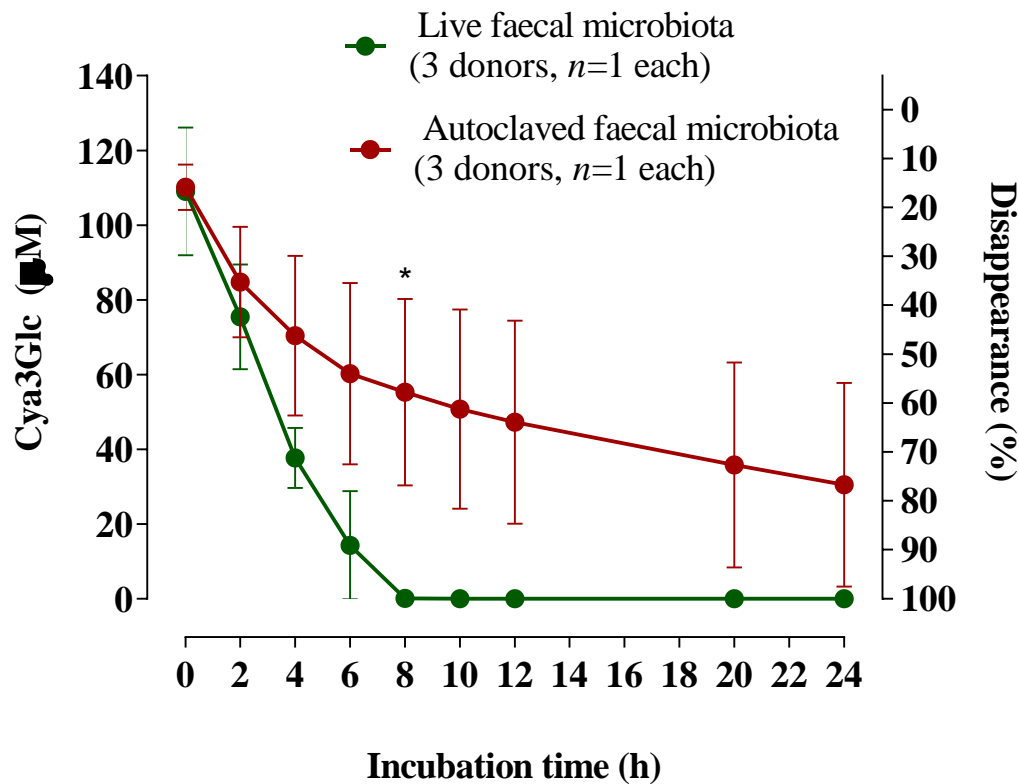


Figure 4. 12. Loss of black rice anthocyanins (C_{theo} of Cya3Glc = 133.6 μM) over time was partly spontaneous and partly due to gut microbiota.

Black rice extract (18 mg, containing 33.36 % w/w Cya3Glc) was dissolved in 1 mL water, filtered and immediately added to colon model vessels pre-filled with sterile media (89 mL) and human faecal slurry (10 mL of a 10 % slurry from a fresh stool) to give a final volume of 100 mL and a Cya3Glc concentration of 133.60 μM (60 $\mu\text{g}/\text{mL}$). Similar vessels were prepared but containing autoclaved faecal slurry rather than fresh faecal slurry. Control vessels contained fresh faecal inoculum and media, but no black rice extract. Incubations were carried out at pH 6.6-7.0 and 37°C, over 24 h. Samples (0.5 mL) were collected at the times shown in the figure, mixed with 0.5 mL of 4 % v/v aqueous formic acid, and after sample preparation (chapter 2, section 2.2.6), analysed using HPLC-DAD to determine the Cya3Glc concentration. The data shown are for 3 replicate incubations for each condition using a single donor faecal sample: donor 01 – S3 (n=1), donor 02 – S1 (n=1), and donor 05 – S2 (n=1). No Cya3Glc was detected in control vessels lacking black rice extract (data not shown). Values represent means \pm SD. Statistical analysis was carried out with one-way ANOVA with Tukey multiple comparisons for each time point and **** $p < 0.0001$; *** $p < 0.001$, ** $p < 0.01$, * $p < 0.05$.

4.4.4. The disappearance of Cya3Glc in a simple anaerobic cabinet stirred vessel human colon model that is not pH controlled

Setting up the batch colon model is laborious and time-consuming and as such, it is difficult to carry out technical replicates in the same donor or different donors. However, in order to do more experiments with more replicates, a simple model for investigating the disappearance of black rice anthocyanin (Cya3Glc) by the human faecal microbiota was tried. Simple human-colon stirred vessels, which are not pH controlled, were placed in an anaerobic cabinet where black rice extract was incubated in the presence of fresh human faecal slurry. In addition, black rice extract was incubated with autoclaved faecal slurry. Control vessels were inoculated with human fresh faecal slurry and no black rice extract was introduced.

Cya3Glc was detected in samples collected from vessels treated with black rice extract, whereas no Cya3Glc was detected in control vessels. Cya3Glc was quantified with a significantly lower concentration than the C_{theo} (133.36 μM). The C_{initial} of Cya3Glc at 0 h time point was $84.5 \pm 5.8 \mu\text{M}$ in the presence of live faecal microbiota and $91.5 \pm 4.5 \mu\text{M}$ in the presence of autoclave faecal slurry. These data showed that the black rice anthocyanin recovery is not the same from samples inoculated with live faecal slurry and samples inoculated with autoclaved faecal slurry. However, at 2 h incubation, the disappearance rate of Cya3Glc in the presence of live faecal microbiota was $13.3 \pm 4.3 \mu\text{M/h}$, whereas the spontaneous degradation of Cya3Glc in the presence of autoclaved faecal microbiota was $5.2 \pm 2.1 \mu\text{M/h}$ (**Figure 4. 13**).

In comparison to the pH-controlled colon model (**Figure 4. 12**), Cya3Glc declined at a slower rate when the uncontrolled pH colon model was used (**Figure 4. 13**). For example, in the presence of live faecal microbiota, Cya3Glc fully disappeared after at 8 h incubation in the samples taken from pH-controlled colon vessels, whereas 22.6 μM of Cya3Glc remained (27 % of the initial quantified Cya3Glc) after 24 h incubation in the absence of pH control. Similarly, with autoclaved faecal microbiota, Cya3Glc declined faster when the incubation occurred in the presence of pH controlled (70 % disappeared at 24 h incubation) than with no controlled pH fermentation (38 % disappeared at 24 h incubation).

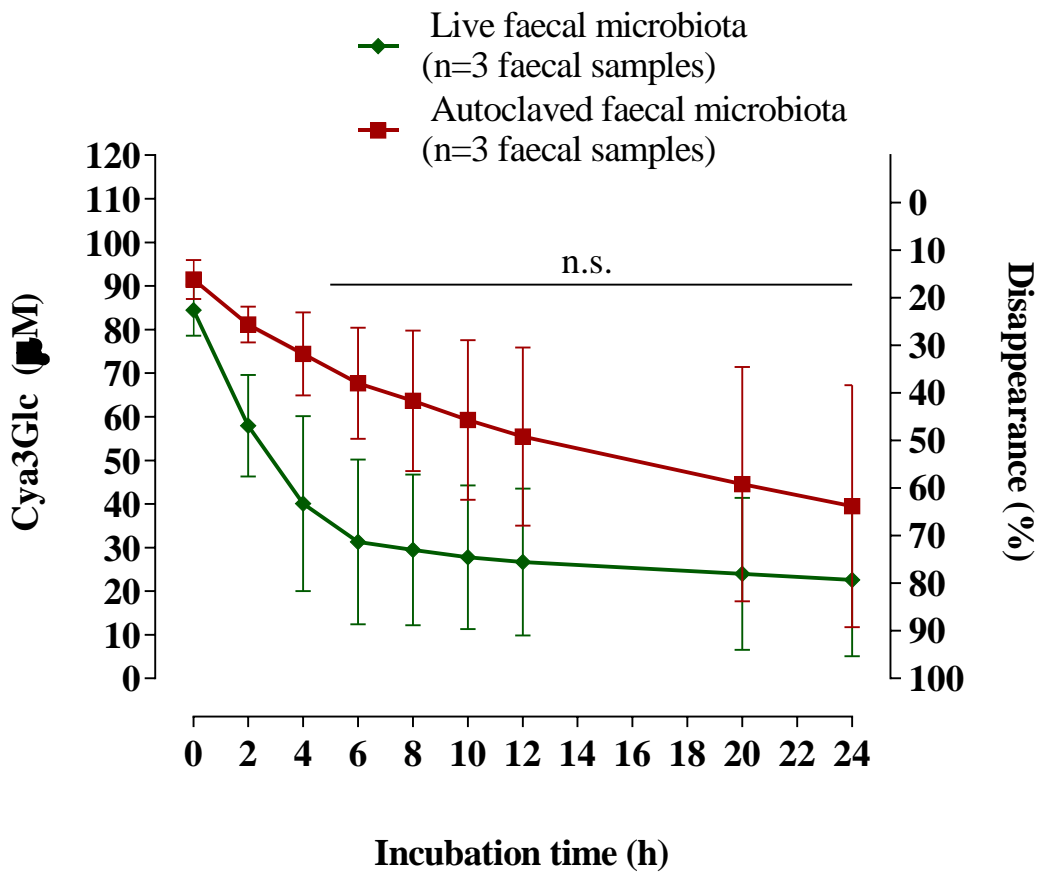


Figure 4. 13. Loss of black rice anthocyanin (C_{theo} of Cya3Glc = 133.60 μ M) using uncontrolled pH model.

Black rice extract (9 mg, containing 33.36 % w/w Cya3Glc) was dissolved in 1 mL water, filtered and immediately added to a colon vessel pre-filled with sterile media (44 mL) and human faecal slurry (5 mL of a 10 % slurry from a fresh stool) to give a final volume of 50 mL and a Cya3Glc concentration of 133.60 μ M (60 μ g/mL). Control vessels were prepared by incubating fresh faecal inoculum in the same media but without black rice extract. Control vessels were prepared by incubating autoclaved faecal samples. Incubation was carried out anaerobically at 37°C, over 24 h. Samples (0.5 mL) were collected at the times shown in the figure, mixed with 0.5 mL of 4 % v/v aqueous formic acid, and after sample preparation (chapter 2, section 2.2.6), analysed using HPLC-DAD to determine the Cya3Glc concentration. No Cya3Glc was detected in control vessels lacking black rice extract (data not shown). The data shown are for 3 replicate incubations for each condition using a single donor faecal sample: donor 01 – S4 (n=1), donor 05 – S2 (n=1), and donor 05 – S3 (n=1). Values represent means \pm SD. Statistical analysis was carried out with one-way ANOVA with Tukey multiple comparisons for each time point and **** $p < 0.0001$; *** $p < 0.001$, ** $p < 0.01$, * $p < 0.05$.

4.4.5. The intra-individual variations in the disappearance of Cya3Glc incubated in the *in-vitro* colon model fermentations.

Having observed that (i) the disappearance of black rice anthocyanin (Cya3Glc) is partly spontaneous and partly driven by faecal microbiota, and (ii) controlling the colon fermentation pH is a critical factor for investigating anthocyanin metabolism by the human gut microbiota, the next step was to investigate whether these processes vary within an individual (i.e., between stool samples collected at different times from the same individual). In order to do this, three different samples (S5, S6, and S7) were collected from donor 01 on different days and were incubated separately with black rice extract (Cya3Glc) using the pH-controlled batch colon model. Control vessels were carried out by inoculating the colon media with fresh faecal slurry, but no black rice extract was added.

No Cya3Glc was detected in samples collected from control vessels. In the black rice-treated vessels, Cya3Glc was detected in the 0 h samples with lower concentrations than the C_{theo} (133.4 μM). At 0 h incubation and in comparison, to vessels inoculated with live gut microbiota, the C_{initial} Cya3Glc from 0 h samples incubated with autoclaved faecal microbiota was slightly higher with an average of 116.4 ± 10.3 but it was 102.4 ± 3.9 μM in the presence of live faecal slurry (**Figure 4. 14**).

However, the average initial disappearance rate (over the first 2 h) of Cya3Glc in the presence of live faecal microbiota was faster (23.2 ± 2.4 $\mu\text{M}/\text{h}$) than the Cya3Glc incubated with autoclaved faecal microbiota (7.9 ± 6.5 $\mu\text{M}/\text{h}$) (**Figure 4. 14B**). In addition, no Cya3Glc was detected after 6 h in samples which were incubated with live faecal microbiota from S5 and S6, while only a very low concentration of Cya3Glc (2.3 μM) was detected in the 8 h sample from donor sample S7.

Conversely, Cya3Glc was detectable in all samples collected over the 24 h incubation from vessels that included autoclaved stool samples. However, the initial quantified concentration of Cya3Glc in samples inoculated with autoclaved stool samples from S6 and S7 was almost the same (110.7 μM with S6 and 110.3 μM with S7), and the initial

spontaneous k_{deg} for Cya3Glc was slightly different in the first 2 h to give initial spontaneous k_{deg} of 7.4 $\mu\text{M}/\text{h}$ for S6 and 11.4 $\mu\text{M}/\text{h}$ for S7.

Later at 24 h incubation, the difference in Cya3Glc concentration in both vessels treated with autoclaved stools from S6 and S7 was significantly different (55.5 μM for S7 and 26.5 μM for S6.), but the overall spontaneous k_{deg} over the 24 h of incubation was quite similar (2.2 $\mu\text{M}/1\text{h}$ for S6 and 2.3 $\mu\text{M}/1\text{h}$ for S7). On the other hand, comparing the spontaneous degradation between S5 and S6, the initial spontaneous k_{deg} after 2 h incubation was 7.4 $\mu\text{M}/1\text{h}$ and 11.4 $\mu\text{M}/1\text{h}$ for S5 and S6, respectively. However, after 24 h incubation, the overall spontaneous k_{deg} was more similar to the initial rate of 2.3 $\mu\text{M}/1\text{h}$ and 3.5 $\mu\text{M}/1\text{h}$, respectively.

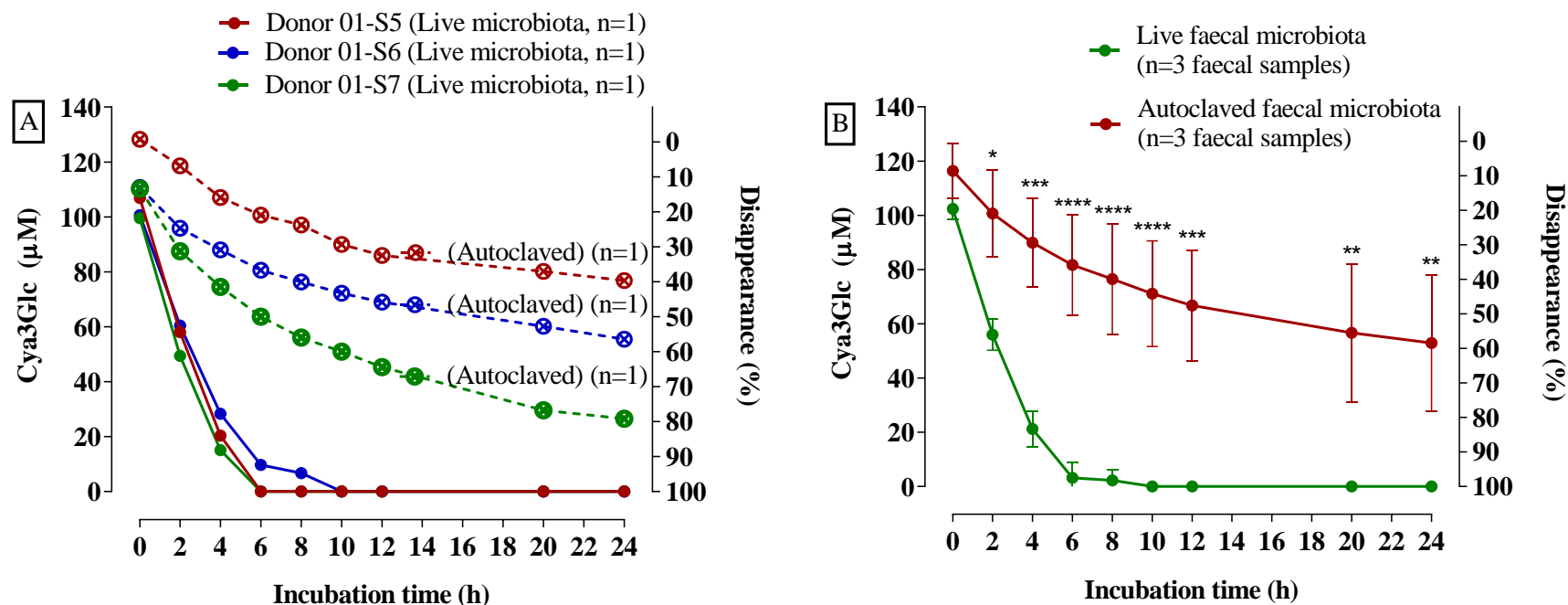


Figure 4. 14. Intra-individual variations in the loss of black rice anthocyanins (C_{theo} of Cya3Glc 133.6 μM) over 24 h.

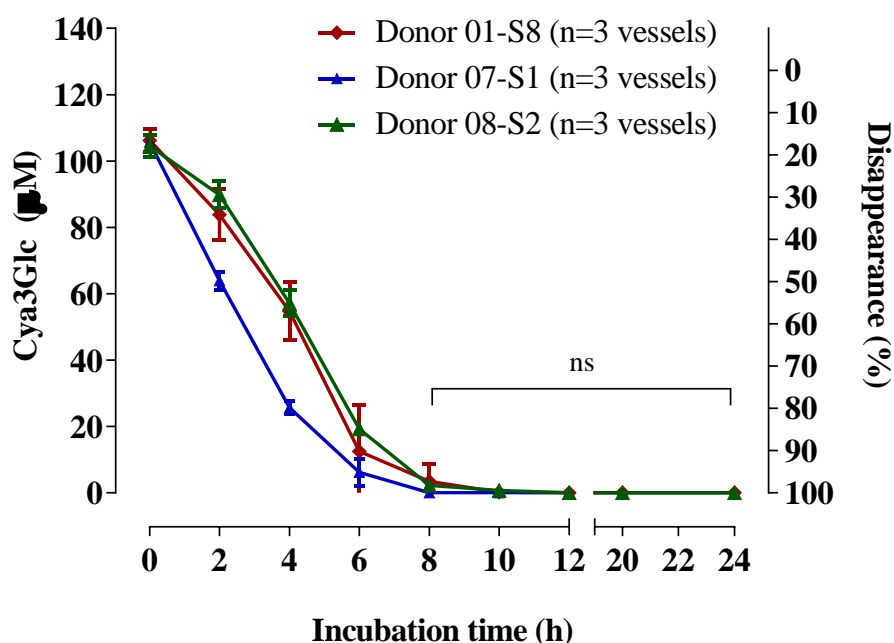
Black rice extract (18 mg, containing 33.36 % w/w Cya3Glc) was dissolved in 1 mL water, filtered and immediately added to a colon model vessel pre-filled with sterile media (89 mL) and human faecal slurry (10 mL of a 10% slurry from a fresh stool) to give a final volume of 100 mL and a Cya3Glc concentration of 133.60 μM (60 $\mu\text{g}/\text{mL}$). Control vessels were prepared by incubating fresh faecal inoculum in the same colon model media but without black rice extract. Incubations were carried out at pH 6.6-7.0 and 37°C, over 24 h. Samples (0.5 mL) were collected at the times shown in the figure, mixed with 0.5 mL of 4 % v/v aqueous formic acid, and after sample preparation (chapter 2, section 2.2.6), analysed using HPLC-DAD to determine the Cya3Glc concentration. No Cya3Glc was detected in control vessels lacking black rice extract (data not shown). The experiments were carried out by using three different faecal samples from the same donor in separate experiments. **A**, data from each donor are presented as one replicate (n=1). **B**, data from the three donors are presented as triplicates (n=3) and values are represented as means \pm SD. Statistical analysis was carried out with one-way ANOVA with Tukey multiple comparisons for each time point and **** $p < 0.0001$; *** $p < 0.001$, ** $p < 0.01$, * $p < 0.05$.

4.4.6. The inter-individual variations in the disappearance of black rice Cya3Glc incubated in the *in-vitro* colon model fermentations.

Next, the inter-individual variations in the disappearance of Cya3Glc, the main black rice anthocyanin, were investigated. In order to investigate this, stool samples were collected from three different donors (Donor 01-S8, 07-S1, and 08-S2) on the same day and faecal slurries were immediately prepared from each of the three stool samples. Each faecal slurry was used to inoculate three different vessels that were treated with the same amount of black rice extract (n=3). In addition, one control vessel was prepared for each donor where the vessel was inoculated with live faecal slurry, but no black rice was introduced. The incubations for all vessels were carried out using a pH-controlled batch colon model over 24 h.

No Cya3Glc was detected in samples collected from control vessels whereas Cya3Glc was detected in samples collected from black-rice-treated vessels. Cya3Glc was detected in 0 h samples at lower concentrations (mean=106.2 μM for donor 01, 105.7 μM for donor 07, and 104.5 μM for donor 08) than the theoretical concentration (133.4 μM) (**Figure 4. 15**). In addition, no Cya3Glc was detected after 6 h in the samples incubated with live faecal microbiota from S5 and S6, while only a small concentration of Cya3Glc was detectable (mean=2.3 μM) after 8 h in the samples from incubations with donor 07.

The initial rate was calculated for the first 2 h for the three donors, which showed there were significant differences between donor 07 ($k_{\text{deg}} 20.9 \pm 1.0 \mu\text{M/h}$) compared to donor 01 ($k_{\text{deg}} 11.2 \pm 2.8 \mu\text{M/h}$) or donor 08 ($k_{\text{deg}} 7.3 \pm 1.8 \mu\text{M/h}$) but no significant difference was shown between donor 07 and donor 08 (**Figure 4. 15**). Cya3Glc had completely disappeared from 8 h samples incubated with live faecal microbiota from donor 07. In contrast, Cya3Glc was detectable until 10 h incubation in samples from both donor 01 and donor 08. However, there was no significant difference between all donors between 8 h and 24 h.



Time (h)	Donor 01 / Donor 07	Donor 01 / Donor 08	Donor 07 / Donor 08
0	ns	ns	ns
2	****	ns	****
4	****	ns	****
6	ns	ns	*

Figure 4. 15. Inter-individual variations in the loss of black rice anthocyanins (C_{theo} of Cya3Glc 133.6 μ M) over 24 h incubated with fresh faecal microbiota.

Black rice extract (18 mg, containing 33.36 % w/w Cya3Glc) was dissolved in 1 mL water, filtered and immediately added to a colon model vessel pre-filled with sterile media (89 mL) and human faecal slurry (10 mL of a 10 % slurry from a fresh stool) to give a final volume of 100 mL and a Cya3Glc concentration of 133.60 μ M (60 μ g/mL). Control vessels were prepared by incubating fresh faecal inoculum in the same colon model media but without black rice extract. Incubation was carried out at pH 6.6-7.0 and 37°C, over 24 h. Samples (0.5 mL) were collected at the times shown in the figure, mixed with 0.5 mL of 4 % v/v aqueous formic acid, and after sample preparation (chapter 2, section 2.2.6), analysed using HPLC-DAD to determine the Cya3Glc concentration. No Cya3Glc was detected in control vessels lacking black rice extract (data not shown). The experiments were carried out by using three different faecal samples from different donors. Each faecal sample was incubated in triplicates. Values represent means \pm SD. Statistical analysis was carried out with one-way ANOVA with Tukey multiple comparisons for each time point and **** $p < 0.0001$; *** $p < 0.001$, ** $p < 0.01$, * $p < 0.05$.

4.4.7. Assessment of the feasibility and viability of micro-organisms when using glycerol-frozen faecal stocks for investigating the disappearance of Cya3Glc during colonic fermentation.

Having demonstrated intra- and inter-individual variations on the disappearance of black rice anthocyanins by human faecal microbiota and, next, the feasibility and viability of microorganisms when using the same stool samples on different occasions to obtain more replicates, using glycerol-frozen faecal stocks was assessed. In addition, the use of glycerol stocks would be important when investigating a large number of samples from clinical trials where the capability to metabolise anthocyanins is investigated in frozen faecal samples. Glycerol-frozen faecal stocks were inoculated into the *in-vitro* colon model vessels to examine the microbial ability to metabolise anthocyanins. Two experiments were conducted using frozen-faecal glycerol stocks which are prepared previously from a fresh faecal sample donated by donor 01-S5. The prepared glycerol-frozen faecal stock contains 37.5 % w/w faecal, 25 % v/v glycerol, and 37.5 % v/v phosphate buffer (BPS) (Chapter 2, section 2.2.3). The first experiment was carried out by thawing the glycerol-frozen stock at room temperature for 30 mins (**Figure 4. 16A**). Then, 2.9 mL of glycerol-frozen faecal stock was used to inoculate the colon vessel. Another 2.9 mL was autoclaved and then added to another vessel to investigate the spontaneous degradation. The experiment was carried out in triplicates. The second experiment was carried out the same way and glycerol-frozen faecal stock from donor 01-S5 was also used to inoculate the colon vessels, but the glycerol-frozen faecal stock was incubated in the anaerobic cabinet for 1 h at 37°C before being added to the colon vessels (**Figure 4. 16B**). Control vessels were also set up for both experiments A and B, inoculated with live glycerol faecal stock with colon media, but no black rice extract was added.

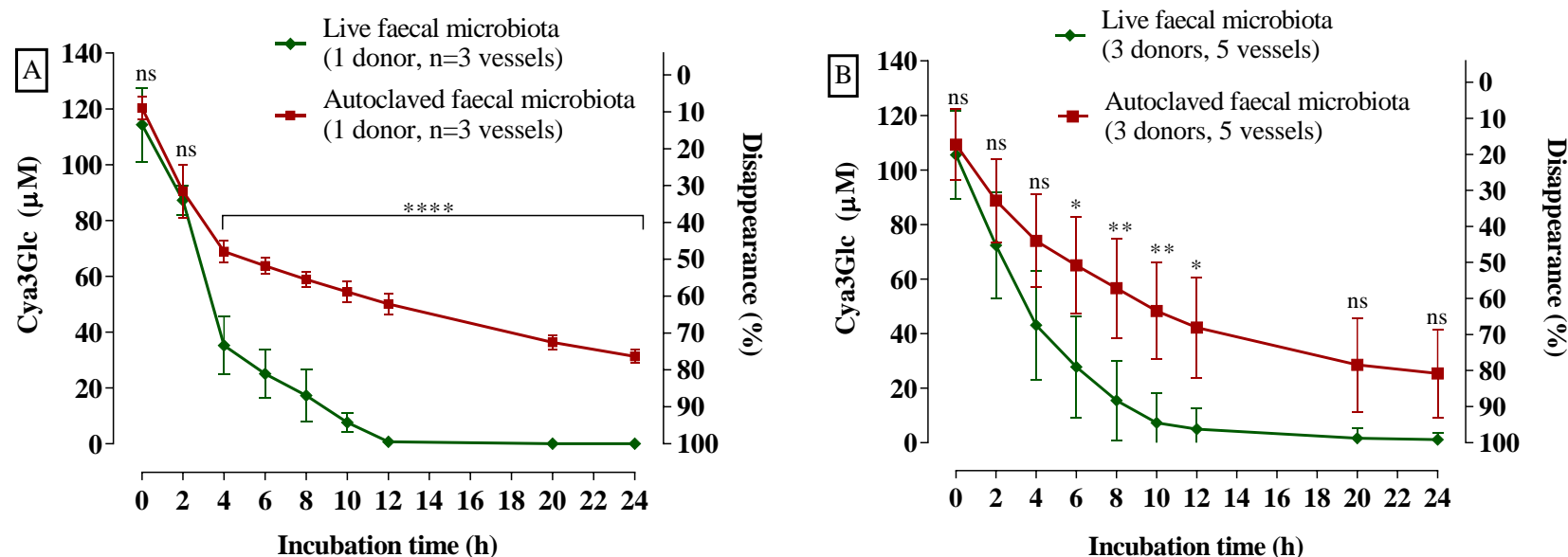


Figure 4. 16. Loss of black rice anthocyanins (C_{theo} of Cya3Glc 133.6 μM) over 24 h fermentations using glycerol-frozen faecal stock.

Black rice extract (18 mg, containing 33.36 % w/w Cya3Glc) was dissolved in 1 mL water, filtered and immediately added to a colon model vessel pre-filled with sterile media (96.4 mL) and glycerol-frozen faecal stocks (2.6 mL of a 37 % stool sample) to give a final volume of 100 mL, 1 % faecal sample, and a Cya3Glc concentration of 133.60 μM (60 $\mu\text{g}/\text{mL}$). Control vessels were prepared by incubating glycerol-frozen faecal stock in the same colon media but without black rice extract. Incubations were carried out at pH 6.6-7.0 and 37°C, over 24 h. Samples (0.5 mL) were collected at the times shown in the figure, mixed with 0.5 mL of 4 % v/v aqueous formic acid, and after sample preparation (chapter 2, section 2.2.6), analysed using HPLC-DAD to determine the Cya3Glc concentration. No Cya3Glc was detected in control vessels lacking black rice extract (data not shown). Glycerol-frozen faecal stock was previously prepared using a fresh faecal sample collected from different donors. **A**, the glycerol-frozen faecal stock (faecal sample from donor 01-S5) was thawed for 30 min at room temperature before inoculating the vessels (n=3). **B**, the glycerol-frozen faecal stocks (faecal samples from donors 01-S1 (n=1), 01-S5 (n=3), and 03-S3 (n=1)) were incubated in the anaerobic cabinet at 37°C for 1 h before the inoculation (n=5). Values represent means \pm SD. Statistical analysis was carried out with one-way ANOVA with Tukey multiple comparisons for each time point and **** $p < 0.0001$; *** $p < 0.001$, ** $p < 0.01$, * $p < 0.05$.

In experiment A or B, no Cya3Glc was detected in control vessels and only detected in the samples collected from vessels incubated with black rice extract (**Figure 4. 16**). However, Cya3Glc declined faster in the presence of live glycerol faecal microbiota. In contrast, in the presence of autoclaved glycerol faecal microbiota, the Cya3Glc declined at a slower rate. Comparing the rate of loss over the first 2 h, no significant difference between the initial k_{deg} rate in the presence of live faecal microbiota ($13.5 \pm 4.2 \mu\text{M/h}$) and the presence of autoclaved faecal microbiota ($14.9 \pm 3.4 \mu\text{M/h}$) when the glycerol-frozen faecal stock was thawed at room temperature for 30 min before the inoculation; whereas, the k_{deg} was significantly different with $23.1 \pm 7.9 \mu\text{M/h}$ and $11.3 \pm 7.3 \mu\text{M/h}$ when the glycerol-frozen faecal stock was incubated anaerobically for 1 h at 37°C.

4.4.8. Disappearance of a mixture of fifteen bilberry anthocyanins during the human *in-vitro* colonic fermentation

In the previous sections, the metabolism of a purified black rice anthocyanin powder that contained one dominant anthocyanin (Cya3Glc; 87 % of total anthocyanins), was investigated. Here, experiments were conducted using a highly purified anthocyanin extract obtained from bilberries (*Vaccinium myrtillus*) which has a much more complex anthocyanin profile. Anthocyanins in the bilberry extract powder were characterised and reported previously described in this chapter (**Section 4.4.1**). The analysis results showed that the bilberry extract powder contained 15 different types of anthocyanins. Although one anthocyanin was only present at trace levels, the other 14 anthocyanins in the bilberry extract were all present in appreciable amounts and were quantified (**Figure 4. 7**) The detected aglycone moieties (anthocyanidins) in bilberry extract were cyanidin, delphinidin, petunidin, peonidin, and malvidin. All of these were present as anthocyanidin-3-monosaccharides where the sugar moiety was either glucose, galactose, or arabinose. The result showed that the total anthocyanins in bilberry extract powder were 262.9 ± 5.5 mg (g dry weight)⁻¹ (**Table 4. 3**).

The different anthocyanins present at different concentrations in the bilberry extract powder indicate that the bilberry extract powder provides a good example for investigating the metabolism of multi-type anthocyanin sources and/or a mixture of anthocyanins by the human gut microbiota. In order to investigate this, bilberry anthocyanin extract was incubated with both fresh faecal slurry and autoclaved faecal slurry. The experiment was carried out by using 5 different fresh faecal stools donated by donors 01 (n=1), 03 (n=2), and 06 (n=2). Control vessels containing non-autoclaved faecal slurry were carried out with no black rice extract introduced (**Figure 4. 17**).

No anthocyanins were detected in control vessels. But all 14 types of bilberry anthocyanins were detected in samples collected from vessels which were treated with bilberry extract (**Figure 4. 18**). The total quantified the concentration of bilberry anthocyanins at 0 h was 187.9 ± 42.5 μ M in the presence of live faecal microbiota. In the presence of autoclaved faecal microbiota, the initial quantified concentration was 203.9 ± 27.6 μ M (**Figure 4. 18B**). The total bilberry anthocyanins declined faster in the

presence of live faecal microbiota with an initial rate of $42.8 \pm 12.7 \mu\text{M/h}$, whereas in the presence of autoclaved faecal microbiota, the disappearance rate was slower with the initial spontaneous k_{deg} of $27.6 \pm 11.4 \mu\text{M/h}$.

Only with live faecal samples from donor 03 (n=2), had the anthocyanins fully disappeared by the 6 h time point. However, the initial k_{deg} from the same donor but different faecal samples (S1 and S6) was significantly different. On the other hand, with faecal samples from donor 06 (n=2), the bilberry anthocyanins fully disappeared at 12 h incubation in sample S1, but very small quantities of anthocyanins remained until 24 h incubation. The same was observed with donor 01-S9, small concentrations of bilberry anthocyanins remained, and they were detected in samples collected at 24 h incubation. Previously black rice anthocyanins disappeared completely between 6 and 12 h in the presence of live microbiota (**Figure 4. 14**), but in some cases with bilberry, anthocyanins were observed even at 24 h. Two reasons may explain this, the initial concentration in bilberry was much higher and different types of anthocyanins were present in bilberry rather than just one major anthocyanin in black rice (Cya3Glc).

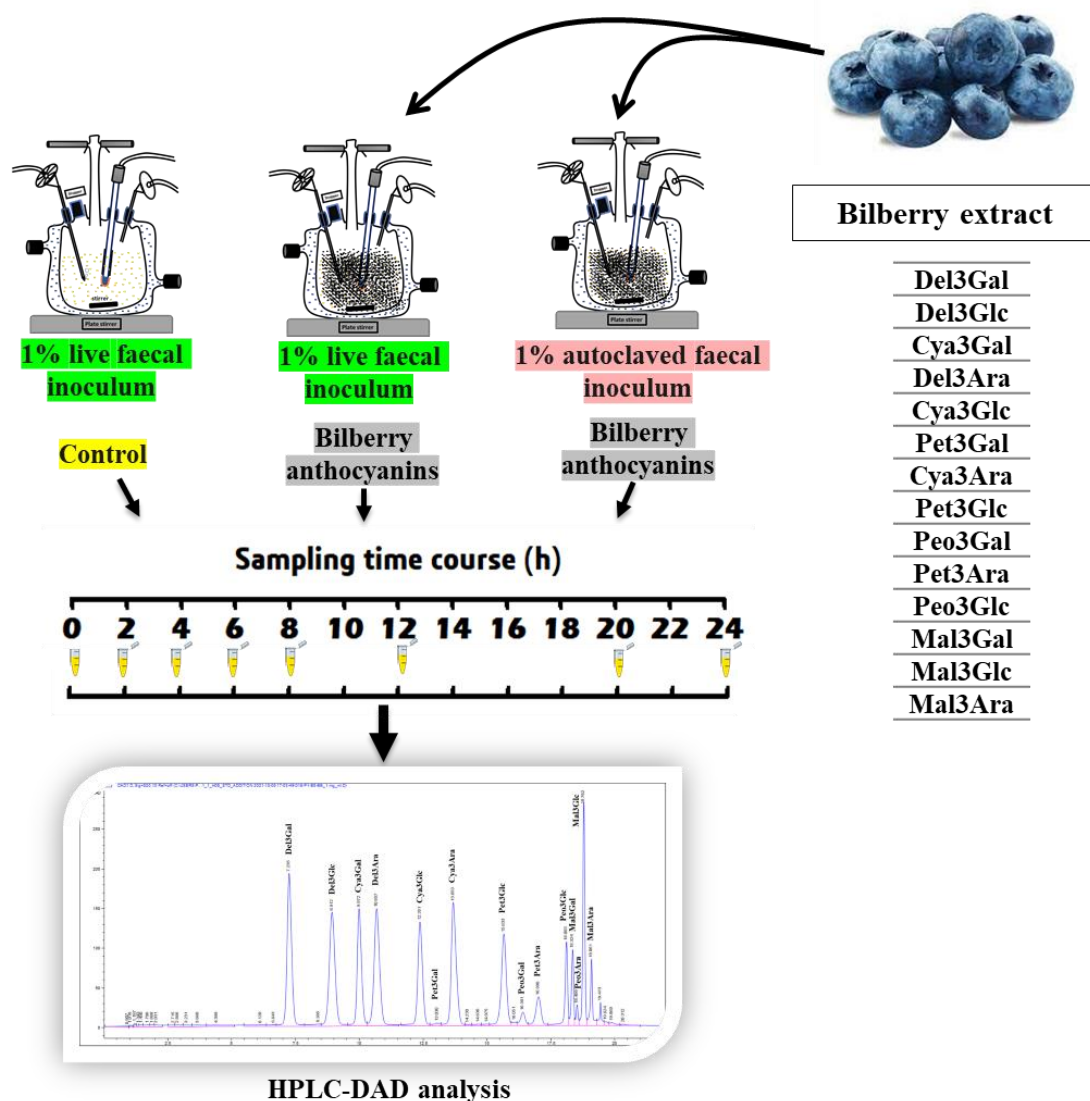


Figure 4. 17. Schematic of experimental design for the metabolism of bilberry anthocyanins by the human faecal microbiota using in-vitro human colon model fermentation.

Bilberry extract powder was incubated with live faecal slurry and separately with autoclaved faecal slurry. Control vessel was prepared by inoculating sterile colon media with live-faecal inoculum and no bilberry extract was added. Incubation was carried out at pH 6.6-7.0 and 37°C, over 24 h with a continuous nitrogen flow. Samples (0.5 mL) were removed at the times shown in the figure, mixed with 0.5 mL of 4 % v/v aqueous formic acid, and after sample preparation (chapter 2, section 2.2.6), analysed using HPLC-DAD to determine the concentrations of the 14 anthocyanins.

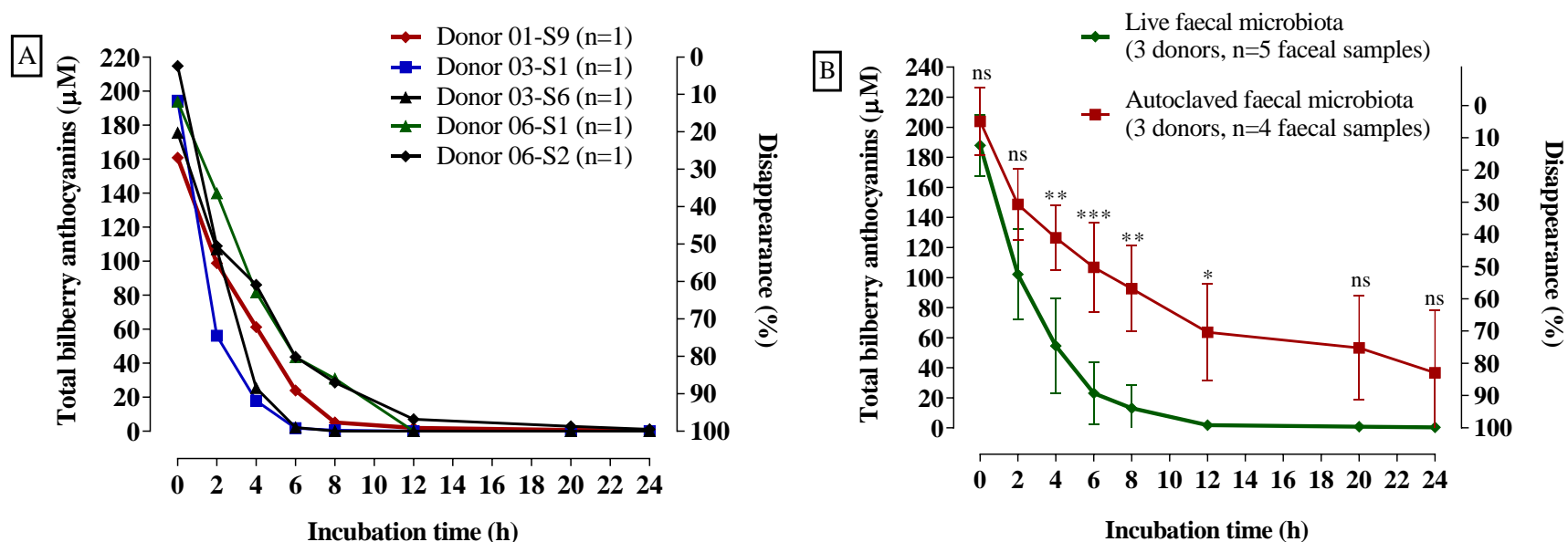


Figure 4. 18. Loss of bilberry anthocyanins (C_{theo} of total anthocyanins = 265 μ M) over 24 h.

Bilberry extract (46 mg, containing 26.2 % w/w anthocyanins) was dissolved in 1 mL water, filtered and immediately added to a colon model vessel pre-filled with sterile media (89 mL) and fresh human faecal slurry (10 mL of a 10 % slurry from a fresh stool) to give a final volume of 100 mL and a total anthocyanin concentration of 265 μ M (120 μ g/mL). Another vessel was prepared in the same way but inoculated with autoclaved faecal slurry. Control vessels were prepared by incubating fresh faecal inoculum in the same media but without bilberry extract. Incubations were carried out at pH 6.6-7.0 and 37°C with continuous nitrogen flow. Samples (0.5 mL) were removed at the times shown in the figure, mixed with 0.5 mL of 4 % v/v aqueous formic acid, and after sample preparation (chapter 2, section 2.2.6) analysed using HPLC-DAD to determine the concentrations of the 14 anthocyanins. No anthocyanins were detected in control vessels lacking bilberry extract (data not shown). The data shown are 5 replicates using donor faecal samples from donor 01 (n=1), donor 03 (n=2), donor 06 (n=2). A, represent separate experiments for the loss of bilberry anthocyanin in the presence of live faecal microbiota with each donor. B, represent the loss of bilberry anthocyanins for all donors (n=5) in the presence of live faecal microbiota and autoclaved faecal slurry; values represent as means \pm SD. Statistical analysis was carried out with one-way ANOVA with Tukey multiple comparisons for each time point and **** $p < 0.0001$; *** $p < 0.001$, ** $p < 0.01$, * $p < 0.05$.

4.4.9. The effect of anthocyanidin B-ring and the conjugated sugars on the disappearance of anthocyanins during colonic fermentation.

Having investigated the metabolism of the total anthocyanins of bilberry by the human faecal microbiota and the differences in k_{deg} between the spontaneous and the gut microbiota-dependent, the same data from the experiment described in the previous section (**Section 4.5.8**) was used again but with the 14 individual anthocyanins in bilberry extract being plotted separately to observe the variations between them in terms of rates of decline. Because the 14 individual anthocyanins in bilberry extract were present at different concentrations, the data for each anthocyanin was normalised to 100 % (i.e., all the individual anthocyanins started at 100 %). The comparison was carried out for the first 8 h of incubation where most of the anthocyanins were still detected in the collected samples.

The data in this section showed that the initial k_{deg} varied between anthocyanins in both gut microbiota-dependent (**Figure 4. 19**) and spontaneous degradation (**Figure 4. 22**). In the presence of live gut microbiota, the nature of aglycone moieties showed to play a role in anthocyanin stability against the activity of faecal microbiota (**Figure 4. 20**). For example, Del3Gal and Cya3Gal showed a high k_{deg} after 2 h incubation, whereas the Mal3Ara showed not only the slowest initial k_{deg} but also the slowest overall k_{deg} in the first 8 h of incubation. All peonidin (Peo) anthocyanins showed medium initial k_{deg} in the first 2 h, however, but also later they showed faster k_{deg} than other anthocyanins at 6 and 8 h incubation. All Del-based anthocyanins showed a higher k_{deg} compared with other aglycones. Malvidin, however, showed the highest stability in the presence of live faecal microbiota. Therefore, in the presence of live faecal microbiota, Del3Gal was the least stable/most rapidly degraded bilberry anthocyanin while Mal3Ara was the most stable/least rapidly degraded bilberry anthocyanin.

Different sugar moieties on the anthocyanins also appeared to affect anthocyanin stability in the presence of live gut microbiota (**Figure 4. 21**). For example, within the same aglycone (i.e., Cya), galactose increased the k_{deg} of the whole molecule of anthocyanins (Cya3Gal), whereas arabinose moiety increased the anthocyanin stability against the

faecal microbiota activity. This may be because there is a difference in the ability of faecal microbiota to hydrolyse arabinose compared to galactose.

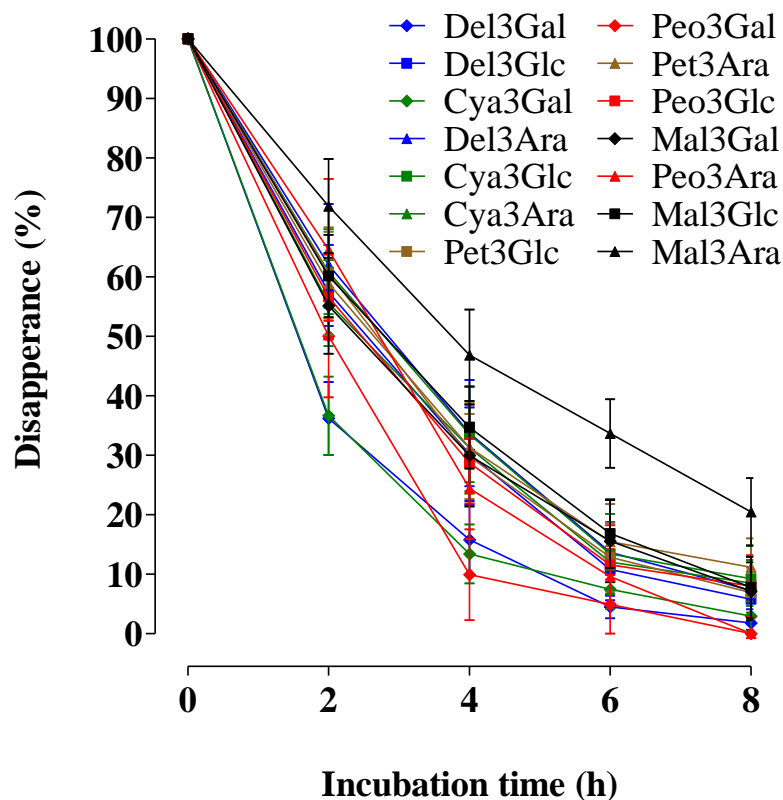


Figure 4. 19. Loss of individual bilberry anthocyanins over the first 8 h in the presence of live faecal microbiota.

Bilberry extract (46 mg, containing 26.2% w/w anthocyanins) was dissolved in 1 mL water, filtered and immediately added to a colon vessel pre-filled with sterile media (89 mL) and human faecal slurry (10 mL of a 10% slurry from a fresh stool) to give a final volume of 100 mL and a total anthocyanin concentration of 265 μ M (120 μ g/mL). Incubations were carried out at pH 6.6-7.0 and 37°C with continuous nitrogen flow. Samples (0.5 mL) were collected at the times shown in the figure, mixed with 0.5 mL of 4% v/v aqueous formic acid, and after sample preparation (chapter 2, section 2.2.6), analysed using HPLC-DAD to determine the concentrations of the 14 individual anthocyanins. All concentrations were normalised to 100% of the initial quantified concentration at 0 h. The data shown are 5 replicates using donor faecal samples from donor 01 (n=1), donor 03 (n=2), donor 06 (n=2). Values represent means \pm SD.

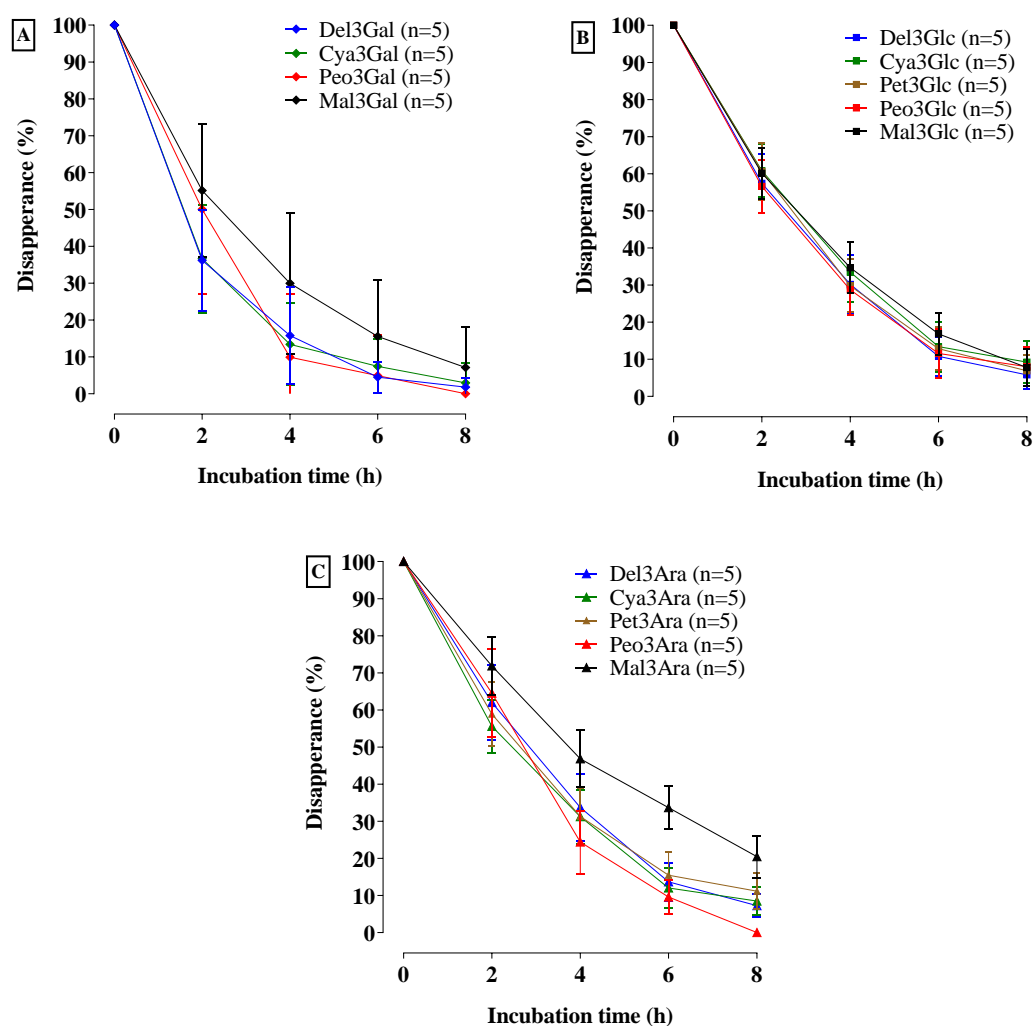


Figure 4. 20. Effect of B-ring on the loss of bilberry anthocyanins which are attached to the same sugar moiety (Galactose (Gal), glucose (Glc), or arabinose (Ara)) over the first 8 h in the presence of live faecal microbiota.

Bilberry extract (46 mg, containing 26.2% w/w anthocyanins) was dissolved in 1 mL water, filtered and immediately added to a colon vessel pre-filled with sterile media (89 mL) and human faecal slurry (10 mL) of a 10% slurry from a fresh stool) to give a final volume of 100 mL and a total anthocyanin concentration of 265 μ M (120 μ g/mL). Incubations were carried out at pH 6.6-7.0 and 37°C with continuous nitrogen flow. Samples (0.5 mL) were collected at the times shown in the figure, mixed with 0.5 mL of 4% v/v aqueous formic acid, and after sample preparation (chapter 2, section 2.2.6), analysed using HPLC-DAD to determine the concentrations of 14 individual anthocyanins. All concentrations were normalised to 100% of the initial quantified concentration at 0 h. The data shown are 5 replicates using donor faecal samples from donor 01 (n=1), donor 03 (n=2), donor 06 (n=2). Values represent means \pm SD. A, loss of bilberry anthocyanins conjugated with galactose. B, loss of bilberry anthocyanins conjugated with glucose. C, loss of bilberry anthocyanins conjugated with arabinose.

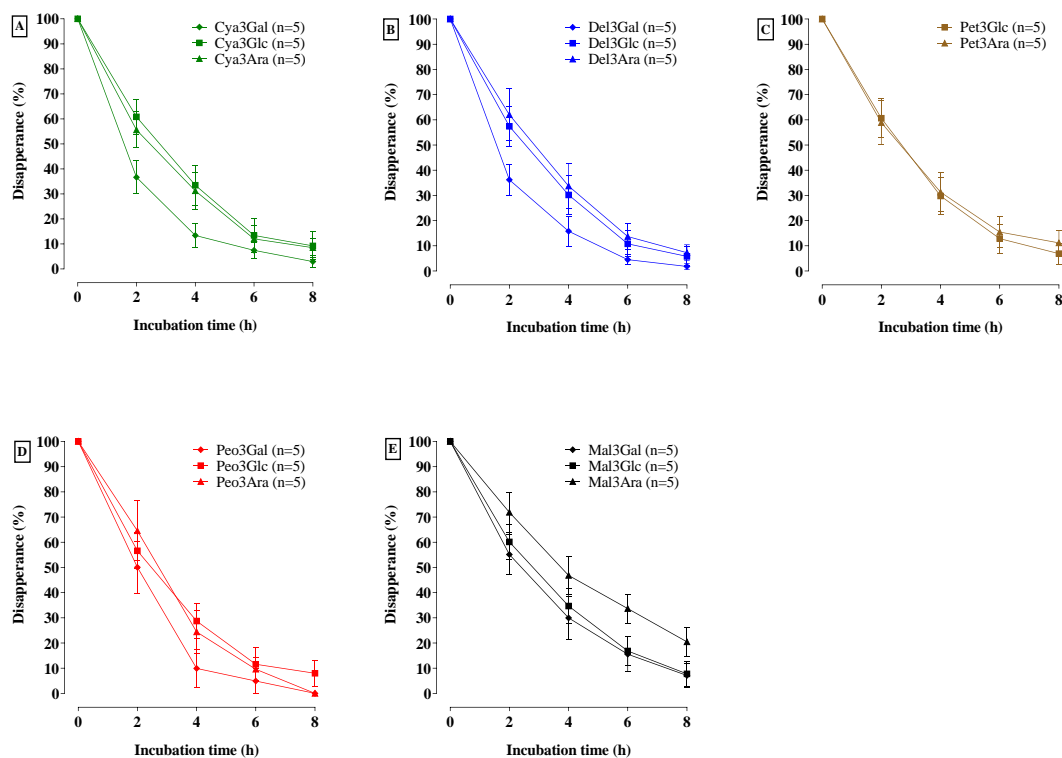


Figure 4. 21. Effects of different sugar substitutions (Galactose (Gal), glucose (Glc) or arabinose (Ara)) on the loss of individual bilberry anthocyanins over the first 8 h in the presence of live faecal microbiota.

Bilberry extract (46 mg, containing 26.2% w/w anthocyanins) was dissolved in 1 mL water, filtered and immediately added to a colon vessel pre-filled with sterile media (89 mL) and human faecal slurry (10 mL of a 10% slurry from a fresh stool) to give a final volume of 100 mL and a total anthocyanin concentration of 265 μ M (120 μ g/mL). Incubations were carried out at pH 6.6-7.0 and 37°C with continuous nitrogen flow. Samples (0.5 mL) were collected at the times shown in the figure, mixed with 0.5 mL of 4% v/v aqueous formic acid, and after sample preparation (chapter 2, section 2.2.6), analysed using HPLC-DAD to determine the 14 individual anthocyanin concentrations. All concentrations were normalised to 100% of the initial quantified concentration at 0 h. The data shown are 5 replicates using donor faecal samples from donor 01 (n=1), donor 03 (n=2), donor 06 (n=2). Values represent means \pm SD. A, loss of the cyanidins of bilberry anthocyanins. B, loss of the delphinidins of bilberry anthocyanins. C, loss of the petunidins of bilberry anthocyanins. D, loss of the peonidins of bilberry anthocyanins. E, loss of the malvidins of bilberry anthocyanins.

In the presence of autoclaved faecal slurries, there were differences in the initial k_{deg} between bilberry anthocyanins over the 2 h incubation period and the overall degradation was consistent with the initial rates of decline (**Figure 4. 22**). For example, the Del-based anthocyanins showed higher rates of decline in the first 2 h, and they kept a constant rate of decline with the highest rate of degradation over the 8 h. In addition, there were no significant differences in the k_{deg} within the same aglycone anthocyanins but have different sugar moieties (**Figure 4. 24**). However, the k_{deg} differences were based on the aglycone, not on the sugar moieties (**Figure 4. 23**).

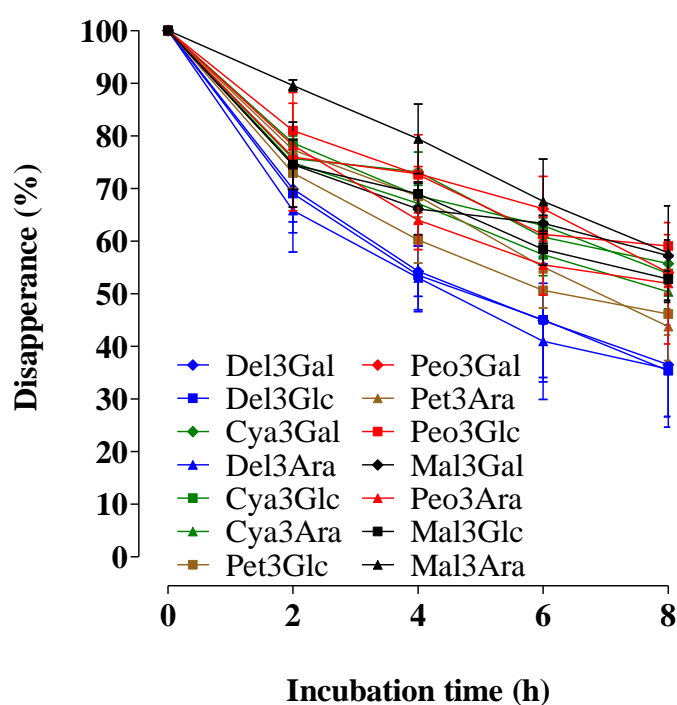


Figure 4. 22. Loss of individual bilberry anthocyanins over the first 8 h in the presence of autoclaved faecal microbiota.

Bilberry extract (46 mg, containing 26.2% w/w anthocyanins) was dissolved in 1 mL water, filtered and immediately added to a colon vessel pre-filled with 89 mL sterile media and 10 mL autoclaved faecal slurry (10% from a fresh stool) to give a final volume of 100 mL and a total anthocyanin concentration of 265 μ M (120 μ g/mL). Incubations were carried out at pH 6.6-7.0 and 37°C with continuous nitrogen flow. Samples (0.5 mL) were collected at the times shown in the figure, mixed with 0.5 mL of 4% v/v aqueous formic acid, and after sample preparation (chapter 2, section 2.2.6), analysed using HPLC-DAD to determine the concentrations of 14 individual anthocyanins. All concentrations were normalised to 100% of the initial quantified concentration at 0 h. The data shown are 5 replicates using donor faecal samples from donor 01 (n=1), donor 03 (n=2), donor 06 (n=2). Values represent means \pm SD.

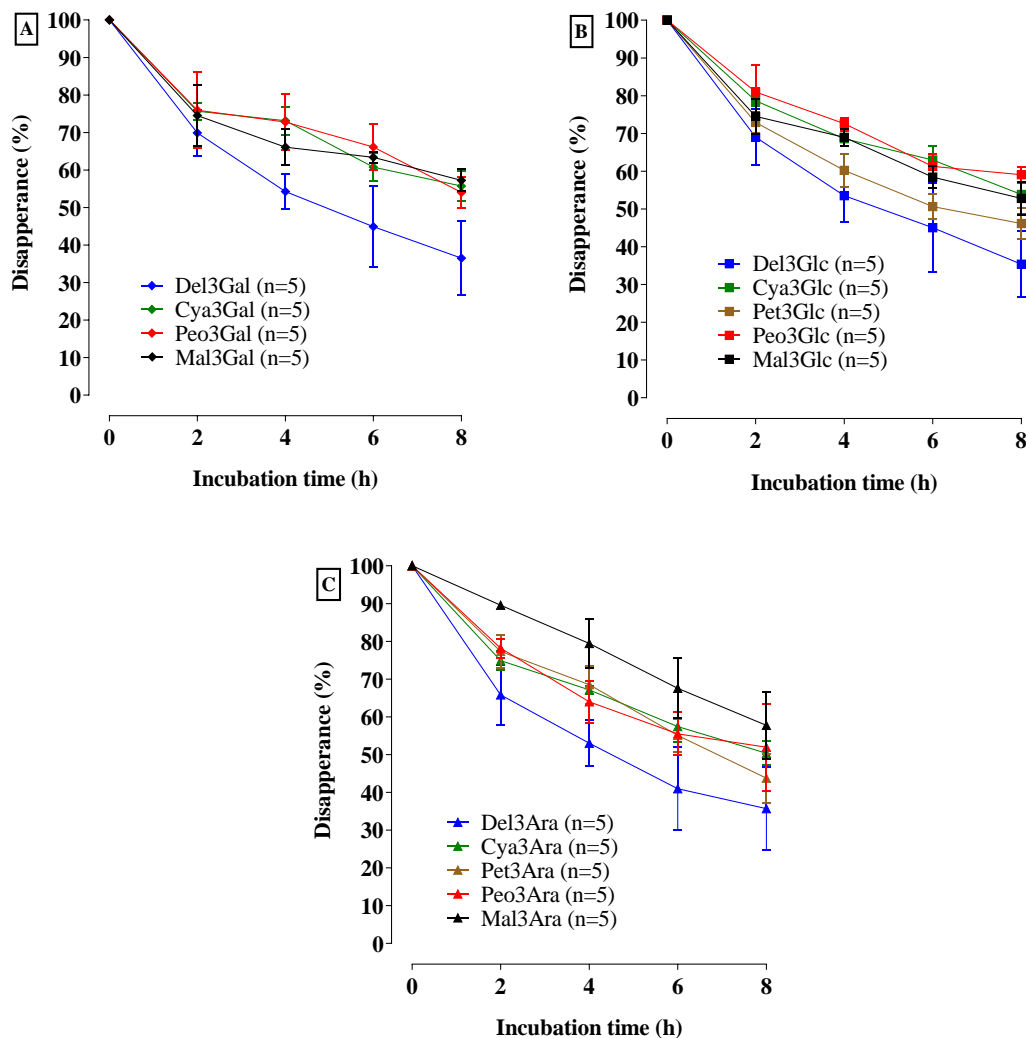


Figure 4. 23. Loss of individual bilberry anthocyanins over the first 8 h in the presence of autoclaved faecal microbiota.

Bilberry extract (46 mg, containing 26.2% w/w anthocyanins) was dissolved in 1 mL water, filtered and immediately added to a colon vessel pre-filled with sterile media (89 mL) and autoclaved human faecal slurry (10 mL of a 10% slurry from a fresh stool) to give a final volume of 100 mL and a total anthocyanin concentration of 265 μ M (120 μ g/mL). Incubations were carried out at pH 6.6-7.0 and 37°C with continuous nitrogen flow. Samples (0.5 mL) were collected at the times shown in the figure, mixed with 0.5 mL of 4% v/v aqueous formic acid, and after sample preparation (chapter 2, section 2.2.6), analysed using HPLC-DAD to determine the concentrations of the 14 individual anthocyanins. All concentrations were normalised to 100% of the initial quantified concentration at 0 h. The data shown are 5 replicates using donor faecal samples from donor 01 (n=1), donor 03 (n=2), donor 06 (n=2). Values represent means \pm SD. **A**, loss of bilberry anthocyanins conjugated with galactose. **B**, loss of bilberry anthocyanins conjugated with glucose. **C**, loss of bilberry anthocyanins conjugated with arabinose.

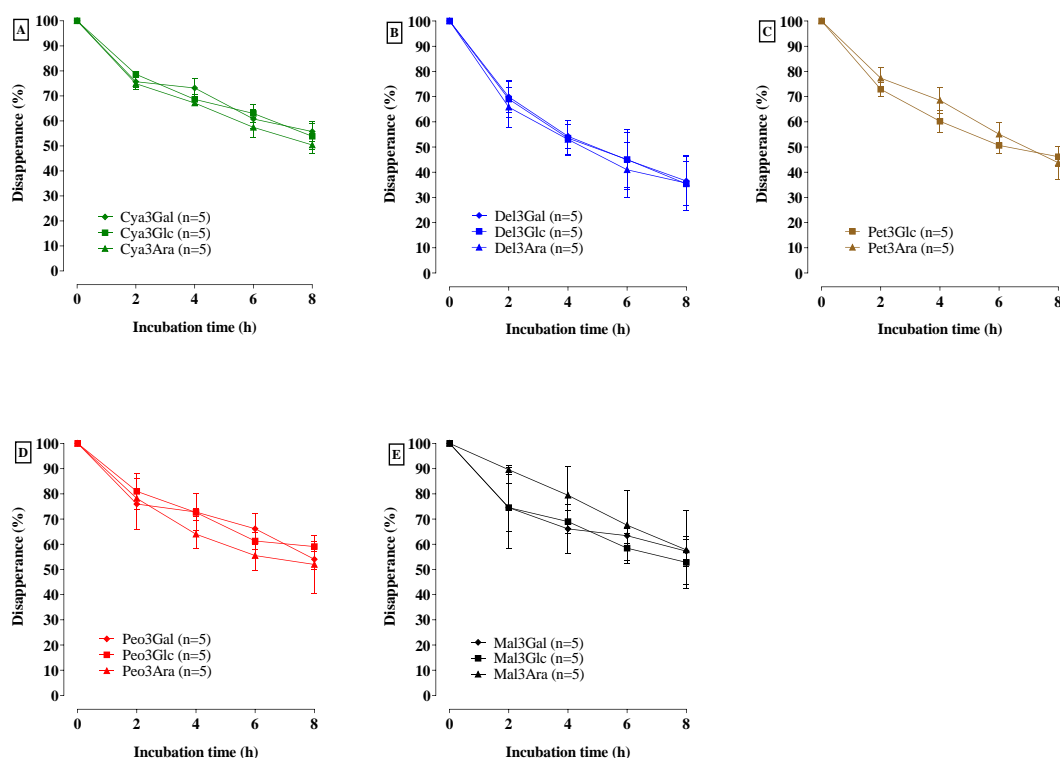


Figure 4. 24. Effects of different sugar substitutions (Galactose (Gal), glucose (Glc) or arabinose (Ara)) on the loss of individual bilberry anthocyanins over the first 8 h in the absence of autoclaved faecal microbiota.

Bilberry extract (46 mg, containing 26.2% w/w anthocyanins) was dissolved in 1 mL water, filtered and immediately added to a colon vessel pre-filled with sterile media (89 mL) and autoclaved human faecal slurry (10 mL of a 10% slurry from a fresh stool) to give a final volume of 100 mL and a total anthocyanin concentration of 265 μ M (120 μ g/mL). Incubations were carried out at pH 6.6-7.0 and 37°C with continuous nitrogen flow. Samples (0.5 mL) were collected at the times shown in the figure, mixed with 0.5 mL of 4% v/v aqueous formic acid, and after sample preparation (chapter 2, section 2.2.6), analysed using HPLC-DAD to determine the concentrations of the 14 individual anthocyanins. All concentrations were normalised to 100% of the initial quantified concentration at 0 h. The data shown are 5 replicates using donor faecal samples from donor 01 (n=1), donor 03 (n=2), donor 06 (n=2). Values represent means \pm SD. **A**, loss of the cyanidins of bilberry anthocyanins. **B**, loss of the delphinidins of bilberry anthocyanins. **C**, loss of the petunidins of bilberry anthocyanins. **D**, loss of the peonidins of bilberry anthocyanins. **E**, loss of the malvidins of bilberry anthocyanins.

On the other hand, in the absence of any faecal materials, the initial k_{deg} between bilberry anthocyanins at 2 h showed different rates, whereas the overall k_{deg} showed a constant k_{deg} for each anthocyanin over the different time points, except for peonidins showed lower k_{deg} after 2 h (**Figure 4. 25**). This contrasts with the anthocyanins incubated with autoclaved samples which showed relatively higher k_{deg} in the first 2 h compared to 4, 6, and 8 h time points. This suggests that faecal material affects the k_{deg} of anthocyanins

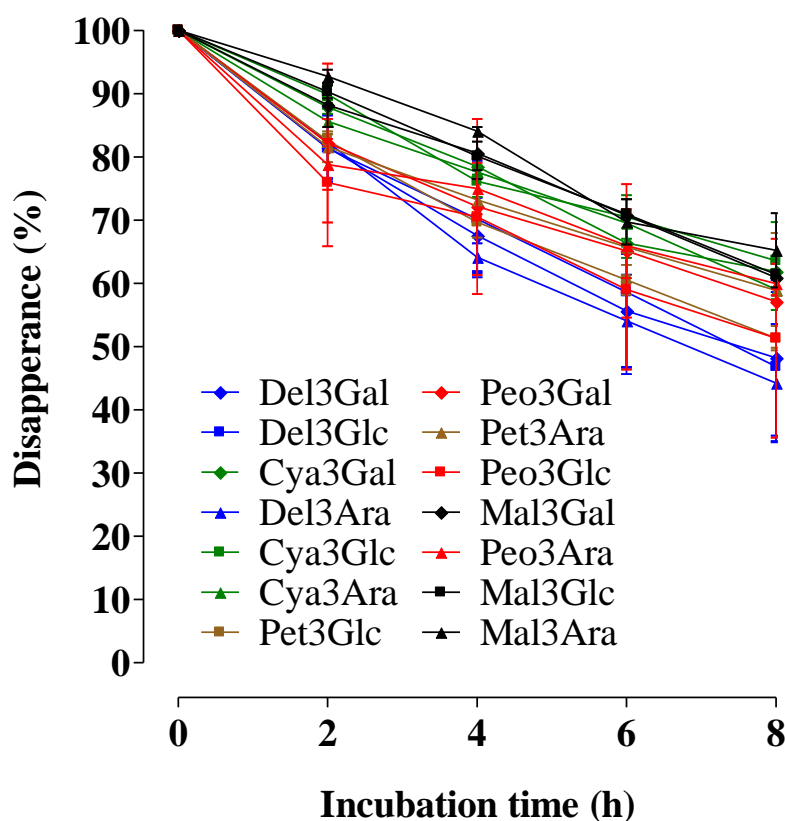


Figure 4. 25. Loss of individual bilberry anthocyanins over the first 8 h only incubated with sterile colon media.

Bilberry extract (46 mg, containing 26.2% w/w anthocyanins) was dissolved in 1 mL water, filtered and immediately added to a colon vessel pre-filled with 89 mL sterile media and 10 mL sterile PBS to give a final volume of 100 mL and a total anthocyanin concentration of 265 μM (120 $\mu\text{g}/\text{mL}$). Incubations were carried out at pH 6.6-7.0 and 37°C with a continuous nitrogen flow. Samples (0.5 mL) were collected at the times shown in the figure, mixed with 0.5 mL of 4% v/v aqueous formic acid, and after sample preparation (chapter 2, section 2.2.6), analysed using HPLC-DAD to determine the concentrations of the 14 individual anthocyanins. All concentrations were normalised to 100% of the initial quantified concentration at 0 h. The data shown are 2 replicates using donor faecal samples from donor 01- S9 (n=1) and donor 03- S2 (n=1). Values represent means \pm SD.

4.5. Discussion

The overall aim of the research described in this chapter was to investigate the metabolism of anthocyanins by the human gut microbiota. In this study, a human *in-vitro* batch colon model was used to incubate and then monitor the rate of loss of anthocyanins. The approaches were to measure the rates of loss of anthocyanins in the presence as well as in absence of live faecal microbiota, to observe variations in the rate of loss of anthocyanin within a person and within individuals, and to relate the rate of loss of anthocyanins to their chemical structures. This was done with a view to furthering our understanding of the metabolism of dietary anthocyanins by the human gut microbiota.

The main findings were that (i) anthocyanins are degraded partly spontaneously and partly due to the activity of faecal microbiota, (ii) the rate of loss of anthocyanins varied between donors but also (iii) varied between faecal samples collected from the same donor but on different occasions, (iv) the B-ring structures and the type of sugar moiety affected the rate of degradation via both the spontaneous and the gut microbiota-dependent routes, (v) controlling the colonic fermentation pH significantly influenced the rate of loss of both spontaneous and gut microbiota-dependent degradations, and (vi) it was feasible to use a glycerol-frozen faecal stock to investigate the gut microbial metabolism of anthocyanins, with the advantage of reducing the intra-individual variation by using the same faecal sample for multiple experiments.

It was demonstrated for the first time in this project that the incubated anthocyanins at physiological range of the human large intestine disappear partly due to a spontaneous process (not requiring live faecal microbiota) and partly due to gut microbiota activity. There are only a few reports of the microbial metabolism of anthocyanins by the gut microbiota. Most of these studies have not considered the potential contribution of spontaneous degradation on anthocyanin disappearance. In line with previous reports, however, the disappearance of anthocyanins occurred faster in the presence of live gut microflora than in incubating anthocyanins without faecal samples. Some of these studies prepared the inoculum from animal gut microflora such as using the content of the large intestine of slaughtered pigs^{89,96} or faeces from germ-free rats²⁴⁰, but the majority of these studies have also used human faecal samples^{88,91,166,173,174,177}. In addition, a few

reports describe experiments using isolated bacterial strains which are commonly found in the human gut such as *Bifidobacteria sp.* and *Lactobacillus sp.*⁹³, and *Actobacillus acidophilus* GIM 1.83 and *Lactobacillus bulgaricus* GIM¹⁷⁶.

In the presence of live faecal microbiota, Aura and others reported that from an initial concentration of 100 μM , Cya3Glc was fully degraded within 2 h when incubation was carried out in the presence of active gut flora¹⁷³. However, Hanske and others showed that only 10 % of the initial concentration of Cya3Glc (100 μM) disappeared within 2 h in the presence of live faecal slurry⁸⁸. Fleschhut and others also reported that after 2 h incubation with live faecal suspension, less than 10 % of the initial concentration of a mixture of Cya3Glc, Mal3Glc, and Peo3Glc remained⁹¹. The current study is novel in that the rate of anthocyanin disappearance was determined in both the presence and absence of live microbiota. While consistent with previous studies that anthocyanins are degraded faster in the presence of the gut microbiota, here it is further demonstrated that the rate of disappearance depends on the initial concentrations.

The novelty of the data in this chapter is that there are significant differences in the k_{deg} of anthocyanins in the presence and absence of live faecal microbiota. This was important to determine the contribution of gut microbiota in anthocyanin degradation compared with spontaneous degradation of anthocyanins. For example, although the disappearance rate was shown to be faster in the presence of live faecal microbiota, the spontaneous degradation of anthocyanin occurred and partly contributed to anthocyanin degradation. In addition, the C_{initial} of anthocyanin was shown to affect the k_{deg} in the presence of live faecal microbiota. For example, the k_{deg} was faster when the C_{initial} of Cya3Glc was 66.8 μM compared to 133.3 μM (**Figure 4. 9** and **Figure 4. 10**). Furthermore, black rice anthocyanin or bilberry anthocyanins fully disappeared between 6 -12 h in the presence of live faecal gut microbiota, while in literature, the complete disappearance of anthocyanins required less time. For example, previous studies investigated authentic or highly purified anthocyanins reported that the complete disappearance occurred by 2 h incubation^{88,89,91,173}. This may suggest that our anthocyanin-rich extracts may contain other phenolics (i.e., protocatechuic acid) which may increase anthocyanin stabilities due to the synergistic effects between phenolic compounds, or contain other compounds (i.e., polysaccharides) that are metabolised by the microbes in preference to anthocyanins.

Another possibility is that the presence of 1% w/v glucose in the prepared colon media is favourable to microbiota as it is an easy source of energy before starting to breakdown anthocyanins, which would delay the anthocyanin degradation process. Glucose is naturally present in the human body and human food. Therefore it is more likely for anthocyanin to be degraded by the gut microbiota for more than 2 h as previous studies show^{89,91,173}. In particular, those studies used phosphate buffer (lack of glucose) as an incubation medium rather than the media components (with 1% glucose) utilised in the current study.

In regards to the spontaneous degradation, results presented in this chapter demonstrated a significant reduction of the initial concentration of anthocyanin over 24 h in the presence of autoclaved faecal slurry (absence of live microbiota). Although some reports in the literature have incubated anthocyanins without microflora and others in the presence of microflora, all of them have not considered the contribution of spontaneous degradation to the overall anthocyanin disappearance. For example, Chen and others reported that the mulberry anthocyanins (Cya3Glc, Cya3Rut, and Del3Rut) were completely degraded by 8 h after incubation with human faecal microflora²⁴⁰, agreeing with the observations in the current study, the authors did not investigate the chemical stability of mulberry anthocyanins. On the other hand, others have investigated the chemical stability of anthocyanins by simply incubating anthocyanin aerobically³⁸ or anaerobically at a neutral pH phosphate buffer^{93,174}. These methods did not mimic the condition of the human gut where the faecal matrix and multi-organisms exist. Therefore, other studies investigated the spontaneous degradation of anthocyanins by inoculating batch-culture fermentation with autoclaved filtered faecal slurry^{89,91,96,173}. The data from these two studies showed a significant decrease in anthocyanin concentration; however, in the experimental material, authors used filtered faecal suspensions from animals such as rats, mice, and pigs which may not represent processes occurring in humans and are not matrix-matched^{89,96}. Meanwhile, other reports showed greater stability of incubated anthocyanins with filtered autoclaved faecal slurry. For example, two reports reported a slight decrease in the initial concentration of incubated anthocyanins with autoclaved filtered faecal suspension^{91,173}. However, since anthocyanins are very unstable compounds at neutral pH³⁸, filtered autoclaved slurry might not be ideal for investigating

the colonic spontaneous degradation of anthocyanins, based on the very reactive pH-dependent intermediates of anthocyanins (like α -diketones)⁹¹ which are likely to interact with other faecal matrix components such as proteins and lipids. Therefore, different stool samples with different matrices might affect the spontaneous degradation, and consequently the microbiota-dependent degradation of anthocyanins.

Inter- and intra-individual variations were described for the first time in both the microbiota-dependent and the spontaneous degradation of the incubated anthocyanins. The differences between individuals were observed to be greater than the differences between stools collected from the same individual. Although the data in this chapter showed slight intra-individual in anthocyanin metabolism, it is possible that this difference is due to the changes that may happen in gut microbiota composition due to daily lifestyle changes such as diets, sleep patterns, and health status²⁴¹. However, the inter-individual variation was shown to be significant. It is possible that this difference is also due to enterotype variations between individuals²⁴².

Data presented in this chapter regarding the metabolism of bilberry anthocyanins goes beyond the existing reports in the literature where only a single or few anthocyanin candidates were investigated *in-vitro*^{88,89,91,177}. Nevertheless, data in this chapter showed considerable differences in anthocyanin k_{deg} between different anthocyanin aglycone (i.e., Cya, Del, Peo, and Mal). For example, Mal showed more stability than others whereas Del showed less stability in both microbiota-derived and spontaneous degradation. Therefore, it is possible that the number of hydroxyl group on B-ring affect the chemical stability of anthocyanin and consequently the gut-microbiota dependent degradations.

In addition to that, the type of sugar moiety in the anthocyanin structure showed to play important role in the k_{deg} of either microbial or spontaneous degradation. Galactose (Gal) decrease the stability of anthocyanins, whereas Arabinose (Ara) was shown to increase the stability of anthocyanins (Gal < Glc < Ara). Glucose and galactose are epimers, which refer to one of a pair of stereoisomers. The only difference between glucose and galactose is the orientation of the -OH group at C-4. Glucose is more stable than galactose and may be less susceptible to the formation of nonspecific glycoconjugates, which are molecules with at least one sugar attached to a protein or lipid. In addition, it was reported that Glc

is more consumable for to cell line than Gal²⁴³. In addition, a report by Ryan and others reported that glucose was utilised more rapidly than galactose by 27 pure oral bacterial cultures²⁴⁴. This indicates that it is easier for bacteria, including gut microbiota, to consume Glc as a carbon source than other sugar moieties such as Gal.

Significant differences were observed in the disappearance rate of the incubated anthocyanins between pH-controlled and non-pH-controlled colon model vessels. In controlled pH colon vessels, the black rice anthocyanin, Cya3Glc, and the various bilberry anthocyanins had almost fully disappeared within 6-12 h of incubation with live faecal microbiota. In contrast, when using uncontrolled pH colon vessels with the same initial concentration of Cya3Glc, a slow disappearance rate was observed over the first 6 h where the degradation stopped, and the complete degradation of Cya3Glc did not occur over the 24 h incubation (**Figure 4. 13**). Conversely, no significant differences were observed in the disappearance rate of the incubated Cya3Glc with or without controlling the pH of the incubation with autoclaved faecal slurry. However, spontaneous degradation was also observed in the absence of pH control. This suggests that the growth of the live microbiota increases the production of organic acids which decreases the medium pH to acidic. This low pH would increase the stability of Cya3Glc, but it may also cause a change in the microbial population that favours microbiota that prosper in low pH conditions or metabolites produced, but which do not have the ability to break down the Cya3Glc. Only one reported study has used a pH-controlled model¹⁷⁷. The authors reported that a mixture of mono-glycoside anthocyanins was almost fully degraded after 10 h incubation in the presence of live faecal inoculum. In addition, these authors reported a 60 % decline of the C_{initial} of Del3Glc within 5 h incubation without faecal microbial fermentation, whereas Mal3Glc was shown to be relatively stable in the same study. This suggests that without the autoclaved faecal materials, the spontaneous degradation depends only on the anthocyanin structure, and no possible reaction with other components could be found in faecal samples such as proteins, and lipids. This strongly suggests that the chemical make-up of the faecal material plays an important role in the spontaneous degradation of anthocyanins. That is, the overall effects of the presence of the faecal microbiome are a mixture of the altered chemistry of the aqueous solution and the presence of live, metabolically active bacteria. On the other hand, the studies which have not used

a controlled pH model fermentation observed a full degradation after a 2 h incubation which is in contrast with the data presented here. However, the colon model media used in this project has a buffering capacity of only 0.5 mM (potassium phosphate), whereas other reports incubated an initial concentration of 100 μ M of anthocyanins in a phosphate buffer ranging between 100 to 150 mM^{89,91,173}. This likely indicates that in the low buffer capacity, the microbiota growth caused a drop in the medium pH which significantly slower the microbial degradation of anthocyanins.

The standard addition method showed that the calculated concentration of Cya3Glc in black rice extract powder was higher by 5 % than using the external standard method. This may happen due to the co-pigmentation effect where non-Cya3Glc compounds in the black rice extract may affect the absorbance properties of Cya3Glc itself at $\epsilon_{520\text{ nm}}$. In addition, all data reported in this chapter showed that the quantified C_{initial} of anthocyanin at 0 h was lower than added anthocyanins (C_{theo}), showing a reduction between 10 and 30 %. This observation was also reported by Hidalgo and others, where the anthocyanin Mal3Glc recovery was calculated to be 85 %¹⁷⁷. This may happen due to the attachment of anthocyanin to the faecal slurry matrix, especially proteins.

4.6. Conclusions

In this chapter, I have investigated the contribution of the human faecal microbiota to the disappearance of anthocyanins. Anthocyanins disappeared partly spontaneous and partly due to the human faecal microbiota activity. The k_{deg} of anthocyanins varied within-person samples as well as between different donors. B-ring substitutions as well as the conjugated sugars affected the rate of loss of anthocyanins, both for the microbiota-dependent and the spontaneous degradation. However, there are very few studies concerning anthocyanin metabolism by the human gut microbiota, and some critical factors need to be considered before conducting the investigation. The spontaneous degradation of anthocyanins contributes directly to the degradation of microbiota-dependent degradation; therefore, incubating anthocyanin with autoclaved faecal microbiota should be considered in the experimental design alongside incubating with live faecal microbiota. Also, the medium itself might change the disappearance rate of anthocyanins since anthocyanins are reactive compounds. In addition, the initial

concentrations may affect the rate of loss where higher concentrations seem to be slower, which may suggest higher concentrations confer partial toxicity to the microbiome and/or just the fact of more initial substrates need more time to be digested. More importantly, controlling the fermentation pH is very critical since anthocyanins are very stable in low pH, and our results showed that the pH is dropping very drastically with 2 h incubation with live faecal microbiota. Due to the intra- and inter-individual variations, the glycerol-frozen faecal stock might be the best option for reproducing the data by using the same faecal sample on different occasions. To conclude, the spontaneous degradation of anthocyanins is contributing roughly 50% of the overall microbiota-dependent degradation. Therefore, further studies on the spontaneous degradation of anthocyanins will be discussed in the following chapter.

Chapter Five

**The spontaneous
degradation of
anthocyanins and
anthocyanidins**

Chapter 5: The spontaneous degradation of anthocyanins and anthocyanidins

5.1. Abstract

Background: In chapter 4 it was shown that the degradation of anthocyanins in the human colon is the result of both spontaneous processes and also microbiota-independent processes, i.e., spontaneous degradation. There is a considerable literature reporting on the spontaneous degradation of anthocyanins, but largely focussed on foods and beverages, or using simple (buffered) solutions under aerobic conditions. However, to the best of my knowledge, nothing has been reported about the spontaneous degradation of anthocyanins in the conditions of the colon.

Aim and methods: The overall aim of the research reported in this chapter was to investigate the spontaneous degradation of anthocyanins (Cya3Glc) as well as anthocyanidins (Cya and Del) in more detail. The specific objectives were to investigate (i) how different matrices affect the rate of spontaneous loss of anthocyanins (colon model media versus phosphate buffer), (ii) the rate of loss of anthocyanins under aerobic and anaerobic conditions, (iii) possible differences in the types and/or profile of breakdown products of anthocyanins between aerobic and anaerobic conditions, (iv) the rate of spontaneous degradation of anthocyanidins (Cya and Del) and appearance of breakdown products, and (v) the effect of initial anthocyanidin concentration on their spontaneous degradation.

Results: In anaerobic conditions and neutral pH, Cya3Glc disappeared faster in colon model media than in phosphate buffer solution with initial degradation rates (k_{deg}) of 17.1 ± 3.8 and 6.9 ± 5.5 $\mu\text{M/h}$, respectively. Data from LC-MS analysis of the breakdown products was consistent with Cya3Glc undergoing classic pH-dependent transformation to give cya hemiketal-Glc, Cya chalcone-Glc, Cya chalcone anionic-Glc and trihydroxyethenylbenzene-Glc (all colourless), but no other products.

Under aerobic condition and neutral pH, the rate of loss of Cya3Glc was faster (k_{deg} , $12.1 \pm 1.3 \mu\text{M/h}$) compared to anaerobic conditions (k_{deg} , $6.9 \pm 5.5 \mu\text{M/h}$), and there was a substantial increase in the number of breakdown products formed under aerobic conditions. These gave rise to various intermediates including PCA, PGA, coumarin-Glc, di- and tri-hydroxyphenyloxoacetic acid, and trihydroxyphenylacetic acid.

Anthocyanidins (Cya and Del) also degraded spontaneously under aerobic conditions and neutral pH. The matrix, pH, initial concentration of anthocyanidin, and buffering capacity of the medium were important parameters that influenced spontaneous degradation. Both Cya and Del initially underwent a classic pH-dependent transformation to give intermediates of chalcones, chalcone anionics, and α -diketones, then underwent oxidation processes. The analysis of Cya showed that PCA, PGA, PGCA, coumarin, di- and tri-hydroxyphenyloxoacetic acid, and trihydroxyphenylacetic acid were the breakdown products. Whereas gallic acid, 3-*O*-methylgallic acid, PGA, PGCA, coumarin, and trihydroxyphenyloxoacetic acid were the breakdown species from Del.

Conclusion: Although anthocyanins showed a pH-dependent transformation in both aerobic and anaerobic conditions, anthocyanins underwent a further series of oxidation processes (non-enzymatic reactions) only in the presence of oxygen. Next, therefore, the enzymatic pathways of anthocyanin metabolism by the human gut microbiota were investigated and presented in the next chapter (Chapter 6).

5.2. Introduction

Anthocyanins have been associated with various biological effects but they are chemically unstable compounds, and their chemical stability is affected by many factors including light, pH, temperature, metal ions, enzymes, and oxygen, amongst others^{82,245}. There is a considerable literature reporting on the spontaneous degradation of anthocyanins, but largely focussed on foods and beverages. A number of studies have used simple (buffered) solutions to investigate the spontaneous degradation of anthocyanins. For example, Kay and others reported that Cya3Glc and its aglycone (cyanidin) degraded spontaneously in phosphate buffered solution under physiological conditions of pH (7.4) and temperature (37°C)³⁸. In addition, Woodward and others

reported that different anthocyanins are degraded spontaneously in neutral-pH phosphate buffer and water⁸⁷. Due to anthocyanin instability and their poor bioavailability, it has been hypothesised that any biological effects associated with anthocyanin consumption can be attributed to their spontaneous and microbial metabolites, rather than the parent compound³⁸. The relative contribution of spontaneous and microbial anthocyanin metabolism *in vivo* is still superficially understood. However, the results from the previous chapter (Chapter 4) showed that the colonic degradation of anthocyanins is partly spontaneous and partly due to gut microbiota activity. Therefore, in this chapter investigations were conducted to understand the spontaneous degradation of anthocyanins in more detail, as the breakdown products are likely to undergo further metabolism by the gut microbiota *in vivo*, and consequently will have implications for health effects associated with an anthocyanin-rich diet. To the best of my knowledge, all reports in the literature to date have concerned the spontaneous degradation in the presence of oxygen and have not considered the anaerobic degradation of anthocyanins. However phenolic acid (B-ring-derived product) and PGA (A-ring-derived product) were reported as the breakdown products of the spontaneous degradation of anthocyanins and anthocyanidins, it has been noticed in these reports that there are some differences in the experimental design. For example, different matrices were used for the incubation of anthocyanins such as water, buffer solutions (with different buffer capacities: 0 mM, 10 mM, and 100 mM) and tissue culture samples. Also, the preparation of a stock standard solution of the authentic compounds was also different or not mentioned. Furthermore, the investigated concentrations of anthocyanins or anthocyanidins were varied which ranged from low concentrations ($20 \mu\text{g mL}^{-1}$) up to very high concentrations ($1000 \mu\text{g mL}^{-1}$). Therefore, the outcome data from these reports was variable. For example, it was accounted for both A-ring and B-ring breakdown products but with less than 30 % molar recovery of the initial concentration of Cya3Glc⁸⁷. In contrast, Kay and others quantified both A- and B-ring breakdown products with 100 % molar recovery of the initial concentration of Cya3Glc and they only reported that protocatechuic acid (PCA) (B-ring-derived) and phloroglucinol aldehyde (PGA) (A-ring-derived) are the main and the end breakdown products of the spontaneous degradation of Cya3Glc and its aglycone³⁸. Therefore, in this chapter, the aerobic and anaerobic spontaneous degradation of anthocyanins and anthocyanidins have been investigated. In addition, the effect of

different factors such as matrix and pH, and initial concentrations were studied in more detail.

5.3. Objectives

The focus of the research reported in this chapter was to understand the spontaneous degradation of anthocyanins and their aglycones. The formation of the new breakdown products was investigated under various conditions. Loss of Cya3Glc and appearance of breakdown products were compared between colon model media and phosphate buffer, and under both aerobic and anaerobic conditions. Both the anthocyanin Cya3Glc and the anthocyanidins Cya and Del were investigated. Therefore, the studies described in this chapter were focused on (1) monitoring the disappearance of Cya3Glc, Cy, and Del during incubation in phosphate buffer and colon media; (2) exploring the loss of Cya3Glc, Cya, and Del in the presence as well as the absence of oxygen, and (3) investigating the formation of their breakdown products in both the presence and absence of atmospheric oxygen. The observations made here will be compared to the results of experiments that were carried out to investigate the microbiota-dependent degradation of anthocyanins reported in the next chapter. Critically, since degradation of anthocyanins in the presence of faecal microbiota will involve both spontaneous and microbiota-dependent processes, the observations made here will allow the microbiota-dependent processes to be distinguished from the spontaneous processes occurring in the colon model experiments.

5.4. Results

5.4.1. The identification of Cya3Glc, Cya, Del, and their breakdown products on HPLC-DAD-MS

A chromatographic separation method was developed for 30 authentic phenolic compounds, as well as for Cya3Glc, Cya, and Del (**Table 5. 1**) on a reversed-phase HPLC column. A range of UV-VIS wavelengths (250, 280, 330, 370, and 520) were set up to determine the best signal response for each compound. The RT for each compound was determined by injecting each authentic standard individually as well as in a mixture of compounds. In addition, the mass fragment ion was observed using MS detector (coupled with HPLC-DAD) using a full scan mode and negative ionisation polarity. The stock

solutions for all compounds were prepared in MeOH (1 mg/mL). Later, they were diluted in both phosphate buffer (pH 6.8) and colon media (pH 6.8).

Cya3Glc, Cya, and Del were best detected at 520 nm at different RT, 14.4, 20.4, and 17.3, respectively (**Table 5. 1**). Whereas the majority of phenolic compounds were best detected at λ (280 nm) (e.g., gallic acid, catechol, PGA), some were best detected at λ (250 nm) (e.g., PCA, PGCA, and pyrogallol), and some at λ (330 nm) (e.g., ferulic acid, and 5-hydroxyferulic acid). The separation method (**Chapter 2, section 2.3.3**) showed good separation of the majority of phenolic compounds (**Figure 5. 1**). However, some compounds overlapped in one peak. For example, the peak at RT 8.2 was shown to be formed from 4 different compounds (peaks no. 6, 19, 20, and 30), but the mass detector could be used to differentiate between them. Furthermore, there was no large difference in RT for phenolic compounds injected individually or within a mixture of other phenolic compounds. Additionally, there was no considerable effect of the matrix on the RT of all compounds.

Table 5. 1. HPLC-DAD-MS identification of Cya3Glc, Cya, and Del.

No	Compound	RT	Best signal (λ)	Parent ion m/z [M-H] ⁻	Other ions m/z [M-H] ⁻
1	Cya3Glc	14.4	520	447.0	895.1, 285
2	Cya	20.4	520	285.1	593.1
3	Del	17.3	520	301.1	625.1, 601.1

Table 5. 2. HPLC-DAD-MS identification of potential breakdown compounds during the spontaneous degradation of Cya3Glc, Cya, and Del.

No	Compound	RT (min)	Best signal (λ)	Parent ion m/z [M-H] ⁻	Other ions m/z [M-H] ⁻
1	Pyrogallol	2.12	250	125.1	251.1
2	Phloroglucinol	1.78	250	125.1	251.1
3	Cinnamic acid	24.83	280	147.2	163.2, 119
4	Ferulic acid	17.25	330	193.2	177.9
5	Sinapic acid	19.01	330	223.2	208
6	4-Hydroxybenzaldehyde	8.23	280	121.1	-
7	Vanillic acid	8.87	250	167.1	358, 152
8	5-hydroxyferulic acid	11.63	330	209.1	207.1, 208.1, 192
9	4-Hydroxybenzoic acid	6.08	250	137.1	-
10	Phloroglucinol aldehyde (PGA)	9.97	280	153.1	-
11	Syringic acid	11.36	280	197.2	418, 182
12	Caffeic acid	9.46	330	179.2	135
13	Gallic acid	2.18	280	169.1	125
14	3-O-methyl-gallic acid	7.11	280	183.1	367.1, 124
15	Protocatechuic acid (PCA)	3.86	250	153.1	09.1
16	Phloroglucinol carboxylic acid (PGCA)	4.53	250	169.1	362, 151
17	Dihydrocaffeic acid	7.79	280	181.2	363.2
18	Dihydroferulic acid	14.94	280	195.2	391
19	3-hydroxy benzoic acid	8.22	250	137.1	275
20	2,4-dihydroxy benzoic acid	8.20	250	153.1	330, 109
21	3,4-dihydroxyphenylacetic acid	4.88	280	167.1	123, 344
22	Homovanillic acid	10.34	280	181.2	137, 2M-H
23	Catechol	4.47	280	109.1	363
24	3,5-dihydroxy benzoic acid	3.80	250	153.1	307, 109
25	3-hydroxy phenyl acetic acid	8.87	280	151.1	107, 303
26	3-(4-hydroxyphenyl) propionic acid	11.73	280	165.2	354
27	Protocatechualdehyde (PCAlD)	5.67	280	137.1	275
28	2,4-dihydroxy benzaldehyde	10.60	280	137.1	-
29	3,4-dihydroxymandelic acid	1.43	280	183.1	367, 165

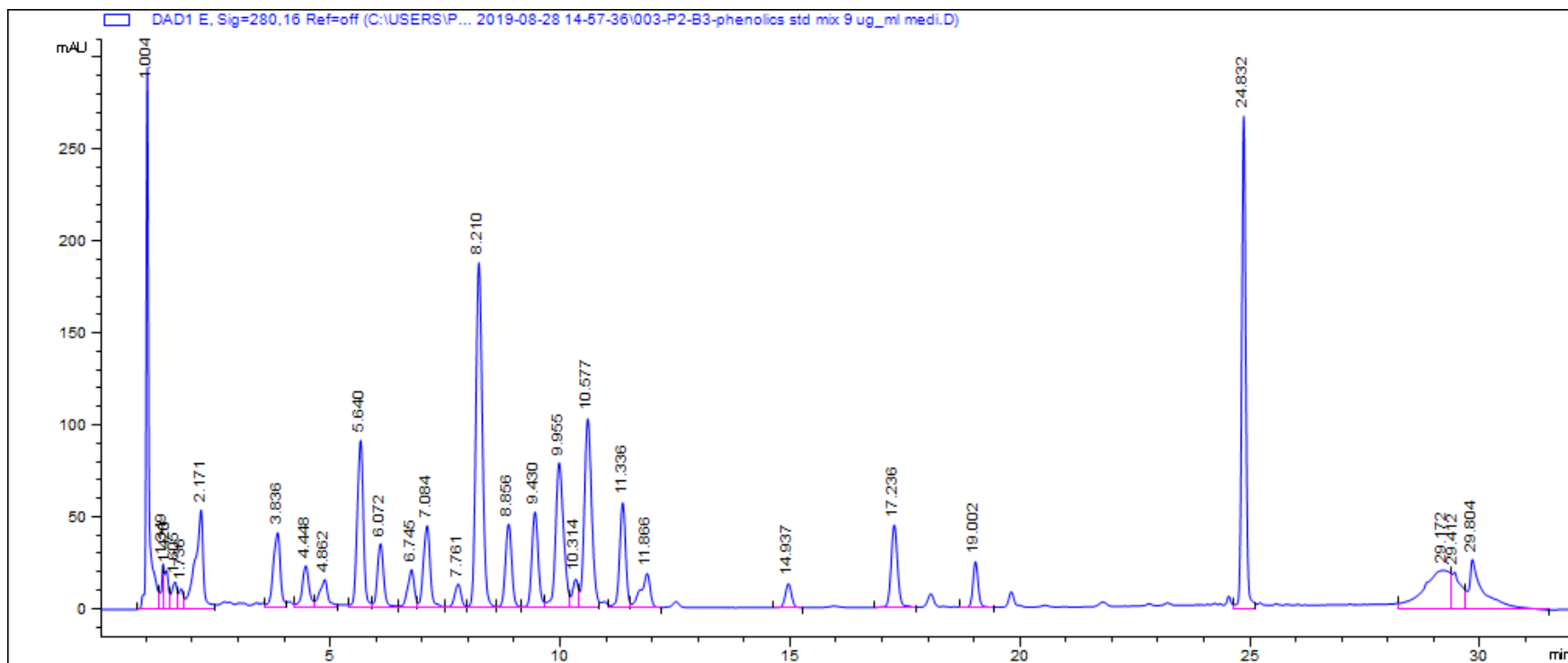


Figure 5. 1. DAD chromatogram λ (280 nm) of a mixture of 30 phenolic compounds dissolved in a 10 mM phosphate buffer (pH 6.8).

5.4.2. The spontaneous degradation of Cya3Glc in colon model media: Anaerobic conditions

Having observed in the previous chapter (**Chapter 4**) that the black rice anthocyanin (Cya3Glc) was degraded spontaneously during the anaerobic incubation of the *in-vitro* colon model fermentations, the degradation of authentic Cya3Glc was carried out to understand the anaerobic spontaneous degradation of anthocyanins. Briefly, authentic Cya3Glc with an initial theoretical concentration (C_{theo}) of 170 μM was incubated in neutral pH colon media at 37°C for 24 h inside an anaerobic cabinet. Samples were collected at 0, 4, 8, 12, 20 and 24 h into HPLC vials. The vials were firmly capped inside the anaerobic cabinet and then immediately taken to be analysed by HPLC-DAD to quantify the Cya3Glc concentrations. A control vial ($t=0$) was prepared using pure Cya3glc but in acidified colon media and immediately injected onto the HPLC column.

Cya3Glc was degraded anaerobically over the 24 h during the anaerobic incubation with colon media (**Figure 5. 2**). No significant difference was observed between the control vial ($t=0$) and treatment vial at 0 h, but there was a significant difference in the concentration of Cya3Glc in the control vial ($t=0$) and treatment vial at 4, 8, 12, 20, and 24 h (all $p<0.0001$). Over the first 4 h, the initial k_{deg} of the spontaneous degradation of Cya3Glc was $17.1 \pm 3.9 \mu\text{M/h}$. In chapter 4, however, Cya3Glc was shown to be degraded spontaneously with an initial k_{deg} of $10 \pm 6.7 \mu\text{M/h}$ in the *in-vitro* colon model which contained colon media with 1 % autoclaved faecal sample (**Chapter 4, Figure 4. 12**). Furthermore, a concentration of Cya3Glc of $22.4 \pm 15.4 \mu\text{M}$ (13 % of C_{initial}) was quantified at 24 h. However, in the *in-vitro* colon model, $30.6 \pm 27.3 \mu\text{M}$ (27.7 % of C_{initial}) of Cya3Glc was detected in the sample collected at 24 h. This difference might be due to the lack of pH control and/or the effect of the faecal matrix on the spontaneous degradation of anthocyanins.

Although the data presented here showed that the overall spontaneous k_{deg} of Cya3Glc is similar to the overall k_{deg} of Cya3Glc during the incubation in the *in-vitro* colon model, phosphate buffer solution has been commonly used in literature to investigate the spontaneous k_{deg} of anthocyanins.

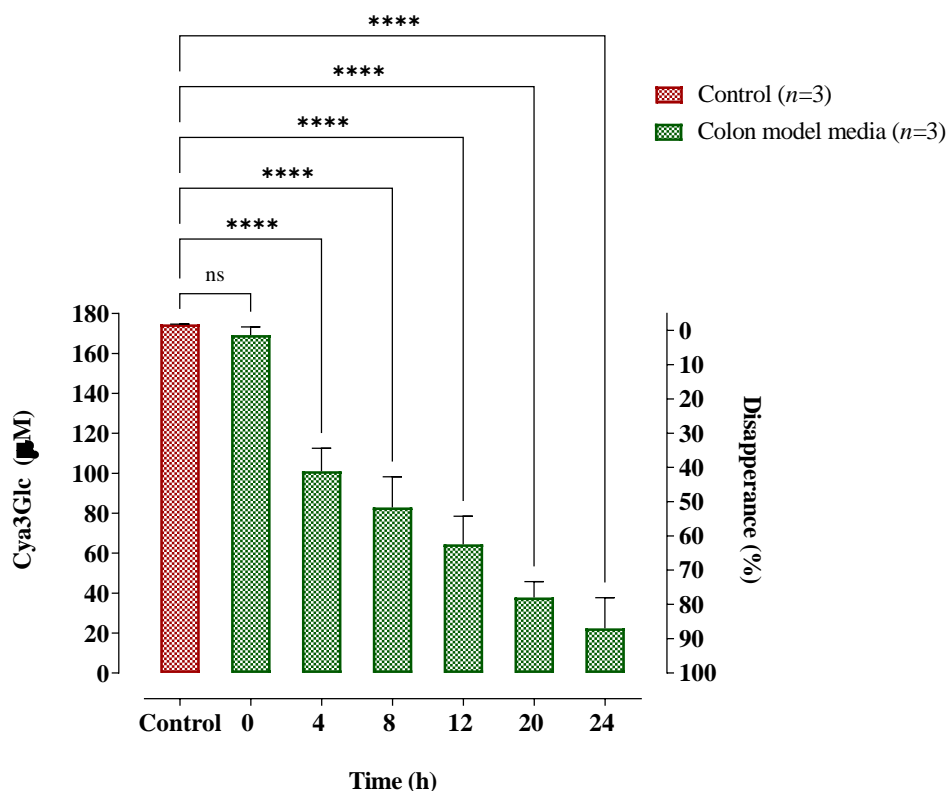


Figure 5. 2. The anaerobic spontaneous degradation of Cya3Glc ($C_{theo} = 170 \mu\text{M}$) under the physiological condition of the colon (neutral pH; 37°C) in colon media.

A colon media (0.5 mM K phosphate, pH 7.0) was prepared and autoclaved then placed in the anaerobic cabinet overnight. On the day of the experiment, a fresh stock solution (SS) of Cya3Glc (2 mg/mL) was prepared by dissolving 2 mg of the authentic compound in 1 mL DMSO. Inside the anaerobic cabinet and in a 10 mL vial, a 168.5 μL of SS was added to 4831.5 μL media to give a final volume of 5 mL with Cya3Glc concentration of 150 μM , then immediately the first sample at 0 h was collected into a 1 mL HPLC vial, capped, taken for HPLC analysis. Other samples were collected for injections at the times shown in the figure to determine the Cya3Glc concentration. External standard curve of serial concentrations of Cya3Glc was prepared in acidified colon model media (4% v/v formic acid). Each experiment was carried out in triplicates. Values represent means \pm SD of three independent experiments. ****Significance from control ($p < 0.0001$) which include pure Cya3Glc standard spiked directly into acidified colon model media at $t=0$, using one-way analysis of variance (ANOVA) with Tukey's Multiple Comparison Test.

5.4.3. The spontaneous degradation of Cya3Glc in phosphate buffered solution: Anaerobic conditions

In the previous section, Cya3Glc was shown to be degraded spontaneously during anaerobic incubation in colon media. However, in the literature, simple buffered solutions were used to investigate the spontaneous degradation of anthocyanins. Therefore, the anaerobic spontaneous degradation of Cya3Glc was investigated in a simple buffer solution at pH 7.4, 37°C. The same method was followed as described in the previous section (Section 5.4.1) for incubating Cya3Glc (C_{theo} of 170 μM) in a phosphate-buffered solution over 24 h. A control vial ($t=0$) was prepared using the authentic Cya3glc, but it was prepared in acidified phosphate buffer solution, and then immediately injected onto the HPLC column.

Cya3Glc was degraded over the 24 h during the anaerobic incubation in phosphate buffer (**Figure 5. 3**). Compared with control, the rate of loss of Cya3Glc was statistically different only at 20 and 24 h ($p<0.05$), whereas no significant differences were observed at 0, 4, 8, 12 h. The error bars showed to be bigger at 20 and 24 h because the results from one replicate showed less degradation rate. However, over the first 4 h, the initial k_{deg} of the anaerobically incubated Cya3Glc in phosphate buffer was $6.9 \pm 5.5 \mu\text{M/h}$, which is substantially slower than the initial k_{deg} of Cya3Glc observed with colon media ($17.1 \pm 3.8 \mu\text{M/h}$). Consequently, the spontaneous k_{deg} is also slower than the spontaneous k_{deg} of the incubated Cya3Glc in the *in-vitro* colon model fermentation with autoclaved faecal sample (**Chapter 4, figure 4.11**). For example, the data presented in **Figure 5. 2** showed that 50 % ($81.8 \pm 45.2 \mu\text{M}$) of the C_{initial} of Cya3Glc was detected in the sample collected at 24 h, but only 13.2 % ($22.4 \pm 15.4 \mu\text{M}$) of the C_{initial} of Cya3Glc was detected in the 24 h sample incubated with colon media and 23 % ($30.6 \pm 27.3 \mu\text{M}$) of the C_{initial} of Cya3Glc was detected from samples collected from the *in-vitro* colon model at the 24 h. This indicated that not only 1 % autoclaved faecal sample, but also different mediums affected the spontaneous degradation of anthocyanins. Therefore, data shown in **Figure 5. 4** showed a significant difference ($p<0.05$) of the spontaneous k_{deg} between the anaerobic k_{deg} of Cya3Glc in colon media and phosphate buffered solution at 4, 8, and 12 h. However, there was no significant difference at 20 and 24 h.

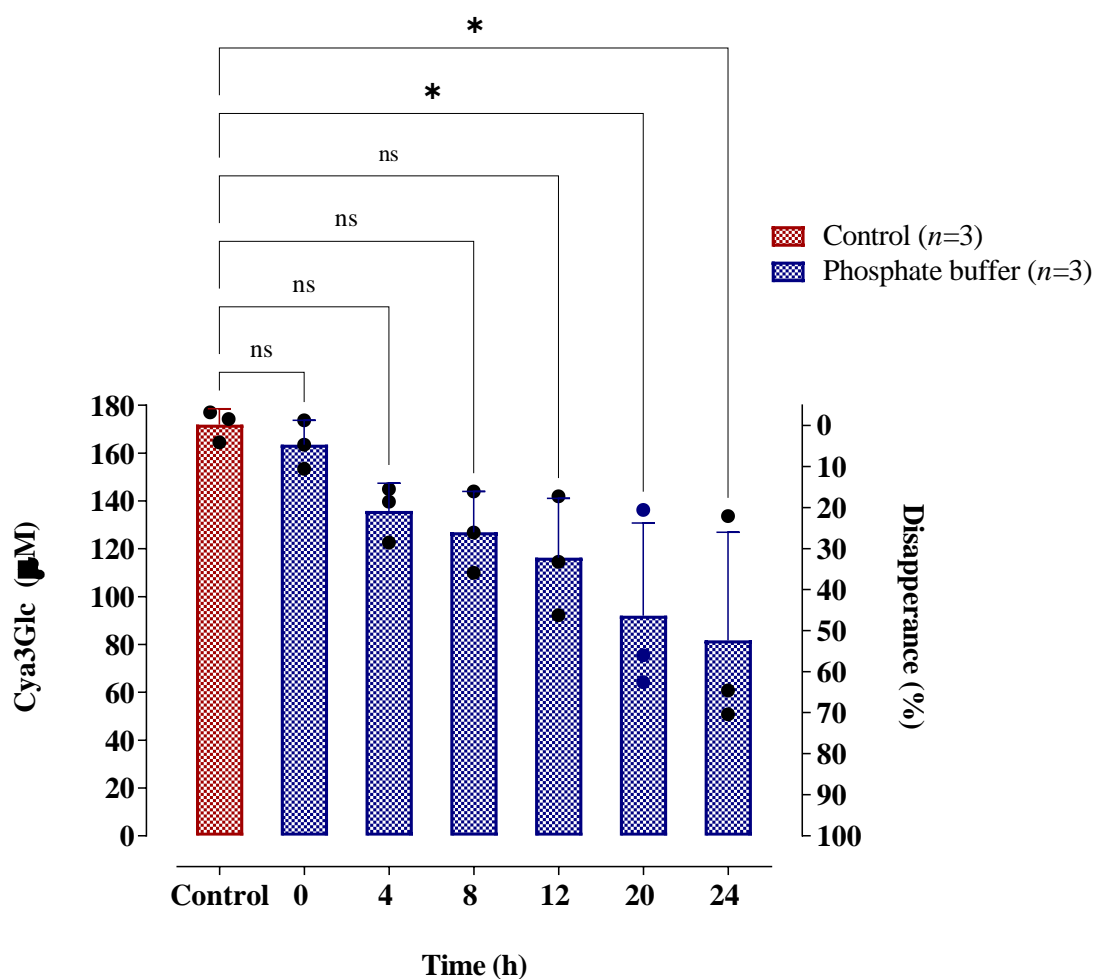


Figure 5. 3. The anaerobic spontaneous degradation of Cya3Glc ($C_{theo} = 170 \mu\text{M}$) under the physiological condition of the colon (neutral pH; 37°C) in phosphate-buffered solution.

A phosphate buffer (10 mM K phosphate, pH 7.4) was prepared and autoclaved then placed in the anaerobic cabinet overnight. On the day of the experiment, a fresh stock solution (SS) of Cya3Glc (2 mg/mL) was prepared by dissolving 2 mg of the authentic compound in 1 mL DMSO. Inside the anaerobic cabinet and in a 10 mL vial, a 168.5 μL of SS was added to 4831.5 μL phosphate solution to give a final volume of 5 mL with Cya3Glc concentration of 150 μM , then immediately the first sample at 0 h was collected into a 1 mL HPLC vial, capped, taken to HPLC analysis. Other samples were collected for injections at the times shown in the figure to determine the Cya3Glc concentration. External standard curve of serial concentrations of Cya3Glc was prepared in acidified phosphate buffer (4% v/v formic acid). Values represent means \pm SD of three independent experiments. *Significance from control ($p < 0.05$) which include pure Cya3Glc standard spiked directly into acidified phosphate buffer at $t=0$, using one-way analysis of variance (ANOVA) with Tukey's Multiple Comparison Test.

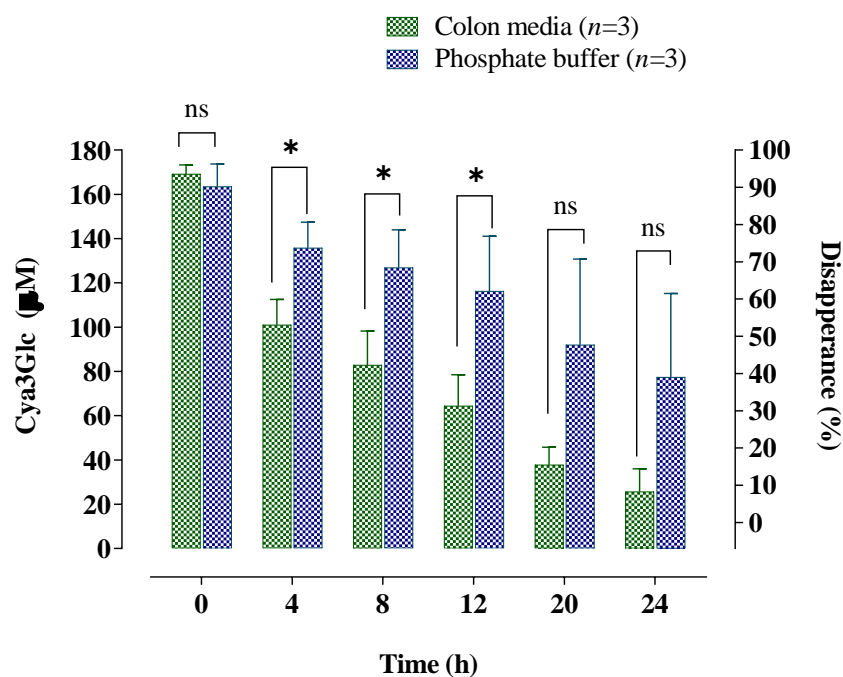


Figure 5. 4. Comparison of the anaerobic spontaneous degradation of Cya3Glc in colon model media and phosphate buffer.

Values represent means \pm SD of three independent experiments. * Significance at comparable time points ($p < 0.05$) in both colon model media and phosphate buffer which include incubated pure Cya3Glc standard, using unpaired t test with two tailed p value.

In literature, however, the spontaneous degradation was investigated in the aerobic condition, showing higher k_{deg} in comparison with the data presented in this section and the previous section (Section 5.4.1). For example, Woodward and others investigated the incubation of Cya3Glc with phosphate buffer (pH 7.4) at 37°C and reported that 15 % of the $C_{initial}$ of Cya3Glc (140 μ M) was detected from sample collected at 24 h. Therefore, it is important to understand the difference between the aerobic and anaerobic spontaneous degradation of anthocyanins in more detail.

5.4.4. The spontaneous degradation of Cya3Glc in colon media and phosphate buffer: Aerobic conditions

Having observed that the authentic standard of Cya3Glc degrades spontaneously during anaerobic incubation in colon media and in phosphate buffer, the next question that was addressed was whether aerobic condition affects the spontaneous k_{deg} . To investigate this, an authentic Cya3Glc (C_{theo} of 170 μM) was incubated aerobically in colon media and phosphate buffer under physiological conditions (neutral pH, 37°C). Briefly, Cya3Glc was incubated in a 1 mL-HPLC vial which was filled with colon media (or phosphate buffer solution) then immediately placed in the HPLC autosampler where the temperature was set at 37°C prior to the incubation. Auto-injections were carried out over 24 h from the same experimental vial to quantify the Cya3Glc using peak areas from DAD at 520 nm.

In both colon media and phosphate buffer, significant loss of the aerobically incubated Cya3Glc was observed over 24 h (**Figure 5. 5**). However, over the first 4 h, the initial k_{deg} of Cya3Glc shown to be faster in colon media ($24 \pm 13.3 \mu\text{M/h}$) than in phosphate buffer ($9.1 \pm 1.5 \mu\text{M/h}$). In the previous chapter (Chapter 4), the spontaneous k_{deg} of the incubated Cya3Glc during the *in-vitro* colon model fermentation was $10 \pm 6.7 \mu\text{M/h}$ over the first 4 h (**Chapter 4, section 4.5.3**). This observation showed that the presence of atmospheric oxygen has a significant effect on the stability of anthocyanins by showing considerable difference between initial k_{deg} of Cya3Glc under the anaerobic and the aerobic conditions. In addition, $47.4 \pm 1.7 \mu\text{M}$ (28 % of the C_{initial}) was detected in the last injection at 24 h from the vial containing phosphate buffered solution and Cya3Glc (**Figure 5. 5**). Whereas Cya3Glc was completely degraded spontaneously by 18 h of the aerobic incubation in colon media.

These data showed that there is a significant matrix effect (from both faecal material and the medium) on the spontaneous k_{deg} of Cya3Glc (**Table 5. 3**). Phosphate buffer could be the proper media for controlling the pH during incubation, but it might not be the best representative to mimic the medium of the gastrointestinal tract under the physiological condition.

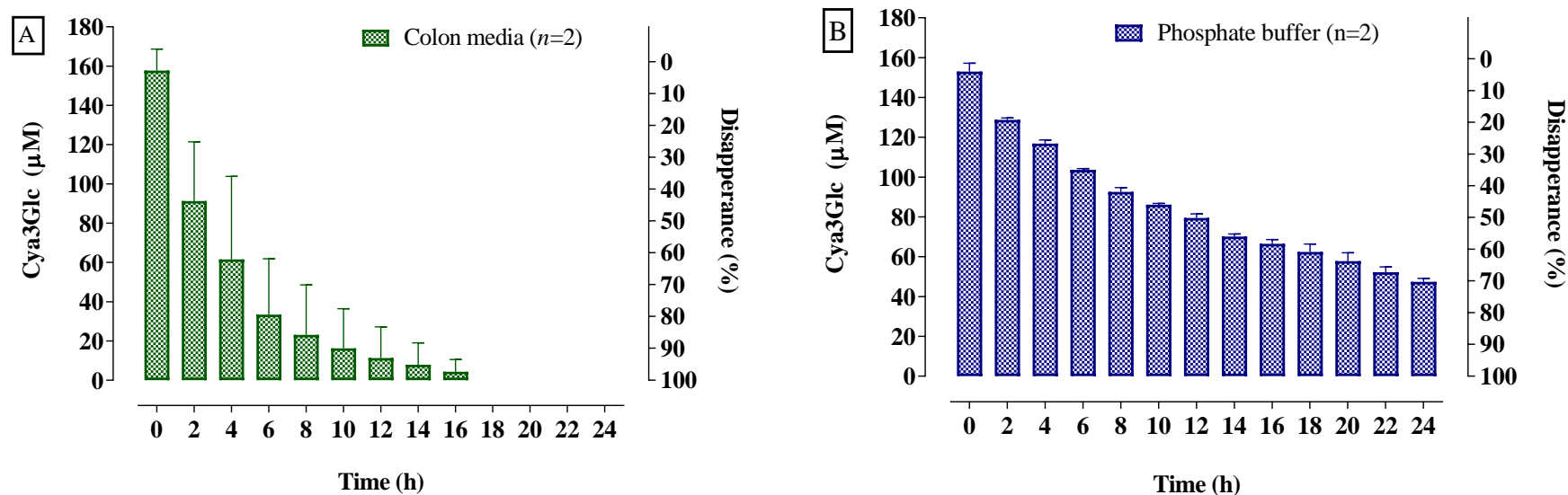


Figure 5. 5. The aerobic spontaneous degradation of Cya3Glc ($C_{theo} = 170 \mu\text{M}$) at physiological condition (neutral pH; 37°C) in colon media and phosphate buffer.

A phosphate buffer (10mM K phosphate, pH 7.4) and colon media (0.5 mM K phosphate, pH 7.0) were prepared and autoclaved. On the day of the experiment, a fresh stock solution (SS) of Cya3Glc (2 mg/mL) was prepared by dissolving 2 mg of the authentic compound in 1 mL DMSO. In 1mL HPLC vials and separate days, two experimental vials ($n=2$) were prepared for each medium by adding 168.5 μL of SS to 4831.5 μL medium) to give a final volume of 5 mL and a Cya3Glc concentration of 150 μM , then immediately the experimental vials were put in LC-DAD autosampler for injections at the times shown in the figure to determine the Cya3Glc concentration. External standard curve of serial concentrations of Cya3Glc was prepared in acidified phosphate buffer or colon media (4% v/v formic acid). Each experiment was carried out in duplicates. Values represent means \pm SD.

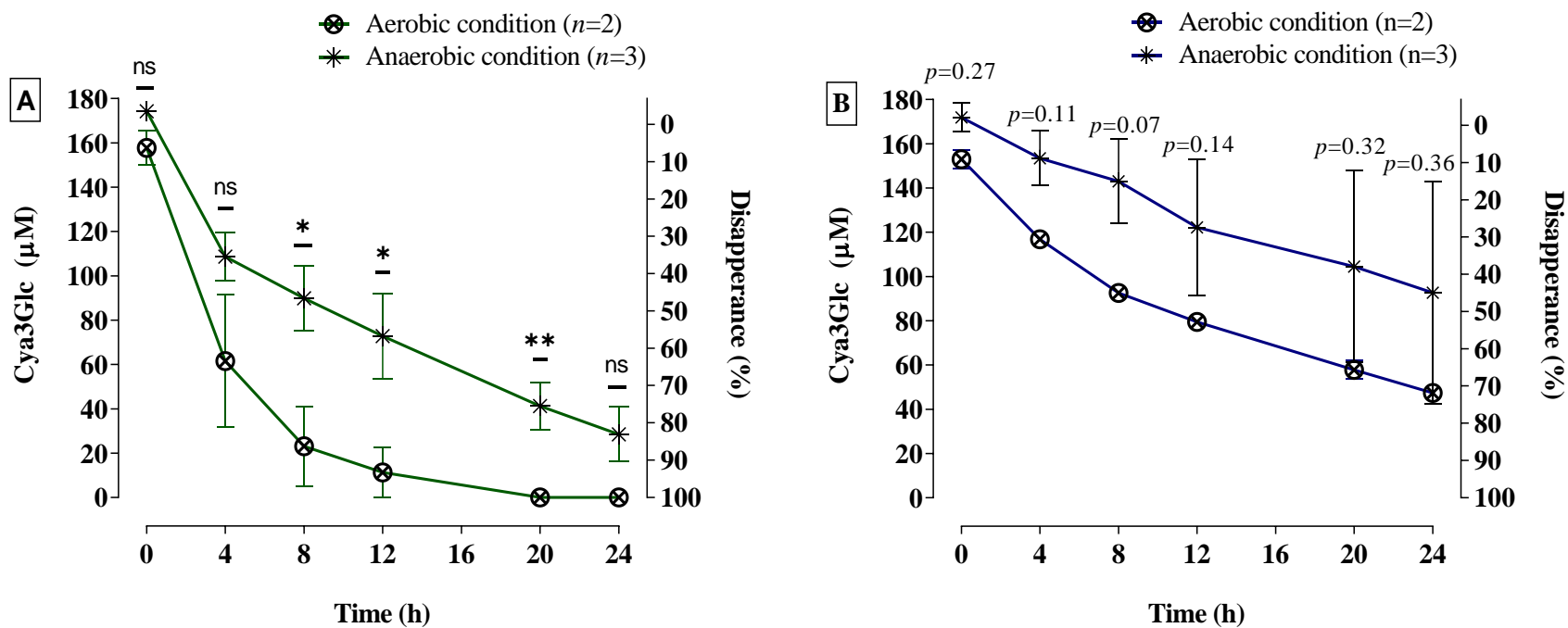


Figure 5. 6. Comparison between aerobic and anaerobic spontaneous degradation of Cya3Glc in colon model media and phosphate buffer.

Where the experiment was carried out in colon media (A) and phosphate buffer (B). Values represent means \pm SD of two independent experiments. * Significance ($p < 0.05$) and ** Significance ($p < 0.01$) from the same time point which include incubated pure Cya3Glc standard in colon model media at different time points, using unpaired t test with two tailed p value.

Table 5. 3. Comparison of the spontaneous degradation of Cya3Glc in different conditions#

		Colon media	Phosphate buffer	<i>in-vitro</i> colon model*	
	C_{theo}	μM	170	170	133.3
Aerobic incubation	C_{initial}	μM	157.7 ± 10.9	152.9 ± 4.2	-
	k_{deg}	$\mu\text{M/h}$	24 ± 13.3	9.1 ± 1.5	-
	C_{end}	μM	0.0	47.4 ± 1.7	-
	$\%_{\text{end}}$	%	0	31	-
Anaerobic incubation	C_{initial}	μM	169.2 ± 4.1	163.5 ± 10.1	110 ± 6
	k_{deg}	$\mu\text{M/h}$	17.1 ± 3.9	6.9 ± 5.5	10.0 ± 6.7
	C_{end}	μM	22.4 ± 15.4	81.7 ± 45.2	30.6 ± 27.3
	$\%_{\text{end}}$	%	13	50	28

C_{theo} = theoretical concentration.

C_{initial} = initial quantified concentration at 0 h.

k_{deg} = degradation rate over the first 4 h.

C_{end} = end detected concentration at 24 h.

$\%_{\text{end}}$ = percent (based on C_{initial}) of quantified concentration at the end of incubation (24 h).

All values are means ± SDs.

* Cya3Glc was incubated in the *in-vitro* colon model vessel which contained colon media with 1% autoclaved faecal sample (chapter 4, Figure 4. 12).

5.4.5. Investigating the breakdown products of the spontaneous degradation of Cya3Glc during anaerobic incubation

The formation of breakdown products from the anaerobic spontaneous degradation of Cya3glc was observed on the DAD using different wavelengths (250, 280, 330, 370, and 520 nm). All newly formed peaks were observed from the UV-VIS chromatograms of the injections from vials containing phosphate buffer but newly formed peaks in the vial containing colon media were not clear and easy to monitor as the chromatogram had a very noisy background presumably from the various components present in colon media. Therefore, all new peaks were observed on the chromatograms created from injections from incubations of Cya3Glc in phosphate buffer solutions, then analysed the parent ions $m/z[M-H]^-$ in full scan mode and picked up some in-source fragments. Afterwards, the identified masses were used later to observe the peak formation over time in both incubations in buffer solutions and colon model media.

In the absence of oxygen, Cya3Glc declined over time. In parallel, new peaks appeared as breakdown products of Cya3Glc over 24 h (**Figure 5. 7**). Some new peaks gave $m/z[M-H]^-$ values greater than that of Cya3Glc ($m/z[M-H]^- = 447$). The new masses (i.e., $m/z[M-H]^- = 465$ and 463) were higher than the mass of Cya3Glc ($m/z[M-2H]^- = 447$), showing that Cya3Glc underwent structural changes and the potential addition of small masses like O_2 and H_2O . This change is due to the pH, and it will be referred to the pH-dependent degradation⁹¹. It is well known that anthocyanins are stable at low pH (pH 1-3). In addition, a $m/z[M-H]^- 329$ was detected during the anaerobic incubation. Furthermore, expected masses such as $m/z[M-H]^- 153$ corresponding to PCA and/or PGA were not detected.

At 0 h, the Cya3Glc peak appeared at RT 14.8 on DAD chromatogram (**Figure 5. 11**), and with $m/z[M-H]^- 447$ on mass spectra chromatogram (**Figure 5. 7A**). The interpretation of mass spectra is usually carried out by assuming that the highest intensity of parent ion on the mass spectra chromatogram as the mass $[M]$ of the compound, and $\pm H$ depends on the ionisation polarity (positive or negative). Extra confirmation of the compound mass $[M]$ and its structural formula might be expected by observing other in-source fragment peaks on mass spectra chromatograms. For example, the mass spectra

obtained from Cya3Glc showed that the highest peak, which accounted for the parent ion, was 447 m/z [M-2H]⁻ (**Figure 5. 7A**). In addition, a m/z [2M-H]⁻ ion of 895.2 appeared to show a dimer of Cya3Glc mass. An in-source fragment of m/z [M-H]⁻ 285 was also shown to confirm the cyanidin after knocking off glucose (Glc) moiety from Cya3Glc. Moreover, spectra peaks with higher masses than the Cya3Glc [M-H]⁻ but smaller than the mass of Cya3Glc dimer [2M-H]⁻ represented an adduct with Cya3Glc might occur during the ionisation. For example, spectra peak of 465.1 [M-H]⁻ accounted for an adduct molecule of H₂O (18 amu) with Cya3Glc.

Another peak appeared at 12.7 min on DAD chromatogram at 0 h incubation (**Figure 5. 11**) with m/z [M-H]⁻ 465 (**Figure 5.7.B**). This would be presumed C-ring fission and the addition of H₂O (18 amu) to Cya3Glc that would form Cya chalcone-Glc in *cis*- form that later transformed to a *trans*- form with less structure energy⁸¹. This mass was shown to be increased over the first 4 h of the incubation in both colon media and phosphate buffer (**Figure 5.6**). Afterwards, it declined faster in colon media while it plateaued over time in the phosphate buffer. *cis/trans*-Cya chalcone-Glc was identified as [M-H]⁻ =465; a dimer [2M-H]⁻ =931.2 and [[M-H]-Glc]⁻ =303 (**Figure 5. 7B**).

After 1 h incubation another peak (RT 7.3) appeared with the mass of m/z [M- H]⁻ 463 (**Figure 5. 6**). This m/z value suggested that Cya chalcone-Glc lost two protons [2H⁺] to form Cya chalcone anionic-Glc. This mass increased over time during the incubation in phosphate buffer to reach its maximum accumulation at 24 h. Whereas the same peak was detected at 24 h in colon media but in a very small amount. This compound was interpreted using mass fragment pattern [M- H]⁻ 463; as a dimer [2M-H]⁻927.2 (**Figure 5. 8C**). Anionic Cya chalcone-Glc is a charged form, thus it is presumably form dimers with high molecular weight which delay it is elution to appear lately at RT 14.1 (**Figure 5. 8D**). Another peak with m/z [M-H]⁻ 329 appeared in both phosphate buffer and colon media, however, it appeared at 4 h in colon media and at 8 h in phosphate buffer (**Figure 5. 7 and Figure 5. 8E**). Nevertheless, this peak in both colon media and phosphate buffer, and the m/z [M-H]⁻ 329 increased over time to reach its maximum accumulation at 24 h (**Figure 5. 7**).

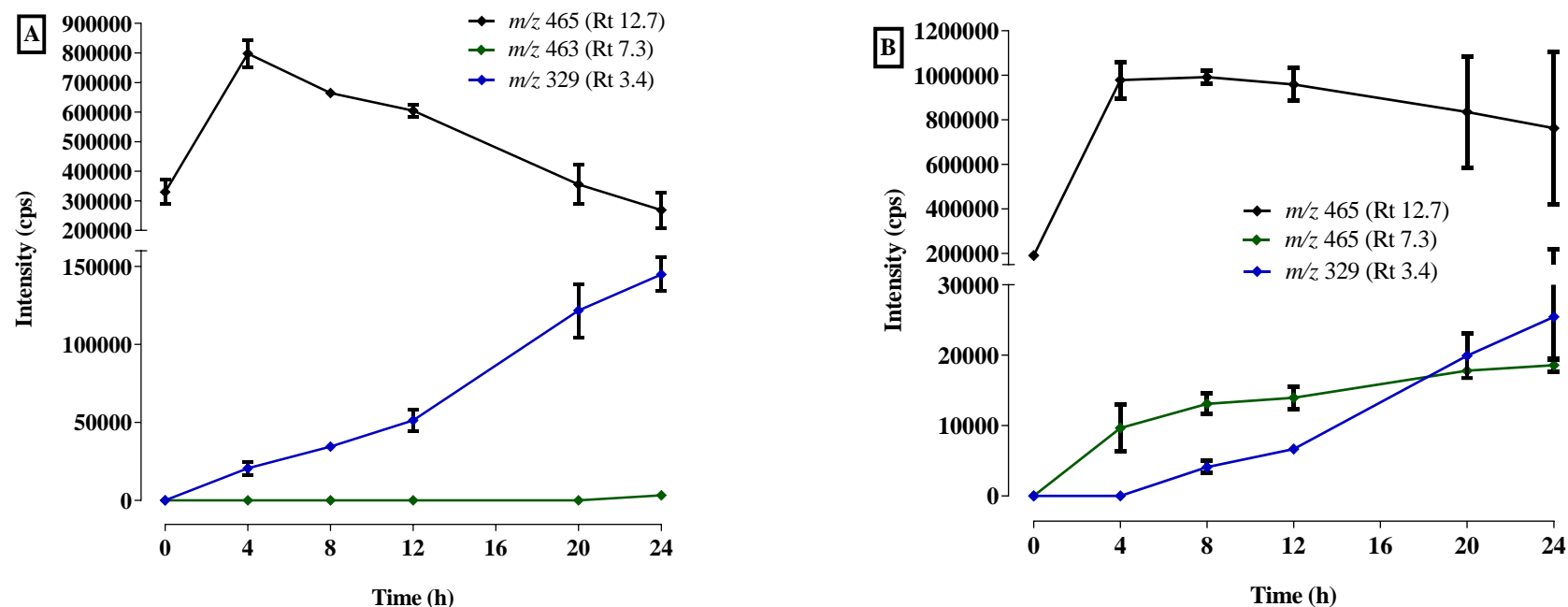
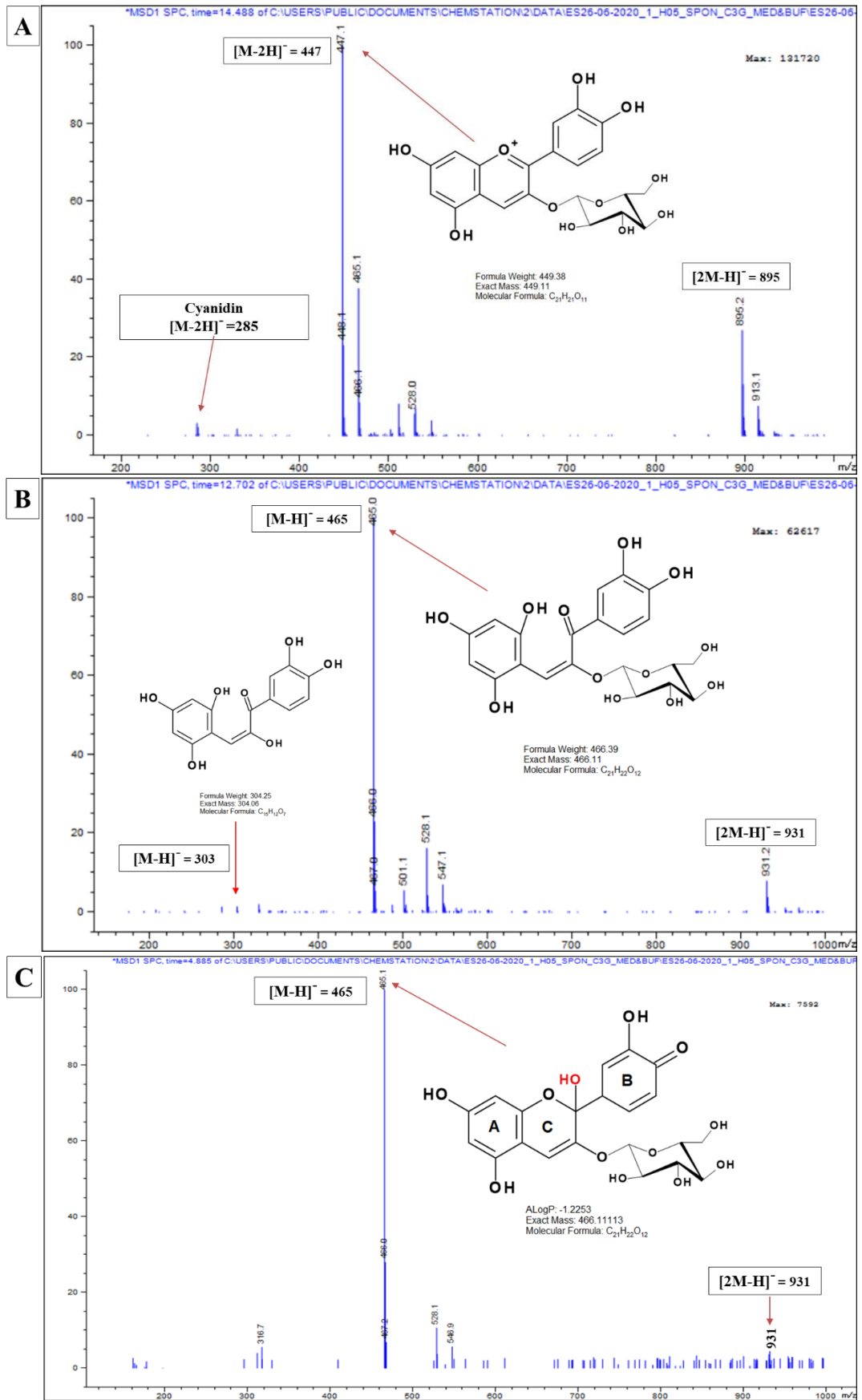


Figure 5. 7. The formation of the breakdown masses (products) during the anaerobic spontaneous degradation of Cya3Glc ($C_{\text{theo}} = 150 \mu\text{M}$) at physiological condition (neutral pH; 37°C) in colon media and phosphate buffer.

Phosphate buffer (A, 10mM K phosphate, pH 7.4) and colon media (B, 0.5 mM K phosphate, pH 7.0) were prepared and autoclaved. Colon media and phosphate buffer were incubated in the anaerobic cabinet overnight at 37°C to carry out the anaerobic degradation in the next day. On the day after, a fresh stock solution (SS) of Cya3Glc (2 mg/mL) was prepared by dissolving 2 mg of the authentic compound in 1 mL DMSO. In the anaerobic cabinet, two experimental vials ($n=2$) were prepared for each medium by adding 168.5 μL of SS to 4831.5 μL medium) to give a final volume of 5 mL and a Cya3Glc concentration of 150 μM . Samples (0.5 mL) were collected at the times shown in the figure, mixed with 0.5 mL of 4% v/v aqueous formic acid then immediately analysed using HPLC-DAD-MS in negative full scan mode to determine the Cya3Glc concentration. External standard curve of serial concentrations of Cya3Glc was prepared in acidified phosphate buffer (4% v/v formic acid). Each experiment was carried out in triplicates. Values represent means \pm SD.



To be continued in the next page.....

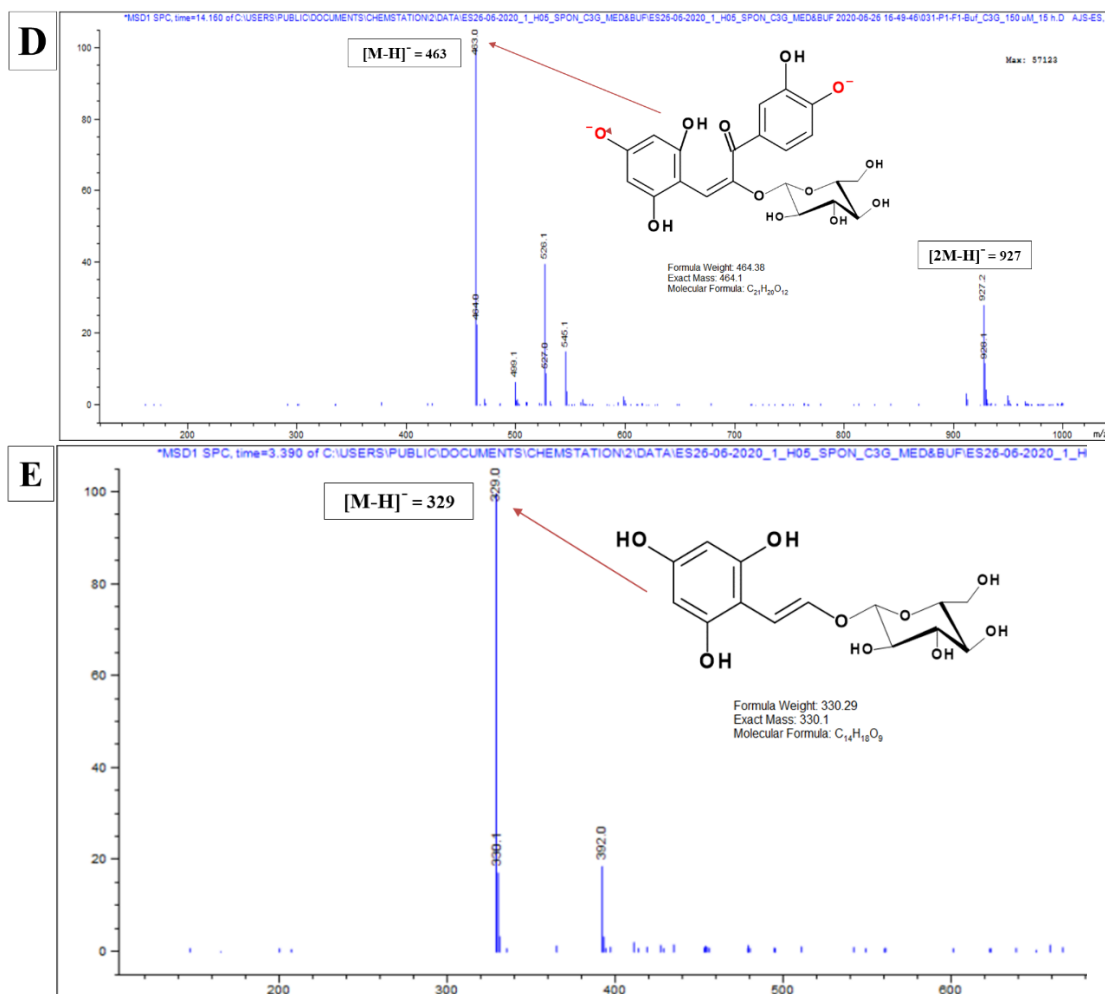


Figure 5. 8. The mass spectra of the peaks corresponding to Cya3Glc and its anaerobic spontaneous breakdown products in phosphate buffer on LC-MS in negative full scan mode, where x axis is $m/z[M-H]^-$ and y axis is the relative abundance (100%).

Cya3Glc (A), Cya chalcone-Glc (B), Cya chalcone-anionic-Glc (C), dimer of Cya chalcone-anionic-Glc (D), and trihydroxyethenylbenzene-Glc (E).

5.4.6. Investigating the breakdown products of the spontaneous degradation of Cya3Glc during the aerobic incubation

The formation of breakdown product peaks from the aerobic spontaneous degradation of Cya3glc was observed also on the DAD using different wavelengths (250, 280, 330, 370, and 520 nm). In addition, all newly formed peaks were observed from the UV-VIS chromatograms of the injections from vials containing phosphate buffer, because the peaks formed from the vial containing colon media were not clear and easy to monitor due to a high and noisy background presumably from colon media ingredients. Therefore, all new peaks were initially observed on the chromatograms created from injections from incubation with phosphate buffer. Afterward the corresponding masses of these new peaks were identified in the colon media samples by extracting these m/z [M-H]⁻ from the full scan to create a targeted MS chromatogram that could be integrated.

With regard to the aerobic spontaneous degradation, Cya3Glc declined at a faster rate over time compared to the anaerobic degradation (**Figure 5. 6**). Four peaks which were detected in the anaerobic degradation of Cya3Glc, were also detected in the aerobic spontaneous degradation of Cya3Glc i.e., *cis/trans*-Cya chalcone-Glc (RT 12.7; m/z [M- H]⁻ 465), Cya chalcone-Glc (RT 7.3; m/z [M-H]⁻ 463), 2,4,6-trihydroxyethenylbenzene-Glc (RT 3.4; m/z [M-H]⁻ 329) and dimer of Cya chalcone-Glc (RT 14.1; m/z [M-H]⁻ 931).

However, nine new peaks were detected as breakdown products during the aerobic degradation of Cya3Glc (**Table 5. 4**). The formation of these peaks was observed over the 24 h (**Figure 5. 9**). Three peaks showed to have higher mass than the mass of Cya3Glc. One peak, m/z [M-H]⁻ 465 (RT 4.8), appeared at 3 h and increased over time up to 24 h. This was interpreted as Cya hemiketal ketone-Glc. Another unknown peak was m/z [M- H]⁻ 495 (RT 7.6) which appeared at 2 h and increased over time to reach its maximum at 24 h. Another peak appeared (RT 14.9; m/z [M-H]⁻ 929) later at 4 h and also showed constant increase over time, and this mass was identified as a dimer of two different molecules, Cya chalcone-Glc (m/z [M-H]⁻ 465) and Cya chalcone anionic (m/z [M-H]⁻ 463). However, there was another new peak, but with lower masses than Cya3Glc, was shown to be increased over time. The peak (RT 6.4; m/z [M-H]⁻355) appeared at 2 h and

consistently increased over time. This peak was identified as coumarin-Glc based on $m/z[M-H]^-$ 355, another ion $m/z[M-H]^-$ 193 for coumarin, and other ion of $m/z[M-H]^-$ 177 (**Figure 5. 9**).

Additionally, five peaks with smaller apparent masses than the $m/z[M-H]^-$ of Cya3Glc appeared to increase over time (**Figure 5. 9** and **Figure 5. 11**). Two peaks were identified using m/z and RT of authentic standards, PCA (RT 3.7; $m/z[M-H]^-$ 153) and PGA (RT 9.7; $m/z[M-H]^-$ 153). However, further structure confirmation was done using fragment ions $[M-H]$ which were 109 and 125 for PCA and PGA, respectively (**Figure 5. 10E** and **5.10F**). The other three peaks were interpreted using the fragment ions from the current ion chromatogram. Therefore, these peaks were identified as 2,4,6- trihydroxyphenyloxoacetic acid (RT 1.4; $m/z[M-H]^-$ 197) with in-source ion fragment of 177, 153 and 125 $[M-H]^-$, 2,4,6- trihydroxyphenylacetic acid (RT 2.3; $m/z[M-H]^-$ 183) with ion fragment of 177, and 139 $[M-H]$, and 3,4- dihydroxyphenylacetic acid (RT 1.7; $m/z[M-H]^-$ 181) with ion fragment of 177, 137 and 109 $[M-H]$ (**Table 5. 4**).

The experimental HPLC vial of the aerobic spontaneous degradation of Cya3Glc was left over 7 days in the same condition (aerobic, 37°C) to inject it again onto HPLC-DAD-MS. The data showed that 3,4-dihydroxyphenylacetic acid (RT 1.7; $m/z[M-H]^-$ 181) remained as the highest peak compared to other peaks (**Appendix 4**).

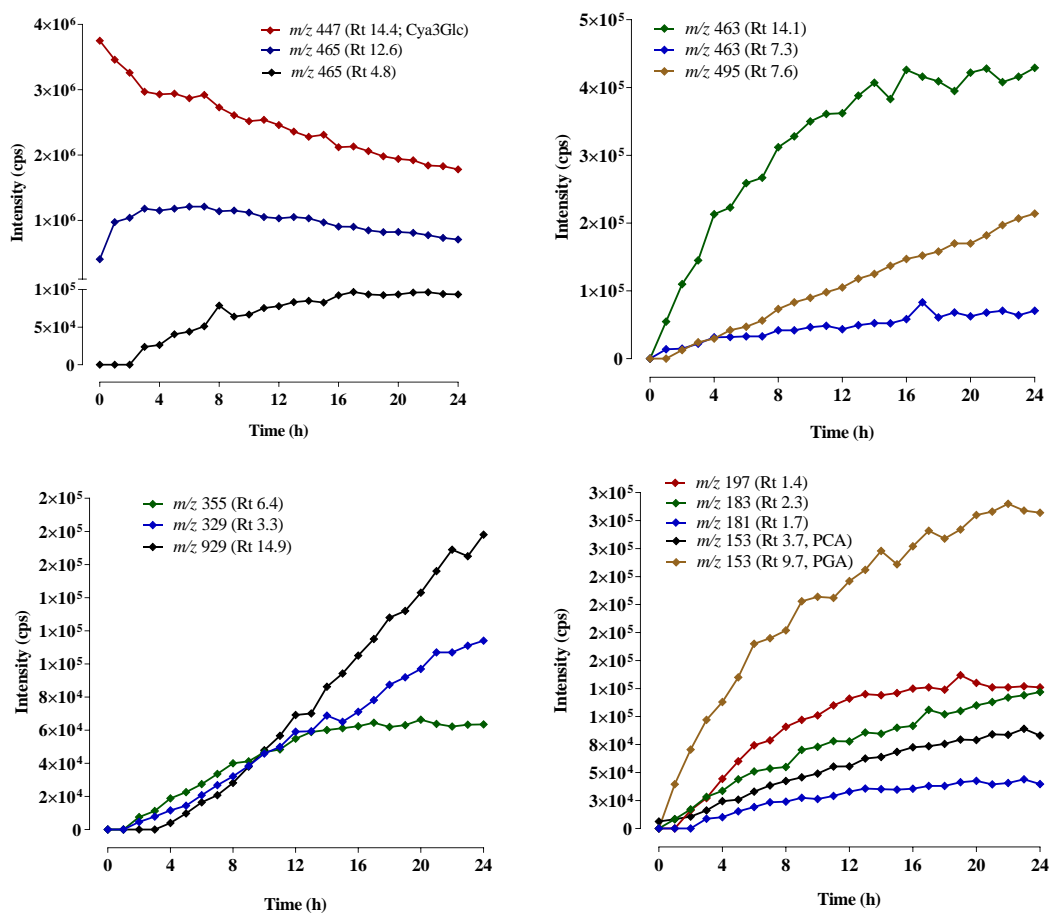
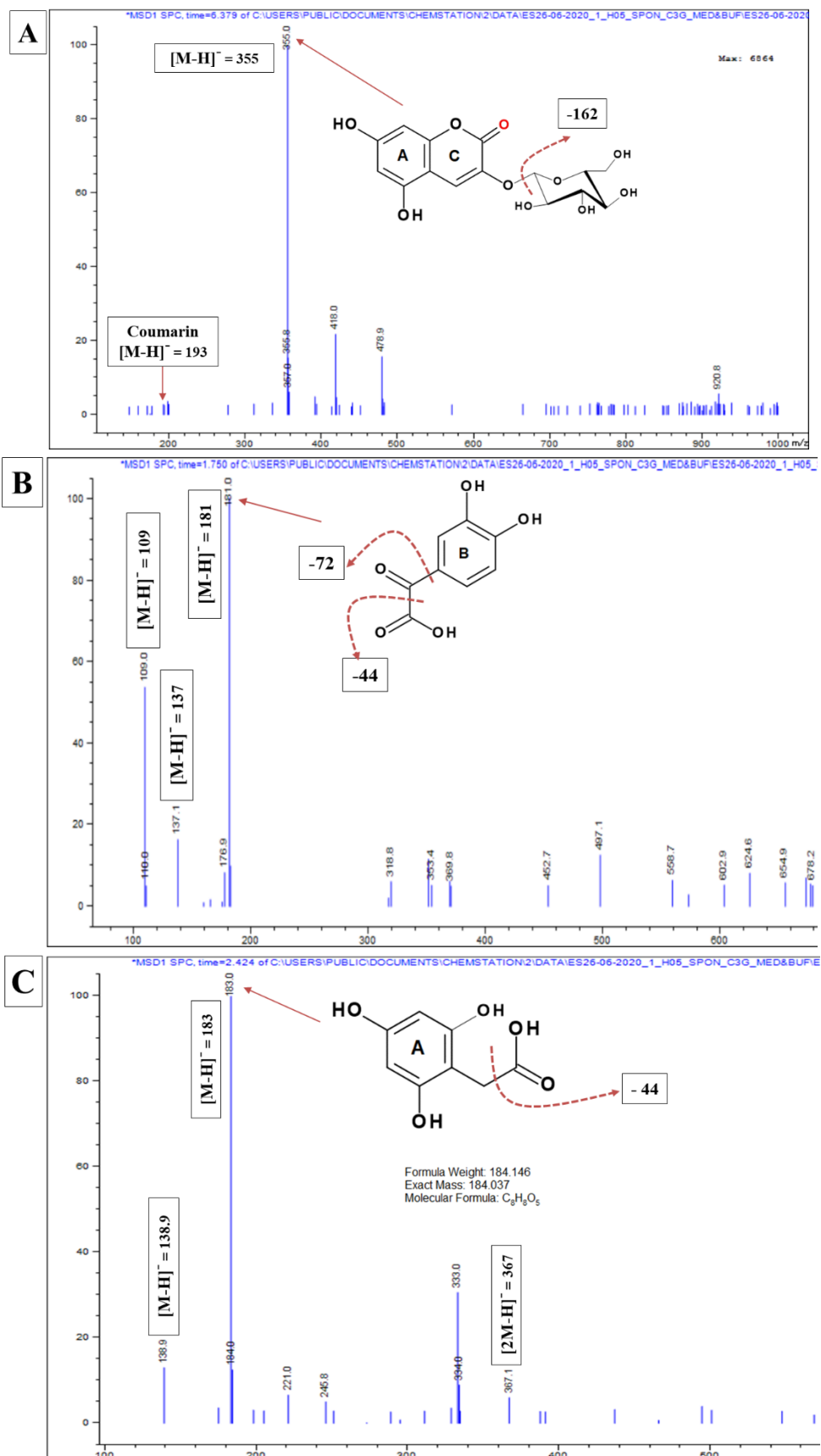


Figure 5. 9. Spontaneous aerobic degradation of Cya3Glc (170 μ M) at neutral pH; 37°C and the formation of breakdown products over 24 h incubation.

A phosphate buffer (10mM K phosphate, pH 7.4) was freshly prepared and then autoclaved. A fresh stock solution (SS) of Cya3Glc (2 mg/mL) was prepared by dissolving 2 mg of the authentic compound in 1 mL DMSO. An experimental vial (n=1) of 150 μ M of Cya3Glc was prepared by adding 33.7 μ L of SS to 966.3 μ L phosphate buffer, and immediately injected through HPLC-DAD-MS (in negative full scan mode) where the autosampler temperature was set at 37°C. Different auto-injections were carried out at the times (shown in the figure) to follow the Cya3Glc concentration and the formation of other breakdown products. External standard curve of serial concentrations of Cya3Glc was prepared in acidified phosphate buffer (4% v/v formic acid). The experiment was carried out twice in total, and similar results were obtained. The data are shown from one experiment.



To be continued in the next page.....

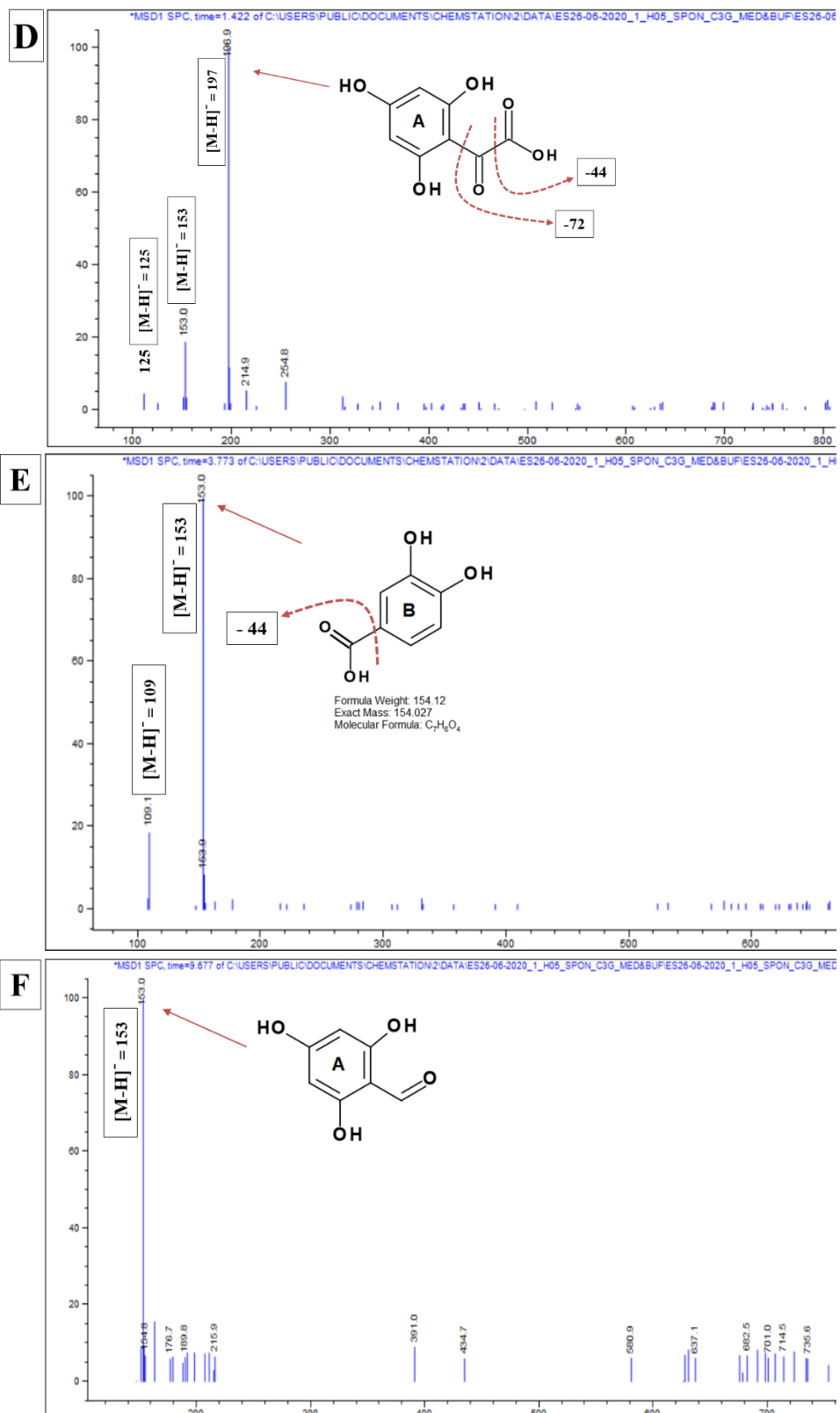


Figure 5. 10. The mass spectra of peaks corresponding to breakdown products from the aerobic spontaneous degradation of Cya3Glc in phosphate buffer on LC-MS in negative full scan mode, where x axis is m/z and y axis is relative abundance (100%).

Coumarin-Glc (A), dihydroxyphenyl-oxo-acetic acid (B), trihydroxyphenyl acetic acid (C), and trihydroxyphenyl-oxo-acetic acid (D), protocatechuic acid (E), and phloroglucinol aldehyde (F).

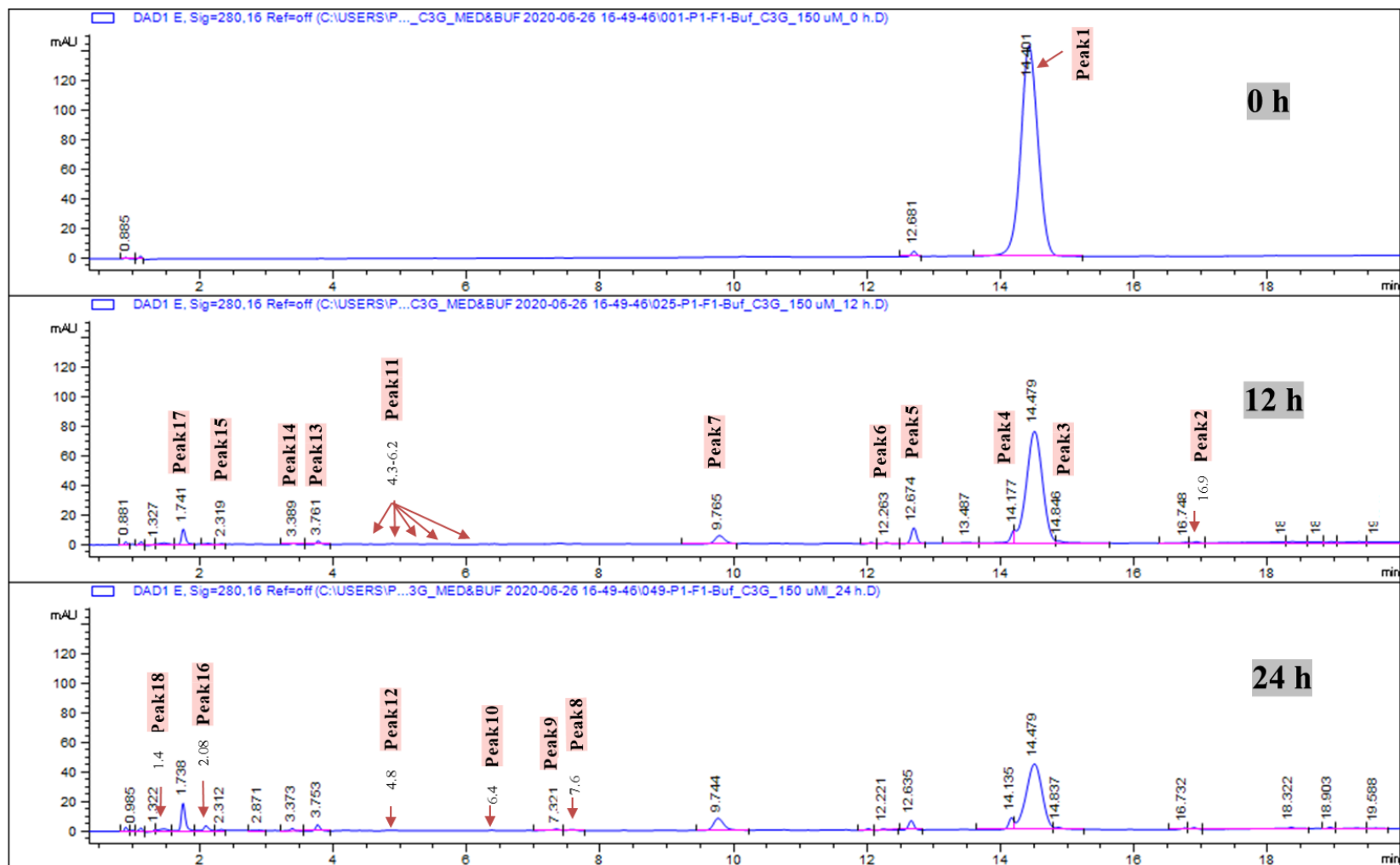


Figure 5. 11. DAD chromatogram λ (280 nm) of the aerobic incubation of Cya3Glc at 0, 12 and 24 h in a 10 mM phosphate buffer (pH 7.4) at 37°C showing the decomposition of Cya3Glc with the formation of new breakdown products.

Table 5. 4. Identification of Cya3Glc and its putative spontaneous breakdown products during aerobic and anaerobic conditions

Peak	RT (min)	Mass (amu)	Parent ion m/z [M-H] ⁻	Other ions m/z [M-H] ⁻	Identified compound	Detection	
						media/ buffer	Aerobic/ anaerobic
1	14.4	449	447	895, 447, 329, 285	Cya3Glc	both	both
2	16.9	768	767	329	Unknown	both	aerobic
3	14.8	930	929	767, 587, 447, 379, 317	Cya chalcone + Cya chalcone anionic	both	aerobic
4	14.1	928	927	463	Cya chalcone anionic-Glc (Dimer)	both	both
5	12.6	466	465	931, 465, 329, 303	<i>cis/trans</i> -Cya chalcone-Glc	both	both
6	12.2	766	765	627, 167, 142	Unknown	buffer	aerobic
7	9.7	154	153	125	Phloroglucinol aldehyde (PGA)	both	aerobic
8	7.6	496	495	198, 175, 161, 142	Cya chalcone anionic-Glc + 2 O	both	aerobic
9	7.3	464	463.1	397, 367, 198, 177	Cya chalcone anionic-Glc	both	both
10	6.4	356	355	193, 177	Coumarin-Glc	both	aerobic
11	4.3, 5.1, 5.4, 6.0, 6.2	344	343	283,197, 177, 153	Dihydroxy-oxo- cyclohexa- dienylacetyl-Glc	both	aerobic but peak appeared at RT 5.4 was detected in anaerobic
12	4.8	466	465	343, 317	Cya hemiketal ketone-Glc	media	aerobic
13	3.7	154	153	109	protocatechuic acid (PCA)	both	aerobic
14	3.4	330	329	196, 177, 153	2,4,6- trihydroxyethenylb enzene-Glc	both	both
15	2.3	184	183	177, 139	2,4,6- trihydroxyphenyl acetic acid	both	aerobic
16	2.0	178	177	169, 125	Unknown	both	aerobic
17	1.7	182	181	177, 137, 109	3,4- dihydroxyphenyl- oxo acetic acid	both	aerobic
18	1.4	198	197	177, 153, 125	2,4,6- trihydroxyphenyl- oxo acetic acid	both	aerobic

5.4.7. The effects of matrix, initial concentration, and buffer capacity on the aerobic spontaneous degradation of anthocyanidins: Cya

In the previous sections, anthocyanins (Cya3Glc) were shown to be degraded spontaneously during aerobic and anaerobic incubations. Previous reports have investigated anthocyanidins^{38,87}. However, it has been noticed that there were variables in the experimental design in these reports. For example, different matrices were used for the incubation of anthocyanidins such as water, buffer solutions (with different buffer capacities) and tissue culture samples. Also, the preparation of stock standard solution of the authentic compounds was also different or not mentioned, and the initial concentration ranged from low concentration (20 $\mu\text{g mL}^{-1}$) up to very high concentrations (1000 $\mu\text{g mL}^{-1}$). Therefore, here the effects of various variables such as matrix, initial concentration, and buffering capacity on the spontaneous k_{deg} were investigated.

The effect of matrix

To investigate this, a stock solution of an authentic Cya was freshly prepared in DMSO, then it was immediately incubated in two HPLC vials: (1) one containing milli-Q water (deionised and filtered water) and (2) the other containing 100 mM phosphate buffer solution with pH 7.4 as reported in the literature where of using simple solution was commonly used. The incubation was carried out at 37°C over 24 h. The initial concentration of Cya in both vials was 1000 $\mu\text{g mL}^{-1}$ as reported in Kay report³⁸. In addition, a high C_{initial} would help to follow up and identify the formation of the breakdown products. The final DMSO percent was 1% in both experiments. At different time points, samples were injected onto HPLC-MS to quantify Cya.

Cya was extensively degraded in phosphate buffer but only slightly degraded in Milli-Q water and the purple colour of Cya remained even after 24 h incubation in water compared to phosphate buffer (**Figure 5. 12**). However, in phosphate buffer solution, dark blue precipitation was formed. Therefore, the solution was centrifuged and then the precipitate was resuspended in Milli-Q water and injected again through HPLC-MS, showing unknown peaks. The main peak appeared at RT 25.4 and accounted for the mass of 290 m/z (**Figure 5. 13**). The mass of catechin and epicatechin is 290 (amu). Therefore, the

injection of authentic standard compound of catechin and (+)-epicatechin was carried out, but both appeared at different retention times from the RT of the peak with mass of 290, confirming it is a different compound.

At 24 h, the pH was measured in both vials by using litmus paper to give pH values of ~ 4 for water and 7 for phosphate buffer solution. Because the pH of milli-Q water is slightly low (~ 6.0), therefore, the same experiment with milli-Q water was repeated but the milli-Q water pH was adjusted to 7.4 using a drop of 1 M NaOH prior to the incubation. However, the colour of the solution was as purple at $t=0$ h incubation which showed that the spontaneous degradation is not completed or did not happen. Regarding breakdown products, only a mass of 304 (putatively Cya chalcone) was detected as the main breakdown product in water and phosphate buffer.

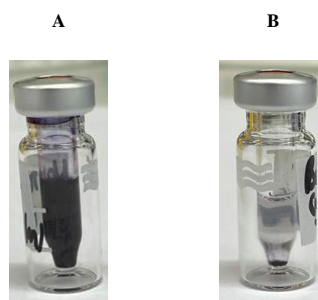


Figure 5. 12. Picture of incubated Cya ($1000 \mu\text{g mL}^{-1}$) in two different matrices after 24 h incubation at 37°C .

A: milli-Q water and B: 100 mM phosphate buffered solution.

The effect of the initial concentration of anthocyanidins

The observation of a precipitate in the previous experiment from the incubation of high amount of Cya ($1000 \mu\text{g mL}^{-1}$) in water and phosphate buffer solutions led to the question of whether the high initial concentration caused reactional saturations or equilibriums which halt the spontaneous reactions. Therefore, the same incubation was carried out again in 100 mM phosphate buffer but with lower initial concentrations of Cya (100 and $500 \mu\text{g mL}^{-1}$) with a final 1 % DMSO. In addition, another experiment with Cya ($500 \mu\text{g mL}^{-1}$) was carried out but the DMSO percentage was increased to 5%. Samples were injected on HPLC to quantify Cya at different time points.

Cya degraded over 24 h in the three experimental vials. No precipitation was formed in the vial containing $100 \mu\text{g mL}^{-1}$ with 1 % DMSO as well as in the vial containing $500 \mu\text{g mL}^{-1}$ with 5 % DMSO (**Figure 5. 14A and B**). However, in the vial containing $500 \mu\text{g mL}^{-1}$ with 1 % DMSO, a dark blue precipitate was formed (**Figure 5. 14C**). Again, the main peak gave a mass of 290 when the precipitate was resuspended and injected onto the HPLC-MS.

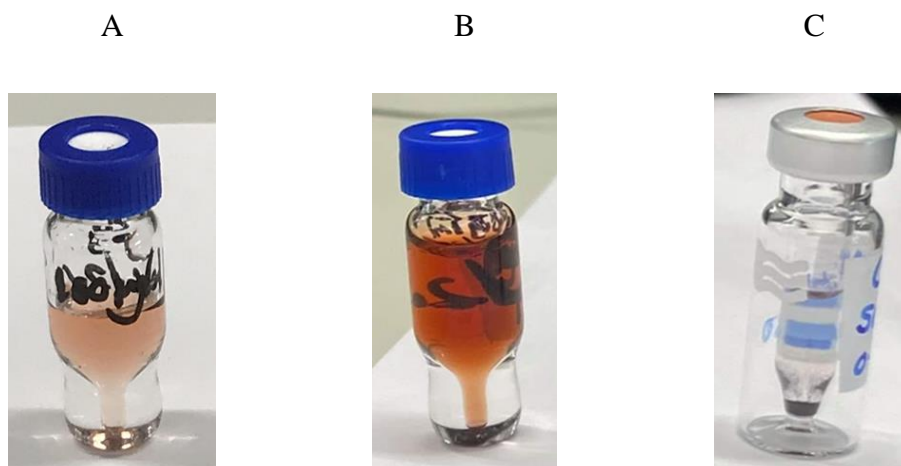


Figure 5. 14. Pictures of incubated authentic Cya (with different concentrations and with different % of DMSO) in phosphate buffered solution (100 mM) at 24 h.

A: $100 \mu\text{g mL}^{-1}$ and 1% DMSO, B: $500 \mu\text{g mL}^{-1}$ in 5% DMSO, and C: $500 \mu\text{g mL}^{-1}$ in 1% DMSO.

The effect of the medium buffer capacity

Having observed that the initial concentration and the DMSO percentage are crucial for Cya solubility and thus for investigation of the spontaneous degradation of anthocyanidins. The pH of the medium is also critical and known to influence the spontaneous degradation of both anthocyanins and anthocyanidins²⁴⁶. Further work was carried out to investigate the spontaneous degradation under the physiological condition (at neutral pH). However, maintaining the pH at neutral pH was essential over the incubation time. Therefore, different phosphate buffered solutions with different buffering capacity strengths were investigated. To examine this, an initial concentration of 150 μ M of Cya was incubated in different solutions with different buffer capacities over 20 h (**Figure 5. 15**). The solutions were as follows: (i) water with no buffering capacity, (ii) colon model media with 0.5 mM buffering capacity, (iii) phosphate buffer with 10mM buffering capacity and (iv) phosphate buffer with 100 mM buffering capacity. Samples were taken over time and injected on HPLC-MS to quantify Cya over time.

Visually, the colour of the solution in vials was slightly different in particular between the colour of the phosphate buffer solution and the colour in colon model media. However, in all experimental vials, Cya degraded over time and no Cya was detected at 20 h injections. However, the pH was measured at 20 h incubation for all vials: water, colon model media, 10 mM phosphate buffer, 100 mM phosphate buffer which showed pH of 4.0, 5.0, 6.8 and 7.4, respectively. This showed that the degradation process and the breakdown products tend to decrease the pH of the medium. But with a higher capacity buffer, the medium system maintains the pH value at physiological pH (neutral) as it occurred with 100 mM phosphate buffer.

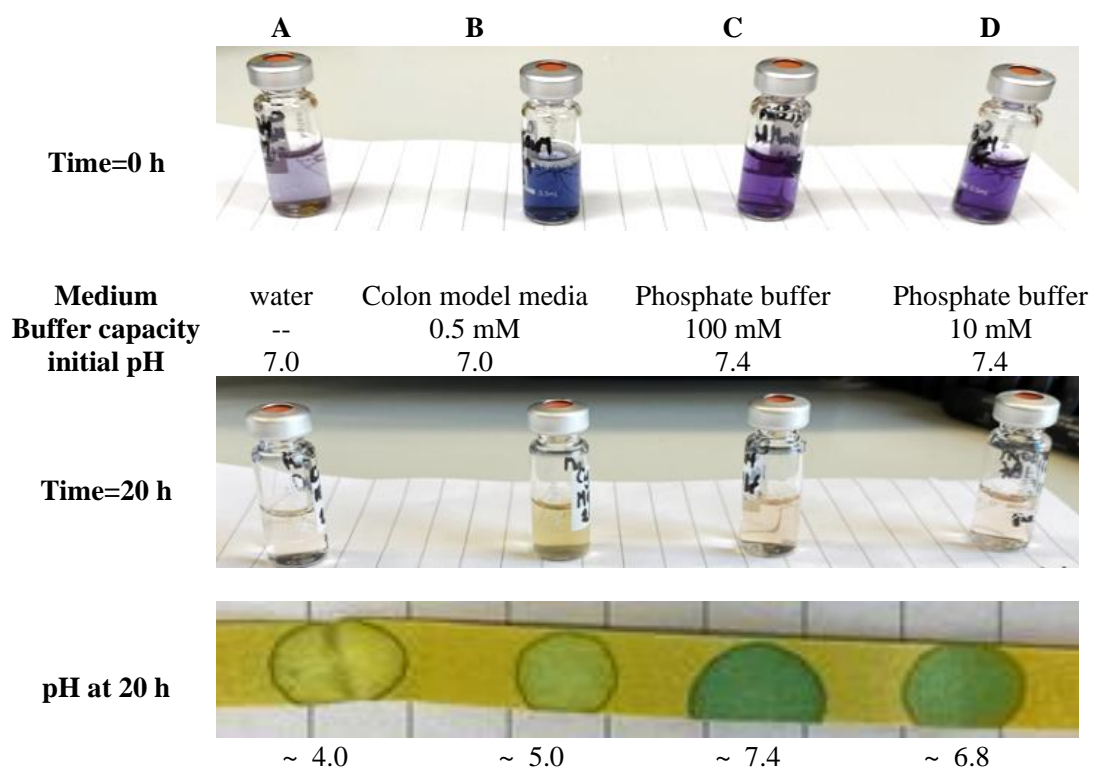


Figure 5. 15. The spontaneous degradation of Cya (150 μ M, with 1.5% DMSO) in different media with different buffer capacities at 0 and 20 h.

A: in water (no buffer capacity, pH 7.0), **B:** in colon model media (0.5mM buffer capacity, pH 7.0), **C:** in phosphate buffer (100 mM, pH 7.4), and **D:** in phosphate buffer (10 mM, pH 7.4).

The effect of the medium pH

The effect of two different medium pHs (6.8 and 7.4) was investigated. To examine this, an initial Cya concentration of 222 μM was incubated in two phosphate-buffered solutions with different pH (6.8 and 7.4 h) over 12 h in HPLC autosampler at 37°C. (Figure 5. 16). Samples were injected by setting up the autosampler for auto injections to quantify Cya over 12 h.

Cya was degraded spontaneously over the time course (Figure 5. 16). Cya was degraded faster in phosphate buffered solution with high pH (7.4) than in solution with pH 6.8. For example, the initial spontaneous decline rate was 93.3 $\mu\text{M}/\text{h}$ in a pH 7.4 solution, whereas it was 31.3 $\mu\text{M}/\text{h}$ in a pH 6.8 solution. In addition, after 12 h incubation, 31.9 μM of Cya was detected in higher pH of 6.8 while 12.9 μM was detected in a buffered solution with pH 7.4.

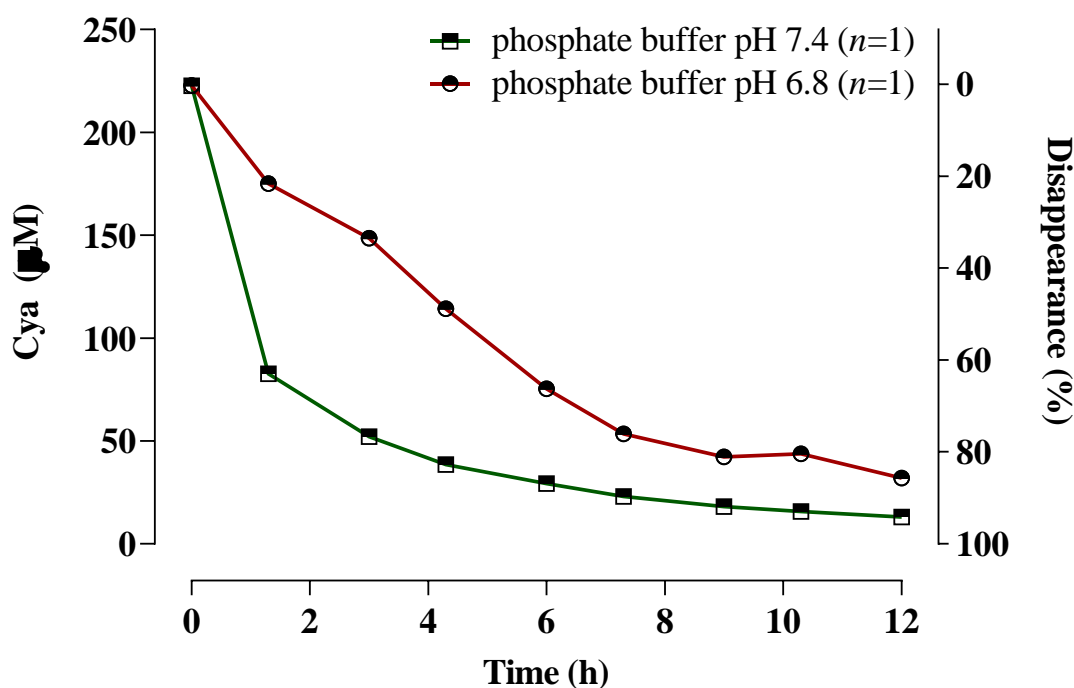


Figure 5. 16. The spontaneous degradation of Cya (222 μM , with 3% DMSO) in two phosphate buffered solutions with different pH (6.8 and 7.4) over 12 h at 37°C.

5.4.8. The spontaneous degradation of anthocyanidins: Cya and Del

In the previous section, the matrix of the medium, the initial concentration of anthocyanidins, the medium buffer capacity, and the pH of the solution showed substantial effects on the spontaneous degradation of anthocyanidins (Cya) and thus the experiment was designed based on findings in the previous section. Therefore, a 100 mM phosphate buffer and initial concentration of anthocyanidins (Cya or Del) of $100 \mu\text{g mL}^{-1}$ in 3% DMSO, were chosen to investigate the spontaneous degradation of authentic compounds of Cya and Del under the physiological conditions (pH 6.8 and 7.4 and 37°C).

Cya and Del were declined over the time course (**Figure 5. 17**). The initial k_{deg} over the first 3 h was relatively slower for Cya ($24.8 \mu\text{M/h}$) than Del ($27.6 \mu\text{M/h}$). However, at 12 h, 85 % of C_{initial} of Cya was degraded and 81% of C_{initial} of Del was degraded. Various breakdown phenolics formed during the time course incubation. For example, PCA and PGA produced in the presence of Cya, whereas gallic acid, PGA, and 3-O-gallic acid formed in the presence of Del.

In regards to Cya breakdown production, the B-ring-derived PCA was shown to be increased over time and reached a C_{max} of $17.4 \mu\text{M}$ at 12 h. PGA, the A-ring product, was also increased over time to reach its C_{max} of $4.2 \mu\text{M}$ at 12 h. However, in the presence of Del, the B-ring gallic acid increased over time but only reached its C_{max} of $1.2 \mu\text{M}$ at 12 h. However, although the A-ring PGA product increased, the increase was over 4.5 h (C_{max} of $3.1 \mu\text{M}$) and then declined to $2.7 \mu\text{M}$ at 12 h. Furthermore, 3-O-methylgallic acid was produced and consistently increased over the time course to reach its C_{max} of $3.7 \mu\text{M}$ at 12 h.

Other unknown peaks were formed during the incubation of both Cya and Del in phosphate buffer (pH 6.8). However, their MS properties of ion fragments were used to tentatively identify these corresponding compounds.

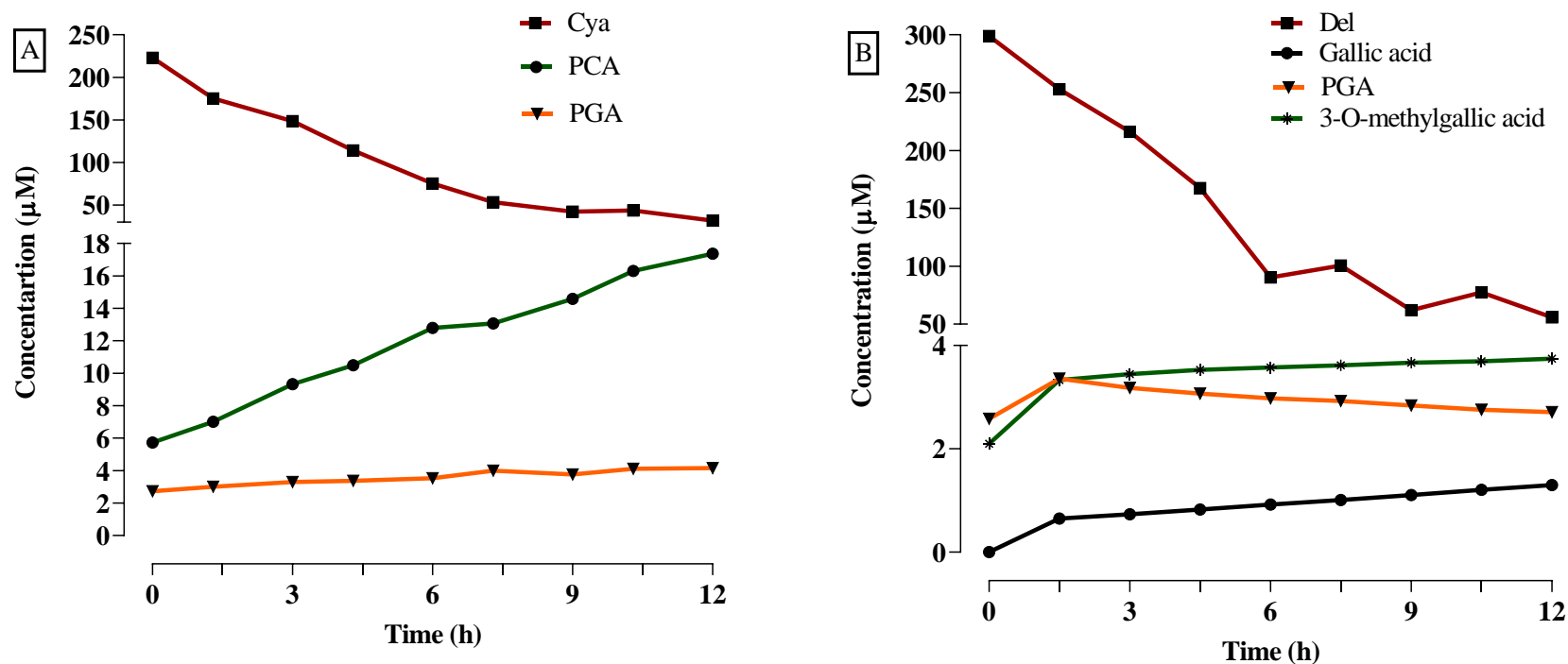


Figure 5. 17. The spontaneous degradation of Cya with C_{initial} of $100 \mu\text{g mL}^{-1}$ ($222 \mu\text{M}$) (A) and Del with C_{initial} of $100 \mu\text{g mL}^{-1}$ ($330 \mu\text{M}$) (B) at physiological condition (neutral pH; 37°C) in phosphate-buffered solution.

A phosphate buffer (10mM K phosphate, pH 6.8) was prepared and autoclaved. On the day of the experiment, a fresh stock solution (SS) of anthocyanidin (1 mg/mL) was prepared by dissolving 1 mg of the authentic compound in 1 mL DMSO. In a 1mL HPLC vial, 100 μL of SS was added to 900 μL phosphate buffered solution to give a final Cya concentration of 222 μM (or 330 μM ; Del), then immediately the experimental vial was incubated in LC-DAD autosampler at 37°C and then injections were carried out at the times shown in the figure (every 90 min) to determine the Cya (or Del) concentration. External standard curve of serial concentrations of Cya (Or Del) was prepared in acidified phosphate buffer (4% v/v formic acid). Each experiment was carried out once.

5.4.9. Identification of breakdown products of the spontaneous degradation of Cya and Del

The breakdown products of Cya and Del were identified by observing new peaks on DAD at different wavelengths (250, 280, 330, 370 nm) (**Figure 5. 18** and **Figure 5. 19**). In addition, all corresponding masses of these new peaks were identified through MS detector. The analysis of breakdown species showed that, in both anthocyanidins (Cya and Del), the formation of chalcones, chalcone α -diketones and chalcone anionic forms are the main peaks of the classic pH-dependent transformation of the flavylium form of anthocyanidins into other intermediates (**Table 5. 5** and **Table 5. 6**). Other peaks appeared which corresponded to polymers of these intermediates together and/or with oxygen or H₂O. The putative mechanism is that the formation of these intermediates occurred when the flavylium form was converted to the hemiketal form (addition of OH) after nucleophilic attack by water molecules (H-O-H) on C2 in C-ring. Due to the neutral pH of the medium, hemiketal lost more hydrogen atoms from its hydroxylic groups to transform the hemiketal anionic form (unstable form). As a result, rearrangement occurred on B-ring of the molecule which decreased the stability of C2 on C-ring. This instability led to two possible fissions on the hemiketal structure. The first cleavage occurred on C-ring between O1 and C2 to give chalcone, chalcone α -diketones and their anionic forms (2H loss). The other possible pathway was after the cleavage happened between C2 and C1' forming coumarin (mass of 194). Later all these previously mentioned intermediates underwent a series of oxidation process in the presence of the atmospheric oxygen forming low molecular weight phenolic compounds such as PCA, PGA, PGCA, dihydroxyphenylacetic acid, dihydroxyphenyl-oxo acetic acid and trihydroxyphenyl-oxo acetic acid from Cya. Similar phenolics formed from Del degradation (because they originated from A-ring) were PGA, PGCA, and trihydroxyphenyl-oxo acetic acid but other B-ring phenolics were identified as gallic acid and 3,4,5-trihydroxyphenyl-oxo acetic acid. However, another B-ring phenolic was identified as 3-O-methylgallic acid but the substitution of the methyl group on the hydroxy group on B-ring was proposed to be formed during the proposed transformation mechanism of the Del hemiketal especially into the anionic forms where the structure is very highly reactive and likely reacts with other components in the medium.

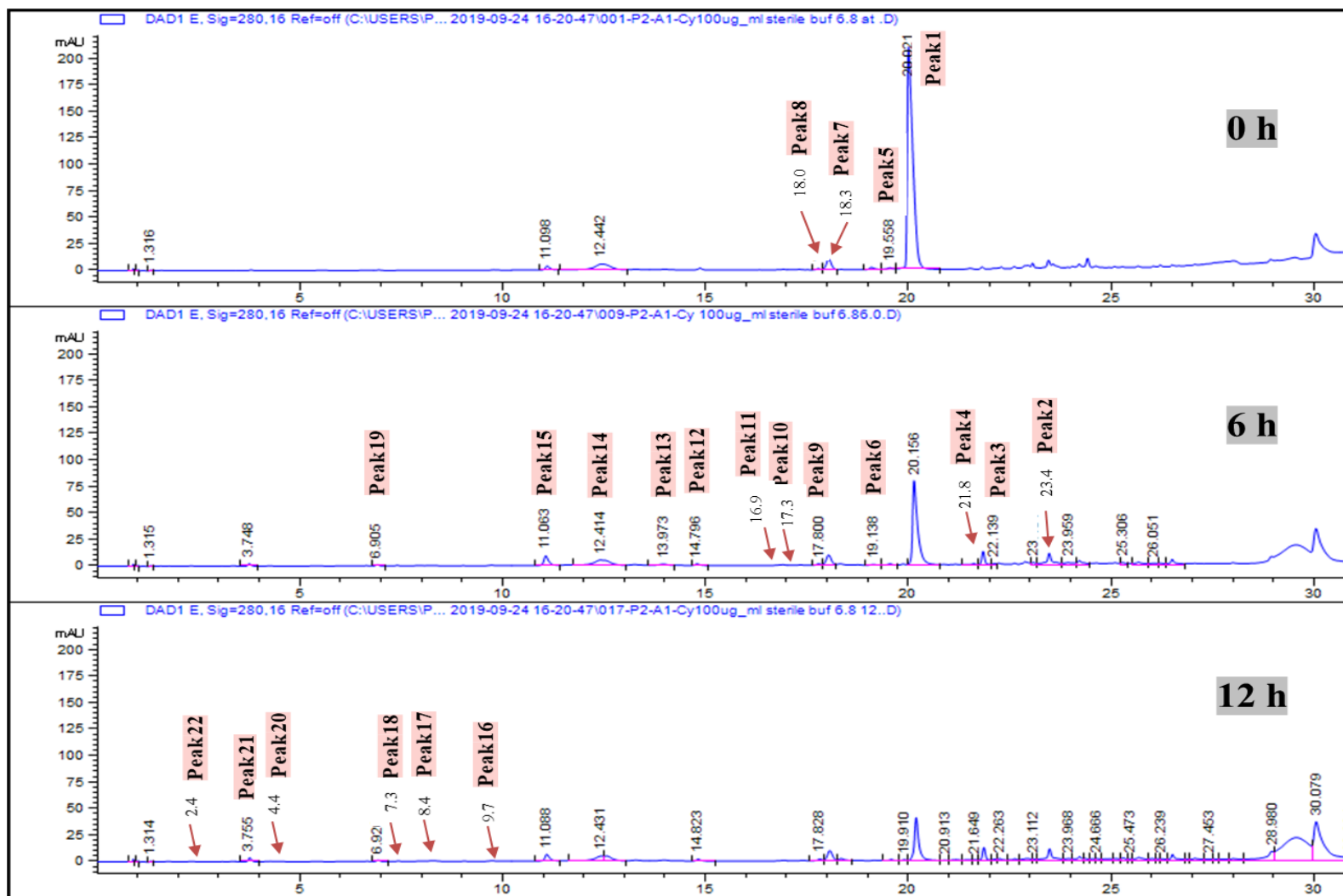


Figure 5. 18. DAD chromatogram λ (280 nm) of the incubation of $100 \mu\text{g mL}^{-1}$ ($222 \mu\text{M}$) Cya at 0, 6 and 12 h incubation in a 100 mM phosphate buffer (pH 6.8) at 37°C showing the decomposition of Cya with the formation of new breakdown products.

Table 5. 5. Identification of Cya and its putative spontaneous breakdown products during aerobic incubation in phosphate buffer pH 6.8 at 37°C.

Peak	RT (min)	Mass (amu)	Parent ion m/z [M-H] ⁻	In-source fragment ions m/z [M-H] ⁻	Identified compound
1	20.0	287	285	125	Cya
2	23.4	602	601	329, 207	2 Cya chalcone anionic
3	22.1	618	617	333, 287, 197	2 Cya chalcone anionic + O
4	21.8	652	651	587	Unknown (dimer)
5	19.5	304	303	181, 165	Cya chalcone
6	19.1	364	363	587, 303, 183, 131	Cya chalcone + 4O
7	18.3	302	301	191, 179, 151	Cya chalcone anionic
8	18.0	304	303	181, 151, 125	Cya chalcone α -diketone
9	17.8	350	349	331, 317	Cya chalcone anionic + 3O
10	17.3	302	301		Cya chalcone anionic
11	16.9	604	603	319, 183, 169	2 Cya chalcone anionic
12	14.7	604	603	331, 303, 179	2 Cya chalcone α -diketone
13	13.9	304	303	195, 167	Cya chalcone or Cya chalcone α -diketone
14	12.4	334	333	301, 167	Cya chalcone anionic + 2O
15	11.0	570	569	333, 331, 165	Unknown
16	9.7	154	153		PGA
17	8.4	194	193	587, 177, 165, 153	Coumarin
18	7.3	320	319	167, 165	Cya chalcone anionic + H ₂ O
19	6.9	320	319	165	Cya chalcone + O
20	4.4	170	169	151	PGCA
21	3.7	154	153	109	PCA
22	3.3	198	197	153, 139, 123	Unknown
23	2.4	184	183	177, 165, 139, 129	2,4,6-trihydroxyphenylacetic acid
24	1.7	182	181	177, 137, 109	3,4-dihydroxyphenyloxoacetic acid
25	1.4	198	197	177, 125	2,4,6-trihydroxyphenyloxoacetic acid

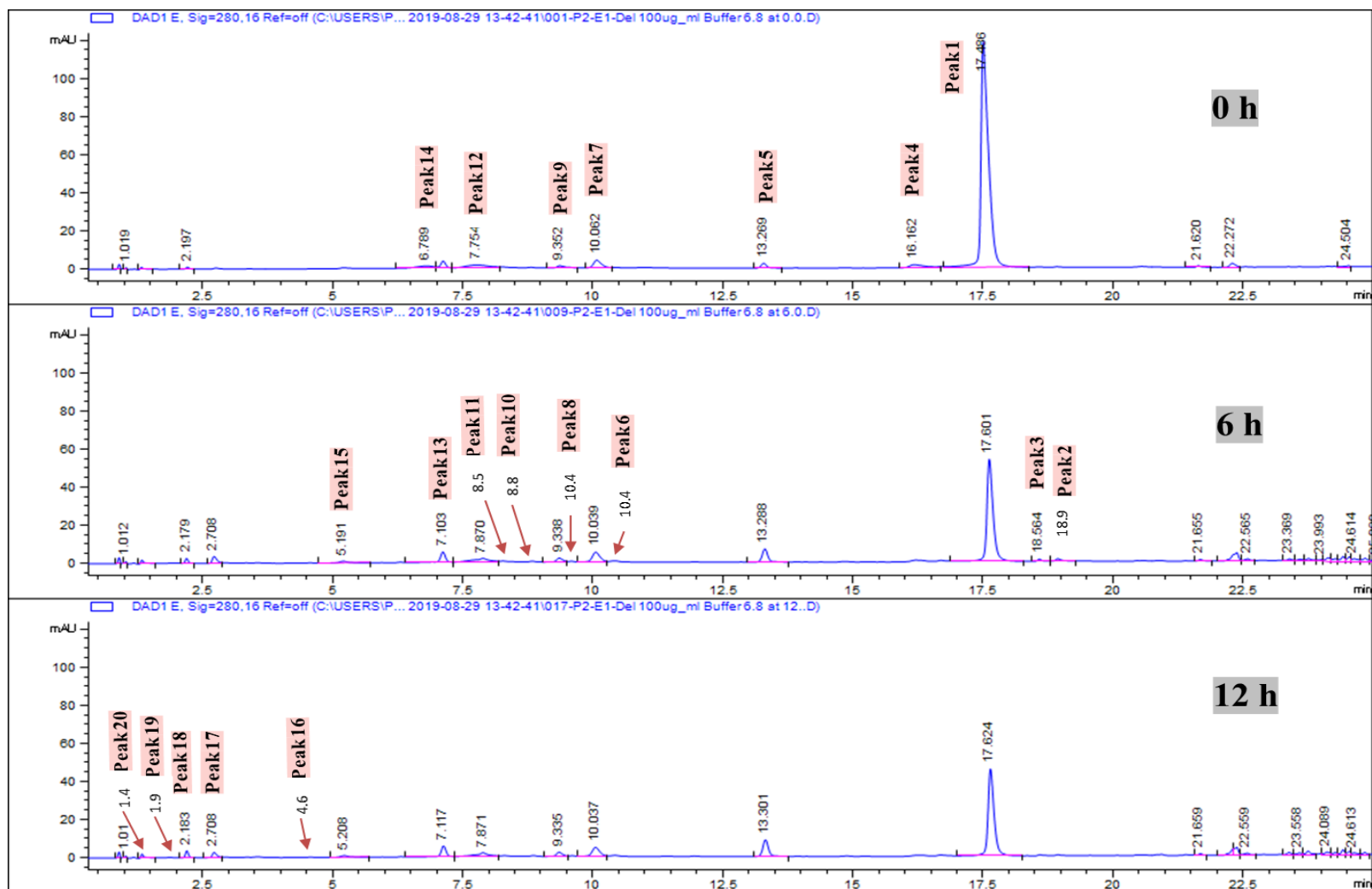


Figure 5. 19. DAD chromatogram λ (280 nm) of the aerobic incubation of Del at 0, 6 and 12 h incubation in a 100 mM phosphate buffer (pH 6.8) at 37°C showing the decomposition of Del with the formation of new breakdown products.

Table 5. 6. Identification of Del and its putative spontaneous breakdown products during aerobic incubation in phosphate buffer pH 6.8 at 37°C

Peak	RT (min)	Mass (amu)	Parent ion m/z [M-H] ⁻	In-source fragment ions m/z [M-H] ⁻	Identified compound
1	17.50	303	301	191, 153	Del
2	18.9	618	617	301	2 Del + O
3	18.5	650	649	301	2 Del + 4O
4	16.1	620	619	319, 301, 174	Del chalcone anionic + Del + H ⁺
5	13.2	366	365	347, 319, 315, 179	Del chalcone anionic + 3O
6	10.4	320	319	153	Del chalcone or Del chalcone α -diketone
7	10.0	154	153		PGA
8	9.6	382	381	331, 319, 317	Del chalcone α -diketone + 4O
9	9.3	318	317	191	Del chalcone anionic
10	8.8	516	515	275, 319, 211	Del chalcone anionic + 198
11	8.5	194	193	153	Coumarin
12	7.8	394	393	361, 319	Del chalcone + 74
13	7.1	184	183	125, 124	3-O-methylgallic acid (B-ring)
14	6.7	348	347	319, 317	Del chalcone anionic + 3O
15	5.1	368	367	317, 179, 153	Del chalcone α -diketone + 3O
18	4.6	170	169	151	PGCA
16	3.3	198	197	177, 153, 137, 122	3,4,5-trihydroxyphenyloxoacetic acid
17	2.7	602	601	301, 177	2 Del (dimer)
18	2.1	170	169	125	Gallic acid
19	1.9	178	177	165, 137, 129	Unknown
20	1.4	198	197	177, 125	2,4,6-trihydroxyphenyloxoacetic acid

5.5. Discussion

The overall aim of this chapter was to investigate the spontaneous degradation of anthocyanins and their aglycones (anthocyanidins) and to relate the spontaneous degradation of anthocyanins to their metabolism by the human faecal microbiota.

The main findings in this chapter were that (i) at neutral pH, anthocyanins (Cya3Glc) and anthocyanidins (Cya and Del) underwent a classic pH-dependent transformation to form colourless intermediates (hemiketal, hemiketal ketone, chalcone, chalcone anionic forms, (ii) only in the presence of atmospheric oxygen, the formed pH-dependent intermediates underwent a series of auto-oxidative processes, forming different simple phenolic compounds (iii) the spontaneous k_{deg} of Cya3Glc was faster in colon media than in phosphate buffer, and during aerobic than anaerobic incubations, (iv) the experiment matrix, initial concentration of anthocyanidin, pH value, and the medium buffering capacity are crucial factors which considerably affected the spontaneous k_{deg} of anthocyanidins and thus the appearance of their breakdown products.

Anthocyanins are stable in an acidic environment; therefore, anthocyanins stay in the flavylium form $[M^+]$. At neutral pH, flavylium form is prone to structural changes. However, some studies proposed that there are two pathways for the spontaneous degradation of anthocyanins: (i) deprotonation (very fast process) where the flavylium cation lose protons (H^+) to form quinoidal base and then quinoidal anionic base and (ii) hydration (relatively slow process) where the structure forms hemiketal and chalcone ^{80,81,83,246,247}. Although these studies were focused on the effect of the pH changes on anthocyanins, they have not considered the effect of atmospheric oxygen. However, in this chapter aerobic and anaerobic spontaneous degradation of anthocyanins at neutral pH were investigated in more detail.

Under colonic conditions (anaerobic, neutral pH, 37°C), Cya3Glc showed a classic pH-dependent degradation where the flavylium cation structure underwent structural transformation (hydration process) (**Figure 5. 20**) mainly in three steps: (i) the nucleophilic attack at C2 position on C-ring by H_2O forming Cya hemiketal-Glc (carbinol pseudobase, $m/z[M-H]^-$ 465), (ii) structure transformations, then (iii) structural fission

occurred on C-ring between O1 and C2 to give Cya chalcone-Glc (m/z [M-H]⁻ 465) as *cis* isomer, and its anionic forms by losing 2H (m/z [M-H]⁻ 463). It was demonstrated previously that *cis* isomers are high-energy structures, therefore these intermediates undergo structure relaxation to be converted to *trans* isomers⁸¹. The later intermediates underwent another fission between C2 and C3 to form 2,4,6-trihydroxyethenylbenzene-Glc (m/z [M-H]⁻ 329). However, almost all previous studies had investigated the spontaneous degradation of anthocyanins in the presence of atmospheric oxygen^{78,82,87,248–252}. Therefore, to the best of my knowledge, this was the first time to report the anaerobic spontaneous degradation of anthocyanins (Cya3Glc).

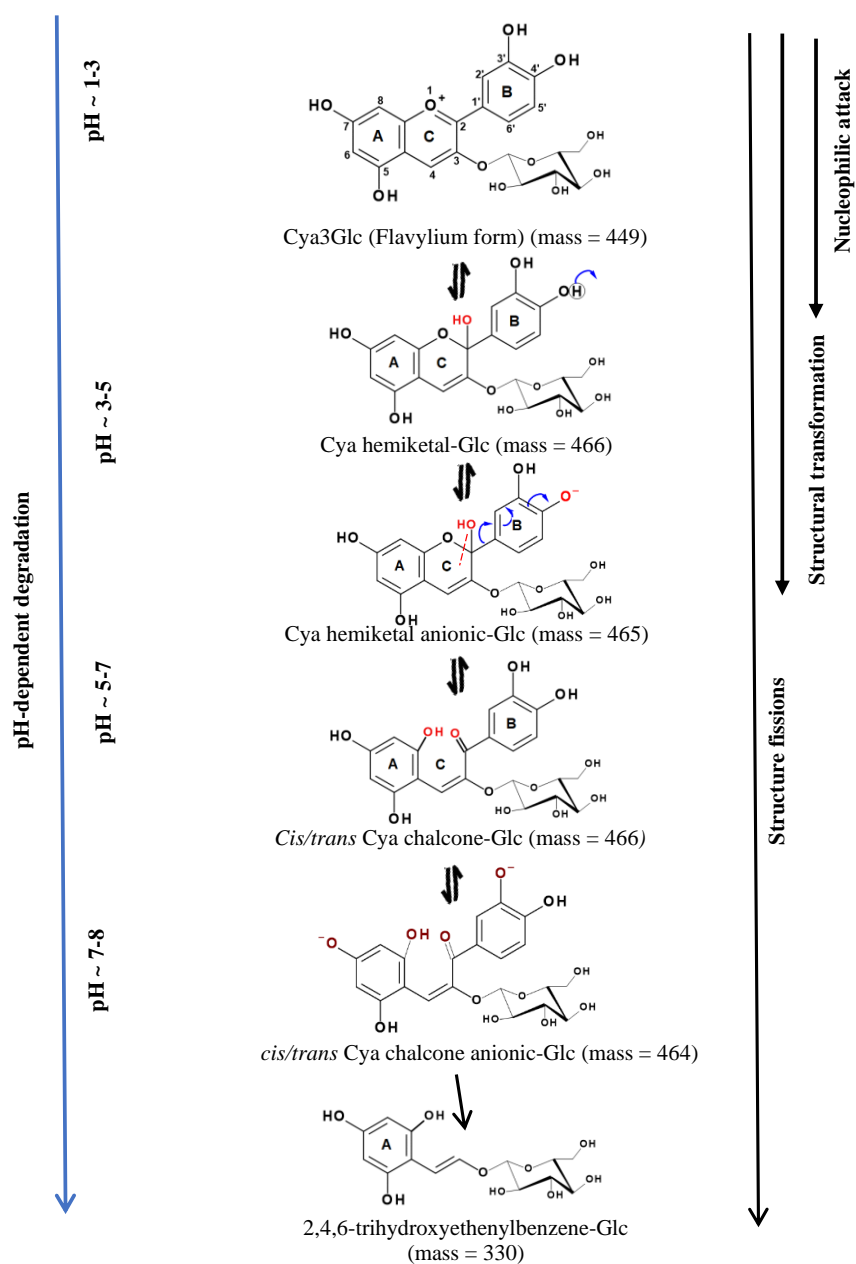


Figure 5. 20. Postulated mechanism of the anaerobic spontaneous degradation of cyanidin-3-*O*-glucoside (Cya3Glc).

In aerobic conditions, Cya3Glc also underwent classic pH-dependent transformation (hydration process). However, there was a substantial increase in the number of breakdown products formed under aerobic compared to anaerobic conditions (Figure 5.21). In the presence of atmospheric oxygen, Cya3Glc underwent a series of oxidation processes which included ring fissions (e.g., three in the C-ring between O1-C2, then between C2-C3 and C3-C4, and another between the C- and B-rings at C2-C1'). These gave rise to various intermediates including (i) Cya chalcone anionic-Glc + 2 O (RT 7.6, $m/z[M-H]^-$ 495), (ii) dimer of Cya chalcone-Glc and Cya chalcone anionic-Glc (RT 14.9, $m/z[M-H]^-$ 929), (iii) coumarin-Glc (RT 6.4, $m/z[M-H]^-$ 355), (iv) trihydroxyethenylbenzene-Glc (RT 3.3, $m/z[M-H]^-$ 329), and (v) phloroglucinol aldehyde (RT 9.7, $m/z[M-H]^-$ 153). In addition, accumulation of phenolic acids such as 2,4,6-trihydroxyphenyloxo acetic acid (RT 1.4, $m/z[M-H]^-$ 197), 2,4,6-trihydroxyphenylacetic acid (RT 2.3, $m/z[M-H]^-$ 183), dihydroxyphenyl-oxo acetic acid (RT 1.7, $m/z[M-H]^-$ 181), and protocatechuic acid (RT 3.7, $m/z[M-H]^-$ 153) occurred across the time-course and suggested that these were the last detectable breakdown products of aerobic spontaneous degradation of Cy3Glc.

In the presence of atmospheric oxygen, the Cya3Glc intermediates underwent further series of auto-oxidation processes (**Figure 5. 21**) including early-stage fission between C2 and C1' to form coumarin-Glc ($m/z[M-H]^-$ 355) which was previously suggested by Brouillard and others²⁴⁸. In agreement with the literature, PCA (B-ring product) and PGA (A-ring product) were identified as spontaneous degradation species from Cya3Glc^{38,87}. In agreement, two reports reported that 2,4,6-trihydroxyphenylacetic acid and coumarin-Glc were putatively identified based on their mass of $m/z[M-H]^-$ 183 and 355, respectively^{245,251}. However, for the first time, two potential phenolics were monitored and identified based on their appearance over time and, based on the mass fragment ions (**Figure 5. 9B-D**), they were interpreted as 3,4-dihydroxyphenyloxoacetic acid ($m/z[M-H]^-$ 181) and 2,4,6-trihydroxyphenyloxoacetic acid ($m/z[M-H]^-$ 197).

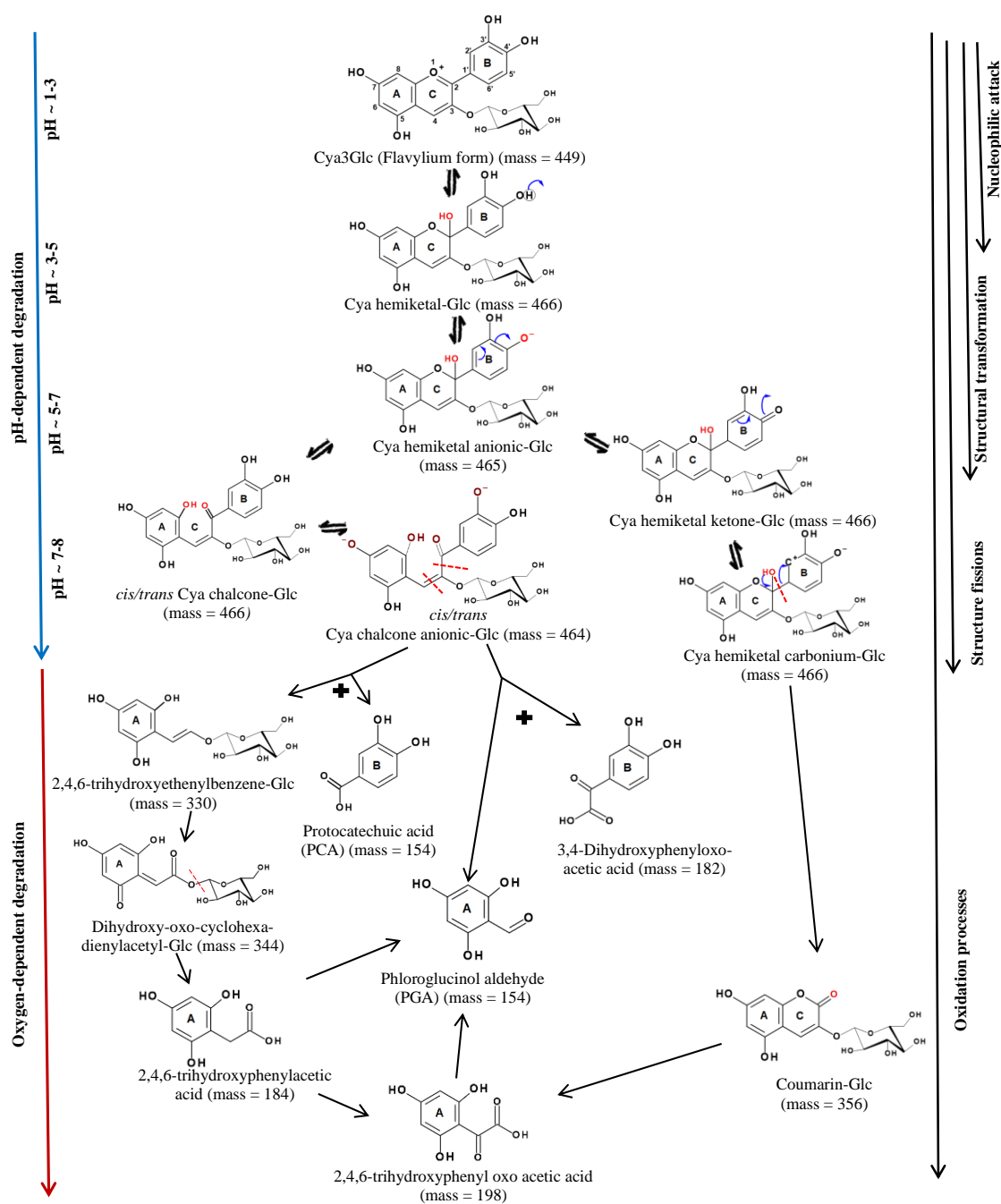


Figure 5. 21. Postulated mechanism of the aerobic spontaneous degradation of cyanidin-3-glucoside (Cya3Glc) during the incubation in 10mM phosphate buffer (6.8 and 7.4 pH) at 37°C.

The recovery of formed phenolics from Cya3Glc or Cya was calculated on the basis that stoichiometric conversion of one mole of parent compound will give rise to one mole each of B-ring and A-ring phenolic compounds. However, the quantified PCA (B-ring) and PGA (A-ring) accounted for no more than 30 % of the initial concentration of Cya3Glc or Cya. This was in contrast to Kay and others who reported that the recovery of Cya3Glc or Cya was equivalent to the PCA and PGA recovered; although, another study reported that the recovery of Cya3Glc or Cya when quantified on a molarity basis, PCA and PGA contributed to no more than 20% of the initial concentration of the parent compounds⁸⁷. However, based on our results and the report by Woodward and others⁸⁷, the rate of decline of Cya3Glc was slower in water (lack of pH control) compared to the phosphate buffer solution. This suggested that a drop in pH occurred during the formation of the breakdown products (especially with carboxylic groups) which consequently increased the anthocyanin stability. In addition, the appearance of these phenolics might play an important role in anthocyanin stability by forming polymers with anthocyanins, or bonding to parent compound, which protects anthocyanins from autoxidation by a steric effect and/or a synergistic effect where the latter is common within phenolic compounds²⁵³.

Here it can be concluded that the spontaneous degradation of anthocyanin and/or anthocyanidins follows kinetic degradation where the reaction rate is slower when the concentrations of breakdown products increase, whereas the rate of the reaction is faster when the concentrations of the breakdown products decrease. The disappearance of formed breakdown products was confirmed when another injection was carried out from the same experimental vial after two weeks of incubating Cya3Glc in phosphate buffered solution which showed the complete disappearance of Cya3Glc as well as the formed breakdown products. This confirmed that the phenolics originating from anthocyanins underwent a destructive process (mainly auto-oxidation) until they were converted to simple aliphatic chain compounds. Therefore, it would be a challenge to quantify the equivalent recovery of breakdown phenolics from the anthocyanin in a system at a specific time, even if the new phenolic acids (di- and tri-hydroxyphenyl-oxo-acetic acids) were included in the quantification.

Other peaks with higher masses (i.e., 768, 928, and 766 amu) than the mass of Cya3Glc (449 amu) were observed during the spontaneous degradation of Cya3Glc. These masses were identified as dimers consisting of formed intermediates (especially with the highly active intermediate, Cya chalcone anionic-Glc). For example, during the incubation of Cya3Glc in aerobic and anaerobic condition, a mass of 928 was detected which is equivalent to 2M of Cya chalcone anionic-Glc dimer. However, only in the presence of oxygen, the formation of a mass of 496 was observed over time with high intensity. This suggests the intermediate (Cya chalcone anionic-Glc) is bonded to two molecules of oxygen (mass 464 + 32).

Other masses were investigated based on the literature^{81,246,252} such as mass 482 (Cyanone), 320 (Cyanone aglycone), 449 (Cya quinoidal base-Glc), and 447 (Cya anionic quinoidal base-Glc) but these masses were not detected. However, the mass of 344 (amu) was detected as 5 different peaks with retention times as 4.7, 5.1, 5.4, 6.0, and 6.2. These masses are putatively correspond to different isomers of the same compound (Dihydroxy-oxo-cyclohexa-dienylacetyl-Glc) which was previously suggested as anthocyanone A by Vallverdú-Queralt and others as A-ring species²⁵⁴.

Anthocyanidins were also investigated (**Figure 5. 22** and **Figure 5. 23**). In the presence of atmospheric oxygen, Cya degraded spontaneously faster compared to Cya3Glc with 85.6 % and 42% of the initial concentration disappearing at 12 h, respectively. The sugar moiety increase the stability of anthocyanin aglycone^{38,87}. At the early stages of degradation, Cya and Del underwent pH-dependent degradation (hydration process) forming intermediates: hemiketal, hemiketal ketone, chalcone, chalcone α -diketone, and their anionic forms (**Figure 5. 22** and **Figure 5. 23**). Further autooxidation reactions occurred to breakdown these intermediates into simple phenolic compounds. For example, in both Cya and Del experiments, cleavage took place between C2 and C1' of the hemiketal ketone to form coumarin (A-ring, mass =194). Other A-ring phenolics appeared from both anthocyanidins and they included 2,4,6-trihydroxyphenyloxoacetic acid (mass=198), PGCA (mass=170), PGA (mass=154). However, the mass of 184 (amu) was only detected in the experiment of Cya and Cya3Glc which indicated it is a Cya breakdown product. Gallic Acid (mass=170) was detected from Del as B-ring phenolic, whereas PCA (mass=154) from Cya and Cya3Glc. Another mass of 182 (amu) was

observed in Cya and Cya3Glc which was tentatively interpreted as 3,4-dihydroxyphenyloxoacetic acid. On the other hand, a mass of 198 (amu) was detected from Del which might correspond to 3,4,6-dihydroxyphenyloxoacetic acid (B-ring). Surprisingly, a high peak at RT 7.1 was observed and quantified as 3-O-methylgallic acid authentic compound and mass fragment ions (m/z [M-H]⁻ 169 and 125). This observation might suggest that the B-ring methylation substitution occurred on the hydroxy group of the B-ring. It is possible also that it happened during the pH-dependent transformation where the formed intermediates are highly active especially such as the chalcone anionic forms where the B-ring hydroxy group loss proton (**Figure 5. 22** and **Figure 5. 23**).

These anthocyanidin breakdown products were formed in the presence of atmospheric oxygen, however, the anaerobic spontaneous degradation of anthocyanidins was not investigated due to lack of time. However, it would be important for future work to investigate the anaerobic spontaneous degradation of anthocyanidins. This will provide further knowledge on whether anthocyanins (i.e., Cya3Glc) only undergo a pH-dependent spontaneous degradation or the absence of the sugar moiety (as in anthocyanidins) contributing to a further degradation of anthocyanidins under the anaerobic degradation.

Comparison between the formed breakdown products from the degradation of incubated anthocyanins and anthocyanidins in neutral pH at 37°C presented in **Table 5. 7**. This comparison showed that pH-dependent degraded compound is similar and occurred in the presence and absence of oxygen. Whereas the majority of detected breakdown products appeared in the presence of oxygen. In addition, some breakdown products appeared only in phosphate buffer solution.

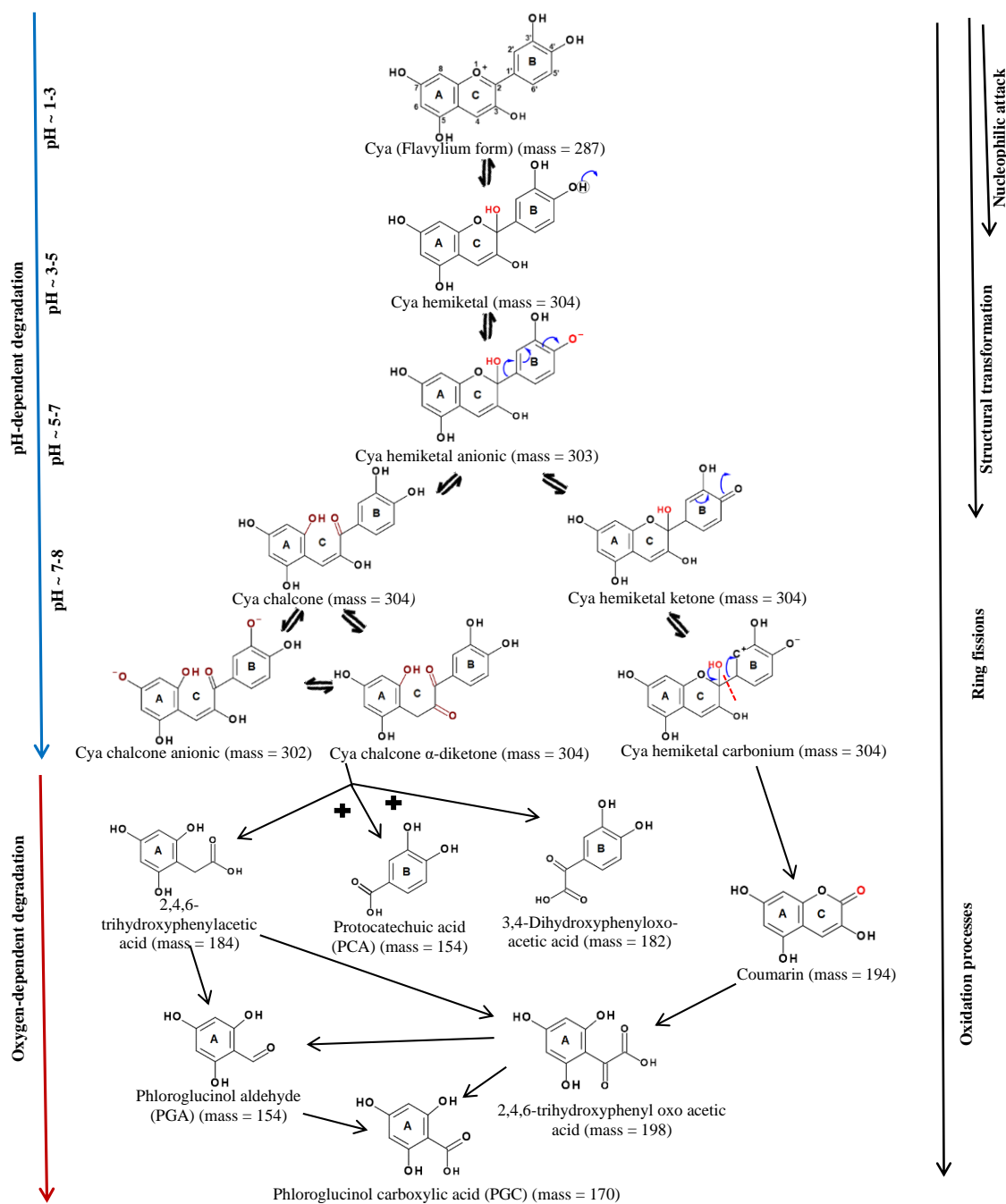


Figure 5. 22. Postulated mechanism of the aerobic spontaneous degradation of 100 $\mu\text{g mL}^{-1}$ Cyanidin (Cya) incubated in 10mM phosphate buffer (6.8 pH) at 37°C.

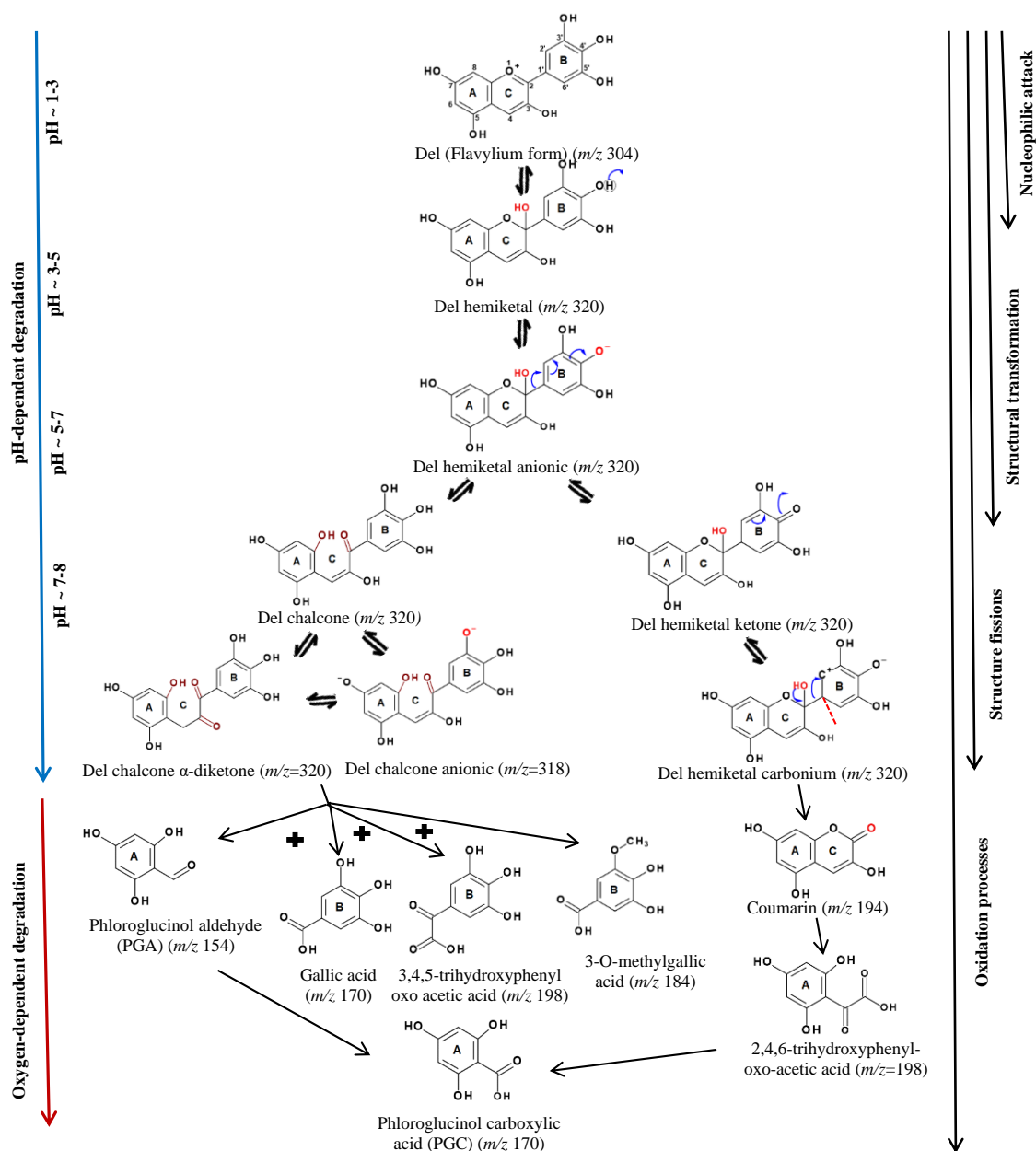


Figure 5. 23. Postulated mechanism of the aerobic spontaneous degradation of 100 $\mu\text{g mL}^{-1}$ delphinidin (Del) incubated in 10mM phosphate buffer (6.8 pH) at 37°C.

Table 5. 7. Comparison between the formed breakdown products from the degradation of incubated anthocyanins and anthocyanidins in neutral pH at 37°C.

No.	Identified compound	Mass (amu)	Origin	Which rings?	Aerobic	Anaerobic	phosphate buffer	colon media
1	Cya hemiketal-Glc	466	Cya3Glc	A & B	Yes	Yes	Yes	Yes
2	<i>cis/trans</i> Cya chalcone-Glc	466	Cya3Glc	A & B	Yes	Yes	Yes	Yes
3	Cya hemiketal ketone-Glc	466	Cya3Glc	A & B	Yes	No	No	Yes
4	<i>cis/trans</i> Cya chalcone anionic-Glc	464	Cya3Glc	A & B	Yes	Yes	Yes	Yes
5	2,4,6-trihydroxyethenylbenzene-Glc	330	Cya3Glc	A	Yes	Yes	Yes	Yes
6	Coumarin-Glc	356	Cya3Glc	A	Yes	No	Yes	Yes
7	Dihydroxy-oxo-cyclohexa-dienyl acetyl-Glc	344	Cya3Glc	A	Yes	No	Yes	Yes
8	2,4,6-trihydroxyphenylacetic acid	184	Cya3Glc	A	Yes	No	Yes	Yes
9	Cya hemiketal	304	Cya	A & B	Yes	Yes	Yes	-
10	Cya Chalcone	304	Cya	A & B	Yes	Yes	Yes	-
11	Cya chalcone anionic	302	Cya	A & B	Yes	Yes	Yes	-
12	Cya chalcone α -diketone	302	Cya	A & B	Yes	Yes	Yes	-
13	Del hemiketal	320	Del	A & B	Yes	Yes	Yes	-
14	Del Chalcone	320	Del	A & B	Yes	Yes	Yes	-
15	Del chalcone anionic	318	Del	A & B	Yes	Yes	Yes	-
16	Del chalcone α -diketone	320	Del	A & B	Yes	Yes	Yes	-
17	3,4,5-trihydroxyphenyloxoacetic acid	198	Del	B	Yes	No	Yes	-
18	3-O-methylgallic acid	184	Del	B	Yes	No	Yes	-
19	Gallic acid	170	Del	B	Yes	No	Yes	-
20	Phloroglucinol aldehyde (PGA)	154	Cya3Glc & Cya & Del	A	Yes	No	Yes	Yes
22	2,4,6-trihydroxyphenyloxoacetic acid	198	Cya3Glc & Cya & Del	A	Yes	No	Yes	Yes
21	Protocatechuic acid (PCA)	154	Cya3Glc & Cya	B	Yes	No	Yes	Yes
22	2,4,6-trihydroxyphenylacetic acid	184	Cya3Glc & Cya	A	Yes	No	Yes	Yes
23	3,4-dihydroxyphenyloxoacetic acid	182	Cya3Glc & Cya	B	Yes	No	Yes	Yes
24	Coumarin	194	Cya & Del	A	Yes	No	Yes	-
25	Phloroglucinol carboxylic acid (PGCA)	170	Cya & Del	A	Yes	No	Yes	-

In addition, various parameters had significant effects on the spontaneous degradation of Cya3Glc, Cya and Del. Woodward and others reported that the spontaneous k_{deg} of anthocyanins and their aglycones were significantly different in water compared to those observed from incubations in phosphate buffered solution⁸⁷. Similarly, Cya3Glc was shown to be degraded faster in colon model media compared to phosphate buffer, although the buffering capacity is lower in colon model media than in phosphate buffer, with 0.5 and 10 mM, respectively. This demonstrates that the other ingredients in colon model media may interact with anthocyanins and thus increases the k_{deg} which suggests that the anthocyanins and the formed intermediates are highly reactive and/or very sensitive compounds. Therefore, phosphate buffer is an ideal media for controlling the pH during the incubation, but it might not be the best representative for mimicking the medium of the gastrointestinal tract under physiological conditions.

Additionally, the spontaneous degradation of Cya was also affected by the initial concentration. For example, a high concentration of Cya ($1000 \mu\text{g mL}^{-1}$) was more stable in water but precipitated in phosphate buffer. The stability of a high concentration of Cya in water would be explained as polymer formation between Cya and its intermediates. However, this higher concentration of Cya precipitated in the presence of phosphate buffer may be due to the higher buffering capacity of this solution or some effect of high phosphate. This was further demonstrated by other experiments which showed that the increase of final DMSO % in the final volume of the experiment increased the solubility of anthocyanins. The buffering capacity of the medium was another important factor influencing the spontaneous degradation of anthocyanins. The lower buffering capacity solution (i.e., water and colon model media) showed decreases in pH values from 7.0 to ~ 4.0 in the case of water and from 7.0 to ~5.0 in the case of colon model media. This decrease in pH increases the stability of anthocyanin and their aglycone^{83,246,255}. This was also further demonstrated when Cya showed a faster decline rate in phosphate buffered solution with pH 7.4 compared with the same solution but with a pH value of 6.8 (Figure 5.15). Although anthocyanin bioavailability is very low, anthocyanin metabolites were shown to be more bioavailable than parent compounds⁹⁹, and there are claims that anthocyanin metabolites are responsible for delivering the health benefits of anthocyanins. Therefore, some recent studies have investigated the health benefits of

some anthocyanin metabolites. However, some factors should be considered when investigating the beneficial effects of anthocyanins such as concentration, temperature, pH, preparation of anthocyanins, and medium ingredients. Nevertheless, a Cya metabolite, PCA, was shown to inhibit the development of esophageal cancer in rats²⁵⁶. Forester and others also demonstrated that three anthocyanin metabolites, PGA (anthocyanin A-ring metabolite), gallic acid (Del B-ring metabolite), and 3-O-methylgallic acid (Peo B-ring metabolite), reduce the human colon cancer cell viability²⁵⁷. Although the majority of the spontaneous metabolites are produced in aerobic condition, the gut microbial metabolites, which will be presented in the next chapter (Chapter 6), are different apart from PCA and PGA. Therefore, it is important to investigate the biological activity of the other spontaneous and microbial metabolites of anthocyanins in future.

5.6. Conclusions

At neutral pH, anthocyanins degrade spontaneously faster under aerobic conditions than anaerobic conditions and disappeared spontaneously faster in colon media than in simple buffered solutions. In aerobic and anaerobic conditions, anthocyanins underwent pH-dependent transformations forming highly reactive intermediates. However, only in the presence of atmospheric oxygen, these intermediates were further degraded and transformed into simple phenolic compounds. Furthermore, the spontaneous degradation of anthocyanins and anthocyanidins was considerably affected by the experimental matrix, initial concentration of anthocyanidins, pH value, and the buffer capacity of medium. Phosphate buffer could be an ideal media for controlling the pH during the incubations, but it might not be the best representative for mimicking the medium of the human gastrointestinal tract under physiological conditions. It can be concluded that spontaneous degradation is critical, and all these factors should be considered in the biological investigations of the health-beneficial role of anthocyanins, in particular *in-vitro* culture models which could lead to variations in results. The spontaneous degradation of anthocyanins is a nonenzymatic degradation which contributes to the production of anthocyanin breakdown products. However, the enzymatic pathways of anthocyanin metabolism by the human gut microbiota were investigated and presented in the next chapter (Chapter 6).

Chapter Six

**Elucidating metabolic
pathways of colonic
degradation of
anthocyanins**

Chapter 6: Elucidating metabolic pathways of colonic degradation of anthocyanins

6.1. Abstract

Background: Anthocyanin metabolites appearing in human blood and urine following consumption of penta-[¹³C]-labelled anthocyanins were shown to be present at orders of magnitude higher concentrations than the intact anthocyanin. However, it is not clear if these breakdown products are produced through spontaneous degradation or microbiota-dependent transformation, or a combination of both. Having reported that the rate of loss of black rice and bilberry anthocyanins was considerably faster in the presence of live faecal inocula compared to autoclaved faecal inocula (Chapter 4) and the nature of the products of spontaneous degradation of anthocyanins (Chapter 5), the next step was to investigate the biotransformation of anthocyanins by the human gut microbiota.

Objectives: (i) Identify and quantify microbiota-dependent metabolites over time during fermentation of black rice and bilberry anthocyanins; (ii) assess the inter- and intra-individual variation in the formation of these anthocyanin-metabolites; (iii) elucidate the metabolic pathways of degradation of anthocyanins by the gut microbiota.

Methods: Samples from experiments presented in chapter 4 were used to investigate the appearance of anthocyanin metabolites by the human gut microbiota. Briefly, an *in-vitro* pH-controlled human colon model was used to incubate black rice and bilberry anthocyanin extracts with the human faecal slurries. UPLC-MS/MS was used to determine the concentration of anthocyanin metabolites over 24 h using a triple quadrupole mass spectrometer in multiple reaction monitoring (MRM) mode and searching for known and other predicted metabolites.

Results: In the presence of gut microbiota, various black rice anthocyanin metabolites were detected that originated from the B-ring including 3,4-dihydroxyphenylacetic acid (DHPAA), protocatechuic acid (PCA), dihydroferulic acid, dihydrocaffeic acid, and catechol. In contrast, there were only two A-ring-derived metabolites

(phloroglucinaldehyde (PGA) and phloroglucinol carboxylic acid (PGCA)). Additional B-ring metabolites were identified from incubations of bilberry anthocyanins, including vanillic acid, gallic acid, syringic acid, PCA, and 3-O-methylgallic acid. Various microbial metabolic pathways were indicated such as [Cya3Glc→PCA→catechol], [Cya3Glc→PGA→PGCA→phloroglucinol], and [Cya3Glc→dihydroferulic acid→dihydrocaffeic acid→4-methylcatechol]. In addition, the formation rate and the maximum concentration (C_{\max}) of the anthocyanin metabolites varied between donors and also between faecal samples collected from the same donor but on different days. Furthermore, it was feasible to use glycerol-frozen faecal stocks for reproducibility purposes, although the C_{\max} was lower compared to using fresh faecal samples.

Conclusions and Future work: From the data presented in this chapter, different enzymatic reactions were involved in anthocyanin catabolism, such as deglycosylation, demethylation, oxidation, and decarboxylation. The production of the microbial anthocyanin metabolites such as catechol, dihydrocaffeic acid, dihydroferulic acid, and 4-methylcatechol was completely microbiota-dependent, providing strong evidence that the gut microbiota is important for the metabolism of anthocyanins. Future research should focus on evaluating the biological effects of these anthocyanin-derived microbial metabolites.

6.2. Introduction

With the state of the art concerning knowledge of anthocyanin ring-fission metabolites and more specifically microbiota-dependent metabolites, the *in-vivo* human studies (such as that described in chapters 1 and 4) reported that anthocyanins degraded into various metabolites before passing through circulation. However, these reports detected conjugated derivatives (sulfates and/or glucuronides) of anthocyanin metabolites such as PCA-sulfates and PCA-glucuronide^{37,99,121}. The estimated concentrations of anthocyanin-derived metabolites were low compared to consumed anthocyanins, i.e. 12 % was excreted after participants consumed 500 mg isotopically labelled Cya3Glc¹⁰⁰. Only one report by Vitaglione and others reported a higher recovery (44 %) of the B-ring-derived PCA in plasma after 2 hours of consuming blood orange juice which contained Cya3Glc¹¹³. But they used the whole fruit in their intervention study which can be

misleading the results because not only anthocyanins, but other polyphenols normally exist in the fruit. This suggested that anthocyanins underwent through degradation process. This agreed with De Ferrars' report which reported that anthocyanin breakdown products and their metabolites are found in blood and urine at orders of magnitude higher concentrations than the intact anthocyanin with 12 % recovery of the initial dose of ^{13}C in the urine sample ⁹⁹. The aforementioned study identified the pharmacokinetic profiles of anthocyanin metabolites following the consumption of a 500 mg oral bolus dose of ^{13}C -labelled Cya3Glc. More importantly, a human study⁹⁹ reported that traces of intact Cya3Glc was detected in faeces as well as its breakdown products (i.e., PCA and PGA) and their derived metabolites such as vanillic acid, ferulic acid, and caffeic acid. This indicated that the consumed anthocyanins are likely to enter the large intestine where they are subject to metabolism by the gut microbiota before they are excreted and/or reabsorbed into circulation ⁸⁹.

There are a few reports of the use of faecal samples in *in-vitro* investigations of the role of gut microbiota in anthocyanin metabolism and the identification of metabolites. These studies have used either animal faeces such as pigs and rats ^{89,96,240} or selected colon-isolated strains ^{93,176}. In a few reports, human faecal samples were used to represent the human gut microbiota, but the fermentation was carried out either in a simple phosphate buffer or a non-pH-controlled model was used for the incubations ^{88,91,173}. As presented in chapter 4 and literature ¹⁵⁷, controlling the *in-vitro* model pH is a critical variable that has a strong effect on human gut microbiota activity. Nevertheless, in the previous *in-vitro* studies, PGA was reported as a A-ring degradant and various phenolic acids as a B-ring degradant. For example, two reports reported that PCA was a major microbial-derived B-ring metabolite from both Cy3Glc and Cya3Rut^{88,173}. Furthermore, vanillic acid⁹¹ and syringic acid¹⁷⁷ were identified as the major B-ring-derived metabolites from Peo3Glc and Mal3Glc, respectively. In this study, investigations of the formation of anthocyanin metabolites were carried out using a pH-controlled batch human colon model which was inoculated with different human faecal samples to assess intra- and inter-individual variations in the formation of anthocyanin metabolites and their microbial pathways.

6.3. Objectives

The overall aim of the research presented in this chapter and chapter 4 was to investigate the metabolism of dietary anthocyanins by the human gut microbiota in some detail. The role of the gut microbiota on the disappearance of anthocyanins was reported and discussed in Chapter 4. Whereas the focus of the research reported herein focused on the metabolic transformation pathways and the production of anthocyanin metabolites and their further metabolism. The *in-vitro* human colon fermentation was used as an experimental model and the metabolism of two sources of dietary anthocyanins (black rice and bilberry) was investigated. Therefore, the studies described in this chapter were focused on (i) Identifying and quantifying the black rice anthocyanin metabolites being produced during *in-vitro* colon fermentation in the presence as well as the absence of live human faecal microbiota; (ii) assessing the inter- and intra-individual variation in the appearance of microbial metabolites during the *in-vitro* colon fermentation of black rice anthocyanins; (iii) identifying and quantifying the microbial metabolites being produced during incubations of bilberry anthocyanin extract in the *in-vitro* colon fermentation, (iv) Determining the microbial metabolic pathways of anthocyanin degradation during the *in-vitro* colon fermentations.

6.4. Results

All figures contain data that are the absolute concentrations as measured in the experimental samples. However, all the concentration values discussed within the text are those obtained after subtraction of the background concentrations at 0 h for each metabolite.

6.4.1. The identification of anthocyanin metabolites

An extensive list of phenolic compounds and other small organic compounds such as aldehydes were investigated as possible black rice anthocyanin metabolites and listed in a report by Percival²⁵⁸. These compounds in the list and others were chosen based on previously published reports⁹⁹. The shortlist in **Table 6. 1** was chosen based on (i) the higher abundances of the peaks corresponding to phenolics in the extensive list after running samples from the colon model experiments, (ii) catabolites that were predicted to

arise from alternative C-ring fissions, and (iii) compounds that might be generated by various microbial metabolic processes such as oxidation, dehydrogenation, hydroxylation, or decarboxylation of the already identified compounds. For metabolite quantification, a separation method was developed in-house using a reverse-phase UPLC column (Percival, Jokioja and Kroon, unpublished) to monitor only specific mass/charge ratio (m/z) values of interest and therefore allow the detection of low concentrations. With assistance from Dr Saha, the acquisition method was set up on the QQQ-MS using MRM mode for the chosen phenolics by separately infusing the authentic phenolic compounds into the MS to confirm the retention times (RT) and to determine the parent mass ions, fragment (daughter) ions, the optimum collision energy (CE), and the best ionisation mode.

All of the experimentally generated phenolic compounds had RTs that matched closely with the RTs of their corresponding authentic standards which, along with the observation of the parent and daughter ion masses at the same time, was strong evidence that the identifications were accurate (**Table 6. 1**; column 2 parentheses versus column 3).

Although the ion peak for the authentic standard 3,4-DHPAA and the ion peaks for the 3,4-DHPAA in the colon model samples gave the same mass [M-H] transitions (167, 123, 95, and 41) which they were detected at slightly different RTs, namely 4.07 and 4.38 min, respectively (**Figure 6. 2**). This could be due to forming isomers of 3,4-DHPAA. Therefore, further investigation was carried out by testing isomeric compounds with the same mass (mass of 168) as 3,4-DHPAA, but the hydroxy groups on the benzene ring shifted into different positions, i.e., 2,4- or 2,5-DHPAA (**Figure 6. 1**). However, these were detected at different RTs, 2.4 and 2.9 min for 2,4-DHPAA and 2,5-DHPAA, respectively. Therefore, I assume that 3,4-DHPAA may form ionic forms²⁵⁹ during the colon model fermentations.

Table 6. 1. UPLC-MS/MS identification (MRM) of potential anthocyanin metabolites during the anaerobic in vitro human colon model fermentation.

No.	Analytical standards Metabolite, (RT _{min}) ^a	Colon model compound identification with MRM ion transitions						
		RT ^b (min)	Mass (amu)	Precursor ion <i>m/z</i> [M-H]	CE ^c	Product ion <i>m/z</i> [M-H]	CE ^c	Other product ions [M] ⁻
1	Pyrogallol, (2.63)	2.65	126.03	125.0	22	78.9	30	51.1
2	Phloroglucinol, (2.28)	2.21	126.03	125.0	18	57.1	46	41.0
3	Cinnamic acid, (7.46)	7.57	148.05	147.0	10	103.0	22	77.1
4	Ferulic acid, (6.28)	6.28	194.06	193.0	18	134.0	10	178.0
5	Sinapic acid, (6.28)	6.29	224.07	223.1	10	207.9	18	193.0
6	4-Hydroxybenzaldehyde, (5.86)	5.87	122.04	121.0	35	92.0	46	119.9
7	Vanillic acid, (5.41)	5.41	168.04	167.0	14	152.0	10, 22	123.3 ^d , 107.9 ^d
8	5-Hydroxy ferulic acid, (5.62)	5.63	210.05	209.0	24	193.9	34	150.1
9	4-Hydroxybenzoic acid, (4.88)	4.88	138.03	137.0	18	93.0	42	39.0
10	Phloroglucinol aldehyde (PGA), (6.11)	6.11	154.03	153.0	14	151.0	26, 34	69.0, 41.0 ^d
11	Syringic acid, (5.57)	5.55	198.05	197.0	14	182.0	22	123.1
12	Caffeic acid, (5.50)	5.51	180.04	179.0	22	134.9	34	106.9
13	Gallic acid (1.56)	1.58	170.02	169.0	14	125.0	22	79.1
14	3- <i>O</i> -methylgallic acid, (5.41)	5.41	184.04	183.0	30	123.9	34	78.1
15	Protocatechuic acid (PCA), (3.12)	3.14	154.03	153.0	22	109.1 ^d	26, 30	53.1, 90.9
16	Phloroglucinol carboxylic acid (PGCA), (3.39)	3.41	170.02	169.0	14	150.9	20, 46	125.0 ^d , 40.9
17	Dihydrocaffeic acid, (5.33)	5.33	182.06	181.1	10	136.9	14	59.0
18	Dihydroferulic acid, (6.14)	6.14	196.07	195.1	14	136.1	30	120.8
19	3-Hydroxy benzoic acid, (4.88)	4.88	138.03	137.0	18	93.0 ^d	26, 66	65, 41.1
20	2,4-Dihydroxy benzoic acid, (2.44)	2.37	154.03	153.0	14	109.1 ^d	18, 42	65.1, 41.0
21	3,4-Dihydroxyphenylacetic acid (3,4-DHPAA), (4.07)	4.38	168.04	167.0	10	123.0	22, 34	95.0, 41.0
22	Homovanillic acid, (5.55)	5.55	182.06	181.1	14	136.9 ^d	14, 14	122, 104.9
23	Catechol, (5.01)	5.03	110.04	109.0	18	91.0	18	53.0
24	3,5-Dihydroxybenzoic acid, (2.13)	2.19	154.03	153.0	10	109.1	14, 22	67.0, 41.0 ^d

25	3-Hydroxyphenylacetic acid, (5.39)	5.39	152.05	151.0	10	106.9	66	41.0
26	3-(4-Hydroxyphenyl) propionic acid, (5.92)	5.92	166.06	165.1	10	120.9	14	59.0
27	Protocatechualdehyde (PCAlD), (5.23)	5.23	138.03	137.0	26	107.9	26, 50	92.0, 41.0
28	2,4-Dihydroxybenzaldehyde, (6.31)	6.31	138.03	137.0	22	91.0	34, 46	65.0 ^d , 41.0
29	3,4-Dihydroxymandelic acid, (1.30)	1.30	184.04	183.0	18	120.9	14	137.1
30	Ellagic acid, (6.17)	6.19	302.01	301.0	30	229.1	34	284.1
31	Hippuric acid, (4.78) ^e	4.80	179.06	180.1	14	105.0	38	76.9
32	<i>p</i> -Coumaric acid, (6.07)	6.07	164.05	163.0	14	119.0	34	93.0
33	Isovanillic acid, (5.55)	5.55	168.04	167.0	18	107.9	10, 42	152.0, 90.9
34	4-Methylcatechol, (6.26)	6.26	124.05	123.0	18	108.0	46, 66	65.0, 41.0
35	4-Hydroxybenzylalcohol, (4.54)	4.54	124.05	123.0	22	104.9	42, 62	65.0, 41.0

^a The retention time (RT) of metabolites using authentic compounds.

^b The retention time (RT) of metabolites in the colon model samples.

^c Abbreviation for collision energy

^d This product ion was neglected in the MRM acquisition method and thus the quantification method. This is because the same product ion originated from two different precursor ions which cause interference giving a higher abundance than it should be.

^e The polarity mode for identification was positive m/z $[M+H]^+$

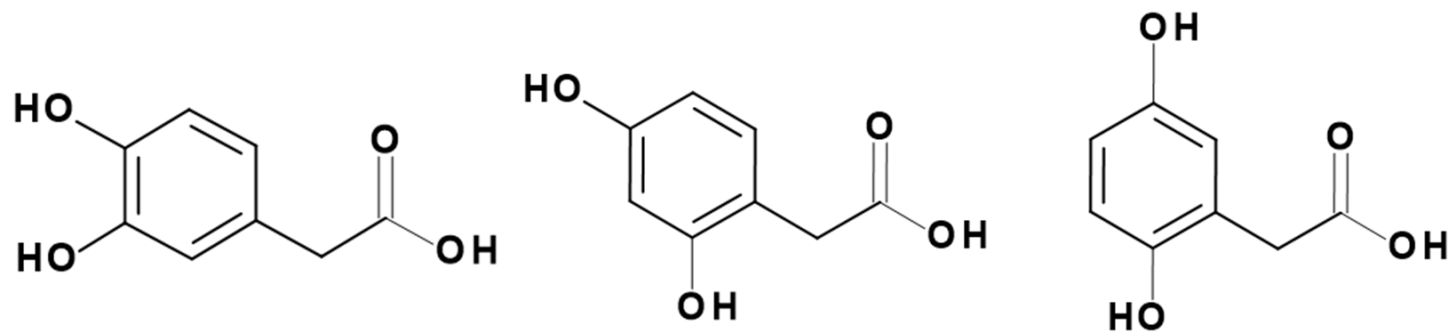


Figure 6. 1. The chemical structures of dihydroxyphenylacetic acid isomers.
3,4-DHPAA (A), 2,4-DHPAA (B), and 2,5-DHPAA (C).

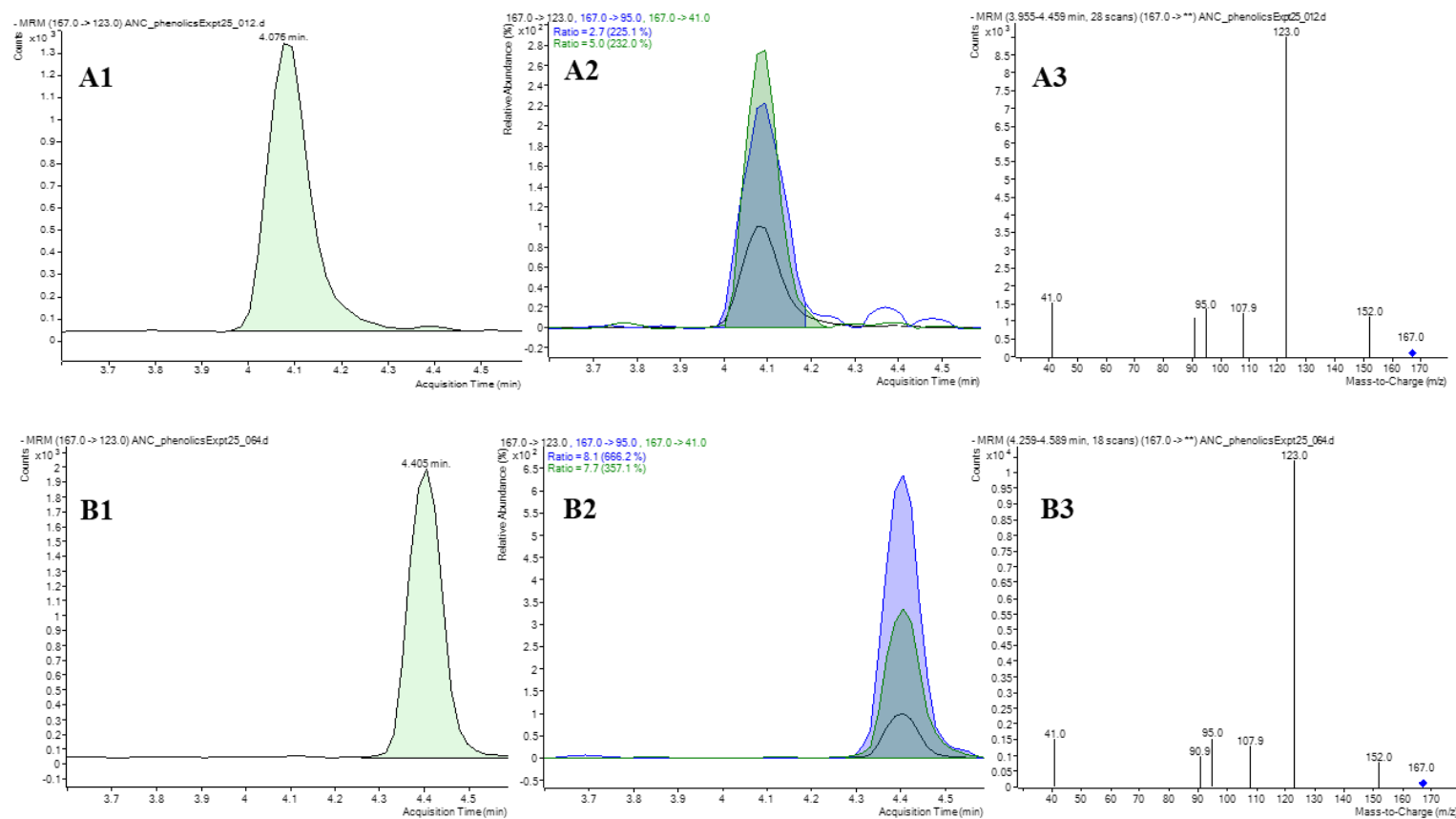


Figure 6. 2. Ms/Ms chromatograms of the ion currents for 3,4-dihydroxyphenylacetic acid (DHPAA).

The mass pair of DHPAA 167-123-95-41 arising in the authentic standard (A) and in the colon model-derived samples (B), where A1 and B1 present the quantifier peak with RTs, A2 and B2 show the quantifier and qualifier ratios of the selective daughter fragment ions, and A3 and B3 present the mass spectrum for both compounds.

6.4.2. The formation of anthocyanin metabolites during incubations of black rice anthocyanin extract in the human *in-vitro* colon model fermentations

Briefly, batch colon model fermentation was used to incubate black rice anthocyanin extract (at low and high Cya3Glc concentrations of 66.8 and 133.6 μM , respectively) with a human faecal inoculum with both fresh and autoclaved faecal slurry. A control vessel containing non-autoclaved faecal slurry, but no black rice extract was also included in the experimental design. Samples were collected and then analysed using UPLC-MS/MS in MRM mode (i.e., searching for predicted metabolites).

In both investigations of low and high concentrations of black rice anthocyanin extract, various metabolites in the presence of live faecal microbiota were detected (**Figure 6. 3, Figure 6. 4, Figure 6. 5, Figure 6. 6**). For example, PCA, PGA, 3,4-DHPAA, and catechol were the main black rice anthocyanin metabolites. Other metabolites were also detected in the presence of live faecal microbiota but at very low concentrations, namely PGCA, dihydrocaffeic acid, dihydroferulic acid, gallic acid, pyrogallol, and 4-hydroxybenzoic acid. The formation rates of the aforementioned metabolites showed significant inter- and intra-individual variations.

Although the detected metabolites were similar in vessels incubated with low or high concentrations of black rice anthocyanins, the maximal concentrations (C_{max}) of these metabolites were higher from vessels incubated with higher concentrations of black rice extract (**Figure 6. 3, Figure 6. 5, and Figure 6. 6**). Some metabolites such as PCA and DHPAA had background concentrations at 0 h. For example, PCA was detected in the 0-h sample, particularly in samples collected from vessels treated with black rice extract powder. This showed that the black rice powder contained some phenolic compounds such as PCA (**Figure 6. 3, Figure 6. 4, Figure 6. 5, and Figure 6. 6**).

Furthermore, in the vessels containing both live faecal microbiota and black rice extract, there were two types of metabolites (initial (or primary) and secondary metabolites) based on the time when they started to appear. The initial metabolites are the ones that were detected at early stages of incubation (within the first 4 h), reached their C_{max} between 4 and 10 h, and then most often declined thereafter (i.e., PCA, PGA, DHPAA, and

dihydroferulic acid). For example, PCA and PGA increased over time to reach C_{\max} between 6 and 8 h, then declined afterwards which likely indicated further steps of metabolism. DHPAA also increased over time at high rates in the first 8 h of incubation, afterward the rate of production or decline was significantly different depending on different faecal samples. In contrast, the secondary metabolites such as catechol, PGCA and dihydrocaffeic acid appeared at later stages of incubation after 6 or 8 h, and their C_{\max} was usually observed between 20 and 24 h (**Figure 6. 3, Figure 6. 4, Figure 6. 5, and Figure 6. 6**). Catechol did not appear initially in the first 6 or 8 h of incubation while it showed to be increased consistently over time between 8 and 24 h, indicating that catechol is a secondary product.

Moreover, dihydrocaffeic acid and dihydroferulic acid appeared only in the vessels containing both live bacteria and black rice extract, but they were detected at very low concentrations. Dihydroferulic acid increased in the initial stages in all experiments to reach C_{\max} between 6-8 h (**Figure 6. 3, Figure 6. 4, Figure 6. 5, and Figure 6. 6**), then either stayed at the same concentration or slightly decreased. Whereas dihydrocaffeic acid was detected only in two experiments at very low concentrations (**Figure 6. 3 and Figure 6. 4**) and it only appeared at later stages of the incubation and reached its C_{\max} at the end of the incubation (20-24 h).

In the vessels containing both autoclaved faecal samples and black rice extract, the appearance of the majority of the metabolites plateaued or slightly decreased. However, PCA slightly increased between 4-6 h (**Figure 6. 3, Figure 6. 5, and Figure 6. 6**). Additionally, 4-hydroxybenzoic acid slightly increased after 8 h incubation in the autoclaved faecal sample. PGA did not increase (**Figure 6. 3 and Figure 6. 6**). Furthermore, DHPAA was massively increased at 24 h in two experiments (**Figure 6. 3 and Figure 6. 4**). However, in the other two experiments (**Figure 6. 3, Figure 6. 5, and Figure 6. 6**), DHPAA was not elevated in the vessels containing autoclaved faecal slurry.

Gallic acid was detected at low concentrations in all vessels (control, black rice treated with fresh slurry, and black rice treated with autoclaved faecal slurry). At 0 h, however, the gallic acid concentration was much higher in vessels with autoclaved faecal slurry than in vessels containing fresh faecal slurries (both control and black rice-treated vessels). However, in both vessels containing live faecal slurries, gallic acid slightly

increased over time to reach the C_{\max} between 4 and 8 h incubation. Afterwards, gallic acid either declined or remained at the same concentration over time. On the other hand, in vessels containing autoclaved faecal slurry, gallic acid concentration remained unchanged over the 24 h incubation or slightly declined. In addition, pyrogallol was only formed in the presence of live faecal microbiota (in both control and black rice-treated vessels), but the formation of pyrogallol started at later time of incubation (8 h). This indicated that pyrogallol is a secondary metabolite. Since it appeared in both vessels containing live faecal slurry (control and black rice treatment vessels), pyrogallol is not a black rice anthocyanin metabolite. However, its appearance correlates with gallic acid since both compounds were formed over time only in the presence of live faecal microbiota. Conversely, 4-hydroxybenzoic acid was detected in control black rice-treated vessels, regardless of whether the vessels were inoculated with fresh faecal or autoclaved faecal slurries. In the presence of live faecal microbiota, the appearance of 4-hydroxybenzoic acid was in the early stage of incubation (from 2 to 6 h), but it appeared at a later time in the presence of autoclaved faecal slurries (**Figure 6. 6**).

Thus, seven metabolites were shown to be microbiota-dependent metabolites which originated from the black rice anthocyanins. In accordance with the chemical structure of the Cya3Glc and the substitution of hydroxyl groups on the A and B rings, the A-ring-derived metabolites were PGA and PGCA, whereas the B-ring-derived metabolites were PCA, DHPAA, catechol, dihydrocaffeic acid, and dihydroferulic acid.

The analysis of black rice anthocyanin extract powder (presented in chapter 4) showed that the powder contains phenolic (anthocyanins) as well as non-phenolic contents. The anthocyanin (phenolic content) content was 38 % w/w (predominantly 88 % Cya3Glc and 6 % Peo3Glc). Therefore, the investigation of pure authentic anthocyanins was carried out to further confirm the production of A- and B-rings metabolites from Cya3Glc as well as Peo3Glc. The results are presented in the next section.

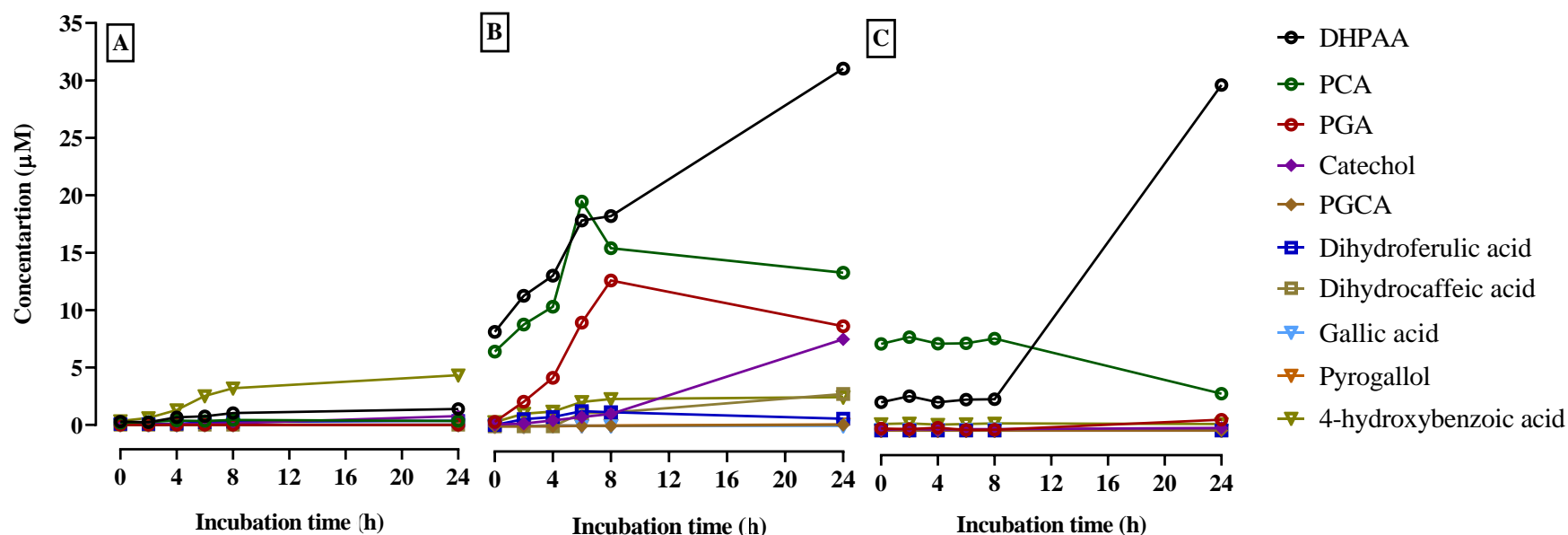


Figure 6.3. The formation of anthocyanin metabolites during batch colon model fermentation over 24 h by using a low concentration of black rice anthocyanin (66.8 μM Cya3Glc).

Black rice extract (18 mg, containing 33.36% w/w Cya3Glc) was dissolved in 1 mL water, filtered and immediately added to colon model vessels pre-filled with sterile media (89 mL) and human faecal slurry (10 mL of a 10% slurry from a fresh stool) to give a final volume of 100 mL and a Cya3Glc concentration of 66.8 μM (30 $\mu\text{g}/\text{mL}$) (B). Similar vessels were prepared but containing autoclaved faecal slurry rather than fresh faecal slurry (C). Control vessels contained fresh faecal inoculum and media, but no black rice extract (A). Incubations were carried out at pH 6.6-7.0 and 37°C, over 24 h. Samples (0.5 mL) were collected at the times shown in the figure, mixed with 0.5 mL of 4% v/v aqueous formic acid, and after sample preparation (Chapter 2, section 2.2.6), analysed using UPLC-MS/MS to determine concentrations of anthocyanin metabolites. The data shown are for 1 replicate incubation using a single donor faecal sample: donor 01 – S1 (n=1).

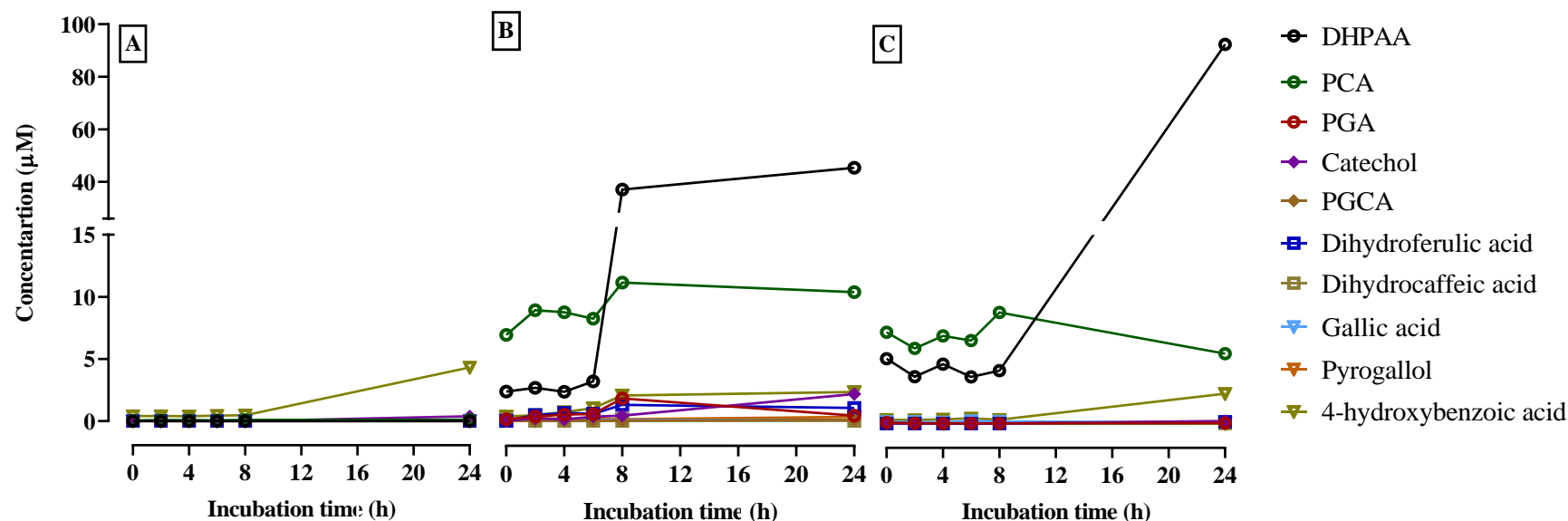


Figure 6. 4. The formation of anthocyanin metabolites during batch colon model fermentation over 24 h by using a low concentration of black rice anthocyanin (66.8 μM Cya3Glc).

Black rice extract (18 mg, containing 33.36% w/w Cya3Glc) was dissolved in 1 mL water, filtered and immediately added to colon model vessels pre-filled with sterile media (89 mL) and human faecal slurry (10 mL of a 10% slurry from a fresh stool) to give a final volume of 100 mL and a Cya3Glc concentration of 66.8 μM (30 μg/mL) (B). Similar vessels were prepared but containing autoclaved faecal slurry rather than fresh faecal slurry (C). Control vessels contained fresh faecal inoculum and media, but no black rice extract (A). Incubations were carried out at pH 6.6-7.0 and 37°C, over 24 h. Samples (0.5 mL) were collected at the times shown in the figure, mixed with 0.5 mL of 4% v/v aqueous formic acid, and after sample preparation (Chapter 2, section 2.2.6), analysed using UPLC-MS/MS to determine concentrations of anthocyanin metabolites. The data shown are for 1 replicate incubation using a single donor faecal sample: donor 01 – S5 (n=1).

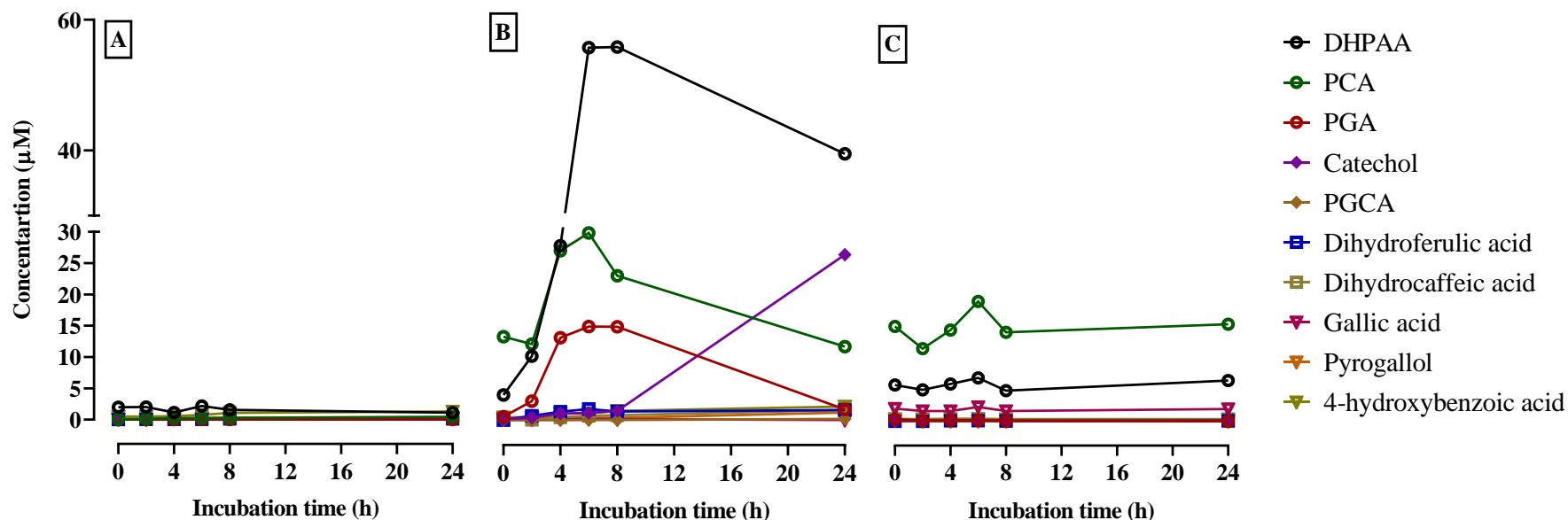


Figure 6. 5. The formation of anthocyanin metabolites during batch colon model fermentation over 24 h by using a high concentration of black rice anthocyanin (133.6 μM Cya3Glc).

Black rice extract (18 mg, containing 33.36% w/w Cya3Glc) was dissolved in 1 mL water, filtered and immediately added to colon model vessels pre-filled with sterile media (89 mL) and human faecal slurry (10 mL of a 10% slurry from a fresh stool) to give a final volume of 100 mL and a Cya3Glc concentration of 133.60 μM (60 $\mu\text{g}/\text{mL}$) (B). Similar vessels were prepared but containing autoclaved faecal slurry rather than fresh faecal slurry (C). Control vessels contained fresh faecal inoculum and media, but no black rice extract (A). Incubations were carried out at pH 6.6-7.0 and 37°C, over 24 h. Samples (0.5 mL) were collected at the times shown in the figure, mixed with 0.5 mL of 4% v/v aqueous formic acid, and after sample preparation (Chapter 2, section 2.2.6), analysed using UPLC-MS/MS to determine concentrations of anthocyanin metabolites. The data shown are for 1 replicate incubation using a single donor faecal sample: donor 01 – S3 (n=1).

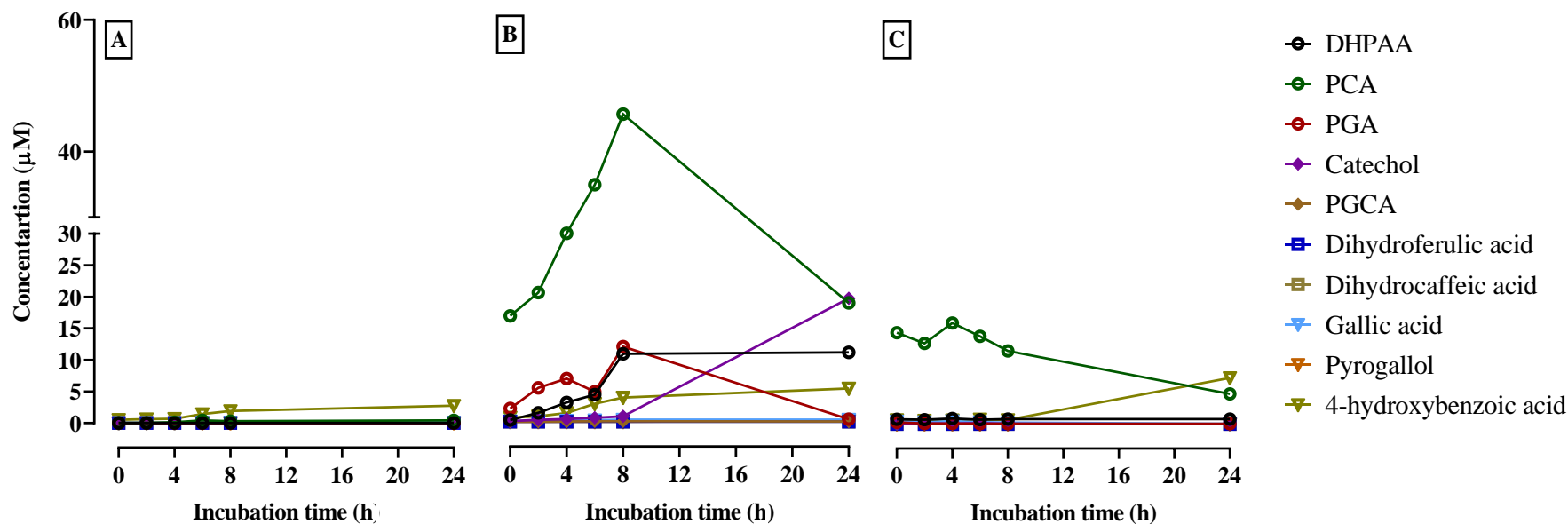


Figure 6. 6. The formation of anthocyanin metabolites during batch colon model fermentation over 24 h by using a high concentration of black rice anthocyanin (133.6 μM Cya3Glc).

Black rice extract (18 mg, containing 33.36% w/w Cya3Glc) was dissolved in 1 mL water, filtered and immediately added to colon model vessels pre-filled with sterile media (89 mL) and human faecal slurry (10 mL of a 10% slurry from a fresh stool) to give a final volume of 100 mL and a Cya3Glc concentration of 133.6 μM (60 $\mu\text{g}/\text{mL}$) (B). Similar vessels were prepared but containing autoclaved faecal slurry rather than fresh faecal slurry (C). Control vessels contained fresh faecal inoculum and media, but no black rice extract (A). Incubations were carried out at pH 6.6-7.0 and 37°C, over 24 h. Samples (0.5 mL) were collected at the times shown in the figure, mixed with 0.5 mL of 4% v/v aqueous formic acid, and after sample preparation (Chapter 2, section 2.2.6), analysed using UPLC-MS/MS to determine concentrations of anthocyanin metabolites. The data shown are for 1 replicate incubation using a single donor faecal sample: donor 05 – S2 (n=1).

6.4.4. The formation of anthocyanin metabolites during the *in-vitro* colonic fermentation of pure anthocyanins

Black rice extract containing 38 % anthocyanins, which predominantly consisted of 87% Cya3Glc and 6 % Peo3Glc, was shown to be degraded and metabolised by the human faecal microbiota into various A- and B-ring-derived metabolites. However, for further confirmation, the microbial degradation of pure authentic Cya3Glc and Peo3Glc was investigated together with the appearance of their metabolites using the *in-vitro* human colon model. Briefly, pure authentic Cya3Glc and Peo3Glc were incubated separately with both fresh faecal slurry and autoclaved faecal slurry. The experiment was carried out using a fresh faecal sample donated by donor 08-S3 (n=1). Control vessels containing non-autoclaved faecal slurry were carried out with no authentic anthocyanin introduced. Samples were collected over 24 h, then analysed using UPLC-MS/MS.

DHPAA, PCA, and PGA were the main metabolites of Cya3Glc (**Figure 6. 7**). While catechol was also present, it was at a very low concentration in the presence of live faecal microbiota, and no significant differences were found in the amount of catechol produced when Cya3Glc has incubated the presence of live and autoclaved faecal slurries. Moreover, PGCA was not detected in all vessels. In addition, dihydroferulic acid appeared between 10 - 20 h at very low concentrations, but it declined after 20 h. Dihydrocaffeic acid was initially detected at 12 h at a very low concentration which slightly increased until 24 h. PGCA was not detected either in the presence or absence of live faecal microbiota. Furthermore, catechol production was very low in the presence of live faecal microbiota and reached its C_{max} (0.65 μM) at 24 h, and C_{max} was 0.49 μM at 24 h in the autoclaved faecal slurry.

Nevertheless, in the presence of live faecal microbiota, the production of B-ring-derived PCA reached the C_{max} of 10.6 μM at 10 h, then it declined to 5.6 μM at 24 h. However, PCA detected in the absence of live faecal microbiota, reached its C_{max} of 1.2 μM at 24 h. Furthermore, in the presence of live faecal microbiota, the A-ring-derived degradation phenolic, PGA, considerably increased over the first 10 h reaching its C_{max} of 9.8 μM at 10 h. Afterwards, PGA declined to 4.8 μM at 24 h. However, in the presence of autoclaved faecal slurry, PGA was detected at a very low concentration at a later time point of

incubation reaching its C_{\max} (0.28 μM) at 24 h. Moreover, DHPAA showed a rapid rise at 8 h with C_{\max} of 5.3 μM in the presence of live faecal microbiota. In the presence of autoclaved stool sample, however, DHPAA reached 3.8 μM at 20 h then spiked to its C_{\max} at 24 h (39.1 μM) (**Figure 6. 7**).

The B-ring-derived metabolites, dihydrocaffeic acid and dihydroferulic acid, were formed over time in the presence of live faecal microbiota but the concentration was very low. However, the production of dihydroferulic acid was higher in the presence of live faecal microbiota with C_{\max} of 0.09 μM at 20 h whereas the C_{\max} was 0.02 μM at 24 h. Conversely, the production of dihydrocaffeic acid was lower in the presence than in the absence of live faecal microbiota. For example, the highest concentration of dihydrocaffeic acid in the presence and absence of live faecal microbiota were 0.03 μM at 24 h and 0.21 μM at 10 h, respectively. The initial appearance of dihydrocaffeic acid occurred at a later stage of incubation, but dihydroferulic acid started to appear at the early stages of incubation but normally declined afterwards. These results suggest that dihydroferulic acid is more likely an intermediate of dihydrocaffeic acid (dihydroferulic acid \rightarrow dihydrocaffeic acid).

On the other hand, the incubation of the purified Peo3Glc showed PGA and vanillic acid and dihydrocaffeic acid are the main metabolites in the live faecal microbiota incubations (**Figure 6. 8**). For example, the A-ring-derived metabolites, PGA, increased in the first 10 h of incubation reaching its C_{\max} of 7.6 μM at 10 h, then it declined to 2.5 μM at 24 h. In addition, vanillic acid increased over the first 12 h with C_{\max} 3.7 μM at 12 h, it further slightly declined to 1.6 μM concentration at 24 h. However, the B-ring-derived dihydrocaffeic acid was present at a low concentration and the formation of dihydrocaffeic acid was at a constant rate after 8 h of incubation in the presence of live faecal microbiota. The C_{\max} detected at 24 h was 0.9 μM .

Moreover, PCA, DHPAA, and catechol were also present in the presence of live faecal microbiota. PCA appeared at 4 h at a very low concentration (0.14 μM), increased (3 fold) between 8 and 12 h (0.48 μM), declined to 0.41 μM at 20 h, then increased again to 0.73 μM at 24 h. The increase in PCA was in parallel with the decline of vanillic acid suggesting that vanillic acid is more likely to be an intermediate compound for PCA (vanillic acid \rightarrow PCA).

DHPAA was detected only in the presence of live faecal microbiota and only at 20 and 24 h with a concentration of 3.0 and 3.8 μM , respectively. Catechol was detected also at very low concentration. However, the formation of catechol was not significant in the presence of live faecal microbiota compared to its formation in the control vessel, which indicated that the majority of catechol formed comes from the faecal sample. In addition, the PGCA was not present in all vessels.

Thus, these data showed that the majority of metabolites formed from black rice anthocyanins are similar to the metabolites formed from the authentic Cya3Glc which is consistent with the fact that the black rice extract anthocyanins are dominated by Cya3Glc (87% total). However, the production of catechol was considerably lower in the incubation of the authentic Cya3Glc than the production from the incubation of black rice anthocyanin extract. Also, the data indicated that dihydroferulic acid originated from Cya3Glc in the black rice extract as a primary metabolite, but dihydrocaffeic acid originated from the Peo3Glc in the black rice extract as a primary metabolite. Therefore, another experiment was carried out by incubating a higher concentration (100 μM) of the authentic Cya3Glc using faecal samples from different donor (01-S10) (data not shown). In this experiment, dihydroferulic acid appeared to be an intermediate of dihydrocaffeic acid (C_{max} , 0.28 μM at 8 h). In addition, 4-methylcatechol appeared in parallel with a decline in dihydrocaffeic acid at 10 h. This might suggest that dihydrocaffeic acid is an intermediate for the formation of 4-methylcatechol (dihydrocaffeic acid \rightarrow 4-methylcatechol), where 4-methylcatechol reached its C_{max} of 0.25 μM at 24 h. Catechol was also observed to be formed over time but at a low concentration compared to the incubation of black rice anthocyanins.

Based on C_{max} and time of appearance, PGA, PCA, and DHPAA were shown to be the main and initial (primary) microbial metabolites from black rice anthocyanins.

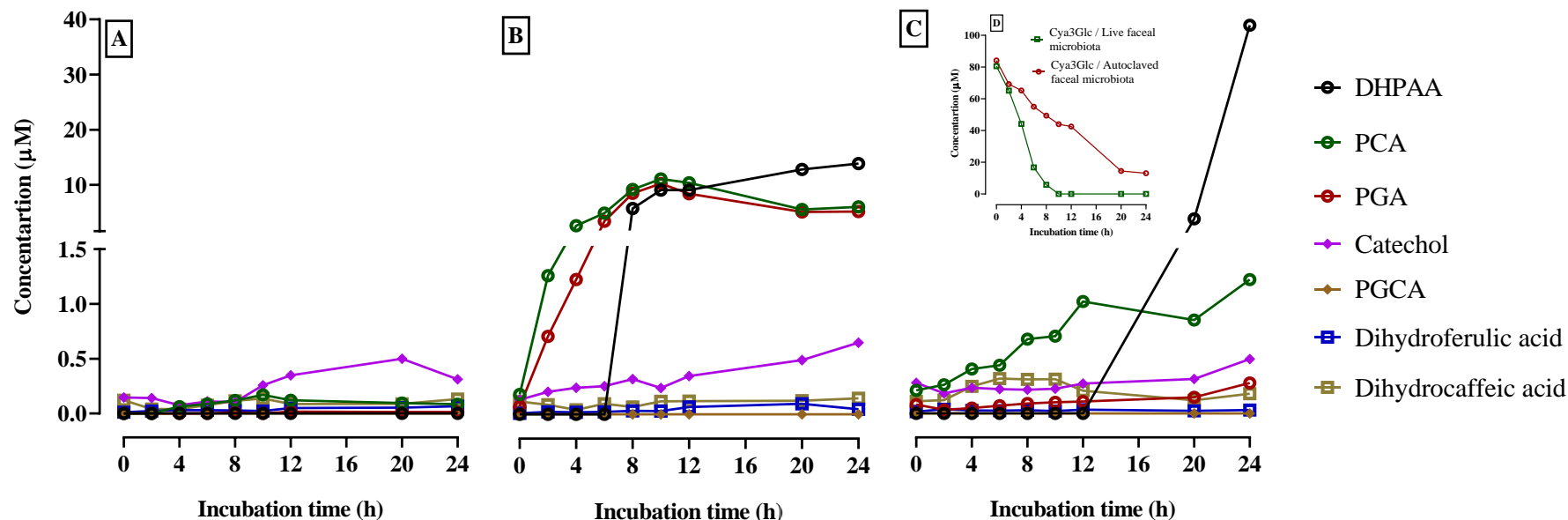


Figure 6. 7. The formation of Cya3Glc metabolites during batch colon model fermentation over 24 h.

A 5 mg/mL of authentic Cya3Glc was dissolved in 1 mL acidified water, and immediately 1 mL was added to colon model vessels pre-filled with sterile media (89 mL) and human faecal slurry (10 mL of a 10% slurry from a fresh stool) to give a final volume of 100 mL and a Cya3Glc concentration of 111.3 µM (50 µg/mL) (B). Similar vessels were prepared but containing autoclaved faecal slurry rather than fresh faecal slurry (C). Control vessel contained fresh faecal inoculum and media, but no Cya3Glc (A). Incubations were carried out at pH 6.6-7.0 and 37°C, over 24 h. Samples (0.5 mL) were collected at the times shown in the figure, mixed with 0.5 mL of 4% v/v aqueous formic acid, and after sample preparation (Chapter 2, section 2.2.6), analysed using HPLC-DAD to determine the Cya3Glc concentration and LC-MS/MS to determine metabolites concentrations. The data shown are for 1 replicate incubation using a single donor faecal sample: donor 08-S3. No Cya3Glc was detected in control vessels (data not shown).

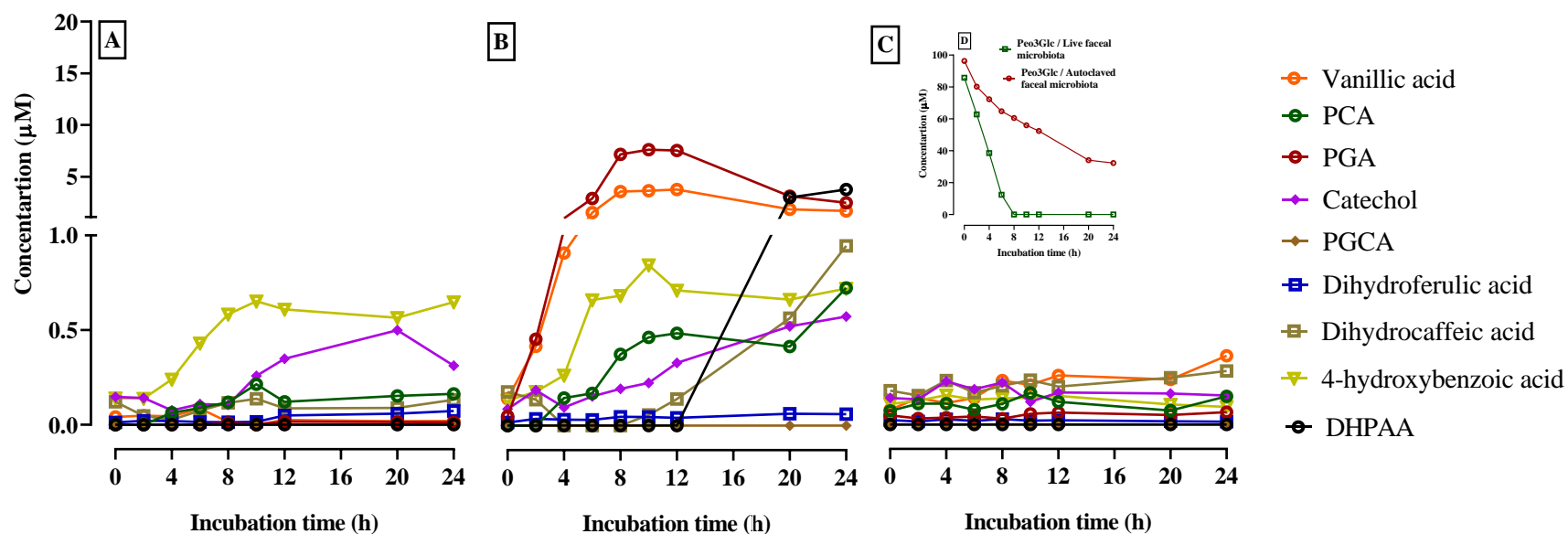


Figure 6. 8. The formation of Peo3Glc metabolites during batch colon model fermentation over 24 h.

A 5 mg/mL of authentic Peo3Glc was dissolved in 1 mL acidified water, and immediately 1 mL was added to colon model vessels pre-filled with sterile media (89 mL) and human faecal slurry (10 mL of a 10% slurry from a fresh stool) to give a final volume of 100 mL and a Peo3Glc concentration of 108 µM (50 µg/mL) (B). Similar vessels were prepared but containing autoclaved faecal slurry rather than fresh faecal slurry (C). Control vessel contained fresh faecal inoculum and media, but no Peo3Glc (A). Incubations were carried out at pH 6.6-7.0 and 37°C, over 24 h. Samples (0.5 mL) were collected at the times shown in the figure, mixed with 0.5 mL of 4% v/v aqueous formic acid, and after sample preparation (Chapter 2, section 2.2.6), analysed using HPLC-DAD to determine the Peo3Glc concentration and LC-MS/MS to determine metabolites concentrations. The data shown are for 1 replicate incubation using a single donor faecal sample: donor 08 – S3. No Peo3Glc was detected in control vessels (data not shown).

6.4.5. The step-by-step metabolic pathway of anthocyanin metabolites

Having confirmed the main black rice metabolites appearing at various times with incubations with pure Cya3Glc, the metabolic pathways of these metabolites were examined using the batch colon model fermentation. The approach was to incubate the early-appearing metabolites directly in the colon model and determine what their breakdown products might be. Thus, PCA, PGA, and DHPAA were incubated with live faecal microbiota and with autoclaved faecal microbiota. Control vessels were carried out by inoculating live faecal microbiota, but no main metabolites were introduced. Samples were collected over time and the metabolites were analysed using UPLC-MS/MS.

In the presence of live faecal microbiota, the rates of decline of the PCA and DHPAA were considerably faster in comparison with the presence of autoclaved faecal samples (**Figure 6. 9** and **Figure 6. 11**). However, PGA was degraded similarly in the presence and absence of live faecal microbiota (**Figure 6. 10**). For PCA the k_{deg} was significantly faster after 8 h of the incubation and was fully degraded at 20 h. Whereas PGA and DHPAA showed slower decline rates, where they were still detected in 24 h samples.

While DHPAA declined in the presence of live faecal microbiota, no predicted breakdown products were identified. However, as they increased in synchrony with the decline of the original compound of PCA or PGA, catechol and PGCA, and phloroglucinol were identified as further-step metabolites (e.g., PCA → catechol and PGA → PGCA → phloroglucinol). Therefore, two pathways of the degradation of Cya3Glc and Peo3Glc were identified using step-by-step metabolic pathway investigations.

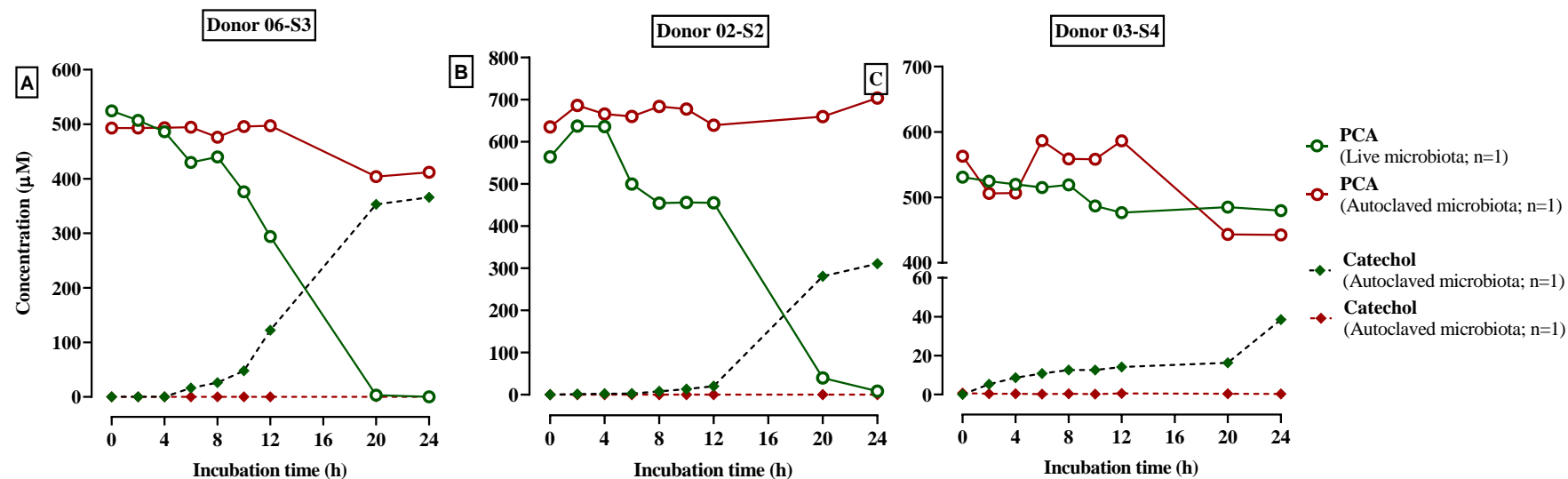


Figure 6.9. Incubations of PCA in the in-vitro colon model over 24 h.

A 25 mg/mL of PCA was prepared in aqueous methanol (50%v/v). A volume of 0.4 mL was added to colon model vessels pre-filled with sterile media (99.6 mL) and human faecal slurry (10 mL of a 10% slurry from a fresh stool) to give a final volume of 100 mL and a concentration of PCA of 100 μg/mL. Similar vessels were prepared but containing autoclaved faecal slurry rather than fresh faecal slurry. Control vessels contained fresh faecal inoculum and media, but no authentic phenolic compounds. Incubations were carried out at pH 6.6-7.0 and 37°C, over 24 h. Samples (0.5 mL) were collected at the times shown in the figures, mixed with 0.5 mL of 4% v/v aqueous formic acid, and after sample preparation (Chapter 2, section 2.2.6), analysed using LC-MS/MS to determine the concentration of the phenolic. The data shown are for 1 replicate incubation for each condition using three individual donor faecal samples: donor 06-S3 (fresh slurry; n=1), donor 02-S2 (fresh slurry; n=1), and donor 03-S4 (glycerol-faecal stock; n=1).

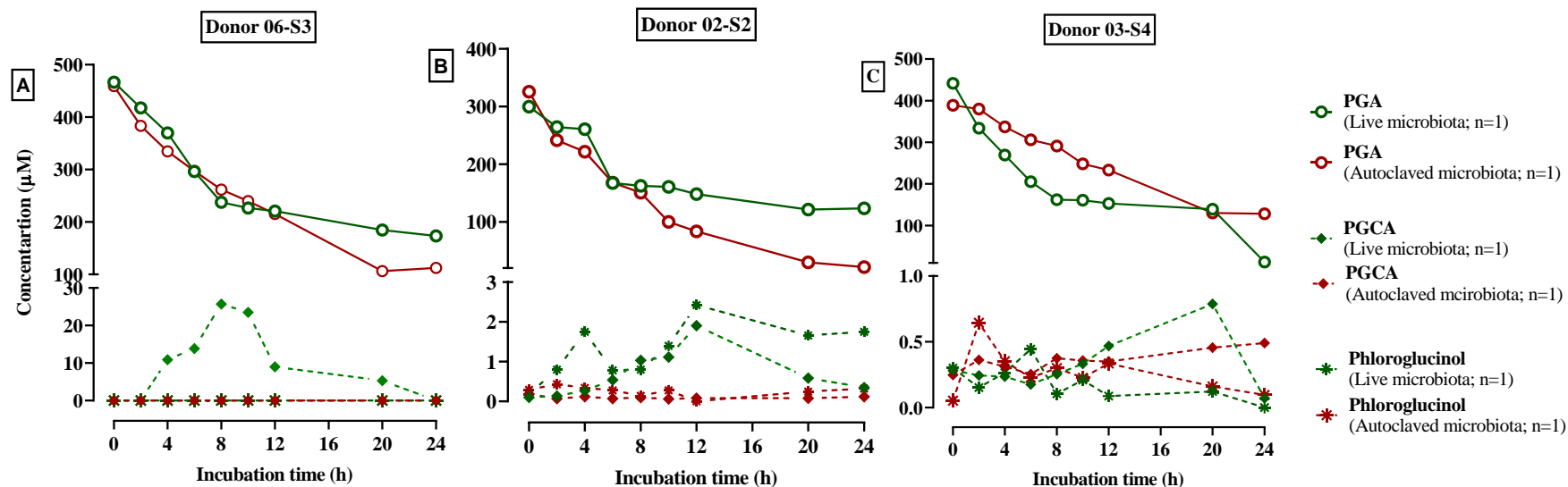


Figure 6.10. Incubations of PGA in the in-vitro colon model over 24 h.

A 25 mg/mL of PGA was prepared in aqueous methanol (50%v/v). A volume of 0.4 mL was added to colon model vessels pre-filled with sterile media (99.6 mL) and human faecal slurry (10 mL of a 10% slurry from a fresh stool) to give a final volume of 100 mL and a concentration of PGA of 100 μg/mL. Similar vessels were prepared but containing autoclaved faecal slurry rather than fresh faecal slurry. Control vessels contained fresh faecal inoculum and media, but no authentic phenolic compounds. Incubations were carried out at pH 6.6-7.0 and 37°C, over 24 h. Samples (0.5 mL) were collected at the times shown in the figures, mixed with 0.5 mL of 4% v/v aqueous formic acid, and after sample preparation (Chapter 2, section 2.2.6), analysed using LC-MS/MS to determine the concentration of the phenolic. The data shown are for 1 replicate incubation for each condition using three individual donor faecal samples: donor 06–S3 (fresh slurry; n=1), donor 02–S2 (fresh slurry; n=1), and donor 03–S4 (glycerol-faecal stock; n=1).

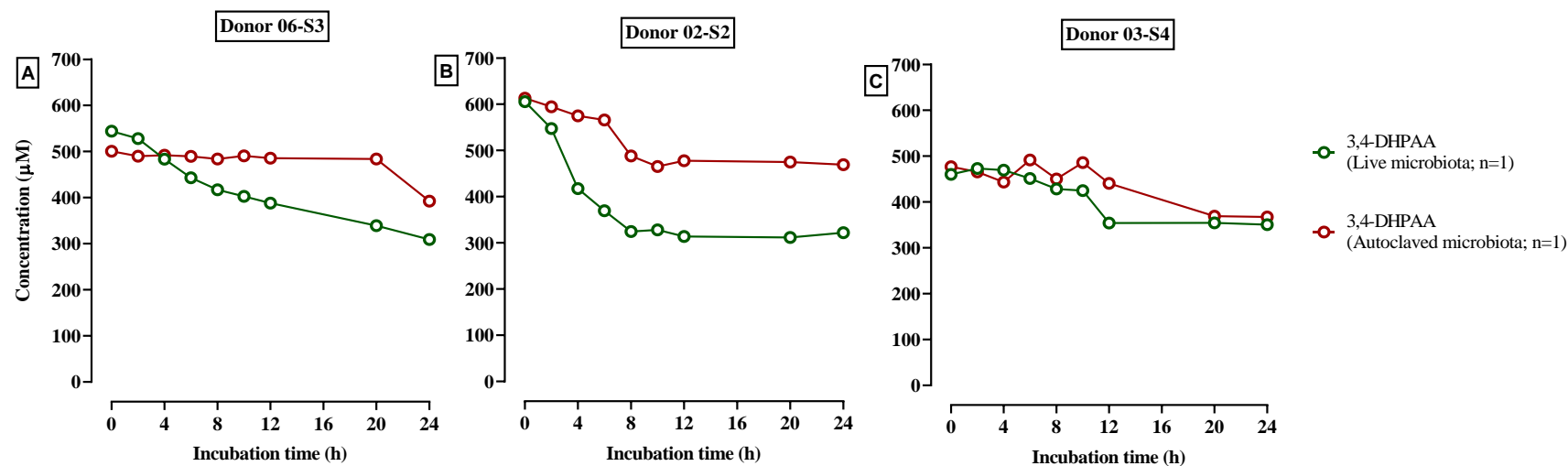


Figure 6.11. Incubations of 3,4-DHPAA in the in-vitro colon model over 24 h.

A 25 mg/mL of 3,4-DHPAA was prepared in aqueous methanol (50% v/v). A volume of 0.4 mL was added to colon model vessels pre-filled with sterile media (99.6 mL) and human faecal slurry (10 mL of a 10% slurry from a fresh stool) to give a final volume of 100 mL and a concentration of 3,4-DHPAA of 100 µg/mL. Similar vessels were prepared but containing autoclaved faecal slurry rather than fresh faecal slurry. Control vessels contained fresh faecal inoculum and media, but no authentic phenolic compounds. Incubations were carried out at pH 6.6-7.0 and 37°C, over 24 h. Samples (0.5 mL) were collected at the times shown in the figures, mixed with 0.5 mL of 4% v/v aqueous formic acid, and after sample preparation (Chapter 2, section 2.2.6), analysed using LC-MS/MS to determine the concentration of the phenolic. The data shown are for 1 replicate incubation for each condition using three individual donor faecal samples: donor 06-S3 (fresh slurry; n=1), donor 02-S2 (fresh slurry; n=1), and donor 03-S4 (glycerol-faecal stock; n=1).

6.4.6. The intra-individual variations in the formation of the black rice anthocyanin metabolites during the human *in-vitro* colon model fermentations

Having observed that the formation of PCA, PGA, 3,4-DHPAA, PGC, catechol, dihydroferulic acid, and dihydrocaffeic acid is driven by live faecal microbiota with different pathways being involved, the next step was to investigate the intra-individual variation (i.e., between stool samples collected at different times from the same individual) in the production of these metabolites. The samples collected from experiments in chapter 4, section 4.5.5, were used to investigate the intra-individual variation. In brief, three different faecal samples (S5, S6, and S7) were collected from donor 01 on different days. Each sample was used to inoculate the *in-vitro* colon model vessels containing black rice anthocyanin extracts. Samples were collected over time and were analysed later using UPLC-MS/MS.

Although the stool samples were collected from sample donor 01, the production of black rice anthocyanin metabolites varied between stool samples collected on different occasions (**Figure 6. 12**). For example, the main metabolite, DHPAA was shown to be formed in the presence of live faecal microbiota to reach the C_{\max} at 6 h for both samples S5 and S7, but it reached C_{\max} at 4 h with S6. Afterwards, DHPAA declined at different rates in the different faecal samples (S5, 6, and 7) (data not shown because they are on a different scale). In addition, PCA, increased over the first 4 h with a C_{\max} of 8.1 and 19.7 μM for S5 and S6, respectively, but it was over 6 h for S7 with C_{\max} of only 2.4 μM . PGA also increased over time. For example, with faecal sample S5, PGA increased over the first 6 h then slightly declined at 8 h before increasing again to reach its C_{\max} of 0.94 μM at 24 h. However, the production of PGA in the presence of the other stool samples (S6 and S7) was notably higher with C_{\max} of 6.0 and 3.3 μM at 8 and 6 h, respectively. Although with S7 PGA declined after 6 h to reach a concentration of 3.3 μM at 8 h and was fully degraded at 20 h, the rate of PGA decline was significantly slower with the faecal sample from S6 which was detected at a concentration of 5.7 μM at 20 h.

Catechol also was detected with different C_{\max} in the different stool samples collected from the same donor. For example, in both S5 and S6, catechol was initially detected at

4 h of incubation and reached C_{\max} at 24 h with a concentration of 2.4 and 3.4 μM , respectively. However, with S7, catechol was detected later (at 8 h) but it reached the C_{\max} (4.7 μM) a little earlier at 20 h, then it slightly declined to reach a concentration of 4.4 μM at 24 h. PGCA was also investigated but was not detected.

Additionally, dihydrocaffeic acid was not detected in inoculations of S7 faecal samples, but it was detected in the other two stool samples. In the presence of S5, dihydrocaffeic acid increased over the 24 h time course and it reached its C_{\max} of 1.1 μM , but in the presence of S6, it was detected initially with background concentration at 0h, which later declined over the first 6 h then it appeared again at 8 h to reach its C_{\max} of 7.7 μM at 24h. Moreover, dihydroferulic acid was also detected but with different formation patterns. With S7, the detected concentration at 0 h gradually disappeared over 24 h, with no additional formation. However, with S5 and S6, there was formation over the first incubation time when dihydroferulic acid reached its C_{\max} (0.8 μM , at 6 h) and (1.0 μM , at 2 h), respectively. However, they declined after reaching the C_{\max} .

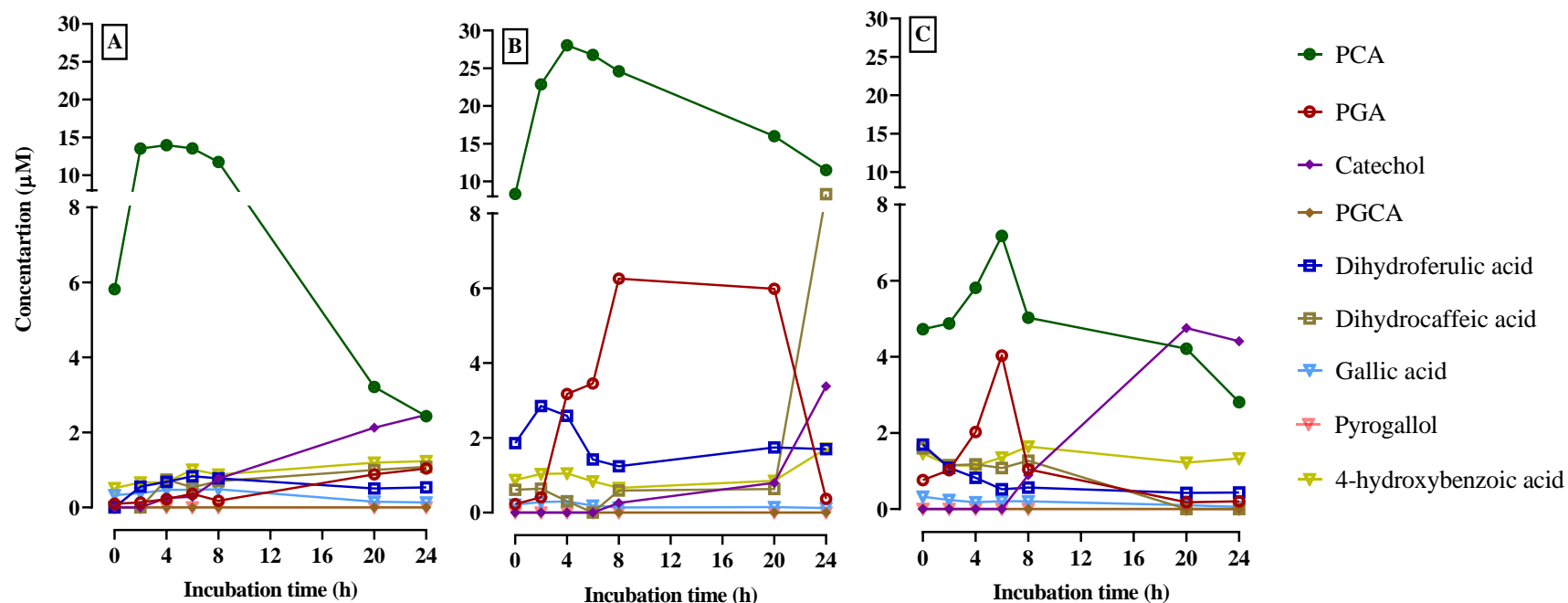


Figure 6.12. The formation of black rice anthocyanin metabolites showing the intra-individual variations in the presence of live faecal microbiota.

Black rice extract (18 mg, containing 33.36% w/w Cya3Glc) was dissolved in 1 mL water, filtered and immediately added to colon model vessels pre-filled with sterile media (89 mL) and human faecal slurry (10 mL of a 10% slurry from a fresh stool) to give a final volume of 100 mL and a Cya3Glc concentration of 133.60 μM (60 $\mu\text{g}/\text{mL}$). Control vessels contained fresh faecal inoculum and media, but no black rice extract (data not shown). Different faecal samples from the same donor were used, where donor 01-S5 (A), donor 01-S6 (B), and donor 01-S7 (C). Incubations were carried out at pH 6.6-7.0 and 37°C, over 24 h. Samples (0.5 mL) were collected at the times shown in the figure, mixed with 0.5 mL of 4% v/v aqueous formic acid, and after sample preparation (Chapter 2, section 2.2.6), analysed using UPLC-MS/MS to determine concentrations of anthocyanin metabolites. The experiments were carried out by using three different faecal samples from the same donor collected on different days and run in separate experiments. The data from each donor are presented as one replicate (n=1).

6.4.7. The inter-individual variations in the formation of the black rice anthocyanin metabolites during the human *in-vitro* colon model fermentations

Next, the inter-individual variations of the formation of black rice anthocyanin metabolites were investigated. In order to investigate this, the same samples collected from experiments performed in chapter 4, section 4.5.6 were used. Briefly, three stool samples were collected from three different donors (Donor 01-S8, 07-S1, and 08-S2) on the same day and faecal slurries were immediately prepared from each of the three stool samples. Each faecal slurry was used to inoculate three different vessels that were treated with the same amount of black rice extract ($n=3$). In addition, control vessels were prepared for each donor where the vessels were inoculated with live faecal slurry, but no black rice was introduced. The incubations for all vessels were carried out using an *in-vitro* pH-controlled batch colon model, where samples were collected over 24 h and analysed using UPLC-MS/MS.

Although PCA, PGA, DHPAA, and catechol were shown to be the main metabolites in the three different donors, their formation rates varied from one donor to another (**Figure 6. 13**). The main metabolite, DHPAA, increased over time to reach the C_{\max} at different time points of the incubation. For example, DHPAA formation reached C_{\max} of $37 \pm 5.3 \mu\text{M}$ (at 10 h), $19 \pm 11 \mu\text{M}$ (at 6 h) and $50 \pm 4.7 \mu\text{M}$ (at 20 h) for donor 01-S8, 07-S1, and 08-S2, respectively. The rates of decline for DHPAA also varied. For example, the DHPAA declined faster over time and fully disappeared after 8 h for donor 07-S1, and after 20 h for donor 01-S8. Whereas for donor 08-S2, the formation of DPHAA occurred over the first 20 h and slightly declined at 24 h.

PCA increased in the early stage of incubation for all donors. PCA reached its C_{\max} at 10 h for both donor 01-S8 ($11.1 \pm 1.1 \mu\text{M}$) and donor 08-S2 ($5.3 \pm 1 \mu\text{M}$), whereas the C_{\max} ($7.3 \pm 1.5 \mu\text{M}$) was at 8 h for donor 07-S1. In all donors, PCA declined gradually after reaching the C_{\max} . PGA increased over the first 6 h in the case of donor 07-S1 (C_{\max} , $1.7 \pm 0.4 \mu\text{M}$), 8 h for both donor 01-S8 (C_{\max} , $2.4 \pm 0.3 \mu\text{M}$) and donor 08-S2 (C_{\max} , $1.6 \pm 0.6 \mu\text{M}$). It was also observed that a constant decrease of PGA after reaching the C_{\max} , but there was a rapid increase of PGA at 24 h for both donors 01-S8 and 08-S2 to reach a concentration which higher than their C_{\max} at 8 h.

Dihydroferulic acid appeared in all donors at the initial stages of incubation (between 4 – 10 h). For example, the C_{\max} for donors 01-S8 ($0.41 \pm 0.12 \mu\text{M}$) and 08-S2 ($0.35 \pm 0.14 \mu\text{M}$) was reached at 6 h. However, with donor 07-S1, the C_{\max} of $0.49 \pm 0.1 \mu\text{M}$ was achieved at 10 h. On the other hand, dihydrocaffeic acid was not detected in the presence of live faecal microbiota from donors 01-S8 and 07-S1. However, it was shown to be produced in donor 08-S2 to reach C_{\max} of $0.75 \pm 0.34 \mu\text{M}$ at 20 h.

Unlike the other main metabolites, catechol steadily increased after 8h for both donor 01-S8 and donor 07-S1, but it was initially increased at 2 h in donor 08-S2, but then showed more substantial increase at 8 h. The C_{\max} for all donors occurred at 20 h, where the C_{\max} for donors 01-S8, 07-S1, and 08-S2 were 6.6 ± 0.8 , 5.5 ± 1.1 , and $8.0 \pm 1.8 \mu\text{M}$, respectively. PGCA was detected in all donors. With donors 01-S8 and 08-S2, for example, PGCA reached its C_{\max} at 12 h with a concentration of 0.24 ± 0.14 and $0.12 \pm 0.05 \mu\text{M}$, respectively. However, at 10 h the C_{\max} of PGCA was $0.09 \pm 0.02 \mu\text{M}$ in the presence of stool sample S1 from donor 07.

Although the main metabolites were detected in all three donors, the results showed that the formation rates of anthocyanin metabolites as well as their k_{deg} are variable and donor dependent. The degradation of initial metabolites showed also that faecal gut microbiota might contribute to the biotransformation of these metabolites into further-step or secondary metabolites.

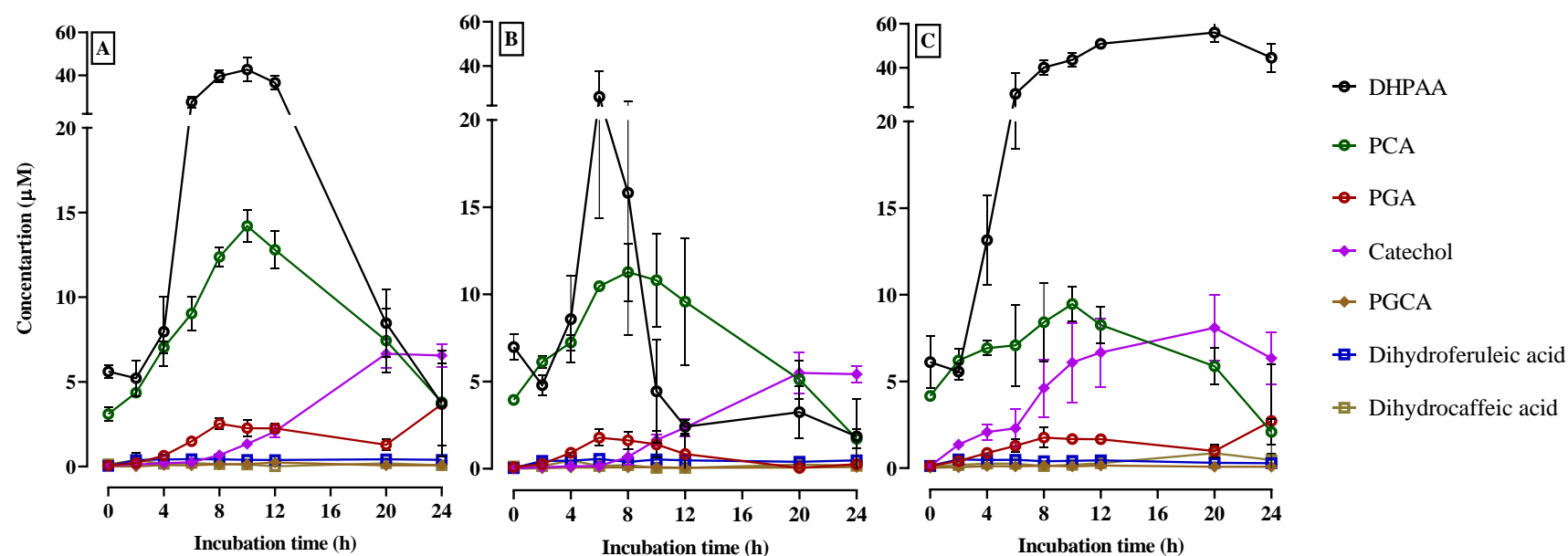


Figure 6.13. The formation of black rice anthocyanin metabolites showing the inter-individual variations in the presence of live faecal microbiota.

Black rice extract (18 mg, containing 33.36% w/w Cya3Glc) was dissolved in 1 mL water, filtered and immediately added to colon model vessels pre-filled with sterile media (89 mL) and human faecal slurry (10 mL of a 10% slurry from a fresh stool) to give a final volume of 100 mL and a Cya3Glc concentration of 133.60 µM (60 µg/mL). Control vessels contained fresh faecal inoculum and media, but no black rice extract (data not shown). Faecal samples were collected on the same day from different donors, where donor 01-S8 (A), donor 07-S1 (B), and donor 08-S2 (C). Incubations were carried out at pH 6.6-7.0 and 37°C, over 24 h. Samples (0.5 mL) were collected at the times shown in the figure, mixed with 0.5 mL of 4% v/v aqueous formic acid, and after sample preparation (Chapter 2, section 2.2.6), analysed using UPLC-MS/MS to determine concentrations of anthocyanin metabolites. The experiments were carried out by using three different faecal samples from different donors collected on the same day. Each faecal sample was incubated in triplicates. Values represent means ± SD.

6.4.8. The formation of black rice anthocyanin metabolites when using glycerol-frozen faecal stocks to inoculate the human *in-vitro* colon model fermentations

Having demonstrated the feasibility and viability of microorganisms in glycerol-frozen faecal stocks in the disappearance of anthocyanins (chapter 4, section 4.5.7), the formation of anthocyanins metabolites was also investigated by using the same samples from experiments presented in chapter 4. Briefly, three stool samples were collected from three different donors (Donor 05-S1, 01-S5, and 03-S3) and glycerol faecal stocks were prepared separately (Chapter 2, section 2.2.3), then stored at - 80°C. On the colon model experiment day, the frozen faecal glycerol stocks were thawed at room temperature for one h before inoculating into colon model vessels which were later treated with black rice extract. In addition, control vessels were prepared for each donor and inoculated only with live faecal slurry, but no black rice was introduced. The incubations for all vessels were carried out using *in-vitro* pH-controlled batch colon model, where samples were collected over 24 h and analysed onto UPLC-MS/MS.

In all three different donors, the production of black rice anthocyanin metabolites was observed. However, the concentrations of metabolites were lower than the concentrations produced from using fresh faecal slurries (**Figure 6. 14**). In addition, both donor 05-S1 and 03-S3 showed similarity in the lower production of most of metabolites, but donor 01-S5 showed higher production, possibly indicating that microbial viability was higher.

To illustrate this, the most abundant metabolites (DHPAA, PCA, PGA, and catechol) were explored in more detail. The production of DHPAA increased up to 8 h of incubation with both donor 05-S1 (C_{\max} , 15.7 μM at 24 h) and 03-S3 (C_{\max} , 29 μM at 24 h), but with donor 01-S5 the production was elevated after 4 h to reach the C_{\max} of 14.2 μM at 12 h, then it is shown to decline to 8.6 μM at 24 h. The formation of PCA was lower in the presence of faecal samples from donors 05-S1 and 03-S3, with a C_{\max} of 0.8 μM at 12 h and 0.5 μM at 10 h, respectively, and higher with donor 01-S5 (C_{\max} of 1.2 μM at 12h). PGA production was also low, although its production was higher (C_{\max} 0.52 μM at 12 h) with donor 05-S1 than the other two; donor 01-S5 (C_{\max} , 0.24 μM at 12 h) and donor 03-S3 (C_{\max} , 0.25 μM at 24 h). The production of catechol was significantly higher in the

presence of donor 01-S5 (C_{\max} 1.9 μM at 24 h). With donor 05-S1 and 03-S3, catechol also reached its C_{\max} but at very low concentrations; 0.04 and 0.06 μM , respectively at 24 h). Dihydroferulic acid was detected in all three donors, however, the production was higher with donor 05-S1 (C_{\max} , 0.15 μM at 24 h) and donor 01-S5 (C_{\max} , 0.18 μM at 12 h) than with donor 03-S3 (C_{\max} , 0.10 μM at 24 h). Furthermore, dihydrocaffeic acid was not detected in donor 03-S3, however, its formation in the other two donors was very limited, even in comparison with the production of other metabolites.

It was noticed that the timing of catechol production corresponded with the decline of PCA. For example, PCA production and then decline were more significant in donor 01-S5 than for the other two donors. Meanwhile, in the same donor 01-S5, catechol was significantly produced (**Figure 6. 14B**). Moreover, the production of PGCA corresponded with the degradation of PGA. For example, in **Figure 6. 14A** the production of PGA was higher in donor 05-S1, and also PGCA was noticeably and in parallel increased in the same donor. This relation might be donor-specific or metabolite-type specific or both.

To conclude, using frozen faecal glycerol stocks is a feasible approach to confirm the reproducibility of results for the same faecal sample. However, the production rates and amounts are significantly lower than those observed when fresh faecal samples are used. It suggested that the freezing process (e.g., storage duration and thawing procedure) might affect microbial viability. Therefore, it should be noted that it is possible for some bacteria to die due to storage conditions which might raise another challenge to use frozen faecal glycerol stocks.

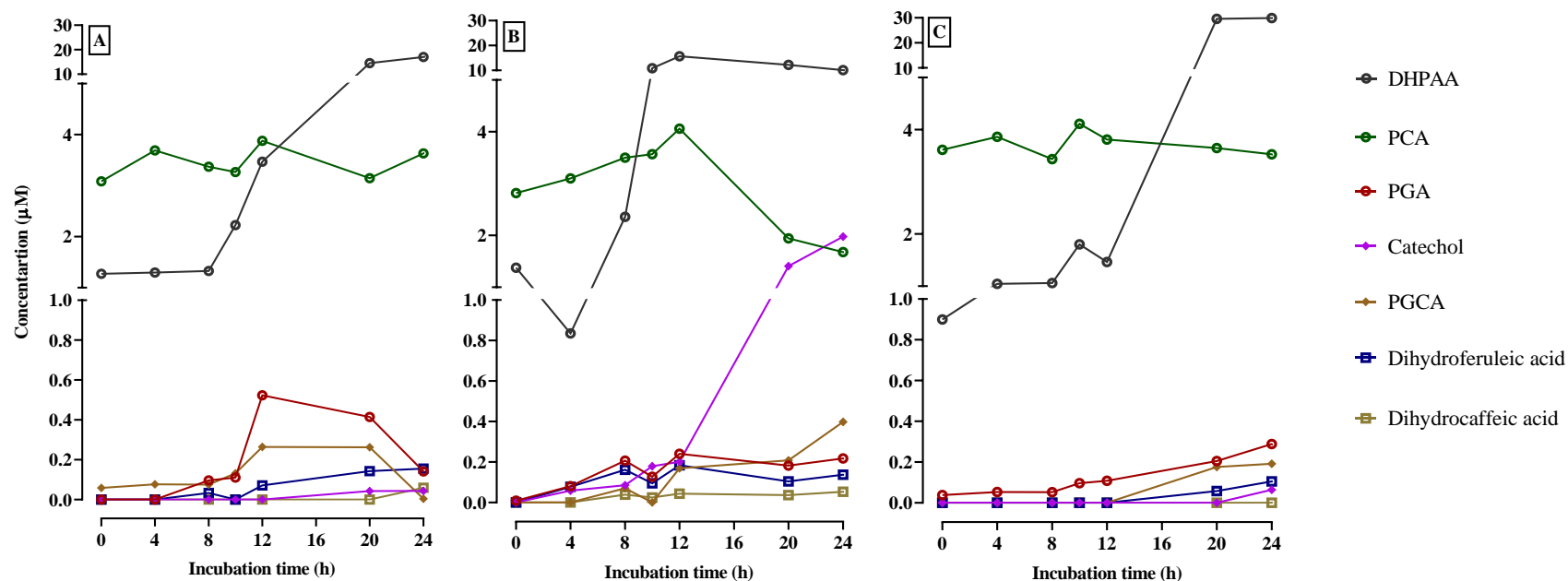


Figure 6.14. The formation of black rice anthocyanin metabolites in the presence of live faecal microbiota using glycerol-frozen faecal stocks.

Black rice extract (18 mg, containing 33.36% w/w Cya3Glc) was dissolved in 1 mL water, filtered and immediately added to colon model vessels pre-filled with sterile media (96.4 mL) and glycerol-frozen faecal stocks (2.6 mL of a 37% stool sample) to give a final volume of 100 mL and a Cya3Glc concentration of 133.60 µM (60 µg/mL). Control vessels contained frozen faecal glycerol stocks and media, but no black rice extract (Data not shown). The faecal samples were collected from different donors on different days before preparing the faecal-glycerol stocks, where donor 05-S1 (A), donor 01-S5 (B), and donor 03-S3 (C). Incubations were carried out at pH 6.6-7.0 and 37°C, over 24 h (data not shown). Samples (0.5 mL) were collected at the times shown in the figure, mixed with 0.5 mL of 4% v/v aqueous formic acid, and after sample preparation (Chapter 2, section 2.2.6), analysed using UPLC-MS/MS to determine concentrations of anthocyanin metabolites the experiments were carried out by using three different frozen faecal glycerol- samples prepared from different donors. The data from each donor are presented as one replicate (n=1).

6.4.9. The formation of anthocyanin metabolites during the fermentation of a mixture of fifteen bilberry anthocyanins in an *in-vitro* colon model

A series of experiments to investigate the loss of different types of anthocyanins in a bilberry extract by the human gut microbiota were described in chapter 4 (section 4.5.8). Here, the formation of the bilberry anthocyanin metabolites was investigated. Briefly, bilberry anthocyanin extract was incubated with both fresh faecal slurry and autoclaved faecal slurry from donor 08-S3 (n=1). A control vessel containing fresh faecal slurry, but no bilberry extract was also included.

In the presence of live faecal microbiota, various phenolic compounds were detected during the *in-vitro* colon fermentation of bilberry anthocyanin extract (**Figure 6. 15**). The main B-ring-derived metabolites gallic acid, PCA, 3-O-methylgallic acid, syringic acid, and vanillic acid, were detected and shown to increase over the first 8 h of incubation. The main A-ring-derived metabolite, PGA, increased over the first 10 h. In addition, catechol and DHPAA were present at high concentrations. In addition, other metabolites were detected but at low concentrations, namely PGCA, 4-methylcatechol, dihydrocaffeic acid, and dihydroferulic acid. A number of metabolites reached their C_{\max} at 10 h. For example, at 10 h, gallic acid, PCA, PGA, and PGCA were detected with a concentration of 3.6 ± 0.5 , 3.3 ± 0.2 , 3.9 ± 0.6 , 0.20 ± 0.08 μM , respectively. Another two metabolites, vanillic acid and syringic acid were elevated to reach their highest concentration at 8 h with a concentration of 0.16 ± 0.08 and 0.10 ± 0.01 μM , respectively. The other metabolites were shown to reach their highest concentration later at 24 h. For example, at 24 h, the highest detected concentration of catechol, dihydroferulic acid, dihydrocaffeic acid, DHPAA, and 4-methylcatechol were 4.8 ± 0.6 , 0.37 ± 0.03 , 0.30 ± 0.07 , 5.3 ± 1.8 , 0.10 ± 0.06 μM , respectively. 3-O-methylgallic acid reached its C_{\max} (0.68 ± 0.43 μM) at 20 h. In the absence of live faecal microbiota, DHPAA was elevated over time to reach a C_{\max} of 18.8 ± 3.43 μM at 20 h. In addition, 4-hydroxybenzoic acid was detected and increased in the presence of live faecal microbiota (after 2 h), however, in the presence of autoclaved faeces, 4-hydroxybenzoic acid was detected later (after 12 h) reaching its highest concentration of 2.1 ± 0.5 μM at 20 h.

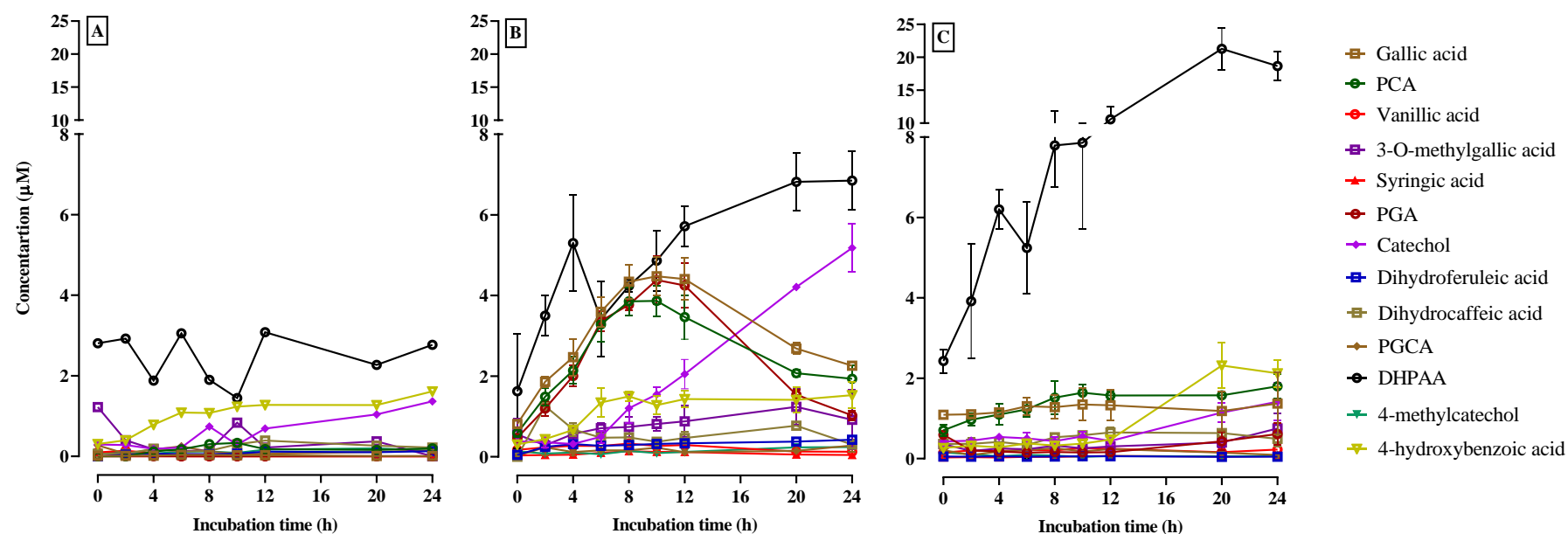


Figure 6. 15. The formation of anthocyanin metabolites during batch colon model fermentation over 24 h by using a concentration of bilberry anthocyanin ($50 \mu\text{g mL}^{-1}$).

Bilberry extract (19.1 mg, containing 26.2% w/w anthocyanins) was dissolved in 1 mL water, filtered and immediately added to colon model vessels pre-filled with sterile media (89 mL) and human faecal slurry (10 mL of a 10% slurry from a fresh stool) to give a final volume of 100 mL and a total anthocyanin concentration of $50 \mu\text{g/mL}$ (B). Similar vessels were prepared but containing autoclaved faecal slurry rather than fresh faecal slurry (C). Control vessel contained fresh faecal inoculum and media, but no bilberry extract (A). Incubations were carried out at pH 6.6-7.0 and 37°C , over 24 h. Samples (0.5 mL) were collected at the times shown in the figure, mixed with 0.5 mL of 4% v/v aqueous formic acid, and after sample preparation (Chapter 2, section 2.2.6), analysed using UPLC-MS/MS to determine concentrations of anthocyanin metabolites. The data shown are for 3 replicate incubations using a single donor faecal sample: donor 08 – S3 (n=1). Data for control presented as one replicate.

6.5. Discussion

The overall aim of the research described in this chapter was to investigate the appearance of anthocyanin-derived microbiota-dependent metabolites from the degradation of anthocyanins by the human gut microbiota. The approach was to measure the formation of the microbial anthocyanin metabolites in the presence and absence of live faecal microbiota and assess whether there are variations both within- and between-individuals.

The main findings in this chapter were that (i) various black rice anthocyanin-derived microbiota-dependent metabolites were detected (PCA, PGA, DHPAA, catechol, PGCA, dihydroferulic acid, and dihydrocaffeic acid) in the presence of live faecal microbiota (ii) the appearance rates and C_{\max} of anthocyanin metabolites varied within a person (in different stool samples collected on different days) and between individuals where samples were collected and the experiment run on the same day, (iii) different metabolic pathways were suggested for the black rice anthocyanins i.e., [Cya3Glc→PCA→catechol] and [Cya3Glc→PGA→PGCA→phloroglucinol], (iv) PGA and corresponding A-ring phenolic acid were also detected from the incubation of the pure authentic Cya3Glc and Peo3Glc, but no significant production of catechol and PGCA, (v) it was feasible to use frozen faecal glycerol stocks to investigate the gut microbial metabolism of anthocyanins, but the production of anthocyanin metabolites was slower in comparison to the corresponding fresh faecal samples, and (vi) various B-ring metabolites (gallic acid, vanillic acid, 3-O-methylgallic acid and syringic acid) were detected during the incubation of bilberry anthocyanin extract with live faecal microbiota.

The novelty of the work in this chapter is that for the first time some microbial metabolites only produced by the gut microbiota were identified. In addition, some gut microbiota-dependent metabolites were initial metabolites while others are secondary and arise from the primary metabolites. Therefore, metabolites were categorised into primary (or initial) and secondary metabolites based on both C_{\max} and the initial time of appearance. For example, the metabolites PCA and PGA were shown to appear at early stages (within the first 2 h) of the fermentation and their C_{\max} were higher compared to other metabolites. Therefore, PCA and PGA were considered primary metabolites. In addition, PCA and PGA appeared to decline after reaching their C_{\max} , suggesting that they started to be

metabolised into secondary metabolites. When PCA and PGA were further investigated separately (Figure 6.9-10), it was confirmed that they were intermediates for the secondary metabolites catechol and PGCA, respectively. The secondary metabolites started to be formed as expected at later stages of fermentation (after 6 h), and they normally reached their C_{\max} at the end of incubation time (between 20 and 24 h). For example, although they are detected at relatively low concentrations, dihydroferulic acid was shown to be an intermediate (primary metabolite) of dihydrocaffeic acid after demethylation process [Cya3Glc→dihydroferulic acid→dihydrocaffeic acid]. Microbial demethylation of compounds has been reported before by Zhang and others who showed that the gut microbiota was able to demethylate the alkaloid drug berberine (via the CYP51 enzyme) and thus improved its intestinal absorption²⁶⁰. Therefore, it is plausible that the faecal microbiota has the capacity to demethylate the methyl group (CH_3) from the methoxy group (O-CH_3) on position 3 on the benzene ring of the dihydroferulic acid by an as yet unknown O-demethylase (**Figure 6. 16** and **Figure 6. 17**).

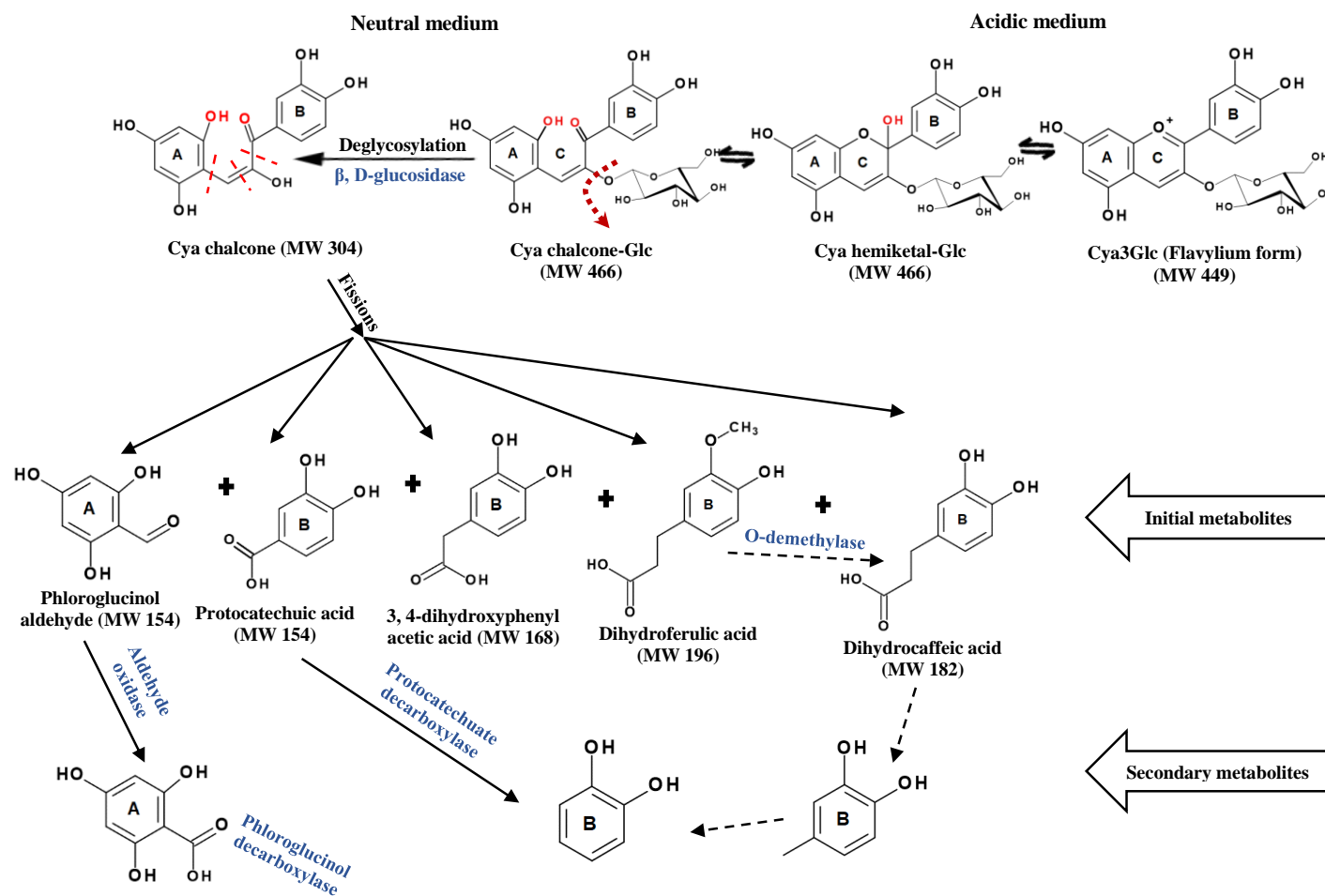


Figure 6. 16. Proposed pathway of colonic biotransformation of Cyanidin-3-O-glucoside (Cya3Glc) by the human gut microbiota, where the solid arrows represent confirmed routes, the dotted arrows represent predicted routes, and MW is an abbreviation for the molecular weight.

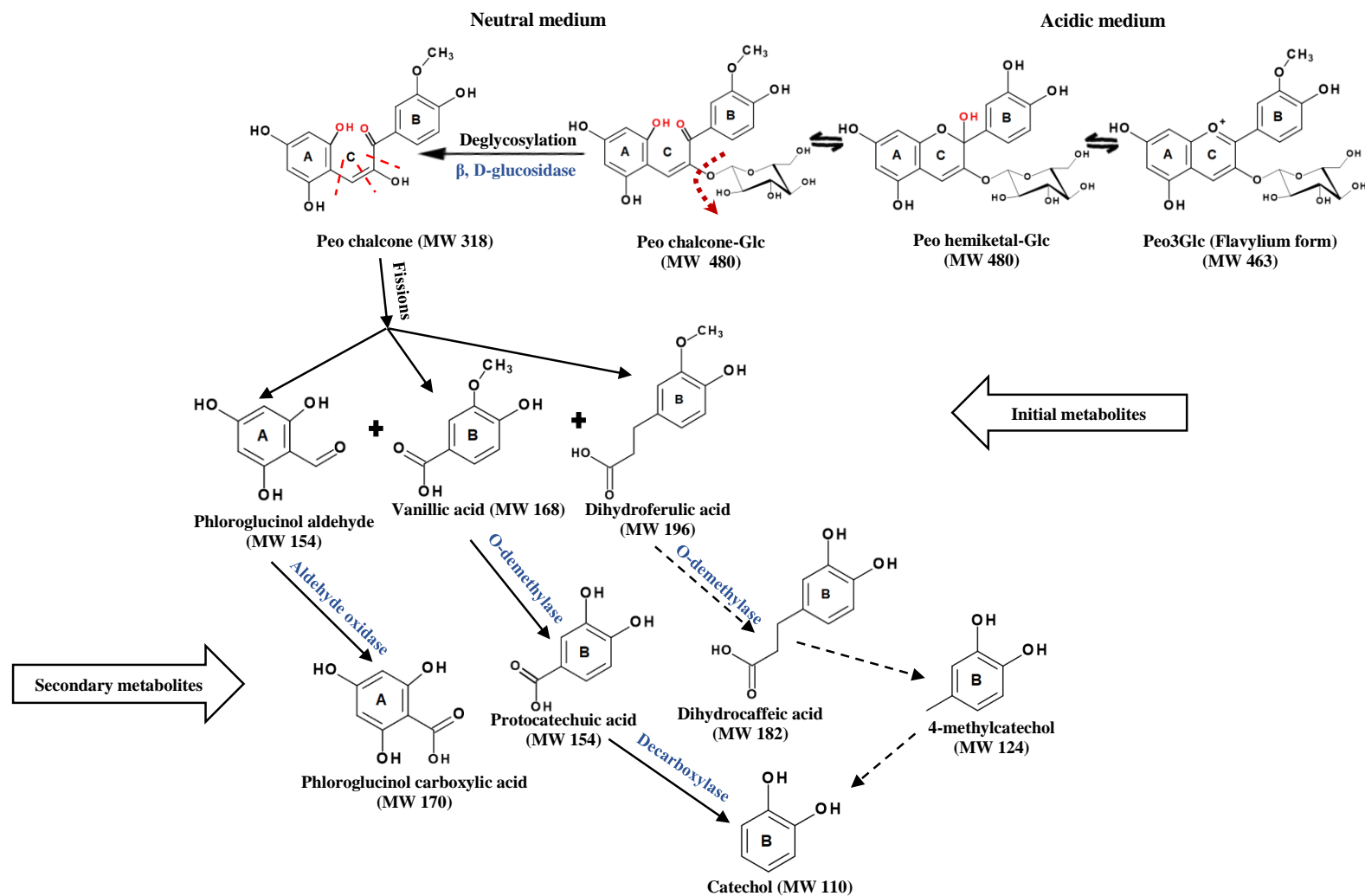


Figure 6. 17. Proposed pathway of the colonic biotransformation of peonidin-3-O-glucoside (Peo3Glc), where the solid arrows represent confirmed routes, the dotted arrows represent anticipated routes, and MW is an abbreviation for the molecular weight.

These data highlight seven microbiota-derived metabolites produced anaerobically in the colon model in the presence of live faecal microbiota from the black rice anthocyanin extract. However, in the vessels containing autoclaved faecal samples, DHPAA was detected at very high concentrations in some incubation with black rice anthocyanins extract (**Figure 6. 3** and **Figure 6. 4**). In addition, DHPAA appeared at the later stage of fermentation in the presence of autoclaved microbiota compared to vessels containing fresh faecal samples. In other experiments, however, no production of DHPAA was observed in the presence of autoclaved faecal slurries (**Figure 6. 5** and **Figure 6. 6**). This suggested that anthocyanins (Cya3Glc) may break down spontaneously. For example, data in Chapter 4 showed that different faecal matrices affect the spontaneous k_{deg} of black rice anthocyanins. However, this spontaneous degradation may be varied depends on the faecal matrix and/or the faecal contents.

The production of these anthocyanin metabolites varied between stool samples (collected from the same donor but on different days) and also varied between stool samples collected from different donors collected on the same day, showing intra- and inter-individual variations respectively. Very few reports have investigated the gut microbial metabolism of anthocyanins using *in-vitro* human colon model studies. Some studies have used the content of large intestine from animal models^{89,96,240}; others have used specific or isolated strains^{93,176}. Furthermore, animal studies have identified the A-ring metabolite PGA and corresponding A-ring-derived phenolic acid (i.e., PCA and gallic acid from Cya3Glc and Del3Glc, respectively). In agreement with an animal study reported by Hanske and others⁸⁸, here it is demonstrated that using the human gut microbiota, PGA and PCA were the main metabolites from Cya3Glc. Although it appeared at late incubation stages in vessels containing autoclaved faecal slurries, DHPAA was defined as a primary metabolite from Cya3Glc because it was formed in the first few hours of incubation with a high concentration compared to the other metabolites.

In addition, although few other reports have used human faecal samples to investigate the microbial metabolism of anthocyanins, they used a simple phosphate buffer, non-pH-controlled models and complex mixture of anthocyanins, the spontaneous degradation of anthocyanins was neglected, and/or the incubation time was for short time. For example, it was reported that the metabolism of Cya3Glc in the presence of human faecal samples

using a simple buffer solution over 2 h¹⁷³, concluding that PCA was the breakdown product of Cya3Glc. Hanske and others increased the incubation time to 25 h for the incubation of pure Cya3Glc with a human stool sample⁸⁸, but no pH-controlled model was used, and the medium was a simple buffer solution. In the current study, the pH-controlled model was used and other metabolites, not only PCA and PGA were identified as microbiota-dependent metabolites. Hanske and others, however, stated that PCA and PGA are the microbial metabolites of Cya3Glc⁸⁸. More recently, two reports used nutrient media to incubate anthocyanins with faecal samples^{174,175}. But they used a non-pH-controlled model in their investigations. However, ¹⁷⁴ reported that syringic acid and tyrosol were the main microbial products from Mal3Glc-rich extract and Peo3Glc-rich extracts, respectively. However, from the data in this chapter, various black rice anthocyanin metabolites were shown to be formed in the presence of live faecal microbiota such as DHPAA, PCA, PGA PGCA, catechol, dihydrocaffeic acid and dihydroferulic acid.

Although black rice anthocyanin extract is a Cya3Glc-rich extract (87.2 % of total black rice anthocyanins), the other main anthocyanin is Peo3Glc (6.2 % of total black rice anthocyanins). Furthermore, in the incubations with authentic Peo3Glc the main B-ring-derived metabolite was vanillic acid, and the main A-ring-derived metabolite was PGA. However, the production of dihydrocaffeic acid was also relatively high. The data is suggesting that dihydrocaffeic acid was produced from Peo3Glc. Although dihydroferulic acid was also shown to be produced from both pure Cya3Glc and Peo3Glc, the C_{max} was relatively low from pure Peo3Glc compared to pure Cya3Glc. From this data, it can be concluded that both compounds might originate from both Cya3Glc and Peo3Glc.

However, on the basis of the time at which they were formed, the primary (or initial) metabolites appeared at the early stages of incubation (between 2-6 h). Dihydroferulic acid was shown to be a primary metabolite whereas dihydrocaffeic acid was shown to be a secondary metabolite in the case of Cya3Glc. However, although the production of dihydroferulic acid from Peo3Glc was very low, dihydroferulic acid was shown to be a primary metabolite and dihydrocaffeic acid a secondary metabolite, suggesting that dihydrocaffeic acid was formed from dihydroferulic acid by demethylation. However,

pure authentic anthocyanins are very expensive, more experiments need to be carried out using more donor replicates to confirm these findings.

In the aerobic condition, it is well established that Cya3Glc breaks down spontaneously into PGA and PCA in equimolar amounts^{38,87}. However, in this chapter, the formation of Cya3Glc breakdown products did not occur under anaerobic conditions of the colon model in the absence of live faecal microbiota. However, in the presence of live faecal microbiota, not only PCA and PGA but also PGCA, catechol, dihydrocaffeic acid and dihydroferulic acid were formed. In addition, the data also showed that in humans, the gut microbial activity is mainly catabolism reactions such as deglycosylation (via β -D-glucosidase), decarboxylation (via decarboxylase) and demethylation (O-demethylase). For example, catechol was produced after the decarboxylation of the intermediate PCA. Therefore, the microbial pathways involved in the degradation of Cya3Glc and Peo3Glc were proposed (**Figure 6. 16 and Figure 6. 17**). The present suggested that A-ring products PGA and the B-ring PCA bio-transformed into PGCA and catechol respectively. In addition, based on the initial formation time, there were initial and secondary metabolites. For example, the dihydroferulic acid was bio-converted into dihydrocaffeic acid which may be converted into 4-methylcatechol, but this would have to be confirmed in future studies.

PCA and PGA, and DHPAA were present at 2 h, reached their C_{\max} within 4 to 10 h, then declined afterwards. Therefore, a metabolite pathway study was assessed by incubating these three phenolics separately using the same *in-vitro* colon model fermentation. The appearance of catechol corresponded with the decline of PCA, suggesting that PCA was entirely converted to catechol and catechol was shown to be relatively stable as it did not degrade further. On the other hand, PGCA was formed in parallel with PGA degradation, however, the formed PGCA was not stable or was rapidly converted to other products. It was suggested that catechol and PGCA are secondary metabolites of Cya3Glc through their intermediates PCA and PGA respectively. Catechol was bio-converted by decarboxylation of the carboxylic group of the PCA. PGCA might lose its carboxylic group to give phloroglucinol (m/z [M-H]⁻ 125), but phloroglucinol was not detected which suggested that phloroglucinol might be unstable or PGCA was not converted to

phloroglucinol. In addition, DHPAA was investigated, but no investigated metabolites were detected as microbial products from 3,4-DHPAA.

Dihydroferulic acid appeared at the early stages of the incubation of Cya3Glc with live microbiota, suggesting that it comes from B-ring of Cya3Glc. But the B-ring of Cya3Glc has two hydroxy groups at positions 3' and 4'. This suggested that Cya3Glc is converted to Peo3glc (by methylation at the 3' hydroxy group) as it has been proposed previously⁸⁸. However, Peo3Glc was searched for at its m/z value, in the colon model sample, but it was not detected. On the basis of this, it is possible that the Cya3Glc underwent a pH-dependent transformation forming Cya chalcone and then Cya chalcone anionic forms (Chapter 5.5), which are highly active. Cya chalcone anionic form might interact with other molecules (such as the component of the colon media or other break down products) and thus a methyl group attached at position 3' to form Peo chalcone. This explanation is supported by the detection of dihydroferulic acid (where a methyl group at 3' on the B-ring).

Studies with pure Cya3Glc confirmed that PCA, PGA, DHPAA, dihydrocaffeic acid, and dihydroferulic acid are microbial metabolites. However, secondary metabolites, catechol and PGCA, showed no significant increase compared to the levels formed during the incubation of black rice anthocyanin extract. This suggested that the non-anthocyanin content in the black rice extract affects the metabolism of anthocyanins. It is also proposed that variations may occur between donors and within the same donor but different faecal samples. Therefore, more donors are needed to investigate the metabolism of the pure Cya3Glc.

The other pure authentic Peo3Glc was metabolised to the B-ring product vanillic acid and the A-ring product PGA. However, other potential B-ring metabolites were identified, e.g. dihydrocaffeic acid started to appear after 8 h incubation. However, the formation was at later stages of the incubation and the formation was increased over time to reach the C_{max} at 20 or 24 h, suggesting that dihydrocaffeic acid is a secondary metabolite from Peo3Glc. The methylated form of dihydrocaffeic acid is dihydroferulic acid. This suggested that the microbiota converted the dihydroferulic acid into dihydrocaffeic acid by demethylation process. Since dihydrocaffeic acid appeared at a late stage of

incubation, it is more likely that dihydroferulic acid underwent a demethylation process as it formed, transforming into dihydrocaffeic acid.

Significant intra-individual variations were observed in the current results. For example, within the same donor 01, the production of PCA was higher with S6 (C_{\max} 19.7 μM at 4 h), whereas the C_{\max} was 2.4 μM after 6 h and 8.1 μM after 4 h incubation with S7 and S5, respectively. More interestingly, although a very low concentration was detected for dihydrocaffeic acid and dihydroferulic acids from samples S5 and S6, both compounds were not detected from sample S7, suggesting that it might be sample specific. Catechol was shown to be a downstream metabolite of PCA. However, the production of catechol was shown to fluctuate regardless of the production of PCA from the same samples. For example, with faecal sample S6, the PCA production was higher (C_{\max} 19.7 μM) than the production of catechol (C_{\max} 3.4 μM). Whereas with S7, the production of PCA was lower (C_{\max} 2.4 μM) than the production of catechol (C_{\max} 4.4 μM). Additionally, no other B-ring-derived metabolites (such as dihydrocaffeic and dihydroferulic acid) were detected with this stool sample (S7). This suggested that S7 has more capacity to convert PCA to catechol, but less capacity to form dihydrocaffeic and dihydroferulic acids. PGA, the intermediate for PGCA, also showed variation between stool samples. However, PGCA was not detected from all stool samples which collected from the same donor 01.

There was also a significant difference in the production of black rice anthocyanin metabolites between different donors (inter-individual variations). For example, the mean C_{\max} of PCA was 11.1, 7.3, and 5.3 μM with donors 01-S8, 07-S1, and 08-S2, respectively. As PCA is an intermediate of catechol (PCA \rightarrow catechol), the C_{\max} of catechol corresponded with the C_{\max} of PCA in the case of donor 01 and 07 (11.1 μM \rightarrow 6.6 μM and 7.3 μM \rightarrow 1.7 μM , respectively). But it was different with donor 08 (5.3 \rightarrow 8.0 μM), suggesting that the capacity to decarboxylate PCA into catechol is donor-specific and also the rate of PCA catabolism to catechol is faster in donor 08. In addition, although dihydroferulic acid was detected at very low concentrations, dihydrocaffeic acid was not detected in both samples from donors 01 and 07. This suggested that there is a lack of demethylation capacity for donors 01 and 07. Furthermore, the PGCA and its intermediate PGA were detected in all three donors.

With regard to gallic acid, it was detected at very low concentrations, and the initial concentration in the 0 h sample was higher in vessels containing autoclaved faecal samples compared to vessels inoculated with fresh faecal samples. The explanation for this might be that the faecal samples contain traces of other polyphenols (e.g., tannins). Gallic acid is the main unit of gallotannin structure ²⁶¹. It is possible that using high temperatures during the autoclave process of the faecal slurry breaks down tannins into gallic acid via hydrolysis (I). However, in the presence of live faecal microbiota, gallic acid was shown to be formed at the initial stages of incubation (2-6 h) then it decreased over time. This showed that the hydrolysis (I) of tannins might occur by enzymatic reaction resulting in the biotransformation of tannins into gallic acid. This enzymatic hydrolysis was previously reported²⁶², but it was by fungi. Furthermore, pyrogallol was formed only in vessels containing live faecal microbiota (Control and black rice-treated vessels). This was previously noted by Hidalgo and others who showed the live gut microbiota transforms gallic acid into pyrogallol by decarboxylation process (II)¹⁷⁷ (**Figure 6. 18**).

4-hydroxybenzoic acid also appeared in control and black rice-treated vessels. It may be concluded that the faecal matrix contains compounds conjugated with 4-hydroxybenzoic acid and during the incubation, the conjugated compounds degraded to release 4-hydroxybenzoic acid. This release occurred earlier in the presence of live gut microbiota possibly due to the ability of bacteria to accelerate the degradation process. But in the presence of autoclaved faecal material, the appearance of 4-hydroxybenzoic acid was later which showed that conjugated compounds might be degraded spontaneously after some time under the colon model conditions.

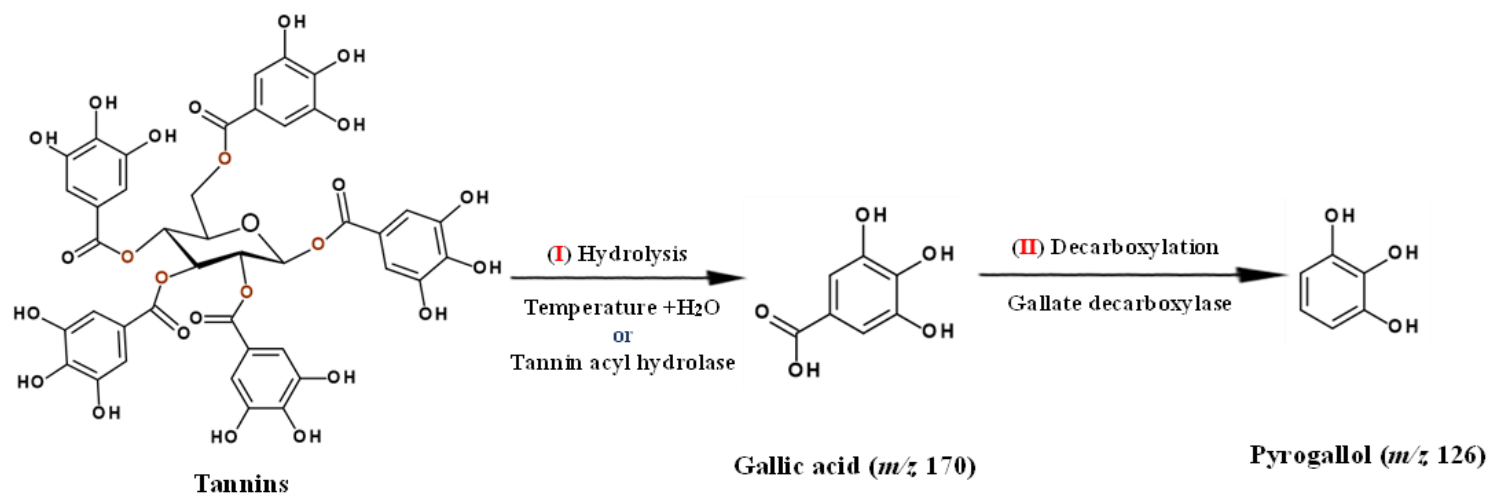


Figure 6. 18. Proposed pathway of the formation of gallic acid and pyrogallol from tannins, in the presence of live faecal microbiota

6.6. Conclusions

Overall, the work in this chapter focused on the production of anthocyanin metabolites by the human gut microbiota and the hypothesised variations within and between individuals. The results in this chapter showed that the human gut microbiota plays an important role in the appearance and production of various anthocyanin metabolites. For example, the formation rates of black rice anthocyanin degradants were significantly faster in the presence of live faecal microbiota. In addition, seven metabolites, PCA, PGA, PGCA, catechol, dihydrocaffeic acid and dihydroferulic acid, were microbiota-dependent metabolites. In addition, the appearance rates of the aforementioned metabolites varied within a person as well as between different individuals. This indicates that different faecal samples from the same donor, but on different days and different individuals have different metabolic capacities. The same individual might have different microbial profiles on different days, showing the dynamic of the human gut microbiota ²⁶³. Furthermore, the human gut microbiota showed catabolism capabilities such as deglycosylation, oxidation, decarboxylation, and demethylation. Therefore, it was clear that the initial metabolites were subjected to further catabolism by gut microbiota, suggesting various metabolic trajectories. These findings are in consensus with the notion that gut microbiota plays an important role in anthocyanin metabolism and give strong evidence why the bioavailability of anthocyanins is very low. Indeed, human studies have reported lower molecular weight metabolites (as conjugated forms) in the circulation or excretion fluids after the consumption of anthocyanins. This is more likely due to entering the circulation, after being produced by gut microbiota, subsequently, anthocyanin-metabolites undergo phase II metabolic reactions (in the liver and/or kidney) and are present in conjugated forms such as glucuronides and sulfatides in the circulation. In chapter 4, although it was demonstrated that the spontaneous degradation of anthocyanins contributes to the overall microbiota-dependent degradation, the microbial anthocyanin-metabolites are considerably different from the breakdown products from the spontaneous degradation (presented in chapter 5). Therefore, it is recommended that further work should focus on the biological activity of both spontaneous breakdown products and microbial metabolites. It is possible that these anthocyanin metabolites confer health benefits to the host, such as anti-inflammatory, anticarcinogenic and antioxidant effects.

Meanwhile, it is important to identify the microbes involved in anthocyanin metabolism, which would provide further information for deep understanding of the metabolic function of the gut microbiota as well as the effects of anthocyanins on the human gut microbiota structure. Therefore, the effect of black rice anthocyanin extract on the gut microbiota structure was investigated and presented in the next chapter (Chapter 7).

Chapter Seven

**The impact of
anthocyanins on the
structure and function of
the human colonic
microbiome**

Chapter 7: The impact of anthocyanins on the structure and function of the human colonic microbiome

7.1. Abstract

Background: Only tiny fraction of ingested anthocyanins are absorbed in the small intestine. In previous chapters, it has been shown that in a model of the human colon, anthocyanins undergo ring fission and some of this occurs spontaneously, but a considerable contribution to anthocyanin transformation is also made by the gut microbiota, and this generates distinct metabolites. Very little is known about whether the gut microbiota is altered upon treatment with anthocyanins and in response to the appearance of ring fission products during fermentation.

Objective: To test the hypothesis that treatment with anthocyanins would alter the structure and function of the human colonic microbiome and that the abundance of species that metabolise the anthocyanins and generate the early anthocyanin breakdown products, would be increased compared to the microbiome in untreated controls.

Methods: A batch *in-vitro* human colon model that was inoculated with fresh human faecal material was used. Vessels were treated with purified anthocyanins from black rice (133.3 μM) or no anthocyanins as controls (n=7 vessels per condition) and incubated over 24 h. Samples were collected at 0, 6, 12, and 24 h and later subjected to DNA extraction, library preparation and shotgun metagenomic sequencing. Sequence data were analysed using in-house bioinformatics pipelines to determine microbiota profiles at the genus and species levels and to predict effects on metabolic pathways.

Results: Black rice anthocyanins only had very modest effects on gut microbiota composition compared to controls and the differences were mainly detected at 6 and 12 h. At the phylum level, black rice anthocyanins increased the abundance of Bacteroidetes and reduced the abundance of Firmicutes at 6 and 12 h. At species level, at 6 h, the relative abundance of *Bacteroides vulgatus* increased by 6 % in the presence of black rice

anthocyanins compared to a 2 % increase in controls. In addition, in the presence of anthocyanins, there were very small increases in *Citrobacter freundii* and *Ruminococcus torques* at 6 and 12 h. However, in both anthocyanin-treated and control samples, *Bifidobacterium longum* dominated the microbial profile at the end of the 24 h fermentation. Additionally, *Klebsiella oxytoca* was shown to be involved in ortho-cleavage degradation pathway of catechol and 4-methylcatechol, but no significant differences were observed between controls and plus anthocyanins treatments. Furthermore, no significant abundance of known microbial genes was observed to be involved in anthocyanin metabolism, such as β -glucosidase and protocatechuate decarboxylase.

Conclusions: The data presented here show that exposure of human colon microbiota to a high concentration of anthocyanins had surprisingly little effect on gut microbiota structure and function. This may indicate that the ability to degrade anthocyanins is widespread among the human gut microbiota and anthocyanin exposure is not particularly selective.

7.2. Introduction

As described in chapter 1 and reported in the literature, anthocyanins are poorly bioavailable. Only a tiny fraction of ingested anthocyanins are absorbed in the small intestine, and the anthocyanins are mainly in conjugated forms (i.e., methyl or sulphate conjugates)^{37,99}.

In the literature and chapter 1, it was hypothesised that the health benefits of anthocyanins are due to the interaction between anthocyanins and the human gut microbiota¹⁶⁸. The beneficial effects of anthocyanins are likely to be explained by the generated anthocyanin metabolites by gut microbiota or by anthocyanins/anthocyanin breakdown products increasing the abundance of beneficial microbes in the human gut¹³⁷ such as *Bifidobacterium spp.* and *Lactobacillus spp.* which have been reported to benefit human health^{161,168,264}. However *in vitro* studies reported that anthocyanins were degraded by the faecal microbiota³⁷, this was also shown in chapters 4 and 6 where anthocyanins

undergo microbial metabolism in a model of the human colon, and this generates distinct metabolites.

Although it was also hypothesised in the literature that anthocyanins may shift the structure of the human gut microbiota, the strength of this relationship is still superficial, especially as these studies showed little evidence for structural changes in the gut microbiota in response to anthocyanin treatments^{137,168}. Nevertheless, few studies reported that structural changes of the gut microbiota were observed. For example, Hildago and others used *in-vitro* incubation of Mal3Glc with faecal gut microbiota¹⁷⁷. They reported that there was considerable growth of *Bifidobacterium spp.* and *Lactobacillus spp.*, whilst gallic acid (a known microbial anthocyanin metabolite) reduced the relative abundance of *Clostridium histolyticum* without negatively affecting beneficial bacteria. This effect is supported by Queipo-Ortuno and others who reported that the growth of *C. histolyticum* in human faeces was decreased when incubated with red wine extract, however, notably red wine comprises a complex mixture of polyphenols so this effect cannot be directly attributed to anthocyanins¹⁹³.

In chapter 1 (Section 1.9), *in-vitro* and animal studies were reviewed for evidence on the effects of anthocyanin consumption on gut microbiota structure. However, the common outcome between *in-vitro*, animal and human studies was that anthocyanins are commonly associated with increases in *Bifidobacterium* and *Lactobacillus* species. However, very little is known about how the gut microbiota is altered upon treatment with anthocyanins and in response to the appearance of ring fission products during fermentation.

7.3. Objectives

The overall aim of the research presented in this chapter was to determine the effects of anthocyanin exposure on the structure and function of the human gut microbiota. The approach was to expose a human faecal microbiome to purified anthocyanins for 24 h and to collect samples periodically for subsequent DNA extraction and metagenomics analysis. The metagenomic sequence data was interrogated to assess changes in the

relative abundance of bacteria compared to a control (without added anthocyanin) and to assess any changes in the relative abundance of bacterial genes.

7.4. Results

In *in-vitro* colon models, purified black rice anthocyanins were used to investigate the impact of anthocyanins on the gut microbiota structure and function. Briefly, twelve *in-vitro* colon model vessels were inoculated with 1% human slurry, where seven vessels (anthocyanin treated) were treated with black rice anthocyanins ($n=7$) and seven vessels (Control) where no black rice anthocyanins were added ($n=7$) (**Figure 7. 1**). Two additional vessels contained only autoclaved colon media as contamination controls ($n=2$). The incubation was carried out over 24 h, and 5 mL samples were collected at 0, 6, 12, and 24 h for DNA extraction (**Chapter 2, section 2.4.2**). The extracted DNA was sequenced using metagenomic shotgun analysis, then the metagenomics dataset was used to perform bioinformatic analysis.

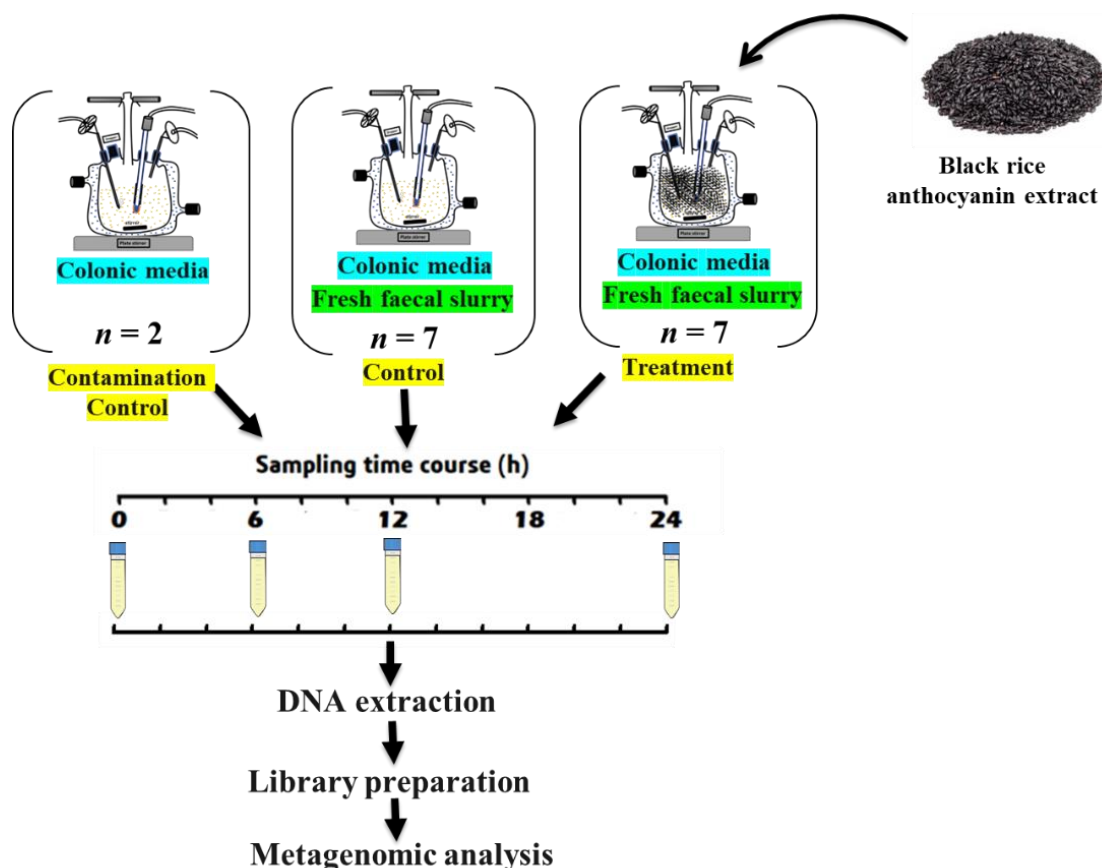


Figure 7. 1. Schematic of experimental design for investigating the effects of black rice anthocyanins on the composition of the human faecal microbiota using an in-vitro human colon model.

Black rice anthocyanins were incubated with fresh faecal slurry, where the faecal sample (S1) was collected on the day of the experiment from donor 08. Control vessels were prepared by inoculating sterile colon media with the same faecal inoculum and no black rice extract was added. Other control vessels were prepared by only incubating sterile colon media for contamination control. Incubation was carried out at pH 6.6-7.0, 37°C, over 24 h. Samples (5 mL) were collected at the times shown in the figure, and DNA was extracted, quantified, and sent for library preparation and metagenomic sequencing.

7.4.1. Bacterial growth during the *in-vitro* colon model fermentations

The first step was performing bacterial counts over the time course of the *in-vitro* colon model fermentation (0, 6, 12, 24 h). The *in-vitro* colon model was prepared as described in chapter 2 (Section 2.2.4-5). The final faecal sample concentration was 1 % w/v in colon media. For counting the bacterial numbers, three samples were collected from three different vessels ($n=3$). Afterwards, serial dilutions (10^{-1} , 10^{-2} , 10^{-3} , 10^{-4} , 10^{-5} , and 10^{-6}) were prepared in sterile deoxygenated PBS and plated onto petri dishes containing colon media agar. The plates were incubated anaerobically for 48 h and then bacterial colonies were counted.

Bacterial colony numbers were similar between control and treatment vessels at 0 and 6 h incubation (**Figure 7. 2**). At 0 h, the number of bacterial colonies was $1.3 \pm 0.17 \times 10^6$ and $1.2 \pm 0.12 \times 10^6$ in control and anthocyanin-treated vessels, respectively. At 6 h incubation, the number of bacterial colonies considerably increased to reach $7.9 \pm 1.5 \times 10^7$ ($\uparrow 6000\%$) and $9.0 \pm 4.8 \times 10^7$ ($\uparrow 7200\%$) in control and treatment samples, respectively. Compared to 6 h, bacterial colony numbers were increased at 12 h in control and anthocyanin-treated samples ($\uparrow 220$ and 260% , respectively), but they were slightly lower in control vessels ($2.6 \pm 0.5 \times 10^8$) compared to treatment vessels ($3.2 \pm 0.4 \times 10^8$). At 24 h, there were no further increases in bacterial colony numbers compared to 12 h samples. For example, the number of bacterial colonies slightly decreased ($\downarrow 14\%$) in treatment vessels to be $2.8 \pm 0.4 \times 10^8$, whereas in control vessels bacterial colony numbers were $1.3 \pm 0.1 \times 10^8$ at 24 h, showing a considerable decline ($\downarrow 50\%$) in viable bacterial cells.

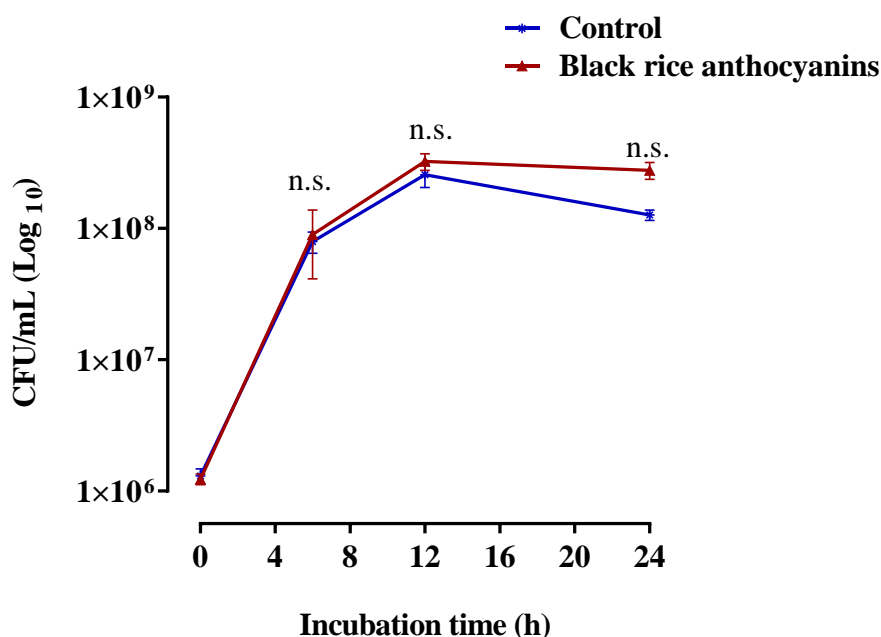


Figure 7. 2. The bacterial growth curve during batch colon model fermentation over 24 h.

Black rice anthocyanin extract was incubated in seven vessels ($n=7$) containing live faecal slurry (treated vessels), where the faecal sample (S1) was collected on the day of the experiment from donor 08. Control vessels ($n=7$) were prepared by inoculating sterile colon media with fresh faecal inoculum and no black rice extract was added (non-treated vessels). Incubations were carried out at pH 6.6-7.0, 37°C , over 24 h. For bacterial growth calculation, three samples (0.5 mL) were collected from both control and treatment vessels at the times shown in the figure. Afterwards, serial dilutions were prepared and spotted on 1% agar colon media. Data are presented as triplicates ($n=3$) and values are represented as means \pm SD. Statistical analysis was carried out with a Mann-Whitney U-test for each time point and **** $p < 0.0001$; *** $p < 0.001$, ** $p < 0.01$, * $p < 0.05$.

7.4.2. Microbial community profiling

For microbial community profiling, host DNA contamination is expected in metagenomics datasets, hence the metagenome was first processed using KneadData to remove host, contaminant, and adapter sequences, then quality control was performed using Trimmomatic (**Chapter 2, section 2.4.5**). Only high quality trimmed, and non-contaminant paired reads (in which both reads passed filtering) were used for downstream analyses. High quality and trimmed reads were used to estimate the microbial composition profiles using MetaPhlAn v3.0.2^{202,203}. MetaPhlAn identifies the microbes and their abundance from metagenomics reads by mapping them to the ChocoPhlAn database of unique clade-specific marker genes. Clades are group of organisms and clade-specific markers are coding sequences that are strongly conserved within the clade's genomes and are sufficiently different to any sequence outside the clade. The marker genes in the ChocoPhlAn database were identified from over 17,000 reference genomes from bacteria, archaea, viruses, and eukaryotes²⁰³.

Heatmaps were used to visualise the relative abundance of the microbial communities. Figure 7.3 shows the heatmaps with hierarchical clustering using the top 50 species, and Bray-Curtis distance for samples and species (**Figure 7. 3**). The microbial profiles for all samples at 0 h were very similar, which is expected as these samples were taken at the start of the experiment and originated from one donor. However, as can be seen from the heatmap profiles, samples collected after 6 h and 12 h were slightly different from those at 0 h, and those collected at 24 h were also different from the 0 h profile as well as the 6 and 12 h profiles, indicating a shift in microbial community over the incubation period. This is further demonstrated in the multidimensional scaling plot (MDS).

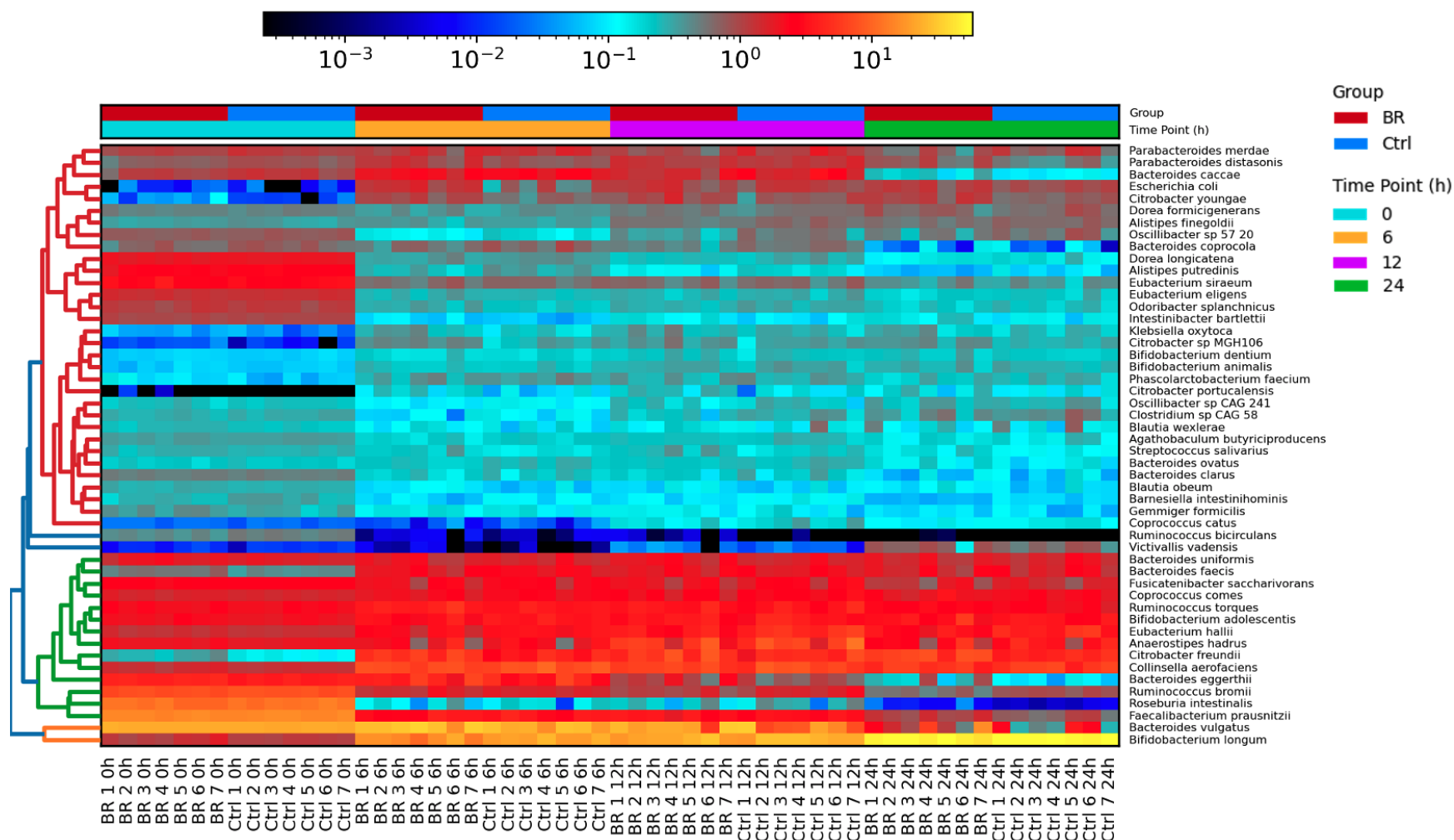


Figure 7.3. Hierarchical clustering of microbial profiles showing samples ordered by time point (columns) for the top 50 species. Clustering by feature (species) was performed with Bray-Curtis distance. As expected, there is a uniform taxonomic profile for samples at 0 h, which then changes over time for both control (Ctrl) and black rice anthocyanin samples (BR).

An MDS plot was constructed to explore the microbial profile at each time point and the effect of anthocyanin treatment on these microbial profiles. The MDS plot (**Figure 7. 4**) shows that there was time dependent clustering of the microbial composition. Three distinct clusters were observed: all 0 h samples were closely clustered together on the right side (red triangles and circles), while the 6h (magenta) and 12h (green) samples were more closely clustered in the middle of the plot with a slight shift of the 12 h, samples to the left, and 24 h samples (blue) clustered on the left. The clustering of the 0 h samples was expected since these samples were collected at the start of the experiment and originated from the same donor. While at 6 and 12 h, most of the control samples tended to cluster on the lower part of the plot compared to the anthocyanin treated samples, the differences in the clustering were not so distinct as to provide a clear separation between the control and the anthocyanin treated samples. As such, the plot shows that samples were clustered depending on time points, and there are no clear differences observed in the microbial composition between treatment and control.

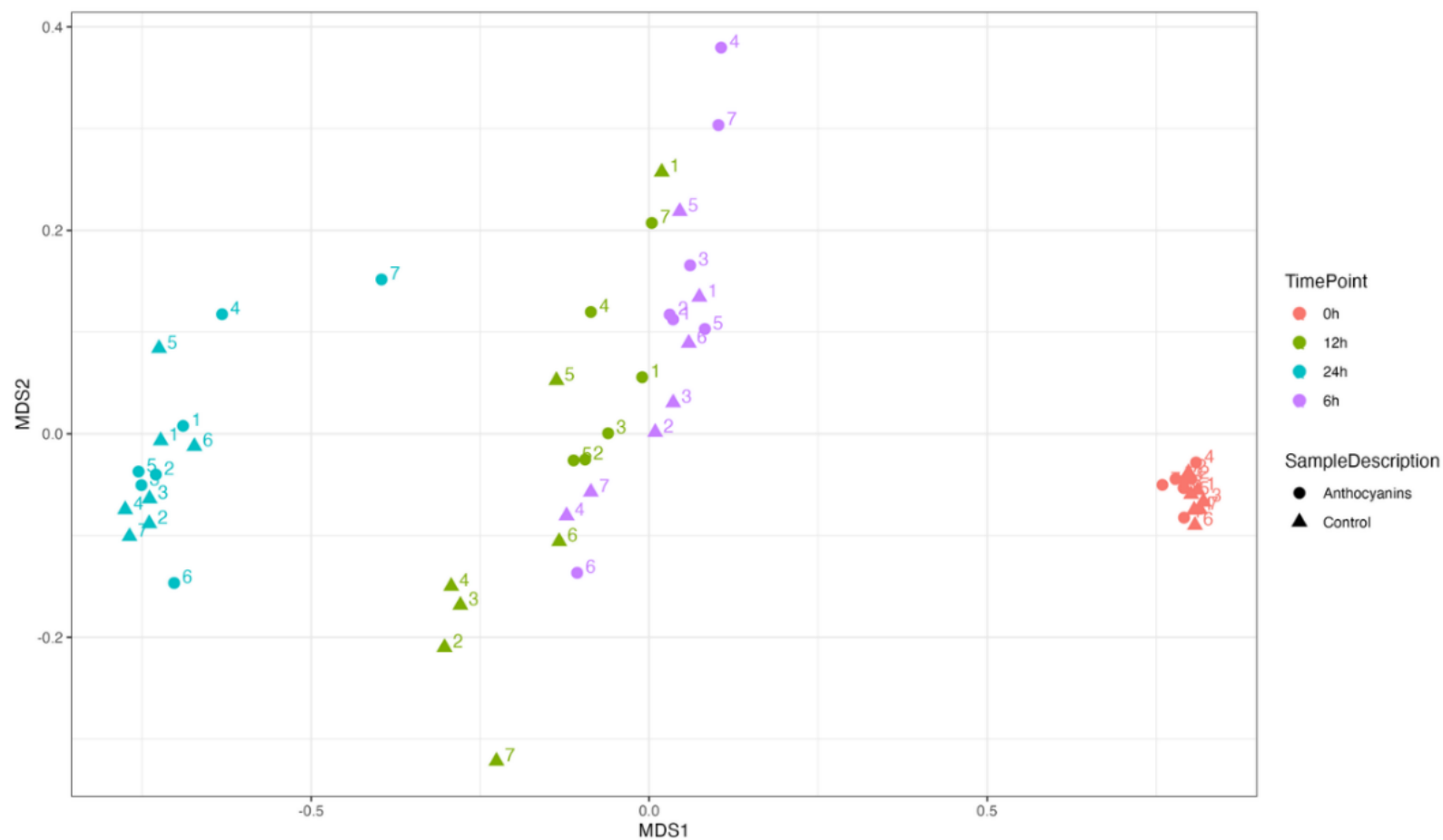


Figure 7. 4. MDS plot where the time point is colour-coded, triangles represent control samples, and circles represent samples from vessels treated with anthocyanins.

The figure shows samples at 0 h (red), 6 h (magenta), 12 h (green) and 24 h (blue). Samples taken at the start and end of the experiment, 0h and 24 h, clearly differed from each other and samples at 6 h and 12 h.

7.4.3. Microbial composition: Taxonomic profiling

Next the relative abundances of the top 10 genera were explored. Although the bar chart showed no clear differences between treatments and controls, the data shown in **Figure 7.5** indicated that the relative abundances at the genus level were different at 6, 12 and 24 h compared to the 0 h samples. For example, the relative abundance of the genus *Bifidobacterium* was shown to increase over time to reach its highest abundance at 24 h. In addition, compared to the relative abundances at 0 h, *Bacteroides* slightly increased at 6 h, then decreased at 12 h and continued to further decrease to its lowest level at 24 h. While at 0 h, *Faecalibacterium*, *Ruminococcus* and *Roseburia* were present at high levels, before declining considerably at 6, 12, and 24 h. The proportion of *Anaerostipes* increased slightly at 12 h compared to 0 and 6 h, but again declined at 24 h. However, the abundance of *Blautia* remained relatively constant over the time course of incubation. Furthermore, the relative abundance of *Citrobacter*, *Collinsella* and *Eubacterium* were relatively lower at 0 h, but they increased at 6 h with the relative the abundance plateauing at 12 h and remaining at constant level until 24 h. No statistically significant differences were observed at the genus level were observed between anthocyanin treated and control vessels.

Following the lack of significant difference in the microbiota at genus level, the effects of anthocyanin treatment on the 10 most abundant species in the dataset were assessed. Specific profile alteration in the faecal microbiota between anthocyanin-treated and non-anthocyanin-treated were observed (**Figure 7.5**). Species profiles for all 0 h samples were similar, both for samples treated with anthocyanins and without. However, the most evident but modest change in community composition was observed at 6 h, where samples treated with anthocyanins had an increase in *Bacteroides vulgatus*, as well as a decrease in *Bifidobacterium longum*. While the relative abundances of some bacterial species changed over time, these changes followed a similar trend in both groups. Overall, there was a slight increase in *Bacteroides vulgatus* in the presence of black rice anthocyanins after 6 h incubation. However, *Bifidobacterium longum* flourished at 12, and 24 h of the incubations in both anthocyanin treated and non-treated vessels.

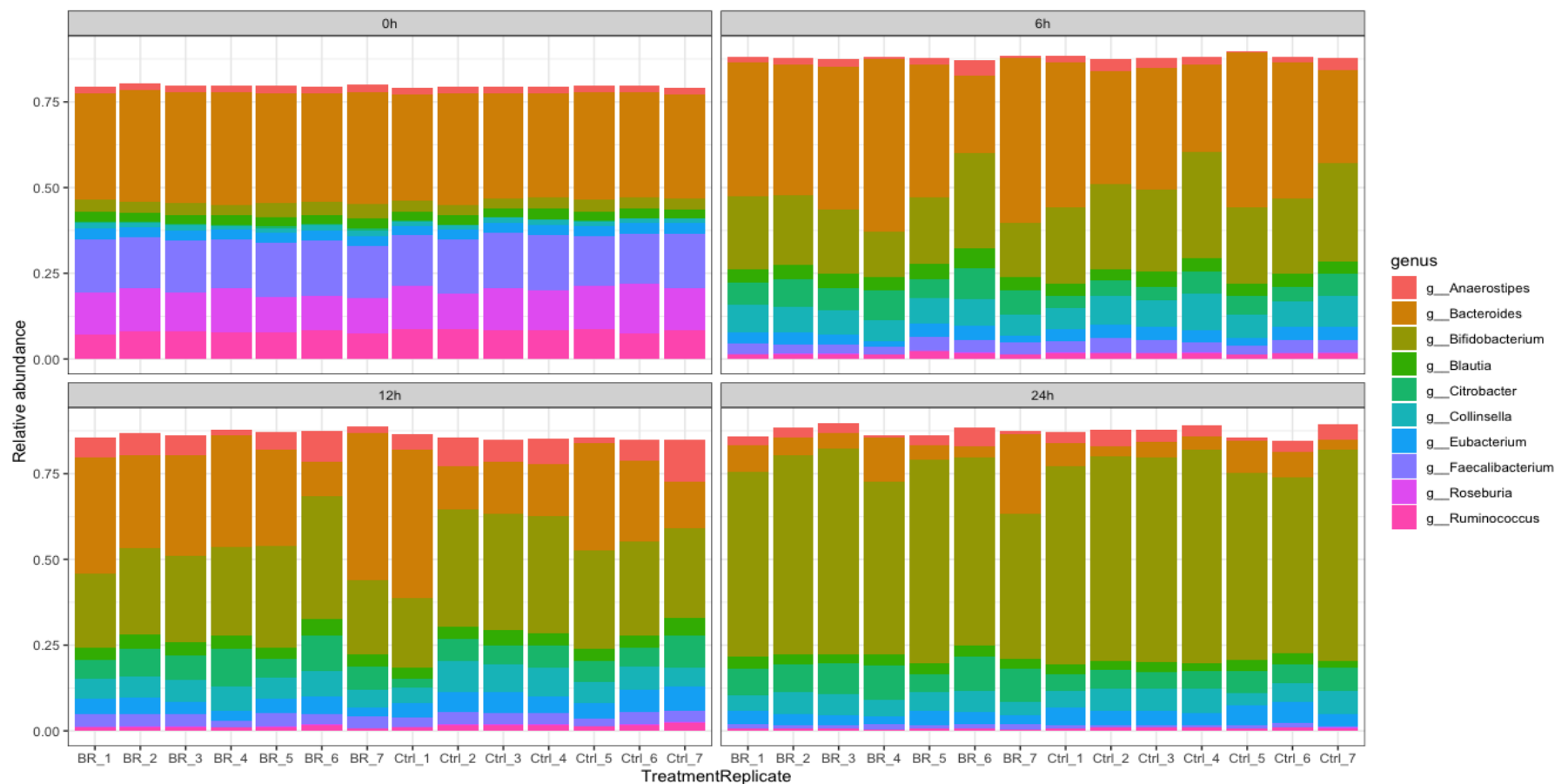


Figure 7. 5. Composition of relative abundances for the 10 most abundant genera for each sample across time at 0, 6, 12, and 24 h. The y-axis shows the relative abundance. Whereas, the x-axis shows the specific samples (treatment and replicate) at different time points, where BR refers to treatment with black rice anthocyanins, while Ctrl refers to control sample where no black rice anthocyanins were introduced.

As can be seen from **Figure 7. 6**, at 24 h *Bifidobacterium longum* was the most predominant species in both the control and treated groups. **Figure 7. 4** indicates that samples at 24 h clustered separately from the samples from 6 and 12 h, as such, the samples from 24 h were eliminated from further analysis. Therefore, the bar chart in **Figure 7. 7** presents the relative abundances of the top 10 most abundant species only at 0, 6, and 12 h time points. *Bacteroides vulgatus* increased over time in anthocyanin treated samples compared to control samples. In addition, in the presence of anthocyanins, the relative abundance of *Citrobacter freundii* was slightly increased but not significantly increased compared to control samples at 6 and 12 h. Compared to control samples, the proportion of *Ruminococcus torques* was also shown to be increased in the presence of anthocyanins but only at 6 h, but it was not statistically significant.

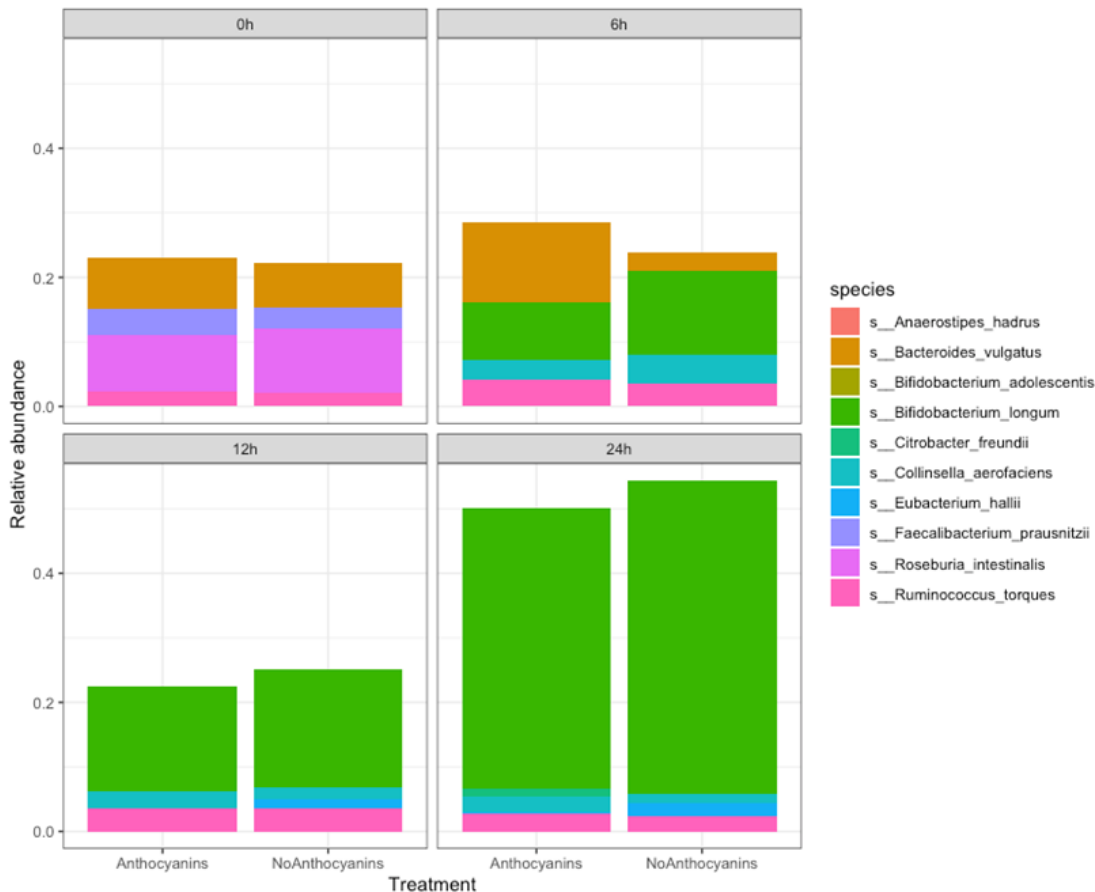


Figure 7. 6. Composition in relative abundances of the top 10 most abundance species in the anthocyanin-treated and non-anthocyanin-treated control samples from the in-vitro colon model collected at 0, 6, 12 and 24 h incubations.

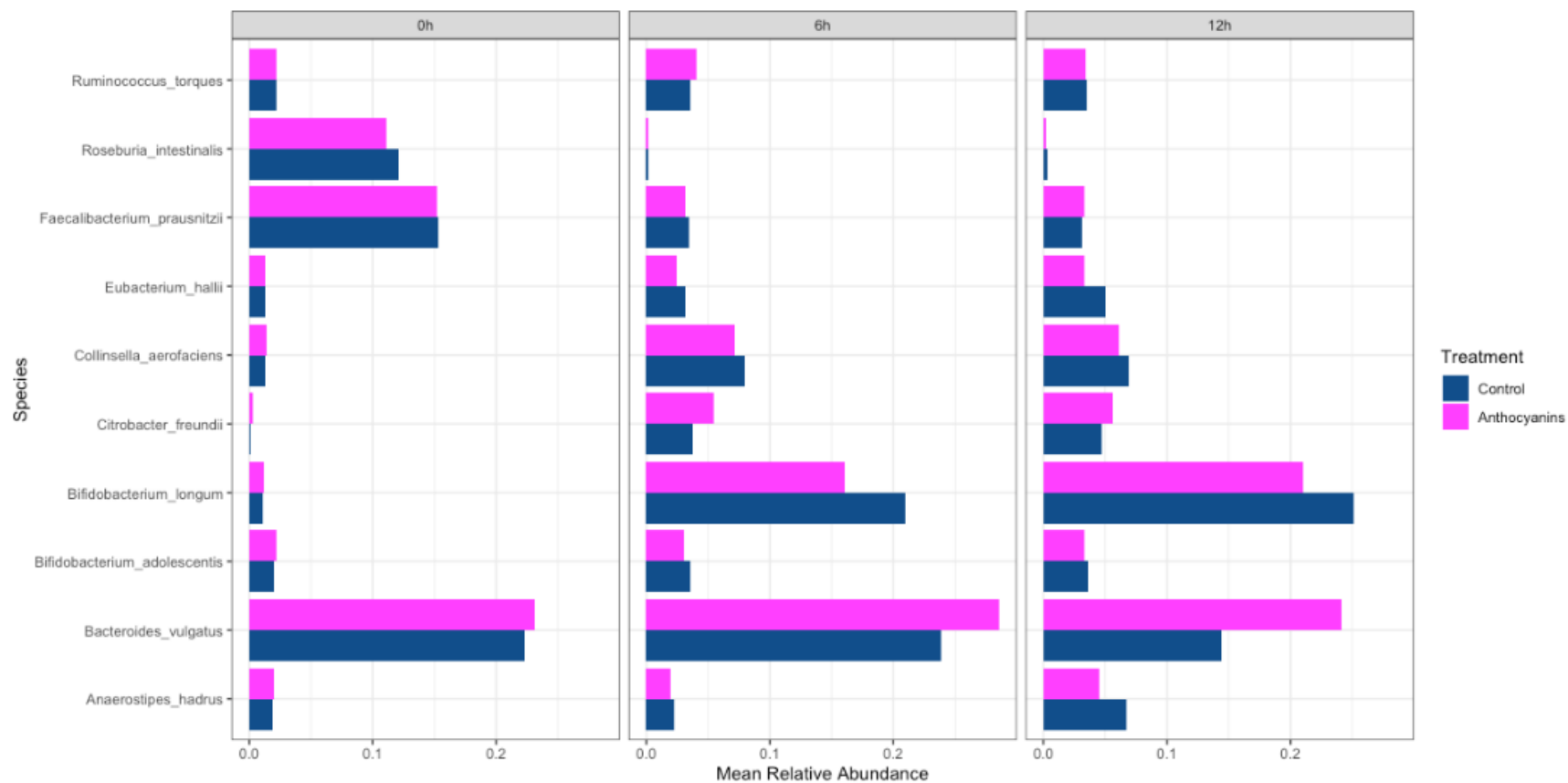


Figure 7. 7. Composition in relative abundances of the top 10 most abundant species in the anthocyanin-treated and non-anthocyanin-treated control samples from the in-vitro colon model at 0, 6, and 12 h time points.

When analyses were carried out at 0, 6 and 12 hr, microbial compositions at the Phylum level were presented using Krona plots²⁶⁵. Similar to reports in the literature, at the start of the experiment, samples at 0 h had a predominance of Firmicutes with an average of 58% of the classified reads, followed by Bacteroidetes with 37% and Actinobacteria with 5% (**Figure 7. 8**).

As incubation time progressed, the microbial composition shifted from what was observed at 0 h and what would be observed in human colonic samples. At 6 h, the microbial composition of control samples had Bacteroidetes as the dominant Phylum (38% of total) followed very closely by Actinobacteria (33%), Firmicutes (23%) and Proteobacteria (6%). However, in samples treated with anthocyanins, Bacteroidetes was also the dominant phylum although with a higher percentage (43%) followed by Actinobacteria (27%), Firmicutes (22%) and Proteobacteria (9%). The proportions of Bacteroidetes and Proteobacteria were higher in samples treated with anthocyanins than observed in control samples, while the proportion of Actinobacteria was slightly lower in the anthocyanin treated samples than in the control samples. However, they were not statistically different.

No significant differences were observed. However, at 12 h, in the control samples the taxonomic composition shifted slightly, and the dominant Phylum became Actinobacteria (36%) followed by Firmicutes (31%), Bacteroidetes (26%) and Proteobacteria (7%). However, in samples treated with anthocyanins, Actinobacteria and Bacteroidetes were the most dominant Phyla (33 and 32%, respectively) followed by Firmicutes (26%) and Proteobacteria (9%). Samples treated with anthocyanins had a higher proportion of Bacteroidetes (32%) compared to Firmicutes (26%), whereas in control samples, the opposite effect was observed, where Firmicutes (31%) had a larger abundance than Bacteroidetes (26%). Finally, samples treated with anthocyanins had higher proportion of Proteobacteria (9%) compared to control samples (7%). A summary of compositional changes at the phylum, genus and species levels is also presented in the following figures (**Figure 7. 9**, **Figure 7. 10**, and **Figure 7. 11**) Next, functional analyses were carried out to determine whether anthocyanin treatment had any effect on specific pathways involved in anthocyanin metabolism.

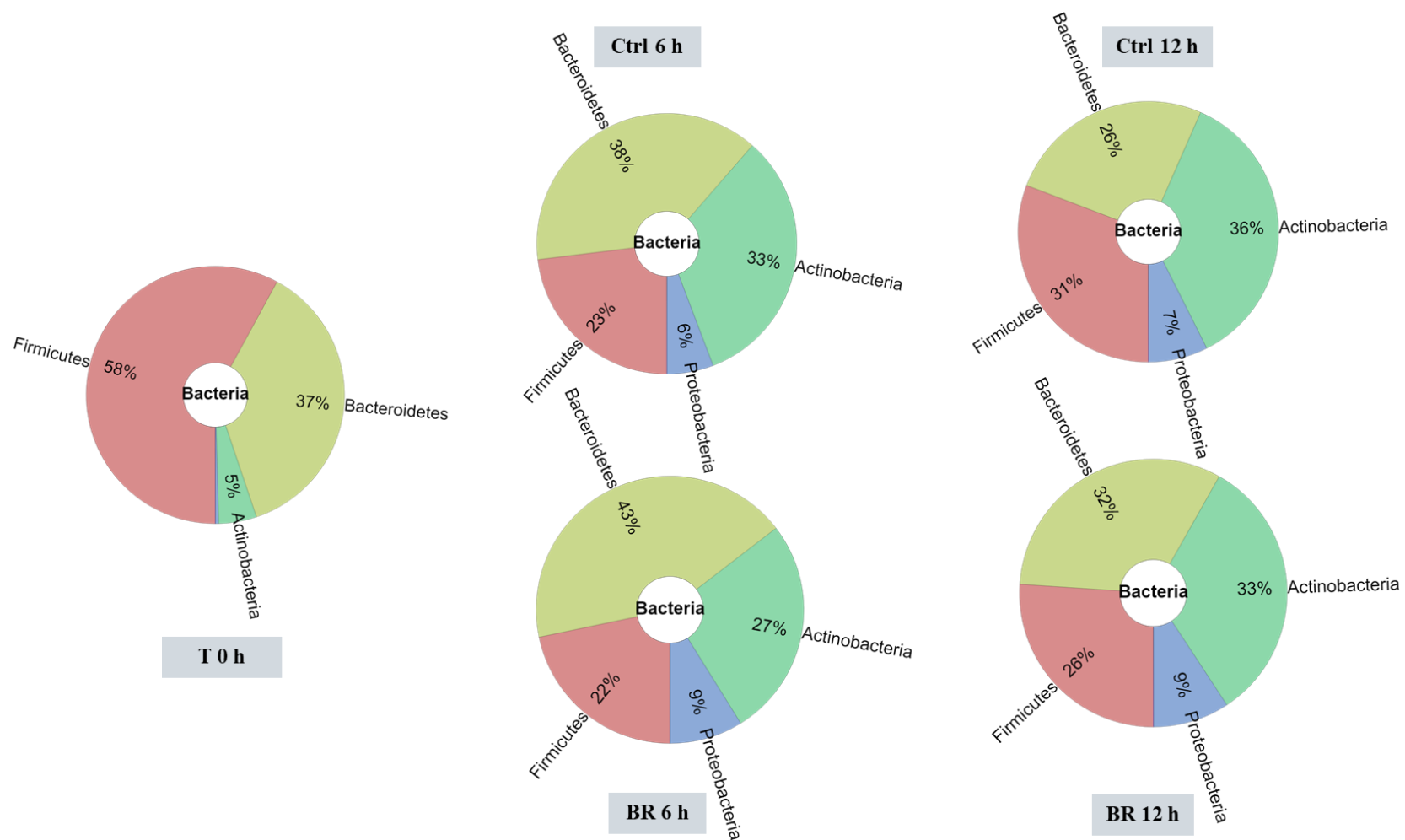


Figure 7. 8. Microbial composition at the Phylum level for samples taken at the start of the experiment (T0), control samples (Ctrl) and samples treated with anthocyanins (BR) at 6h and 12h.

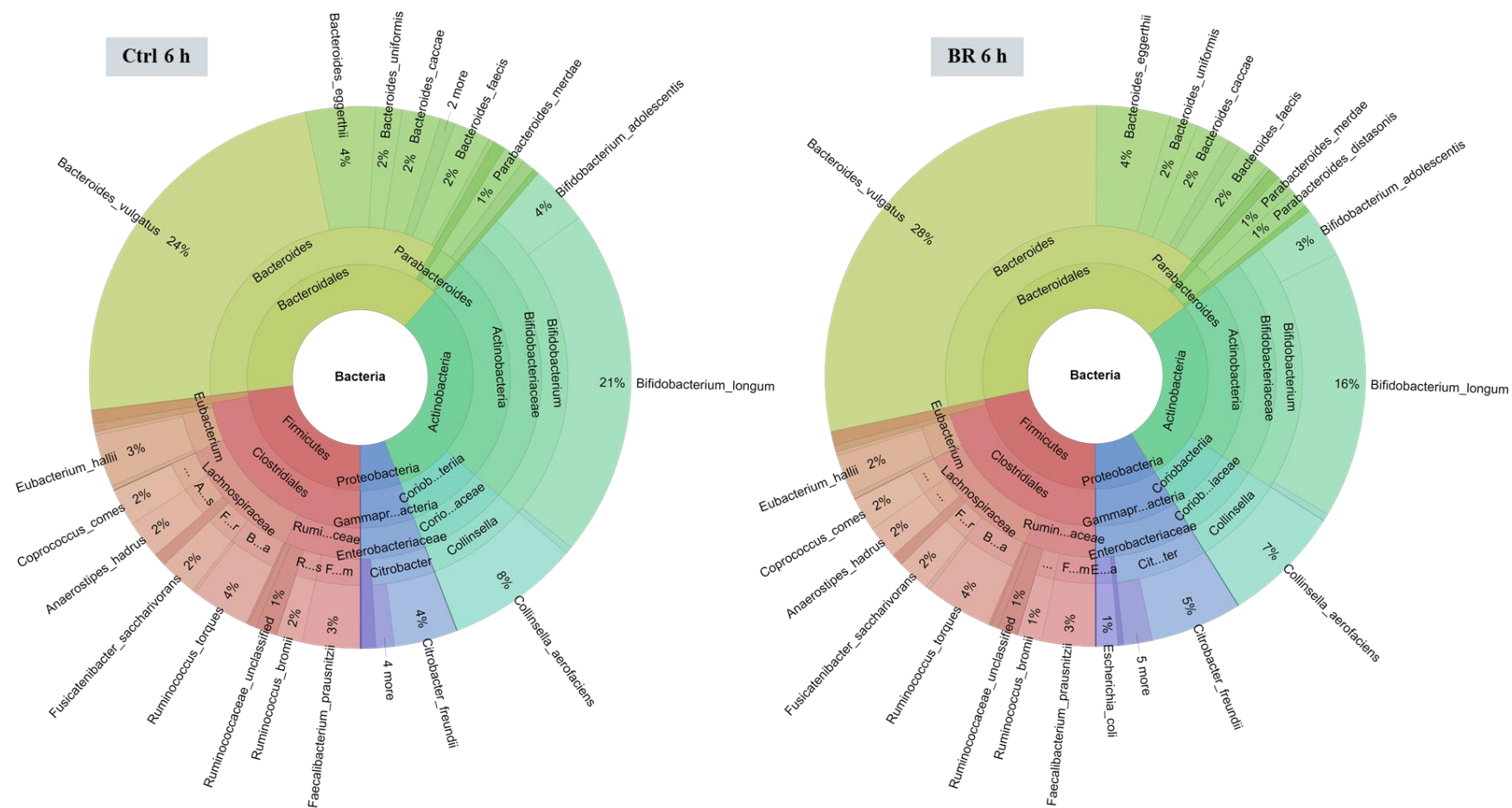


Figure 7. 10. Microbial composition at the species level for control samples (Ctrl) and treated anthocyanins (BR) at 6 h (T6).

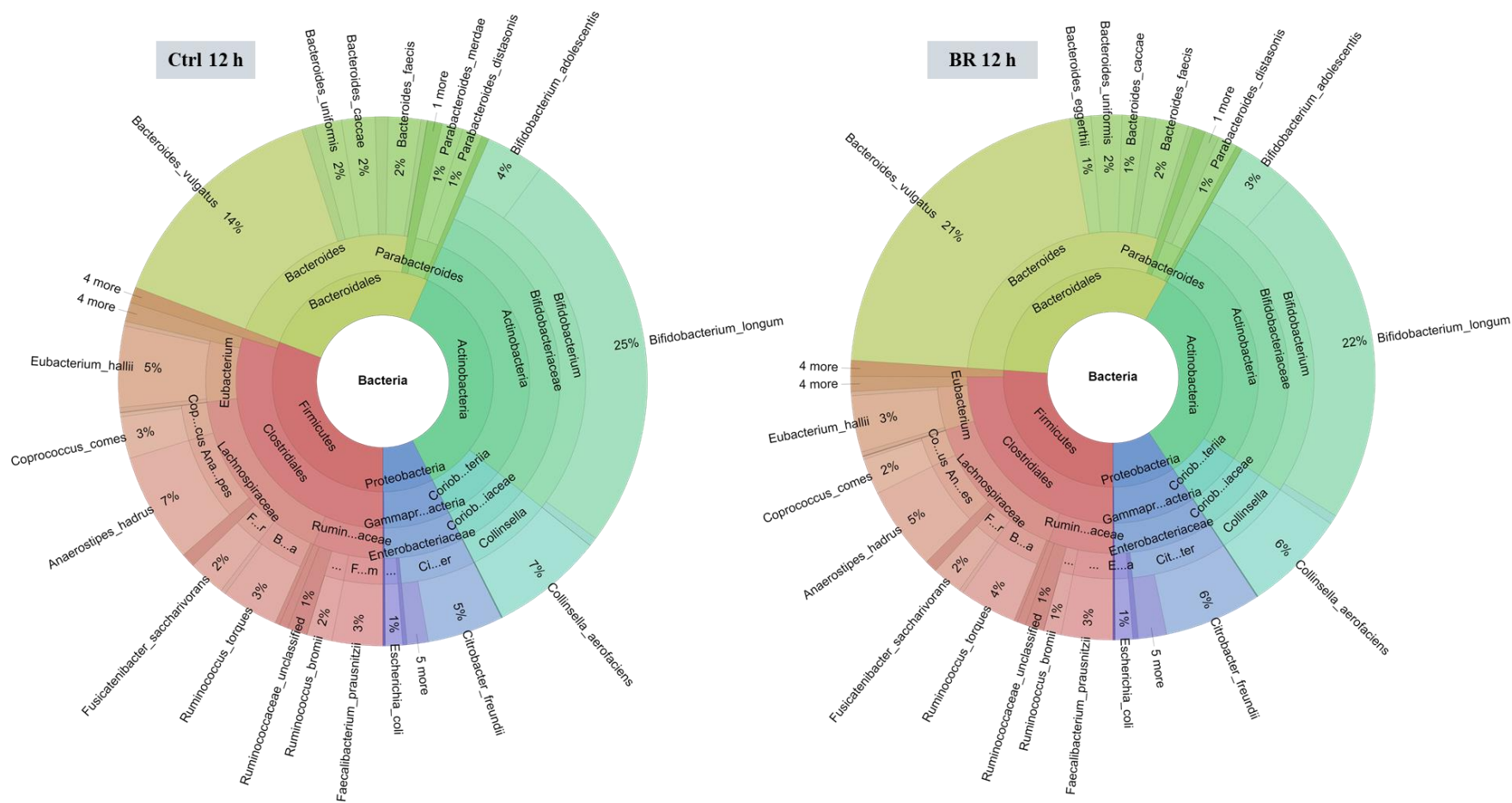


Figure 7. 11. Microbial composition at the species level for control samples (Ctrl) and treated anthocyanins (BR) at 12 h (T12).

7.4.4. Functional analysis: Pathways

After pre-processing of the metagenomics dataset, Metabolic Reconstruction and Pathway Analysis using HUMAnN3 (**Chapter 2, section 2.4.7**) was used for functional analysis. MaAsLin2, selecting Linear Model (LM) method, was used to test the association between Pathway relative abundances and the effect of anthocyanins in the microbiome (**Chapter 2, section 2.4.8**). Whole-genome shotgun metagenomics has the advantage of sequencing to a high enough resolution to study community structures, phylogenetic composition, species diversity, metabolic capacity, and functional diversity and to facilitate maximal capture of organismal and functional data of the microbiota ²⁶⁶. HUMAnN3 was employed for profiling the abundance of microbial metabolic pathways and other molecular functions. MaAsLin2 is used to find associations between community total abundances with the effect of the treatment over time (**Chapter 2, section 2.4.8**)

Several metabolic pathways were chosen from several hundred that were considered likely to be relevant to anthocyanin metabolism to show the metabolic capacity of the gut microbiota, such as anaglycolysis pathway (Glycolysis III), catechol degradation III (ortho-cleavage pathway), catechol degradation to β -keto adipate, cinnamate degradation to 2-oxopent-4-enoate, 3-hydroxycinnamate degradation to 2-oxopent-4-enoate, and 4-methylcatechol degradation (ortho cleavage). The metabolic pathways were not differed between controls and anthocyanin treatments, the genes for enzymes involved in certain pathways were present at both 6 and 12 h. These pathways are related to catechol that show different effect due to treatment and time. For example, the abundance of genes in the ortho-cleavage pathway of catechol degradation to β -keto adipate (**Figure 7. 12**) and 4-methylcatechol degradation (**Figure 7. 13**) were shown to be different (but not statistically different) between controls (Ctrl) and black rice anthocyanin treated (BR) samples. In both figures, *Klebsiella oxytoca* was the dominant species involved in both ortho-cleavage pathways of catechol and 4-methylcatechol degradation. Although the data show differences over time between samples at the start of the experiment (T0) and samples at 6 and 12 h, no statistical differences were observed between control samples (Ctrl) and black rice treated samples (BR) at 6 and 12 h.

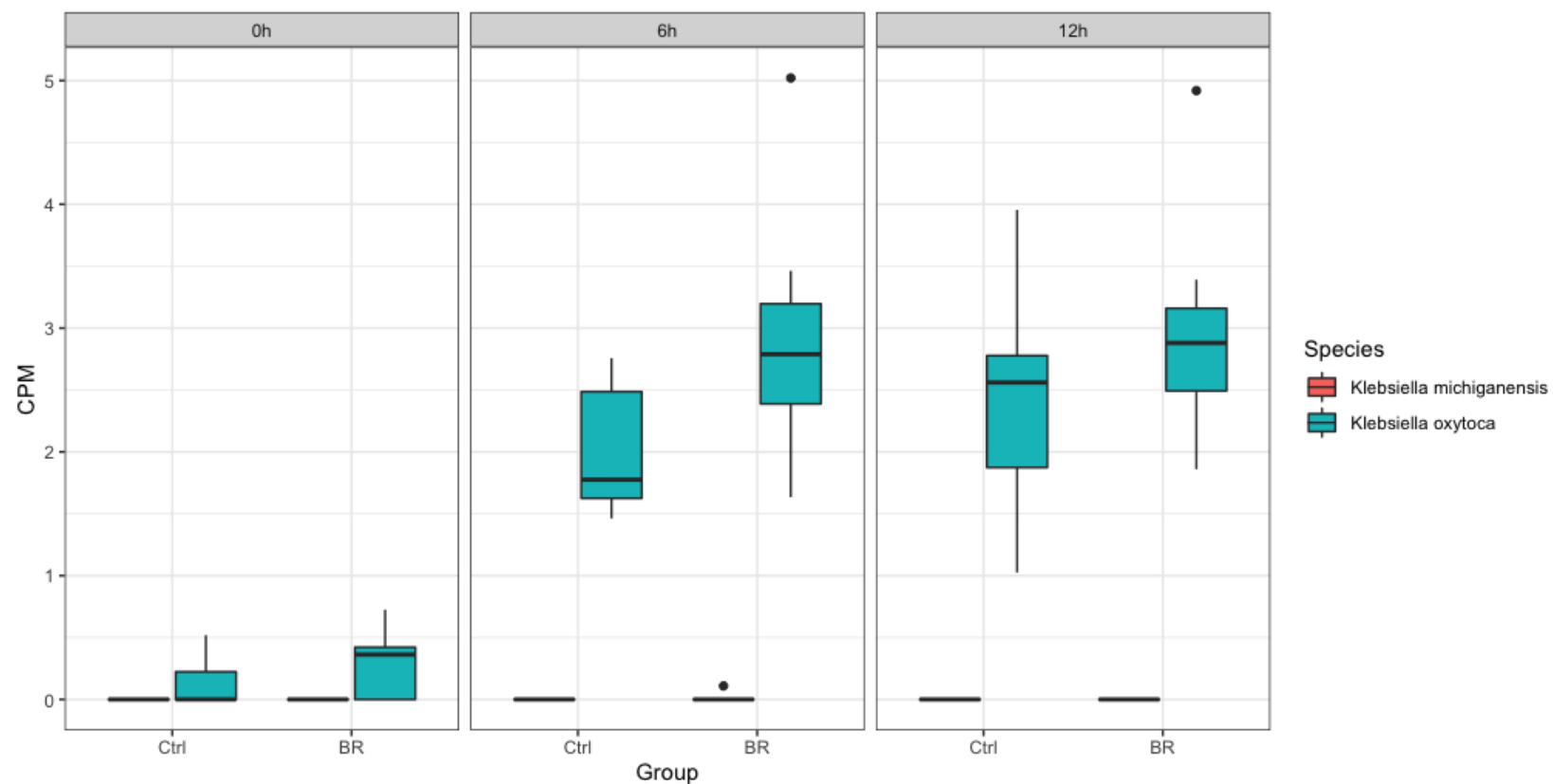


Figure 7. 12. The effect of anthocyanin treatment and time on ortho-cleavage pathway of catechol degradation to β -keto adipate.

The black rice anthocyanins (BR) were incubated into seven colon model vessels which was inoculated with 1% faecal slurry, whereas other seven vessels were only inoculated with 1 % faecal slurry (Ctrl). The y axis shows the abundance of genes expressed as counts per million reads mapped (CPM).

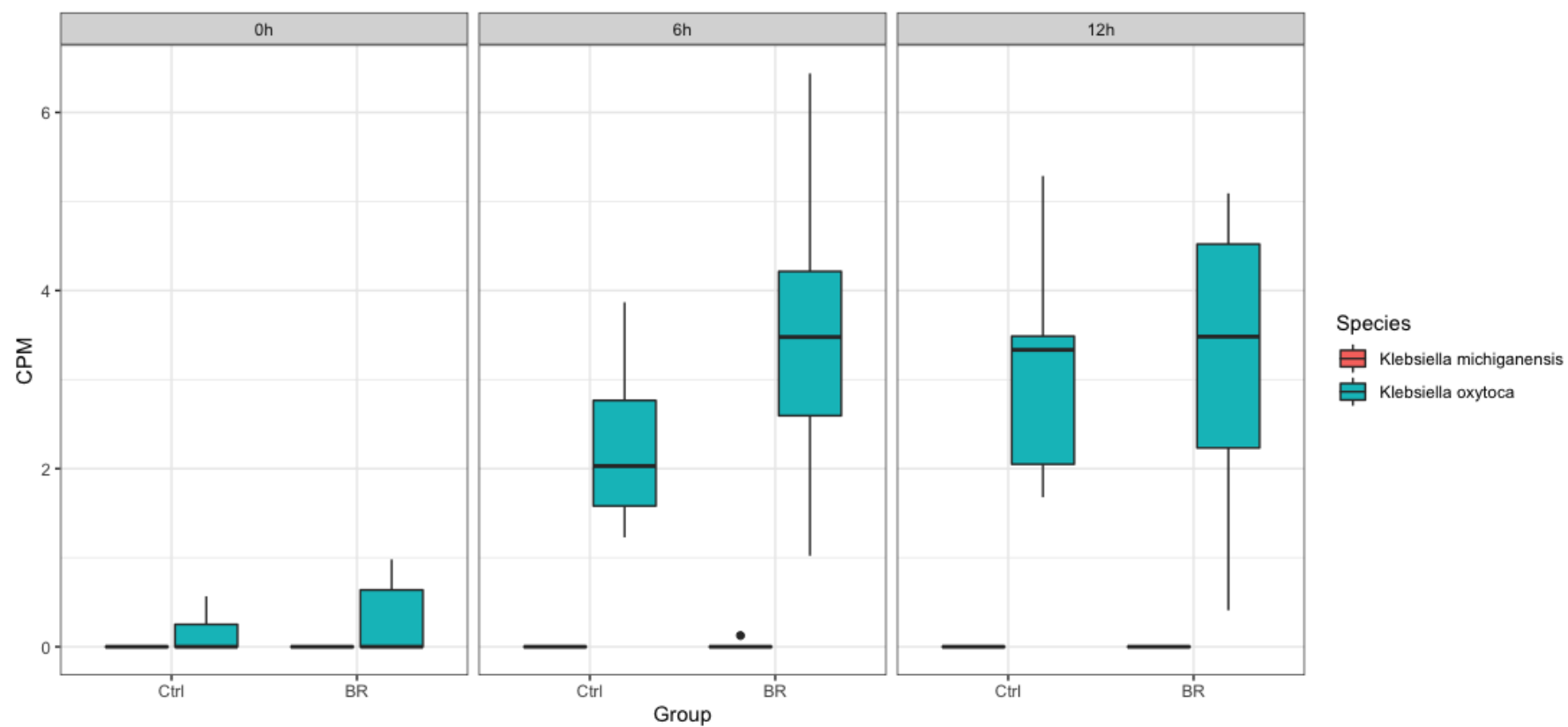


Figure 7. 13. The effect of anthocyanin treatment and time on ortho-cleavage pathway of 4-methylcatechol degradation.

The black rice anthocyanins (BR) were incubated into seven colon model vessels which was inoculated with 1% faecal slurry, whereas other seven vessels were only inoculated with 1 % faecal slurry (Ctrl). The y axis shows the abundance of genes expressed as counts per million reads mapped (CPM).

7.4.5. Functional analysis: Enzyme commission categories

In addition to investigating some metabolic pathways, enzyme commission (EC) categories were also investigated. Enzyme commission numbers (EC numbers) is a numerical classification system that is used to group enzymes on the basis of the chemical reactions that they catalyse. By using the gene family abundances, HUMAnN3 is used to reconstruct the abundance to enzyme commission (EC) categories in the microbiome using the function `humann_regroup_table` (**Chapter 2., section 2.4.7**). MaAsLin2 is used to find associations between community total abundances with the effect of the treatment over time (**Chapter 2, section 2.4.8**). MaAsLin2 was used for selecting Linear Model (LM) method to test the association between EC category relative abundances and the effect of anthocyanins in the microbiome.

The same approach of using EC category relative abundances was carried out and hundreds of EC categories were investigated. Only few EC categories showed the most significant changes in terms of the interaction of treatment and time for samples treated with anthocyanins at 6h and 12h. At 6 h, 20 EC categories were selected that show the most significant changes over time by black rice anthocyanin treatment (BR) (**Table 7. 1**). At 12 h, 20 EC categories that show the most significant changes over time by BR were also selected (**Table 7. 2**). However, there were no apparent changes in the abundance of any genes encoding any of the identified enzymes in response to treatment versus control at both 6 and 12 h. For example, β -glucosidase has been reported to be involved in metabolism of anthocyanins and other flavonoids, which play important role in hydrolysing the sugar moieties from their aglycones^{93,176}. Therefore, 1,4- β - glucosidase was examined where *Roseburia intestinalis* and *Roseburia intestinalis* CAG 13 were shown to be involved in, but no significant difference neither between controls and BR treatments or within the same treatment over time (**Figure 7. 14**). In addition, catechol 1,2-dioxygenase was also investigated which showed increase over time in both controls and BR treatments where *Klebsiella oxytoca* and *Klebsiella michiganensis* were shown to be involved (**Figure 7. 15**). But no significant difference between controls and BR treatments was detected.

Table 7. 1. The 20 EC categories that show the most significant changes by BR anthocyanin treatment at 6h.

Feature	Treatment.Time	coef	stderr	N	N.not.0	pval	qval
2.4.1.20..Cellobiose.phosphorylase	BR.6h	-0.0104895	0.00022129	41	41	4.84E-34	1.79E-30
3.6.3.40..Teichoic.acid.transporting.ATPase	BR.6h	-0.0128894	0.00030545	41	41	2.96E-32	4.39E-29
3.4.13.19..Membrane.dipeptidase	BR.6h	-0.009607	0.00024136	41	41	2.32E-31	2.15E-28
3.6.3.23..Oligopeptide.transporting.ATPase	BR.6h	-0.0032694	8.30E-05	41	14	3.31E-31	2.23E-28
3.2.1.91..Cellulose.1.4.beta.cellobiosidase..non.reducing.end.	BR.6h	-0.0090989	0.00023808	41	41	9.71E-31	5.54E-28
3.5.4.2..Adenine.deaminase	BR.6h	-0.0141788	0.00038099	41	41	2.47E-30	1.22E-27
3.5.2.14..N.methylhydantoinase..ATP.hydrolyzing.	BR.6h	-0.00954	0.00025963	41	38	3.86E-30	1.69E-27
3.2.1.74..Glucan.1.4.beta.glucosidase	BR.6h	-0.0111952	0.00030593	41	38	4.46E-30	1.72E-27
2.7.1.35..Pyridoal.kinase	BR.6h	0.00703876	0.00020093	41	41	2.06E-29	5.66E-27
2.1.1.148..Thymidylate.synthase..FAD.	BR.6h	-0.0109538	0.00031491	41	41	2.64E-29	6.99E-27
1.3.1.74..2.alkenal.reductase..NAD.P.....	BR.6h	-0.0084342	0.00024299	41	41	2.84E-29	7.03E-27
1.10.9.1..Plastoquinol..plastocyanin.reductase	BR.6h	-0.0097879	0.00028441	41	35	3.83E-29	8.61E-27
3.6.3.15..Sodium.transporting.two.sector.ATPase	BR.6h	-0.0087261	0.00025666	41	41	5.86E-29	1.21E-26
2.1.1.191..23S.rRNA..cytosine.1962..C.5...methyltransferase	BR.6h	-0.009002	0.00026653	41	41	7.38E-29	1.40E-26
4.1.99.14..Spore.photoproduct.lyase	BR.6h	-0.0087054	0.00025908	41	38	8.84E-29	1.60E-26
1.3.99.22..Coproporphyrinogen.dehydrogenase	BR.6h	-0.009319	0.00027824	41	41	9.90E-29	1.75E-26
6.3.5.6..Asparaginyl.tRNA.synthase..glutamine.hydrolyzing.	BR.6h	-0.0104751	0.00031456	41	41	1.21E-28	2.09E-26
1.5.1.7..Saccharopine.dehydrogenase..NAD.....L.lysine.forming.	BR.6h	-0.0108025	0.00033566	41	41	3.98E-28	6.02E-26
4.4.1.8..Cystathionine.beta.lyase	BR.6h	0.00989867	0.00031664	41	41	1.09E-27	1.33E-25
4.1.1.32..Phosphoenolpyruvate.carboykinase..GTP.	BR.6h	-0.0070916	0.00022823	41	41	1.35E-27	1.58E-25

Table 7. 2. The 20 EC categories that show the most significant changes for treated samples with BR anthocyanins at 12h.

Feature	Treatment.Time	coef	stderr	N	N.not.0	pval	qval
2.4.1.20..Cellobiose.phosphorylase	BR.12h	-0.010171206	0.000233257	41	41	9.29E-33	1.72E-29
3.6.3.23..Oligopeptide.transporting.ATPase	BR.12h	-0.003269412	8.75E-05	41	14	2.11E-30	1.12E-27
3.4.13.19..Membrane.dipeptidase	BR.12h	-0.009190724	0.000254421	41	41	7.02E-30	2.48E-27
3.2.1.91..Cellulose.1.4.beta.cellulosidase..non.reducing.end.	BR.12h	-0.008985947	0.000250954	41	41	9.56E-30	3.22E-27
3.6.3.40..Teichoic.acid.transporting.ATPase	BR.12h	-0.011182593	0.00032197	41	41	2.78E-29	7.03E-27
3.2.1.74..Glucan.1.4.beta.glucosidase	BR.12h	-0.01103248	0.000322473	41	38	4.71E-29	1.03E-26
3.5.2.14..N.methylhydantoinase..ATP.hydrolyzing.	BR.12h	-0.008728843	0.000273678	41	38	5.44E-28	7.61E-26
6.3.5.6..Asparaginyl.tRNA.synthase..glutamine.hydrolyzing.	BR.12h	-0.010575706	0.000331577	41	41	5.44E-28	7.61E-26
1.10.9.1..Plastoquinol..plastocyanin.reductase	BR.12h	-0.009425623	0.000299793	41	35	8.96E-28	1.15E-25
2.1.1.148..Thymidylate.synthase..FAD.	BR.12h	-0.010314468	0.000331943	41	41	1.35E-27	1.58E-25
2.7.1.35..Pyridal.kinase	BR.12h	0.006579224	0.000211801	41	41	1.36E-27	1.58E-25
1.3.1.74..2.alkenal.reductase..NAD.P.....	BR.12h	-0.007884543	0.000256134	41	41	1.87E-27	2.07E-25
4.1.99.14..Spore.photoproduct.lyase	BR.12h	-0.008361987	0.000273093	41	38	2.25E-27	2.38E-25
3.6.3.15..Sodium.transporting.two.sector.ATPase	BR.12h	-0.008117595	0.000270544	41	41	4.54E-27	4.55E-25
3.2.1.4..Cellulase	BR.12h	-0.013889909	0.000472542	41	41	9.25E-27	8.80E-25
1.1.1.244..Methanol.dehydrogenase	BR.12h	-0.006653433	0.000230067	41	41	1.62E-26	1.51E-24
3.5.4.2..Adenine.deaminase	BR.12h	-0.011443702	0.000401599	41	41	2.70E-26	2.36E-24
2.1.1.191..23S.rRNA..cytosine.1962..C.5...methyltransferase	BR.12h	-0.007879556	0.000280948	41	41	4.68E-26	3.93E-24
4.4.1.8..Cystathionine.beta.lyase	BR.12h	0.009268408	0.000333771	41	41	6.59E-26	5.37E-24
1.5.1.7..Saccharopine.dehydrogenase..NAD.....L.lysine.forming.	BR.12h	-0.0096473	0.000353817	41	41	1.24E-25	9.44E-24

3.2.1.74: Glucan 1,4-beta-glucosidase

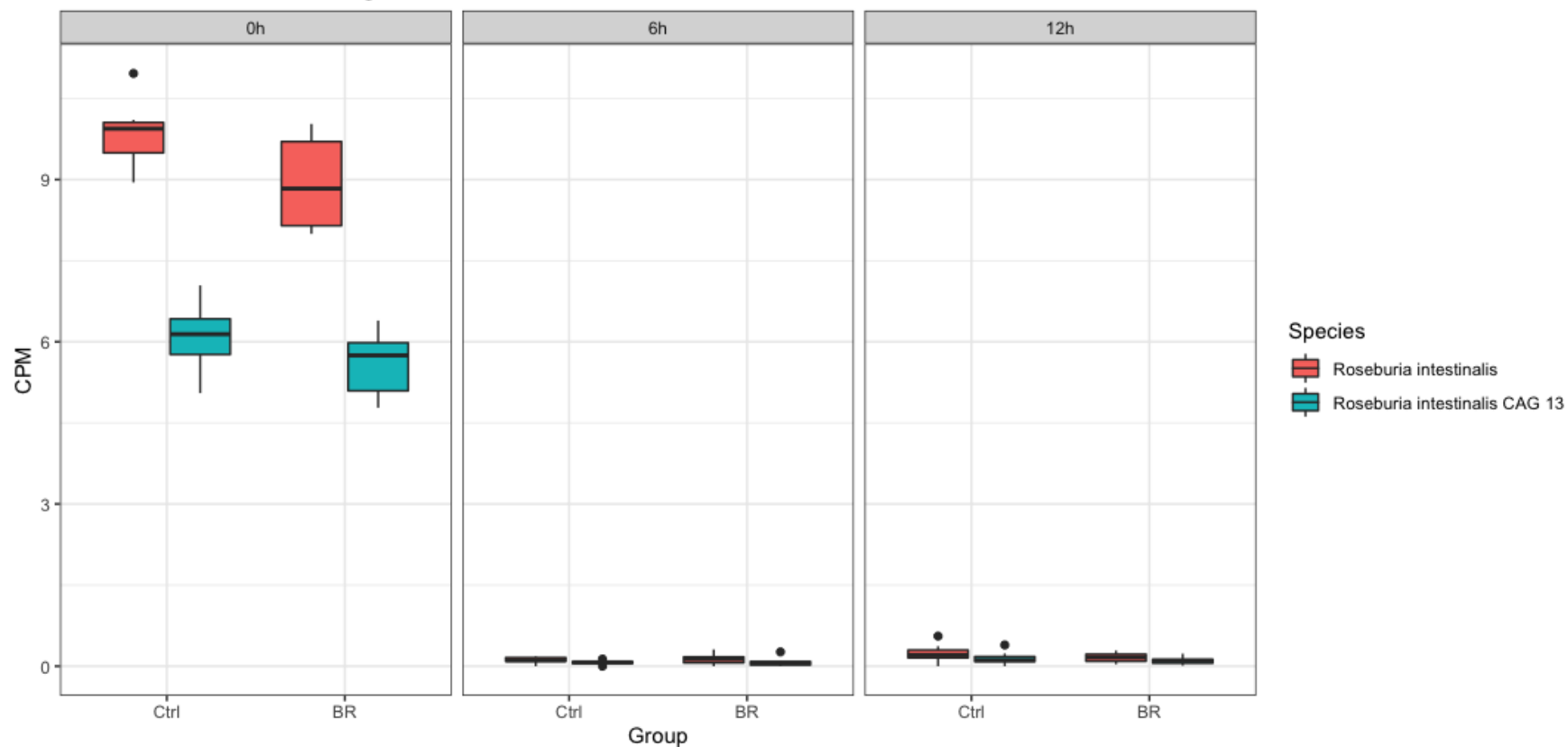


Figure 7. 14. The relative abundances of species level for the EC glucan 1,4- β -glucosidase that presented different relative abundances due to anthocyanin treatment and time.

Relating community-total abundance to the groups and time points showed that both samples treated with anthocyanins (BR) and controls (Ctrl) exhibit no enrichment of the genes involved in production of 1,4- β -glucosidase at 6 h and 12 h. The y axis shows the abundance of genes expressed as counts per million reads mapped (CPM).

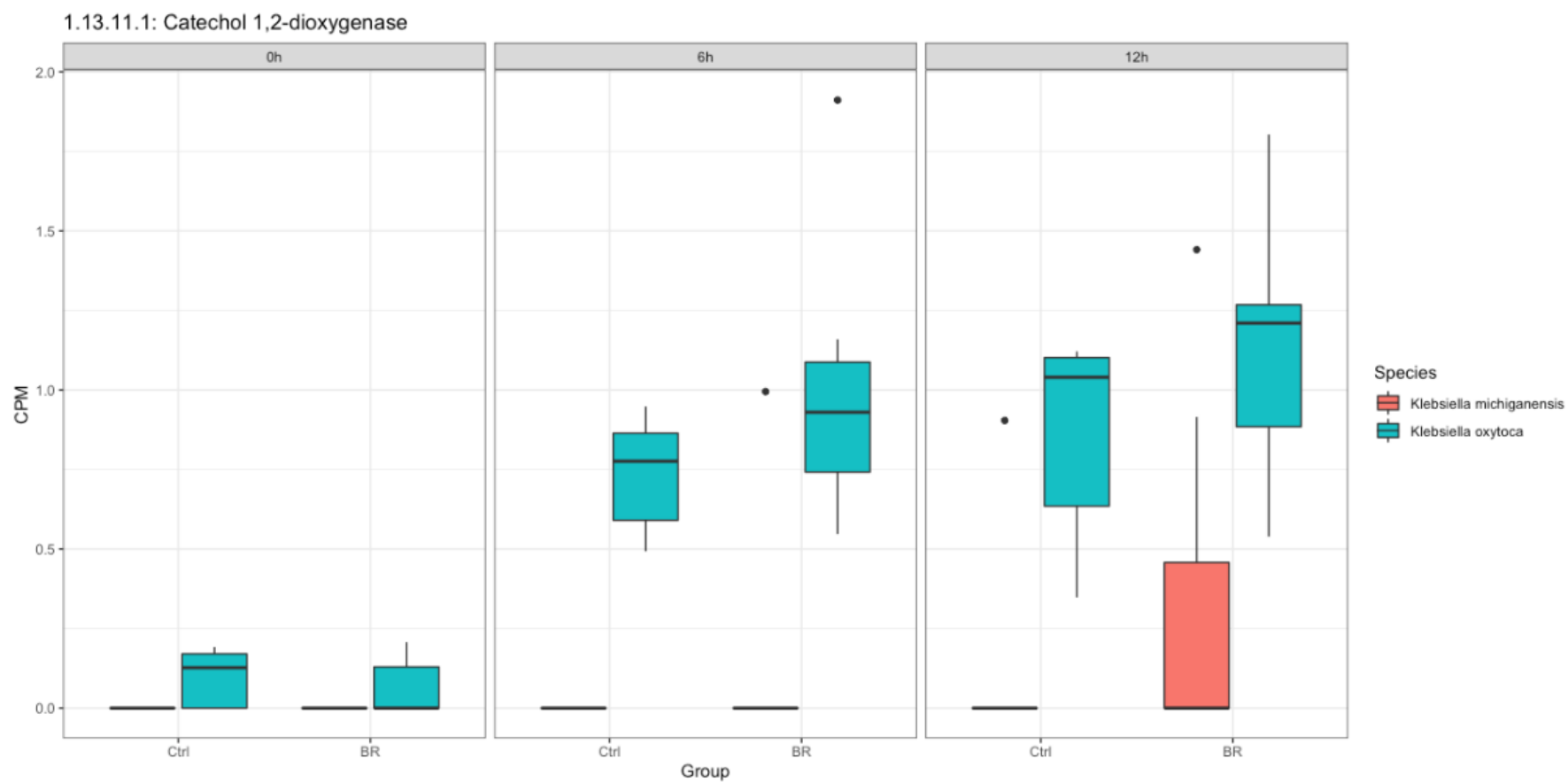


Figure 7. 15. The relative abundance for Pathway 1.13.11.1: Catechol 1,2-dioxygenase, compared the relative abundance for the two *Klebsiella* species in the pathway: *Klebsiella oxytoca* and *Klebsiella michiganensis*.

Relating community-total abundance to the groups and time points showed that samples treated with anthocyanins exhibit a higher enrichment of the pathway compared to control samples at 6 h and 12 h. The y axis shows the abundance of genes expressed as counts per million reads mapped (CPM).

7.5. Discussion

The aim of this chapter was to determine how treatment with anthocyanins affects the structure and function of the human colonic microbiome, which was assessed using an *in-vitro* human colon model and comparing anthocyanin treatments to controls, and monitoring over time using shotgun metagenomics.

The main findings in this chapter were that (i) mild effects (but not statistically different) were observed with black rice anthocyanins on the gut microbiota composition of one donor, (ii) black rice anthocyanins reduced the abundance of the phylum *Firmicutes* and increased the abundance of the phylum *Bacteroidetes* but no statistical significant was observed, (iii) *Bacteroides vulgatus* was considerably increased (not significant difference) at 6 h in the presence of black rice anthocyanins, (iv) *Bifidobacterium longum* dominated the microbial profiles at the end of incubations in both control and treatment, and (v) the genes putatively involved in the ortho-cleavage degradation pathway of catechol were shown to be present in *Klebsiella oxytoca* and increased in the presence of anthocyanins, although this was not significant.

Data presented in this chapter showed mild changes with no significant differences on the gut microbiome structure after the treatment of black rice anthocyanin extract. However, several studies that have investigated the effect of anthocyanins on the gut microbiota profile have reported that anthocyanins increase the abundance of beneficial *Bifidobacteria* and *Lactobacilli* species^{2,164,177,192,195}. Data presented in this chapter, however, showed no substantial effect on these genera after black rice anthocyanin treatments. This may suggest that anthocyanins may not modulate the composition of the human gut microbiota. This is in agreement with a human study reported by Percival, who stated that no significant effects of black rice and bilberry anthocyanins on the structure of the participants' gut microbiota²⁵⁸. Although the mild or may be no-effect of anthocyanins on the gut microbiota composition were shown in this chapter, the data was obtained from the use of a faecal sample from a single donor. In chapter 4 and 6, different inter-individual variations were shown in the metabolism of anthocyanins. Therefore, it is possible that this variation in between individuals in anthocyanin metabolism is also exist for the notion of anthocyanins are able to alter the gut microbiota composition.

However, this was in contrast with a human study reported by Percival, (2021) which examined multiple donors, but there were no significant changes on the gut microbiota composition by consuming anthocyanins. Therefore, for future *in-vitro* work, it would be worthwhile to investigate the effects of anthocyanin treatments on the structure and function of the gut faecal microbiome using faecal sample from different individuals.

The phyla Bacteroidetes and Firmicutes constitute a dominant part of the human gut microbiota, together accounting for 90% of the human gut bacterial species¹⁴³. Although there are debates on good and bad bacteria in the literature¹⁶¹, several reports have shown that many *Bacteroides* species are able to deliver beneficial effects to the host compared to Firmicutes¹⁸⁹. Data presented in this chapter showed that there was a slight shift at phylum level in the relative abundance of Bacteroidetes when in the presence of black rice anthocyanins, where Bacteroidetes increased over Firmicutes at 6 and 12 h. Consequently, at the species level, the major change was *Bacteroides vulgatus* which was shown to be increased in the presence of black rice anthocyanins over other species at 6 h. However, no significant difference was observed.

There is conflicting evidence in the literature regarding whether anthocyanins are able to alter the gut microbiota composition²⁴⁷. The *in-vitro* studies showed an increase in *Bifidobacterium* spp., *Lactobacillus* spp and *Enterococcus* spp. in response to anthocyanin treatments^{166,177,196}. However, animal studies have shown that anthocyanin intervention can increase the abundance of Actinobacteria^{267,268}. The inhibition of *Clostridium* spp. (i.e., *C. histolyticum* which is pathogenic in humans) by anthocyanins has also been reported¹³⁷. However, in this chapter, a mild increase (but not significant) in the abundance of Bacteroides was observed in response to the presence of black rice anthocyanins. This variation between *in-vitro* and *in-vivo* studies may be due to the host effect (genetic polymorphisms or upper GI metabolism) of the animal. In addition, the difference between some *in-vitro* studies and the study presented in this chapter is that the model used in this chapter was pH-controlled and the method used to determine the structure of gut microbiota was microbiome shotgun sequencing. Whereas in the literature, they did not control the pH, and the determination method of the microbiota used was fluorescent in situ hybridisation (FISH)¹³⁷.

Although there is no significant difference, data presented in this chapter showed that the greatest changes of faecal gut microbiota composition due to black rice anthocyanins supplement were only observed at 6 and 12 h. In chapters 4 and 6, the black rice anthocyanins were observed to be fully degraded between 6 and 10 h causing various metabolites to appear (i.e., PCA, PGA, and catechol) at these times or thereafter during the *in-vitro* colon model fermentations. This might suggest that anthocyanins themselves rather than anthocyanin metabolites modulate the composition of the gut microbiota. There are several other pieces of evidence to support this notion. Firstly, as shown in chapter 6, the C_{\max} of anthocyanin metabolites observed in the colon model fermentations were very low (typically between 1-10 μM compared to C_{initial} of the anthocyanins (133.3 μM). Secondly, bacterial catabolism generates a mixture of diverse metabolites in the culture and not all of these may affect the gut microbiota. Thirdly, gut microbial anthocyanin metabolism is a multistep process and eventually generates non-aromatic (Aliphatic) metabolites that are fully degraded by the microbiota.

It was also reported in the literature that genes known to be implicated in anthocyanin metabolism, such as β -glucosidase were involved^{93,173,176}. In chapter 6, the microbial metabolic pathways of black rice anthocyanins (Cya3Glc and Peo3Glc) were investigated; thus, enzymatic reactions were expected based on the appearance of various metabolites. For example, the metabolic pathway forming catechol from Cya3Glc is [Cya3Glc \rightarrow PCA \rightarrow catechol]; therefore, β -glucosidase and protocatechuate decarboxylase were expected to be observed from this metabolic pathway. However, no genes for enzymes were observed to be significantly more abundant when in the presence of black rice anthocyanins. One of the barriers in terms of understanding the role of the gut microbiota in anthocyanin metabolism is that few of the enzymes known to be involved in anthocyanin metabolism have been identified or characterised as well as β -glucosidase. It is highly likely that several of the reactions involved in anthocyanin metabolism can be carried out by multiple enzymes. It should be acknowledged that the metagenomic dataset can only be used to see if genes are present in the profiled microbiota but cannot provide any information relating to gene expression.

A recent human study reported that catechol and its phase 2 conjugates (sulfate conjugate) were major metabolites excreted in urine and were positively correlated with the

microbial species *Bacteroides finegoldii* and *Bacteroides salyersiae* after black rice anthocyanin consumption (Percival, 2021). However, only the abundance of *Bacteroides vulgatus* was relatively increased in black rice treatments compared to controls. This shows that the genera of *Bacteroides* may be involved in anthocyanins metabolism and thus their relative abundance increased in the presence of anthocyanins. However, the different observations between the two studies (the colon model and the human study) with respect to *Bacteroides* at the species level between may have due to the effect of the host (upper GI tract) in the *in-vivo* study²⁵⁸, or due to using a single donor in the study presented in this chapter which a limitation to data shown on various species of *Bacteroides*.

There are strengths in the study presented in this chapter. For example, studying the changes of the faecal gut microbiota in response to anthocyanin using a pH control *in-vitro* colon model has not been reported before. In addition, previous studies have not used the high throughput sequencing (metagenomics) which provides more information than other methods used. However, the study in this chapter investigated only one donor, which could mean that individual variations would not be able to be confirmed. This may affect the conclusion on the effects of anthocyanins on the gut microbiota composition.

7.6. Conclusions

The work in this chapter assessed the impact of anthocyanins on the human gut microbiome, showing mild effects of black rice anthocyanins on the structure and function of the human gut microbiome. Overall, the data presented does not support the hypothesis that consuming anthocyanins alters the structure and function of the human gut microbiota. However, the identification of gut microbiota species associated and/or involved in anthocyanins metabolism is still in its infancy, as such it is not possible to draw a fully informed conclusion with respect to whether anthocyanin consumption modulates the human gut microbiome. Despite this, *Bacteroides vulgatus* was observed to be relatively increased (but not significant) at 6 h in the presence of black rice anthocyanins. It is likely that this is due to functional metagenomics data only providing information regarding the abundance of a gene in the metagenome and not its expression, limiting the conclusions that can be drawn from this data. Furthermore, it is possible that

using the faecal microbiome from a single donor is not representative enough to see changes in the microbiome composition. Therefore, future work could focus on the isolated bacteria that are known to be involved in the biotransformation of anthocyanins into phenolic metabolites, such as catechol, PCA, and PGA. This may further our understanding of how the human gut microbiota metabolise anthocyanins differently and how this may affect an individuals' response to dietary anthocyanins, and the health effects associated with anthocyanins consumption.

Chapter Eight

General Discussion

Chapter 8: General discussion

8.1. Summary of main findings

The overall aim of the research presented in this thesis was to investigate the interactions between dietary anthocyanins and the human gut microbiota, using *in-vitro* colonic batch fermentation models. The specific objectives were to investigate (1) the role of the human gut microbiota in the metabolism of dietary anthocyanins and (2) the impact of anthocyanins on the structure and function of the human gut microbiota. The main findings were as follows:

- The colonic loss of anthocyanins was partly spontaneous and partly due to the activities of the gut microbiota, with the k_{deg} being considerably faster in the presence of live faecal microbiota compared to autoclaved faecal microbiota.
- The pH of colonic fermentations, the hydroxylation pattern of the anthocyanin B-ring, and the type of sugar moiety were important factors affecting the k_{deg} of anthocyanins via both spontaneous and gut microbiota-dependent processes.
- Several metabolites including 3,4-DHPAA, PCA, PGA, catechol, PGCA, 4-methylcatechol, dihydrocaffeic acid, and dihydroferulic acid were identified as microbiota-dependent metabolites from the fermentation of black rice anthocyanins.
- Two microbial metabolic pathways were indicated, i.e., [Cya3Glc \rightarrow PCA \rightarrow catechol] and [Cya3Glc \rightarrow PGA \rightarrow PGCA \rightarrow phloroglucinol] during the colonic fermentation of Cya3Glc.
- In contrast, it was shown that in the absence of live gut microbiota, anthocyanins and anthocyanidins underwent a classic pH-dependent transformation to form

colourless intermediates (hemiketal, hemiketal ketone, chalcone, chalcone anionic forms) in the colon model.

- There was considerable between-donor variation in microbiota-dependent degradation of anthocyanins.
- Within-donor, between stool variation in microbiota-dependent degradation, was modest, but for spontaneous degradation, differences were more substantial.
- Only in the presence of atmospheric oxygen did anthocyanins (i.e., Cya3Glc) undergo a series of auto-oxidative processes that formed products such as 2,4,6-trihydroxyphenyloxoacetic acid, 3,4-dihydroxyphenyloxoacetic acid, and coumarin-Glc).
- The impact of exposing human faecal microbiota to black rice anthocyanins was modest, with only small differences (but non-statistically significant) compared to controls observed at phylum and genus level at 6, and 12 h (small reduction in the abundance of Firmicutes and small increase in Bacteroidetes (mainly *Bacteroides vulgatus*)).

8.2. Discussion points

8.2.1. *In-vitro* studies of anthocyanin degradation under aerobic conditions cannot be used to determine degradation in anaerobic environments such as the colon

A healthy gut is characterized by a low level of oxygen, neutral pH, and by the presence of large bacterial communities of anaerobes²⁶⁹. However, several reports of *in-vitro* studies investigating the spontaneous degradation of anthocyanins at neutral pH were conducted in aerobic conditions^{38,87}. This opens a new discussion on whether the aerobic spontaneous degradation of anthocyanins is relevant to what happens in the colon or not. Aerobic conditions have relevance for anthocyanin stability/degradation during food processing, in the mouth and oesophagus (but only for a short time) and the stomach (although here the acidic conditions will increase the stability of anthocyanins). However,

data presented in this thesis (Chapter 5) show that aerobic conditions are not a suitable mimic of the colon where the pH is neutral, and it is anaerobic. The research presented in chapter 5 showed that spontaneous degradation of anthocyanins was slower in the anaerobic condition than in the aerobic one. In addition, in the absence of oxygen, anthocyanins underwent pH-dependent structural changes of anthocyanin flavylium into chalcones and chalcones anionic forms (colourless forms) and no PCA or PGA was detected. In contrast, various breakdown products (including PCA and PGA as previously reported) were shown to be formed in the presence of oxygen^{38,87}. However, based on the evidence in chapter 5, the appearance of simple phenolic compounds (including PCA and PGA) in the colon condition is mainly due to the gut microbiota activity. This provides important information for future *in-vitro* colonic studies to differentiate between the spontaneous and microbiota-dependent processes of phenolic compounds. Therefore, the biological activity of microbial metabolites should be, for example, investigated under anaerobic condition rather than in the presence of oxygen. This may further the research on that topic to investigate the biological effect of these metabolites in both aerobic and anaerobic environments.

8.2.2. *In-vitro* studies of anthocyanin metabolism need to use appropriate models

To date, only one study has investigated the metabolism of anthocyanins using a pH-controlled *in-vitro* model¹⁷⁷. However, all other *in-vitro* studies have used simple buffer solutions to investigate the metabolism of anthocyanins^{88,89,91,93,96,166,170,173–176,240,260}. In this thesis, data presented in chapter 4 showed that controlling the pH of the *in-vitro* colon model is a critical parameter for studying anthocyanin metabolism by the gut microbiota. For example, data was presented (figure 4.13 in chapter 4) showing that both spontaneous and gut microbiota-dependent rates of degradation of anthocyanins were substantially reduced in an uncontrolled pH model.

Several of the cited reports in the previous paragraph used simple buffers to maintain the pH near neutral, e.g., 150 mM phosphate buffer⁸⁹, 130 mM carbonate phosphate buffer

¹⁷⁰, and 100 mM phosphate buffer ^{88,91}. These buffers may maintain the pH at the beginning of incubation, but it is more likely to lose their buffer capacity over a long period of fermentation due to the continuous production of acids associated with bacterial growth. In addition, the use of high buffer capacity solutions introduces significant concentrations of buffer salts into the media which may affect the overall growth of the faecal microbiota or could select some species over others. During this project, the effect of low and high buffer capacity solutions was investigated, and it was demonstrated that there were differences in the growth of two gut microbiota species (*Escherichia coli* and *Lactobacillus lactis*) over time (**Appendix 7**). It is also possible that the presence of high concentrations of buffer salts not only affects the rate of microbial degradation of anthocyanins, but also the nature of the anthocyanin metabolite products of degradation. Therefore, further work should be carried out to establish the effects of buffer salts on anthocyanin degradation. Furthermore, *in-vitro* studies investigating the impact of anthocyanins on the gut microbiota composition also need to consider the effect of the salts used in the media.

8.2.3. Is PCA an important metabolite of anthocyanin degradation in humans?

The earliest reports of the bioavailability of anthocyanins from plant foods were in the late 1990s and only described the appearance of the intact anthocyanins in the urine of participants²⁷⁰. The first report of the bioavailability of a ring-fission metabolite from anthocyanins was that of Vitaglione and others who concluded that PCA was the major human metabolite of Cya3Glc that was present in blood orange juice and this single metabolite accounted for 44 mol% of the ingested Cya3Glc¹¹³. Since this report was published, there has been a steep increase in the year-on-year number of papers published concerned with establishing putative biological effects of PCA (**Figure 8. 1**). However, in this thesis (Chapter 6), data has been presented to show that PCA is a microbiota-dependent metabolite and not the most accumulated metabolite at 24 h but as an intermediate to the formation of catechol. In addition, a number of other potentially important metabolites of Cya3Glc were found to be accumulating and were identified, including 3,4-DHPAA, catechol, dihydroferulic acid, dihydrocaffeic acid and PCGA. Indeed, the report by Vitaglione ¹¹³ also contradicts more recent human bioavailability

studies reported by De Ferrars⁹⁹ and Percival²⁵⁸ where PCA was not a major accumulating metabolite of purified forms of Cya3Glc (**Table 8. 1**). For example, Percival (2021) reported that catechol sulfate was the most abundant metabolite of Cya3Glc among other important metabolites (i.e., PCA-3-O-sulfate, PCA-3-O-glucuronide, catechol glucuronide, and homovanillic sulfate, homoPCA (DHPAA), and homovanillic sulfate) in participants who had consumed highly purified black rice anthocyanins. Similarly, De Ferrars paper reported that ferulic acid, 4-hydroxybenzaldehyde, vanillic acid, PCA-sulfate, PCA-glucuronide, and vanillic acid sulfate were the main metabolites identified and quantified in urine after ingestion of penta[¹³C]-Cya3Glc⁹⁹. In agreement with De Ferrars and Percival reports^{99,258}, the *in-vitro* colon model fermentation data presented in Chapter 6 showed that the most abundant metabolites accumulating as a result of metabolism in a human faecal-inoculated colon model were 3,4-DHPAA, PCA, PGA, catechol, PGCA, dihydroferulic acid, and dihydrocaffeic acid. In addition, the C_{max} of PCA was shown to be ~ 10 % of incubated Cya3Glc. Therefore, the data in this thesis suggested that PCA is not the major or the accumulating Cya3Glc metabolite, but others (e.g., catechol) are important metabolites which they may significantly contribute to the beneficial properties of consumed anthocyanins.

Table 8. 1. Comparison between different human studies on the protocatechuic acid (PCA) recoveries.

	Vitaglione et al., (2007) ¹¹³	De Ferrars et al., (2014) ⁹⁹	Percival, (2021) ²⁵⁸
Ingested Cya3Glc	Red orange juice (71 mg Cya3Glc)	¹³ C-labelled Cya3Glc (500 mg)	Purified black rice anthocyanins (320 mg/day Cya3Glc)
Intervention time	24 h	48 h	28 days
PCA in serum	44 %	0.004 %	n.d.
PCA in urine (mol%)	n.d.	0.01	0.06
PCA in faeces (mol%)	41.6	0.07	N/D

n.d., a compound not detected; N/D, a compound not determined (not investigated).

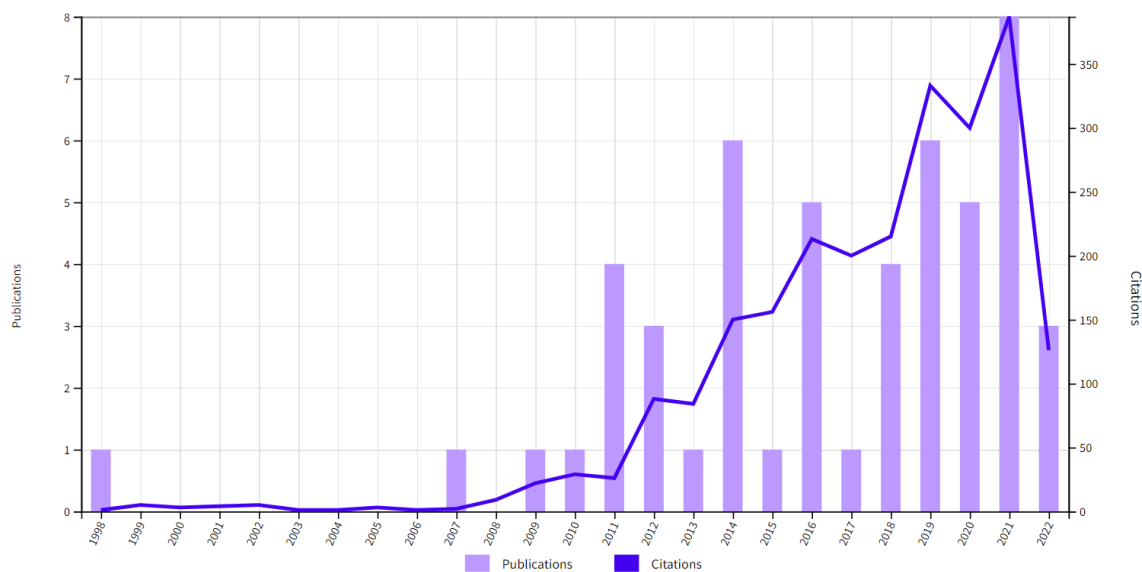


Figure 8. 1. Times cited and publications over time of protocatechuic acid (PCA) and its relationship to human health.

(Source: Web of Science; last access June 2022; the search keyword: protocatechuic acid (PCA) and human health).

8.2.4. Which anthocyanin metabolites should be studied for their possible biological activity with relevance to human health?

The data in this thesis provides evidence that the gut microbiota metabolise anthocyanins into various simple phenolic compounds arising from initial ring fission events. These metabolites may be important in delivering the health benefits of anthocyanin-rich foods bearing in mind the poor bioavailability of anthocyanins. In the opinion of the author, the three best studies describing the human ring fission metabolites of Cya3Glc are that reports of de Ferrars⁹⁹, Percival²⁵⁸ and this thesis. Both published reports show that PCA-sulfate, PCA-glucuronide, Isovanillic acid sulfate, and homovanillic sulfate are important human metabolites of Cya3Glc while the Percival report²⁵⁸ also provides evidence that catechol-sulfate is indeed the most abundant metabolite, and it has been noted that De Ferrars report⁹⁹ did not search for this compound and so would not have detected it using LC-MS in multiple reaction monitoring (MRM) mode. However, the data in this thesis confirms that these metabolites (but not in conjugated forms) are formed through the activity of the human faecal microbiota and accumulate to the highest concentrations in a humanised colon model. In addition, Percival report²⁵⁸ showed other conjugated metabolites were B-ring Cya3Glc metabolites (i.e., catechol sulfate, catechol glucuronide,

vanillic acid glucuronide, homoPCA sulfate, PCA glucuronide, PCA sulfate, and dihydrocaffeic acid sulfate). Therefore, the most important Cya3Glc metabolites (based on their concentrations), and those that should be the priority for future *in vitro* investigations of their putative biological activities are:

- Catechol-sulfate (e.g., catechol-3-*O*-sulfate or catechol-4-*O*-sulfate)
- PCA-sulfate (e.g., PCA-3-*O*-sulfate or PCA-4-*O*-sulfate)
- Isovanillic acid sulfate
- Catechol-glucuronide
- DHPAA
- Homovanillic acid sulfate
- Dihydrocaffeic acid sulfate

Finally, the research conducted in this thesis reinforced that these metabolites accumulate but only in unconjugated forms, showing novel Cya3Glc metabolites generated by the human gut microbiota such as DHPAA, catechol, PGCA, dihydrocaffeic acid, and dihydrocaffeic acid. Therefore, the beneficial effects of anthocyanins could be due to these new microbial metabolites and/or the action of a collection of metabolites. The effect of collective metabolites is more physiologically relevant since the biological cells are prone to different metabolites at the same time. In addition, the biological effects of conjugated forms of the aforementioned metabolites would be worthwhile to be included in the *in-vitro* and *in-vivo* studies.

8.2.5. Biomarkers of microbiota-dependent degradation of anthocyanins

In-vitro and human studies regarding the gut microbiota metabolites have focused on the B-ring phenolic acid (e.g., PCA from Cya3Glc) as the main metabolite and it has also been proposed as a biomarker metabolite of anthocyanin consumption^{88,89,91,93,96,113,170,173,174,176,177,237,240}. In addition, although in the colon environment (anaerobic) the production of the B-ring phenolic acids is mainly microbiota-dependent, (evidence presented in Chapter 6), B-ring phenolic acids are probably not a good biomarker of microbiota-dependent anthocyanin degradation. That is because data presented in this thesis (Chapter 5) and elsewhere in the literature^{38,87} shows that B-ring phenolic acids of anthocyanins (such as PCA from Cya3Glc) can also

be formed by non-enzymatic oxidative processes when anthocyanins are exposed to aerobic conditions at neutral pH. In addition, those phenolic acids (i.e., PCA, gallic acid, vanillic acid and 4-hydroxybenzoic acid) are common phenolic compounds found in many plant foods^{271,272}. Therefore, biomarkers of microbiota-dependent metabolism of anthocyanins must focus on those generated by microbial enzymatic processes to distinguish them from the products of spontaneous degradation. Although other flavonoids have some similarities to anthocyanin structures, catechol and 4-methylcatechol (as well as their conjugated forms) could be good candidates for microbial biomarkers of anthocyanin metabolism in the human body. Data presented in chapters 5 and 6 showed that the formation of catechol and 4-methylcatechol, dihydroferulic acid, and dihydrocaffeic acid are microbiota-dependent. They are, therefore, good candidates for investigating if there is a human metabotype concerning anthocyanin metabolism. There is pretty convincing evidence that metabotypes arising from differences in gut microbiota-dependent metabolism of other polyphenols such as ellagic acid/ellagitannins (which generate urolithins^{186–188,201,273}) and the isoflavone daidzein (which generates equol^{274,275}) are associated with different outcomes in human dietary intervention studies with foods and extracts rich in these polyphenols.

8.2.6. Current limitations in microbial gene annotation are preventing the identification of the microbial genes responsible for observed metabolic steps (Redundancy issues).

In spite of the fast development of powerful bioinformatics approaches, full interpretation of the content of mixed microbial genomes remains a challenging task²⁷⁶. Various public genome sequence databases and associated resources are available worldwide, however, the quality of the annotations depends largely on the original dataset providers, with erroneous or incomplete annotations often carried over into the public resources and these are difficult to correct²⁷⁷. This limitation might affect the outcomes of research on the changes of microbiota profiles. In chapter 7 as well as the report by Percival showed no significant impact of anthocyanins on the structure and function of the gut microbiota²⁵⁸. This limitation opens a discussion on the way of collecting data and how to be stored in one common database a robust reference for public access. This is because the current datasets in these different resources have different degrees of precision and resolution due

to diverse annotation methods. In addition to that, public resources, such as NCBI's RefSeq, further process microbial genome data from primary resources ²⁷⁸.

8.2.7. Impact of polyphenols on the structure and function of the human gut microbiota

There are several reports now in the literature ^{88,93,96,174,177,258} as well as in this thesis that the gut microbiota plays important role in anthocyanin metabolism. In contrast, studies of the impact of anthocyanins on the composition of the human gut microbiota are currently very limited, and overall, there is not much evidence that consumption of anthocyanins has significant effects on the structure and function of the gut microbiota. A recent systematic review of the effect of anthocyanins on intestinal health reported that consumption of diets rich in anthocyanins increased the abundance of Bacteroidetes and reduced the abundance of Firmicutes ¹⁹⁰. However, the data presented in this review was mainly generated from animal studies with more purified anthocyanins and/or from studies where laboratory animals were fed whole foods and the effect could not be attributed to the anthocyanins. There is only one placebo-controlled study of the effects of regular daily consumption of isolated anthocyanins on gut microbiota structure and function in humans (Percival, 2021), and in that report no significant effects on the gut microbiota profile were detected after consumption of purified anthocyanin extracts for 28 days. In agreement with Percival (2021), data in Chapter 7 showed that there were only small effects on the structure and function of the human gut microbiota following incubations of faecal gut microbiota with a purified anthocyanin extract.

Another factor which could play a role in changing the gut microbiota composition is the metabolites formed from anthocyanins by the gut microbiota. The *in-vitro* studies showed that the gut microbiota catabolise anthocyanins into simple phenolics, mainly the A-ring PGA and B-ring phenolic acid (i.e., PCA from Cya3Glc) ^{88,89,237,240,91,93,96,170,173,174,176,177}. This notion was supported in this thesis by the data presented in Chapters 4 and 6. However, reports have proposed that anthocyanin consumption can modulate gut microbial populations and that the composition of the gut microbiota largely dictates how anthocyanins are metabolised ^{160,165,166,169,268}. Therefore, more work will be needed to investigate whether only anthocyanins or all ingredients in anthocyanin-rich food have

the effect to alter the gut microbiota composition. Additional studies conducted both in humans and using in vitro models (such as colon models) are required to confirm if anthocyanins are largely benign with regard to their ability to affect gut microbiota structure and function, and to investigate if anthocyanin ring-fission metabolites are active in this regard.

8.3. Strengths and limitations of the research

The work presented in this thesis has provided several new insights into the role of the human gut microbiota in anthocyanin metabolism, and there are several strengths in the way the research was conducted. For example, a controlled pH model under anaerobic conditions was used here while other reports in the literature followed the use of simple buffered solutions to investigate the microbial degradation of anthocyanins. In addition, a highly purified anthocyanin extract was used here, which provides strong evidence that the metabolism and effects observed are due to the anthocyanins and not the other components in complex foods. Furthermore, autoclaving the human faecal slurries as an additional control was critical to show the contribution of both spontaneous processes and of microbiota-dependent processes in the degradation of anthocyanins.

However, there are some limitations and weaknesses. The colon model only reflects the conditions of the human colon, and the observations obtained from these experiments cannot reflect transformations that potentially occur in the upper gut, particularly the ileum, where the structure of the microbiota community differs^{279,280}. By using faecal glycerol stocks, it is possible that freezing may have affected the viability of certain species over others which might have affected the results of anthocyanin metabolism experiments, although there was little evidence of this occurring. Indeed, the consistency of my observations with those from animal and human intervention studies suggests that it is an excellent model for studying the metabolism of anthocyanins in the human colon. Due to the inter-individual variations, another potential weakness is that the metagenomic analysis for investigating the impact of anthocyanin on gut microbiota structure was carried out using one single donor. It is also worth noting that the metagenomic analysis only provides data on the relative abundance of genes (DNA) and does not provide any information of whether or not the expression of particular genes is being affected, which

would require qRT-PCR assays for target genes or transcriptomics for genome wide expression analysis (of mRNA).

8.4. Recommendations for future work

This thesis provides new insights into the colonic metabolism of anthocyanins (black rice and bilberry) and makes new observations on the role of the human gut microbiota in the metabolism and bioavailability of anthocyanins. The main findings were novel showing the importance of gut microbiota in the metabolism of anthocyanins and how a different set of metabolites are products of microbial metabolism compared to spontaneous degradation of anthocyanins. These findings open the way for new questions to be asked and investigated in future research.

- It is very important to focus on spontaneous degradation as microbial-dependent degradation of anthocyanins, considering the difference between the aerobic and anaerobic spontaneous degradation of anthocyanins to reflect the physiological condition of the human gut.
- Furthermore, although the majority of *in-vitro* experiments in the literature were carried out using the uncontrolled-pH colon model, in this thesis controlling the pH of the fermentation was shown to be an important factor in anthocyanin metabolism by the human gut microbiota. Therefore, more work needs to be carried out using pH-controlled systems for further investigations of other anthocyanin-rich extracts and/or different purified anthocyanin such as delphinidin, pelargonidin and petunidin.
- Data presented in this thesis, in combination with data presented in reports by de Ferrars⁹⁹ and Percival²⁵⁸, show that the most abundant human metabolites of Cya3Glc are Catechol-sulfates, PCA-sulfate, Isovanillic acid sulfate, Catechol-glucuronide, DHPAA (HomoPCA), Homovanillic acid sulfate, Dihydrocaffeic acid sulfate, and yet these have hardly been investigated for

their possible biological activities. PCA is a relatively minor metabolite and yet there are >100 reports of studies of its biological activities determined predominantly using cultured mammalian cell models but also animal feeding studies, but very few for catechol-sulfates, the most abundant metabolite. Therefore, future research needs to focus on determining relevant biological activities for the most abundant anthocyanin metabolites which for Cya3Glc are phase-2 conjugates of catechol (catechol-O-sulfates), PCA (-sulfate and -glucuronide), dihydrocaffeic acid (sulfates), and dihydroferulic acid (-sulfate and -glucuronide). Those metabolites could be also investigated separately and in pooled mixtures to determine their biological activities.

- There is little known of the molecular processes by which the gut microbiota metabolises anthocyanins. It would seem likely that these processes involve at least enzymes such as PCA decarboxylase (that would convert PCA to catechol) among others but may also require transporters to affect the uptake of the anthocyanins by bacterial cells, and/or cofactors and may even utilise bacterial microcompartments. A combination of genetic studies and *in-vitro* molecular and biochemical studies could be undertaken to advance understanding of these processes which will help explain the inter-individual variation and potentially provide targets for manipulation, e.g., using specific dietary components.
- The data present in this thesis showed that there are various breakdown products resulting from the aerobic spontaneous degradation of anthocyanins. In chapter 1, an overview of the spontaneous degradation was presented and showed that mainly two breakdown products were shown to be a result of aerobic spontaneous degradation of anthocyanins (the A-ring PGA and the B-ring phenolic acid). However, other breakdown products were putatively identified in chapter 5 as new spontaneous products of the degradation of anthocyanins. The biological activities of these metabolites would also be investigated.

- In addition, future work should aim to isolate bacteria involved in anthocyanin metabolism. This work would be carried out by enriching bacteria using an *in-vitro* colon model and then plating the end-point sample on agar colon media which is also supplemented with anthocyanins. Three different treatment vessels (0, 0.1, and 1 % glucose colon media) are recommended alongside control (no anthocyanin; 1 % glucose). For the incubation, continuous feeding of anthocyanins to faecal gut microbiota would be carried out using an *in-vitro* colon model over 60 h. The feeding process with anthocyanins would be carried out over 5 times (5 cycles: cycle = 12 h). The inoculation of the first cycle should be with a 1 % fresh faecal sample, then at the end of each cycle, 5 mL is needed to inoculate the following cycle which contained 95 mL of fresh colon media and anthocyanins. At the end of incubation of cycle 5, 1 mL sample will be collected from each treatment to be streaked and then incubated anaerobically on Petri dishes.
- The metagenomic analysis presented in chapter 7 shows no significant impact of black rice anthocyanins on the structure and functions of the human gut microbiota. The limitation of the work in chapter 7 was that only one stool from one donor was investigated. However, the results in chapters 4 and 6 show individual variations in anthocyanin metabolism. Therefore, it is recommended for future work to investigate more faecal samples from the same donor as well as from different donors. Furthermore, it is entirely possible that the main effects of anthocyanins on the gut microbiome are to alter the expression of specific microbial genes rather than alter the relative composition of the microbiome, and studies of gene expression should also be undertaken.

References

References

1. Anantharaju PG, Gowda PC, Vimalambike MG, Madhunapantula S V. An overview on the role of dietary phenolics for the treatment of cancers. *Nutr J*. 2016;15(1):1-16. doi:10.1186/s12937-016-0217-2
2. Wang J, Xu J, Gong X, Yang M, Zhang C, Li M. Biosynthesis, chemistry, and pharmacology of polyphenols from Chinese *Salvia* species: A review. *Molecules*. 2019;24(1):1-23. doi:10.3390/molecules24010155
3. Tsao R. Chemistry and biochemistry of dietary polyphenols. *Nutrients*. 2010;2(12):1231-1246. doi:10.3390/nu2121231
4. Rashmi HB, Negi PS. Phenolic acids from vegetables: A review on processing stability and health benefits. *Food Res Int*. 2020;136(May):109298. doi:10.1016/j.foodres.2020.109298
5. El Khawand T, Courtois A, Valls J, Richard T, Krisa S. A review of dietary stilbenes: sources and bioavailability. *Phytochem Rev*. 2018;17(5):1007-1029. doi:10.1007/s11101-018-9578-9
6. Cook NC, Samman S. Flavonoids-Chemistry, metabolism, cardioprotective effects, and dietary sources. *J Eur Ceram Soc*. 1996;63(SUPPL. 1):66-76. doi:10.1016/S0955-2863(95)00168-9
7. Egert S, Rimbach G. Which sources of flavonoids: Complex diets or dietary supplements? *Adv Nutr*. 2011;2(1):8-14. doi:10.3945/an.110.000026
8. Yao LH, Jiang YM, Shi J, et al. Flavonoids in food and their health benefits. *Plant Foods Hum Nutr*. 2004;59(3):113-122. doi:10.1007/s11130-004-0049-7
9. Thilakarathna SH, Vasantha Rupasinghe HP. Flavonoid bioavailability and attempts for bioavailability enhancement. *Nutrients*. 2013;5(9):3367-3387.

doi:10.3390/nu5093367

10. Cassidy A. Berry anthocyanin intake and cardiovascular health. *Mol Aspects Med.* 2018;61:76-82. doi:10.1016/j.mam.2017.05.002
11. Wallace TC, Giusti MM. Anthocyanins. *Advances in Nutrition. Am Soc Nutr.* 2015;(8):620-622. doi:10.3945/an.115.009233.Clinical
12. Castañeda-Ovando A, Pacheco-Hernández M de L, Páez-Hernández ME, Rodríguez JA, Galán-Vidal CA. Chemical studies of anthocyanins: A review. *Food Chem.* 2009;113(4):859-871. doi:10.1016/j.foodchem.2008.09.001
13. Crozier A, Jaganath IB, Clifford MN. Dietary phenolics: Chemistry, bioavailability and effects on health. *Nat Prod Rep.* 2009;26(8):1001-1043. doi:10.1039/b802662a
14. Prior RL, Wu X. Anthocyanins: Structural characteristics that result in unique metabolic patterns and biological activities. *Free Radic Res.* 2006;40(10):1014-1028. doi:10.1080/10715760600758522
15. Konczak I, Zhang W. Anthocyanins - More than nature's colours. *J Biomed Biotechnol.* 2004;2004(5):239-240. doi:10.1155/S1110724304407013
16. Khoo HE, Azlan A, Tang ST, Lim SM. Anthocyanidins and anthocyanins: Colored pigments as food, pharmaceutical ingredients, and the potential health benefits. *Food Nutr Res.* 2017;61(1). doi:10.1080/16546628.2017.1361779
17. Tsuda T. Dietary anthocyanin-rich plants: Biochemical basis and recent progress in health benefits studies. *Mol Nutr Food Res.* 2012;56(1):159-170. doi:10.1002/mnfr.201100526
18. Smeriglio A, Barreca D, Bellocco E, Trombetta D. Chemistry, Pharmacology and Health Benefits of Anthocyanins. *Phyther Res.* 2016;1286(March):1265-1286.

doi:10.1002/ptr.5642

19. Jokioja J, Yang B, Linderborg KM. Acylated anthocyanins: A review on their bioavailability and effects on postprandial carbohydrate metabolism and inflammation. *Compr Rev Food Sci Food Saf.* 2021;20(6):5570-5615. doi:10.1111/1541-4337.12836
20. Giusti MM, Wrolstad RE. Acylated anthocyanins from edible sources and their applications in food systems. *Biochem Eng J.* 2003;14(3):217-225. doi:10.1016/S1369-703X(02)00221-8
21. He F, Liang NN, Mu L, et al. Anthocyanins and their variation in red wines I. Monomeric anthocyanins and their color expression. *Molecules.* 2012;17(2):1571-1601. doi:10.3390/molecules17021571
22. Horbowicz M, Grzesiuk A, DEBski H, Kosson R. Anthocyanins of Fruits and Vegetables - Their Occurrence, Analysis and Role in Human. *Veg Crop Res Bull.* 2008;68(April):5-22. doi:10.2478/v10032-008-0001-8
23. Delgado-Vargas F, Paredes-López O. *Natural Colorants for Food and Nutraceutical Uses.*; 2002. doi:10.1201/9781420031713
24. Delgado-Vargas F, Jimenez AR, Paredes-Lopez O. *Critical Reviews in Food Science and Nutrition. Natural Pigments: Carotenoids, Anthocyanins, and Betalains — Characteristics, Biosynthesis, Processing, and Stability.* Vol 40.; 2010.
25. Tanaka Y, Sasaki N, Ohmiya A. Biosynthesis of plant pigments: Anthocyanins, betalains and carotenoids. *Plant J.* 2008;54(4):733-749. doi:10.1111/j.1365-313X.2008.03447.x
26. Boulton R. The copigmentation of anthocyanins and its role in the color of red wine: A critical review. *Am J Enol Vitic.* 2001;52(2):67-87.

27. Ananga A, Georgiev V, Ochieng J, Phills B, Tsolova V. The Mediterranean Genetic Code - Grapevine and Olive. *Mediterr Genet Code - Grapevine Olive*. 2013;(December 2016):1998-2002. doi:10.5772/3442
28. Huang D. Dietary antioxidants and health promotion. *Antioxidants*. 2018;7(1):7-9. doi:10.3390/antiox7010009
29. Pojer E, Mattivi F, Johnson D, Stockley CS. The case for anthocyanin consumption to promote human health: A review. *Compr Rev Food Sci Food Saf*. 2013;12(5):483-508. doi:10.1111/1541-4337.12024
30. Wu X, Beecher GR, Holden JM, Haytowitz DB, Gebhardt SE, Prior RL. Concentrations of anthocyanins in common foods in the United States and estimation of normal consumption. *J Agric Food Chem*. 2006;54(11):4069-4075. doi:10.1021/jf0603001
31. Patras A, Brunton NP, O'Donnell C, Tiwari BK. Effect of thermal processing on anthocyanin stability in foods; mechanisms and kinetics of degradation. *Trends Food Sci Technol*. 2010;21(1):3-11. doi:10.1016/j.tifs.2009.07.004
32. Zoratti L, Sarala M, Carvalho E, et al. Monochromatic light increases anthocyanin content during fruit development in bilberry. *BMC Plant Biol*. 2014;14(1):1-10. doi:10.1186/s12870-014-0377-1
33. Passeri V, Koes R, Quattrocchio FM. New challenges for the design of high value plant products: Stabilization of anthocyanins in plant vacuoles. *Front Plant Sci*. 2016;7(FEB2016):1-9. doi:10.3389/fpls.2016.00153
34. Rapisarda P, Bellomo SE, Intelisano S. Storage temperature effects on blood orange fruit quality. *J Agric Food Chem*. 2001;49(7):3230-3235. doi:10.1021/jf0100321
35. Remini H, Mertz C, Belbahi A, Achir N, Dornier M, Madani K. Degradation

- kinetic modelling of ascorbic acid and colour intensity in pasteurised blood orange juice during storage. *Food Chem.* 2015;173:665-673.
doi:10.1016/j.foodchem.2014.10.069
36. Clifford MN. Anthocyanins - Nature, occurrence and dietary burden. *J Sci Food Agric.* 2000;80(7):1063-1072. doi:10.1002/(SICI)1097-0010(20000515)80:7<1063::AID-JSFA605>3.0.CO;2-Q
37. McGhie TK, Walton MC. The bioavailability and absorption of anthocyanins: Towards a better understanding. *Mol Nutr Food Res.* 2007;51(6):702-713. doi:10.1002/mnfr.200700092
38. Kay CD, Kroon PA, Cassidy A. The bioactivity of dietary anthocyanins is likely to be mediated by their degradation products. *Mol Nutr Food Res.* 2009;53(SUPPL. 1):92-101. doi:10.1002/mnfr.200800461
39. Cevallos-Casals BA, Cisneros-Zevallos L. Stoichiometric and kinetic studies of phenolic antioxidants from Andean purple corn and red-fleshed sweetpotato. *J Agric Food Chem.* 2003;51(11):3313-3319. doi:10.1021/jf034109c
40. Lao F, Sigurdson GT, Giusti MM. Health Benefits of Purple Corn (*Zea mays* L.) Phenolic Compounds. *Compr Rev Food Sci Food Saf.* 2017;16(2):234-246. doi:10.1111/1541-4337.12249
41. Prior RL, Lazarus SA, Cao G, Muccitelli H, Hammerstone JF. Identification of procyanidins and anthocyanins in blueberries and cranberries (*Vaccinium* spp.) Using high-performance liquid chromatography/mass spectrometry. *J Agric Food Chem.* 2001;49(3):1270-1276. doi:10.1021/jf001211q
42. Mikulic-Petkovsek M, Schmitzer V, Slatnar A, et al. Investigation of anthocyanin profile of four elderberry species and interspecific hybrids. *J Agric Food Chem.* 2014;62(24):5573-5580. doi:10.1021/jf5011947

43. Bräunlich M, Slimestad R, Wangensteen H, Brede C, Malterud KE, Barsett H. Extracts, anthocyanins and procyanidins from *Aronia melanocarpa* as radical scavengers and enzyme inhibitors. *Nutrients*. 2013;5(3):663-678. doi:10.3390/nu5030663
44. Meng L, Zhu J, Ma Y, et al. Composition and antioxidant activity of anthocyanins from *Aronia melanocarpa* cultivated in Haicheng, Liaoning, China. *Food Biosci*. 2019;30(April 2018). doi:10.1016/j.fbio.2019.100413
45. Kallithraka S, Aliaj L, Makris DP, Kefalas P. Anthocyanin profiles of major red grape (*Vitis vinifera* L.) varieties cultivated in Greece and their relationship with in vitro antioxidant characteristics. *Int J Food Sci Technol*. 2009;44(12):2385-2393. doi:10.1111/j.1365-2621.2008.01869.x
46. Gorinstein S, Caspi A, Libman I, et al. Red grapefruit positively influences serum triglyceride level in patients suffering from coronary atherosclerosis: Studies in vitro and in humans. *J Agric Food Chem*. 2006;54(5):1887-1892. doi:10.1021/jf058171g
47. Benmeziane F, Cadot Y, Djamai R, Djermoun L. Determination of major anthocyanin pigments and flavonols in red grape skin of some table grape varieties (*Vitis vinifera* SP.) by high-performance liquid chromatography-photodiode array detection (HPLC-DAD). *Oeno One*. 2016;50(3):125-135. doi:10.20870/oenone.2016.50.3.56
48. Espley R V., Hellens RP, Putterill J, Stevenson DE, Kutty-Amma S, Allan AC. Red colouration in apple fruit is due to the activity of the MYB transcription factor, MdMYB10. *Plant J*. 2007;49(3):414-427. doi:10.1111/j.1365-313X.2006.02964.x
49. Karlsen A, Paur I, Bøhn SK, et al. Bilberry juice modulates plasma concentration of NF- κ B related inflammatory markers in subjects at increased risk of CVD. *Eur J Nutr*. 2010;49(6):345-355. doi:10.1007/s00394-010-0092-0

50. Mauray A, Felgines C, Morand C, Mazur A, Scalbert A, Milenkovic D. Bilberry anthocyanin-rich extract alters expression of genes related to atherosclerosis development in aorta of apo E-deficient mice. *Nutr Metab Cardiovasc Dis.* 2012;22(1):72-80. doi:10.1016/j.numecd.2010.04.011
51. Wang SY, Lin HS. Antioxidant activity in fruits and leaves of blackberry, raspberry, and strawberry varies with cultivar and developmental stage. *J Agric Food Chem.* 2000;48(2):140-146. doi:10.1021/jf9908345
52. Mallery SR, Budendorf DE, Larsen MP, et al. Effects of human oral mucosal tissue, saliva, and oral microflora on intraoral metabolism and bioactivation of black raspberry anthocyanins. *Cancer Prev Res.* 2011;4(8):1209-1221. doi:10.1158/1940-6207.CAPR-11-0040
53. Teng H, Fang T, Lin Q, Song H, Liu B, Chen L. Red raspberry and its anthocyanins: Bioactivity beyond antioxidant capacity. *Trends Food Sci Technol.* 2017;66:153-165. doi:10.1016/j.tifs.2017.05.015
54. Xie C, Kang J, Chen JR, Nagarajan S, Badger TM, Wu X. Phenolic acids are in vivo atheroprotective compounds appearing in the serum of rats after blueberry consumption. *J Agric Food Chem.* 2011;59(18):10381-10387. doi:10.1021/jf2025264
55. Bunea A, Rugină D, Sconța Z, et al. Anthocyanin determination in blueberry extracts from various cultivars and their antiproliferative and apoptotic properties in B16-F10 metastatic murine melanoma cells. *Phytochemistry.* 2013;95:436-444. doi:10.1016/j.phytochem.2013.06.018
56. Del Bo' C, Roursgaard M, Porrini M, Loft S, Møller P, Riso P. Different effects of anthocyanins and phenolic acids from wild blueberry (*Vaccinium angustifolium*) on monocytes adhesion to endothelial cells in a TNF- α stimulated proinflammatory environment. *Mol Nutr Food Res.* 2016;60(11):2355-2366. doi:10.1002/mnfr.201600178

-
57. Talavéra S, Felgines C, Texier O, et al. Anthocyanin metabolism in rats and their distribution to digestive area, kidney, and brain. *J Agric Food Chem.* 2005;53(10):3902-3908. doi:10.1021/jf050145v
58. Igwe EO, Charlton KE, Roodenrys S, Kent K, Fanning K, Netzel ME. Anthocyanin-rich plum juice reduces ambulatory blood pressure but not acute cognitive function in younger and older adults: a pilot crossover dose-timing study. *Nutr Res.* 2017;47:28-43. doi:10.1016/j.nutres.2017.08.006
59. Usenik V, Štampar F, Veberič R. Anthocyanins and fruit colour in plums (*Prunus domestica* L.) during ripening. *Food Chem.* 2009;114(2):529-534. doi:10.1016/j.foodchem.2008.09.083
60. Sandhu AK, Huang Y, Xiao D, Park E, Edirisinghe I, Burton-Freeman B. Pharmacokinetic Characterization and Bioavailability of Strawberry Anthocyanins Relative to Meal Intake. *J Agric Food Chem.* 2016;64(24):4891-4899. doi:10.1021/acs.jafc.6b00805
61. Sirijan M, Pipattanawong N, Saeng-On B, Chaiprasart P. Anthocyanin content, bioactive compounds and physico-chemical characteristics of potential new strawberry cultivars rich in-anthocyanins. *J Berry Res.* 2020;10(3):397-410. doi:10.3233/JBR-190487
62. Sadilova E, Stintzing FC, Carle R. Anthocyanins, colour and antioxidant properties of eggplant (*Solanum melongena* L.) and violet pepper (*Capsicum annuum* L.) peel extracts. *Zeitschrift fur Naturforsch - Sect C J Biosci.* 2006;61(7-8):527-535. doi:10.1515/znc-2006-7-810
63. Karimi A, Kazemi M, Samani SA, Simal-Gandara J. Bioactive compounds from by-products of eggplant: Functional properties, potential applications and advances in valorization methods. *Trends Food Sci Technol.* 2021;112(April):518-531. doi:10.1016/j.tifs.2021.04.027

64. Wiczowski W, Szawara-Nowak D, Topolska J. Red cabbage anthocyanins: Profile, isolation, identification, and antioxidant activity. *Food Res Int.* 2013;51(1):303-309. doi:10.1016/j.foodres.2012.12.015
65. Pedro AC, Granato D, Rosso ND. Extraction of anthocyanins and polyphenols from black rice (*Oryza sativa* L.) by modeling and assessing their reversibility and stability. *Food Chem.* 2016;191:12-20. doi:10.1016/j.foodchem.2015.02.045
66. Sriseadka T, Wongpornchai S, Rayanakorn M. Quantification of flavonoids in black rice by liquid chromatography- negative electrospray ionization tandem mass spectrometry. *J Agric Food Chem.* 2012;60(47):11723-11732. doi:10.1021/jf303204s
67. Zhang H, Shao Y, Bao J, Beta T. Phenolic compounds and antioxidant properties of breeding lines between the white and black rice. *Food Chem.* 2015;172:630-639. doi:10.1016/j.foodchem.2014.09.118
68. Hansen AS, Marckmann P, Dragsted LO, Finné Nielsen IL, Nielsen SE, Grønbæk M. Effect of red wine and red grape extract on blood lipids, haemostatic factors, and other risk factors for cardiovascular disease. *Eur J Clin Nutr.* 2005;59(3):449-455. doi:10.1038/sj.ejcn.1602107
69. Tsang C, Higgins S, Duthie GG, et al. The influence of moderate red wine consumption on antioxidant status and indices of oxidative stress associated with CHD in healthy volunteers. *Br J Nutr.* 2005;93(2):233-240. doi:10.1079/bjn20041311
70. Zhao X, Yuan Z. Anthocyanins from Pomegranate (*Punica granatum* L.) and Their Role in Antioxidant Capacities in Vitro. *Chem Biodivers.* 2021;18(10). doi:10.1002/cbdv.202100399
71. Aviram M, Rosenblat M, Gaitini D, et al. Pomegranate juice consumption for 3 years by patients with carotid artery stenosis reduces common carotid intima-

- media thickness, blood pressure and LDL oxidation. *Clin Nutr.* 2004;23(3):423-433. doi:10.1016/j.clnu.2003.10.002
72. Aviram M, Dornfeld L, Rosenblat M, et al. Pomegranate juice consumption reduces oxidative stress, atherogenic modifications to LDL, and platelet aggregation: Studies in humans and in atherosclerotic apolipoprotein E-deficient mice. *Am J Clin Nutr.* 2000;71(5):1062-1076. doi:10.1093/ajcn/71.5.1062
73. Legua P, Melgarejo P, Martínez JJ, Martínez R, Hernández F. Evaluation of spanish pomegranate juices: Organic acids, sugars, and anthocyanins. *Int J Food Prop.* 2012;15(3):481-494. doi:10.1080/10942912.2010.491931
74. Bellomo MG, Fallico B. Anthocyanins, chlorophylls and xanthophylls in pistachio nuts (*Pistacia vera*) of different geographic origin. *J Food Compos Anal.* 2007;20(3-4):352-359. doi:10.1016/j.jfca.2006.04.002
75. Niu J, Zhang G, Zhang W, et al. Anthocyanin concentration depends on the counterbalance between its synthesis and degradation in plum fruit at high temperature. *Sci Rep.* 2017;7(1):1-16. doi:10.1038/s41598-017-07896-0
76. Liu Y, Tikunov Y, Schouten RE, Marcelis LFM, Visser RGF, Bovy A. Anthocyanin biosynthesis and degradation mechanisms in Solanaceous vegetables: A review. *Front Chem.* 2018;6(MAR). doi:10.3389/fchem.2018.00052
77. Zhang L, Wang L, Zeng X, Chen R, Yang S, Pan S. Comparative transcriptome analysis reveals fruit discoloration mechanisms in postharvest strawberries in response to high ambient temperature. *Food Chem X.* 2019;2:100025. doi:10.1016/j.fochx.2019.100025
78. Oren-Shamir M. Does anthocyanin degradation play a significant role in determining pigment concentration in plants? *Plant Sci.* 2009;177(4):310-316. doi:10.1016/j.plantsci.2009.06.015

79. Peterson ME, Daniel RM, Danson MJ, Eisenthal R. The dependence of enzyme activity on temperature: Determination and validation of parameters. *Biochem J.* 2007;402(2):331-337. doi:10.1042/BJ20061143
80. Zhao CL, Chen ZJ, Bai XS, et al. Structure-activity relationships of anthocyanidin glycosylation. *Mol Divers.* 2014;18(3):687-700. doi:10.1007/s11030-014-9520-z
81. Brouillard R, Lang J. The hemiacetal– cis -chalcone equilibrium of malvin, a natural anthocyanin. *Can J Chem.* 1990;68(5):755-761. doi:10.1139/v90-119
82. Moldovan B, David L, Chisbora C, Cimpoi C. Degradation kinetics of anthocyanins from european cranberrybush (*viburnum opulus l.*) fruit extracts. Effects of temperature, pH and storage solvent. *Molecules.* 2012;17(10):11655-11666. doi:10.3390/molecules171011655
83. Oliveira J, Mateus N, De Freitas V. Previous and recent advances in pyranoanthocyanins equilibria in aqueous solution. *Dye Pigment.* 2014;100(1):190-200. doi:10.1016/j.dyepig.2013.09.009
84. Yahia EM, Ornelas-Paz J de J. *Chemistry, Stability, and Biological Actions of Carotenoids.*; 2009. doi:10.1002/9780813809397.ch7
85. Zhou Y, Singh BR. Effect of Light on Anthocyanin Levels in Submerged, Harvested Cranberry Fruit. *J Biomed Biotechnol.* 2004;2004(5):259-263. doi:10.1155/S1110724304403027
86. Remini H, Dahmoune F, Sahraoui Y, Madani K, Kapranov VN, Kiselev EF. Recent Advances on Stability of Anthocyanins. *Rudn J Agron Anim Ind.* 2018;13(4):257-286. doi:10.22363/2312-797x-2018-13-4-257-286
87. Woodward G, Kroon P, Cassidy A, Kay C. Anthocyanin stability and recovery: Implications for the analysis of clinical and experimental samples. *J Agric Food*

- Chem.* 2009;57(12):5271-5278. doi:10.1021/jf900602b
88. Hanske L, Engst W, Loh G, Sczesny S, Blaut M, Braune A. Contribution of gut bacteria to the metabolism of cyanidin 3-glucoside in human microbiota-associated rats. *Br J Nutr.* 2013;109(8):1433-1441. doi:10.1017/S0007114512003376
89. Keppler K, Humpf HU. Metabolism of anthocyanins and their phenolic degradation products by the intestinal microflora. *Bioorganic Med Chem.* 2005;13(17):5195-5205. doi:10.1016/j.bmc.2005.05.003
90. Kuntz S, Rudloff S, Asseburg H, et al. Uptake and bioavailability of anthocyanins and phenolic acids from grape/blueberry juice and smoothie in vitro and in vivo. *Br J Nutr.* 2015;113(7):1044-1055. doi:10.1017/S0007114515000161
91. Fleschhut J, Kratzer F, Rechkemmer G, Kulling SE. Stability and biotransformation of various dietary anthocyanins in vitro. *Eur J Nutr.* 2006;45(1):7-18. doi:10.1007/s00394-005-0557-8
92. Justesen U, Arrigoni E. Electrospray ionisation mass spectrometric study of degradation products of quercetin, quercetin-3-glucoside and quercetin-3-rhamnoglucoside, produced by in vitro fermentation with human faecal flora. *Rapid Commun Mass Spectrom.* 2001;15(7):477-483. doi:10.1002/rcm.250
93. Ávila M, Hidalgo M, Sánchez-Moreno C, Pelaez C, Requena T, Pascual-Teresa S de. Bioconversion of anthocyanin glycosides by Bifidobacteria and Lactobacillus. *Food Res Int.* 2009;42(10):1453-1461. doi:10.1016/j.foodres.2009.07.026
94. Goszcz K, Deakin SJ, Duthie GG, Stewart D, Megson IL. Bioavailable Concentrations of Delphinidin and Its Metabolite, Gallic Acid, Induce Antioxidant Protection Associated with Increased Intracellular Glutathione in Cultured Endothelial Cells. *Oxid Med Cell Longev.* 2017;2017(Ldl).

doi:10.1155/2017/9260701

95. Kamonpatana K, Giusti MM, Chitchumroonchokchai C, et al. Susceptibility of anthocyanins to ex vivo degradation in human saliva. *Food Chem.* 2012;135(2):738-747. doi:10.1016/j.foodchem.2012.04.110
96. Forester SC, Waterhouse AL. Identification of cabernet sauvignon anthocyanin gut microflora metabolites. *J Agric Food Chem.* 2008;56(19):9299-9304. doi:10.1021/jf801309n
97. Fang J. Bioavailability of anthocyanins. *Drug Metab Rev.* 2014;46(4):508-520. doi:10.3109/03602532.2014.978080
98. Stahl W, Van Den Berg H, Arthur J, et al. Bioavailability and metabolism. *Mol Aspects Med.* 2002;23(1-3):39-100. doi:10.1016/S0098-2997(02)00016-X
99. De Ferrars RM, Czank C, Zhang Q, et al. The pharmacokinetics of anthocyanins and their metabolites in humans. *Br J Pharmacol.* 2014;171(13):3268-3282. doi:10.1111/bph.12676
100. Czank C, Cassidy A, Zhang Q, et al. Human metabolism and elimination of the anthocyanin, cyanidin-3-glucoside: A ¹³C-tracer study. *Am J Clin Nutr.* 2013;97(5):995-1003. doi:10.3945/ajcn.112.049247
101. Milbury PE, Cao G, Prior RL, Blumberg J. Bioavailability of elderberry anthocyanins. *Mech Ageing Dev.* 2002;123(8):997-1006. doi:10.1016/S0047-6374(01)00383-9
102. Mülleder U, Murkovic M, Pfannhauser W. Urinary excretion of cyanidin glycosides. *J Biochem Biophys Methods.* 2002;53(1-3):61-66. doi:10.1016/S0165-022X(02)00093-3
103. Fernandes I, Faria A, Calhau C, de Freitas V, Mateus N. Bioavailability of

- anthocyanins and derivatives. *J Funct Foods*. 2014;7(1):54-66.
doi:10.1016/j.jff.2013.05.010
104. Talavéra S, Felgines C, Texier O, et al. Anthocyanins are efficiently absorbed from the small intestine in rats. *J Nutr*. 2004;134(9):2275-2279.
doi:10.1093/jn/134.9.2275
105. Passamonti S, Vrhovsek U, Vanzo A, Mattivi F. The stomach as a site for anthocyanins absorption from food. *FEBS Lett*. 2003;544(1-3):210-213.
doi:10.1016/S0014-5793(03)00504-0
106. Felgines C, Talavéra S, Texier O, et al. Absorption and metabolism of red orange juice anthocyanins in rats. *Br J Nutr*. 2006;95(5):898-904.
doi:10.1079/bjn20061728
107. Kay CD, Pereira-Caro G, Ludwig IA, Clifford MN, Crozier A. Anthocyanins and Flavanones Are More Bioavailable than Previously Perceived: A Review of Recent Evidence. *Annu Rev Food Sci Technol*. 2017;8(December):155-180.
doi:10.1146/annurev-food-030216-025636
108. Mueller D, Jung K, Winter M, Rogoll D, Melcher R, Richling E. Human intervention study to investigate the intestinal accessibility and bioavailability of anthocyanins from bilberries. *Food Chem*. 2017;231:275-286.
doi:10.1016/j.foodchem.2017.03.130
109. Ichiyanagi T, Shida Y, Rahman MM, Hatano Y, Konishi T. Bioavailability and tissue distribution of anthocyanins in bilberry (*Vaccinium myrtillus* L.) extract in rats. *J Agric Food Chem*. 2006;54(18):6578-6587. doi:10.1021/jf0602370
110. De Ferrars RM, Czank C, Saha S, et al. Methods for isolating, identifying, and quantifying anthocyanin metabolites in clinical samples. *Anal Chem*. 2014;86(20):10052-10058. doi:10.1021/ac500565a

111. Manach C, Williamson G, Morand C, Scalbert A, Rémésy C. Bioavailability and bioefficacy of polyphenols in humans. I. Review of 97 bioavailability studies. *Am J Clin Nutr*. 2005;81(1 Suppl):230-242. doi:10.1093/ajcn/81.1.230s
112. de Pascual-Teresa S, Moreno DA, García-Viguera C. Flavanols and anthocyanins in cardiovascular health: A review of current evidence. *Int J Mol Sci*. 2010;11(4):1679-1703. doi:10.3390/ijms11041679
113. Vitaglione P, Donnarumma G, Napolitano A, et al. Protocatechuic acid is the major human metabolite of cyanidin-glucosides. *J Nutr*. 2007;137(9):2043-2048. doi:10.1093/jn/137.9.2043
114. Xie L, Lee SG, Vance TM, et al. Bioavailability of anthocyanins and colonic polyphenol metabolites following consumption of aronia berry extract. *Food Chem*. 2016;211:860-868. doi:10.1016/j.foodchem.2016.05.122
115. Milbury PE, Vita JA, Blumberg JB. Anthocyanins are bioavailable in humans following an acute dose of cranberry juice. *J Nutr*. 2010;140(6):1099-1104. doi:10.3945/jn.109.117168
116. Mullen W, Edwards CA, Serafini M, Crozier A. Bioavailability of pelargonidin-3-O-glucoside and its metabolites in humans following the ingestion of strawberries with and without cream. *J Agric Food Chem*. 2008;56(3):713-719. doi:10.1021/jf072000p
117. Kay CD, Mazza G, Holub BJ. Anthocyanins exist in the circulation primarily as metabolites in adult men. *J Nutr*. 2005;135(11):2582-2588. doi:10.1093/jn/135.11.2582
118. Frank T, Janßen M, Netzel M, et al. Pharmacokinetics of Anthocyanidin-3-Glycosides Following Consumption of Hibiscus sabdariffa L. Extract. *J Clin Pharmacol*. 2005;45(2):203-210. doi:10.1177/0091270004270561

-
119. Bitsch R, Netzel M, Frank T, Strass G, Bitsch I. Bioavailability and biokinetics of anthocyanins from red grape juice and red wine. *J Biomed Biotechnol.* 2004;2004(5):293-298. doi:10.1155/S1110724304403106
120. Bitsch I, Janßen M, Netzel M, Straß G, Frank T. Bioavailability of anthocyanidin-3-glycosides following consumption of elderberry extract and blackcurrant juice. *Int J Clin Pharmacol Ther.* 2004;42(05):293-300. doi:10.5414/CP42293
121. Kay CD, Mazza G, Holub BJ, Wang J. Anthocyanin metabolites in human urine and serum. *Br J Nutr.* 2004;91(6):933-942. doi:10.1079/bjn20041126
122. Felgines C, Talavéra S, Gonthier MP, et al. Strawberry anthocyanins are recovered in urine as glucuro- and sulfoconjugates in humans. *J Nutr.* 2003;133(5):1296-1301. doi:10.1093/jn/133.5.1296
123. Nielsen ILF, Dragsted LO, Ravn-haren G, Freese R, Rasmussen SE. Absorption and excretion of black currant anthocyanins in humans and watanabe heritable hyperlipidemic rabbits. *J Agric Food Chem.* 2003;51(9):2813-2820. doi:10.1021/jf025947u
124. Mazza G, Kay CD, Cottrell T, Holub BJ. Absorption of anthocyanins from blueberries and serum antioxidant status in human subjects. *J Agric Food Chem.* 2002;50(26):7731-7737. doi:10.1021/jf0206901
125. Rechner AR, Kuhnle G, Hu H, et al. The Metabolism of Dietary Polyphenols and the Relevance to Circulating Levels of Conjugated Metabolites. *Free Radic Res.* 2002;36(11):1229-1241. doi:10.1080/246-1071576021000016472
126. Wu X, Cao G, Prior RL. Absorption and metabolism of anthocyanins in elderly women after consumption of elderberry or blueberry. *J Nutr.* 2002;132(7):1865-1871. doi:10.1093/jn/132.7.1865

127. Murkovic M, Mülleder U, Adam U, Pfannhauser W. Detection of anthocyanins from elderberry juice in human urine. *J Sci Food Agric*. 2001;81(9):934-937. doi:10.1002/jsfa.910
128. Netzel M, Strass G, Janssen M, Bitsch I, Bitsch R. Bioactive Anthocyanins Detected in Human Urine after Ingestion of Blackcurrant Juice. *J Environ Pathol Toxicol Oncol*. 2001;20(2):7. doi:10.1615/JEnvironPatholToxicolOncol.v20.i2.20
129. Tsuda T, Horio F, Uchida K, Aoki H, Osawa T. Dietary cyanidin 3-O- β -D-glucoside-rich purple corn color prevents obesity and ameliorates hyperglycemia in mice. *J Nutr*. 2003;133(7):2125-2130. doi:10.1093/jn/133.7.2125
130. Tsuda T, Shiga K, Ohshima K, Kawakishi S, Osawa T. Inhibition of lipid peroxidation and the active oxygen radical scavenging effect of anthocyanin pigments isolated from *Phaseolus vulgaris* L. *Biochem Pharmacol*. 1996;52(7):1033-1039. doi:10.1016/0006-2952(96)00421-2
131. Reis JF, Monteiro VVS, Souza Gomes R, et al. Action mechanism and cardiovascular effect of anthocyanins: A systematic review of animal and human studies. *J Transl Med*. 2016;14(1):1-16. doi:10.1186/s12967-016-1076-5
132. Lila MA. Anthocyanins and human health: An in vitro investigative approach. *J Biomed Biotechnol*. 2004;2004(5):306-313. doi:10.1155/S111072430440401X
133. Acquaviva R, Russo A, Galvano F, et al. Cyanidin and cyanidin 3- O - β -D-glucoside as DNA cleavage protectors and antioxidants. *Cell Biol Toxicol*. 2003;19(4):243-252. doi:10.1023/B:CBTO.0000003974.27349.4e
134. Lazzé MC, Pizzala R, Savio M, Stivala LA, Prosperi E, Bianchi L. Anthocyanins protect against DNA damage induced by tert-butyl-hydroperoxide in rat smooth muscle and hepatoma cells. *Mutat Res - Genet Toxicol Environ Mutagen*. 2003;535(1):103-115. doi:10.1016/S1383-5718(02)00285-1

135. de Sousa Moraes LF, Sun X, Peluzio M do CG, Zhu M-J. Anthocyanins/anthocyanidins and colorectal cancer: What is behind the scenes? *Crit Rev Food Sci Nutr.* 2019;59(1):59-71. doi:10.1080/10408398.2017.1357533
136. Li D, Wang P, Luo Y, Zhao M, Chen F. Health benefits of anthocyanins and molecular mechanisms: Update from recent decade. *Crit Rev Food Sci Nutr.* 2017;57(8):1729-1741. doi:10.1080/10408398.2015.1030064
137. Igwe EO, Charlton KE, Probst YC, Kent K, Netzel ME. A systematic literature review of the effect of anthocyanins on gut microbiota populations. *J Hum Nutr Diet.* 2019;32(1):53-62. doi:10.1111/jhn.12582
138. Turnbaugh PJ, Ley RE, Hamady M, Fraser-liggett C, Knight R, Gordon JI. The human microbiome project: exploring the microbial part of ourselves in a changing world. *Nature.* 2007;449(7164):804-810. doi:10.1038/nature06244.The
139. Schwartz A. *Microbiota of the Human Body: Implications in Health and Disease. Preface.* Vol 902.; 2016.
140. Tierney BT, Yang Z, Lubber JM, et al. The Landscape of Genetic Content in the Gut and Oral Human Microbiome. *Cell Host Microbe.* 2019;26(2):283-295.e8. doi:10.1016/j.chom.2019.07.008
141. Anhê FF, Varin T V., Le Barz M, et al. Gut Microbiota Dysbiosis in Obesity-Linked Metabolic Diseases and Prebiotic Potential of Polyphenol-Rich Extracts. *Curr Obes Rep.* 2015;4(4):389-400. doi:10.1007/s13679-015-0172-9
142. Loftus M, Hassounh SAD, Yooseph S. Bacterial associations in the healthy human gut microbiome across populations. *Sci Rep.* 2021;11(1):1-14. doi:10.1038/s41598-021-82449-0
143. Rinninella E, Raoul P, Cintoni M, et al. What is the healthy gut microbiota composition? A changing ecosystem across age, environment, diet, and diseases.

- Microorganisms*. 2019;7(1). doi:10.3390/microorganisms7010014
144. Round JL, Mazmanian SK. The gut microbiota shapes intestinal immune responses during health and disease. *Nat Rev Immunol*. 2009;9(5):313-323. doi:10.1038/nri2515
145. Jandhyala SM, Talukdar R, Subramanyam C, Vuyyuru H, Sasikala M, Reddy DN. Role of the normal gut microbiota. *World J Gastroenterol*. 2015;21(29):8836-8847. doi:10.3748/wjg.v21.i29.8787
146. Vieira-Silva S, Falony G, Darzi Y, et al. Species-function relationships shape ecological properties of the human gut microbiome. *Nat Microbiol*. 2016;1(8). doi:10.1038/nmicrobiol.2016.88
147. Le Chatelier E, Nielsen T, Qin J, et al. Richness of human gut microbiome correlates with metabolic markers. *Nature*. 2013;500(7464):541-546. doi:10.1038/nature12506
148. Johnson CL, Versalovic J. The human microbiome and its potential importance to pediatrics. *Pediatrics*. 2012;129(5):950-960. doi:10.1542/peds.2011-2736
149. Dueñas M, Muñoz-González I, Cueva C, et al. A Survey of Modulation of Gut Microbiota by Dietary Polyphenols. *Biomed Res Int*. 2015;2015(4):1-15. doi:10.1155/2015/850902
150. Clemente JC, Ursell LK, Parfrey LW, Knight R. The impact of the gut microbiota on human health: An integrative view. *Cell*. 2012;148(6):1258-1270. doi:10.1016/j.cell.2012.01.035
151. Baothman OA, Zamzami MA, Taher I, Abubaker J, Abu-Farha M. The role of Gut Microbiota in the development of obesity and Diabetes. *Lipids Health Dis*. 2016;15(1):1-8. doi:10.1186/s12944-016-0278-4

-
152. Bäckhed F, Ley RE, Sonnenburg JL, Peterson DA, Gordon JI. Host-bacterial mutualism in the human intestine. *Science* (80-). 2005;307(5717):1915-1920. doi:10.1126/science.1104816
153. Clapp M, Aurora N, Herrera L, Bhatia M, Wilen E, Wakefield S. Gut Microbiota's Effect on Mental Health: The Gut-Brain Axis. *Clin Pract*. 2017;7(4):131-136. doi:10.4081/cp.2017.987
154. Shehata E, Parker A, Suzuki T, et al. Microbiomes in physiology: insights into 21st-century global medical challenges. *Exp Physiol*. 2022;107(4):257-264. doi:10.1113/EP090226
155. Wang Z, Klipfell E, Bennett BJ, et al. Gut flora metabolism of phosphatidylcholine promotes cardiovascular disease. *Nature*. 2011;472(7341):57-65. doi:10.1038/nature09922
156. Tuohy KM, Fava F, Viola R. "The way to a man's heart is through his gut microbiota" - Dietary pro- and prebiotics for the management of cardiovascular risk. *Proc Nutr Soc*. 2014;73(2):172-185. doi:10.1017/S0029665113003911
157. Day-Walsh P, Shehata E, Saha S, et al. The use of an in-vitro batch fermentation (human colon) model for investigating mechanisms of TMA production from choline, l-carnitine and related precursors by the human gut microbiota. *Eur J Nutr*. 2021;60(7):3987-3999. doi:10.1007/s00394-021-02572-6
158. Duda-Chodak A, Tarko T, Satora P, Sroka P. Interaction of dietary compounds, especially polyphenols, with the intestinal microbiota: a review. *Eur J Nutr*. 2015;54(3):325-341. doi:10.1007/s00394-015-0852-y
159. Ozdal T, Sela DA, Xiao J, Boyacioglu D, Chen F, Capanoglu E. The reciprocal interactions between polyphenols and gut microbiota and effects on bioaccessibility. *Nutrients*. 2016;8(2):1-36. doi:10.3390/nu8020078

160. Tian L, Tan Y, Chen G, et al. Metabolism of anthocyanins and consequent effects on the gut microbiota. *Crit Rev Food Sci Nutr*. 2019;59(6):982-991. doi:10.1080/10408398.2018.1533517
161. Magne F, Gotteland M, Gauthier L, et al. The firmicutes/bacteroidetes ratio: A relevant marker of gut dysbiosis in obese patients? *Nutrients*. 2020;12(5). doi:10.3390/nu12051474
162. Stojanov S, Berlec A, Štrukelj B. The influence of probiotics on the firmicutes/bacteroidetes ratio in the treatment of obesity and inflammatory bowel disease. *Microorganisms*. 2020;8(11):1-16. doi:10.3390/microorganisms8111715
163. Yong E. Gut microbial “enterotypes” become less clear-cut. *Nature*. 2012;(March):1-2. doi:10.1038/nature.2012.10276
164. Vendrame S, Guglielmetti S, Riso P, Arioli S, Klimis-Zacas D, Porrini M. Six-week consumption of a wild blueberry powder drink increases Bifidobacteria in the human gut. *J Agric Food Chem*. 2011;59(24):12815-12820. doi:10.1021/jf2028686
165. Zhou L, Xie M, Yang F, Liu J. Antioxidant activity of high purity blueberry anthocyanins and the effects on human intestinal microbiota. *LWT - Food Sci Technol*. 2019:108621. doi:10.1016/j.lwt.2019.108621
166. Zhang X, Yang Y, Wu Z, Weng P. The Modulatory Effect of Anthocyanins from Purple Sweet Potato on Human Intestinal Microbiota in Vitro. *J Agric Food Chem*. 2016;64(12):2582-2590. doi:10.1021/acs.jafc.6b00586
167. Kay CD. Aspects of anthocyanin absorption, metabolism and pharmacokinetics in humans. *Nutr Res Rev*. 2006;19(1):137-146. doi:10.1079/nrr2005116
168. Faria A, Fernandes I, Norberto S, Mateus N, Calhau C. Interplay between anthocyanins and gut microbiota. *J Agric Food Chem*. 2014;62(29):6898-6902.

doi:10.1021/jf501808a

169. Morais CA, de Rosso VV, Estadella D, Pisani LP. Anthocyanins as inflammatory modulators and the role of the gut microbiota. *J Nutr Biochem*. 2016;33:1-7. doi:10.1016/j.jnutbio.2015.11.008
170. Aura AM. Microbial metabolism of dietary phenolic compounds in the colon. *Phytochem Rev*. 2008;7(3):407-429. doi:10.1007/s11101-008-9095-3
171. Most J, Penders J, Lucchesi M, Goossens GH, Blaak EE. Gut microbiota composition in relation to the metabolic response to 12-week combined polyphenol supplementation in overweight men and women. *Eur J Clin Nutr*. 2017;71(9):1040-1045. doi:10.1038/ejcn.2017.89
172. Moco S, Martin FPJ, Rezzi S. Metabolomics view on gut microbiome modulation by polyphenol-rich foods. *J Proteome Res*. 2012;11(10):4781-4790. doi:10.1021/pr300581s
173. Aura AM, Martin-Lopez P, O'Leary KA, et al. In vitro metabolism of anthocyanins by human gut microflora. *Eur J Nutr*. 2005;44(3):133-142. doi:10.1007/s00394-004-0502-2
174. López De Las Hazas MC, Mosele JI, Macià A, Ludwig IA, Motilva MJ. Exploring the Colonic Metabolism of Grape and Strawberry Anthocyanins and Their in Vitro Apoptotic Effects in HT-29 Colon Cancer Cells. *J Agric Food Chem*. 2017;65(31):6477-6487. doi:10.1021/acs.jafc.6b04096
175. Zheng F, Han M, He Y, et al. Biotransformation of anthocyanins from *Vitis amurensis* Rupr of “Beibinghong” extract by human intestinal microbiota. *Xenobiotica*. 2019;49(9):1025-1032. doi:10.1080/00498254.2018.1532132
176. Cheng JR, Liu XM, Chen ZY, Zhang YS, Zhang YH. Mulberry anthocyanin biotransformation by intestinal probiotics. *Food Chem*. 2016;213:721-727.

doi:10.1016/j.foodchem.2016.07.032

177. Hidalgo M, Oruna-Concha MJ, Kolida S, et al. Metabolism of anthocyanins by human gut microflora and their influence on gut bacterial growth. *J Agric Food Chem.* 2012;60(15):3882-3890. doi:10.1021/jf3002153
178. Durazzo A, Lucarini M, Souto EB, et al. Polyphenols: A concise overview on the chemistry, occurrence, and human health. *Phyther Res.* 2019;33(9):2221-2243. doi:10.1002/ptr.6419
179. Larkin T, Price WE, Astheimer L. The key importance of soy isoflavone bioavailability to understanding health benefits. *Crit Rev Food Sci Nutr.* 2008;48(6):538-552. doi:10.1080/10408390701542716
180. Kerimi A, Kraut NU, da Encarnacao JA, Williamson G. The gut microbiome drives inter- and intra-individual differences in metabolism of bioactive small molecules. *Sci Rep.* 2020;10(1):1-12. doi:10.1038/s41598-020-76558-5
181. Arumugam M, Raes J, Pelletier E, et al. Enterotypes of the human gut microbiome. *Nature.* 2011;473(7346):174-180. doi:10.1038/nature09944
182. Mena P, Favari C, Acharjee A, et al. Metabotypes of flavan-3-ol colonic metabolites after cranberry intake: elucidation and statistical approaches. *Eur J Nutr.* 2022;61(3):1299-1317. doi:10.1007/s00394-021-02692-z
183. Mena P, Ludwig IA, Tomatis VB, et al. Inter-individual variability in the production of flavan-3-ol colonic metabolites: preliminary elucidation of urinary metabotypes. *Eur J Nutr.* 2019;58(4):1529-1543. doi:10.1007/s00394-018-1683-4
184. Hazim S, Curtis PJ, Schär MY, et al. Acute benefits of the microbial-derived isoflavone metabolite equol on arterial stiffness in men prospectively recruited according to equol producer phenotype: A double-blind randomized controlled

- trial. *Am J Clin Nutr*. 2016;103(3):694-702. doi:10.3945/ajcn.115.125690
185. Tomás-Barberán FA, González-Sarrías A, García-Villalba R, et al. Urolithins, the rescue of “old” metabolites to understand a “new” concept: Metabotypes as a nexus among phenolic metabolism, microbiota dysbiosis, and host health status. *Mol Nutr Food Res*. 2017;61(1):1500901. doi:10.1002/mnfr.201500901
186. García-Mantrana I, Calatayud M, Romo-vaquero M, Espín JC, Selva M V, Collado MC. Urolithin Metabotypes Can Determine the Modulation of Gut Microbiota in Healthy Individuals. *Nutrients*. 2019;11:1-13.
187. Selma M V., González-Sarrías A, Salas-Salvadó J, et al. The gut microbiota metabolism of pomegranate or walnut ellagitannins yields two urolithin-metabotypes that correlate with cardiometabolic risk biomarkers: Comparison between normoweight, overweight-obesity and metabolic syndrome. *Clin Nutr*. 2018;37(3):897-905. doi:10.1016/j.clnu.2017.03.012
188. González-Sarrías A, García-Villalba R, Romo-Vaquero M, et al. Clustering according to urolithin metabotype explains the interindividual variability in the improvement of cardiovascular risk biomarkers in overweight-obese individuals consuming pomegranate: A randomized clinical trial. *Mol Nutr Food Res*. 2017;61(5):1600830. doi:10.1002/mnfr.201600830
189. Cao SY, Zhao CN, Xu XY, et al. Dietary plants, gut microbiota, and obesity: Effects and mechanisms. *Trends Food Sci Technol*. 2019;92(July):194-204. doi:10.1016/j.tifs.2019.08.004
190. Verediano TA, Stampini Duarte Martino H, Dias Paes MC, Tako E. Effects of anthocyanin on intestinal health: A systematic review. *Nutrients*. 2021;13(4). doi:10.3390/nu13041331
191. Bresciani L, Angelino D, Vivas EI, et al. Differential Catabolism of an Anthocyanin-Rich Elderberry Extract by Three Gut Microbiota Bacterial Species.

- J Agric Food Chem.* 2020;68(7):1837-1843. doi:10.1021/acs.jafc.9b00247
192. Zhu Y, Sun H, He S, et al. black rice GCMS. 2018.
193. Queipo-Ortuño MI, Boto-Ordóñez M, Murri M, et al. Influence of red wine polyphenols and ethanol on the gut microbiota ecology and biochemical biomarkers. *Am J Clin Nutr.* 2012;95(6):1323-1334. doi:10.3945/ajcn.111.027847
194. Chen L, Jiang B, Zhong C, et al. Chemoprevention of colorectal cancer by black raspberry anthocyanins involved the modulation of gut microbiota and SFRP2 demethylation. *Carcinogenesis.* 2018;39(3):471-481. doi:10.1093/carcin/bgy009
195. Espley R V., Butts CA, Laing WA, et al. Dietary flavonoids from modified apple reduce inflammation markers and modulate gut microbiota in mice. *J Nutr.* 2014;144(2):146-154. doi:10.3945/jn.113.182659
196. Flores G, Ruiz del Castillo ML, Costabile A, Klee A, Bigetti Guergoletto K, Gibson GR. In vitro fermentation of anthocyanins encapsulated with cyclodextrins: Release, metabolism and influence on gut microbiota growth. *J Funct Foods.* 2015;16:50-57. doi:10.1016/j.jff.2015.04.022
197. Gibson GR, Wang X. Regulatory effects of bifidobacteria on the growth of other colonic bacteria. *J Appl Bacteriol.* 1994;77(4):412-420. doi:10.1111/j.1365-2672.1994.tb03443.x
198. Sender R, Fuchs S, Milo R. Revised Estimates for the Number of Human and Bacteria Cells in the Body. *PLoS Biol.* 2016;14(8):1-14. doi:10.1371/journal.pbio.1002533
199. Kellingray L, Tapp HS, Saha S, Doleman JF, Narbad A, Mithen RF. Consumption of a diet rich in Brassica vegetables is associated with a reduced abundance of sulphate-reducing bacteria: A randomised crossover study. *Mol*

- Nutr Food Res.* 2017;61(9):1-11. doi:10.1002/mnfr.201600992
200. Bolger AM, Lohse M, Usadel B. Trimmomatic: A flexible trimmer for Illumina sequence data. *Bioinformatics.* 2014;30(15):2114-2120. doi:10.1093/bioinformatics/btu170
201. Bresciani L, Angelino D, Vivas EI, et al. Differential Catabolism of an Anthocyanin-Rich Elderberry Extract by Three Gut Microbiota Bacterial Species. *J Agric Food Chem.* 2019. doi:10.1021/acs.jafc.9b00247
202. Segata N, Waldron L, Ballarini A, Narasimhan V, Jousson O, Huttenhower C. Metagenomic microbial community profiling using unique clade-specific marker genes. *Nat Methods.* 2012;9(8):811-814. doi:10.1038/nmeth.2066
203. Beghini F, McIver LJ, Blanco-Míguez A, et al. Integrating taxonomic, functional, and strain-level profiling of diverse microbial communities with biobakery 3. *Elife.* 2021;10:1-42. doi:10.7554/eLife.65088
204. Franzosa EA, McIver LJ, Rahnavard G, et al. Species-level functional profiling of metagenomes and metatranscriptomes. *Nat Methods.* 2018;15(11):962-968. doi:10.1038/s41592-018-0176-y
205. Suzek BE, Wang Y, Huang H, McGarvey PB, Wu CH. UniRef clusters: A comprehensive and scalable alternative for improving sequence similarity searches. *Bioinformatics.* 2015;31(6):926-932. doi:10.1093/bioinformatics/btu739
206. Karp PD, Caspi R. A survey of metabolic databases emphasizing the MetaCyc family. *Arch Toxicol.* 2011;85(9):1015-1033. doi:10.1007/s00204-011-0705-2
207. Caspi R, Dreher K, Karp PD. The challenge of constructing, classifying, and representing metabolic pathways. *FEMS Microbiol Lett.* 2013;345(2):85-93. doi:10.1111/1574-6968.12194

208. Caspi R, Billington R, Keseler IM, et al. The MetaCyc database of metabolic pathways and enzymes-a 2019 update. *Nucleic Acids Res.* 2020;48(D1):D455-D453. doi:10.1093/nar/gkz862
209. Mallick H, Rahnavard A, McIver LJ, et al. Multivariable association discovery in population-scale meta-omics studies. *PLoS Comput Biol.* 2021;17(11):1-27. doi:10.1371/journal.pcbi.1009442
210. Płotka-Wasyłka J, Rutkowska M, Owczarek K, Tobiszewski M, Namieśnik J. Extraction with environmentally friendly solvents. *TrAC - Trends Anal Chem.* 2017;91:12-25. doi:10.1016/j.trac.2017.03.006
211. Ignat I, Volf I, Popa VI. A critical review of methods for characterisation of polyphenolic compounds in fruits and vegetables. *Food Chem.* 2011;126(4):1821-1835. doi:10.1016/j.foodchem.2010.12.026
212. Cvjetko Bubalo M, Ćurko N, Tomašević M, Kovačević Ganić K, Radojčić Redovniković I. Green extraction of grape skin phenolics by using deep eutectic solvents. *Food Chem.* 2016;200:159-166. doi:10.1016/j.foodchem.2016.01.040
213. Chemat F, Vian MA, Ravi HK, et al. Review of alternative solvents for green extraction of food and natural products: Panorama, principles, applications and prospects. *Molecules.* 2019;24(16). doi:10.3390/molecules24163007
214. Heinonen J, Farahmandazad H, Vuorinen A, Kallio H, Yang B, Sainio T. Extraction and purification of anthocyanins from purple-fleshed potato. *Food Bioprod Process.* 2016;99:136-146. doi:10.1016/j.fbp.2016.05.004
215. Lima ÁS, Oliveira BS de, Shabudin SV, Almeida M, Freire MG, Bica K. Purification of anthocyanins from grape pomace by centrifugal partition chromatography. *J Mol Liq.* 2021;326:115324. doi:10.1016/j.molliq.2021.115324
216. Silva DT da, Pauletto R, Cavalheiro S da S, et al. Natural deep eutectic solvents

- as a biocompatible tool for the extraction of blueberry anthocyanins. *J Food Compos Anal.* 2020;89(January):103470. doi:10.1016/j.jfca.2020.103470
217. Shehata E, Grigorakis S, Loupassaki S, Makris DP. Extraction optimisation using water/glycerol for the efficient recovery of polyphenolic antioxidants from two *Artemisia* species. *Sep Purif Technol.* 2015;149:462-469. doi:10.1016/j.seppur.2015.06.017
218. Katsampa P, Valsamedou E, Grigorakis S, Makris DP. A green ultrasound-assisted extraction process for the recovery of antioxidant polyphenols and pigments from onion solid wastes using Box-Behnken experimental design and kinetics. *Ind Crops Prod.* 2015;77:535-543. doi:10.1016/j.indcrop.2015.09.039
219. Ito VC, Lacerda LG. Black rice (*Oryza sativa* L.): A review of its historical aspects, chemical composition, nutritional and functional properties, and applications and processing technologies. *Food Chem.* 2019;301(April):125304. doi:10.1016/j.foodchem.2019.125304
220. Lätti AK, Riihinen KR, Kainulainen PS. Analysis of anthocyanin variation in wild populations of bilberry (*Vaccinium myrtillus* L.) in Finland. *J Agric Food Chem.* 2008;56(1):190-196. doi:10.1021/jf072857m
221. Müller D, Schantz M, Richling E. High Performance Liquid Chromatography Analysis of Anthocyanins in Bilberries (*Vaccinium myrtillus* L.), Blueberries (*Vaccinium corymbosum* L.), and Corresponding Juices. *J Food Sci.* 2012;77(4):340-345. doi:10.1111/j.1750-3841.2011.02605.x
222. Pereira-Caro G, Watanabe S, Crozier A, Fujimura T, Yokota T, Ashihara H. Phytochemical profile of a Japanese black-purple rice. *Food Chem.* 2013;141(3):2821-2827. doi:10.1016/j.foodchem.2013.05.100
223. Aboufarrag H, Hollands WJ, Percival J, Philo M, Savva GM, Kroon PA. No Effect of Isolated Anthocyanins from Bilberry Fruit and Black Rice on LDL

- Cholesterol or other Biomarkers of Cardiovascular Disease in Adults with Elevated Cholesterol: A Randomized, Placebo-Controlled, Cross-Over Trial. *Mol Nutr Food Res.* 2022;2101157:1-9. doi:10.1002/mnfr.202101157
224. Apostolakis A, Grigorakis S, Makris DP. Optimisation and comparative kinetics study of polyphenol extraction from olive leaves (*Olea europaea*) using heated water/glycerol mixtures. *Sep Purif Technol.* 2014;128:89-95. doi:10.1016/j.seppur.2014.03.010
225. Red AE, Aldini G. Effect of Extraction Solvent and Temperature on Polyphenol. 2021.
226. Rupasinghe HPV, Kathirvel P, Huber GM. Ultrasonication-assisted solvent extraction of quercetin glycosides from “Idared” apple peels. *Molecules.* 2011;16(12):9783-9791. doi:10.3390/molecules16129783
227. Rakotondramasy-Rabesiaka L, Havet JL, Porte C, Fauduet H. Estimation of effective diffusion and transfer rate during the protopine extraction process from *Fumaria officinalis* L. *Sep Purif Technol.* 2010;76(2):126-131. doi:10.1016/j.seppur.2010.09.030
228. Seikova I, Simeonov E, Ivanova E. Protein leaching from tomato seed- Experimental kinetics and prediction of effective diffusivity. *J Food Eng.* 2004;61(2):165-171. doi:10.1016/S0260-8774(03)00083-9
229. Morsli F, Grigorakis S, Halahlah A, Poulianiti KP, Makris DP. Appraisal of the combined effect of time and temperature on the total polyphenol yield in batch stirred-tank extraction of medicinal and aromatic plants: The extraction efficiency factor. *J Appl Res Med Aromat Plants.* 2021;25(August):100340. doi:10.1016/j.jarmap.2021.100340
230. Alara OR, Abdurahman NH. Kinetics studies on effects of extraction techniques on bioactive compounds from *Vernonia cinerea* leaf. *J Food Sci Technol.*

- 2019;56(2):580-588. doi:10.1007/s13197-018-3512-4
231. Hobbi P, Okoro OV, Delporte C, et al. Kinetic modelling of the solid–liquid extraction process of polyphenolic compounds from apple pomace: influence of solvent composition and temperature. *Bioresour Bioprocess*. 2021;8(1). doi:10.1186/s40643-021-00465-4
232. Manach C, Scalbert A, Morand C, Rémésy C, Jiménez L. Polyphenols: Food sources and bioavailability. *Am J Clin Nutr*. 2004;79(5):727-747. doi:10.1093/ajcn/79.5.727
233. Thursby E, Juge N. Introduction to the human gut microbiota. *Biochem J*. 2017;474(11):1823-1836. doi:10.1042/BCJ20160510
234. Illiano P, Brambilla R, Parolini C. The mutual interplay of gut microbiota, diet and human disease. *FEBS J*. 2020;287(5):833-855. doi:10.1111/febs.15217
235. Singh RK, Chang HW, Yan D, et al. Influence of diet on the gut microbiome and implications for human health. *J Transl Med*. 2017;15(1):1-17. doi:10.1186/s12967-017-1175-y
236. Stevens JF, Maier CS. The chemistry of gut microbial metabolism of polyphenols. *Phytochem Rev*. 2016;15(3):425-444. doi:10.1007/s11101-016-9459-z
237. Cheng M, Zhang X, Guo XJ, Wu ZF, Weng PF. The interaction effect and mechanism between tea polyphenols and intestinal microbiota: Role in human health. *J Food Biochem*. 2017;41(6):1-9. doi:10.1111/jfbc.12415
238. Bolca S, Van de Wiele T, Possemiers S. Gut metabotypes govern health effects of dietary polyphenols. *Curr Opin Biotechnol*. 2013;24(2):220-225. doi:10.1016/j.copbio.2012.09.009

239. Aboufarrag H. Interactions between anthocyanins, cholesterol metabolism and PON-1 in relation to HDL quality and CVD risk. 2019;(September).
<https://ueaeprints.uea.ac.uk/id/eprint/74189/>.
240. Chen Y, Li Q, Zhao T, et al. Biotransformation and metabolism of three mulberry anthocyanin monomers by rat gut microflora. *Food Chem.* 2017;237:887-894.
doi:10.1016/j.foodchem.2017.06.054
241. O'Toole PW, Jeffery IB. Gut microbiota and aging. *Science (80-)*. 2015;350(6265):1214-1215. doi:10.1126/science.aac8469
242. Cardona F, Andrés-Lacueva C, Tulipani S, Tinahones FJ, Queipo-Ortuño MI. Benefits of polyphenols on gut microbiota and implications in human health. *J Nutr Biochem.* 2013;24(8):1415-1422. doi:10.1016/j.jnutbio.2013.05.001
243. Wilkens CA, Altamirano C, Gerdtzen ZP. Comparative metabolic analysis of lactate for CHO cells in glucose and galactose. *Biotechnol Bioprocess Eng.* 2011;16(4):714-724. doi:10.1007/s12257-010-0409-0
244. Ryan CS, Kleinberg I. A comparative study of glucose and galactose uptake in pure cultures of human oral bacteria, salivary sediment and dental plaque. *Arch Oral Biol.* 1995;40(8):743-752. doi:10.1016/0003-9969(95)00028-N
245. Rodriguez-Amaya DB. Update on natural food pigments - A mini-review on carotenoids, anthocyanins, and betalains. *Food Res Int.* 2019;124(March 2018):200-205. doi:10.1016/j.foodres.2018.05.028
246. Março PH, Poppi RJ, Scarminio IS, Tauler R. Investigation of the pH effect and UV radiation on kinetic degradation of anthocyanin mixtures extracted from *Hibiscus acetosella*. *Food Chem.* 2011;125(3):1020-1027.
doi:10.1016/j.foodchem.2010.10.005
247. Fernandes I, Marques C, Évora A, et al. *Anthocyanins: Nutrition and Health.*;

2019. doi:10.1007/978-3-319-78030-6_79
248. Brouillard R, Iacobucci GA, Sweeny JG. Chemistry of Anthocyanin Pigments. 9. UV-Visible Spectrophotometric Determination of the Acidity Constants of Apigeninidin and Three Related 3-Deoxyflavylium Salts. *J Am Chem Soc.* 1982;104(26):7585-7590. doi:10.1021/ja00390a033
249. Soldatkina LM, Novotna VO, Salamon I. Degradation Kinetics of Anthocyanins in Acidic Aqueous Extracts of Berries. *Odesa Natl Univ Herald Chem.* 2017;22(1(61)):55-66. doi:10.18524/2304-0947.2017.1(61).94711
250. Dangles O, Fenger JA. The chemical reactivity of anthocyanins and its consequences in food science and nutrition. *Molecules.* 2018;23(8). doi:10.3390/molecules23081970
251. Fenger JA, Robbins RJ, Collins TM, Dangles O. The fate of acylated anthocyanins in mildly heated neutral solution. *Dye Pigment.* 2020;178(March):108326. doi:10.1016/j.dyepig.2020.108326
252. Hrazdina G. Reactions of the anthocyanidin-3,5-diglucosides: Formation of 3,5-di-(O- β -d-glucosyl)-7-hydroxy coumarin. *Phytochemistry.* 1971;10(5):1125-1130. doi:10.1016/S0031-9422(00)89950-1
253. Sang S, Lee MJ, Hou Z, Ho CT, Yang CS. Stability of tea polyphenol (-)-epigallocatechin-3-gallate and formation of dimers and epimers under common experimental conditions. *J Agric Food Chem.* 2005;53(24):9478-9484. doi:10.1021/jf0519055
254. Vallverdú-Queralt A, Meudec E, Ferreira-Lima N, et al. A comprehensive investigation of guaiacyl-pyranoanthocyanin synthesis by one-/two-dimensional NMR and UPLC-DAD-ESI-MSn. *Food Chem.* 2016;199:902-910. doi:10.1016/j.foodchem.2015.12.089

255. Bondre S, Patil P, Kulkarni A, Pillai MM. Study on isolation and purification of anthocyanins and its application as pH indicator. *Int J Adv Biotechnol Res*. 2012;3(3):698-702. <http://www.bipublication.com>.
256. Peiffer DS, Zimmerman NP, Wang LS, et al. Chemoprevention of esophageal cancer with black raspberries, their component anthocyanins, and a major anthocyanin metabolite, protocatechuic acid. *Cancer Prev Res*. 2014;7(6):574-584. doi:10.1158/1940-6207.CAPR-14-0003
257. Forester SC, Choy YY, Waterhouse AL, Oteiza PI. The anthocyanin metabolites gallic acid, 3-O-methylgallic acid, and 2,4,6-trihydroxybenzaldehyde decrease human colon cancer cell viability by regulating pro-oncogenic signals. *Mol Carcinog*. 2014;53(6):432-439. doi:10.1002/mc.21974
258. Percival JR. The Role of the Human Gut Microbiota in the Metabolism of Dietary Anthocyanins. 2021;(September).
259. Waksmundzka-Hajnos M. Chromatographic separations of aromatic carboxylic acids. *J Chromatogr B Biomed Appl*. 1998;717(1-2):93-118. doi:10.1016/S0378-4347(98)00257-6
260. Zhang ZW, Cong L, Peng R, et al. Transformation of berberine to its demethylated metabolites by the CYP51 enzyme in the gut microbiota. *J Pharm Anal*. 2021;11(5):628-637. doi:10.1016/j.jpha.2020.10.001
261. Khanbabaee K, van Ree T. Tannins: Classification and definition. *Nat Prod Rep*. 2001;18(6):641-649. doi:10.1039/b101061l
262. Herrera Bravo de Laguna I, Toledo Marante FJ, Mioso R. Enzymes and bioproducts produced by the ascomycete fungus *Paecilomyces variotii*. *J Appl Microbiol*. 2015;119(6):1455-1466. doi:10.1111/jam.12934
263. Kolodziejczyk AA, Zheng D, Elinav E. Diet–microbiota interactions and

- personalized nutrition. *Nat Rev Microbiol.* 2019;17(12):742-753.
doi:10.1038/s41579-019-0256-8
264. Burcelin R, Garidou L, Pomié C. Immuno-microbiota cross and talk: The new paradigm of metabolic diseases. *Semin Immunol.* 2012;24(1):67-74.
doi:10.1016/j.smim.2011.11.011
265. Ondov BD, Bergman NH, Phillippy AM. Interactive metagenomic visualization in a Web browser. *BMC Bioinformatics.* 2011;12(1):385. doi:10.1186/1471-2105-12-385
266. Shah N, Tang H, Doak TG, Ye Y. Comparing bacterial communities inferred from 16S rRNA gene sequencing and shotgun metagenomics. *Pacific Symp Biocomput 2011, PSB 2011.* 2011:165-176. doi:10.1142/9789814335058_0018
267. Overall J, Bonney SA, Wilson M, et al. Metabolic effects of berries with structurally diverse anthocyanins. *Int J Mol Sci.* 2017;18(2).
doi:10.3390/ijms18020422
268. Lacombe A, Li RW, Klimis-Zacas D, et al. Lowbush Wild Blueberries have the Potential to Modify Gut Microbiota and Xenobiotic Metabolism in the Rat Colon. *PLoS One.* 2013;8(6):1-8. doi:10.1371/journal.pone.0067497
269. Rigottier-Gois L. Dysbiosis in inflammatory bowel diseases: The oxygen hypothesis. *ISME J.* 2013;7(7):1256-1261. doi:10.1038/ismej.2013.80
270. Lapidot T, Harel S, Granit R, Kanner J. Bioavailability of Red Wine Anthocyanins as Detected in Human Urine. *J Agric Food Chem.* 1998;46(10):4297-4302. doi:10.1021/jf980007o
271. Herrmann K, Nagel CW. Occurrence and content of hydroxycinnamic and hydroxybenzoic acid compounds in foods. *Crit Rev Food Sci Nutr.* 1989;28(4):315-347. doi:10.1080/10408398909527504

272. Robbins RJ. Phenolic acids in foods: An overview of analytical methodology. *J Agric Food Chem.* 2003;51(10):2866-2887. doi:10.1021/jf026182t
273. Tomás-Barberán FA, García-Villalba R, González-Sarrías A, Selma M V., Espín JC. Ellagic acid metabolism by human gut microbiota: Consistent observation of three urolithin phenotypes in intervention trials, independent of food source, age, and health status. *J Agric Food Chem.* 2014;62(28):6535-6538. doi:10.1021/jf5024615
274. Rafii F. The Role of Colonic Bacteria in the Metabolism of the Natural Isoflavone Daidzin to Equol. *Metabolites.* 2015;5(1):56-73. doi:10.3390/metabo5010056
275. Mayo B, Vázquez L, Flórez AB. Equol: A Bacterial Metabolite from The Daidzein Isoflavone and Its Presumed Beneficial Health Effects. *Nutrients.* 2019;11(9):2231. doi:10.3390/nu11092231
276. Vallenet D, Calteau A, Dubois M, et al. MicroScope: an integrated platform for the annotation and exploration of microbial gene functions through genomic, pangenomic and metabolic comparative analysis. *Nucleic Acids Res.* October 2019. doi:10.1093/nar/gkz926
277. Markowitz VM, Mavromatis K, Ivanova NN, Chen IMA, Chu K, Kyrpides NC. IMG ER: A system for microbial genome annotation expert review and curation. *Bioinformatics.* 2009;25(17):2271-2278. doi:10.1093/bioinformatics/btp393
278. Bocs S. AMIGene: Annotation of Microbial Genes. *Nucleic Acids Res.* 2003;31(13):3723-3726. doi:10.1093/nar/gkg590
279. Kastl AJ, Terry NA, Wu GD, Albenberg LG. The Structure and Function of the Human Small Intestinal Microbiota: Current Understanding and Future Directions. *Cmgh.* 2020;9(1):33-45. doi:10.1016/j.jcmgh.2019.07.006

280. Mailhe M, Ricaboni D, Vitton V, et al. Repertoire of the gut microbiota from stomach to colon using culturomics and next-generation sequencing. *BMC Microbiol.* 2018;18(1):1-11. doi:10.1186/s12866-018-1304-7

Appendix 1

Product Specifications of the Black Rice and Bilberry Extracts Used in the *in-vitro* Colon Model Study

Appendix 1

These figures are with reference to the methods applied in Chapter 4. Product specifications of the black rice and bilberry extracts used in the in-vitro colon model study



CERTIFICATE OF ANALYSIS

CERTIFICATE NO. 2018060711

PRODUCT	: BLACK RICE EXTRACT POWDER		
PRODUCT NO.	: BR-30	DATE OF MANUFACTURE	: Jun. 4, 2017
BATCH NO.	: 170602 BR-30	DATE OF CERTIFICATE	: Jun. 11, 2017
EXPIRY DATE	: Jun. 3, 2020	SPECIFICATION NO.	: (A0)000

ANALYSIS ITEMS	SPECIFICATIONS	METHOD	RESULTS
CHARACTERISTICS	Purple Black Powder	VISUAL INSPECTION	CONFORMED
※HEAVY METALS	20ppm Max.	Eur. Ph. 2.4.8	CONFORMED
※CADMIUM	1ppm Max.	Eur. Ph. 2.4.27	CONFORMED
※LEAD	3ppm Max.	Eur. Ph. 2.4.27	CONFORMED
※MERCURY	0.1ppm Max.	Eur. Ph. 2.4.27	CONFORMED
LOSS ON DRYING	5.0% Max.	Eur. Ph. 2.8.17	3.8%
ASH	3.0% Max.	Eur. Ph. 2.4.16	0.4%
※PESTICIDES	In accordance to EC Regulation No. 396/2005 and modifications		CONFORMED
ANTHOCYANINS: Content of Anthocyanins by HPLC (on dry basis, expressed as Cyanidin 3-O-glucoside)	30.0% Min.	In-house method	36.9%
CYANIDIN 3-O-GLUCOSIDE: Content of Cyanidin 3-O-glucoside by HPLC (on dry basis)	20.0% Min.	In-house method	33.9%
MICROBIOLOGY		Eur. Ph. 2.6.12 and 2.6.13	
TOTAL PLATE COUNT	<5,000cfu/g		<10cfu/g
YEAST & MOLD	<500cfu/g		<10cfu/g
BILE-TOLERANT GRAM-NEGATIVE BACTERIA	<100cfu/g		<10cfu/g
ESCHERICHIA COLI	Absence/g		CONFORMED
SALMONELLA	Absence/10g		CONFORMED
※AFLATOXINS		Eur. Ph. 2.8.18	
SUM OF AFLATOXIN B1, B2, G1 AND G2	< 4ppb		COMPLIES
AFLATOXIN B1	< 2ppb		COMPLIES
※BENZO(a)PYRENE	< 10ppb	In-house method	CONFORMED
※SUM OF BENZO(a)PYRENE, BENZO(a)ANTHRACENE, BENZO(b)FLUORANTHENE, CHRYSENE	< 50ppb	In-house method	CONFORMED

* Periodic test (not carried out batch by batch) for which BGG tests batches randomly every year.
Complies: BGG can provide a Certificate of Compliance for this test with historical data from tested batches

QUALITY CONTROL MANAGER *XyHong*

Beijing Gingko Group
Your natural partner

CHECK *Junfang Yao*

ANALYST *WqSun*

Room 1706, Tower A, Building 1, Tianzuo International Center,
No. 12 Zhongguancun South Avenue, Haidian District, Beijing, China, 100081
Phone: +86 (0) 10 5970 5209 Fax: +86 (0) 10 5970 5660
www.bggworld.com

Appendix figure 1. 1. Product specifications of the black rice extract used in the in-vitro colon model study.



CERTIFICATE OF ANALYSIS

CERTIFICATE NO. 2018060712

PRODUCT	: BILBERRY EXTRACT POWDER (<i>Myrti</i> PRO)		
PRODUCT NO.	: GC-021J	DATE OF MANUFACTURE	: May 18, 2017
BATCH NO.	: 170511 GC-021J	DATE OF CERTIFICATE	: May 25, 2017
EXPIRY DATE	: May 17, 2020	SEPCIFICATION NO.	: (A1)000

ANALYSIS ITEMS	SPECIFICATIONS	METHOD	RESULTS
CHARACTERISTICS	PURPLE BLACK POWDER	VISUAL INSPECTION	CONFORMED
IDENTIFICATION	HPLC COMPLIES	Eur. Ph. monograph 2394	CONFORMED
LOSS ON DRYING	5.0% Max.	Eur. Ph. 2.8.17	4.2%
ASH	3.0% Max.	Eur. Ph. 2.4.16	0.2%
PH	3.0-4.5	Eur. Ph. 2.2.3	3.2
*HEAVY METALS	20ppm Max.	Eur. Ph. 2.4.8	COMPLIES
*LEAD	3ppm Max.	Eur. Ph. 2.4.27	COMPLIES
*CADMIUM	1ppm Max.	Eur. Ph. 2.4.27	COMPLIES
*MERCURY	0.1ppm Max.	Eur. Ph. 2.4.27	COMPLIES
*PESTICIDES	EC NO. 396/2005 & MODIFICATIONS		COMPLIES
FREE ANTHOCYANIDINS Free Anthocyanidins by HPLC	1.0% Max.	Eur. Ph. monograph 2394	0.5%
ANTHOCYANIDINS Content of Anthocyanins by UV (on dry basis)	25.0% Min	In-house method	26.1%
ANTHOCYANINS Content of Anthocyanins by HPLC (on dry basis, expressed as Cyanidin 3-O-glucoside chloride)	36.0% Min	Eur. Ph. monograph 2394	36.7%
MICROBIOLOGY TOTAL PLATE COUNT	<5,000cfu/g	Eur. Ph. 2.6.12 and 2.6.13	<10cfu/g
YEAST & MOLD	<500cfu/g		<10cfu/g
BILE-TOLERANT GRAM-NEGATIVE BACTERIA	<100cfu/g		<10cfu/g
ESCHERICHIA COLI	Absence/g		CONFORMED
SALMONELLA	Absence/10g		CONFORMED
*AFLATOXINS		Eur. Ph. 2.8.18	
SUM OF AFLATOXIN B1, B2, G1 AND G2	< 4ppb		COMPLIES
AFLATOXIN B1	< 2ppb		COMPLIES
*BENZO(a)PYRENE	< 10ppb	In-house method	COMPLIES
*SUM OF BENZO(a)PYRENE, BENZ(a)ANTHRACENE, BENZO(b)FLUORANTHENE, CHRYSENE	< 50ppb	In-house method	COMPLIES

* Periodic test (not carried out batch by batch) for which BGG tests batches randomly every year.
Complies: BGG can provide a Certificate of Compliance for this test with historical data from tested batches

QUALITY CONTROL MANAGER *lyhera* CHECK *Jf yao* ANALYST *Wq Sun*

Beijing Gingko Group
Your natural partner

Room 1706, Tower A, Building 1, Tianzuo International Center,
No. 12 Zhongguancun South Avenue, Haidian District, Beijing, China, 100081
Phone: +86 (0) 10 5970 5209 Fax: +86 (0) 10 5970 5660
www.bggworld.com

Appendix figure 1. 2. Product specifications of the bilberry extract used in the in-vitro colon model study.

Appendix 2

**The molar extinction
coefficient of common
anthocyanins**

Appendix 2

Appendix table 2. 1. The molar extinction coefficient ($\epsilon_{520\text{nm}}$) of six common anthocyanins.

Anthocyanin	Prepared authentic standard				Absorbance (520 nm)			$\epsilon = A/l \cdot c$ ($M^{-1}cm^{-1}$)				$\epsilon_{520\text{ nm}}$ (mean \pm S.D.)
	Anthocyanin chloride		Anthocyanin		R1	R2	R3	R1	R2	R3	Mean	
	Prepared concentration (mmol/L)	Exact mass (g/mole)	Exact mass (g/mole)	Actual concentration (mmol/L)								
Cya3Glc	0.03711	484.077	449.108	0.03443	0.855	0.853	0.855	24833	24775	24833	24813	25200 \pm 300
	0.03181			0.02951	0.747	0.746	0.747	25312	25278	25312	25301	
	0.02783			0.02582	0.653	0.655	0.654	25288	25365	25326	25326	
Peo3Glc	0.03599	498.092	463.123	0.03346	0.783	0.782	0.782	23400	23370	23370	23380	24100 \pm 600
	0.03085			0.02868	0.688	0.687	0.687	23988	23953	23953	23965	
	0.02699			0.02510	0.621	0.621	0.622	24745	24745	24785	24758	
Mal3Glc	0.03380	528.103	493.134	0.03156	0.834	0.837	0.837	26426	26521	26521	26490	26250 \pm 500
	0.02897			0.02705	0.723	0.717	0.719	26727	26505	26579	26604	
	0.02535			0.02367	0.605	0.607	0.609	25560	25645	25729	25645	
Del3Glc	0.03583	500.072	465.103	0.03333	0.998	0.993	0.993	29944	29794	29794	29844	30300 \pm 400
	0.03072			0.02857	0.878	0.871	0.874	30734	30489	30594	30606	
	0.02688			0.02500	0.758	0.763	0.763	30324	30524	30524	30458	
Pel3Glc	0.04618	468.082	433.113	0.04273	0.746	0.748	0.748	17459	17506	17506	17491	17600 \pm 300
	0.03848			0.03561	0.620	0.622	0.621	17413	17469	17441	17441	
	0.03298			0.03052	0.548	0.548	0.549	17956	17956	17988	17967	
Pet3Glc	0.03479	514.087	479.118	0.03242	0.834	0.827	0.832	25725	25509	25663	25632	26022 \pm 400
	0.02982			0.02779	0.727	0.723	0.727	26162	26018	26162	26114	
	0.02609			0.02431	0.640	0.639	0.641	26321	26280	26362	26321	

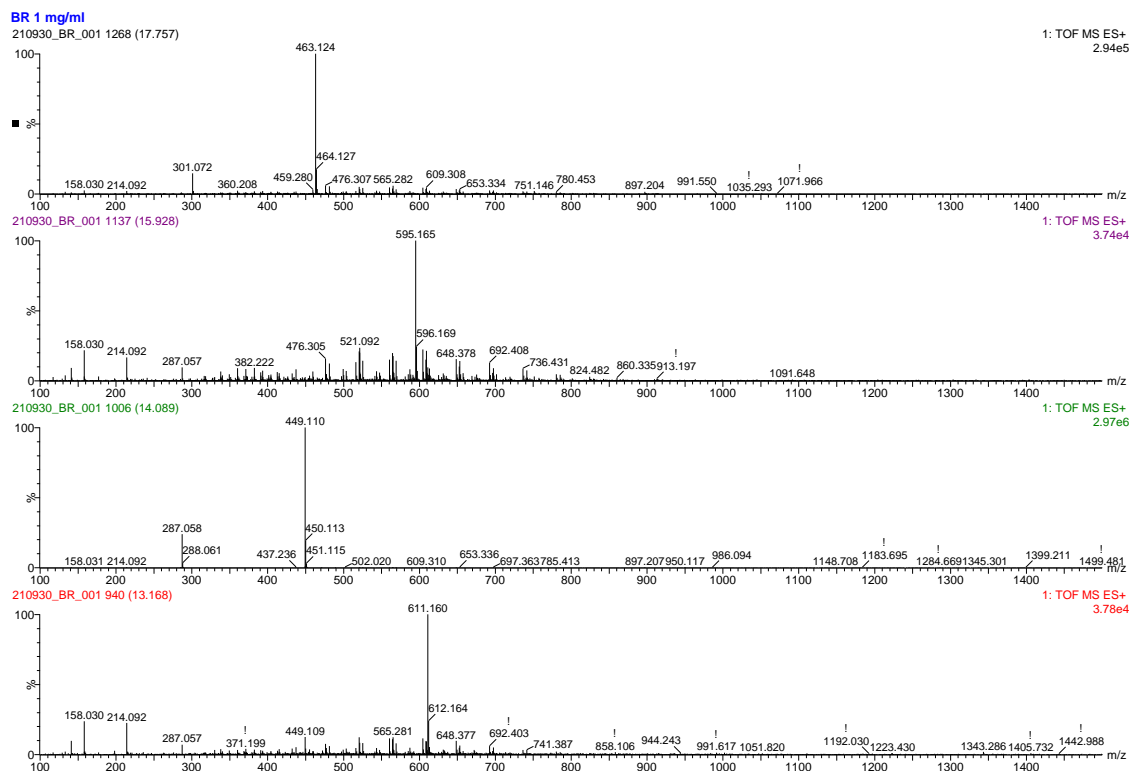
Extinction coefficient ($\epsilon_{520\text{ nm}}$) for 6 pure anthocyanins was established in a freshly prepared acidified aqueous (2% v/v formic acid, pH=2.06). The $\epsilon_{520\text{ nm}}$ for Cya3Glc was $25147.3 \pm 289.1 M^{-1} cm^{-1}$.

Appendix 3

**Mass spectrum of anthocyanins of
black rice and bilberry extract
powders**

Appendix 3

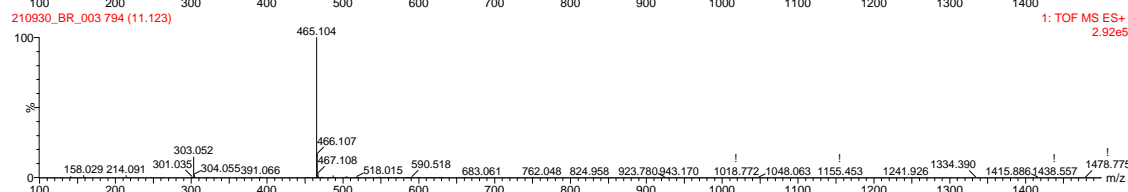
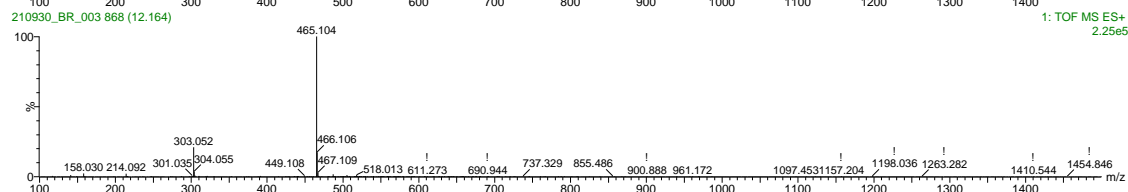
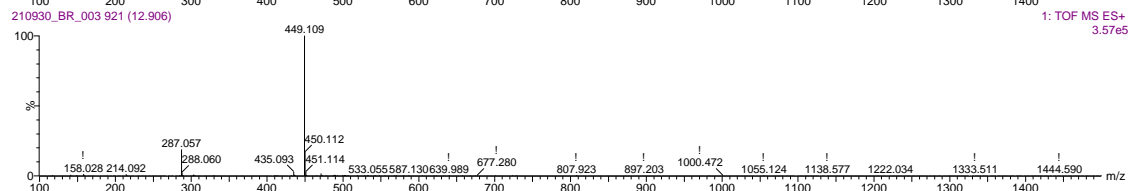
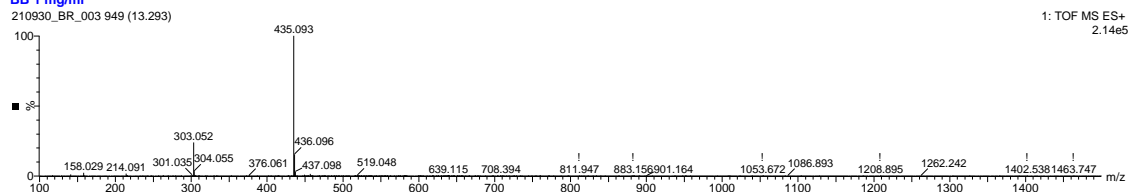
The following figures with reference to the data presented in Chapter 4



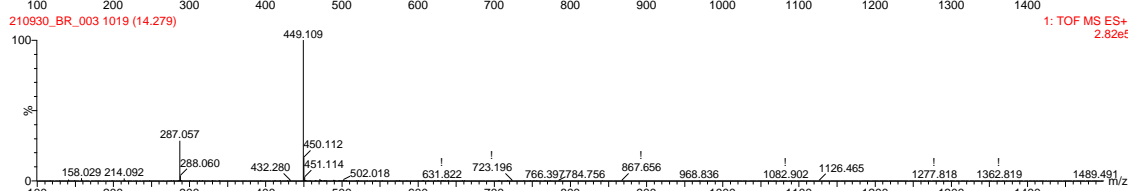
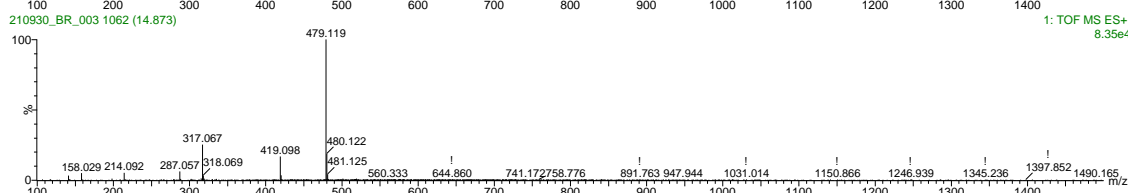
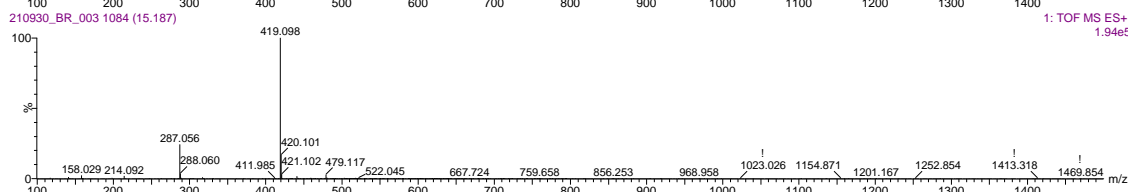
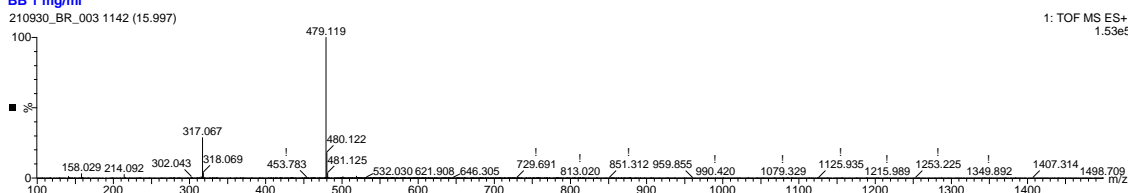
Appendix figure 3. 1. Signals corresponding to the $m/z[M+H]^+$ of anthocyanins in black rice extract.

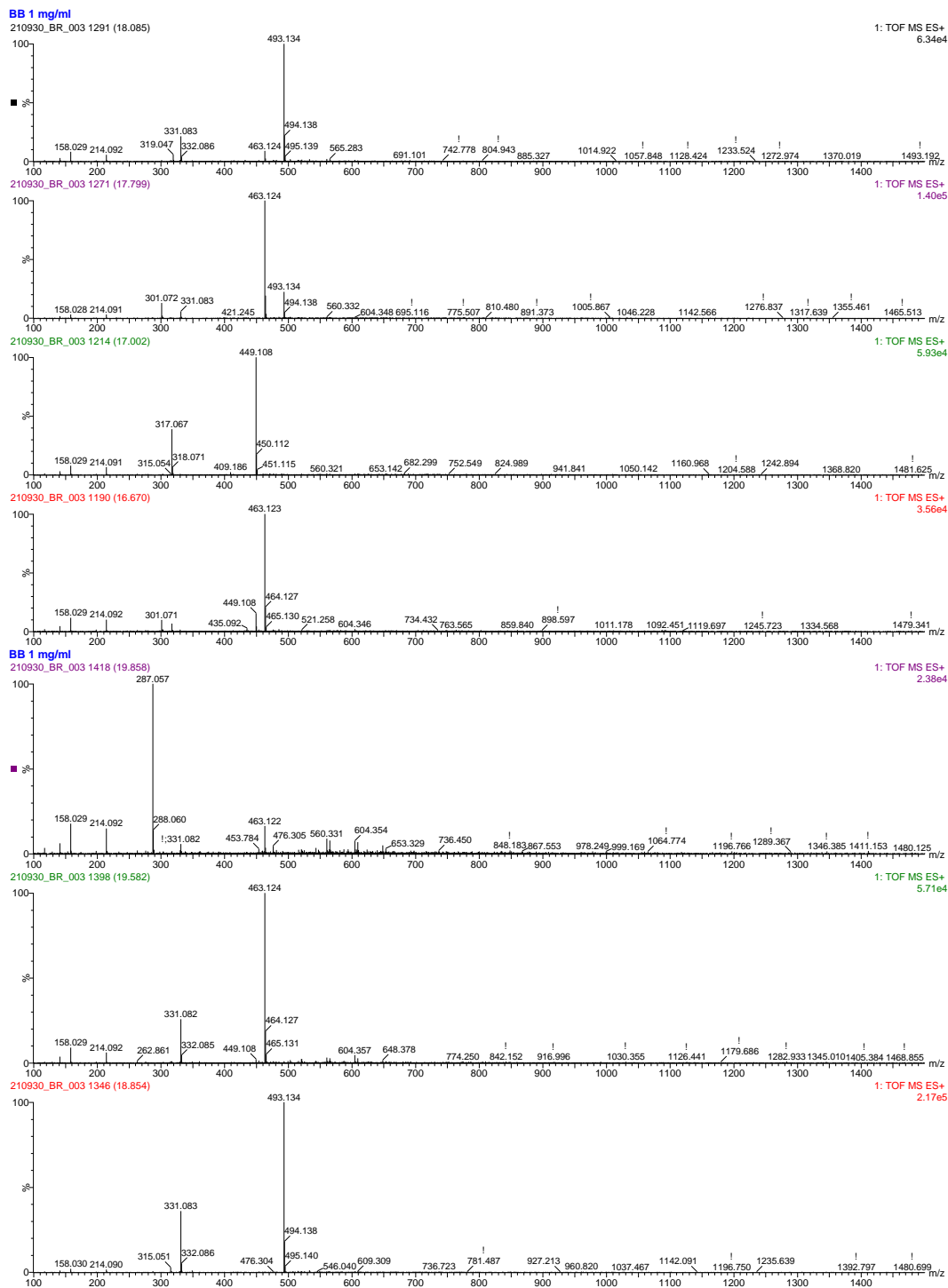
A fresh stock solution of black rice extract powder (1 mg/mL) was prepared in acidified water (2% formic acid). A 10 μ L of prepared stock solution was injected through HPLC-ESI-TOF. Both low and high energy ionisation were scanned alongside with DAD detector at 500 nm. A gradient elution was performed using 1% v/v formic acid in water as solvent A, and 1% v/v formic acid in acetonitrile as solvent B.

BB 1 mg/ml



BB 1 mg/ml





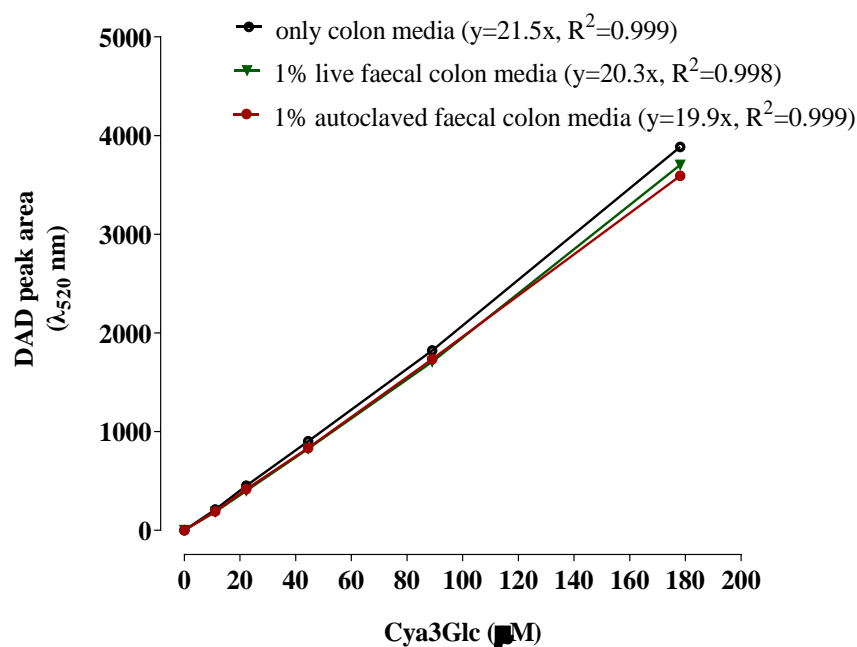
Appendix figure 3. 2. Signals corresponding to the $m/z[M+H]^+$ of anthocyanins in bilberry extract.
A fresh stock solution of black rice extract powder (1 mg/mL) was prepared in acidified water (2% formic acid). A 10 μ L of prepared stock solution was injected through HPLC-ESI-TOF. Both low and high energy ionisation were scanned alongside with DAD detector at 500 nm. A gradient elution was performed using 1% v/v formic acid in water as solvent A, and 1% v/v formic acid in acetonitrile as solvent B

Appendix 4

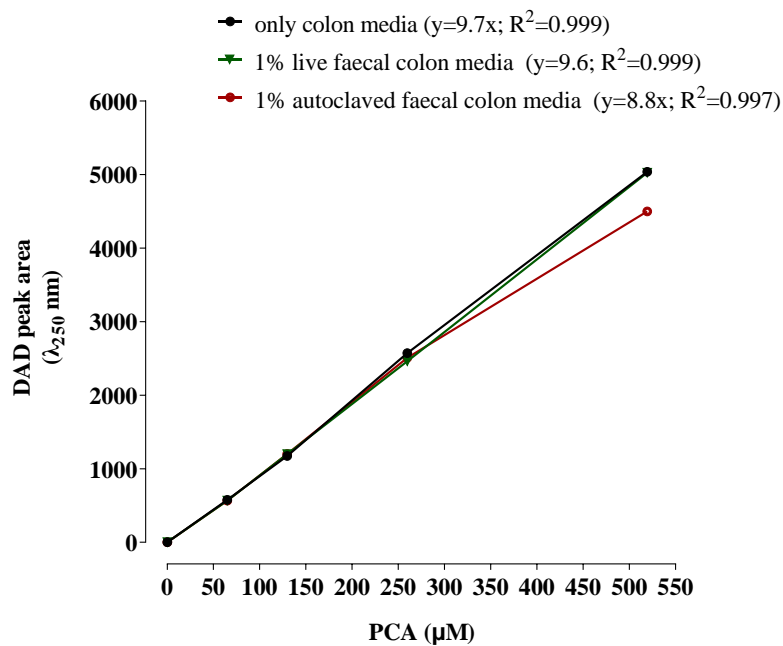
External standard curves and the effect of matrix on the detection and quantification of anthocyanins and their metabolites

Appendix 4

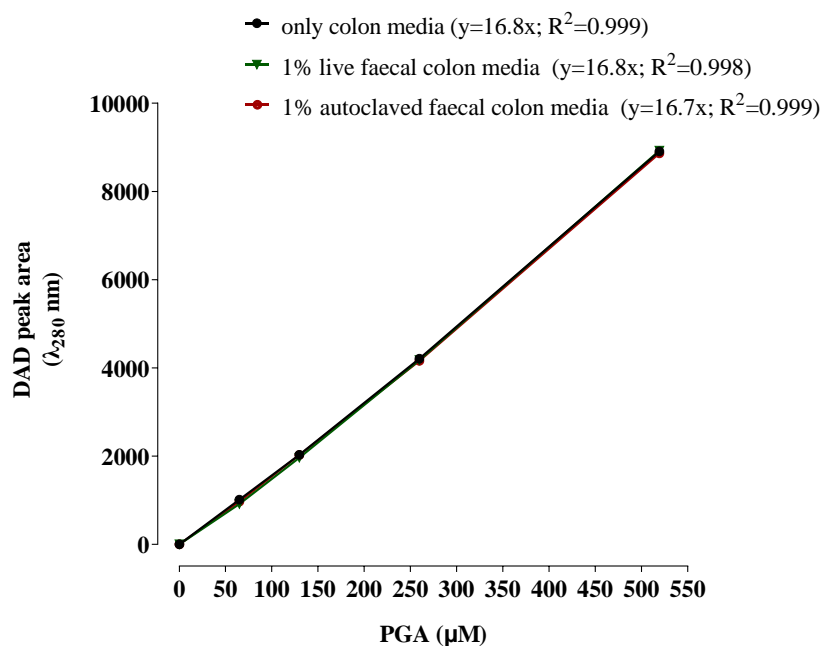
The following figures with reference to the data presented in Chapter 4 and 6



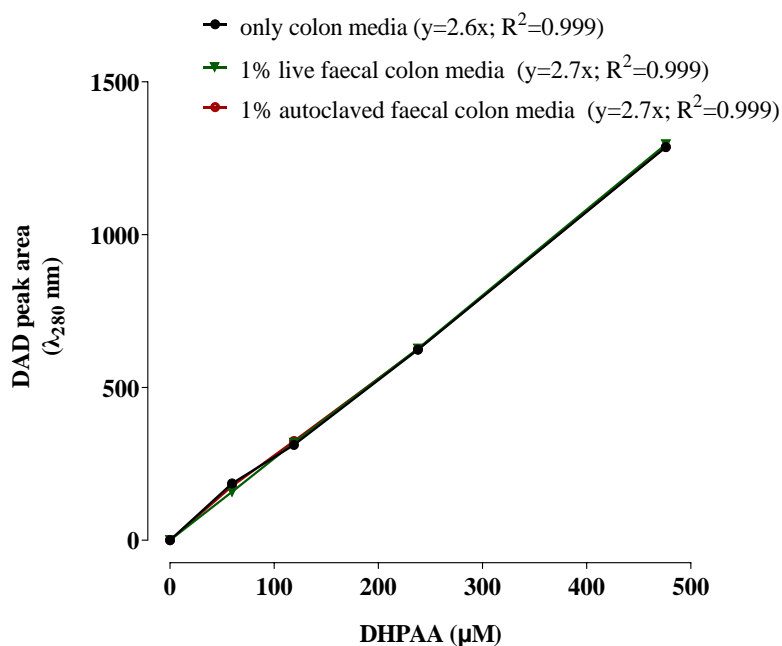
Appendix figure 4. 1. Standard curves in different matrices showing the effect of faecal materials on the detection of Cya3Glc



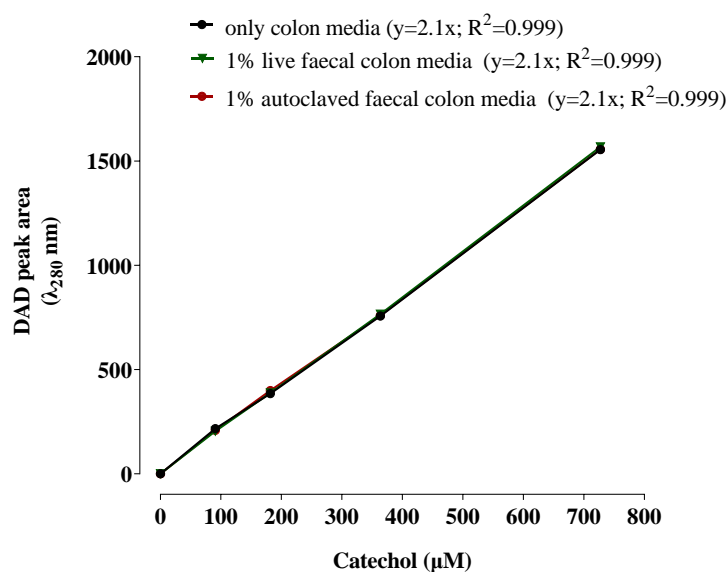
Appendix figure 4. 2. Standard curves in different matrices showing the effect of faecal materials on the detection of PCA.



Appendix figure 4. 3. Standard curves in different matrices showing the effect of faecal materials on the detection of PGA.



Appendix figure 4. 4. Standard curves in different matrices showing the effect of faecal materials on the detection of 3,4-DHPAA.



Appendix figure 4. 5. Standard curves in different matrices showing the effect of faecal materials on the detection of catechol.

Appendix table 4. 1. The effect of in-vitro colon model fermentation on the signal responses of different phenolic metabolites

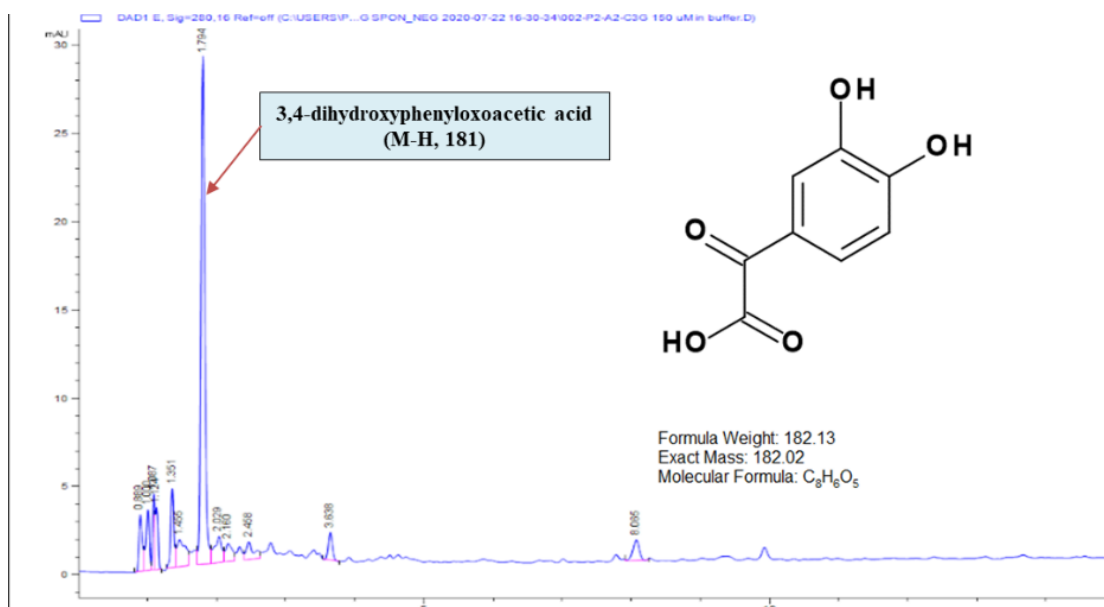
No.	Metabolite	RT	Slope		0-24 h changes
			0 h	24 h	
1	Pyrogallol	2.9	17.95	17.72	-0.23
2	Phloroglucinol	2.64	0.69	0.81	0.12
3	Ferulic acid	6.38	5.9	5.52	-0.38
4	Sinapic acid	6.36	2.26	2.3	0.04
5	Vanillic acid	5.53	2.41	3.27	0.86
6	4-Hydroxybenzoic acid	5.1	23.46	39.78	16.32
7	Phloroglucinol aldehyde (PGA)	6.28	31.61	40.05	8.44
8	Syringic acid	5.65	0.18	0.11	-0.07
9	Caffeic acid	5.63	70.39	109.47	39.08
10	Gallic acid	1.68	57.9	44.9	-13
11	3-O-methyl-gallic acid	5.53	295.82	345.97	50.15
12	Protocatechuic acid (PCA)	3.56	71.385	43.31	-28.075
13	2,4,6- tri hydroxy benzoic acid (PGCA)	3.87	43.65	104.8	61.15
14	Dihydrocaffeic acid	5.48	11.01	13.61	2.6
15	Dihydroferulic acid	6.24	6.34	8.87	2.53
16	2,4 dihydroxy benzoic acid	2.85	0.25	0.39	0.14
22	3,4 dihydroxy phenyl acetic acid (DHPAA)	5.47	3.01	2.16	-0.85
24	Catechol	5.25	17.02	21.87	4.85

Appendix 5

DAD chromatograms

Appendix 5

The following figures with reference to the data presented in Chapter 5.



Appendix figure 5. 1. DAD chromatogram λ (280 nm) of the aerobic incubation of Cya3Glc after 7 days incubation in a 10 mM phosphate buffer (pH 7.4) at 37°C showing the decomposition of Cya3Glc with the formation of new breakdown products.

Appendix 6

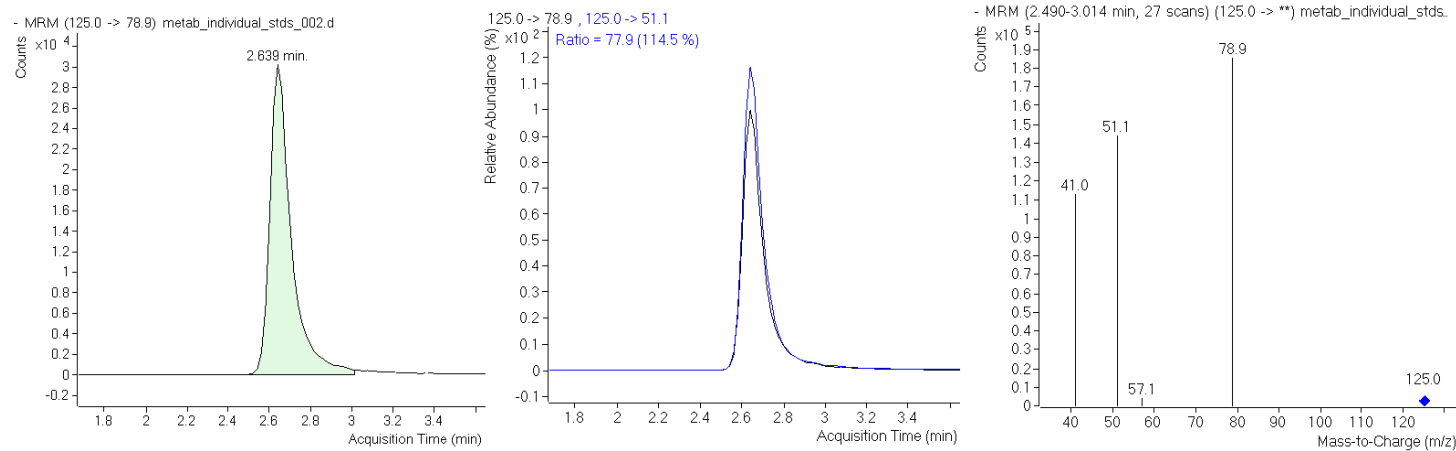
Ms/Ms chromatograms of the ion currents for various metabolites

Appendix 6

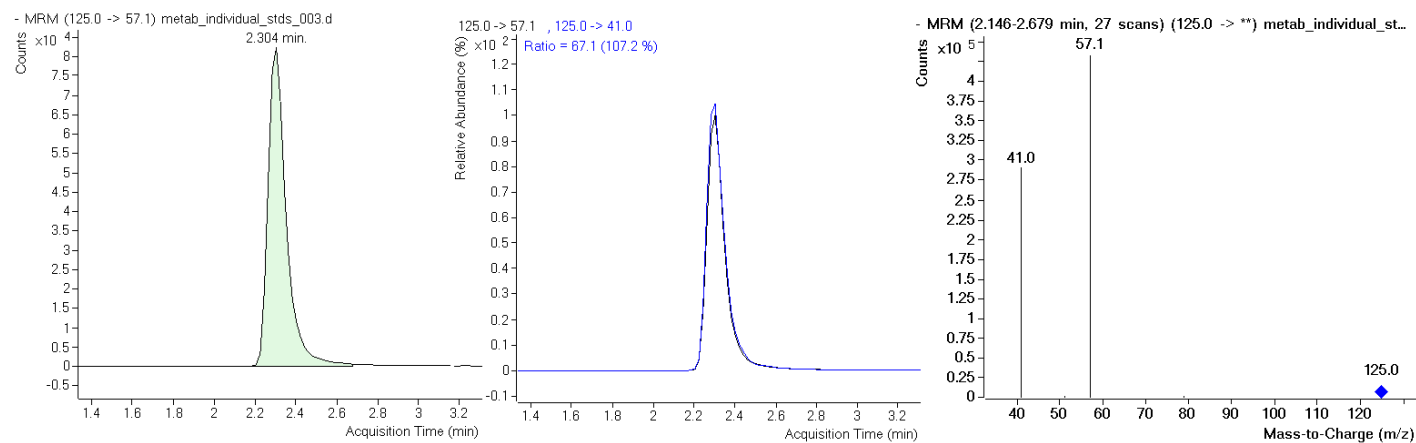
The following figure with reference to the method applied in chapter 6, showing Ms/Ms chromatograms of the ion currents for various metabolites which show the mass pair, the quantifier peak, the quantifier and qualifier ratios of the selective daughter fragment ions, and the mass spectrum of each authentic compound.

Method: Machine Triple quad (6490) Column T3. Gradient was 1% B at injection for 1 minute, increased to 5% at 3 min, 60% at 8 min, 99% at 8.5 min and then re-equilibrated to initial conditions over 3.5 min; where the solvent A= ammonium acetate 10 mM in water; B = ammonium acetate 10 mM in ACN.

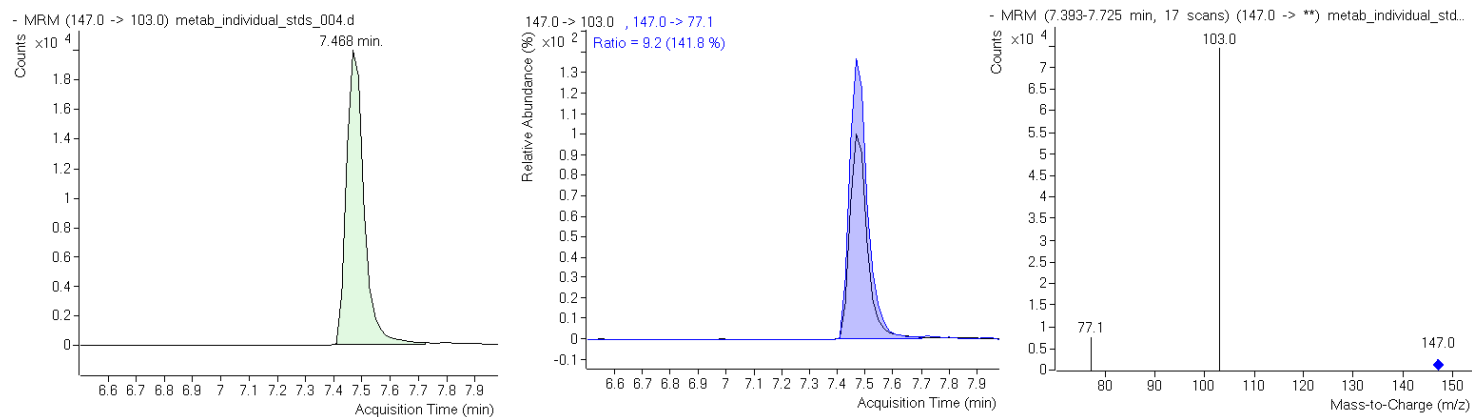
1- Pyrogallol



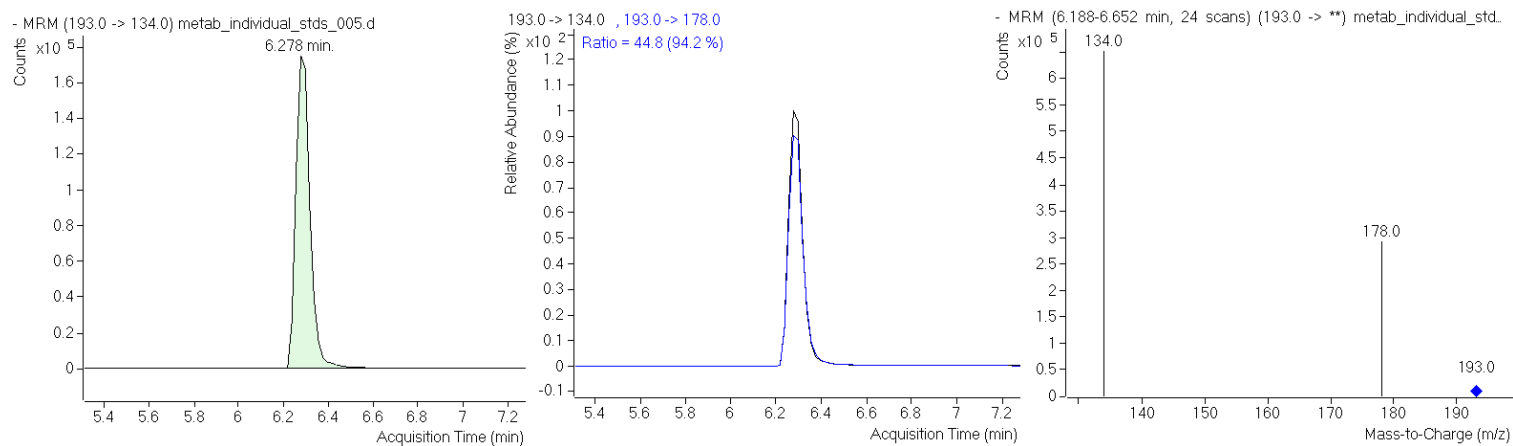
2- Phloroglucinol



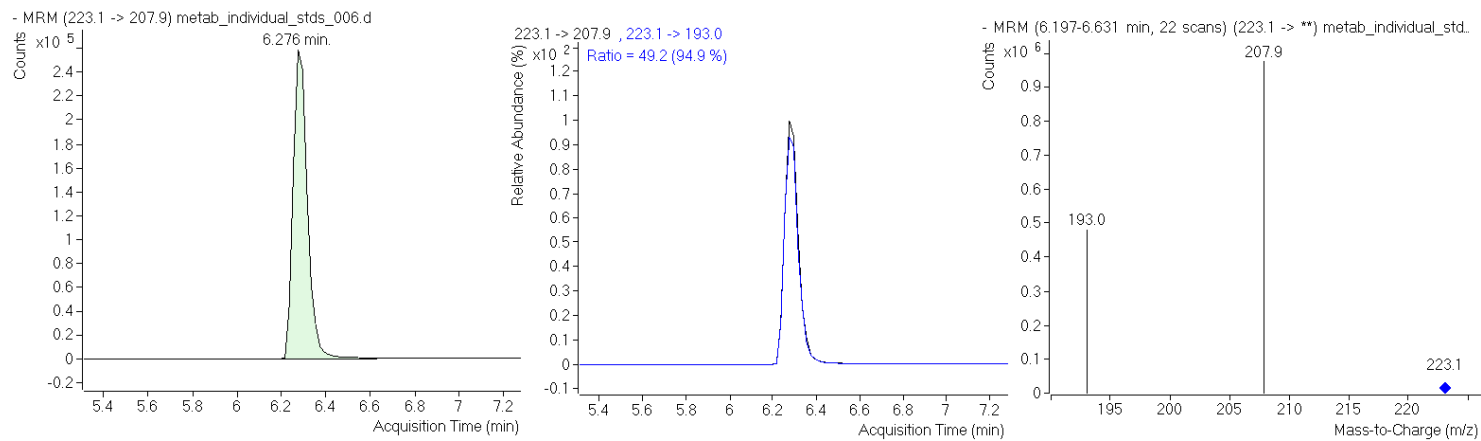
3- Cinnamic acid



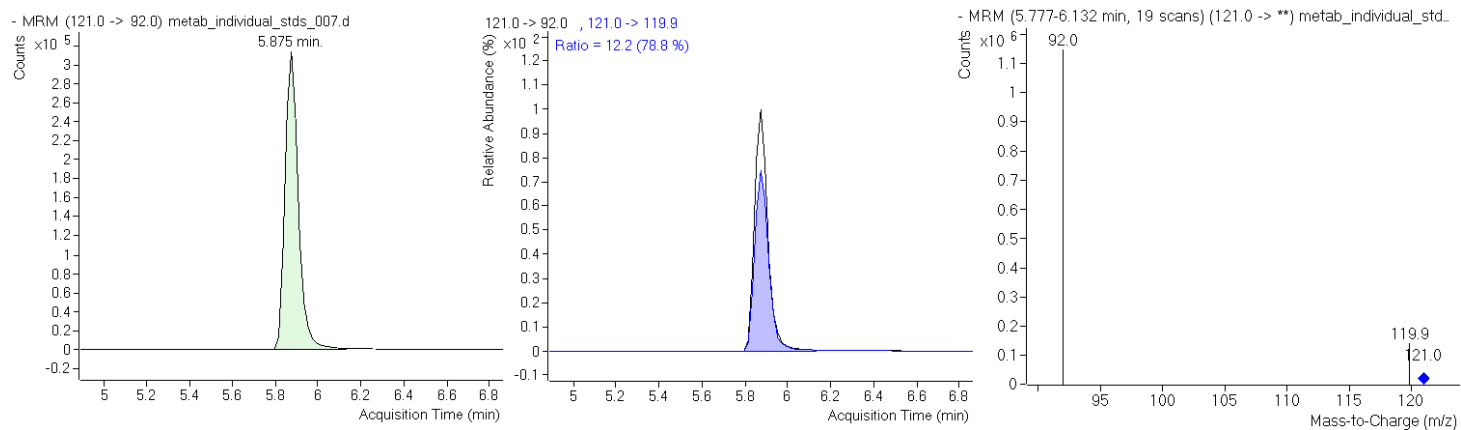
4- Ferulic acid



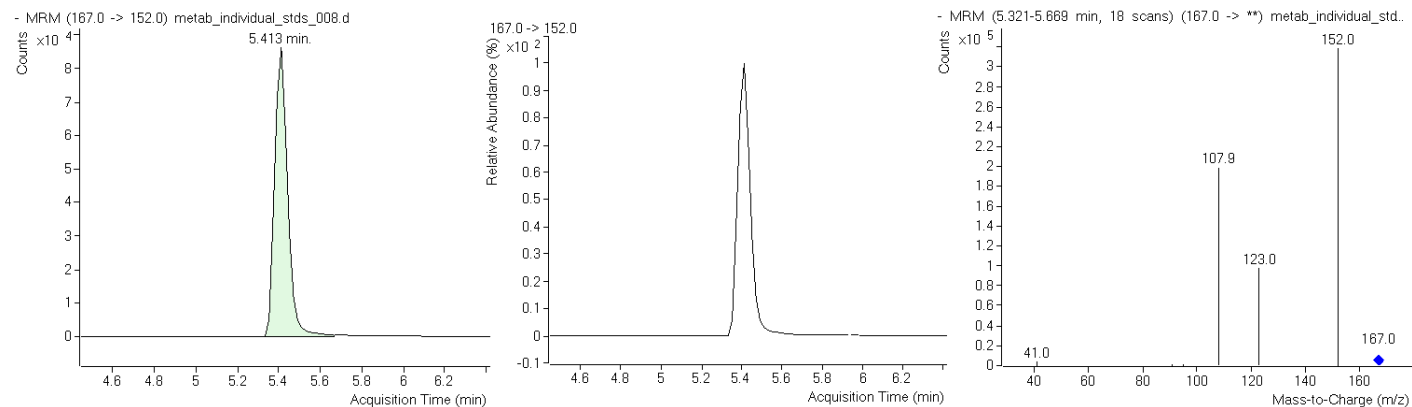
5- Sinapic acid



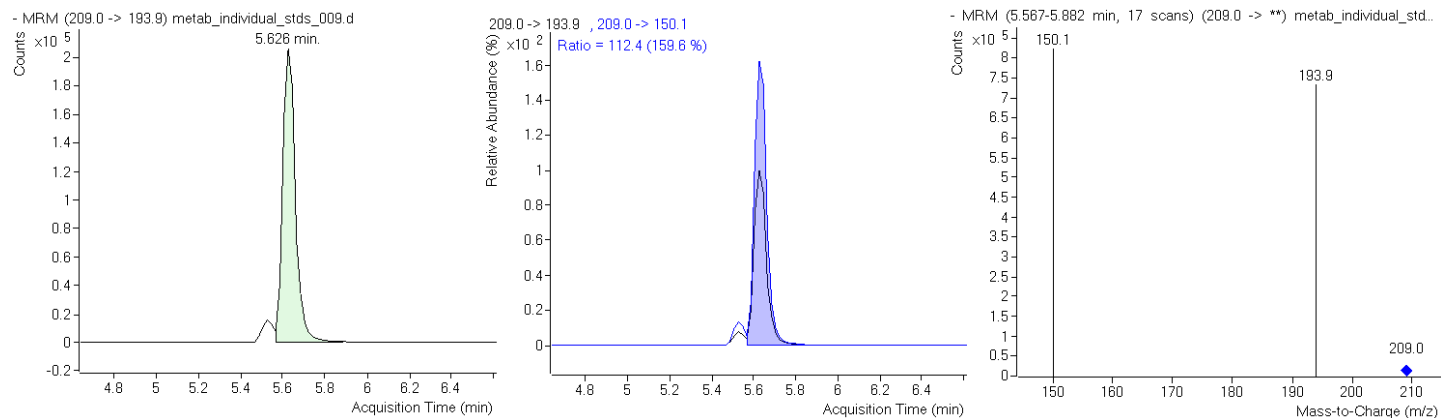
6- 4-hydroxybenzaldehyde



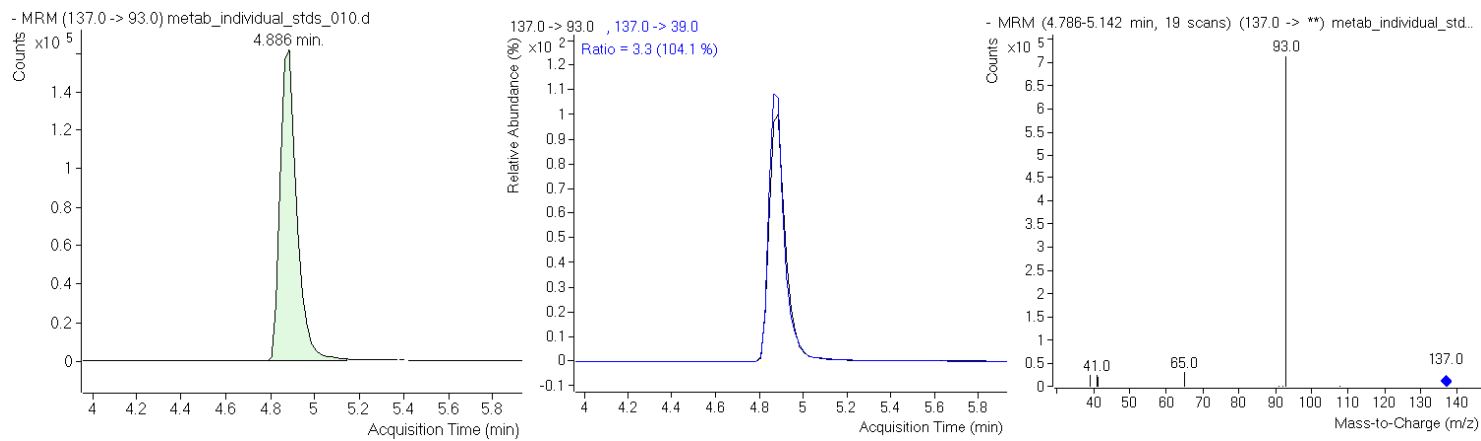
7- Vanillic acid



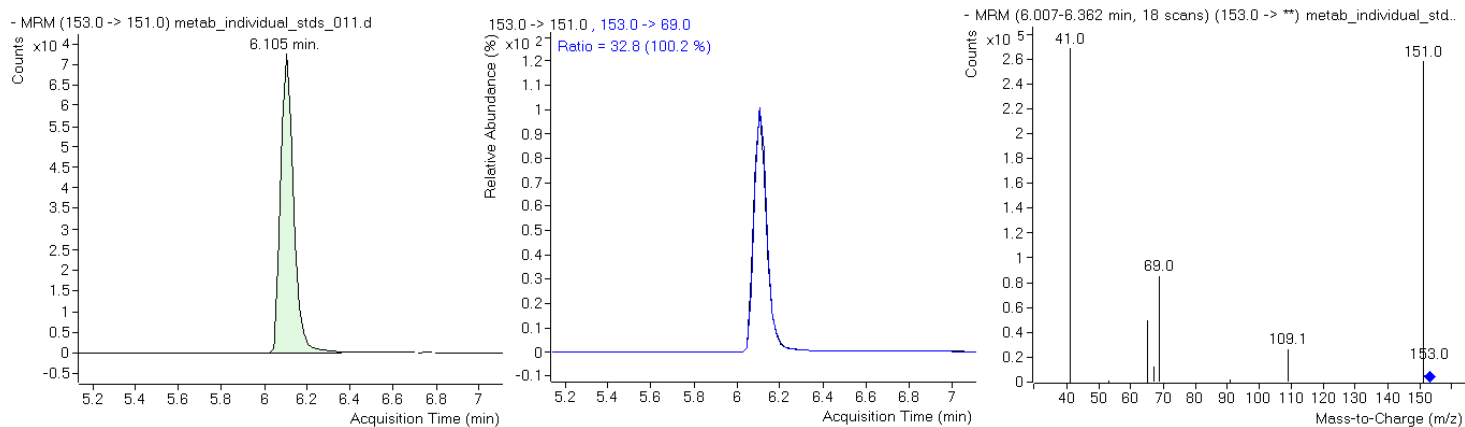
8- 5-hydroxyferulic acid



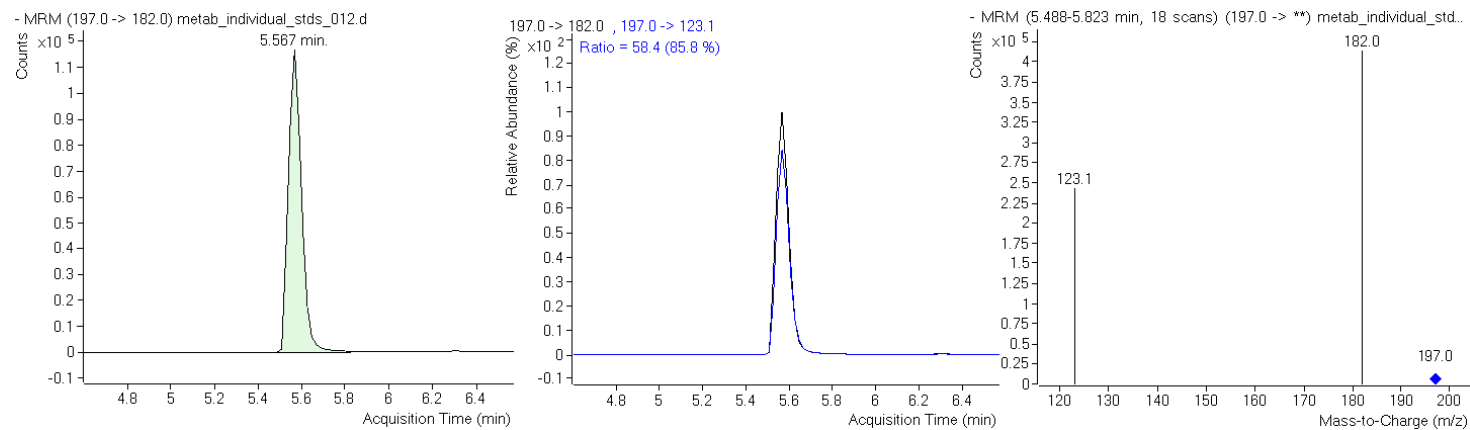
9- 4-hydroxybenzoic acid



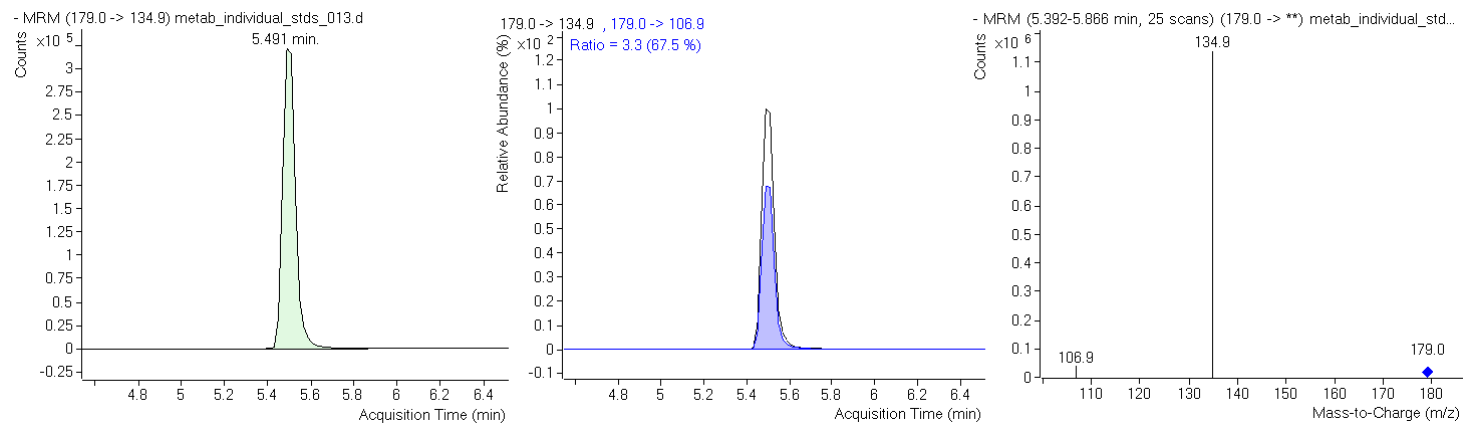
10- Phloroglucinol aldehyde (PGA)



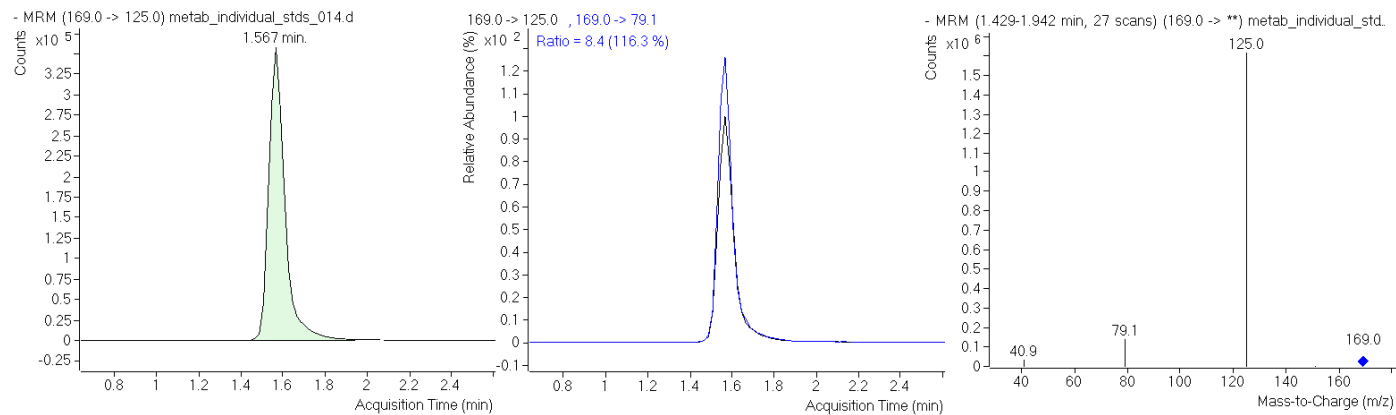
11- Syringic acid



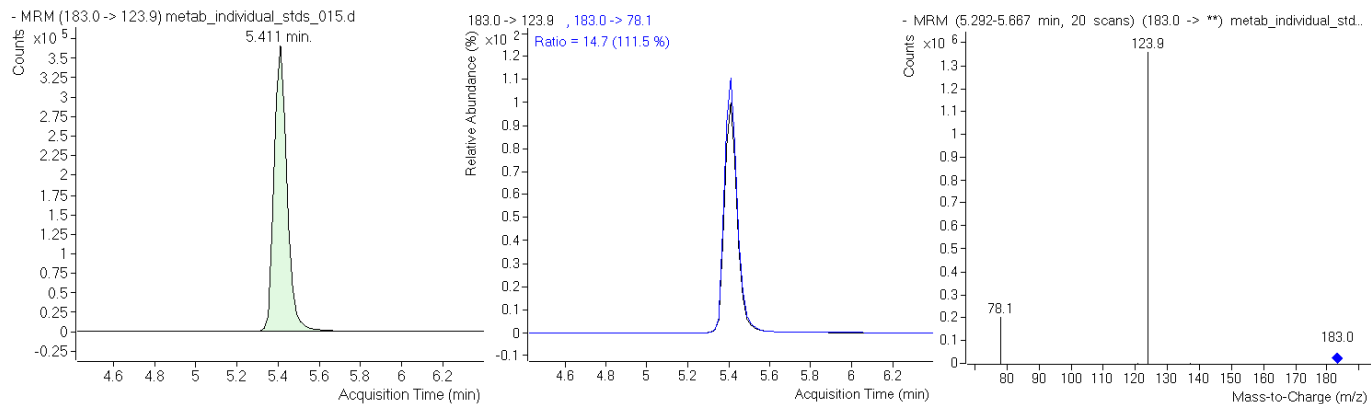
12- Caffeic acid



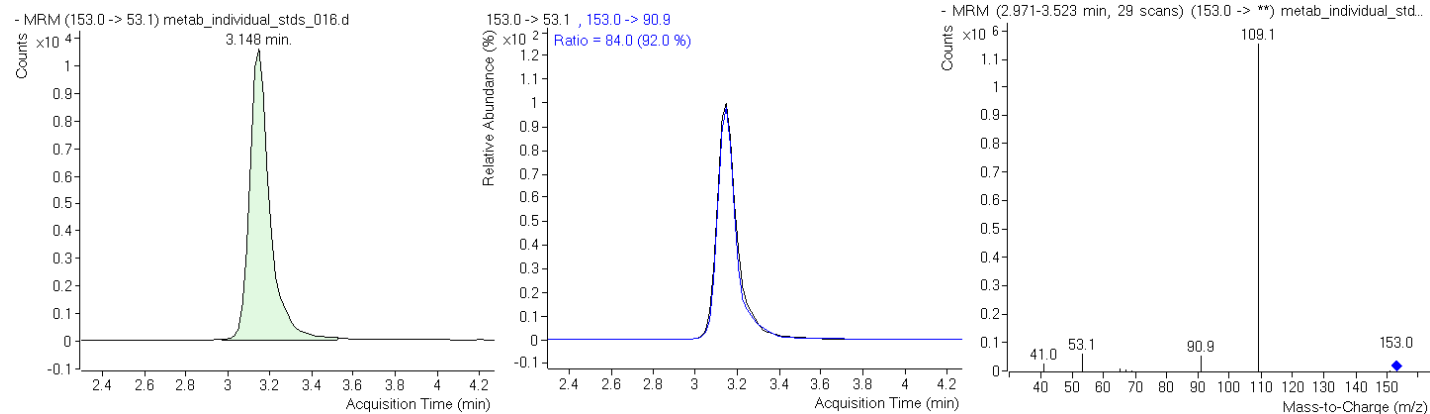
13- Gallic acid



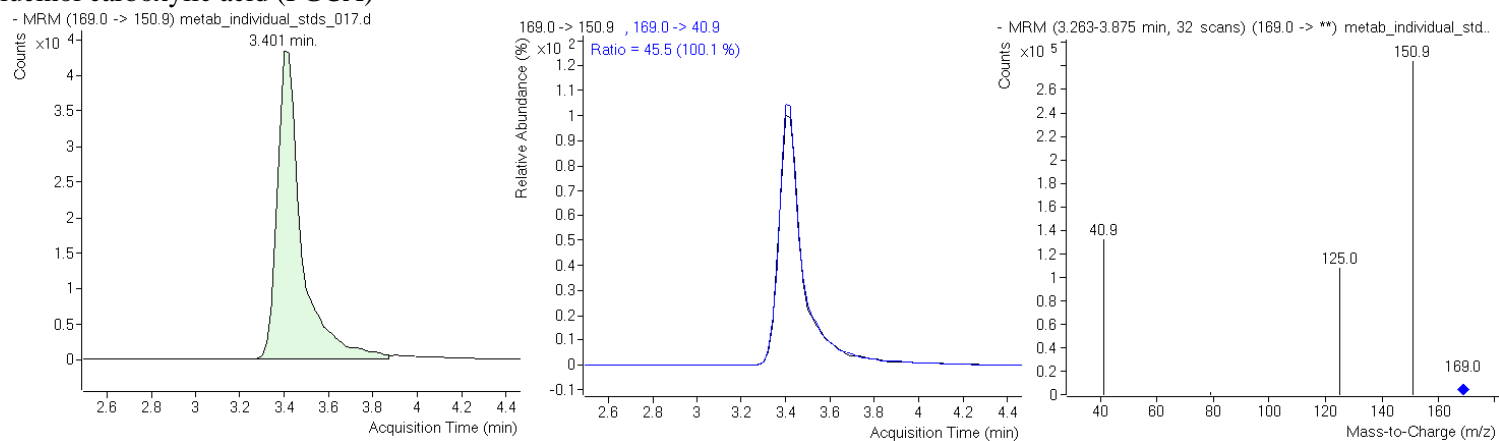
14- 3-O-methylgallic acid



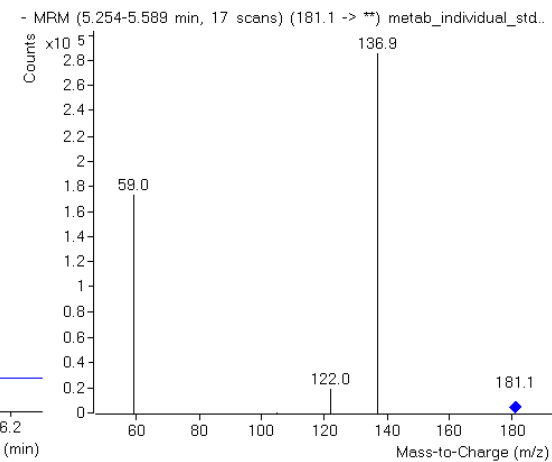
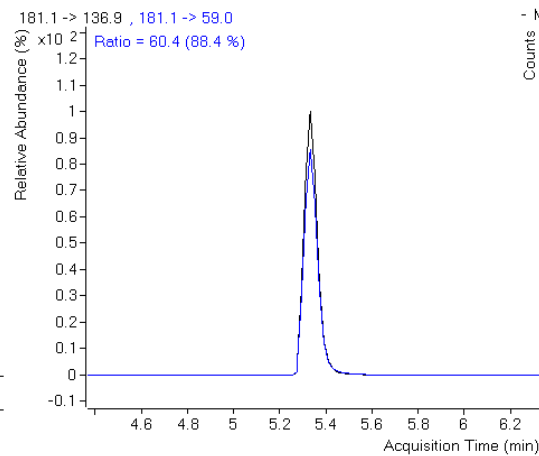
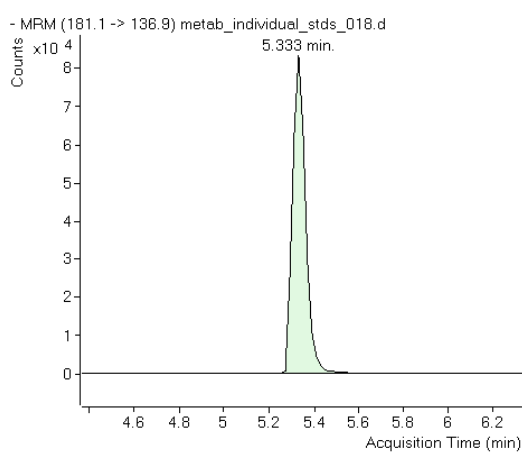
15- Protocatechuic acid (PCA)



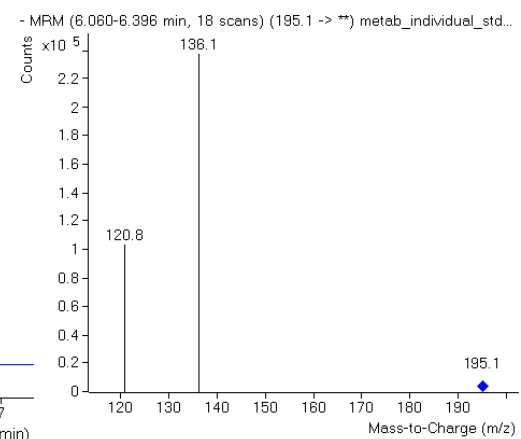
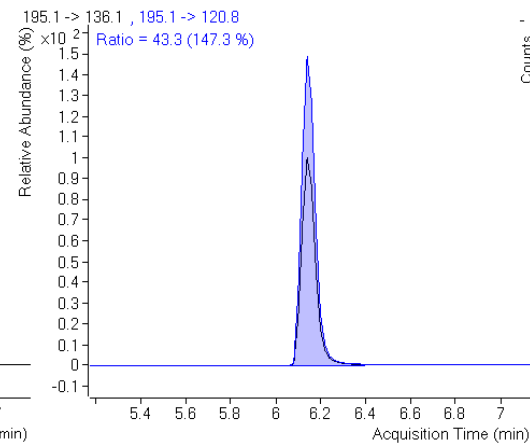
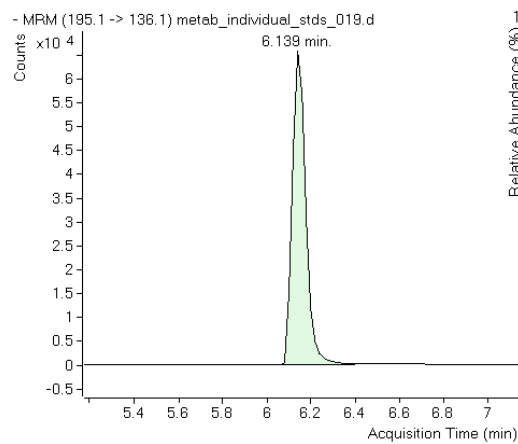
16- Phloroglucinol carboxylic acid (PGCA)



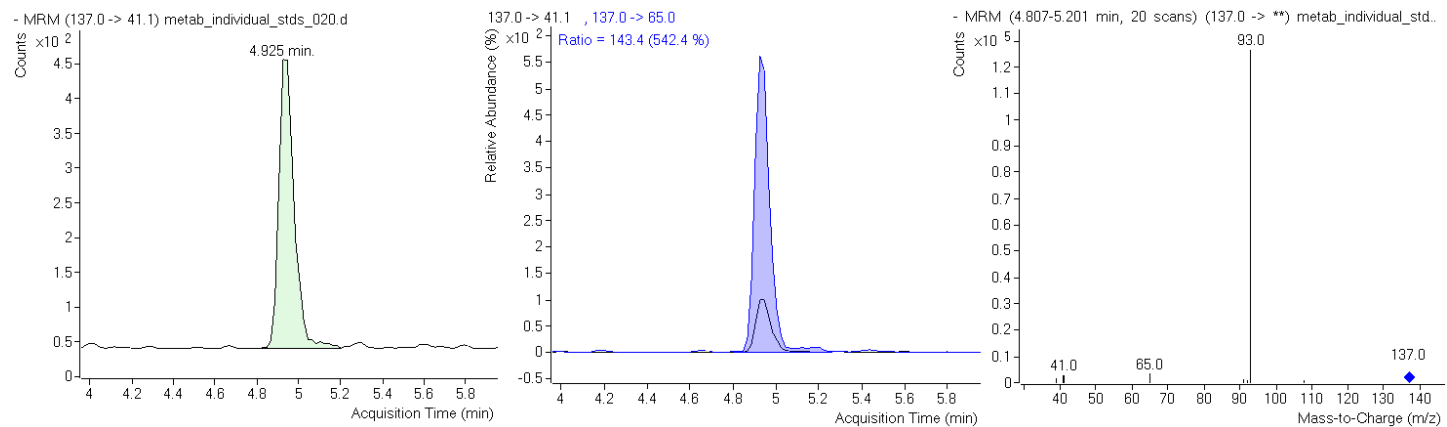
17- Dihydrocaffeic acid



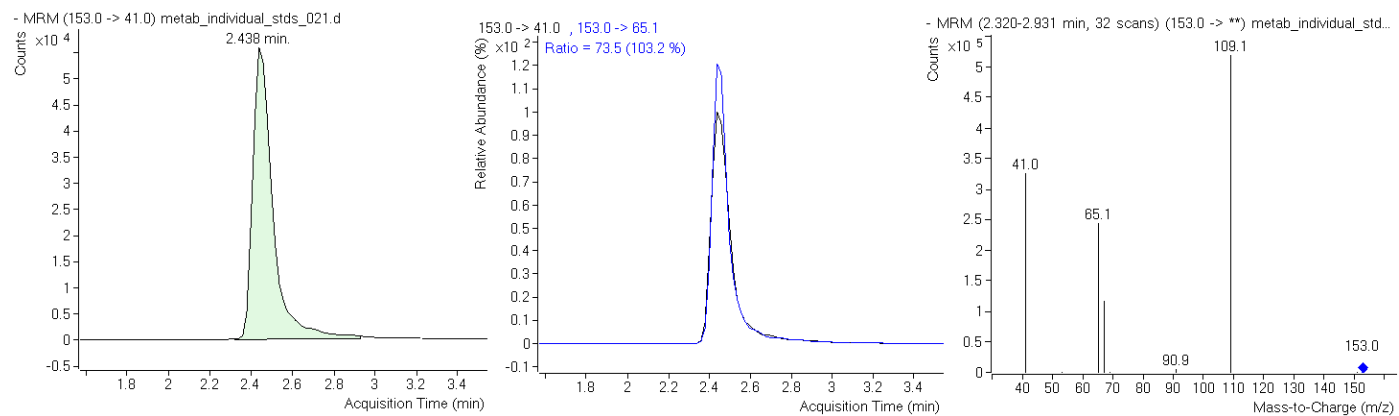
18- Dihydroferulic acid



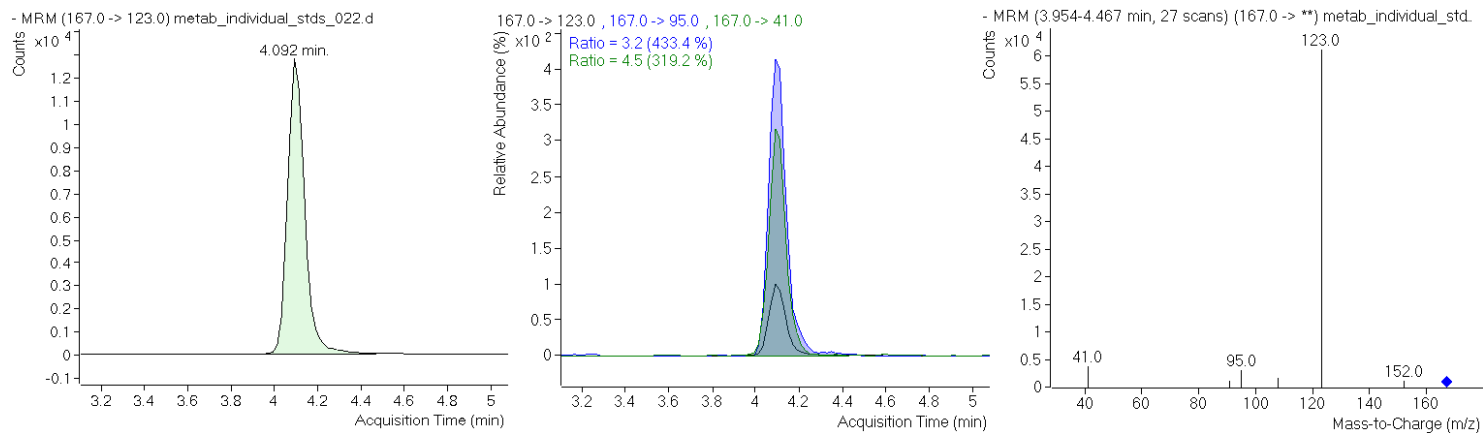
19- 3-hydroxybenzoic acid



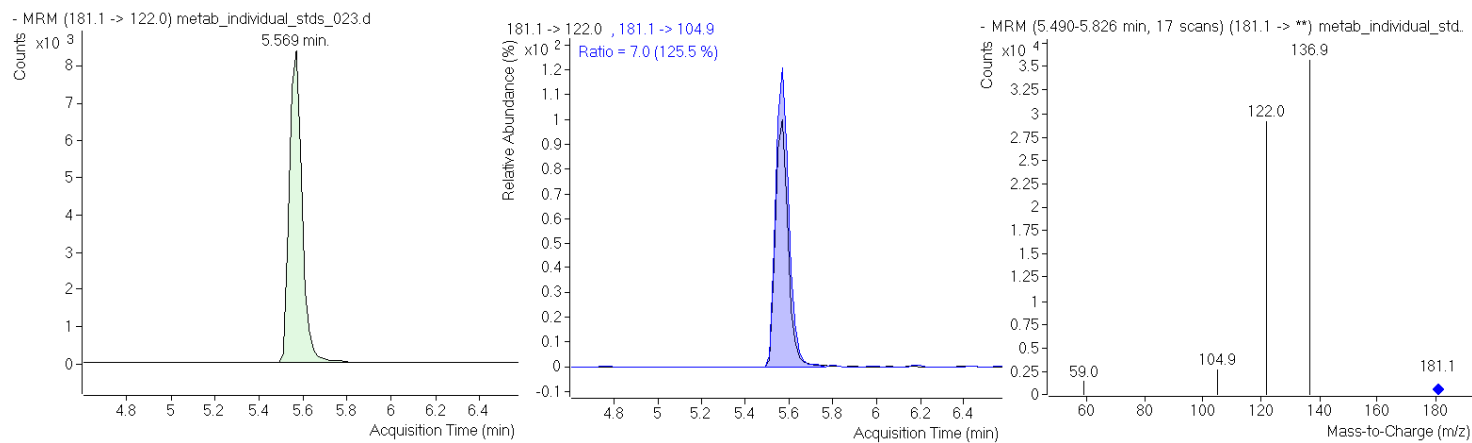
20- 2,4-dihydroxybenzoic acid



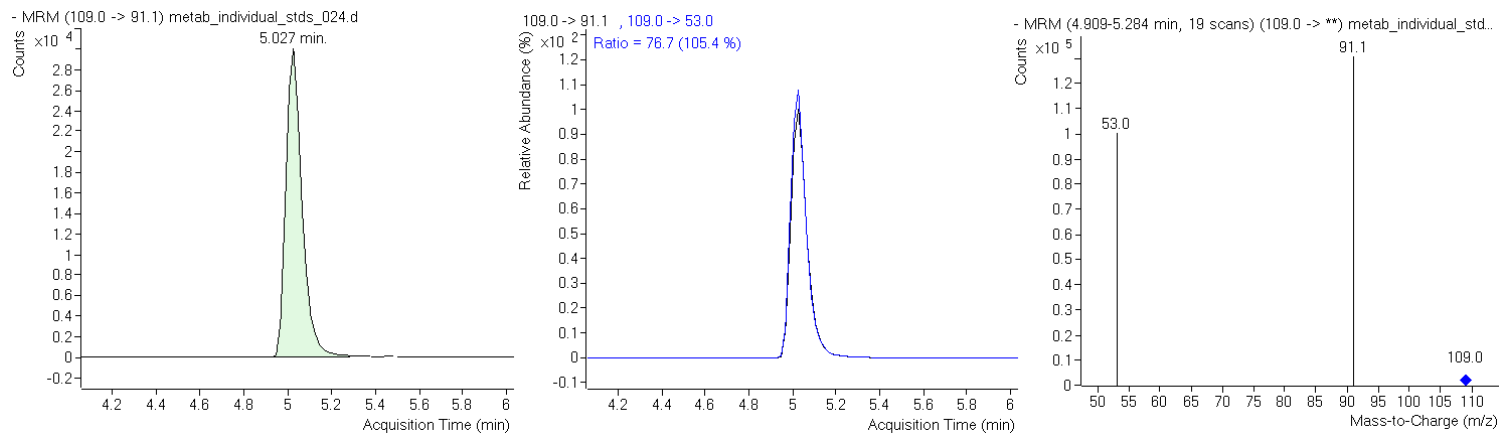
21- 3,4-dihydroxyphenylacetic acid (DHPAA)



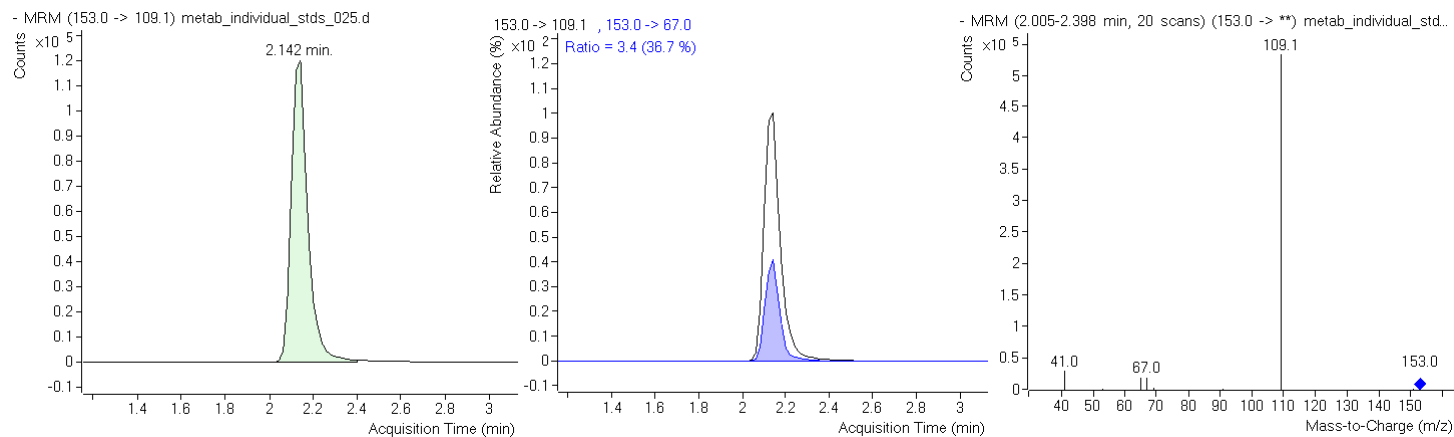
22- Homovanillic acid



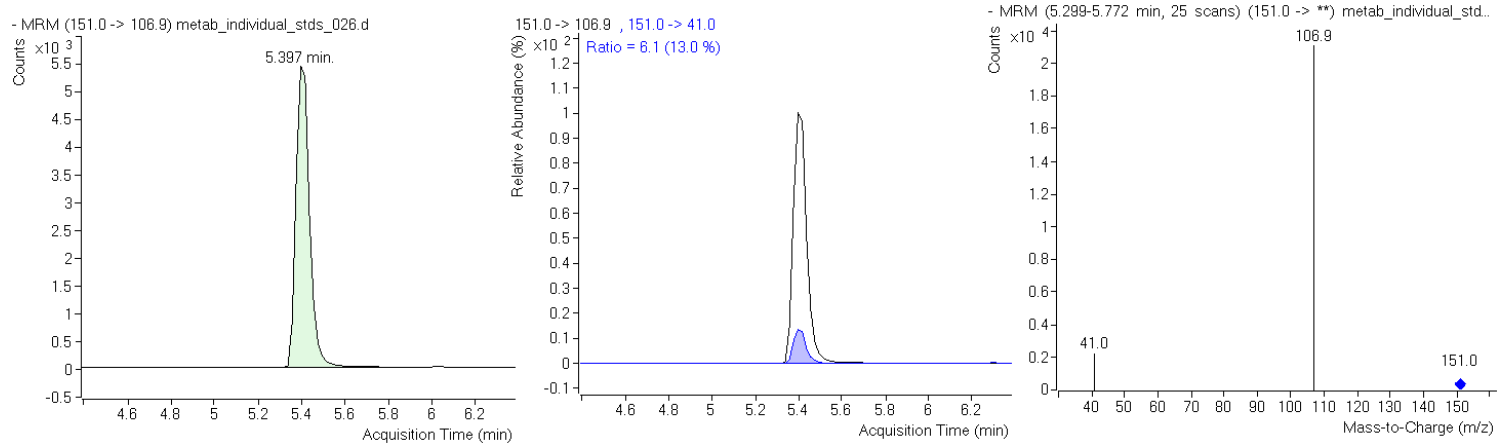
23- Catechol



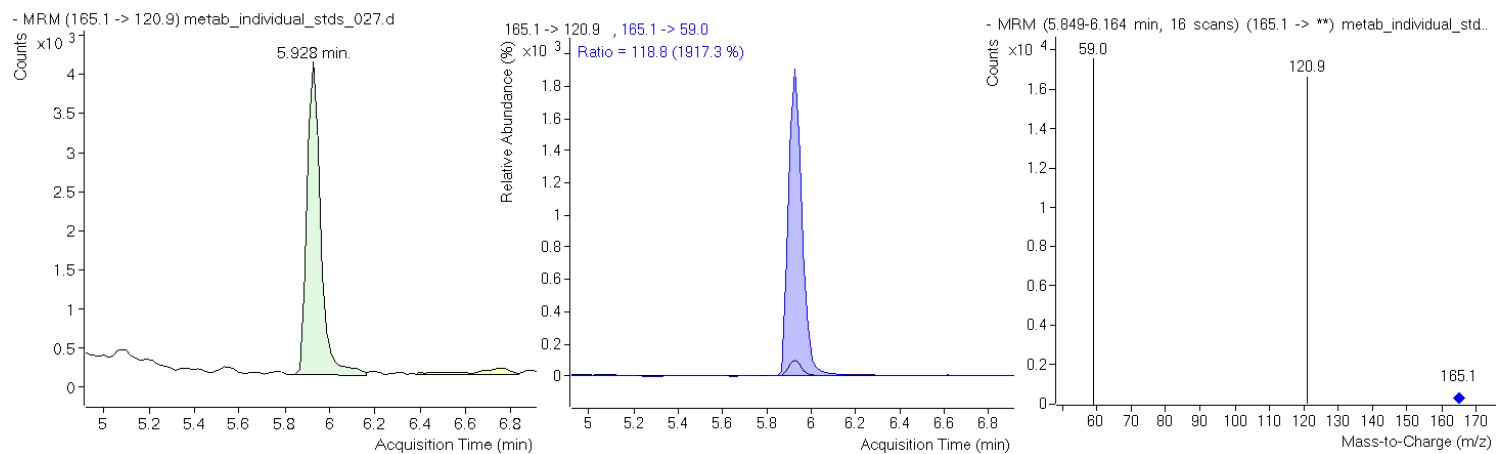
24- 3,5-dihydroxybenzoic acid



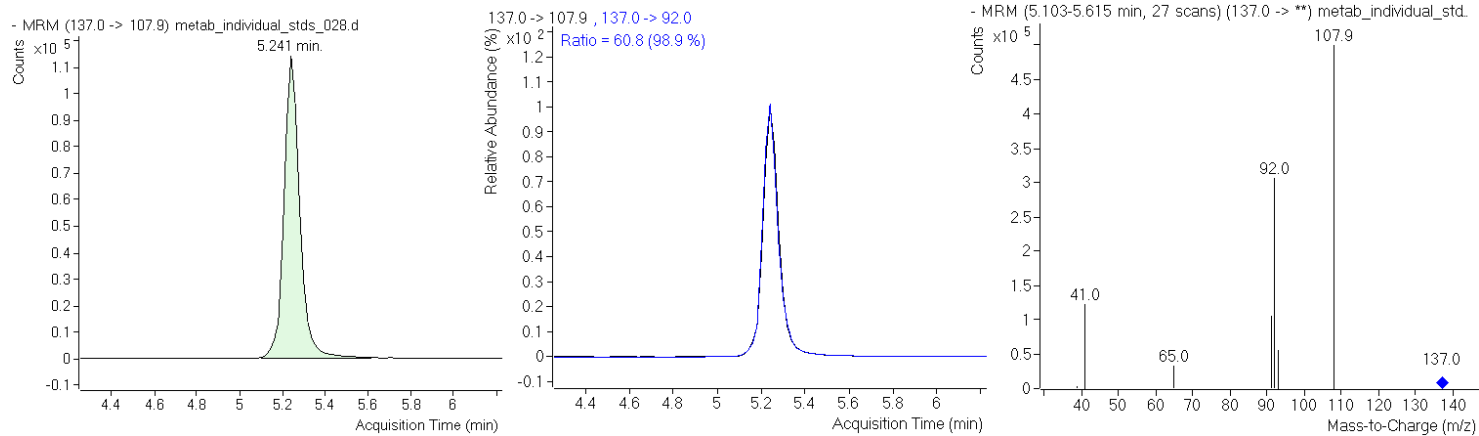
25- 3-hydroxyphenylacetic acid



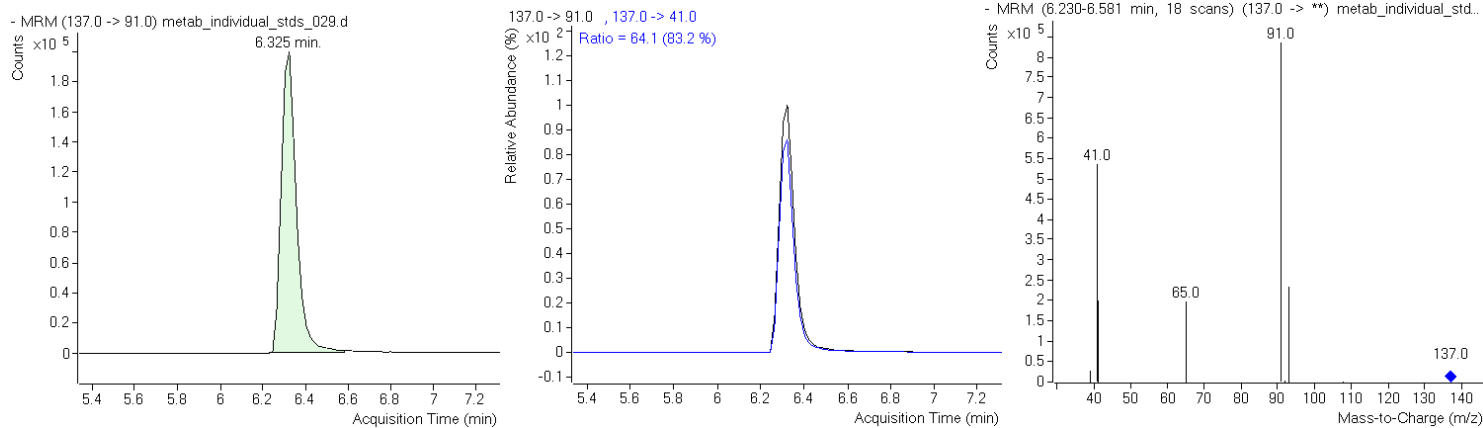
26- 3-(4-hydroxyphenyl)propionic acid



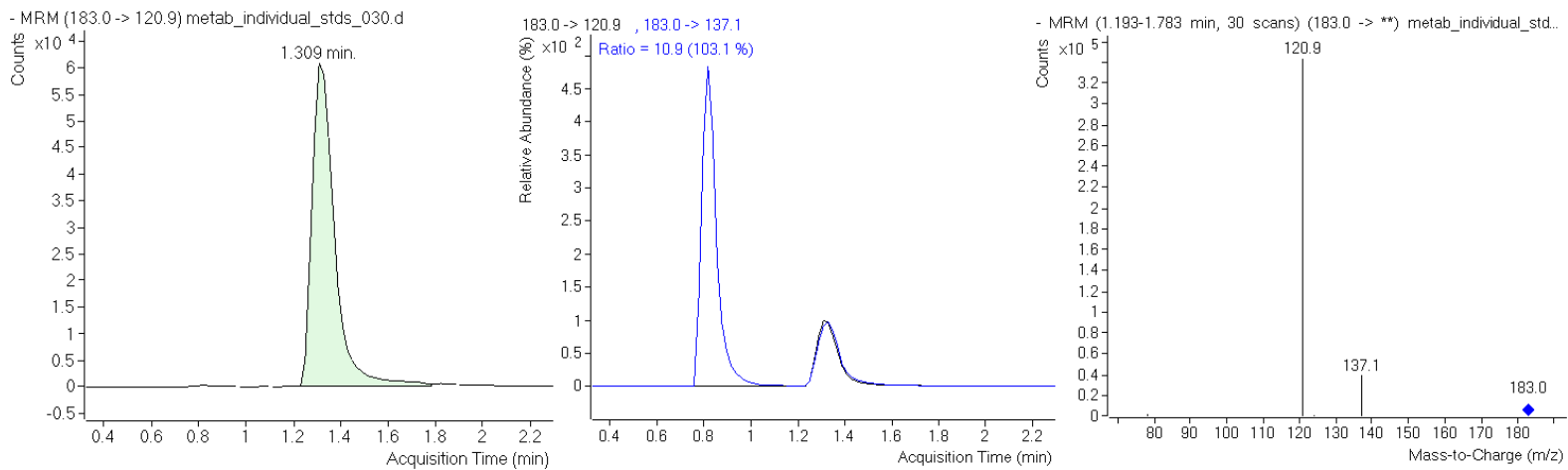
27- PCAld



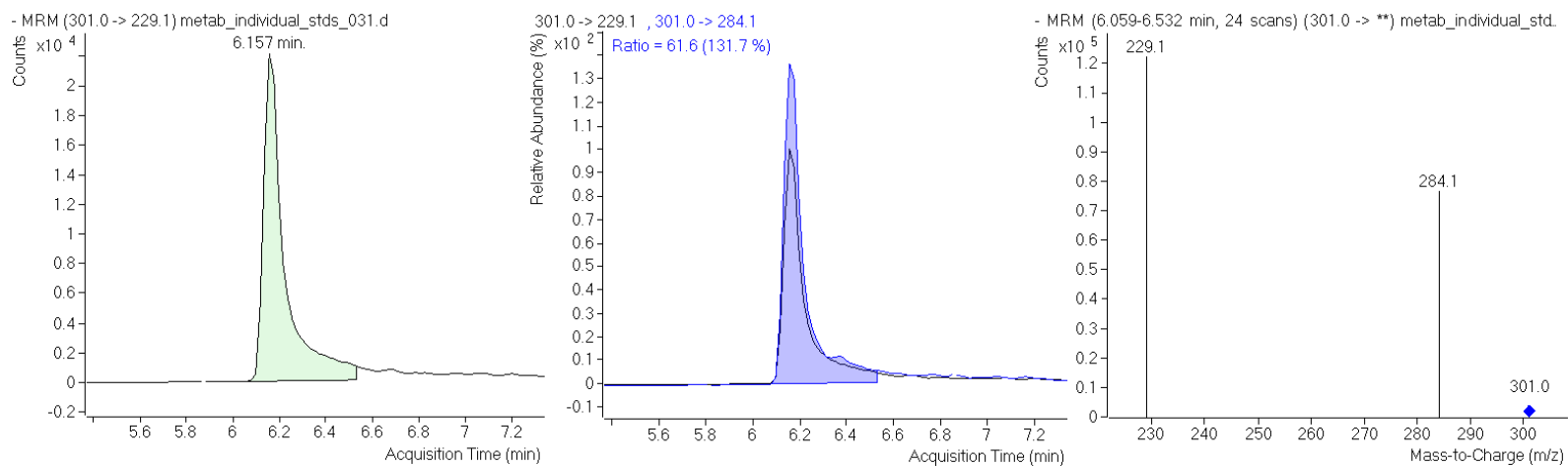
28- 2,4-dihydroxybenzaldehyde



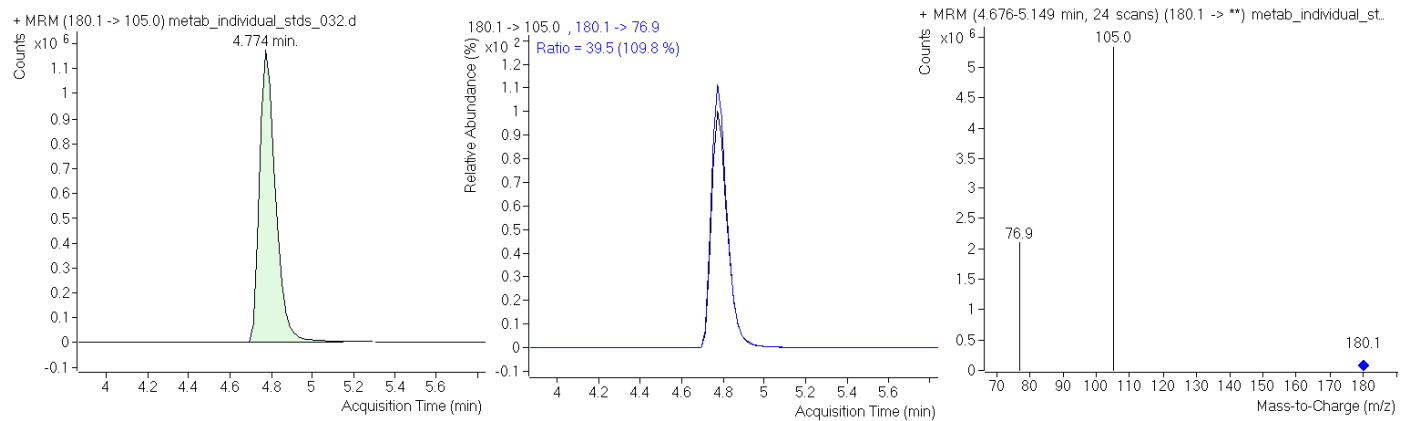
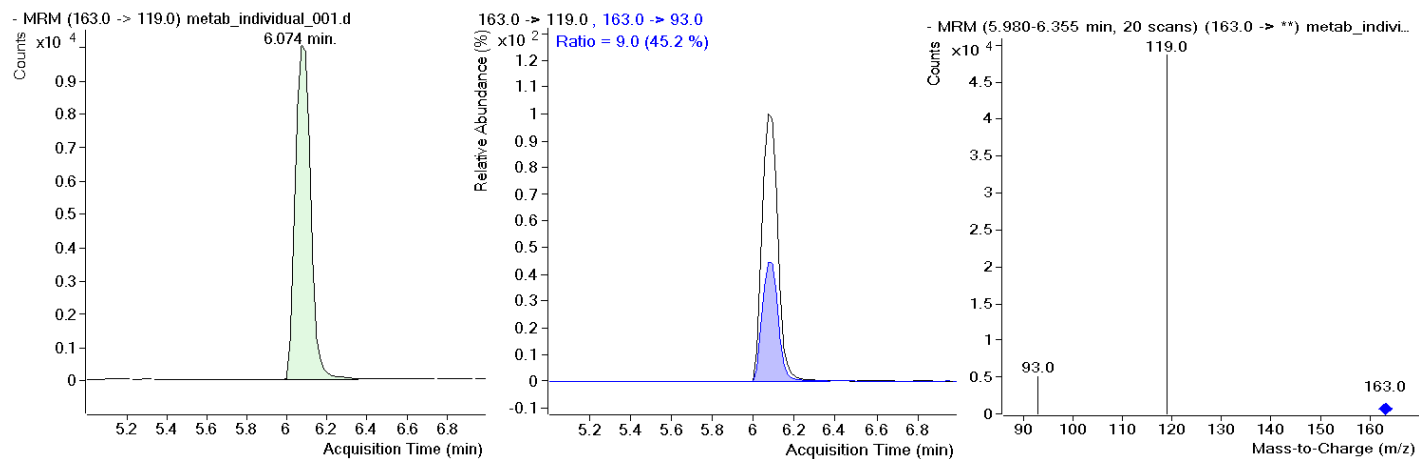
29- 3,4-dihydroxymandelic acid



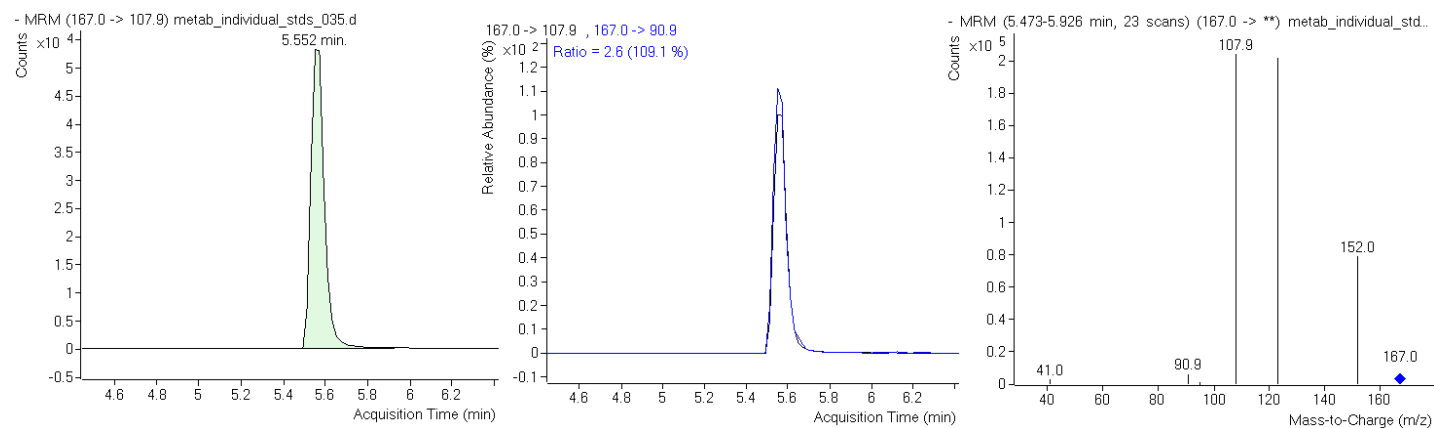
30- Ellagic acid



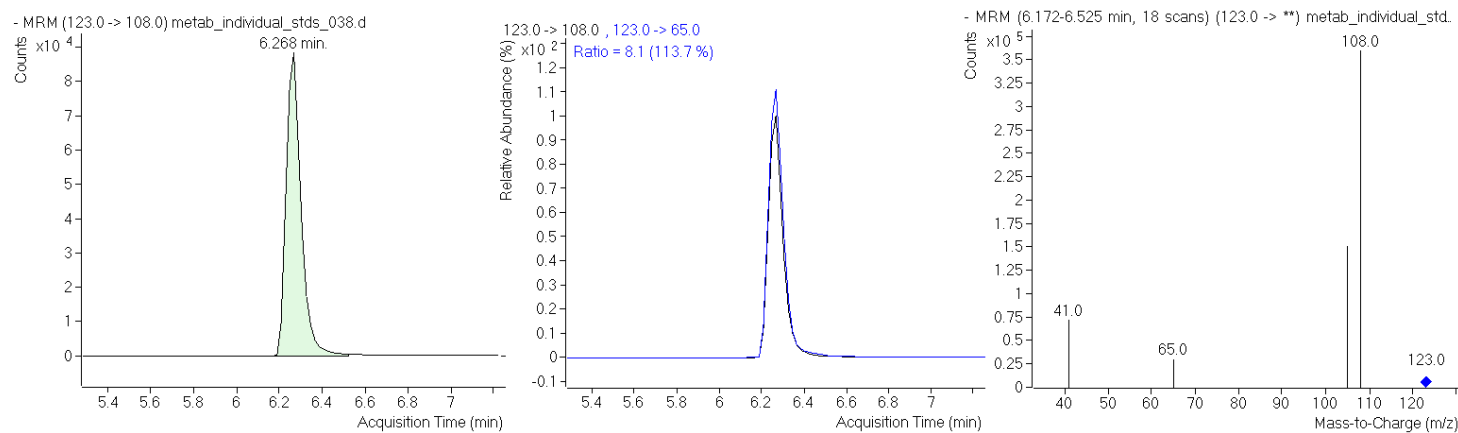
31- Hippuric acid

32- *p*-Coumaric acid

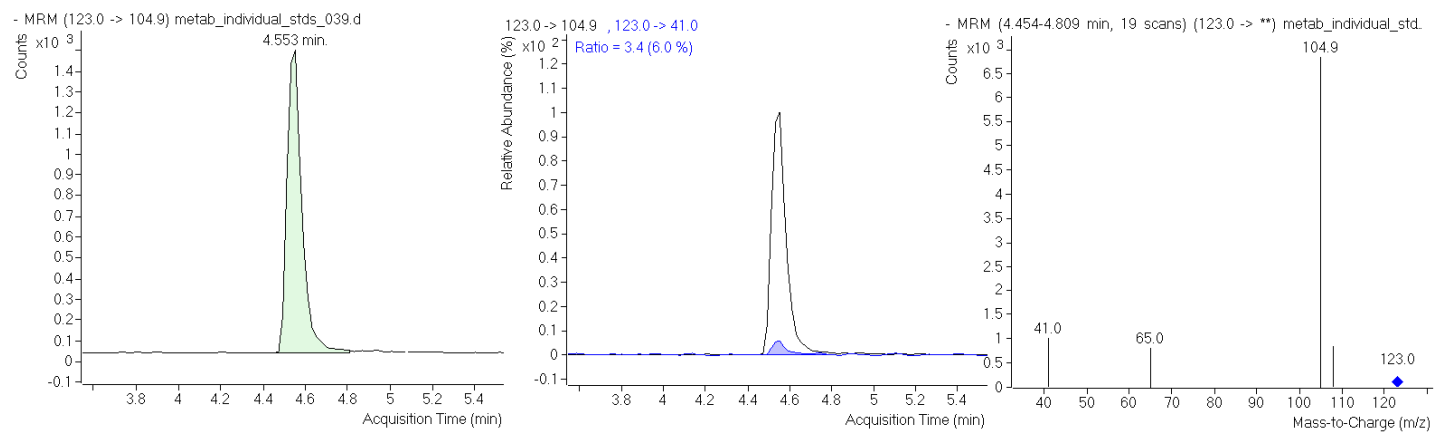
33- Isovanillic acid



34- 4-methylcatechol



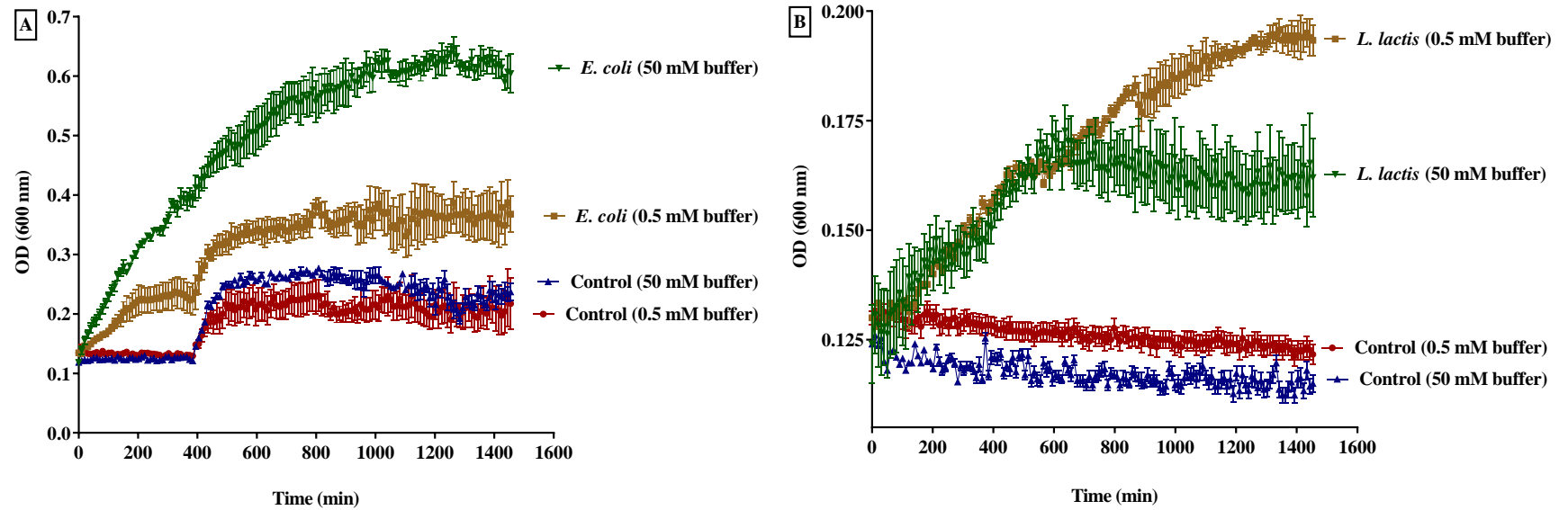
35- 4-hydroxybenzyl alcohol



Appendix 7

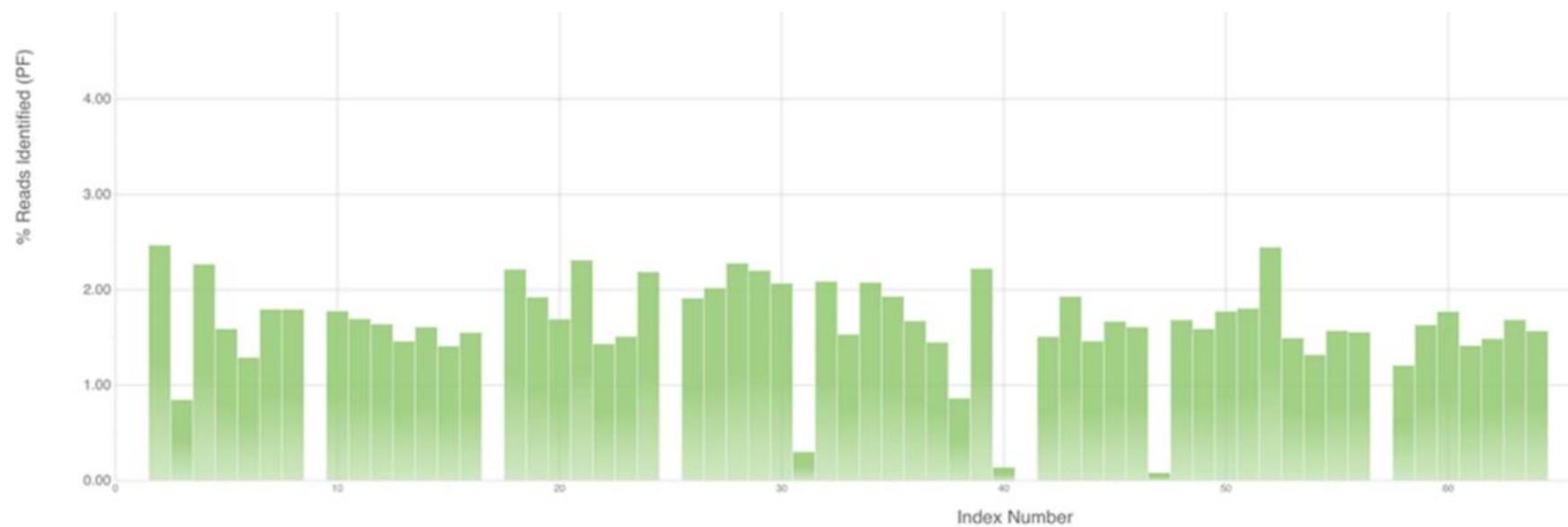
Sequencing data

Appendix 7



Appendix figure 7. 1. The growth curves of *E. Coli* and *L. lactis* in low and high-capacity phosphate buffer media.

These figures and tables are with reference to the methods applied in Chapter 7.



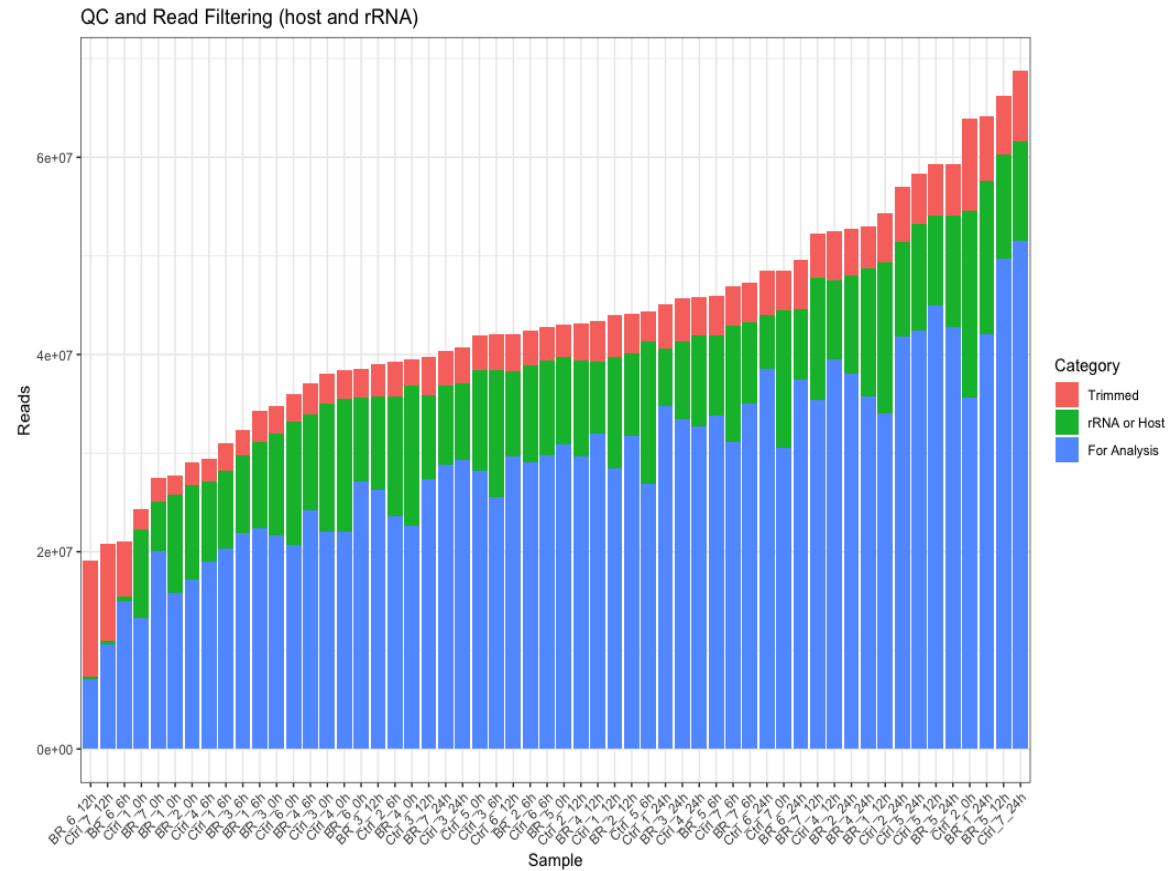
Appendix figure 7. 2. Bar plot chart showing the quantified DNA in all samples.

Quantification of DNA in control (n=7), black rice treatment (n=7), and contamination control (n=2) samples over 24 h of incubation.

Appendix table 7. 1. The following table show the summary of the quality control, trimming and decontamination for the raw sequencing data.

Sample	Group	Time Point (h)	Raw Reads	Trimmed Reads	% Trimmed Reads	Passed QC and Trimming	% Passed QC and Trimming	non rRNA Reads	% non rRNA Reads	Non hg37	% Non hg37	Reads for Downstream Analysis	% Reads for downstream analysis
BR_1_0h	BR_1	0	27,717,491	1,987,225	7.2	25,730,266	92.8	15,992,443	62.2	16,639,510	64.7	15,874,288	57.3
BR_1_6h	BR_1	6	34,292,677	3,107,086	9.1	31,185,591	90.9	22,561,987	72.3	23,218,758	74.5	22,410,584	65.4
BR_1_12h	BR_1	12	54,358,758	5,036,619	9.3	49,322,139	90.7	34,231,238	69.4	35,773,832	72.5	33,985,284	62.5
BR_1_24h	BR_1	24	64,159,997	6,601,629	10.3	57,558,368	89.7	42,343,888	73.6	44,114,677	76.6	42,096,015	65.6
BR_2_0h	BR_2	0	29,054,062	2,346,066	8.1	26,707,996	91.9	17,294,365	64.8	17,945,424	67.2	17,166,437	59.1
BR_2_6h	BR_2	6	42,467,902	3,531,153	8.3	38,936,749	91.7	29,260,046	75.1	30,122,806	77.4	29,055,880	68.4
BR_2_12h	BR_2	12	44,068,898	3,993,098	9.1	40,075,800	90.9	31,989,716	79.8	32,690,734	81.6	31,760,806	72.1
BR_2_24h	BR_2	24	52,789,736	4,725,650	9	48,064,086	91	38,208,403	79.5	39,103,763	81.4	38,011,532	72.0
BR_3_0h	BR_3	0	34,813,521	2,892,014	8.3	31,921,507	91.7	21,767,730	68.2	22,473,459	70.4	21,608,917	62.1
BR_3_6h	BR_3	6	32,308,468	2,504,953	7.8	29,803,515	92.2	22,009,554	73.8	22,617,996	75.9	21,859,014	67.7
BR_3_12h	BR_3	12	38,962,626	3,174,861	8.1	35,787,765	91.9	26,443,767	73.9	27,130,552	75.8	26,266,095	67.4
BR_3_24h	BR_3	24	45,721,948	4,427,593	9.7	41,294,355	90.3	33,666,135	81.5	34,355,627	83.2	33,485,204	73.2
BR_4_0h	BR_4	0	39,500,592	2,651,140	6.7	36,849,452	93.3	22,757,120	61.8	23,678,893	64.3	22,590,768	57.2
BR_4_6h	BR_4	6	37,035,994	3,145,406	8.5	33,890,588	91.5	24,378,936	71.9	25,063,316	74	24,217,483	65.4
BR_4_12h	BR_4	12	43,349,152	4,039,537	9.3	39,309,615	90.7	32,232,389	82	32,839,154	83.5	32,025,231	73.9
BR_4_24h	BR_4	24	53,016,209	4,333,056	8.2	48,683,153	91.8	35,881,006	73.7	36,937,623	75.9	35,704,976	67.3
BR_5_0h	BR_5	0	43,046,615	3,267,704	7.6	39,778,911	92.4	31,146,960	78.3	31,842,583	80	30,922,113	71.8
BR_5_6h	BR_5	6	45,971,679	4,002,558	8.7	41,969,121	91.3	34,051,481	81.1	34,698,305	82.7	33,806,022	73.5

Processing the sequencing data: removal of host sequences and quality control using KneadData

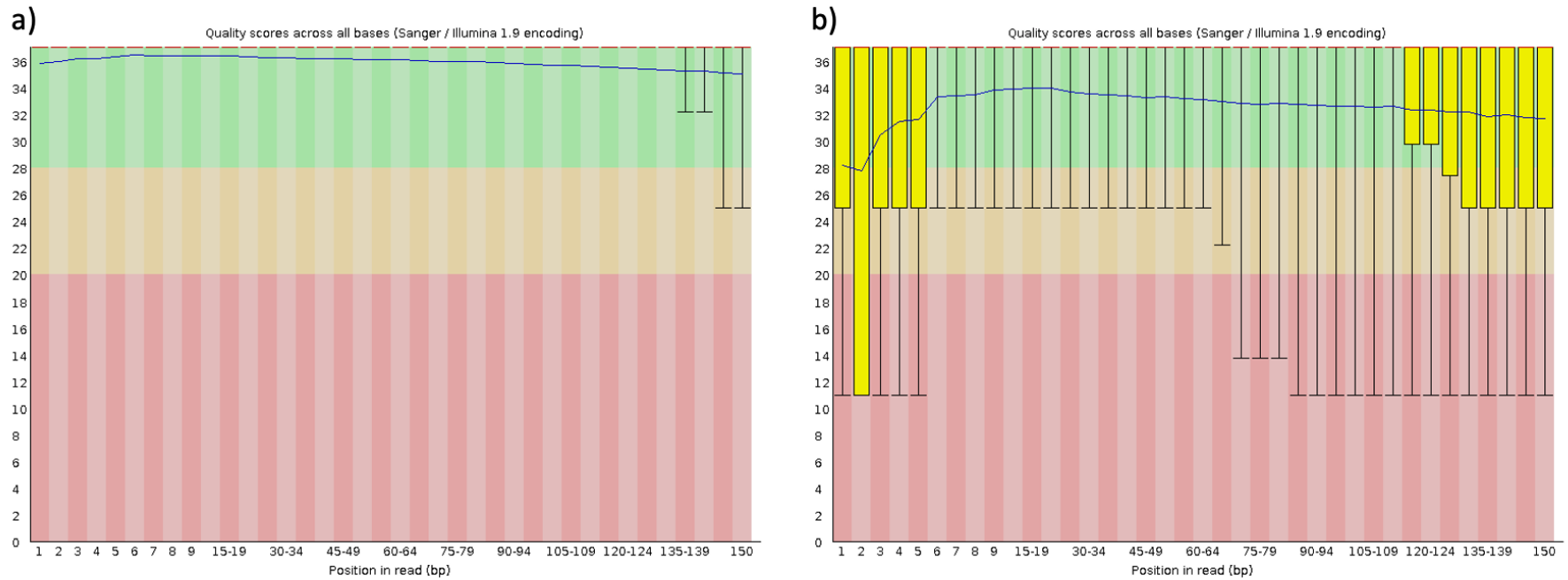


Appendix figure 7. 3. Bar plot summarising read quality of rRNA or host sequences.

In red is the number of reads trimmed due to low quality, the number of adaptor sequences or short reads, in green is the number discarded reads, either rRNA or host sequences, and in blue is the number of reads used for downstream analysis. Most of the sequencing samples for the control and treatment groups are of high sequencing quality. The only exception is sample BR-6-12h, which has very small proportion of reads surviving QC.

Appendix table 7. 2. The table below shows the summary statistics for this sample compared to other black rice (BR) samples.

Sample	Group	Time Point (h)	Raw Reads	Trimmed Reads	% Trimmed Reads	Passed QC and Trimming	% Passed QC and Trimming	non rRNA Reads	% non rRNA Reads	Non hg37	% Non hg37	Reads for Downstream Analysis	% Reads for downstream analysis
BR_6_0h	BR_6	0	38,530,163	2,908,998	7.5	35,621,165	92.5	27,348,447	76.8	27,988,920	78.6	27,150,669	70.5
BR_6_6h	BR_6	6	21,002,270	5,504,598	26.2	15,497,672	73.8	15,160,626	97.8	15,184,746	98	15,001,728	71.4
BR_6_12h	BR_6	12	19,075,486	11,800,648	61.9	7,274,838	38.1	7,151,356	98.3	7,109,118	97.7	7,034,823	36.9
BR_6_24h	BR_6	24	49,629,139	4,964,162	10.0	44,664,977	90.0	37,745,915	84.5	38,381,191	85.9	37,503,889	75.6
BR_7_0h	BR_7	0	27,431,503	2,420,584	8.8	25,010,919	91.2	20,267,312	81	20,692,038	82.7	20,115,803	73.3
BR_7_6h	BR_7	6	47,293,232	3,993,387	8.4	43,299,845	91.6	35,247,958	81.4	36,056,678	83.3	35,009,951	74.0
BR_7_12h	BR_7	12	52,221,844	4,486,620	8.6	47,735,224	91.4	35,592,458	74.6	36,647,788	76.8	35,350,073	67.7
BR_7_24h	BR_7	24	40,310,898	3,522,044	8.7	36,788,854	91.3	29,007,156	78.8	29,686,986	80.7	28,848,362	71.6



Appendix figure 7. 4. The per base sequencing quality for this sample compared to a high-quality sample (BR-5-12h).

Figure a) shows the sequencing quality for sample BR-5-12h, which is an example of a sample with high per base sequencing quality; figure b) shows the per base sequence quality plot for BR-6-12h, for which only 38.1% of the paired-end raw reads survive quality control and trimming.

Appendix table 7. 3. Summary of quality control, adapter trimming and decontamination of sequencing data for all controls samples

Sample	Group	Time Point (h)	Raw Reads	Trimmed Reads	% Trimmed Reads	Passed QC and Trimming	% Passed QC and Trimming	non rRNA Reads	% non rRNA Reads	Non hg37	% Non hg37	Reads for Downstream Analysis	% Reads for downstream analysis
Media_1_0h	Media_1	0	22	NA	NA	NA	NA	NA	NA	NA	NA	NA	NA
Media_1_6h	Media_1	6	383	NA	NA	NA	NA	NA	NA	NA	NA	NA	NA
Media_1_12h	Media_1	12	42,975,408	5,035,996	11.7	37,939,412	88.3	30,205,941	79.6	30,696,337	80.9	29,099,623	67.7
Media_1_24h	Media_1	24	12,330,768	1,027,797	8.3	11,302,971	91.7	9,475,512	83.8	9,461,479	83.7	9,159,362	74.3
Media_2_0h	Media_2	0	37	NA	NA	NA	NA	NA	NA	NA	NA	NA	NA
Media_2_6h	Media_2	6	37	NA	NA	NA	NA	NA	NA	NA	NA	NA	NA
Media_2_12h	Media_2	12	14	NA	NA	NA	NA	NA	NA	NA	NA	NA	NA
Media_2_24h	Media_2	24	36	NA	NA	NA	NA	NA	NA	NA	NA	NA	NA
Negative_1	Negative_1	NA	25	NA	NA	NA	NA	NA	NA	NA	NA	NA	NA
Negative_2	Negative_2	NA	35	NA	NA	NA	NA	NA	NA	NA	NA	NA	NA
Negative_3	Negative_3	NA	16	NA	NA	NA	NA	NA	NA	NA	NA	NA	NA
Negative_4	Negative_4	NA	19	NA	NA	NA	NA	NA	NA	NA	NA	NA	NA
Water_1	Water_1	NA	35	NA	NA	NA	NA	NA	NA	NA	NA	NA	NA
Water_2	Water_2	NA	13	NA	NA	NA	NA	NA	NA	NA	NA	NA	NA
Water_3	Water_3	NA	10	NA	NA	NA	NA	NA	NA	NA	NA	NA	NA
Water_4	Water_4	NA	15	NA	NA	NA	NA	NA	NA	NA	NA	NA	NA

Most of the control samples (negative and positive controls) returned almost no sequencing reads, which is expected. However, there are 2 media samples with high number of reads, Media-1-12h and Media-1-24h, see table below. However, taxonomic classification of these control samples found that all reads map to only *Clostridium butyricum*, which is most likely contamination.

Appendix 8

A review

**Microbiomes in Physiology:
Insights into 21st-Century Global
Medical Challenges**

Appendix 8



Received: 17 November 2021 | Accepted: 17 January 2022

DOI: 10.1111/EP090226



SYMPOSIUM REVIEW

Microbiomes in physiology: insights into 21st-century global medical challenges

Emad Shehata^{1,2} | Aimée Parker¹ | Toru Suzuki³ | Jonathan. R. Swann⁴ |
Jotham Suez⁵ | Paul. A. Kroon¹ | Priscilla Day-Walsh¹

¹Quadram Institute Bioscience, Food Innovation and Health & Gut Microbes in Health and Disease Programmes, Quadram Institute Bioscience, Norwich, UK

²Chemistry of Flavour and Aroma Department, National Research Centre, Dokki, Cairo, Egypt

³Department of Cardiovascular Sciences and NIHR Leicester Biomedical Research Centre, University of Leicester, Glenfield Hospital, Leicester, UK

⁴Faculty of Medicine, School of Human Development and Health, University of Southampton, Southampton, UK

⁵W. Harry Feinstone Department of Molecular Microbiology and Immunology, Johns Hopkins Bloomberg School of Public Health, Baltimore, MD, USA

Correspondence

Priscilla Day-Walsh, Quadram Institute Bioscience, Food Innovation and Health & Gut Microbes in Health and Disease Programmes, Quadram Institute Bioscience, Rosalind Franklin Road, Norwich Research Park, Norwich, Norfolk NR4 7UQ, UK.
Email: priscilla.day-walsh@quadram.ac.uk

Funding information

Biotechnology and Biological Sciences Research Council, Grant/Award Numbers: BB/R012512/1, BBS/E/F/000PR10343, BBS/E/F/000PR10346, BBS/E/F/000PR10347, BB/R012490/1, BBS/E/F/000PR10353, BBS/E/F/000PR10355, BBS/E/F/000PR10356; Newton-Mosharafa Scholarship Fund from the Egyptian Ministry of Higher Education (Cultural Affairs and Mission sector), the British Council and the British Embassy in Egypt; National Institute for Health Research (Leicester Biomedical Research Centre); Medical Research Council (MRC) UK Consortium on Metabolic Phenotyping (MAP/UK)

Edited by: Jeremy Ward

Abstract

The human gut microbiome is a key factor in the development of metabolic diseases and antimicrobial resistance, which are among the greatest global medical challenges of the 21st century. A recent symposium aimed to highlight state-of-the-art evidence for the role of the gut microbiome in physiology, from childhood to adulthood, and the impact this has on global disease outcomes, ageing and antimicrobial resistance. Although the gut microbiome is established early in life, over time the microbiome and its components including metabolites can become perturbed due to changes such as dietary habits, use of antibiotics and age. As gut microbial metabolites, including short-chain fatty acids, secondary bile acids and trimethylamine-N-oxide, can interact with host receptors including G protein-coupled receptors and can alter host metabolic fluxes, they can significantly affect physiological homeostasis leading to metabolic diseases. These metabolites can be used to stratify disease phenotypes such as irritable bowel syndrome and adverse events after heart failure and allow informed decisions on clinical management and treatment. While strategies such as use of probiotics, prebiotics and faecal microbiota transplantation have been proposed as interventions to treat and prevent metabolic diseases and antimicrobial resistance, caution must be exercised, first due to the potential of probiotics to enhance antimicrobial resistance gene reservoirs, and second, a 'healthy gut microbiome' that can be used as a biobank for transplantation is yet to be defined. We highlight that sampling other parts of the gastrointestinal tract may produce more representative data than the faecal microbiome alone.

KEYWORDS

antibiotic resistance, cardiovascular physiology, faecal microbiota transplantation, inflammaging, irritable bowel syndrome, neuroimmunology, probiotics, resistome

This is an open access article under the terms of the [Creative Commons Attribution License](https://creativecommons.org/licenses/by/4.0/), which permits use, distribution and reproduction in any medium, provided the original work is properly cited.

© 2022 The Authors. *Experimental Physiology* published by John Wiley & Sons Ltd on behalf of The Physiological Society

Experimental Physiology. 2022; 107:257–264.

[wileyonlinelibrary.com/journal/eph](https://onlinelibrary.com/journal/eph) | 257

1 | INTRODUCTION

The microbiome is critical to physiological homeostasis, influencing health and disease status in the host. The human body contains trillions of microbes encompassing bacteria, archaea, viruses and microeukaryotes (Zhang et al., 2019). In the current report, the gut microbiome consists of symbiotic or pathobionts that are resident in the host and opportunistic pathogens that are acquired from the environment or other parts of the body (Casadevall & Pirofski, 1999; Chow et al., 2011). While opportunistic pathogens can cause acute effects, pathobionts are only able to cause deleterious effects to host health in certain circumstances, such as when the immune system has become compromised. Commensals/symbionts contribute to the maintenance of physiological homeostasis as well as providing colonisation resistance to opportunistic pathogens (Hornef, 2015). Acute deleterious effects of pathogens in physiology can lead to infections and in extreme cases cause bacteraemia leading to sepsis and death. This has led to heavy overuse of antibiotics to combat infections, which has provided the selective pressure that is driving increases in antibiotic resistance (Ahmed, 2005; Casadevall & Pirofski, 1999; Lau et al., 2004).

As well as harbouring antimicrobial resistance genes, the gut microbiome may also influence systemic physiological functions by competing for essential nutrients or digesting complex molecules to produce substrates for host energy metabolism and cell signalling (Martin et al., 2019). The gut microbiota can therefore also cause subtle but chronic physiological effects, which contribute to the epidemic of metabolic/inflammatory diseases such as diabetes, cardiovascular disease and neurodegenerative diseases (Suez et al., 2018; Wang et al., 2020). Coupled to antibiotic resistance, metabolic diseases are among the leading global medical challenges of our time, posing a socio-economic burden worldwide. Nevertheless, mechanisms through which the microbiome influences physiology remain relatively poorly understood. It is envisaged that advances in sampling techniques, multi-omic approaches (genomic, transcriptomic, methylomic, proteomic, metabolomic), and bioinformatic tools will increase the resolution at which these pan-kingdom interactions can be studied, thus expanding our understanding of the influence of the microbiome on host physiology in health and disease. Such advances will likely revolutionise future clinical practices in disease prevention, treatment and management.

The most compelling evidence for the influence of microbes on human physiology comes from bacterial/viral infections, where a coordinated systemic reaction that evokes a signalling cascade is manifested by a raised body temperature, muscle weakness and pain, and, if poorly managed, results in multi-organ failure and subsequently death (Stearns-Kurosawa et al., 2011). Thus, understanding systemic host responses not only to exogenous microbes but also the microbiome in general is critical. Whether microbiomes are favourable to the host depends on the types and strains that make up the microbiome species and how they interact with the host and other members of the microbial community, which is further influenced by factors such as diet, general health and the environment. The focus of the "Micro-

New Findings

- **What is the topic of this review?**

The role of the gut microbiome in physiology and how it can be targeted as an effective strategy against two of the most important global medical challenges of our time, namely, metabolic diseases and antibacterial resistance.

- **What advances does it highlight?**

The critical roles of the microbiome in regulating host physiology and how microbiome analysis is useful for disease stratification to enable informed clinical decisions and develop interventions such as faecal microbiota transplantation, prebiotics and probiotics. Also, the limitations of microbiome modulation, including the potential for probiotics to enhance antimicrobial resistance gene reservoirs, and that currently a 'healthy microbiome' that can be used as a biobank for transplantation is yet to be defined.

biomes in Physiology" symposium, which took place virtually on the 14th July 2021 at the main Physiological Society meeting and the current report is on the role of the gut microbiome in regulating physiological functions locally in the gut and remotely in various gut-organ axes, including the heart, the liver and the brain.

2 | MICROBES ACROSS THE LIFESPAN

The overall composition of the microbiome is determined by early life events such as mode of delivery, breastfeeding and frequency of antibiotic use. However, the abundance of each microbe may fluctuate across the lifespan due to factors such as age, diet, lifestyle, cultural practices and geographical location (Arbolea et al., 2012; Johnson & Versalovic, 2012). In general, greater microbial diversity and functional redundancy provide resilience to perturbation by the aforementioned factors, and therefore are associated with beneficial impacts on the health of the host (Vieira-Silva et al., 2016).

The presence of microbial genes within the host critically impacts on host metabolic fluxes, with the production of certain metabolites being detrimental and of others beneficial to the health of the host. Microbial metabolism of certain essential dietary precursors can also confer a competitive nutrition partitioning environment between the host and the microbiome. Both microbiota composition and the resulting biochemical products have been shown to change over the life course. For example, the metabolic capacity of the intestinal microbiota to degrade complex carbohydrates to

SYMPOSIUM HIGHLIGHTS

1. The core microbial composition and diversity of the gut is established early in life (within 3 years after birth). Microbial diversity, composition and function can fluctuate over the life course with alterations in microbial metabolite production during critical periods of development contributing to chronic diseases in both childhood and adulthood.
2. While to date a 'healthy microbiome' has not been defined owing to intra- and inter-individual variations in the core microbiome, various microbial products can be used, due to their common functionality, to stratify host disease phenotypes such as irritable bowel syndrome and cardiovascular disease and can predict clinical outcomes after hospitalisation from diseases such as heart failure.
3. Plasma trimethylamine N-oxide (TMAO) is an example of a microbially derived metabolite shown to be an important prognostic marker of adverse events after heart failure and all-cause mortality and is comparable to traditional markers such as B-type natriuretic peptide (BNP) and N-terminal (NT)-pro-hormone BNP (NT-proBNP). Currently, there are no specific drugs that effectively and specifically alter the microbiome to reduce TMAO burden.
4. While there is a debate as to whether alterations in microbial structure and their metabolites such as TMAO may be causative, a mere correlation or indeed a symptom of disease, recent studies using faecal microbiota transplantation and conventionalised animal models indicate that the microbiome has direct/causative effects on host physiology, including effects on inflammaging. The supplementation of TMAO has direct atherogenic effects. In general, high microbial trimethylamine (TMA) production is indicative of altered microbiome composition and structure.
5. The microbiome can also affect the host's health by supporting pathogenic bacteria. This may be mediated by metabolic cross-feeding, whereby commensal species produce metabolites, which support the growth of pathogens and pathobionts. In addition, the microbiome can serve as a reservoir for antimicrobial resistance genes, which can transfer horizontally to pathogenic bacteria. While probiotics have been widely used to prevent or treat diseases (potentially through the modulation of the microbiome), and have been postulated to reduce resistance genes, it has been shown that probiotics may increase and exacerbate the number of antimicrobial resistance genes enhanced by antibiotics.
6. Most data on the diversity and function of the microbiome have been inferred from sampling the faecal microbiome but emerging evidence suggests that the faecal microbiome may misrepresent effects of probiotics on the intestinal microbiome community and the abundance of resistance genes in the gastrointestinal (GI) tract. Therefore, the use of direct sampling from the GI tract is paramount in future research.

short-chain fatty acids (SCFAs) declines with age, while the capacity to transform essential nutrients and proteins into toxic compounds such as trimethylamine-N-oxide (TMAO) and indole sulphates increases with age (Agus et al., 2021; Lee et al., 2020; Rios-Covian et al., 2020). At the symposium, Swann discussed age-dependent variability in the neurobiochemical profiles of mice across the lifecourse, with fluctuations in several microbially derived metabolites. This included metabolites such as 3-indoxyl-sulphate, γ -aminobutyric acid, TMAO, hippurate and phenylacetylglutamine (Swann et al., 2020). While certain metabolites were abundant during the neonatal period and declined into adulthood, others gradually increased with age, and some peaked in abundance at puberty before returning to neonatal levels in adulthood (Swann et al., 2020). As many of these compounds are involved in brain function and development, it is important to characterise whether these fluctuations and their timings would affect developmental plasticity, neonatal growth trajectory and the risk of disease in both childhood and adulthood. Indeed, exposure to certain environmental and nutritional cues during critical periods of growth and development have been shown to influence the risk of developing disease both in early life and in adulthood according to the 'thrifty phenotype' or 'the developmental origins of health and disease' hypothesis (Farshim et al., 2016; Hales & Barker, 2001; Hanson & Gluckman, 2014; Osman et al., 2021).

At the symposium, a direct impact of the microbiome on age-associated inflammation in the brain was described by Parker who reported that faecal microbiota transplantation (FMT) treatment was effective in switching from an age-associated chronic low-grade inflammatory phenotype (inflammaging) and a younger less inflammatory phenotype (Parker et al., 2021). Young mice receiving microbiota from aged mice exhibited an elevated inflammatory phenotype, whereas age-associated serum and brain inflammatory changes in mice could be reduced or reversed by transplantation with microbiota from young donor mice (Parker et al., 2021). Regulatory effects of the FMT treatments were observed in the intestinal epithelial barrier and in the retina. The authors identified serotonergic signalling together with altered lipid and vitamin metabolism as possible mechanisms through which the microbiome may influence age-associated inflammation and functional decline in the gut and the central nervous system. The debate over whether microbes directly impact on physiology has been compounded by limited knowledge available on the mechanisms through which microbially derived compounds alter physiological homeostasis. For example, while in some cases, TMAO produced by the microbiome has been suggested to play an important role in neural development, others have demonstrated an influence of TMAO on brain ageing and cognitive decline (Li et al., 2018; Vuong et al., 2020). Additionally, there are

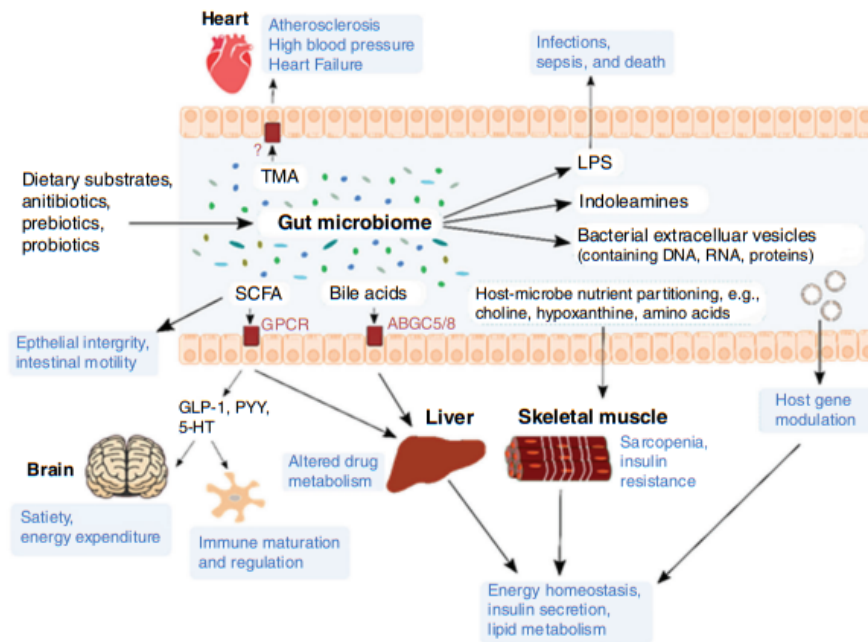


FIGURE 1 Effects of microbially derived components on host physiology. GLP-1, glucagon-like peptide-1; LPS, lipopolysaccharide; PYY, peptide YY

a substantial number of studies showing associations between high plasma levels of TMAO and metabolic diseases, as well as adverse secondary events after heart failure with further studies showing direct atherogenic effects of TMAO in both humans and mice (Brunton et al., 2020; Geng et al., 2018; Tan et al., 2019).

3 | MICROBIAL COMPONENTS, CELL SIGNALLING AND DISEASE STRATIFICATION

In their talks, Swann and Parker highlighted various signalling pathways that are affected by microbially derived compounds (such as metabolites, cell wall components and extracellular vesicles), which can regulate immune function, metabolic homeostasis and brain function (Figure 1). Among the metabolites, SCFAs are perhaps the most-studied gut microbially derived metabolites. SCFAs interact with a range of receptors such as G protein-coupled receptors (GPCRs) on host cells, both locally in the gut and in remote organs such as the brain, heart and the liver. Through their interaction with GPCRs, SCFAs have been shown to modulate the secretion of hormones including glucagon-like peptide-1 and peptide YY, which impact on the brain functions such as mood, appetite, food intake and energy expenditure (Frost et al., 2014; Modasia et al., 2020). In the gut, SCFAs are also utilised by intestinal epithelial and colonic cells as

energy sources, positively promoting gut barrier integrity, as well as maintaining low intestinal pH that is unfavourable to opportunistic pathogens and pathobionts (Pérez-Reytor et al., 2021). Nevertheless, SCFAs may also be used by pathogens such as *Salmonella*, *Clostridium* and *Citrobacter* species as a cue for expressing virulence genes (Zhang et al., 2020). This is a particularly good example of how the interaction of specific microbial species with the complex multi-organism gut microbiome may influence disease risk. In irritable bowel syndrome (IBS) patients with constipation (IBS-C), reduced levels of SCFAs in faecal samples are coupled with reduced levels of acetate in mucosal biopsies (Mars et al., 2020). Although SCFAs derive from dietary fibre, these observations were independent of dietary fibre intake suggesting that other factors may influence the availability of SCFAs. Recent data suggest that SCFAs may derive from the metabolism of L-carnitine to trimethylamine, a pathway highlighted by Suzuki at the symposium (Suzuki et al., 2021) and discussed below in relation to the atherogenic phenotype (Rajakovich et al., 2021). In their talk, Swann further demonstrated that in contrast to IBS-C patients, IBS patients with diarrhoea (IBS-D) present higher levels of tryptophan and its indoleamine microbial metabolite, tryptamine, which again acts locally to regulate intestinal motility by interacting with serotonin receptor-4 (Swann et al., 2020). This was coupled with increased amounts of unconjugated bile acids and decreased amounts of primary bile acids in IBS-D patients (Mars et al., 2020). Another microbial metabolite,

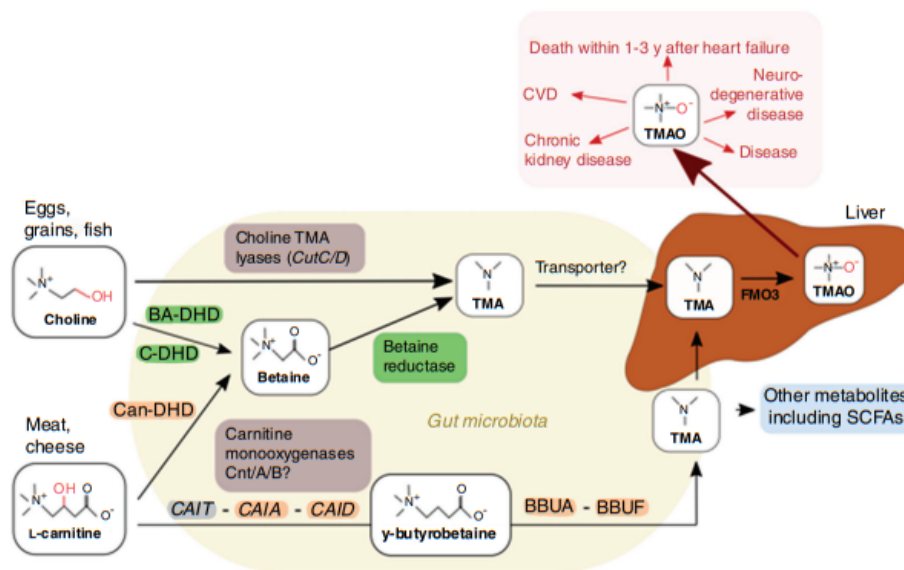


FIGURE 2 Mechanisms of TMA production by the gut microbiota. BA-DH, betaine aldehyde dehydrogenase; BBUA-BBUF, gamma-butyrobetaine utilization genes A to F; C-DH, CAIA, crotonobetainyl-CoA reductase; CAID, carnitiny-CoA dehydratase; CAIT, carnitine/gamma-butyrobetaine antiporter; Can-DH, carnitine dehydrogenase choline dehydrogenase; Cnt/A/B, carnitine monooxygenase subunits A/B; CutC/D, choline trimethylamine-lyase C/D; CVD, cardiovascular disease; FMO3, flavin monooxygenase 3

hypoxanthine, provides an excellent example of competitive nutritional partitioning between the microbiota and the host (Swann et al., 2020). Hypoxanthine is an important energy source for intestinal epithelial cells, promoting epithelial cell development and recovery from injury, however, Swann demonstrated increased hypoxanthine use by the gut microbiome with decreased levels being observed in IBS-C patients (Mars et al., 2020). As such, alterations in microbiota composition and metabolites during critical developmental periods may prove detrimental to health.

4 | STRATIFYING DISEASE OUTCOMES AND CLINICAL DECISIONS BASED ON MICROBIAL METABOLITES: THE CASE OF TRIMETHYLAMINE OXIDE AND HEART FAILURE

The possibility of stratifying patients and guiding clinical decisions based on metabolic profiles was highlighted by Suzuki. Plasma TMAO levels were shown to be a strong predictor of adverse secondary events after heart failure compared to traditional markers such as N-terminal pro-B-type natriuretic peptide (NT-proBNP) (Senthong et al., 2016; Suzuki et al., 2016). TMAO is produced in the liver by flavin-containing monooxygenase isoform 3 (FMO3) following oxidation of trimethylamine (TMA), a derivative of essential dietary components L-carnitine and choline, found in high quantities in red meat and eggs,

respectively (Figure 2) (Koeth et al., 2013). The metabolism of choline to TMA seems to involve the direct choline-TMA lyase pathway (Day-Walsh et al., 2021). However, the metabolism of L-carnitine involves the formation of an obligate intermediate, γ -butyrobetaine, which is further metabolised in a multistep process involving several gene clusters to produce TMA and other metabolites including SCFAs, such as acetate and butyrate, which have been shown to be the end-products in this process (Day-Walsh et al., 2021; Rajakovich et al., 2021). The factors that regulate the formation of TMA from carnitine are yet to be understood although it seems that this pathway may be more important in the production of the atherogenic TMA than that involving choline. In their talk, Suzuki further highlighted that the associations of TMAO with adverse events after heart failure are influenced by geographical location, being higher in individuals from Norway, the Netherlands, Germany, Sweden and the United Kingdom than in those from Italy and Greece (Suzuki et al., 2019). Of note, this geographical variation was shown to be independent of polymorphisms in the FMO3 gene along with diet, indicating that there is a yet unknown factor influencing the predictive capacity of TMAO on all-cause mortality and death after heart failure.

To date, it has been difficult to clarify the compositions or indeed microbial species that can be used to predict disease phenotypes in the host. However, the abundant microbial metabolites provide an opportunity to profile and characterise individuals who may be at risk of not only heart failure but other metabolic diseases as well

as hospitalisation and adverse events after hospitalisation including death. In their talk, Suzuki demonstrated that heart failure patients presenting high levels of TMAO when they are admitted to the hospital might still have high levels after treatment; that is to say, current treatments of heart failure patients and management of their future risk do not target their TMAO status. This presents an opportunity to stratify patients who may be at risk and to make clinically relevant informed decisions based on microbial metabolites. Nevertheless, there is an urgent need for therapies that can target the microbiome to reduce the burden of TMAO in those at risk, as current medications such as β -blockers do not target the microbiome.

5 | MANIPULATING THE MICROBIOME FOR THE BENEFIT OF THE HOST: PROBIOTICS, PREBIOTICS AND FAECAL MICROBIOTA TRANSPLANTATION

Supplementation with live probiotic microorganisms has been proposed as a means for beneficially altering the microbiome, for example by reducing the production of disease-associated metabolites (including TMAO) or reducing the burden of pathobionts and commensals carrying antibiotic resistance genes. As highlighted by Swann probiotics, including those commonly used as dietary supplements, could support health by preventing the colonisation of pathobionts in preterm babies (Alcon-Giner et al., 2020). However, in their talk, Suez highlighted the complexity and limitations of using probiotics in adults, as the colonisation success of supplemented probiotics shows high inter-individual variations, which may underlie heterogeneity in probiotics' efficacy (Zmora et al., 2018). For example, members of the gut microbiome encode for antibiotic resistance genes, creating a reservoir (resistome) that can transfer horizontally to pathogens and pathobionts, facilitating the emergence of antibiotic-resistant strains. In their work, Suez demonstrated that probiotics can reduce the reservoir of antibiotic resistance genes in the human gut, but only in individuals permissive (receptive) to probiotic colonisation (Montassier et al., 2021).

In addition to being a major contributor to the expansion of the gut resistome, the use of antibiotics perturbs the gut microbiome, leading to dysbiosis associated with an elevated risk for non-communicable diseases. Probiotics are often consumed in conjunction with antibiotic therapy to prevent detrimental effects of antibiotics on the microbiome. In their talk, Suez reported that, surprisingly, probiotics delay, rather than facilitate recovery of microbiome diversity from a course of antibiotics. Furthermore, probiotics contributed to an expansion in the number of antibiotic resistance genes in the gut, and in particular increased the abundance of the clinically relevant vancomycin resistance gene (*VanG*) (Suez et al., 2018).

In addition to probiotics, nutraceutical compounds such as complex carbohydrates and polyphenols have been investigated for their capacity to alter the microbiome for the benefit of the host (prebiotics). While the increase in certain microbes in response to these nutraceuticals may suggest beneficial effects, caution has to be exercised as metabolic cross-feeding may promote the

growth of a beneficial species, which will consequently produce metabolites that facilitate the survival of pathobionts (Eloe-Fadrosh & Rasko, 2013; Mohajeri et al., 2018). FMT has also been proposed as a mode to increase microbial diversity or rebalance a dysbiotic microbial composition resulting from infection or ageing for example. As demonstrated by Parker et al., FMT from young donors proved effective in preventing age-associated symptoms and inflammation (Parker et al., 2021). In the context of the resistome, Suez demonstrated that FMT was more effective than probiotic supplementation at restoring the resistome back to pre-antibiotic status. However, the complexity of the microbiome and variations between individuals make it difficult to pinpoint a 'healthy' or optimal microbial composition that can be used as a biobank to treat all those with gut dysbiosis.

6 | CURRENT LIMITATIONS AND THE FUTURE OF THE MICROBIOME IN MEDICAL PHYSIOLOGY

The microbiome offers a unique albeit challenging opportunity to improve host metabolic physiology and revolutionise future clinical practices in disease prevention, treatment and management. However, there was a consensus among the speakers at the symposium on the requirement for the standardisation of sampling and experimental approaches, which will greatly improve our ability to understand the role of the microbiome in physiology. In particular, Swann highlighted the need for averaging longitudinal data from an individual collected from multiple sampling points while Suez demonstrated the disparity between the microbiome and resistome within the stool sample and that from different sites within the gastrointestinal tract. To date, most research has focused on the bacterial component (bacteriome) of the microbiome, but there is an increasing appreciation of the importance of the viral (virome) and fungal (mycobiome) fractions of the microbiome, which is likely to become more apparent as our ability to study these elements evolves, in particular as the bacteriome along with its metabolome is also substantially influenced by phage predation (Hsu et al., 2019).

Thus, it is evident that many of the non-communicable diseases proposed to be influenced by the microbiome coupled to antimicrobial resistance pose major socio-economic challenges. Understanding the role of the microbiome in physiology and how it can be harnessed to underpin the development of effective therapies and preventative treatments will require a coordinated multidisciplinary research effort by physiologists, microbiologists, nutritionists, clinicians and partnerships with commercial organisations.

ACKNOWLEDGEMENTS

The authors gratefully acknowledge the support of the Biotechnology and Biological Sciences Research Council (BBSRC); this research was funded by the BBSRC Institute Strategic Programme Food Innovation and Health BB/R012512/1 and its constituent projects BBS/E/F/000PR10343, BBS/E/F/000PR10346 and BBS/E/F/000PR10347. A.P. was funded by the BBSRC Institute Strategic

Programme Grant Gut Microbes and Health (BB/R012490/1) and its constituent projects BBS/E/F/000PR10353, BBS/E/F/000PR10355 and BBS/E/F/000PR10356. E.S. was funded by the Newton-Mosharafa Scholarship Fund from the Egyptian Ministry of Higher Education (Cultural Affairs and Mission sector), the British Council and the British Embassy in Egypt. T.S. was funded by the National Institute for Health Research (Leicester Biomedical Research Centre) and the Medical Research Council (MRC) UK Consortium on MetAbolic Phenotyping (MAP/UK).

COMPETING INTERESTS

Authors declare no conflict of interest.

AUTHOR CONTRIBUTIONS

Conception or design of the work: P.D.-W. and E.S. Acquisition, analysis or interpretation of data for the work: P.D.-W., A.P., T.S., J.R.Sw., J.Su., P.A.K. and P.D.-W. Drafting of the work or revising it critically for important intellectual content: P.D.-W., A.P., T.S., J.R.Sw., J.Su., P.A.K. and P.D.-W. All authors have read and approved the final version of this manuscript and agree to be accountable for all aspects of the work in ensuring that questions related to the accuracy or integrity of any part of the work are appropriately investigated and resolved. All persons designated as authors qualify for authorship, and all those who qualify for authorship are listed.

ORCID

Emad Shehata  <https://orcid.org/0000-0002-8698-4797>

Jotham Suez  <https://orcid.org/0000-0003-3836-972X>

Priscilla Day-Walsh  <https://orcid.org/0000-0003-4947-3725>

REFERENCES

- Agus, A., Clément, K., & Sokol, H. (2021). Gut microbiota-derived metabolites as central regulators in metabolic disorders. *Gut*, 70(6), 1174–1182. <https://doi.org/10.1136/gutjnl-2020-323071>
- Ahmed, N. (2005). 23 years of the discovery of *Helicobacter pylori*: Is the debate over? *Annals of Clinical Microbiology and Antimicrobials*, 4, 17. <https://doi.org/10.1186/1476-0711-4-17>
- Alcon-Giner, C., Dalby, M. J., Caim, S., Ketskemeti, J., Shaw, A., Sim, K., Lawson, M. A. E., Kiu, R., Leclaire, C., Chalklen, L., Kujawska, M., Mitra, S., Fardus-Reid, F., Belteki, G., Mccoll, K., Swann, J. R., Kroll, J. S., Clarke, P., & Hall, L. J. (2020). Microbiota supplementation with *Bifidobacterium* and *Lactobacillus* modifies the preterm infant gut microbiota and metabolome: An observational study. *Cell Reports Medicine*, 1(5), 100077. <https://doi.org/10.1016/j.xcr.2020.100077>
- Arboleya, S., Binetti, A., Salazar, N., Fernández, N., Solís, G., Hernández-Barranco, A., Margolles, A., Los Reyes-Gavilán, C. G., & Gueimonde, M. (2012). Establishment and development of intestinal microbiota in preterm neonates. *FEMS Microbiology Ecology*, 79(3), 763–772. <https://doi.org/10.1111/j.1574-6941.2011.01261.x>
- Brunt, V. E., Goscia-Ryan, R. A., Casso, A. G., Vandongen, N. S., Ziemba, B. P., Sapsinsley, Z. J., Richey, J. J., Zigler, M. C., Neilson, A. P., Davy, K. P., & Seals, D. R. (2020). Trimethylamine-N-oxide promotes age-related vascular oxidative stress and endothelial dysfunction in mice and healthy humans. *Hypertension*, 76(1), 101–112. <https://doi.org/10.1161/HYPERTENSIONAHA.120.14759>
- Casadevall, A., & Pirofski, L.-A. (1999). Host-pathogen interactions: Redefining the basic concepts of virulence and pathogenicity. *Infection and Immunity*, 67(8), 3703–3713. <https://doi.org/10.1128/IAI.67.8.3703-3713.1999>
- Chow, J., Tang, H., & Mazmanian, S. K. (2011). Pathobionts of the gastrointestinal microbiota and inflammatory disease. *Current Opinion in Immunology*, 23(4), 473–480. <https://doi.org/10.1016/j.coi.2011.07.010>
- Day-Walsh, P., Shehata, E., Saha, S., Savva, G. M., Nemeckova, B., Speranza, J., Kellingray, L., Narbad, A., & Kroon, P. A. (2021). The use of an in-vitro batch fermentation (human colon) model for investigating mechanisms of TMA production from choline, L-carnitine and related precursors by the human gut microbiota. *European Journal of Nutrition*, 60(7), 3987–3999. <https://doi.org/10.1007/s00394-021-02572-6>
- Eloe-Fadrosh, E. A., & Rasko, D. A. (2013). The human microbiome: From symbiosis to pathogenesis. *Annual Review of Medicine*, 64, 145–163. <https://doi.org/10.1146/annurev-med-010312-133513>
- Farshim, P., Walton, G., Chakrabarti, B., Givens, I., Saddy, D., Kitchen, I., R Swann, J., & Bailey, A. (2016). Maternal weaning modulates emotional behavior and regulates the gut-brain axis. *Science Reports*, 6, 21958. <https://doi.org/10.1038/srep21958>
- Frost, G., Sleeth, M. L., Sahuri-Arisoylu, M., Lizarbe, B., Cerdan, S., Brody, L., Anastasovska, J., Ghourab, S., Hankir, M., Zhang, S., Carling, D., Swann, J. R., Gibson, G., Viardot, A., Morrison, D., Louise Thomas, E., & Bell, J. D. (2014). The short-chain fatty acid acetate reduces appetite via a central homeostatic mechanism. *Nature Communications*, 5, 3611. <https://doi.org/10.1038/ncomms4611>
- Geng, J., Yang, C., Wang, B., Zhang, X., Hu, T., Gu, Y., & Li, J. (2018). Trimethylamine N-oxide promotes atherosclerosis via CD36-dependent MAPK/JNK pathway. *Biomedicine & Pharmacotherapy*, 97, 941–947. <https://doi.org/10.1016/j.biopha.2017.11.016>
- Hales, C. N., & Barker, D. J. P. (2001). The thrifty phenotype hypothesis. *British Medical Bulletin*, 60, 5–20. <https://doi.org/10.1093/bmb/60.1.5>
- Hanson, M. A., & Gluckman, P. D. (2014). Early developmental conditioning of later health and disease: Physiology or pathophysiology? *Physiological Reviews*, 94(4), 1027–1076. <https://doi.org/10.1152/physrev.00029.2013>
- Hornef, M. (2015). Pathogens, commensal symbionts, and pathobionts: Discovery and functional effects on the host. *ILAR Journal*, 56(2), 159–162. <https://doi.org/10.1093/ilar/ilv007>
- Hsu, B. B., Gibson, T. E., Yeliseyev, V., Liu, Q., Lyon, L., Bry, L., Silver, P. A., & Gerber, G. K. (2019). Dynamic modulation of the gut microbiota and metabolome by bacteriophages in a mouse model. *Cell Host & Microbe*, 25(6), 803–814.e805. <https://doi.org/10.1016/j.chom.2019.05.001>
- Johnson, C. L., & Versalovic, J. (2012). The human microbiome and its potential importance to pediatrics. *Pediatrics*, 129(5), 950–960. <https://doi.org/10.1542/peds.2011-2736>
- Koeth, R. A., Wang, Z., Levison, B. S., Buffa, J. A., Org, E., Sheehy, B. T., Britt, E. B., Fu, X., Wu, Y., Li, L., Smith, J. D., Donato, J. A., Chen, J., Li, H., Wu, G. D., Lewis, J. D., Warrier, M., Brown, J. M., Krauss, R. M., ... Hazen, S. L. (2013). Intestinal microbiota metabolism of L-carnitine, a nutrient in red meat, promotes atherosclerosis. *Nature Medicine*, 19(5), 576–585. <https://doi.org/10.1038/nm.3145>
- Lau, S. K. P., Woo, P. C. Y., Woo, G. K. S., Fung, A. M. Y., Wong, M. K. M., Chan, K.-M., Tam, D. M. W., & Yuen, K.-Y. (2004). *Eggerthella hongkongensis* sp. nov. and *Eggerthella sinensis* sp. nov., two novel *Eggerthella* species, account for half of the cases of *Eggerthella bacteremia*. *Diagnostic Microbiology and Infectious Disease*, 49(4), 255–263. <https://doi.org/10.1016/j.diagmicrobio.2004.04.012>
- Lee, J., Venna, V. R., Durgan, D. J., Shi, H., Hudobenko, J., Putluri, N., Petrosino, J., Mccullough, L. D., & Bryan, R. M. (2020). Young versus aged microbiota transplants to germ-free mice: Increased short-chain fatty acids and improved cognitive performance. *Gut Microbes*, 12(1), 1–14. <https://doi.org/10.1080/19490976.2020.1814107>
- Li, D., Ke, Y., Zhan, R., Liu, C., Zhao, M., Zeng, A., Shi, X., Ji, L., Cheng, S., Pan, B., Zheng, L., & Hong, H. (2018). Trimethylamine-N-oxide promotes brain aging and cognitive impairment in mice. *Aging Cell*, 17(4), e12768. <https://doi.org/10.1111/acel.12768>

- Mars, R. A. T., Yang, Yi, Ward, T., Houtti, M.o, Priya, S., Lekatz, H. R., Tang, X., Sun, Z., Kalari, K. R., Korem, T., Bhattarai, Y., Zheng, T., Bar, N., Frost, G., Johnson, A. J., Van Treuren, W., Han, S., Ordog, T., Grover, M., ... Kashyap, P. C. (2020). Longitudinal multi-omics reveals subset-specific mechanisms underlying irritable bowel syndrome. *Cell*, 182(6), 1460–1473.e17. <https://doi.org/10.1016/j.cell.2020.08.007>
- Martin, A. M., Sun, E. W., Rogers, G. B., & Keating, D. J. (2019). The influence of the gut microbiome on host metabolism through the regulation of gut hormone release. *Frontiers in Physiology*, 10, 428. <https://doi.org/10.3389/fphys.2019.00428>
- Modasia, A., Parker, A., Jones, E., Stentz, R., Brion, A., Goldson, A., Defernez, M., Wileman, T., Ashley Blackshaw, L., & Carding, S. R. (2020). Regulation of enteroendocrine cell networks by the major human gut symbiont *Bacteroides thetaotaomicron*. *Frontiers in Microbiology*, 11, 575595. <https://doi.org/10.3389/fmicb.2020.575595>
- Mohajeri, M. H., Brummer, R. J. M., Rastall, R. A., Weersma, R. K., Harmsen, H. J. M., Faas, M., & Eggersdorfer, M. (2018). The role of the microbiome for human health: From basic science to clinical applications. *European Journal of Nutrition*, 57(1), 1–14. <https://doi.org/10.1007/s00394-018-1703-4>
- Montassier, E., Valdés-Mas, R., Batard, E., Zmora, N., Dori-Bachash, M., Suez, J., & Elinav, E. (2021). Probiotics impact the antibiotic resistance gene reservoir along the human GI tract in a person-specific and antibiotic-dependent manner. *Nature Microbiology*, 6(8), 1043–1054. <https://doi.org/10.1038/s41564-021-00920-0>
- Osman, A., Zuffa, S., Walton, G., Fagbodu, E., Zanos, P., Georgiou, P., Kitchen, I., Swann, J., & Bailey, A. (2021). Post-weaning A1/A2 β -casein milk intake modulates depressive-like behavior, brain μ -opioid receptors, and the metabolome of rats. *iScience*, 24(9), 103048. <https://doi.org/10.1016/j.isci.2021.103048>
- Parlier, A., Romano, S., Ansoerge, R., Aboelnoer, A., Le Gall, G., Savva, G. M., Telatin, A., Jones, E., Baker, D., Rudder, S., Blackshaw, L. A., Jeffery, G., & Carding, S. R. (2021). Heterochronic fecal microbiota transfer reverses hallmarks of the aging murine gut, eye and brain. *SSRN Electronic Journal*. <http://doi.org/10.2139/ssrn.3811833>
- Pérez-Reytor, D., Puebla, C., Karahanian, E., & García, K. (2021). Use of short-chain fatty acids for the recovery of the intestinal epithelial barrier affected by bacterial toxins. *Frontiers in Physiology*, 12(721), 650313. <https://doi.org/10.3389/fphys.2021.650313>
- Rajakovich, L. J., Fu, B., Bollenbach, M., & Balskus, E. P. (2021). Elucidation of an anaerobic pathway for metabolism of l-carnitine-derived gamma-butyrobetaine to trimethylamine in human gut bacteria. *Proceedings of the National Academy of Sciences, USA*, 118(32), e2101498118. <https://doi.org/10.1073/pnas.2101498118>
- Rios-Covian, D., González, S., Nogacka, A. M., Arboleya, S., Salazar, N., Gueimonde, M., & De Los Reyes-Gavilán, C. G. (2020). An overview on fecal branched short-chain fatty acids along human life and as related with body mass index: Associated dietary and anthropometric factors. *Frontiers in Microbiology*, 11, 973. <https://doi.org/10.3389/fmicb.2020.00973>
- Senthong, V., Wang, Z., Fan, Y., Wu, Y., Hazen, S. L., & Tang, W. H. W. (2016). Trimethylamine N-oxide and mortality risk in patients with peripheral artery disease. *Journal of the American Heart Association*, 5(10), e004237. <https://doi.org/10.1161/JAHA.116.004237>
- Stearns-Kurosawa, D. J., Osuchowski, M. F., Valentine, C., Kurosawa, S., & Remick, D. G. (2011). The pathogenesis of sepsis. *Annual Review of Pathology*, 6, 19–48. <https://www.annualreviews.org/doi/10.1146/annurev-pathol-011110-130327>
- Suez, J., Zmora, N., Zilberman-Schapira, G., Mor, U., Dori-Bachash, M., Bashardes, S., Zur, M., Regev-Lehavi, D., Ben-Zeev Brik, R., Federici, S., Horn, M., Cohen, Y., Moor, A. E., Zeevi, D., Korem, T., Kotler, E., Harmelin, A., Itzkovitz, S., Maharshak, N., ... Elinav, E. (2018). Post-antibiotic gut mucosal microbiome reconstitution is impaired by probiotics and improved by autologous FMT. *Cell*, 174(6), 1406–1423.e16. <https://doi.org/10.1016/j.cell.2018.08.047>
- Suzuki, T., Heaney, L. M., Bhandari, S. S., Jones, D. J. L., & Ng, L. L. (2016). Trimethylamine N-oxide and prognosis in acute heart failure. *Heart*, 102(11), 841–848. <https://doi.org/10.1136/heartjnl-2015-308826>
- Suzuki, T., Yazaki, Y., Voors, A. A., Jones, D. J. L., Chan, D. C. S., Anker, S. D., Cleland, J. G., Dickstein, K., Filippatos, G., Hillege, H. L., Lang, C. C., Ponikowski, P., Samani, N. J., Van Veldhuisen, D. J., Zannad, F., Zwinderman, A. H., Metra, M., & Ng, L. L. (2019). Association with outcomes and response to treatment of trimethylamine N-oxide in heart failure: Results from BIOSTAT-CHF. *European Journal of Heart Failure*, 21(7), 877–886. <https://doi.org/10.1002/ehf.1338>
- Swann, J. R., Spitzer, S. O., & Diaz Heijtz, R. (2020). Developmental signatures of microbiota-derived metabolites in the mouse brain. *Metabolites*, 10(5), 172. <https://doi.org/10.3390/metabo10050172>
- Tan, Y., Sheng, Z., Zhou, P., Liu, C., Zhao, H., Song, L., Li, J., Zhou, J., Chen, Y., Wang, L., Qian, H., Sun, Z., Qiao, S., Xu, B., Gao, R., & Yan, H. (2019). Plasma trimethylamine N-oxide as a novel biomarker for plaque rupture in patients with ST-segment-elevation myocardial infarction. *Circulation Cardiovascular Interventions*, 12(1), e007281. <https://doi.org/10.1161/circinterventions.118.007281>
- Vieira-Silva, S., Falony, G., Darzi, Y., Lima-Mendez, G., Garcia Yunta, R., Okuda, S., Vandeputte, D., Valles-Colomer, M., Hildebrand, F., Chaffron, S., & Raes, J. (2016). Species-function relationships shape ecological properties of the human gut microbiome. *Nature Microbiology*, 1(8), 16088. <https://doi.org/10.1038/nmicrobiol201688>
- Vuong, H. E., Pronovost, G. N., Williams, D. W., Coley, E. J. L., Siegler, E. L., Qiu, A., Kazantsev, M., Wilson, C. J., Rendon, T., & Hsiao, E. Y. (2020). The maternal microbiome modulates fetal neurodevelopment in mice. *Nature*, 586(7828), 281–286. <https://doi.org/10.1038/s41586-020-2745-3>
- Wang P.-X., Deng X.-R., Zhang C.-H., & Yuan H.-J. (2020). Gut microbiota and metabolic syndrome. *Chinese Medical Journal*, 133(7), 808–816. <https://doi.org/10.1097/cm9.0000000000000696>
- Zhang, S., Dogan, B., Guo, C., Herlekar, D., Stewart, K., Scherl, E. J., & Simpson, K. W. (2020). Short chain fatty acids modulate the growth and virulence of pathosymbiont *Escherichia coli* and host response. *Antibiotics*, 9(8), 462. <https://doi.org/10.3390/antibiotics9080462>
- Zhang, Z., Tang, H., Chen, P., Xie, H., & Tao, Y. (2019). Demystifying the manipulation of host immunity, metabolism, and extraintestinal tumors by the gut microbiome. *Signal Transduction and Targeted Therapy*, 4(1), 41. <https://doi.org/10.1038/s41392-019-0074-5>
- Zmora, N., Zilberman-Schapira, G., Suez, J., Mor, U., Dori-Bachash, M., Bashardes, S., Kotler, E., Zur, M., Regev-Lehavi, D., Brik, R. B.-Z., Federici, S., Cohen, Y., Linevsky, R., Rothschild, D., Moor, A. E., Ben-Moshe, S., Harmelin, A., Itzkovitz, S., Maharshak, N., ... Elinav, E. (2018). Personalized gut mucosal colonization resistance to empiric probiotics is associated with unique host and microbiome features. *Cell*, 174(6), 1388–1405.e21. <https://doi.org/10.1016/j.cell.2018.08.041>

How to cite this article: Shehata, E., Parker, A., Suzuki, T., Swann, J. R., Suez, J., Kroon, P. A., & Day-Walsh, P. (2022). Microbiomes in physiology: insights into 21st century global medical challenges. *Experimental Physiology*, 107, 257–264. <https://doi.org/10.1113/EP090226>

Appendix 9

Original

**Development and Validation of a
LC-MS/MS Technique for the
Analysis of Short Chain Fatty
Acids in Tissues and Biological
Fluids Without Derivatisation
Using Isotope Labelled Internal
Standards**

Appendix 9



Article

Development and Validation of a LC-MS/MS Technique for the Analysis of Short Chain Fatty Acids in Tissues and Biological Fluids without Derivatisation Using Isotope Labelled Internal Standards

Shikha Saha ¹, Priscilla Day-Walsh ¹, Emad Shehata ^{1,2}  and Paul Anthony Kroon ^{1,*}

¹ Quadram Institute Bioscience, Norwich Research Park, Norwich NR4 7UQ, UK; shikha.saha@quadram.ac.uk (S.S.); priscilla.day-walsh@quadram.ac.uk (P.D.-W.); emad.shehata@quadram.ac.uk (E.S.)

² National Research Centre, Chemistry of Flavour and Aroma Department, Dokki, Cairo 12622, Egypt

* Correspondence: paul.kroon@quadram.ac.uk



Citation: Saha, S.; Day-Walsh, P.; Shehata, E.; Kroon, P.A. Development and Validation of a LC-MS/MS Technique for the Analysis of Short Chain Fatty Acids in Tissues and Biological Fluids without Derivatisation Using Isotope Labelled Internal Standards. *Molecules* **2021**, *26*, 6444. <https://doi.org/10.3390/molecules26216444>

Academic Editor: Yannis Dotsikas

Received: 15 September 2021

Accepted: 22 October 2021

Published: 26 October 2021

Publisher's Note: MDPI stays neutral with regard to jurisdictional claims in published maps and institutional affiliations.



Copyright: © 2021 by the authors. Licensee MDPI, Basel, Switzerland. This article is an open access article distributed under the terms and conditions of the Creative Commons Attribution (CC BY) license (<https://creativecommons.org/licenses/by/4.0/>).

Abstract: The gut microbiota is critical to the maintenance of physiological homeostasis and as such is implicated in a range of diseases such as colon cancer, ulcerative colitis, diabetes, cardiovascular diseases, and neurodegenerative diseases. Short chain fatty acids (SCFAs) are key metabolites produced by the gut microbiota from the fermentation of dietary fibre. Here we present a novel, sensitive, and direct LC-MS/MS technique using isotopically labelled internal standards without derivatisation for the analysis of SCFAs in different biological matrices. The technique has significant advantages over the current widely used techniques based on sample derivatization and GC-MS analysis, including fast and simple sample preparation and short LC runtime (10 min). The technique is specific and sensitive for the quantification of acetate, butyrate, isobutyrate, isovalerate, lactate, propionate and valerate. The limits of detection were all 0.001 mM except for acetate which was 0.003 mM. The calibration curves for all the analytes were linear with correlation coefficients $r^2 > 0.998$. The intra- and inter-day precisions in three levels of known concentrations were <12% and <20%, respectively. The quantification accuracy ranged from 92% to 120%. The technique reported here offers a valuable analytical tool for use in studies of SCFA production in the gut and their distribution to host tissues.

Keywords: gut microbiota; kidney; diabetes; neurodegenerative; cardiovascular; plasma; milk; lactate; butyrate; acetate; propionate

1. Introduction

The gut microbiota has emerged as critical to human metabolism and physiological homeostasis and is thus implicated in a range of metabolic, inflammatory, and neurological diseases [1–3]. Short chain fatty acids (SCFAs), which include butyrate, propionate and acetate, are key metabolites produced by the gut microbiota from the fermentation of dietary fibre and resistant starch [4,5]. While not necessarily a SCFA, lactate produced from dietary fibre can also serve as a precursor for SCFAs and as a marker of lactic acid bacteria such as *Lactobacillus* and *Lactococcus* among many others [6]. Additionally, microbial fermentation of dietary amino acids such as leucine, isoleucine and valine result in the formation of branched short chain fatty acids (BSCFAs) as stereo isomers of the SCFAs butyrate and valerate, which have been proposed as markers of microbial protein metabolism with a particular emphasis on their positive correlation with obesity, ageing, and metabolic diseases [7,8].

As well as providing energy for colonic cells important for gut barrier integrity, SCFAs have emerged as energy substrates for colonic and liver cells and as signalling molecules influencing a range of metabolic and physiological pathways in the liver, brain, kidney, and

the immune system [3,9]. Additionally, due to their low pH, SCFA are critical in preventing the colonization of pathogenic microbes [10]. In vitro and in vivo studies have shown that the disruption of microbial composition and diversity can affect the bioavailability of both SCFA and BSCFAs leading to diseases such as colon cancer, ulcerative colitis, diabetes, cardiovascular diseases, and neurodegenerative diseases [3,11]. While the bioavailability and function of SCFA and BSCFA is usually extrapolated from caecal contents and plasma levels, little is known regarding the bioavailability of these compounds in peripheral organs such as the liver, kidney, and the brain, possibly due to methodological limitations. Nevertheless, SCFA have been proposed to elicit their physiological effects by interacting with G protein coupled receptors (GPR) such as GPR41 and GPR43 and serotonergic receptors [12]. Therefore, it is important to know physiological levels of SCFAs, lactate and BSCFA (referred to as SCFAs) in these tissues as this may help to determine whether their effects are local, directly inducing cell signalling at the target tissue or are mediated remotely through second messenger signalling molecules.

Several techniques have been used for the analysis of SCFA in biological fluids including nuclear magnetic resonance (NMR) spectroscopy, capillary electrophoresis (CE), gas chromatography mass spectrometry (GC-MS), high performance liquid chromatography (HPLC), size-exclusion chromatography and liquid chromatography-tandem mass spectrometry (LC-MS/MS). The drawbacks of utilising the first four techniques were critically reviewed by Primec, et al. [13]. While to date GC-MS remains an instrument of choice for SCFA analysis owing to its affordability, high sensitivity and resolution, the laborious multi-step sample cleanup process which typically involves ultra-sonication, shaking during incubation, centrifugation followed by filtration, derivatisation, drying and sample dilution may lead to poor analyte recovery and reductions in reproducibility and accuracy, as well as low throughput. This makes this technique far from ideal for the analysis of these metabolites in a large number of samples [13–15]. Likewise, HPLC has been used for the analysis of SCFAs in complex biological samples with clean-up steps and drawbacks similar to those used in GC-MS [16–18]. While a number of studies have also employed LC-MS/MS, the analysis of SCFA has still required sample filtration and derivatisation using one of the available reagents such as tris (2,4,6-trimethoxyphenyl) phosphonium propylamine (TMPP) bromide or carboxylic acids such as 4-[2-(*N,N*-diethylamino)ethylaminosulfonyl]-7-(2-aminoethylamino)-2,1,3-benzoxadiazole (DAABD-AE) as well as 3-nitrophenylhydrazine (3NPH) followed by the addition of 3-nitrophenylhydrazine hydrochloride *N*-(3-dimethylaminopropyl)-*N'*-ethylcarbodiimide hydrochloride [19–23]. The only LC-MS/MS technique that has been utilised to measure SCFA in plasma, without derivatisation, required a post neutralization technique before MS detection and with the use of hydrochloric acid (HCl) in the mobile phases, which is a very harsh condition for HPLC columns and would shorten its lifespan should the use of large sample numbers be required [24]. The technique monitored only ammonium adducts of SCFAs with only propionate, acetate, butyrate and valerate being detected. Additionally, most of the other aforementioned techniques did not simultaneously measure lactate and BSCFAs. Simultaneous detection of SCFA, lactate and BSCFAs is also important as several studies have shown that while the SCFA may not change in response to treatment, BSCFAs may change, and vice versa [23,25,26]. Thus, it is evident that there is a requirement for a robust, sensitive, high throughput, column friendly technique for measuring not only SCFAs but also lactate and BSCFAs in biological samples including plasma, faeces, in vitro fermented faecal samples, milk, and other tissues such as liver, kidney, skeletal muscle, etc.

Here we present a sensitive, simple, and high throughput technique without derivatisation for LC-MS/MS (MRM) based analysis of SCFAs, in mouse and human faecal and mouse liver, kidney, brain, skeletal muscle, spleen samples and microbial fermentation media.

2. Results

2.1. Mass Spectrometry Conditions

To obtain precursor and products ions of acetate, lactate, propionate, butyrate, isobutyrate, valerate and isovalerate in electrospray ionization mode, Agilent MassHunter automated Optimizer software was used. The collision energy was used from 0 to 80 by 10 CE step increments in negative and positive polarity modes. The fragmentor value was constant at 380 V. The positive polarity produced more intense product ions for all compounds except lactate. Lactate produced a more intense peak in negative ion mode. The precursor ion and the product ion with the highest signal to noise (S/N) value and the highest peak intensity was selected for the quantifier ion and the other product ion was selected for the qualifier ions. Table 1 summarizes the monitored ions and the optimized MS operating parameters of the analytes and internal standards.

Table 1. LC-MS/MS parameters of SCFA.

Analyte	Retention Time (mins)	Precursor Ion (m/z)	Product Ion (m/z)	Collision Energy	Cell Accelerator Energy	Polarity
Acetate	1.5 (2.3) *	61.1	43	16	4	Positive
D4-Acetate	1.5 (2.3) *	65.1	47	14	4	Positive
Butyrate	3.7 (4.9) *	89.1	43.1	14	4	Positive
13C2-Butyrate	3.7 (4.9)	91.1	44	14	4	Positive
Isobutyrate	2.9 (4.9) *	89.1	43.1	14	4	Positive
D6-Isobutyrate	2.9 (4.9)	95	49	14	4	Positive
Iso-Valerate	4.2 (5.4) *	103.1	43	14	4	Positive
D9-Isovalerate	4.2 (5.4) *	112.2	50.2	18	4	Positive
Lactate	1.7 (2.0) *	89	42.9	10	5	Negative
13C3-Lactate	1.7 (2.0) *	92	46	10	4	Negative
Propionate	2.3 (3.6) *	75	29	18	4	Positive
D2-Propionate	2.3 (3.6) *	77	31.1	14	4	Positive
Valerate	4.7 (5.4) *	103.1	75	10	4	Positive
D9-Valerate	4.7 (5.4) *	112.1	80	10	4	Positive

Note: * The figures in parentheses indicate the retention times obtained using a Phenomenex PFP column.

2.2. Chromatographic Separations

We aimed to develop a technique with a short run time and good sensitivity for the analysis of SCFAs, stereo isomers and lactate in a wide range of matrices. As such the Waters Acquity UPLC HSS T3 C18 1.8 μm , Acquity UPLC BEH C18 1.7 μm , Kinetex-C18 1.7 μm , Kinetex-PFP 1.7 μm , Kinetex-XB-C18 1.7 μm , Luna Omega 1.6 polar C18 and Thermo Scientific Hypercarb (Porous Graphitic Carbon, PGC) columns were tested to achieve an optimal retention of SCFAs. Good retention and peak shapes were achieved on Kinetex-PFP 1.7 μm , Kinetex-XB-C18 1.7 μm , and Luna Omega 1.6 polar C18 column using 0.1% formic acid in both water and acetonitrile. However, butyrate and isobutyrate, valerate and isovalerate isomeric compounds could not be separated by these columns. Therefore, another column was tried to separate stereo-isomeric compounds. Thermo Scientific Hypercarb (porous graphitic carbon, PGC) 3 μm (50 mm \times 2.1 mm) column and guard column was used to separate these seven analytes. Using this column, a good separation, good retention time and peak shape were obtained for all analytes. Isomeric compounds also were separated using mobile phase 0.1% formic acid in water and acetonitrile; Hypercarb column surface is a flat sheet of hexagonally arranged carbon atoms with a very large polynuclear aromatic compounds which is stereo-selective and allowed separation of geometric-isomers [27]. Additionally, it is stable at all pH ranges (0–14), high temperatures and aggressive mobile phases.

The separation of isobutyrate and butyrate, isovalerate and valerate without derivatization on PGC column is shown in the Figure 1A,B. Chromatographic separation for these isomers is necessary for accurate quantification because isobutyrate and butyrate molecular ions and fragmentations are the same and isovalerate and valerate have the same parent

ions and fragmentation ions. Isomeric compounds could not be separated using normal silica base C18 column without derivatisation of SCFA.

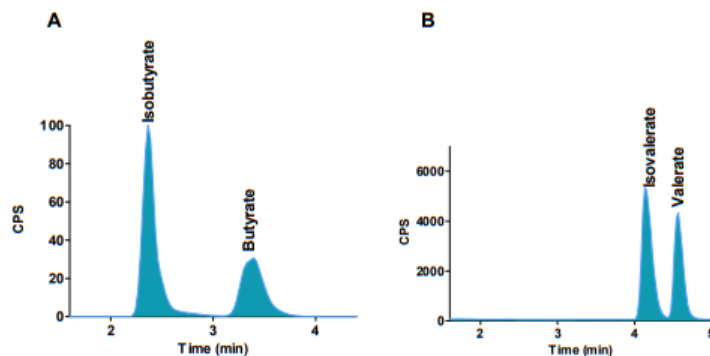


Figure 1. Separation of isomers and stereoisomers of SCFAs using PGC column. (A) Isobutyrate and butyrate, (B) Isovalerate and valerate.

2.3. Method Performance

Linearity, accuracy, precision, recovery and sample stability were studied for validation. These are acceptable criteria for validation of developed methods for publication and future use in biological samples [28]. Method validation was performed using human batch fermentation (colon model) media, mouse faecal samples and various mouse tissues by choosing an appropriate matrix [29].

2.3.1. Linearity and Sensitivity

Endogenous SCFAs are presented in all biological matrices, calibration curves were constructed in aqueous solutions using a stable isotopically labelled internal standard technique for quantification. Isotopically labelled internal standards and analytes contributed to similar chromatographic properties and mass spectroscopic responses, which allowed for the correction of matrix effect variation between the different matrices and the aqueous calibration curve [30,31]. A wide range of concentrations (0.001 mM–10 mM) were studied for calibration curves for all compounds. The least-squares regression calibration curve was $r^2 = 0.998$ for all compounds (Table 2).

Table 2. Method performance data for individual SCFAs, BSCFAs and lactate in acidified water.

Analyte	R ²	Precision (n = 6) (Intra-Day) R.S.D. %			Precision (n = 5) (Inter-Day) R.S.D. %			Accuracy (R.S.D. %)			LOD (mM)	LOQ (mM)
		L	M	H	L	M	H	L	M	H		
Acetate	0.998	11.3	3	2.9	19.3	4.1	6.1	98.2	103	96.6	0.003	0.009
Butyrate	0.999	4.6	2.4	3.6	16.7	5.4	4.5	120.4	102.1	99.8	0.001	0.003
Isobutyrate	0.999	2	1.7	2	10.2	7.4	2.3	107.8	107.9	102.6	0.001	0.003
Isovalerate	0.998	6	3.2	2.7	11.8	4.2	4.7	120	119.3	100.2	0.001	0.003
Lactate	0.999	2.6	2	1.7	9.5	7.6	2.2	120	104.9	98.6	0.001	0.003
Propionate	0.999	5.2	2	1.7	10	9	3.9	119.8	108.4	105.2	0.001	0.003
Valerate	0.998	8	4.4	3.9	14.7	8.4	5.3	116.3	111.4	92.9	0.001	0.003

The optimization software for MRM transition optimization for acetate, butyrate, isobutyrate, isovalerate, lactate, propionate and valerate showed the specific and most sensitive transition at m/z 61 > 43, 89 > 43, 89 > 43, 103 > 43, 89 > 43, 75 > 29 and 103 > 75 respectively. All mentioned SCFAs were well retained and separated well on the PGC

column using a gradient mobile phase with the overall runtime of 10 min. LOD and LOQ values for all compounds are shown in the validation data (Table 2).

2.3.2. Precision and Accuracy

To evaluate intra-day precision replicate ($n = 6$), analysis of three levels of known concentrations (low, medium and high) were spiked in 0.5% orthophosphoric acidified water and analysed by the current techniques. The precision was calculated from the relative standard deviation. The CV (%) was less than 12% for intra-day precision. Inter-day precision was evaluated by analysing the same three levels of concentration samples in acidified water for 5 days. The CV (%) values were <20%. Precision and accuracy data are presented in Table 2.

2.3.3. Carry-Over Effect

For the quantification of metabolites in biological samples by LC-MS/MS, the carry over effect is a common problem. An agilent 1290 series high performance auto sampler with an injection program was used to minimize carry-over effects in this study. No signals were detected in any of the blank samples run amongst SCFA-containing samples, indicating that there was little or no carry over occurring.

2.3.4. Recovery and Matrix Effect

For recovery calculation, known concentrations of individual SCFAs were spiked into the appropriate matrices, and after extraction the samples were quantified using an LC-MS/MS techniques. Nine different matrices were used to determine recovery. The lowest recovery was observed with lactate in the mouse brain samples at about 47%. (See Tables 3 and 4).

The matrix effect on individual analytes were assessed to compare the peak area of the respective isotopically labelled internal standard in post extracted matrix to that in aqueous solution. No matrix effect was noticed for isobutyrate and propionate analysis in Table 3 matrices. However, in the colon model fermented sample, very little matrix effect was found for these compounds, and no matrix effect was observed for butyrate in this matrix (Table 4). The highest matrix effect was observed in spleen matrix for butyrate (76% signal response compared to water), isovalerate (80%) and valerate (84%) analysis, (see Tables 3 and 4).

2.3.5. Sample Stability

All standards and isotope labelled internal standards were prepared in water except for isobutyrate, valerate and isovalerate and their internal standards were prepared in ethanol. Density and purity were considered for stock solution preparation. Stock solutions were kept at -20°C for 6 months, and no changes were observed. The stability of the extracted samples was evaluated at 4°C for 72 h. No significant changes were noticed in sample stability over this time period.

2.4. Quantification of SCFAs in Human Colon Model Fermentation Samples

Colon model fermentation media from three donors each were carried out in duplicates at different time points (0 to 48 h), samples ($n = 6$) were diluted with the addition of 0.5% orthophosphoric acid in methanol containing all isotopically labelled internal standards and subsequently analysed on the LC-MS/MS. All SCFAs peaks were identified in all samples. Figure 2A–F show the 7 SCFA peaks and retention times for all analytes detected in a colon model sample. Figure 2A–L show the corresponding labelled internal standards of SCFAs in colon model samples. The calibration curves constructed from the authentic standards with concentrations of 0–10 mM were linear with a correlation r^2 value of >0.999.

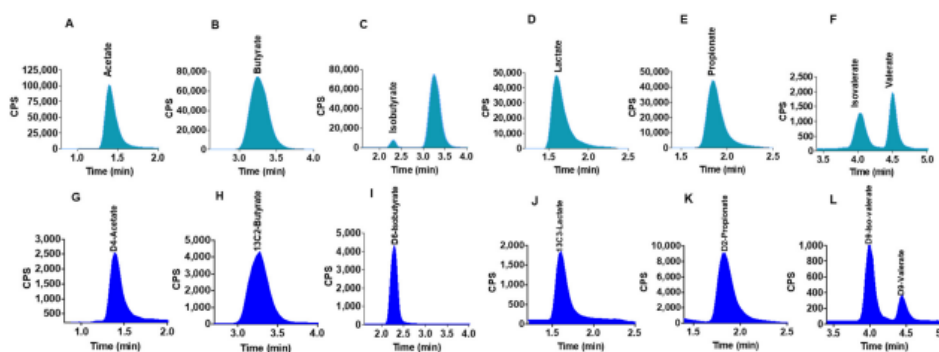
Table 3. Recovery and matrix effect of spiked individual SCFAs, BSCFAs and lactate in appropriate matrices.

Sample Name	Acetate		Butyrate		Isobutyrate		Isovalerate		Lactate		Propionate		Valerate	
	Recovery (%)	Matrix Effect (%)												
Brain	69	0	89	5	82	0	92	22	47	22	79	0	93	57
Faecal	107	0	112	50	103	0	115	46	102	24	100	0	121	56
Kidney	89	17	97	33	96	0	107	34	96	37	104	0	109	53
Liver	81	32	96	53	97	0	115	65	64	38	95	0	105	75
Milk	95	34	79	11	76	0	112	0	97	0	92	0	109	0
Muscle	71	0	89	4	94	0	107	31	75	52	91	0	108	59
Plasma	96	17	89	0	80	0	107	0	64	0	95	0	109	0
Spleen	95	14	98	76	93	0	111	80	95	38	99	0	100	84

Recovery was calculated as (final calculated concentration-non spike concentration/added known concentration) × 100.

Table 4. Recovery and matrix effect of spiked individual SCFAs, BSCFAs and lactate in spiked colon models.

Analytes Added	Measured Conc. (mM), Mean	Recovery (%)	CV (%)	Matrix Effect (%)
Acetate				
0	1.97	-	5.79	43.2
L (0.1 mM)	2.07	98	0.33	42.7
M (1.0 mM)	3.10	113	0.02	42.5
H (10 mM)	11.6	97	1.88	37.7
Butyrate				
0	0.13	-	-	0
L (0.1 mM)	0.25	120	3.85	0
M (1.0 mM)	1.21	108	0.01	0
H (10 mM)	10.1	100	0.61	0
Isobutyrate				
0	0.05	-	2.04	2.50
L (0.1 mM)	0.17	116	3.64	11.21
M (1.0 mM)	1.12	107	0.02	9.47
H (10 mM)	9.83	98	1.60	14.98
Isovalerate				
0	0.01	-	6.25	18.44
L (0.1 mM)	0.12	109	5.09	17.52
M (1.0 mM)	1.01	100	0.04	16.57
H (10 mM)	8.85	88	1.39	18.41
Lactate				
0	0.16	-	5.90	23.98
L (0.1 mM)	0.28	117	1.96	29.43
M (1.0 mM)	1.21	105	0.02	32.08
H (10 mM)	9.61	95	0.87	22.78
Propionate				
0	0.15	-	8.48	7.13
L (0.1 mM)	0.27	116	5.64	14.85
M (1.0 mM)	1.24	109	0.01	10.67
H (10 mM)	9.81	97	0.12	16.08
Valerate				
0	0.02	-	20.18	10.86
L (0.1 mM)	0.14	117	5.26	9.41
M (1.0 mM)	1.22	120	0.05	3.01
H (10 mM)	10.0	100	1.94	7.36

**Figure 2.** LC-MS generated SCFA peaks in colon model fermentation samples. (A–F) peaks detected in colon model fermentation samples. (G–L) corresponding labelled internal standards of SCFA in colon model samples.

2.5. Quantification of SCFAs in Mouse Liver Samples

Liver samples ($n = 15$) from animal study were extracted by 0.5% orthophosphoric acid and analysed by the current LC-MS/MS method. All analytes were detected in the liver samples. Figure 3A–F show the detected analytes in the liver samples and Figure 3G–L show the corresponding isotopically labelled internal standards in the liver samples.

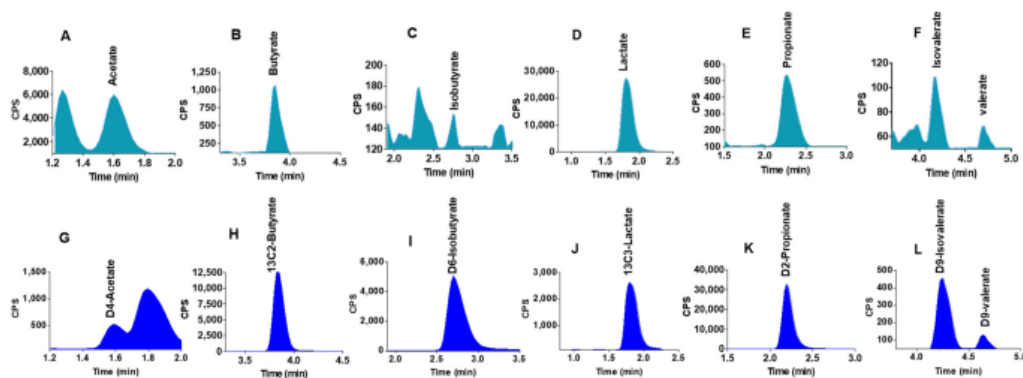


Figure 3. LC-MS generated SCFA peaks in mouse liver samples. (A–F) peaks detected in mouse liver samples. (G–L) corresponding labelled internal standards of SCFA in mouse liver samples.

3. Discussion

The LC-MS/MS technique has great advantages in providing analytical capacity for the simultaneous detection of human metabolites in different biological matrices [32]. SCFAs have been previously analysed in different materials by HPLC using derivatisation techniques which are less sensitive due to the requirement of UV detection and laborious sample preparation as well as long run times (~65 min) rendering them low throughput. Although GC-MS has been widely employed to analyse SCFAs, it has a wide range of drawbacks as described by Primec, et al., 2017 [13]. Since then another technique utilising GC-MS without derivatisation was developed but still required liquid-liquid extraction [33]. Further, LC-MS techniques requiring sample derivatisation have also been used, some involving a very short run time (14 min) and covering a wide range of gut derived metabolites, but once again they require longer sample preparation including sample filtration, which is time consuming and laborious [21,34–36]. A technique with a non-derivatisation step has been developed to analyse SCFAs in plasma using LC-MS, but this requires post neutralization techniques before MS detection and with the use of HCl in the mobile phases, which is very harsh for the HPLC column [24]. Additionally, this technique did not involve simultaneous analysis of stereo isomers and lactate in a wide range of matrices. Studies requiring the analysis of a large number of samples in a wide range of matrices would need the implementation of a fast and simple sample preparation and non-derivatisation high-throughput technique that prevents sample loss. The LC-MS techniques reported to date for quantifying SCFAs have not been tested or validated for use with a wide range of tissues and complex fermentation media which is paramount to future studies that aim to understand the physiological role of these microbial derived metabolites in health and disease. Here we provide a technique with a short run time and good sensitivity for the analysis of SCFAs, stereo isomers and lactate in a wide range of matrices. A brief summary of the aforementioned techniques in comparison to the current one is shown in Table 5.

Table 5. A comparison of previous techniques with the new technique reported here.

Methodological Consideration	GC-MS	HPLC	LC-MS/MS	Current
Derivatization	Yes	No	Yes	No
Sensitivity	μM range	mM range	μM range	μM range
Instrument run time	Long	Long	Medium	short
Sample preparation	Laborious	Simple	Laborious	Simple
BSCFA detection	Yes	No	Yes	Yes
Lactate detection	No	Yes	No	Yes
Tested matrices	4	3	3	9
Sample preparation time	Long	Long	Long	Short (~10 min)
Instrument run time	14–45 min	45–75 min	14–35 min	10 min

Thus, we have developed a new validated technique which does not require sample derivatisation and allows the analysis SCFAs and related metabolites simultaneously in different matrices, employing isotopically labelled internal standards to correct for error in sample preparation, matrix effect and instrumental variation using PGC column. Researchers can also use the common C18-phase columns (Kinetex-XB and Luna Omega polar) or Kinetex-PPF column for the analysis of the five compounds; acetate, butyrate, lactate, propionate and valerate without isomeric compound (isobutyrate and isovalerate) analysis in different matrices, although this would not allow the separation of the stereoisomers.

To our knowledge, this is the first report describing a LC-MS/MS technique for the analysis of SCFAs and related metabolites with a wider application in complex biological fluids and tissues. This technique requires less laborious, fast sample preparative steps with a short LC-MS/MS run time ($T = 10$ min), allowing the analysis of a large number of samples from a wide range of tissues and fluids within a day. The LC-MS/MS technique described in this study allows the analysis of very low levels of SCFAs (0.001 mM) in different matrices. To assess matrix effects, the same concentration of corresponding isotopically labelled internal standards were spiked in different matrices after carrying out extraction as described in the methods section. We found a significant difference in the peak area of labelled internal standards in the different matrices using the electrospray ionization source. Therefore, isotopically labelled internal standards were used, as they are very important for accurate quantification of these compounds in different matrices. While a few studies have demonstrated the bioavailability of SCFA in the human brain and in portal, hepatic, and venous blood, to our knowledge this is the first study to show direct bioavailability of SCFAs in other mouse tissues including the liver, skeletal muscle, kidney and spleen [37–39].

Methodology Limitations: It is noteworthy that some areas of method performance are not ideal, for example the matrix effect in the brain, liver and plasma samples may lead to a low recovery rate for lactate. However, this should not compromise the accuracy for lactate measurements in these tissue samples, as when analyses are carried out in the same matrix, the low recovery rate does not affect quantification accuracy, particularly as this effect is counteracted by the use of isotopically labelled internal standards with quantification carried out using a standard curve. Nevertheless, this stresses the requirement that standard curves be carried out in the same matrices. The poor recovery of lactate, which was measured simultaneously with SCFAs, is consistent with a previous study where lactate recovery from supernatants of bacterial culture was 25% [40]. In the GC-MS techniques described by Primec, et al. although lactic acid was measured from the same samples as SCFA, it is important to note that lactate was measured separately after methylation. Low recovery has no hinderance in measuring the analyte as long as it is consistent across the batches [13]. To our knowledge, no other techniques employing LC/MS/MS have analysed lactate along with SCFAs, although lactate has previously been analysed using LC/MS/MS along with other organic acids [32]. Future studies may wish

to examine the recovery of lactate after pretreatment using trichloro acetic acid, formic acid or perchloric acid.

4. Materials and Methods

4.1. Chemical and Reagents

Acetic, butyric, *d*₄-acetic, ¹³C₂-butyric, isobutyric, isovaleric, lactic, propionic, and valeric acids, were purchased from Sigma® (Dorset, UK). D₆-isobutyric, D₉-isovaleric, ¹³C₃-lactic, D₂-propionic and D₉-valeric acids were purchased from Toronto research chemicals (Toronto, Canada). Ortho-phosphoric and formic acid was obtained from Lichropur (Dorset, UK). Semi-skimmed milk was bought from ALDI supermarket (Essen, Germany). Human plasma (K2EDTA) was purchased from BioIVT (Royston, UK). All solvents with high purity grade were used for LC-MS/MS analysis.

4.2. Colon Model Fermentation Media and Mouse Tissue Samples

4.2.1. Colon Model Study Participants

An in vitro batch fermentation (human colon) model as described by Day-Walsh et al., 2021 was used to study microbial production of SCFAs, lactate and BSCFAs without supplementation of complex carbohydrates [41]. Fresh faecal samples were obtained from participants who were recruited onto the QIB Colon Model study. The study consisted of men and women aged 18 years or older who met the following inclusion criteria: a normal bowel habit with an average Bristol Stool Chart type of 3–5, they had regular defecation of between three times per day and three times per week and had no diagnosed chronic gastrointestinal health problems such as inflammatory bowel disease, irritable bowel syndrome, or celiac disease. Prior to sample donation, participants were not pregnant, or breast feeding, had not taken antibiotics or probiotics within the four weeks and had no gastrointestinal complaints such as vomiting or diarrhea within the last 72 h, and had not recently had an operation requiring general anaesthetic. Samples were collected after an informed consent from all participating subjects and a trial approval (registered at <http://www.clinicaltrials.gov> (accessed on 21 October 2021) (NCT02653001)). Fresh human faecal slurry from three different donors were used for the study in duplicates. Samples were collected at 0, 4, 8, 12, 24 and 48 h and kept at −20 °C immediately until analysis.

4.2.2. Animals and Sample Processing

All experimental protocols and procedures were reviewed and approved by the Animal Welfare and Ethical Review Body (AWERB) at the University of East Anglia, and they were conducted in accordance with the provisions of the Animals (Scientific Procedures) Act 1986 (ASP) and the LASA Guiding Principles for Preparing for and Undertaking Aseptic Surgery (2010) as described by Day, et al., 2018 [42]. Tissues were collected and frozen on dry ice immediately and transferred to −20 °C until processing. Faecal samples were collected prior to animal sacrifice.

4.2.3. Sample Processing

SCFAs from all samples were extracted in 0.5% orthophosphoric acid as outlined by Zhao et al., 2005 and Garcia-Villalba et al., 2012 [15,43]. Samples were thawed on ice, centrifuged and 10 µL of the supernatant was mixed with 90 µL 0.5% orthophosphoric acid containing all isotopically labelled internal standards (5 mM for acetate, 0.25 mM for lactate and 0.5 mM the other five). Samples were further centrifuged at 15,000 rpm for 10 min and the supernatant was transferred to the chromatography vials for analysis using LC-MS. For tissue samples, tissues were pulverized using a pestle and mortar under dry ice and mixed into a homogenous powder. 30 mg of each tissue was mixed with 200 µL of 0.5% orthophosphoric acid in water and homogenized using the Precellys 24 lysis homogeniser at 6000 rpm for 2 cycles for 30 s (Bertin Technologies, Montigny-le Bretonneux, France). After centrifugation for 10 min at 4 °C, 45 µL of the supernatant was mixed with 5 µL of 0.5% orthophosphoric acid containing all isotopically labelled internal standards

(conc. 0.5 mM for all except lactate, lactate conc. was 0.25 mM). Other sample extraction methods including 100% methanol in 0.5% orthophosphoric acid (85% orthophosphoric acid diluted in methanol) and 50% methanol in 0.5% orthophosphoric acid were also trialed, but these gave a cloudy mixture that did not separate completely even after centrifugation at 15,000 rpm for 15 min.

Plasma and semi-skimmed milk (50 μ L) were mixed with 100 μ L methanol containing isotopically labeled internal standards (1 mM for acetate, 0.25 mM lactate and 0.5 mM other analyses) and vortexed. Samples were kept for 5 min on the ice to complete protein precipitation. After centrifugation for 10 min at 4 $^{\circ}$ C at 15,000 rpm, samples were transferred to HPLC vials and analysed by the present LC-MS/MS technique.

4.3. LC-MS/MS Analysis

All SCFAs authentic standards were reconstituted in acidified Milli-Q[®] water to prepare stock solutions at the concentration of 100 mM. All stock solutions were kept at -20 $^{\circ}$ C. A standard curve was produced from stock solutions daily. A standard curve was produced with serial dilutions from the highest concentration (10 mM to 0.001 mM). All serial dilutions were prepared prior to each run. An Agilent 6490 Triple Quad MS mass spectrometer (Agilent Technologies, Santa Clara, CA, USA) equipped with an Agilent 1290 HPLC system (Agilent Technologies, Santa Clara, CA, USA) was used for the analysis of SCFA. The LC flow rate was 0.15 mL/min. The column used for the analysis was a Thermofisher PGC 3 μ m (50 mm \times 2.1mm) or Phenomenex 1.8 μ m (100 mm \times 2.1 mm PFP column with guard column. The column temperature and auto sampler were maintained at 40 $^{\circ}$ C and 4 $^{\circ}$ C, respectively. 2 μ L was used for the injection volume. Samples were analysed using 0.1% formic acid in water (mobile phase A) and 0.1% formic acid in acetonitrile (mobile phase B). The gradient was started with 0% B, increased 60% B within 4 min, after washing for 2 min using 100% mobile phase B and equilibration was for another 4 min using 100% mobile phase A. The equilibration time was kept a little bit longer (4 min), because of PGC column packing material. The total run was 10 min. The 6490 MS/MS system was equipped with an electrospray ionization (ESI) source operated in positive and negative-ion detection mode. Nitrogen gas was used for nebulation, desolvation, and collision. The analytes were monitored in multiple-reaction monitoring (MRM) mode. The MRM precursor, product ions and collision energy were optimized by Agilent optimizer software. The transitions of precursor ions to product ions (m/z) and some optimized MS operating parameters of the analyte are described in Table 1. The source parameters were: gas temperature of 200 $^{\circ}$ C with a gas flow of 16 L/minute, a sheath gas temperature of 300 $^{\circ}$ C with a sheath gas flow of 11 L/minute, a nebuliser pressure of 50 psi and capillary voltage of 3500 V for positive polarity, and a Nozzle Voltage 1000 V. The iFunnel parameters were: high pressure radio frequency (RF) of 150 V and low-pressure RF of 60 V. The LC eluent flow was sprayed into the mass spectrometer interface without splitting. Identification was achieved based on retention time of authentic SCFA standards and by product ions monitor.

4.4. Method Validation

4.4.1. Linearity

Seven authentic standards were spiked in acidified water to construct calibration curves for all compound analysis. The concentrations versus peak area ratio (analyte peak area/internal standard peak area) were plotted to construct the calibration curves.

4.4.2. Sensitivity

Diluted solution of individual analytes was injected to get LOD and LOQ values. LOD was calculated as signal to noise ratio at least three times higher than the baseline noise. LOQ was calculated at a signal to noise ratio 10 times higher than the baseline noise of each compound.

4.4.3. Precision and Accuracy

Intra-day precision and accuracy were calculated by analysis of replicates spiked in acidified water at concentrations of 0.01 (L), 0.5 (M) and 5 (H) mM for all SCFA ($n = 6$ at each level) on the same day. To assess the inter-day precision and accuracy, spiked replicates of the same concentration level ($n = 6$) were analysed on five different days. The relative standard deviation (R.S.D. %) of the replicate analyses was used for precision calculation. Accuracy was calculated by comparison of expected concentrations with the measured concentrations of the spiked samples. A R.S.D. % of 20% was deemed acceptable for both precision and accuracy.

4.4.4. Carry-Over Effect

To assess carry-over effects, water was injected after an injection of the highest concentration of each standard. Agilent 1200 series high performance auto sampler with an injection program was used to minimize carry-over effects.

4.4.5. Recovery and Matrix Effect (or Ion Suppression)

Three different levels (Low: 0.1 mM, Medium: 1 mM and High: 10 mM, $n = 3$) of the seven analytes were added to the in vitro batch fermentation sample to assess recovery. After samples were processed according to Section 4.3 and analysed by the present technique, the recovery was calculated as (final calculated concentration-non spike concentration/added known concentration) $\times 100$.

The recovery of known concentration (1 mM) in six different animal tissues, milk and plasma were assessed by spiking individual analytes and analysed by LC-MS/MS. The above formula was used to calculate the recovery in different matrices.

The matrix effect was calculated by the post-extraction spike method as indicated by RSC guidelines for LC-MS measurements [28]. The endogenous individual analytes are present in different matrices, therefore isotope labelled internal standards were used to assess matrix effects. The same concentrations (0.5 mM except lactate 0.25 mM for all tissues, milk and plasma, 5 mM acetate, 0.25 mM lactate and 0.5 mM others for in vitro batch fermentation sample) of individual compounds (isotope labelled internal standards) were spiked in different extracted matrices and acidified (0.5% ortho-phosphoric acid) The equation (Peak area in water-peak area in matrices/peak area in water) $\times 100$ was used to assess the LC-MS/MS matrix effect for all analytes.

4.5. Data Analysis

Data files were exported and analysed on an Agilent MassHunter Quantitative analysis B.06.00/Build 6.0.388.0 (Agilent Technologies, Santa Clara, CA, USA) The software integrates the peak area for the metabolites which is then exported as an Excel document. The concentration of the SCFAs was calculated using the equation of the standard curve and the peak area ratio (analyte peak area/internal standard peak area) of the SCFA.

5. Conclusions

We have developed a new LC-MS technique for SCFAs analysis that involves less laborious sample preparative steps, does not require sample derivatisation and uses isotopically labelled internal standards to account for matrix effects which allows accurate measurement of SCFAs, BSCFAs and lactate in different biological matrices using LC-MS/MS. The application of this analytical tool to ex vivo and in vitro models will be instrumental in carrying out mechanistic studies to elucidate biological profiles and physiological effects of SCFAs and their related metabolites contributing to our overall understanding of the role of the microbiome in health and disease.

Author Contributions: Conceptualization, S.S. and P.D.-W.; methodology, S.S.; software, S.S.; validation, S.S. and P.D.-W.; formal analysis, S.S.; investigation, S.S., P.D.-W. and E.S.; resources, P.A.K.; data curation, S.S.; writing—original draft preparation, P.D.-W. and S.S.; writing—review and editing, S.S., P.D.-W., E.S. and P.A.K.; visualization, S.S., P.D.-W. and P.A.K.; supervision, P.A.K.; project administration, P.A.K.; funding acquisition, P.A.K. All authors have read and agreed to the published version of the manuscript.

Funding: The author(s) gratefully acknowledge the support of the Biotechnology and Biological Sciences Research Council (BBSRC); This research was funded by the BBSRC Institute Strategic Programme Food Innovation and Health BB/R012512/1 and its constituent projects BBS/E/F/000PR10343, BBS/E/F/000PR10346 and BBS/E/F/000PR10347, The European Union Seventh Framework Programme ([FP7/2007–2013] under grant agreement n° 245121 and Emad Shehata was funded by the Newton-Mosharafa Scholarship Fund from the Egyptian Ministry of Higher Education (Cultural Affairs and Mission sector), the British Council and the British Embassy in Egypt grant number).

Institutional Review Board Statement: The QIB Colon Model Study, was approved by the QIB (formally Institute of Food Re-search) Human Research Governance committee (IFR01/2015), and Lon-don—Westminster Research Ethics Committee (15/LO/2169).

Informed Consent Statement: Informed consent was obtained from all subjects involved in the study.

Data Availability Statement: The data presented in this study are available on request from the corresponding author.

Acknowledgments: We acknowledge Simon Carding and Aimee Parker from the Quadram Institute Bioscience (QIB) for providing mouse brain samples, Naiara Beraza and Sian Seaman also from QIB for providing mouse faecal samples and David Vauzour from the University of East Anglia for his assistance in the animal studies.

Conflicts of Interest: The authors declare no conflict of interest.

Sample Availability: Standards from which the compounds were analysed are available from the stated commercial manufacturers. Biological samples are not available.

References

1. Blaak, E.E.; Canfora, E.E.; Theis, S.; Frost, G.; Groen, A.K.; Mithieux, G.; Nauta, A.; Scott, K.; Stahl, B.; van Harsselaar, J.; et al. Short chain fatty acids in human gut and metabolic health. *Benef Microbes* **2020**, *11*, 411–455. [[CrossRef](#)] [[PubMed](#)]
2. Holmes, Z.C.; Silverman, J.D.; Dressman, H.K.; Wei, Z.; Dallow, E.P.; Armstrong, S.C.; Seed, P.C.; Rawls, J.F.; David, L.A. Short-Chain Fatty Acid Production by Gut Microbiota from Children with Obesity Differs According to Prebiotic Choice and Bacterial Community Composition. *mBio* **2020**, *11*, e00914–20. [[CrossRef](#)] [[PubMed](#)]
3. Silva, Y.P.; Bernardi, A.; Frozza, R.L. The Role of Short-Chain Fatty Acids From Gut Microbiota in Gut-Brain Communication. *Front. Endocrinol.* **2020**, *11*, 25. [[CrossRef](#)] [[PubMed](#)]
4. Brown, C.T.; Davis-Richardson, A.G.; Giongo, A.; Gano, K.A.; Crabb, D.B.; Mukherjee, N.; Casella, G.; Drew, J.C.; Ilonen, J.; Knip, M.; et al. Gut microbiome metagenomics analysis suggests a functional model for the development of autoimmunity for type 1 diabetes. *PLoS ONE* **2011**, *6*, e25792. [[CrossRef](#)] [[PubMed](#)]
5. Koh, A.; De Vadder, F.; Kovatcheva-Datchary, P.; Bäckhed, F. From Dietary Fiber to Host Physiology: Short-Chain Fatty Acids as Key Bacterial Metabolites. *Cell* **2016**, *165*, 1332–1345. [[CrossRef](#)]
6. Saez-Lara, M.J.; Gomez-Llorente, C.; Plaza-Diaz, J.; Gil, A. The role of probiotic lactic acid bacteria and bifidobacteria in the prevention and treatment of inflammatory bowel disease and other related diseases: A systematic review of randomized human clinical trials. *BioMed Res. Int.* **2015**, *2015*, 505878. [[CrossRef](#)]
7. Rios-Covian, D.; González, S.; Nogacka, A.M.; Arboleya, S.; Salazar, N.; Gueimonde, M.; de los Reyes-Gavilán, C.G. An Overview on Fecal Branched Short-Chain Fatty Acids Along Human Life and as Related With Body Mass Index: Associated Dietary and Anthropometric Factors. *Front. Microbiol.* **2020**, *11*, 973. [[CrossRef](#)]
8. Agus, A.; Clément, K.; Sokol, H. Gut microbiota-derived metabolites as central regulators in metabolic disorders. *Gut* **2021**, *70*, 1174–1182. [[CrossRef](#)]
9. Zhang, J.; Zhang, H.; Liu, M.; Lan, Y.; Sun, H.; Mai, K.; Wan, M. Short-Chain Fatty Acids Promote Intracellular Bactericidal Activity in Head Kidney Macrophages From Turbot (*Scophthalmus maximus* L.) via Hypoxia Inducible Factor-1 α . *Front Immunol.* **2020**, *11*, 615536. [[CrossRef](#)] [[PubMed](#)]
10. Parada Venegas, D.; De la Fuente, M.K.; Landskron, G.; González, M.J.; Quera, R.; Dijkstra, G.; Harmsen, H.J.M.; Faber, K.N.; HERNANDEZ, M.A. Short Chain Fatty Acids (SCFAs)-Mediated Gut Epithelial and Immune Regulation and Its Relevance for Inflammatory Bowel Diseases. *Front Immunol.* **2019**, *10*, 277. [[CrossRef](#)] [[PubMed](#)]

11. Carretta, M.D.; Quiroga, J.; López, R.; Hidalgo, M.A.; Burgos, R.A. Participation of Short-Chain Fatty Acids and Their Receptors in Gut Inflammation and Colon Cancer. *Front. Physiol.* **2021**, *12*, 662739. [[CrossRef](#)] [[PubMed](#)]
12. Sun, M.; Wu, W.; Liu, Z.; Cong, Y. Microbiota metabolite short chain fatty acids, GPCR, and inflammatory bowel diseases. *J. Gastroenterol.* **2017**, *52*, 1–8. [[CrossRef](#)] [[PubMed](#)]
13. Primec, M.; Mičetić-Turk, D.; Langerholc, T. Analysis of short-chain fatty acids in human feces: A scoping review. *Anal. Biochem.* **2017**, *526*, 9–21. [[CrossRef](#)]
14. Chai, L.; Luo, Q.; Cai, K.; Wang, K.; Xu, B. Reduced fecal short-chain fatty acids levels and the relationship with gut microbiota in IgA nephropathy. *BMC Nephrol.* **2021**, *22*, 209. [[CrossRef](#)] [[PubMed](#)]
15. Zhao, G.; Nyman, M.; Jönsson, J.A. Rapid determination of short-chain fatty acids in colonic contents and faeces of humans and rats by acidified water-extraction and direct-injection gas chromatography. *Biomed Chromatogr.* **2006**, *20*, 674–682. [[CrossRef](#)] [[PubMed](#)]
16. Kotani, A.; Miyaguchi, Y.; Kohama, M.; Ohtsuka, T.; Shiratori, T.; Kusu, F. Determination of short-chain fatty acids in rat and human feces by high-performance liquid chromatography with electrochemical detection. *Anal. Sci.* **2009**, *25*, 1007–1011. [[CrossRef](#)] [[PubMed](#)]
17. Wang, H.-Y.; Wang, C.; Guo, L.-X.; Zheng, Y.-F.; Hu, W.-H.; Dong, T.T.X.; Wang, T.-J.; Tsim, K.W.K. Simultaneous determination of short-chain fatty acids in human feces by HPLC with ultraviolet detection following chemical derivatization and solid-phase extraction segmental elution. *J. Sep. Sci.* **2019**, *42*, 2500–2509. [[CrossRef](#)] [[PubMed](#)]
18. Tahara, Y.; Yamazaki, M.; Sukigara, H.; Motohashi, H.; Sasaki, H.; Miyakawa, H.; Haraguchi, A.; Ikeda, Y.; Fukuda, S.; Shibata, S. Gut Microbiota-Derived Short Chain Fatty Acids Induce Circadian Clock Entrainment in Mouse Peripheral Tissue. *Sci. Rep.* **2018**, *8*, 1395. [[CrossRef](#)] [[PubMed](#)]
19. Higashi, T.; Ichikawa, T.; Inagaki, S.; Min, J.Z.; Fukushima, T.; Toyo'oka, T. Simple and practical derivatization procedure for enhanced detection of carboxylic acids in liquid chromatography–electrospray ionization–tandem mass spectrometry. *J. Pharm. Biomed. Anal.* **2010**, *52*, 809–818. [[CrossRef](#)]
20. Liebisch, G.; Ecker, J.; Roth, S.; Schweizer, S.; Öttl, V.; Schött, H.F.; Yoon, H.; Haller, D.; Holler, E.; Burkhardt, R.; et al. Quantification of Fecal Short Chain Fatty Acids by Liquid Chromatography Tandem Mass Spectrometry–Investigation of Pre-Analytic Stability. *Biomolecules* **2019**, *9*, 121. [[CrossRef](#)]
21. Song, H.E.; Lee, H.Y.; Kim, S.J.; Back, S.H.; Yoo, H.J. A Facile Profiling Method of Short Chain Fatty Acids Using Liquid Chromatography–Mass Spectrometry. *Metabolites* **2019**, *9*, 173. [[CrossRef](#)] [[PubMed](#)]
22. Mueller, N.T.; Zhang, M.; Juraschek, S.P.; Miller, E.R.; Appel, L.J. Effects of high-fiber diets enriched with carbohydrate, protein, or unsaturated fat on circulating short chain fatty acids: Results from the OmniHeart randomized trial. *Am. J. Clin. Nutr.* **2020**, *111*, 545–554. [[CrossRef](#)] [[PubMed](#)]
23. Sharma, M.; Arora, I.; Stoll, M.L.; Li, Y.; Morrow, C.D.; Barnes, S.; Berryhill, T.F.; Li, S.; Tollefsbol, T.O. Nutritional combinatorial impact on the gut microbiota and plasma short-chain fatty acids levels in the prevention of mammary cancer in Her2/neu estrogen receptor-negative transgenic mice. *PLoS ONE* **2020**, *15*, e0234893. [[CrossRef](#)] [[PubMed](#)]
24. van Eijk, H.M.H.; Bloemen, J.G.; Dejong, C.H.C. Application of liquid chromatography–mass spectrometry to measure short chain fatty acids in blood. *J. Chromatogr. B.* **2009**, *877*, 719–724. [[CrossRef](#)] [[PubMed](#)]
25. Schäpe, S.S.; Krause, J.L.; Engelmänn, B.; Fritz-Wallace, K.; Schattenberg, F.; Liu, Z.; Müller, S.; Jehlich, N.; Rolle-Kampczyk, U.; Herberth, G.; et al. The Simplified Human Intestinal Microbiota (SIHUMix) Shows High Structural and Functional Resistance against Changing Transit Times in In Vitro Bioreactors. *Microorganisms* **2019**, *7*, 641. [[CrossRef](#)] [[PubMed](#)]
26. Calderón-Pérez, L.; Gosálbes, M.J.; Yuste, S.; Valls, R.M.; Pedret, A.; Llauroadó, E.; Jimenez-Hernandez, N.; Artacho, A.; Pla-Pagà, L.; Companys, J.; et al. Gut metagenomic and short chain fatty acids signature in hypertension: A cross-sectional study. *Sci. Rep.* **2020**, *10*, 6436. [[CrossRef](#)] [[PubMed](#)]
27. Stewart, M.A. Porous Graphitic Carbon-Based Metabolomics and Development of an Alternative Biomass-Derived Carbon Stationary Phase. Ph.D. Thesis, University of York, York, UK, 2013.
28. Sargent M. (Ed.) *Guide to Achieving Reliable Quantitative LC-MS Measurements*; RSC Analytical Methods Committee: Cambridge, UK, 2013.
29. van de Merbel, N.C. Quantitative determination of endogenous compounds in biological samples using chromatographic techniques. *TrAC Trends Anal. Chem.* **2008**, *27*, 924–933. [[CrossRef](#)]
30. Bao, X.; Wu, J.; Shuch, B.; LoRusso, P.; Bindra, R.S.; Li, J. Quantitative Profiling of Oncometabolites in Frozen and Formalin-Fixed Paraffin-Embedded Tissue Specimens by Liquid Chromatography Coupled with Tandem Mass Spectrometry. *Sci. Rep.* **2019**, *9*, 11238. [[CrossRef](#)] [[PubMed](#)]
31. Wu, J.; Wiegand, R.; LoRusso, P.; Li, J. A stable isotope-labeled internal standard is essential for correcting for the interindividual variability in the recovery of lapatinib from cancer patient plasma in quantitative LC-MS/MS analysis. *J. Chromatogr. B Anal. Technol. Biomed. Life Sci.* **2013**, *941*, 100–108. [[CrossRef](#)] [[PubMed](#)]
32. Al Kadhi, O.; Melchini, A.; Mithen, R.; Saha, S. Development of a LC-MS/MS Method for the Simultaneous Detection of Tricarboxylic Acid Cycle Intermediates in a Range of Biological Matrices. *J. Anal. Methods Chem.* **2017**, *2017*, 5391832. [[CrossRef](#)]
33. Lotti, C.; Rubert, J.; Fava, F.; Tuohy, K.; Mattivi, F.; Vrhovsek, U. Development of a fast and cost-effective gas chromatography–mass spectrometry method for the quantification of short-chain and medium-chain fatty acids in human biofluids. *Anal. Bioanal. Chem.* **2017**, *409*, 5555–5567. [[CrossRef](#)]

34. Zeng, M.; Cao, H. Fast quantification of short chain fatty acids and ketone bodies by liquid chromatography-tandem mass spectrometry after facile derivatization coupled with liquid-liquid extraction. *J. Chromatogr. B Anal. Technol. Biomed. Life Sci.* **2018**, *1083*, 137–145. [[CrossRef](#)] [[PubMed](#)]
35. Chan, J.C.Y.; Kioh, D.Y.Q.; Yap, G.C.; Lee, B.W.; Chan, E.C.Y. A novel LCMSMS method for quantitative measurement of short-chain fatty acids in human stool derivatized with ¹²C- and ¹³C-labelled aniline. *J. Pharm. Biomed. Anal.* **2017**, *138*, 43–53. [[CrossRef](#)] [[PubMed](#)]
36. Liao, H.Y.; Wang, C.Y.; Lee, C.H.; Kao, H.L.; Wu, W.K.; Kuo, C.H. Development of an Efficient and Sensitive Chemical Derivatization-Based LC-MS/MS Method for Quantifying Gut Microbiota-Derived Metabolites in Human Plasma and Its Application in Studying Cardiovascular Disease. *J. Proteome Res.* **2021**, *20*, 3508–3518. [[CrossRef](#)]
37. Oldendorf, W.H. Carrier-mediated blood-brain barrier transport of short-chain monocarboxylic organic acids. *Am. J. Physiol.* **1973**, *224*, 1450–1453. [[CrossRef](#)]
38. Bachmann, C.; Colombo, J.-P.; Berüter, J. Short chain fatty acids in plasma and brain: Quantitative determination by gas chromatography. *Clin. Chim. Acta* **1979**, *92*, 153–159. [[CrossRef](#)]
39. Cummings, J.H.; Pomare, E.W.; Branch, W.J.; Naylor, C.P.; Macfarlane, G.T. Short chain fatty acids in human large intestine, portal, hepatic and venous blood. *Gut* **1987**, *28*, 1221–1227. [[CrossRef](#)] [[PubMed](#)]
40. De Baere, S.; Eeckhaut, V.; Steppe, M.; De Maesschalck, C.; De Backer, P.; Van Immerseel, F.; Croubels, S. Development of a HPLC–UV method for the quantitative determination of four short-chain fatty acids and lactic acid produced by intestinal bacteria during in vitro fermentation. *J. Pharm. Biomed. Anal.* **2013**, *80*, 107–115. [[CrossRef](#)] [[PubMed](#)]
41. Day-Walsh, P.; Shehata, E.; Saha, S.; Savva, G.M.; Nemeckova, B.; Speranza, J.; Kellingray, L.; Narbad, A.; Kroon, P.A. The use of an in-vitro batch fermentation (human colon) model for investigating mechanisms of TMA production from choline, l-carnitine and related precursors by the human gut microbiota. *Eur. J. Nutr.* **2021**, *60*, 3987–3999. [[CrossRef](#)]
42. Day, P.E.L.; Chambers, K.F.; Winterbone, M.S.; García-Blanco, T.; Vauzour, D.; Kroon, P.A. Validation of control genes and a standardised protocol for quantifying gene expression in the livers of C57BL/6 and ApoE^{−/−} mice. *Sci. Rep.* **2018**, *8*, 8081. [[CrossRef](#)] [[PubMed](#)]
43. García-Villalba, R.; Giménez-Bastida, J.A.; García-Conesa, M.T.; Tomás-Barberán, F.A.; Carlos Espin, J.; Larrosa, M. Alternative method for gas chromatography-mass spectrometry analysis of short-chain fatty acids in faecal samples. *J. Sep. Sci.* **2012**, *35*, 1906–1913. [[CrossRef](#)] [[PubMed](#)]

Appendix 10

Original

**The Use of an *in-vitro* Batch
Fermentation (human colon)
Model for Investigating
Mechanisms of TMA Production
from Choline, L-carnitine and
Related Precursors by the Human
Gut Microbiota**

Appendix 10

European Journal of Nutrition (2021) 60:3987–3999
<https://doi.org/10.1007/s00394-021-02572-6>

ORIGINAL CONTRIBUTION



The use of an *in-vitro* batch fermentation (human colon) model for investigating mechanisms of TMA production from choline, L-carnitine and related precursors by the human gut microbiota

Priscilla Day-Walsh¹ · Emad Shehata^{1,2} · Shikha Saha¹ · George M. Savva¹ · Barbora Nemeckova¹ · Jasmine Speranza^{1,3,4} · Lee Kellingray¹ · Arjan Narbad¹ · Paul A. Kroon¹

Received: 11 February 2021 / Accepted: 19 April 2021 / Published online: 2 May 2021
 © The Author(s) 2021

Abstract

Purpose Plasma trimethylamine-N-oxide (TMAO) levels have been shown to correlate with increased risk of metabolic diseases including cardiovascular diseases. TMAO exposure predominantly occurs as a consequence of gut microbiota-dependent trimethylamine (TMA) production from dietary substrates including choline, carnitine and betaine, which is then converted to TMAO in the liver. Reducing microbial TMA production is likely to be the most effective and sustainable approach to overcoming TMAO burden in humans. Current models for studying microbial TMA production have numerous weaknesses including the cost and length of human studies, differences in TMA(O) metabolism in animal models and the risk of failing to replicate multi-enzyme/multi-strain pathways when using isolated bacterial strains. The purpose of this research was to investigate TMA production from dietary precursors in an *in-vitro* model of the human colon.

Methods TMA production from choline, L-carnitine, betaine and γ -butyrobetaine was studied over 24–48 h using an *in-vitro* human colon model with metabolite quantification performed using LC–MS.

Results Choline was metabolised via the direct choline TMA-lyase route but not the indirect choline–betaine–TMA route, conversion of L-carnitine to TMA was slower than that of choline and involves the formation of the intermediate γ -BB, whereas the Rieske-type monooxygenase/reductase pathway for L-carnitine metabolism to TMA was negligible. The rate of TMA production from precursors was choline > carnitine > betaine > γ -BB. 3,3-Dimethyl-1-butanol (DMB) had no effect on the conversion of choline to TMA.

Conclusion The metabolic routes for microbial TMA production in the colon model are consistent with observations from human studies. Thus, this model is suitable for studying gut microbiota metabolism of TMA and for screening potential therapeutic targets that aim to attenuate TMA production by the gut microbiota.

Trial registration number NCT02653001 (<http://www.clinicaltrials.gov>), registered 12 Jan 2016.

Keywords Phosphatidylcholine · Lecithin · TMAO · Fish odour syndrome · Carnitine · Betaine · γ -Butyrobetaine · Cardiovascular disease · Metabolic disease · Human gut microbiota

Introduction

It is well established that the human gut microbiota produce substrates that are both beneficial and deleterious to health [1–3]. In particular, the metabolism of dietary substrates such as choline and L-carnitine to trimethylamine (TMA) and subsequently to trimethylamine oxide (TMAO) by a hepatic enzyme flavin-containing monooxygenase 3 (FMO3) is of interest due to the strong associations of high circulating TMAO concentrations with the risk of numerous metabolic diseases and the risk of death from heart failure [4–6]. Whether or not TMAO is causally linked to disease

✉ Paul A. Kroon
paul.kroon@quadram.ac.uk

¹ Quadram Institute Bioscience, Norwich Research Park, Norwich NR4 7UQ, UK

² Chemistry of Flavour and Aroma Dept, National Research Centre, 33 El Buhouth St, Giza 12622, Dokki, Egypt

³ Foundation “Prof. Antonio Imbesi”, University of Messina, Piazza Pugliatti 1, 98122 Messina, Italy

⁴ Department of Chemical, Biological, Pharmaceutical and Environmental Sciences, University of Messina, Polo Universitario dell’Annunziata, 98168 Messina, Italy

risk remains contentious, but there is a growing consensus that changes in microbial production of TMA are indicative of alterations in gut microbiota composition and diversity [7–10], i.e. that high levels of circulatory TMAO reflect gut dysbiosis in some way. In addition, because they are essential for methylation processes, lipid membrane generation, lipid metabolism and neurotransmitter production, excessive metabolism of choline and L-carnitine by the gut microbiota may deprive the host of these essential substrates and increase the risk of metabolic diseases such as diabetes, cardiovascular diseases and neurodegenerative diseases [11]. Accordingly, there is considerable interest in developing effective and sustainable interventions that effectively reduce TMA production, and, therefore, host TMAO burden.

The requirement for the gut microbiota in the metabolism of choline to TMA was elegantly demonstrated by Tang et al. who showed that the metabolism of phosphatidylcholine (PC)/lecithin to TMA, and subsequently TMAO, could be suppressed by the administration of broad-spectrum antibiotics, without suppressing the production of choline and betaine [10]. Metagenomic and transcriptomics approaches have played a crucial role in identifying genes, enzymes and pathways that are involved in TMA production [12, 13]. However, the presence of genes in microbial genomes that are predicted to be capable of degrading choline and L-carnitine is not always indicative of functional capacity of the microbe to produce TMA [14, 15]. Consequently, animal, human and *in-vitro* single-strain studies have been employed to functionally characterise the pathways and species involved in the metabolism of choline, L-carnitine, betaine and γ -BB. Of note are the requirement of a glycol radical enzyme choline TMA-lyase (CutC) along with its activating enzyme (CutD) for the metabolism of choline to TMA, [15–17]. The importance of bacterial microcompartments in choline metabolism has also been demonstrated using bacterial pure cultures [18]. In mice, using PC as a substrate, it was reported that TMA can be formed as a result of multiple steps (PC \rightarrow choline \rightarrow betaine \rightarrow TMA), although betaine was a poor substrate for the production of TMAO [19, 20]. Another study incorporating experiments with single bacterial strains, live human faecal microbes and mouse caecal cell lysates provided evidence that the metabolism of choline to TMA could be inhibited by a choline analogue 3,3-dimethyl-1-butanol (DMB) [21]. Nevertheless, in humans it is still unclear which pathways are predominant for the metabolism of choline to TMA. The absolute requirement of the gut microbiota in the metabolism of L-carnitine to TMA has also been demonstrated, in single-strain, animal and human studies [22, 23]. Using a combination of bioinformatics and strain-specific approaches, it was shown that the Rieske-type two component L-carnitine oxygenase/reductases (CntA/Bs) are required for microbial dependent degradation of L-carnitine to TMA [14]. In another report,

it was shown that the concentration of TMAO in plasma peaked 24 h (h) after oral L-carnitine administration [22]. Using both human and animal studies, Koeth et al. provided evidence that γ -BB is an obligate intermediate formed during the metabolism of L-carnitine to TMA with the major site for γ -BB production being the small bowel, proximal to that of TMA production [22].

Here we describe the use of an *in-vitro* batch fermentation model to study the metabolic pathways for TMA production from dietary substrates such as choline, L-carnitine, betaine and γ -BB in humans. This model has been widely used to investigate the microbial metabolism of various other nutrients [24, 25]. We hypothesised that the conversion of these substrates into TMA in a batch model faithfully replicate the findings from previously reported studies of TMA production in human, animal and *in-vitro* studies. In testing the human colon model for this purpose, we anticipate being able to study the human gut microbiota-dependent conversion of these substrates to TMA in more detail, and demonstrate that this model is suitable for studies that seek to find dietary interventions that reduce the production of TMA. Our specific objective was to measure the changes in the concentration of TMA and associated metabolites over an extended period (24 h) in the colon model when incubated with TMA precursors. We also explored whether DMB, which had previously been shown to inhibit TMA production from choline *in-vivo* and in single-strain models [21], would inhibit the metabolism of choline to TMA in the human *in-vitro* colon model. In addition, we investigate whether the conversion of these substrates to TMA could be replicated using a simple anaerobic environment without pH control.

Materials and methods

Materials

Trichloroacetic acid (TCA), heptafluorobutyric acid (HFBA), γ -BB (3-(carboxypropyl)trimethylammonium chloride) and choline chloride-(trimethyl-d9) were purchased from Sigma-Aldrich. All unlabelled methylamines except γ -BB, all solvents unless otherwise stated, acetic acid, and ammonium acetate were purchased from Fisher Scientific Limited. Labelled internal standards [(d9-TMA), d9-TMAO and d9-carnitine] were purchased from Cambridge Isotope Laboratories. Fermanc 260 pH control units were from Electrolab, and Stomacher 400 from Seward. 3,3-Dimethyl-1-butanol (DMB) was purchased from VWR™.

Study design

An *in-vitro* batch fermentation model was used to study the microbial metabolism of choline, betaine, L-carnitine and γ -BB. Faecal samples were obtained from participants recruited onto the QIB Colon Model study. Men and women aged 18 years or older who live/work within 10 miles of the Norwich Research Park were recruited if they satisfied the following criteria: participants who were assessed to have a normal bowel habit, regular defecation between three times a day and three times a week, with an average stool type of 3–5 on the Bristol Stool Chart, and no diagnosed chronic gastrointestinal health problems, such as irritable bowel syndrome, inflammatory bowel disease, or coeliac disease. Participants were asked further questions immediately prior to donating a stool sample to confirm that they had not taken antibiotics or probiotics within the last 4 weeks, had not experienced a gastrointestinal complaint, such as vomiting or diarrhoea, within the last 72 h, were not currently pregnant or breast-feeding, and had not recently had an operation requiring general anaesthetic. The study was approved by the Quadram Institute Bioscience (formally Institute of Food Research) Human Research Governance committee (IFR01/2015), and London—Westminster Research Ethics Committee (15/LO/2169). The informed consent of all participating subjects was obtained, and the trial is registered at <http://www.clinicaltrials.gov> (NCT02653001). Twenty-one fresh human faecal slurry from five different donors were used for choline inoculations. For L-carnitine, betaine and γ -BB inoculations, samples from three donors were used in eight, four and six fermentation experiments, respectively, with each donor being used at least once for each substrate.

Each substrate was added to vessels to give a target concentration of 2000 $\mu\text{mol/L}$. A blank vessel was inoculated with PBS and human faecal slurry. Concentrations of TMA and the related precursors were measured at baseline, then at 2, 4, 6, 8, 10, 12 and 24 h. In three subsequent experiments, 2000 or 10,000 $\mu\text{mol/L}$ DMB was added to vessels treated with choline. Finally, similar substrate concentrations for choline, L-carnitine, betaine, γ -BB were also used for the anaerobic fermentations without pH control.

In-vitro batch fermentations

Batch fermentation *in-vitro* human colon model experiments were carried out as previously described by Parmanand et al. and depicted in supplementary Fig. 1 [24]. All vessels were assembled, sealed and autoclaved before each experiment. Twenty-four h prior to experiments, colon model media (2 g/L each of peptone water, yeast extract and NaHCO_3 , 0.1 g NaCl, 0.04 g/L each of K_2HPO_4 and KH_2PO_4 , 0.01 g each of $\text{MgSO}_4 \cdot 7\text{H}_2\text{O}$, $\text{CaCl}_2 \cdot 6\text{H}_2\text{O}$, 2 ml Tween, 10 g/L D-glucose, 10 μl vitamin

K, 0.5 g/L each of cysteine and bile salts) was added into vessels and continuously supplied with oxygen free nitrogen with continuous stirring throughout the experiment as described by Parmanand et al. [24]. On the day of treatments, a fresh human faecal sample was diluted 1/10 w/v with phosphate buffer and homogenised using a Stomacher 400 for 45 s at 230 RPM to generate the faecal slurries that were used as inocula. Master stocks of 1 M of each of L-carnitine (99+%), choline chloride (99%), betaine hydrochloride (99% extra pure) and γ -BB (technical grade) were prepared in PBS and filter sterilised using 0.22 μm Minisart filters. To achieve a final concentration of 2000 $\mu\text{mol/L}$, 220 μl of the substrate stocks were added separately to vessels containing faecal slurry (final concentration of 1 g stool per 100 mL colon model contents) and made up to a final volume of 110 ml with growth media. Based on a published average of the number of microorganisms in 1 g of wet stool [25], the 1.1 g of stool used in each fermentation vessel is expected to contain an average of 0.96×10^{11} microorganisms. In selected experiments using choline as substrate, DMB was also added to a final concentration of either 2000 or 10,000 $\mu\text{mol/L}$ to estimate the extent to which DMB was able to inhibit TMA formation from choline. pH was maintained at 6.6–7.2 using Fermac 260 pH control units and pumps that automatically added either 1 M HCL or 1 M NaOH when the pH was out of this range. The vessels were maintained at 37 °C using a circulating water jacket. Samples were collected every two hours for 12 h and then at 20 h and 24 h and frozen immediately at -20 °C. It is worth noting that while each substrate stock was generated and added to give an expected final concentration of 2000 $\mu\text{mol/L}$, the concentrations of some substrates measured at the beginning of experiments were materially lower than 2000 $\mu\text{mol/L}$. It was possible that this was due to complexing of the substrates with faecal components (e.g., fibre/undigested food) such that they were lost in the pellet after the centrifugation step to clarify samples before analysis. Quantification of the substrates in PBS alone gave concentration estimates for betaine and L-carnitine that were approximately 2000 $\mu\text{mol/L}$, and 1611 and 1685 $\mu\text{mol/L}$ for γ -BB and choline, respectively. It was shown that the choline was contaminated with TMA, and that the sum of choline plus TMA gave a total concentration of approximately 2000 $\mu\text{mol/L}$. The γ -BB used was technical grade, and although it was not contaminated with TMA, it was presumably contaminated with one or more unknown substances. This is further clarified in Table 1 where the concentrations listed in column 4 ('Measured in PBS') are the best estimates of the total concentration of each substrate in the experiments and the concentrations listed in column 3 ('Measured in 1% faecal matrix') likely best reflect the available (in solution) concentrations.

Table 1 Analysis of TMA substrates and TMA in the complete colon model matrix and in PBS

Substrate	Theoretical conc ^a (μmol/L)	Measured in 1% faecal matrix (μmol/L)	Measured in PBS (μmol/L)	Measured TMA conc ^a (μmol/L)	Sum of substrate (PBS)+TMA (μmol/L)
Blank	0	n.d	n.d	n.d	0
Choline	2000	1742	1685	234	1919
Betaine	2000	1883	1936	n.d	1936
L-Carnitine	2000	1658	2087	n.d	2087
γ-BB	2000	1536	1611	n.d	1611

The concentrations of the substrates that had been supplemented to achieve a 2000 μmol/L concentration in a 1% faecal slurry in colon model media (colon model starting conditions) were lower than expected (column 3). This was not due to the matrix affecting the quantification as standard curves were matrix-matched. Since this effect may have been due to binding of substrates to matrix components (e.g., fibre from the faecal sample), we also measured the substrate concentrations in PBS which gave modestly higher estimates for betaine and γ-BB and a significantly higher estimate for L-carnitine (2087 versus 1658 mol/L; column 4). A significant concentration of TMA was observed in the choline supplemented samples but not in any of the samples supplemented with the other substrates (column 5); this was a consistent observation across different batches of choline. Together, these observations show that (i) the supplementations with betaine and L-carnitine were within 4% of the target concentration of 2000 μmol/L, (ii) that a significant proportion (~20%) of the L-carnitine was not in the aqueous phase and may not be available for metabolism by the gut microbiota, (iii) that supplementations with choline achieved concentrations of about 1750 μmol/L and were contaminated with TMA that roughly accounted for the 'missing' choline, and (iv) γ-BB supplementations only achieved concentrations around 1600 μmol/L, presumably due to contamination of the purchased γ-BB material

Metabolite quantification using LC–MS/MS

Serial dilutions of all metabolites were prepared in 1% filtered faecal slurry to match the matrix of the samples for the calibration curves. Prior to analysis, samples were filtered and 5 μl of sample was mixed with 25 μl of 50% trichloroacetic acid (TCA) and kept at 4 °C for 5 min for deproteinisation. 70 μl of isotopically labelled internal standards (d9-choline, d9-TMA, d9-TMAO and d9-carnitine) prepared in 0.2 M acetic acid were added to the samples and the serially diluted standards, and microcentrifuged at maximum speed for 5 min. 5 μl of the mixture was transferred to chromatography vials containing 95 μl milliQ water for analysis with LC–MS/MS (Agilent Technologies, USA). Briefly, Mobile phase A contained 10 mM ammonium acetate and 0.05% heptafluorobutyric acid (HFBA) in water while mobile phase B consisted of 10 mM ammonium acetate, 0.05% HFBA in 90% methanol. The gradient was started with 0.2 ml/min flow from 2% mobile phase B which was increased by 10% within 1.54 min and after washing for 4 min, equilibration was for another 2.5 min. The total run was 8 min. The separation was carried out on Waters C8 (100 X2.1 mm, 1.7 μm) column and temperature was kept at 35 °C. The 6490 MS/MS system equipped with an electrospray ionization (ESI) source operated in positive-ion detection mode was used. Nebulisation, desolvation and collision was carried out using nitrogen gas and multiple-reaction monitoring (MRMs) mode was used with an Agilent optimizer software to optimise ion and energy collision. A gas flow

of 12 L/min with gas temperature of 200 °C were used along with the temperature of 300 °C and flow rate of 11 L/min for sheath gas. 50 psi, 3500, 1000 V, were used for nebuliser pressure, capillary voltage and nozzle voltage, respectively. The iFunnel radio frequencies (RF) were 150 V RF for high pressure and 60 V for low pressure RF. The flow of LC eluent was sprayed into MS interface without splitting. Retention times and MRM transition (precursor/product) ions were used to identify and quantify the metabolites (Table 2). Sample peak area/isotopically labelled internal standards peak area ratios were used to calculate concentrations using standard curves.

Table 2 Retention times and target ion masses for metabolite identification and quantification using LC–MS/MS

Compound	Retention time (min)	Precursor ion (m/z)	Product ion (m/z)
Betaine	0.84	118.2	58.1
L-Carnitine	0.95	162.2	43.1
D9-L-Carnitine	0.93	171.2	43.1
Choline	1.59	104.2	45.1
D9-Choline	1.59	113.8	49.2
TMA	1.70	60.6	44.1
D9-TMA	1.68	69.4	49.2
TMAO	1.43	76.1	58.1
D9-TMAO	1.45	85.2	66.1
γ-BB	1.12	146.2	86.9

Statistical analysis

To assess whether choline, betaine, L-carnitine and γ -BB are all metabolised to TMA in the multi-species batch fermentation human *in-vitro* colon model, we compared the increase in the concentrations of TMA over 24 h to the increase in the untreated 'Blank' fermentations. To account for within-sample correlation in outcomes, and the observation that standard deviation of TMA concentration was proportional to the mean values in each condition, a linear weighted mixed model was used to estimate the differences between production from different substrates, with regression weights set to a power of the residual variance. A random effect of substrate for groups defined by sample was included in the model. The average marginal effect of adding each substrate on TMA produced was estimated, as well as all pairwise differences between substrates. The packages nlme (version 3.1–139) and emmeans (version 1.3.4) in R statistical software (version 3.6.1) were used to perform the statistical analysis [26–28]. All trajectories of metabolite levels over time periods under each treatment condition, and the difference in choline metabolism without DMB or with 2 or 10 mM/L DMB are described graphically, both as means within treatment groups and for each fermentation individually.

Results

Significant production of TMA from choline, L-carnitine and γ -BB but limited production from betaine

The change in TMA concentration after incubation of the human faecal inoculum with each substrate was assessed after 24 h, and the data are presented in Fig. 1 and Supplementary Table I. Differences in production between substrates with confidence intervals are shown in Supplementary Table 1. Average TMA increased between 0 and 24 h for all treatments, including the blank. Large variations were observed in TMA production in different experiments (Supplementary Fig. 2, 3).

TMA produced after 24 h from choline is consistently greater and was on average significantly higher than that produced from other substrates (Fig. 2 and Supplementary Table 1). TMA produced from betaine was low in all cases. At 24 h, TMA from L-carnitine and γ -BB was highly variable across experiments, ranging between 0 and 1000 $\mu\text{mol/L}$, with no differences in average production between the two (Fig. 2 and Supplementary Table 1).

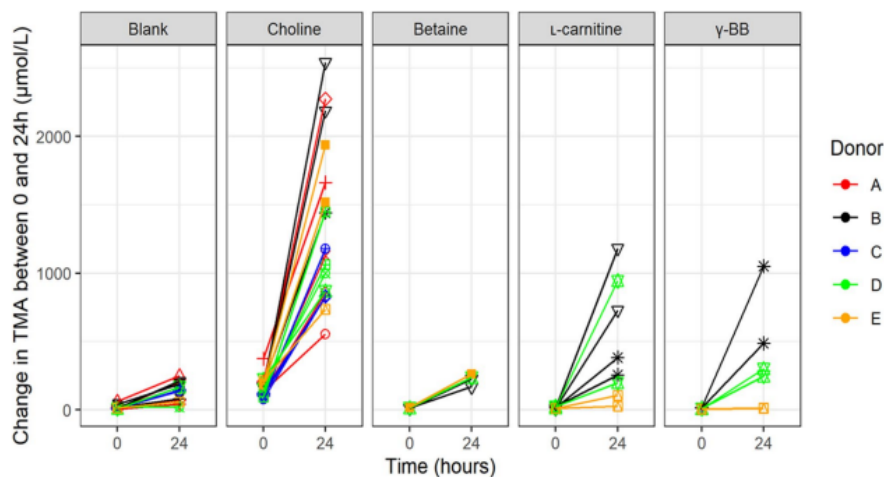


Fig. 1 Change in TMA between 0 and 24 h in each batch fermentation seeded with faecal samples of five different donors. Fermentation stratified by substrate added. Colours correspond to donors and marker shapes to individual experiments. There is a high intra-class

correlation between replicate fermentations within experiments, but little intra-class correlation within donors beyond this. Variation in the levels of TMA produced across experiments is high for each substrate, despite similar levels of substrate being utilised

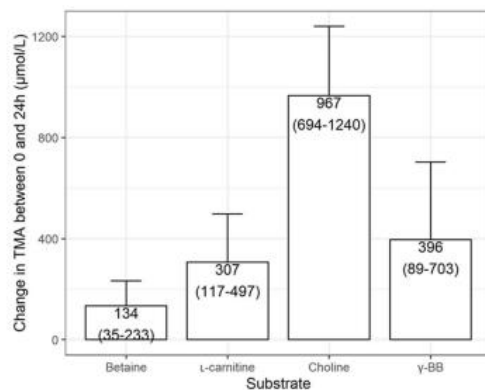


Fig. 2 Estimated mean TMA produced from each substrate over 24 h. Estimates were obtained by mixed effects regression models of the difference between TMA concentration at 0 and 24 h (as described in the statistical methods). The effect of each substrate is calculated with correction for the production of TMA observed in blank vessel without added substrates. Error bars represent 95% confidence intervals

Metabolic pathways for individual substrates

The trajectories for substrate metabolism and TMA production varied between treatments. Figure 3 shows the average trajectory of each measured metabolite over time under each treatment condition. Trajectories in individual fermentations are shown in Supplementary Fig. 4. In the blank, an increase in TMA was observed at 20 and 24 h (Fig. 3a).

The direct choline TMA-lyase pathway is the predominant route of colonic TMA production from choline with little or no contribution from the betaine aldehyde-choline dehydrogenase-betaine reductase pathway

In the choline inoculated fermentations, the concentration of choline started to decline between 6 and 8 h and continued to do so until 24 h by which time it was almost completely utilised in all experiments (Fig. 3b). TMA levels started to increase from the baseline concentration between 6 and 8 h which corresponded with the decrease in baseline levels of choline. It is possible that betaine could be an intermediate in the metabolism of choline to TMA which in theory can occur via the aldehyde/choline dehydrogenase /betaine reductase pathway. However, we

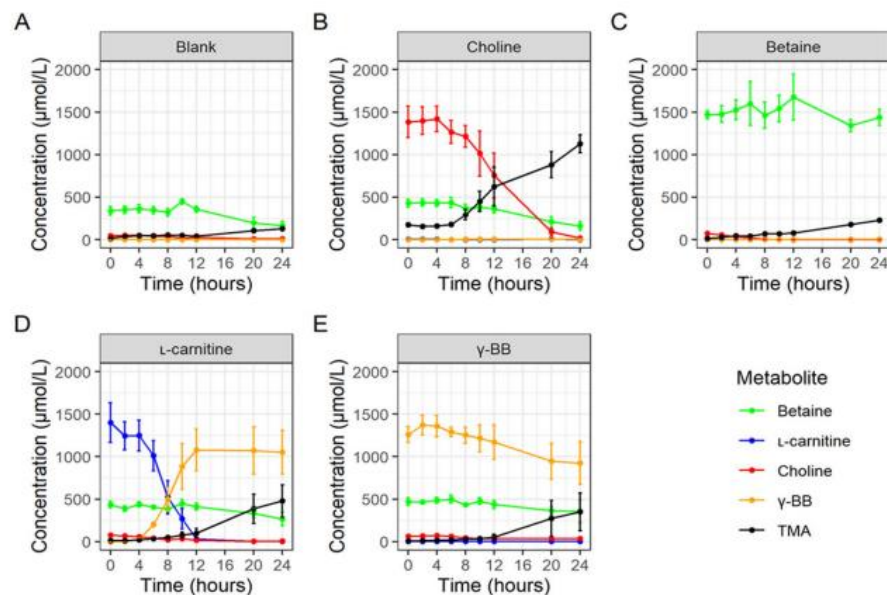


Fig. 3 The average trajectory of all metabolites. With no added substrate (a) and following supplementation with each substrate (b–e). Error bars represent standard errors

did not observe a significant decrease in betaine values when it was used as the substrate (Fig. 3c). However, we did observe modest increases in the concentrations of TMA in betaine-supplemented incubations, and although some of this could be accounted for by reductions in the concentrations of choline and other substrates present in the baseline samples, the final concentration of TMA was significantly higher than observed in the blank incubations, suggesting that some of this TMA may have come from the metabolism of betaine. Additional evidence that there was at least a slow production of TMA from betaine was the observation that background betaine concentrations declined slowly across 24 h in all the non-betaine-supplemented incubations (Fig. 3a, b, d, e). It is also interesting to note that the absolute concentration of betaine in baseline samples, which originates from the faecal inoculum, was substantial (almost 500 $\mu\text{mol/L}$), which is consistent with a very slow rate of conversion of betaine to TMA and, therefore, the accumulation of unmetabolized betaine in the human colon. Overall, and taken together with the observation here that appearance of TMA closely mirrored the disappearance of choline, the data presented do not support the notion that the indirect pathway via betaine is a significant route of TMA production from choline by human gut microbiota.

The metabolism of L-carnitine to TMA requires the γ -butyrobetainyl-CoA:carnitine CoA transferase-carnitine TMA-lyase pathway with formation of γ -BB as an intermediate and does not occur via the Rieske-type monooxygenase or the L-carnitine dehydrogenase pathway

In the L-carnitine supplemented fermentations, the concentration of L-carnitine declined steadily from 6 h until 12 h, by which time it was no longer detectable (Fig. 3d), whilst only a minimal increase in the concentration of TMA was observed during this time. However, there were substantial increases in γ -BB concentrations up to and peaking at 12 h, and these closely corresponded with the disappearance of L-carnitine. Taken together, the observations that (i) the choline observed at baseline also declined from 6 h, (ii) at no timepoint did the concentration of betaine increase and (iii) the concentration of betaine was lower at 24 h than at 0 h, all support the notion that little if any betaine is formed from L-carnitine by the human gut microbiota (Supplementary Fig. 4). Therefore, the production of TMA from carnitine likely occurs via the γ -butyrobetainyl-CoA:carnitine CoA transferase-carnitine TMA-lyase pathway with the formation of γ -BB as an intermediate.

γ -BB is metabolised to TMA but not to L-carnitine, and at a slower rate than the conversion of choline to TMA

In the γ -BB-supplemented fermentations, the concentration of γ -BB declined slowly and by only approximately one third (equivalent to $\sim 450 \mu\text{mol/L}$) after 24 h, following a 6–8 h lag phase (Fig. 3e). A minimal increase in TMA concentrations were observed across 0–8 h and then increased moderately up to 24 h, reaching a concentration similar to the loss of γ -BB (Fig. 3e). L-carnitine concentrations did not change over the 24 h period. Similar to that observed with choline, the background choline in γ -BB-supplemented fermentations declined after a lag of around 8–10 h (Supplementary Fig. 4). These observations are consistent with TMA being produced directly from γ -BB (albeit rather slowly) and not via L-carnitine as an intermediate.

The concentrations of TMA from L-carnitine and γ -BB inoculated fermentations were also measured at 48 h in a single experiment with two replicates per treatment (Supplementary Fig. 5). In the L-carnitine supplemented fermentations, production of TMA increased further between 24 and 48 h to a final concentration of 1541 $\mu\text{mol/L}$, which corresponded to 93 mol% of the starting concentration of available L-carnitine (1658 $\mu\text{mol/L}$, Table 1). In the γ -BB-supplemented fermentations, the concentration of TMA reached 1311 $\mu\text{mol/L}$ at 28 h, accounting for 85 mol% of available γ -BB (1536 $\mu\text{mol/L}$, Table 1). These observations demonstrate that the rate of production of TMA from choline > carnitine > γ -BB, which is reflected in the concentrations of TMA at 24 h, but that given longer incubation (e.g., 48 h) there is almost complete transformation of all three substrates.

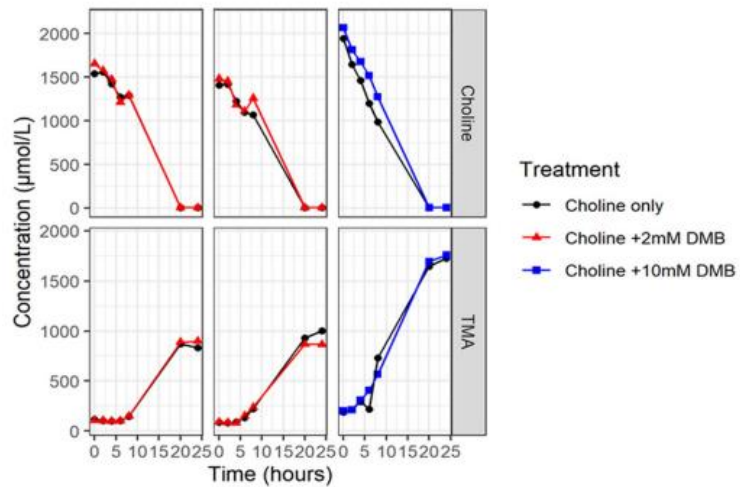
No evidence of inhibition of choline metabolism to TMA by dimethyl-1-butanol (DMB)

DMB has been reported to be an effective inhibitor of TMA production from choline; it has been tested on the basis that it is a structural analogue of choline and this is the basis of its mode of action, i.e., as an inhibitor of microbial choline TMA-lyases (cutC/cutD). Figure 4 illustrates the effects of DMB on choline metabolism. Neither the 2 mM nor the 10 mM DMB concentrations influenced choline metabolism and TMA production at any timepoint compared to choline alone. These data show that even high concentrations of DMB are not effective at inhibiting production of TMA from choline in this faecal-inoculated model of the human colon.

pH control is required TMA production in batch fermentation of human colon models

We also examined the potential conversion of the various TMA precursors using stirred vials in anaerobic cabinets

Fig. 4 The effects of DMB on TMA production from choline in three independent experiments. The graph is stratified by experiment to enable a direct comparison between paired fermentations with and without DMB added. There was no effect of adding DMB on TMA production or choline concentration at any stage over the time period tested

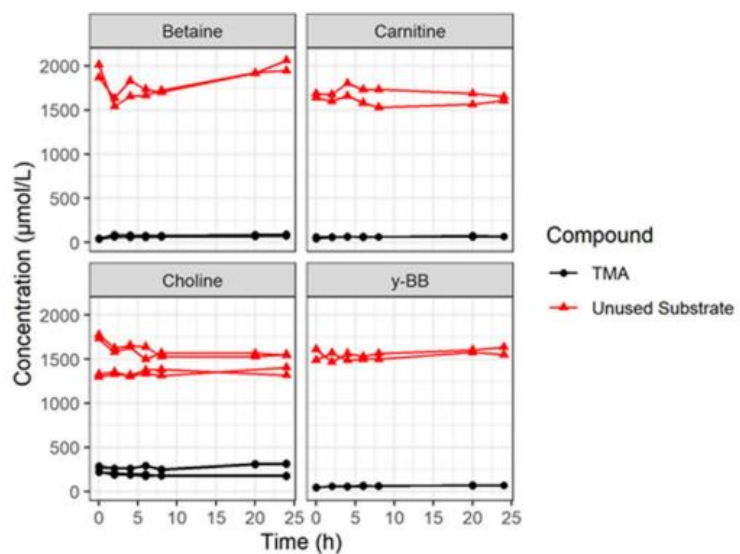


in which the fermentations proceed without pH control. Under this condition neither choline, L-carnitine, betaine or γ -BB declined over time and there was no increase in TMA, clearly showing that none of the substrates were metabolised to produce TMA (Fig. 5). This contrasts with reports for cultures of single-strain bacteria and human faecal bacterial cell isolates where in incubations without pH control, these substrates were reported to be metabolised to TMA [22].

Discussion

The overall aim of the research reported here was to investigate the metabolism of choline, L-carnitine, betaine and γ -BB to TMA in an *in-vitro* batch fermentation model, and in doing so determine how closely the model replicates the production of TMA that has been previously reported in humans. The main findings were that (i) TMA was produced from all three dietary precursors, as well as from the

Fig. 5 The fermentation of TMA substrates under anaerobic conditions without pH control. There was no fermentation of any of the substrate and no TMA production in anaerobic conditions without pH control, although only a few experiments were carried out ($n=3$ for choline and 2 for betaine, L-carnitine and γ -BB)



metabolic intermediate γ -BB, (ii) that the relative rates of production of TMA from the substrates was choline > carnitine > γ -BB > betaine, (iii) that all the previously described metabolic routes to TMA production reported in humans were replicated in this *in-vitro* pH-controlled batch colon model and (iv) that no metabolism to TMA occurred from any substrate when fermentations were performed in the absence of pH control.

Unlike in mice, we show that betaine in humans is not formed as an intermediate of choline to TMA metabolism. Instead, almost all choline is metabolised via the direct choline to TMA route, potentially involving the choline TMA-lyases, suggesting that it is the predominant route. There was minimal TMA production in the betaine inoculations and very little betaine disappearance, indicating that in humans the contribution of betaine to TMA production is minimal if at all. Interestingly, background betaine also declined in the inoculations where choline, and L-carnitine were used as substrates. This may suggest that betaine metabolism requires bacteria or enzymes involved in the metabolism of choline, L-carnitine, and γ -BB, i.e., that are only induced in response to available substrates.

In line with others, we demonstrate that the metabolism of L-carnitine to TMA involves the formation of γ -BB as an intermediate and that the Rieske-type carnitine oxygenase/reductase pathways are not involved in this metabolism by human colonic microbiota [22].

We further demonstrate that while the metabolism of choline to TMA is fast, the production of TMA from L-carnitine is much slower. We provide evidence that this is due to the requirement for γ -BB to be formed as an intermediate. More specifically, we have shown that the rate of conversion of γ -BB to TMA is very slow (Fig. 3e), and this is consistent with our observation of significant accumulation of γ -BB in carnitine supplemented fermentations (Fig. 3d), i.e., the very slow rate of conversion of γ -BB to TMA is rate-limiting in carnitine conversion. Nevertheless, if given sufficient time for complete conversion (24 h for choline and 48 h for L-carnitine), similar levels of TMA were achieved. In a review by Fennema et al. it was proposed that betaine may be formed as an intermediate of L-carnitine by L-carnitine dehydrogenase and metabolised further by betaine reductase to form TMA [29], but this was not observed in the model used here.

After inoculation, the concentration of choline started to decline at 6 h, and in most cases it had completely disappeared within 20 h. Increases in TMA concentrations started after 6 h and coincided with the timepoint at which choline concentrations started to decline, strongly suggesting that TMA was directly synthesised from choline. Betaine has been proposed as a possible intermediate in the metabolism of choline to TMA in mice [19–21, 29, 30]. However, at no time-point did we detect betaine in choline supplemented fermentations. Since the rate of production of TMA from

betaine was slow relative to the rate of production of TMA from choline (Fig. 3b, c, respectively), these data are in keeping with the notion that all the TMA produced in choline supplemented fermentations is a result of direct conversion via a single enzyme-catalysed step, i.e., via the choline TMA-lyase (CutC/CutD).

As in all experiments where choline was not supplemented as a substrate, background choline declined significantly, we can postulate that some of the TMA may have originated from choline and some from the metabolism of betaine via the glycine betaine transmethylase and then to TMA by decarboxylation. However, we did not measure the concentration of dimethylglycine in this study. Further studies using isotopically labelled betaine would be required to ascertain this. As the expression of CutC/D enzymes has been demonstrated in 100% of all people examined, while between 6 and 21% of people are estimated to lack the betaine metabolising *grdH* enzymes, it is possible faecal samples from participants involved in our study lacked the *grdH* enzymes [31, 32].

Interestingly, although there were high intra-class correlation in TMA production between replicates within the same experiment there were no such correlations with respect to different stool samples from the same donors. This indicates that the capacity to produce TMA in faecal samples collected from the same donor on different days was variable. This is consistent with previous reports that have shown there is high intra-individual variation in plasma TMAO levels over a 1–2 year period, although the source of these variations is not clear and warrants further investigation [33–35]. Nevertheless, future human studies investigating the impact of interventions aimed at reducing TMA production will need to take these variabilities into account by multiple sampling over a period of time and using stable isotopes where necessary.

We sought to replicate previous studies to determine whether DMB could also inhibit the metabolism of choline to TMA in the *in-vitro* batch fermentation model. We were unable to show inhibition of choline metabolism to TMA by DMB at 2 and 10 mM. This shows that investigating TMA precursors in the context of complex bacterial mixtures is crucial as only a fraction of bacterial strains may be inhibited by DMB [21]. Wang et al. further demonstrated that DMB administered orally, but not subcutaneously, was effective at reducing TMAO production from choline indicating that this is a gut microbial dependent inhibition [21]. These discrepancies could be due to differences in the microbiota composition between humans and animals.

In the fermentations with L-carnitine we demonstrate the disappearance of L-carnitine from 6 h after the start of the fermentations, which did not correspond with the observed increase in TMA concentration. However, the disappearance of L-carnitine corresponded with the appearance of γ -BB at

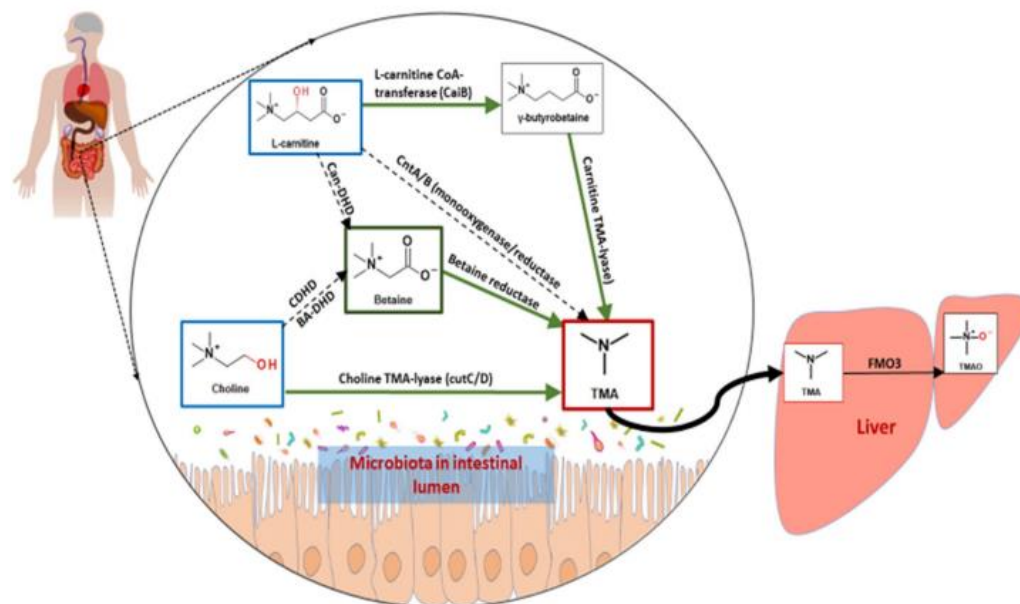


Fig. 6 Pathways for the metabolism of choline, betaine, L-carnitine and γ -BB by human gut microbiota. This is based on data reported here and previously by others [5, 10, 12, 19–22, 32]. In humans, choline is metabolised to TMA via the choline TMA-lyase pathway, betaine is not formed as an intermediate of choline to produce TMA via the choline dehydrogenase (CHDH)/betaine aldehyde dehydrogenase (BADH) > betaine reductase pathway, nor is it formed as an intermediate of L-carnitine via the L-carnitine dehydrogenase pathway. There is no direct conversion of L-carnitine to TMA via the Rieske-type C L-carnitine oxygenase/reductase pathway,

instead L-carnitine is first converted to γ -BB by γ -butyrobetainyl-CoA:carnitine CoA transferases which is then converted to TMA by the L-carnitine TMA lyases. It is possible that betaine may be converted to dimethylglycine by glycine betaine trimethylase and then to TMA by decarboxylation although the evidence for this is weak. Dashed black lines are pathways shown not to be functional in this model; solid green lines indicate pathways we have demonstrated to be important for TMA production in the *in-vitro* human colonic fermentation model

8 h which peaked and plateaued at 12 h and slowly disappeared at 20–24 h, corresponding with TMA production. These observations confirm previous findings in animal and human studies showing that the formation of γ -BB as an intermediate of L-carnitine was obligatory for the formation of TMA. We further confirmed the direct metabolism of γ -BB to TMA by carrying out fermentations in the presence of γ -BB substrate, and we show metabolic dynamics similar to choline where the disappearance of γ -BB corresponds with the appearance of TMA, albeit at a far lower rate in comparison to choline at 24 h. In contrast to the proposed pathway of TMA formation from γ -BB via L-carnitine, where γ -BB may be metabolised to L-carnitine by γ -BB hydroxylase, which is subsequently metabolised to TMA by the Rieske-type carnitine reductase/oxidase, there was no significant formation of TMA production at 8 and 12 h when L-carnitine was completely used up [14, 29]. In addition, at no point did we observe an increase in L-carnitine

in the γ -BB fermentations. This once again highlights the need to study microbial functions in the context of the complex microbiota. These observations complement studies by Koeth et al. and Rath et al. who demonstrated that only a small proportion of individual's stool samples expressed L-carnitine oxygenase CntA/B and that their function is dependent on the availability of molecular oxygen [12, 22].

The fact that there was no direct conversion of L-carnitine to TMA demonstrates that the model used here was strictly anaerobic. Our observations regarding TMA production from L-carnitine and choline were in close agreement with previous reports from studies carried out in humans and serve to validate the utility of this model for investigating mechanisms of TMA production in the human colon. Based on the data obtained using this model, we have provided a schematic that shows which metabolic pathways are important for TMA metabolism in humans, and which are not (Fig. 6). We further show that the results generated using

the *in-vitro* colon model could not be replicated using the non-pH controlled anaerobic fermentations where none of the substrates declined over time and there was no increase in TMA. This is in contrast to other studies that have used anaerobic fermentations without pH control and have demonstrated choline and L-carnitine metabolism to TMA [15, 16, 18, 21]. In the absence of complex microbiota mixtures, pure cultures may indeed be able to metabolise choline to TMA without pH control, although where a mixture of microbiota is present, other bacteria may outcompete TMA-producing bacteria. Thus, anaerobic fermentations without pH control are not suitable for investigating the mechanisms involved in the production of TMA from its dietary precursors when using multi-species bacterial mixtures, including human faecal samples.

Conclusion

Using the pH controlled *in-vitro* batch fermentation human colon model, we show that in humans, the choline TMA-lyase pathway is the major pathway for the production of TMA from choline. Unlike in mice, betaine is not formed as an intermediate of choline for the production of TMA, nor is betaine produced as an intermediate of L-carnitine to produce TMA, although very small quantities of TMA may be produced from betaine. Complementing previously reported data from human and animal studies we show that γ -BB is an intermediate for the metabolism of L-carnitine to TMA. We could not show the direct metabolism of L-carnitine to TMA via the Rieske-type carnitine oxygenase/reductase pathway. While strain-specific models are important for identifying bacterial species and compartments for the production of TMA from its dietary precursors, they must always be accompanied by models which include complex microbiota mixtures similar to those found in the human gut and under pH regulation. This model offers an invaluable tool for increasing our understanding of the metabolic pathways of TMA production including identifying further microorganisms that are involved in TMA production and metabolism, such as Archaea. We envisage that this model will also be useful for studies aiming to identify potential dietary or pharmacological inhibitors of TMA production in the human gut.

Strengths and limitations

One strength of this study is that we were able to use a validated human colon model to investigate the metabolism of TMA precursors separately and investigate their microbial dependent degradation in the presence of complex microbiota species and independent of host enzymes that may also degrade some of these TMA precursors. Another is that the

results presented here are consistent with those reported previously from *in-vivo* studies using human participants and animals, with the exception of betaine, which we show is not an intermediate in the metabolism of choline and L-carnitine. A weakness of this research is that the colon model only reflects conditions in the colon, and our observations may not reflect transformations that potentially occur in the upper gut, particularly the ileum, where the structure of the bacterial communities differ. However, the consistency of our observations with those from animal and human intervention studies suggests that it is an excellent model for studying TMA production in the human colon.

Supplementary Information The online version contains supplementary material available at <https://doi.org/10.1007/s00394-021-02572-6>.

Author's contributions PD contributed to experimental design, carried out the experimental work, data analysis and interpretation and wrote the manuscript, ES contributed to experimental design and experimental work, SS developed the LC-MS/MS methodology and assisted in metabolite analysis, GS carried out statistical data analysis and contributed to manuscript writing, BN contributed to experimental work, JS contributed to experimental work and PK provided original ideas and contributed to experimental design, data interpretation, and the writing of the manuscript.

Funding This research was funded by the Biotechnology and Biological Sciences Research Council (UK) through the Institute Strategic Programme Grants 'Food and Health' (Grant No. BB/J004545/1) and 'Food Innovation and Health' (Grant No. BB/R012512/1 and its constituent projects BBS/E/F/000PR10343, BBS/E/F/000PR10346 and BBS/E/F/000PR10347) to the Quadram Institute Bioscience. Emad Shehata was funded by the Newton-Mosharafa Scholarship Fund from the Egyptian Ministry of Higher Education (Cultural Affairs and Mission sector), the British Council and the British Embassy in Egypt. GS is supported by the BBSRC Core Capability Grant BB/CCG1860/1.

Declarations

Conflict of interest None of the authors declared a conflict of interest.

Open Access This article is licensed under a Creative Commons Attribution 4.0 International License, which permits use, sharing, adaptation, distribution and reproduction in any medium or format, as long as you give appropriate credit to the original author(s) and the source, provide a link to the Creative Commons licence, and indicate if changes were made. The images or other third party material in this article are included in the article's Creative Commons licence, unless indicated otherwise in a credit line to the material. If material is not included in the article's Creative Commons licence and your intended use is not permitted by statutory regulation or exceeds the permitted use, you will need to obtain permission directly from the copyright holder. To view a copy of this licence, visit <http://creativecommons.org/licenses/by/4.0/>.

References

1. Backhed F, Ding H, Wang T, Hooper LV, Koh GY, Nagy A, Semenkovich CF, Gordon JI (2004) The gut microbiota as an

- environmental factor that regulates fat storage. *Proc Natl Acad Sci U S A* 101:15718–15723. <https://doi.org/10.1073/pnas.0407076101>
2. Pedersen HK, Gudmundsdottir V, Nielsen HB, Hyötyläinen T, Nielsen T, Jensen BAH, Forslund K, Hildebrand F, Prifti E, Falony G, Le Chatelier E, Levenez F, Doré J, Mattila I, Plichta DR, Pöhö P, Helligren LI, Arumugam M, Sunagawa S, Vieira-Silva S, Jørgensen T, Holm JB, Tröšt K, Kristiansen K, Brix S, Raes J, Wang J, Haasen T, Bork P, Brunak S, Oresic M, Ehrlich SD, Pedersen O, Consortium M (2016) Human gut microbes impact host serum metabolome and insulin sensitivity. *Nature* 535:376–381. <https://doi.org/10.1038/nature18646>
 3. Chang Y, Chen Y, Zhou Q, Wang C, Chen L, Di W, Zhang Y (2020) Short-chain fatty acids accompanying changes in the gut microbiome contribute to the development of hypertension in patients with preeclampsia. *Clin Sci (Lond)* 134:289–302. <https://doi.org/10.1042/cs20191253>
 4. Suzuki T, Yazaki Y, Voors AA, Jones DJL, Chan DCS, Anker SD, Cleland JG, Dickstein K, Filippatos G, Hillege HL, Lang CC, Ponikowski P, Samani NJ, van Veldhuisen DJ, Zannad F, Zwinderman AH, Metra M, Ng LL (2019) Association with outcomes and response to treatment of trimethylamine N-oxide in heart failure: results from BIOSTAT-CHF. *Eur J Heart Fail* 21:877–886. <https://doi.org/10.1002/ehfj.1338>
 5. Tang WH, Wang Z, Kennedy DJ, Wu Y, Buffa JA, Agatista-Boyle B, Li XS, Levison BS, Hazen SL (2015) Gut microbiota-dependent trimethylamine N-oxide (TMAO) pathway contributes to both development of renal insufficiency and mortality risk in chronic kidney disease. *Circ Res* 116:448–455. <https://doi.org/10.1161/circresaha.116.305360>
 6. Reiner MF, Müller D, Gobatto S, Stalder O, Limacher A, Bonetti NR, Pasvèrk L, Mean M, Rodondi N, Aujesky D, Angelillo-Scherer A, Matter CM, Luscher TF, Camici GG, von Eckardstein A, Beer JH (2019) Gut microbiota-dependent trimethylamine-N-oxide (TMAO) shows a U-shaped association with mortality but not with recurrent venous thromboembolism. *Thromb Res* 174:40–47. <https://doi.org/10.1016/j.thromres.2018.12.011>
 7. Collins HL, Drazul-Schrader D, Sulpizio AC, Koster PD, Williams Y, Adelman SJ, Owen K, Sanli T, Bellamine A (2016) L-Carnitine intake and high trimethylamine N-oxide plasma levels correlate with low aortic lesions in ApoE(-/-) transgenic mice expressing CETP. *Atherosclerosis* 244:29–37. <https://doi.org/10.1016/j.atherosclerosis.2015.10.108>
 8. Nowinski A, Ufnal M (2018) Trimethylamine N-oxide: a harmful, protective or diagnostic marker in lifestyle diseases? *Nutrition* 46:7–12. <https://doi.org/10.1016/j.nut.2017.08.001>
 9. Narath SH, Mautner SI, Svehlikova E, Schultes B, Pieber TR, Sinner FM, Gander E, Libiseller G, Schimek MG, Sourij H, Magnes C (2016) An untargeted metabolomics approach to characterize short-term and long-term metabolic changes after bariatric surgery. *PLoS One* 11:e0161425. <https://doi.org/10.1371/journal.pone.0161425>
 10. Tang WHW, Wang ZE, Levison BS, Koeth RA, Britt EB, Fu XM, Wu YP, Hazen SL (2013) Intestinal microbial metabolism of phosphatidylcholine and cardiovascular risk. *New Engl J Med* 368:1575–1584. <https://doi.org/10.1056/nejmoa1109400>
 11. Janeiro MH, Ramirez MJ, Milagro FI, Martinez JA, Solas M (2018) Implication of Trimethylamine N-Oxide (TMAO) in disease: potential biomarker or new therapeutic target. *Nutrients* 10:1398. <https://doi.org/10.3390/nu10101398>
 12. Rath S, Heidrich B, Pieper DH, Vital M (2017) Uncovering the trimethylamine-producing bacteria of the human gut microbiota. *Microbiome* 5:54. <https://doi.org/10.1186/s40168-017-0271-9>
 13. Martinez-del Campo A, Bodea S, Hamer HA, Marks JA, Haiser HJ, Turnbaugh PJ, Balskus EP (2015) Characterization and detection of a widely distributed gene cluster that predicts anaerobic choline utilization by human gut bacteria. *mBio* 6(2):e00042. <https://doi.org/10.1128/mBio.00042-15>
 14. Zhu Y, Jameson E, Crosatti M, Schafer H, Rajakumar K, Bugg TD, Chen Y (2014) Carnitine metabolism to trimethylamine by an unusual Rieske-type oxygenase from human microbiota. *Proc Natl Acad Sci U S A* 111:4268–4273. <https://doi.org/10.1073/pnas.1316569111>
 15. Romano KA, Vivas EI, Amador-Noguez D, Rey FE (2015) Intestinal microbiota composition modulates choline bioavailability from diet and accumulation of the proatherogenic metabolite trimethylamine-N-oxide. *mBio* 6:e02481. <https://doi.org/10.1128/mBio.02481-14>
 16. Craciun S, Balskus EP (2012) Microbial conversion of choline to trimethylamine requires a glycol radical enzyme. *Proc Natl Acad Sci U S A* 109:21307–21312. <https://doi.org/10.1073/pnas.1215689109>
 17. Kalnins G, Kuka J, Grinberga S, Makrecka-Kuka M, Liepirsh E, Dambrova M, Tars K (2015) Structure and function of CutC choline lyase from human microbiota bacterium *Klebsiella pneumoniae*. *J Biol Chem* 290:21732–21740. <https://doi.org/10.1074/jbc.M115.670471>
 18. Jameson E, Fu T, Brown IR, Paszkiewicz K, Purdy KJ, Frank S, Chen Y (2016) Anaerobic choline metabolism in microcompartments promotes growth and swarming of *Proteus mirabilis*. *Environ Microbiol* 18:2886–2898. <https://doi.org/10.1111/1462-2920.13059>
 19. Wang Z, Klipfell E, Bennett BJ, Koeth R, Levison BS, Dugar B, Feldstein AE, Britt EB, Fu X, Chung YM, Wu Y, Schauer P, Smith JD, Allayee H, Tang WH, DiDonato JA, Lusis AJ, Hazen SL (2011) Gut flora metabolism of phosphatidylcholine promotes cardiovascular disease. *Nature* 472:57–63. <https://doi.org/10.1038/nature09922>
 20. Wang Z, Tang WH, Buffa JA, Fu X, Britt EB, Koeth RA, Levison BS, Fan Y, Wu Y, Hazen SL (2014) Prognostic value of choline and betaine depends on intestinal microbiota-generated metabolite trimethylamine-N-oxide. *Eur Heart J* 35:904–910. <https://doi.org/10.1093/eurheartj/ehu002>
 21. Wang Z, Roberts AB, Buffa JA, Levison BS, Zhu W, Org E, Gu X, Huang Y, Zamanian-Daryoush M, Culley MK, DiDonato AJ, Fu X, Hazen JE, Krajcik D, DiDonato JA, Lusis AJ, Hazen SL (2015) Non-lethal inhibition of gut microbial trimethylamine production for the treatment of atherosclerosis. *Cell* 163:1585–1595. <https://doi.org/10.1016/j.cell.2015.11.055>
 22. Koeth RA, Wang Z, Levison BS, Buffa JA, Org E, Sheehy ET, Britt EB, Fu X, Wu Y, Li L, Smith JD, DiDonato JA, Chen J, Li H, Wu GD, Lewis JD, Warrier M, Brown JM, Krauss RM, Tang WH, Bushman FD, Lusis AJ, Hazen SL (2013) Intestinal microbiota metabolism of L-carnitine, a nutrient in red meat, promotes atherosclerosis. *Nat Med* 19:576–585. <https://doi.org/10.1038/nm.3145>
 23. Rebouche CJ, Mack DL, Edmonson PF (1984) L-Carnitine dissimilation in the gastrointestinal tract of the rat. *Biochemistry* 23:6422–6426. <https://doi.org/10.1021/bi00321a022>
 24. Parmanand BA, Kellingray L, Le Gall G, Basit AW, Fairweather-Tait S, Nbarad A (2019) A decrease in iron availability to human gut microbiome reduces the growth of potentially pathogenic gut bacteria: an in vitro colonic fermentation study. *J Nutr Biochem* 67:20–27. <https://doi.org/10.1016/j.jnutbio.2019.01.010>
 25. Sender R, Fuchs S, Milo R (2016) Revised estimates of the number of human and bacterial cells in the body. *PLoS Biol* 14:e1002533–e1002533. <https://doi.org/10.1371/journal.pbio.1002533>
 26. Takagi R, Sasaki K, Sasaki D, Fukuda I, Tanaka K, Yoshida K, Kondo A, Osawa R (2016) A Single-batch fermentation system to simulate human colonic microbiota for high-throughput

- evaluation of prebiotics. *PLoS One* 11:e0160533. <https://doi.org/10.1371/journal.pone.0160533>
27. Lenth R, Singmann H, Love J, Buerkner P, Herve M (2019) Package 'emmeans' (version 1.3. 4). stimated marginal means, aka least-squares means. <https://CRAN.R-project.org/package=emmeans>. Accessed 2 Feb 2021
 28. Pinheiro J, Bates D, DebRoy S, Sarkar D, R Core Team (2019). nlme: Linear and nonlinear mixed effects models. R package version 3.1–139. <https://CRAN.R-project.org/package=nlme>. Accessed 2 Feb 2021
 29. Team RC (2018) R: A language and environment for statistical computing. Vienna, Austria: R Foundation for Statistical Computing. <https://www.R-project.org/>. Accessed 2 Feb 2021
 30. Fennema D, Phillips IR, Shephard EA (2016) Trimethylamine and Trimethylamine N-Oxide, a Flavin-containing Monooxygenase 3 (FMO3)-Mediated Host-microbiome metabolic axis implicated in health and disease. *Drug Metab Dispos* 44:1839–1850. <https://doi.org/10.1124/dmd.116.070615>
 31. Serra AL, Mariscotti JF, Barra JL, Lucchesi GI, Domenech CE, Lisa AT (2002) Glycine betaine transmethylase mutant of *Pseudomonas aeruginosa*. *J Bacteriol* 184:4301–4303. <https://doi.org/10.1128/jb.184.15.4301-4303.2002>
 32. Jameson E, Doxey AC, Airs R, Purdy KJ, Murrell JC, Chen Y (2016) Metagenomic data-mining reveals contrasting microbial populations responsible for trimethylamine formation in human gut and marine ecosystems. *Microb Genom* 2:e000080. <https://doi.org/10.1099/mgen.0.000080>
 33. Rath S, Rud T, Pieper DH, Vital M (2020) Potential TMA-producing bacteria are ubiquitously found in mammalia. *Front Microbiol* 10:2966. <https://doi.org/10.3389/fmicb.2019.02966>
 34. Kühn T, Rohrmann S, Sookthai D, Johnson T, Katzke V, Kaaks R, von Eckardstein A, Müller D (2017) Intra-individual variation of plasma trimethylamine-N-oxide (TMAO), betaine and choline over 1 year. *Clin Chem Lab Med* 55:261–268. <https://doi.org/10.1515/cclm-2016-0374>
 35. McEntyre CJ, Lever M, Chambers ST, George PM, Slow S, Elmslie JL, Florkowski CM, Lunt H, Krebs JD (2015) Variation of betaine, N, N-dimethylglycine, choline, glycerophosphorylcholine, taurine and trimethylamine-N-oxide in the plasma and urine of overweight people with type 2 diabetes over a two-year period. *Ann Clin Biochem* 52:352–360. <https://doi.org/10.1177/0004563214545346>